frontiers | Research Topics

Drug-resistance in cancer cells: A new wine in an old bottle

Edited by
Leonardo Freire-de-Lima, Takeo Tatsuta and Seung-Yeol Park

Published in
Frontiers in Oncology
Frontiers in Pharmacology

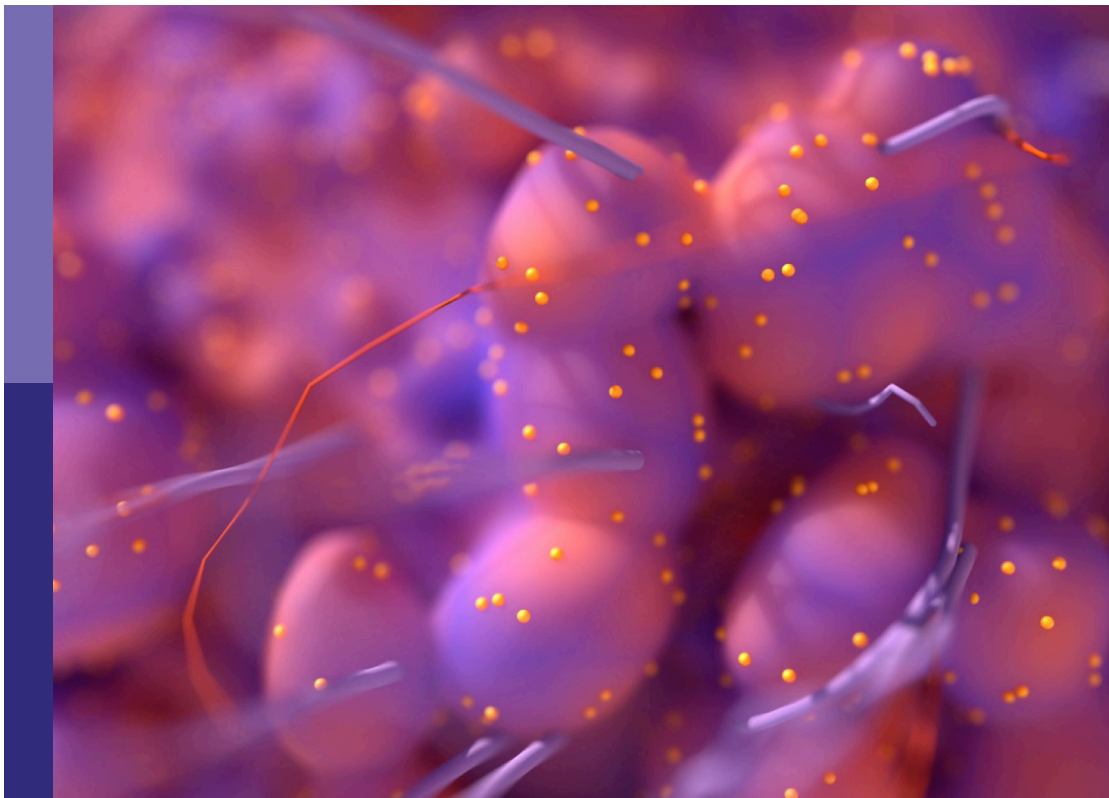

ISSN 1664-8714
ISBN 978-2-83251-848-9
DOI 10.3389/978-2-83251-848-9

About Frontiers

Frontiers is more than just an open access publisher of scholarly articles: it is a pioneering approach to the world of academia, radically improving the way scholarly research is managed. The grand vision of Frontiers is a world where all people have an equal opportunity to seek, share and generate knowledge. Frontiers provides immediate and permanent online open access to all its publications, but this alone is not enough to realize our grand goals.

Frontiers journal series

The Frontiers journal series is a multi-tier and interdisciplinary set of open-access, online journals, promising a paradigm shift from the current review, selection and dissemination processes in academic publishing. All Frontiers journals are driven by researchers for researchers; therefore, they constitute a service to the scholarly community. At the same time, the *Frontiers journal series* operates on a revolutionary invention, the tiered publishing system, initially addressing specific communities of scholars, and gradually climbing up to broader public understanding, thus serving the interests of the lay society, too.

Dedication to quality

Each Frontiers article is a landmark of the highest quality, thanks to genuinely collaborative interactions between authors and review editors, who include some of the world's best academicians. Research must be certified by peers before entering a stream of knowledge that may eventually reach the public - and shape society; therefore, Frontiers only applies the most rigorous and unbiased reviews. Frontiers revolutionizes research publishing by freely delivering the most outstanding research, evaluated with no bias from both the academic and social point of view. By applying the most advanced information technologies, Frontiers is catapulting scholarly publishing into a new generation.

What are Frontiers Research Topics?

Frontiers Research Topics are very popular trademarks of the *Frontiers journals series*: they are collections of at least ten articles, all centered on a particular subject. With their unique mix of varied contributions from Original Research to Review Articles, Frontiers Research Topics unify the most influential researchers, the latest key findings and historical advances in a hot research area.

Find out more on how to host your own Frontiers Research Topic or contribute to one as an author by contacting the Frontiers editorial office: frontiersin.org/about/contact

Drug-resistance in cancer cells: A new wine in an old bottle

Topic editors

Leonardo Freire-de-Lima — Federal University of Rio de Janeiro, Brazil
Takeo Tatsuta — Tohoku Medical and Pharmaceutical University, Japan
Seung-Yeol Park — Pohang University of Science and Technology, Republic of Korea

Topic Coordinator

Leonardo Marques da Fonseca — Federal University of Rio de Janeiro, Brazil

Citation

Freire-de-Lima, L., Tatsuta, T., Park, S.-Y., eds. (2023). *Drug-resistance in cancer cells: A new wine in an old bottle*. Lausanne: Frontiers Media SA. doi: 10.3389/978-2-83251-848-9

Table of contents

frontiers | Frontiers in Oncology

TYPE Editorial
PUBLISHED 22 February 2023
DOI 10.3389/fonc.2023.1161008

OPEN ACCESS

EDITED AND REVIEWED BY
Olivier Feron,
Université catholique de Louvain, Belgium

*CORRESPONDENCE
Leonardo Marques da Fonseca
lfonseca@biof.ufrj.br
Takeo Tatsuta
t-takeo@tohoku-mpu.ac.jp
Seung-Yeol Park
seungpark@postech.ac.kr
Leonardo Freire-de-Lima
leolima@biof.ufrj.br

SPECIALTY SECTION
This article was submitted to Pharmacology of Anti-Cancer Drugs, a section of the journal Frontiers in Oncology

RECEIVED 07 February 2023
ACCEPTED 13 February 2023
PUBLISHED 22 February 2023

CITATION
Fonseca LM, Tatsuta T, Park S-Y and Freire-de-Lima L (2023) Editorial: Drug-resistance in cancer cells: A new wine in an old bottle.
Front. Oncol. 13:1161008.
doi: 10.3389/fonc.2023.1161008

Editorial: Drug-resistance in cancer cells: A new wine in an old bottle

Leonardo Marques da Fonseca[1]*, Takeo Tatsuta[2]*, Seung-Yeol Park[3]* and Leonardo Freire-de-Lima[1]*

[1]Universidade Federal do Rio de Janeiro, Instituto de Biofísica Carlos Chagas Filho, Laboratório de Biologia Celular de Glicoconjugados, Rio de Janeiro, Brazil, [2]Division of Cell Recognition, Institute of Molecular Biomembrane and Glycobiology, Tohoku Medical and Pharmaceutical University, Sendai, Japan, [3]Department of Life Sciences, POSTECH, Pohang, Gyeongbuk, Republic of Korea

KEYWORDS

cancer, ATP binding casette transporter, signaling pathways, chemotherapeutic agents, chemoresistance

Editorial on the Research Topic:
Drug-resistance in cancer cells: A new wine in an old bottle

Cancer is a major challenge to physicians everywhere, and among its malignancy factors, drug resistance, especially multidrug resistance (MDR) phenotypes stand to be one of the most important challenges. This is why we made a call for papers regarding MDR, its causes, and factors that might affect or are directly related to MDR. At the time of writing this editorial, a total of fourteen articles, six review articles and eight original research articles, have been published in this special issue, with over eighteen thousand views up until now.

Negri et al. report that exosomes from resistant hepatocarcinoma cells can induce resistance in sensitive cells in a process that can be reverted by vitamin D. Ye et al., in their work, propose a novel combination therapy strategy to circumvent drug resistance, using a proteolysis targeting chimera (PROTAC) aimed at BCR-ABL1 mutants, characteristic of chronic myeloid leukemia and tyrosine kinase inhibitors. Narayanan et al. provide us with an evaluation of the anticancer potential of sixteen thiazolyl hydrazone derivates of 1-indanone, remarking that one of them, IHT-6, shows promise in the treatment of p53 mutant colorectal cancers, going as far as providing a possible mechanism of action for the drug. Zeng et al., in their research, show that A011, a sigma-2 receptor ligand shows promising toxicity levels against both parental and resistant MCF-7 cells, which is capable of inhibiting ABCB1 transport activity and downregulating ABCG2 expression. A study involving ovarian cancer patients performed by Oplawski et al. shows a correlation between the levels of antigen CA-125 (associated with drug resistance) and patients that have undergone chemotherapy treatment along with surgery. The work of Indorato et al. evaluates mutations in the Eg5 mitotic kinesin and how they translate into resistance phenotypes, predicting that inhibitors may work or not depending on the binding site for Eg5. Ye et al. provide us with an insightful study of drug-delivery strategies for docetaxel and curcumin *via* liposomes, showing that the co-delivery system is more efficient than the free drugs against MCF-7 tumors in mice. The work of Szymczyk et al. shows us that

activation of Akt by either the canonical or alternative pathways is essential for the protective effect against drugs affecting tubulin polymerization in cancer cells.

We also received very insightful review articles that put established knowledge in a new perspective. Xia et al. summarize the regulatory mechanisms of m6A modification in the drug therapy of digestive system malignancies. Li et al. supply a compendium of the understanding of the mechanism of ferroptosis based on the System Xc−/GSH/GPX4 axis in the treatment of drug-resistant solid tumors. Barreto et al. provide an insight into the immunophenotypic characteristics and mechanisms of resistance presented by LSCs and also suggest possible alternatives for the treatment of patients. Zhou et al. judiciously review the more recent works on the emerging role and underlying mechanisms of ncRNAs involved in cancer drug resistance and focus on their clinical applications as biomarkers and therapeutic targets in cancer treatment. Cheng et al. review predictive factors for anti-PD-1/PD-L1 immunotherapy in EC, demonstrating resistance mechanisms to PD-1/PD-L1 blockade. The work of Very and Yazidi-Belkoura summarizes recent evidence that cancer therapeutics affect cellular *O*-GlcNAcylation, and reciprocally, that *O*-GlcNAcylation modulates the response of cancer cells to therapies. It also shows the benefits of targeting *O*-GlcNAcylation as a novel therapeutic strategy for cancer.

This compilation of studies provides a great insight into cancer therapy and drug resistance, covering various subjects from the underlying causes of MDR to ways of circumventing it. Readers will undoubtedly benefit from this material.

Author contributions

LF, TT, S-YP, and LF-d-L wrote the paper. All the authors read and approved the final version of the manuscript.

Acknowledgments

The Editors are deeply grateful to all authors who contributed with original articles and reviews on this Research Topic, which addresses such an important issue in oncobiology.

Conflict of interest

The authors declare that the research was conducted in the absence of any commercial or financial relationships that could be construed as a potential conflict of interest.

Publisher's note

frontiers | Frontiers in Oncology

ORIGINAL RESEARCH
published: 25 April 2022
doi: 10.3389/fonc.2022.874091

Vitamin D Reverts the Exosome-Mediated Transfer of Cancer Resistance to the mTOR Inhibitor Everolimus in Hepatocellular Carcinoma

Mariarosaria Negri[1†], Feliciana Amatrudo[1†], Annalisa Gentile[1], Roberta Patalano[1], Tatiana Montò[1], Cristina de Angelis[1], Chiara Simeoli[1], Rosa Pirchio[1], Renata Simona Auriemma[1], Annamaria Colao[1,2], Rosario Pivonello[1,2] and Claudia Pivonello[1]*

[1] Dipartimento di Medicina Clinica e Chirurgia, Sezione di Endocrinologia, Università Federico II di Napoli, Naples, Italy, [2] United Nations Educational, Scientific and Cultural Organization (UNESCO) Chair for Health Education and Sustainable Development, Federico II University, Naples, Italy

Several multi-kinase inhibitors were widely tested as potential first-line or second-line therapy in patients with advanced hepatocellular carcinoma (HCC). However, acquired drug resistance limits their clinical efficacy. Exosomes are microvesicles secreted by tumor and stromal cells that participate in many biological processes, including drug resistance. The current study evaluated the capability of exosomes derived from everolimus (EVE)-resistant HCC cells in inducing drug resistance in parental human HCC cells and the effect of 1,25(OH)$_2$Vitamin D (VitD) treatment in restoring EVE sensitivity. The internalization of exosomes from EVE-resistant (EveR) cells into parental cells conferred the transmission of aggressive phenotype by promoting the transition of epithelial-to-mesenchymal phenotype, as demonstrated by immunofluorescence, and the acquisition of EVE resistance, as demonstrated by cell proliferation and colony formation assays. Moreover, the internalization of exosomes from EveR into parental cells induced deregulation of the mTOR pathway mainly by triggering the activation of the serine/threonine protein kinase Akt, involved in the cellular survival pathway, as demonstrated by Western blot analysis. Interestingly, the treatment with VitD prevented exosome-induced EVE resistance in HCC cells, significantly inhibiting cell proliferation but also partially reducing colony and size number when combined with EVE compared with control. In conclusion, the results of the current study demonstrated that exosomes derived from EveR cells could induce EVE resistance in EVE-sensitive HCC cells and that VitD can revert the exosome-induced EVE resistance by resensitizing to EVE treatment.

Keywords: exosomes, HCC, everolimus, drug resistance, PI3K/Akt/mTOR pathway

OPEN ACCESS

Edited by:
Leonardo Freire-de-Lima, Federal University of Rio de Janeiro, Brazil

Reviewed by:
Daniele Vergara, University of Salento, Italy
Raphael Carmo Valente, Federal University of Rio de Janeiro, Brazil

***Correspondence:**
Claudia Pivonello
claudia.pivonello@unina.it;
cpivonello@gmail.com

†These authors have contributed equally to this work

Specialty section:
This article was submitted to Pharmacology of Anti-Cancer Drugs, a section of the journal Frontiers in Oncology

Received: *11 February 2022*
Accepted: *22 March 2022*
Published: *25 April 2022*

Citation:
Negri M, Amatrudo F, Gentile A, Patalano R, Montò T, de Angelis C, Simeoli C, Pirchio R, Auriemma RS, Colao A, Pivonello R and Pivonello C (2022) Vitamin D Reverts the Exosome-Mediated Transfer of Cancer Resistance to the mTOR Inhibitor Everolimus in Hepatocellular Carcinoma. Front. Oncol. 12:874091. doi: 10.3389/fonc.2022.874091

INTRODUCTION

Hepatocellular carcinoma (HCC) is the most frequent among primary liver cancers and represents the fourth most common cause of cancer-related death worldwide (1). Cancer surveillance is applied to patients with a high risk to develop HCC, such as patients with cirrhosis, hepatitis B, and chronic hepatitis C with liver fibrosis, with the aim to detect tumors at early stages in order to increase the opportunity to use curative treatments and improve survival (1, 2). Nevertheless, regrettably, HCC is often diagnosed at advanced stages (1, 2). Currently, available or emerging systemic therapies, including multi-kinase inhibitors, used in advanced stages, still have limited efficacy with a scarce impact on overall survival (2). As observed in several types of cancers, systemic therapy often results in the reduction of tumor size but rarely succeeds in eradicating the totality of cancer cells, mainly for the acquisition of drug resistance, which is responsible for therapy failure (3). The phenotypic diversity of neoplastic cells that characterizes a tumor mass is considered a major driver of the development of resistance to medical therapy (3). Drug resistance development can involve several concomitant causes and mechanisms, including the drug efflux mechanisms, the persistence of cancer stem cells, the switch of the epithelial–mesenchymal transition (EMT), and the role of cancer-secreted microRNAs (miRNAs) and exosomes in the tumor microenvironment (4). Exosomes are the smallest extracellular vesicles with a diameter size ranging between 40 and 150 nm and a spherical shape bounded by a lipid bilayer membrane (5). Carrying a multitude of diverse biological factors, the exosomes can play a role in the different physiological and pathological processes (5). The different content of exosomes likely reflects the phenotypic states of the cells in physiological and pathological conditions. Interestingly, the exosomal cargoes can be conveyed to the neighboring or distant cells modulating the phenotype of these target cells (5) and, therefore, among the several effects, altering their capability to respond to the medical treatment. A previous study demonstrated that HCC cell-derived exosomes promoted resistance to the multikinase inhibitor sorafenib in *in vitro* and *in vivo* HCC models, and exosomes derived from highly invasive tumors could trigger stronger drug resistance (6). However, to the best of our knowledge, no studies have reported the ability of exosomes from HCC cell lines resistant to mTOR inhibitors in inducing drug resistance in HCC parental cells. Therefore, the primary aim of the current study was to investigate whether exosomes released by human everolimus (EVE)-resistant cell lines, JHH-6 and PLC/PRF/5, were able to induce EVE resistance in JHH-6 and PLC/PRF/5 parental cells. Moreover, the recent literature highlights the ability of 1,25(OH) vitamin D (VitD) to reverse the pharmacological resistance acquired in different tumor models and at different levels including the regulation of cancer stem cell growth (7), the EMT (7), and the regulation of specific miRNAs (7, 8). In particular, a recent work of the authors have demonstrated that a pre-treatment with VitD was able to restore the sensitivity to EVE in EVE-resistant HCC cell lines by regulating the EMT process and by reducing oncogene expression through the upregulation of miR-375 expression (8). Therefore, the secondary aim of the current study was to explore the role of VitD in the exosome-mediated transfer of cancer EVE resistance in HCC cell models.

MATERIALS AND METHODS

Cell Cultures and Compounds

Human HCC cell lines PLC/PRF/5 and JHH-6 were used for the study. Parental cells were cultured as previously described (8). PLC/PRF/5- and JHH-6-resistant cells (EveR) were obtained by continuous culture of cell lines in the presence of EVE 10^{-8} M for at least 4 months (8). PLC/PRF/5 and JHH-6 parental cells were treated for 16 days with exosomes isolated from PLC/PRF/5 EveR and JHH-6 EveR cells and defined Exo EveR along with the text. Briefly, 1×10^6 PLC/PRF/5 parental cells, 0.5×10^6 JHH-6 parental cells, 2×10^6 PLC/PRF/5 EveR cells, and 1.5×10^6 JHH-6 EveR cells were seeded simultaneously in four different 75-cm^3 flasks in the presence of cell culture exosome-free medium (fetal bovine serum, exosome-depleted, One Shot format, Gibco). Exactly every 3 days, the exosomes were extracted by EveR exosome-free medium by the Cell Culture Exosome Purification Midi Kit [Norgen Biotek Corp. (Canada)] according to the manufacturer's instructions and inoculated in the flasks of both parental cells, respectively. When parental cells reached the confluence, they were detached by trypsin, split, and seeded again in order to complete the exosome-treatment cycle. After 16 days of exosome internalization, the cells were collected for the activity assays. Exosome-treatment protocol has been shown and detailed in **Supplementary Figure 1**. All cell lines were grown at 37°C in a humidified atmosphere with 5% CO_2.

EVE [Selleck Chemicals (UK)] was dissolved in DMSO 100% and stored at −80°C. Fresh aliquots were defrosted prior to each new experiment. Serial dilutions were prepared using DMSO 40% reaching final concentrations of 0.04% in the medium in each well.

Exosomal Protein Extraction and Western Blot

PLC/PRF/5 parental cells (1.5×10^6), (1×10^6) JHH-6 parental cells, (2×10^6) PLC/PRF/5 EveR cells, and (1.5×10^6) JHH-6 EveR cells were seeded in 75-cm^3 flasks in the presence of cell culture exosome-free medium (fetal bovine serum, exosome-depleted, One Shot format, Gibco). Cells were grown in adhesion for 3 days, after which they reached 70% of confluence. Exo EveR cells were grown as described in the protocol detailed in **Supplementary Figure 1**. Parental, EveR, Exo EveR PLC/PRF/5, and JHH-6 cell pellets were harvested and lysed for protein extraction.

Moreover, proteins were also isolated from exosomes released in exosome-free medium of Exo EveR cells by using an ultracentrifuge according to the following protocol. The medium was centrifuged at $300 \times g$ for 10 min at 4°C to remove cell debris. Subsequently, the medium was subjected to 3 other ultracentrifugations to eliminate, based on their size, the large vesicles ($2{,}000 \times g$ for 30 min at 4°C) and medium vesicles

(16,500 × *g* for 30 min at 4°C) and obtain only the smaller vesicles (exosomes) (120,000 × *g* for 2 h at 4°C). The pellet, composed only of exosomes, is stored at −80°C until protein extraction.

Exosomal proteins were isolated in NP40 buffer supplemented with protease phosphatase inhibitor cocktail and an additional 2.0% SDS on ice for 30 min. The homogenate was centrifuged for 15 min at 1,200 × *g* and 4°C, and the supernatant was collected and stored at −80°C until use. Exosomal protein concentrations were determined photometrically with a bicinchoninic acid (BCA) Protein Assay Kit (Thermo Scientific, USA).

After protein heat denaturation at 95°C for 10 min, 5 μg of total extracts was used for immunoblotting. Exosomal proteins were separated by 8% SDS-PAGE and then electroblotted onto a nitrocellulose membrane for 90 min in a TransBlot apparatus. After a blocking treatment for 1 h with 5% milk, the nitrocellulose filters were probed with primary antibodies specific for ALIX (EPR15314-33, Abcam), TSG101 [EPR7130 (B), Abcam], and CD9 (EPR2949, Abcam) overnight. Subsequently, filters were hybridized with peroxidise-conjugated secondary antibodies and immunoreactive bands were detected by the ECL system. After a chemiluminescent reaction, the blot was exposed to ImageQuant Las 4000 (GE Healthcare).

Exosomes Isolation and Staining

PLC/PRF/5 parental cells (1.5×10^6), (1×10^6) JHH-6 parental cells, (2×10^6) PLC/PRF/5 EveR cells, and (1.5×10^6) JHH-6 EveR cells were seeded in 75-cm^3 flasks and grown in 10 ml of exosome-free medium. After 3 days, the cells reached 70% confluence. The medium of EveR cells was collected and exosomes were isolated from cell culture exosome-free medium by using the Cell Culture Exosome Purification Midi Kit [Norgen Biotek Corp. (Canada)] according to the manufacturer's instructions. Ten milliliters of cell culture media was transferred in a conical tube and centrifuged at 1,000 RPM for 15 min to remove any cells and debris. The cell-free media was transferred into a new 15-ml conical tube where 2.5 μl of ExoC Buffer was added for every 1 ml of cell-free media and 400 μl of Slurry E resin was then supplemented. The solution was mixed well by vortexing for 10 s, left at room temperature for 10 min, and then centrifuged for 2 min at 2,000 RPM. The supernatant was discarded and 400 μl of ExoR Buffer was applied to the slurry pellet; it was mixed well by vortexing for 10 s and the resuspended slurry pellet was incubated at room temperature for 10 min. After incubation, the resuspended pellet was vortexed for 10 s and centrifuged for 2 min at 500 RPM. Lastly, the supernatant was transferred to a Mini Filter Spin column assembled with an elution tube and was centrifuged for 1 min at 6,000 RPM. The flowthrough contained the purified exosomes.

Subsequently, in order to resuspend the exosomes in PBS 1X, the Exo-spin Exosome Purification Kit [Cell Guidance Systems (UK)] was used. Extracted exosomes (200 μl) were added to the column and it was centrifuged for 1 min at 50 × *g*; the eluate was discarded. The column was placed in a new Eppendorf and 200 μl of PBS 1X was added to the column and centrifuged at 50 × *g* for 60 s. The exosomes were then marked with PKH67 Green Fluorescent membrane staining [Sigma-Aldrich (USA)]. PKH67 dye (1 μl) was diluted in 500 μl of diluent C. Final dye (250 μl) was mixed with 200 μl of exosomes in PBS 1X for 4 min.

The reaction was stopped by adding an equal volume of PBS 1X and FBS exosome-free (1:1) to this mix, for 3 min. To remove the excess dye, the Exo-spin Exosome Purification Kit [Cell Guidance Systems (UK)] was used as previously described and the colored exosomes were contained in the eluate.

The stained exosomes were inoculated in μ-Dish 35 mm (IBIDI, Germany), previously prepared with PLC/PRF/5 and JHH-6 parental cells at 70% confluence to evaluate the exosome uptake after about 18 h. Images were visualized on an inverted microscope, Olympus IX51, equipped for fluorescence and phase-contrast microscopy (Olympus, Milan, Italy) and were captured at 40× magnification.

mRNA Isolation and RT-qPCR

mRNA isolation from parental and resistant cells was carried out as previously described (9). mRNA expression pattern of single components of mTOR pathway, including mTOR, p70S6k, and 4eBP1, was assessed by SYBR Green-based RT-qPCR performed with specific sets of primer sequences as previously reported (10). The final product was subjected to graded temperature-dependent dissociation to verify that only one product was amplified. Reactions were run in duplicate, and each reaction was repeated thrice on a StepOne Plus real-time PCR machine (Applied Biosystems Foster City, CA, USA). The relative expression levels of each transcript analyzed in each sample were normalized using the housekeeping gene β-actin.

Cell Proliferation Assay

After trypsinization, PLC/PRF/5 parental, EveR and Exo EveR cells (1.5×10^4) and JHH-6 parental, EveR and Exo EveR cells (1.5×10^3) were plated in 1 ml of complete culture medium in 24 well plates for 6 days, respectively. The plates were then placed in an incubator in 5% CO_2 at 37°C. After 24 h, VitD 10^{-7} M and EVE were added to each well at different concentrations, ranging between 10^{-11} and 10^{-7} M. Controls were vehicle-treated. Plates were further incubated at 37°C and 5% CO_2. The medium was changed and VitD and EVE were freshly added every 3 days. After 6 days of treatment, cells were harvested for DNA measurement. Measurement of total DNA content, representative for the number of cells, was performed using the bisbenzimide fluorescent dye (Hoechst 33258) (Boehring Diagnostics, La Jolla, CA), as previously described (11).

Immunofluorescence Staining

Immunofluorescence staining was performed as previously described (8, 10). The cells were incubated with primary antibodies against Vimentin (Abcam, ab92547, rabbit monoclonal, dilution 1/250) and E-cadherin (Santa Cruz, sc-21791, mouse monoclonal, dilution 1/100) for 1.5 h. Slides were then washed thrice in 0.1% Triton/PBS for 5 min and incubated with the secondary antibodies for 1 h (Millipore, AP124F, goat anti-mouse, FITC conjugated, dilution 1/500; ImmunoReagent, Gtx-Rb-003-DRHO, goat anti-rabbit, TRITC conjugated, dilution 1/500). Nuclei were stained with 4,6-diamidino-2-

phenylindole (DAPI) (Lonza Group Ltd, Basel, Switzerland), diluted in PBS 1X 1:40,000. Images were visualized on an inverted microscope, Olympus IX51, equipped for fluorescence and phase-contrast microscopy (Olympus, Milan, Italy) and were captured at 40× magnification and acquired with Olympus IX2-LWUCD 6A14956 Digital Camera F-View II (Olympus, Milan, Italy).

Colony-Forming Assay

Colony-forming assay was performed as previously described (8). Parental PLC/PRF/5, EveR, and Exo EveR cells (500 cell/ml) were plated into six-well culture dishes and cultured in complete medium for 21 days. After 24 h of adhesion, cells were treated with EVE 10^{-10} M and/or VitD 10^{-7} M, whereas in control cells, vehicles were added. Every 3 days, a fresh medium was replaced and drugs and vehicles were readded. After 21 days, formed colonies were stained (12) and counted. Moreover, the dimension of colonies was evaluated by ImageJ software as integrated density.

Cell Lysis and Western Blot

Cell lysis and WB analysis were performed as previously described (9). Primary antibodies specific for Akt (#9272, Cell Signaling Technology, Italy), p70S6k (H-9) (sc-8418) (Santa Cruz Biotechnology Inc.), 4eBP1 (53H11) (#9644, Cell Signaling Technology, Italy), pAkt (ser473) (#9271, Cell Signaling Technology, Italy), pp70S6k (Thr389) (#9206, Cell Signaling Technology, Italy), p4eBP1 (Ser65) (#9456, Cell Signaling Technology, Italy), and β-actin (A4700; Sigma-Aldrich, Italy) were probed on nitrocellulose filters overnight. Peroxidase-conjugated secondary antibodies (Donkey anti-Rabbit IgG, DkxRb-003-DHRPX, ImmunoReagents, Inc) (Goat anti-Mouse IgG, GtxMu-003-DHRPX, ImmunoReagents, Inc) used were probed for 1 h. Immunoreactive bands were detected by the ECL system and the blot was exposed to ImageQuant Las 4000 (GE Healthcare).

Statistical Analysis

All the experiments were performed in quadruplicate and were replicated three times with the exception of Western blot analysis that was replicated two times. All statistical analyses were performed using GraphPad software. Based on the number of groups to compare, differences between controls and treated groups were determined by Student's *t*-test or ANOVA. *p*-values less than 0.05 were considered statistically significant.

RESULTS

Evaluation of Exosomes' Extraction From Cell Media

To confirm that the vesicular structures isolated by JHH-6 and PLC/PRF/5 EveR cell media are exosomes, proteins from the plasma and endosomal membranes, including programmed cell death 6-interacting protein (ALIX), tumor susceptibility gene 101 (TSG101), and cluster of differentiation 9 (CD9), were used as markers. As shown in **Figure 1A**, the specific and selective markers ALIX and TSG101 are both expressed in the exosomes released by JHH-6 and PLC/PRF/5 EveR, while CD9 is only expressed in the exosomes released by JHH-6 EveR. In the exosomal samples of both cell lines, no expression of the cytoskeleton marker, β-actin, confirmed the purity of the exosomal samples.

Exosomes From HCC EveR Cells Internalize in HCC Parental Cells

To explore whether the exosomes from donor JHH-6 and PLC/PRF/5 EveR cells could be transferred to recipient JHH-6 and PLC/PRF/5 parental cells, the uptake of labeled exosome was investigated. As shown in **Figure 1B**, JHH-6 and PLC/PRF/5 EveR cell-derived exosomes, labeled with PKH67 Green Fluorescent Cell Linker, were inoculated with JHH-6 and PLC/PRF/5 parental cells and green staining in the parental cells was observed within 18 h, confirming the exosome incorporation.

Exosomes Induce Mesenchymal-Like Markers in Parental Cells

Tumor progression and the development of drug resistance are dependent on several molecular factors including the crosstalk between tumor cells and their microenvironment. Exosomes released by tumor cells represent a means of communication between cells; therefore, they might take an active role in the transmission of drug resistance. To further investigate the effect of exosome cross-talk on spreading drug resistance signals, it has been tested whether, in parental cells, the incorporation of exosomes released by EveR cells could induce EMT that has been demonstrated to confer resistance to many types of therapeutic agents on tumor cells. Considering the well-known mesenchymal phenotype of parental JHH-6 (13, 14), the EMT has been investigated only the PLC/PRF/5 cell line. As shown in **Figure 2**, PLC/PRF/5 parental cells and PLC/PRF/5 EveR cells mainly express E-cadherin and vimentin, respectively. Interestingly, when exosomes released by PLC/PRF/5 EveR cells were incorporated by the recipient PLC/PRF/5 parental cells in the latter, a significant gain of EMT marker vimentin ($p < 0.01$) was observed.

Exosome Internalization Induces Drug Resistance in HCC Parental Cells

To investigate whether EveR-derived exosome internalization has a role in the acquisition of resistance to EVE in parental cells, cell proliferation assay was performed in JHH-6 and PLC/PRF/5 parental, EveR, and Exo EveR cells after the exposure to escalating doses of EVE, from 10^{-11} M to 10^{-7} M, for 6 days. As shown in **Figures 3A, B** (green line), both HCC cell lines, continuously cultured for at least 4 months in the presence of EVE 10^{-8} M, acquired drug resistance to the cytostatic effect of escalating doses of EVE, confirming our previous results (8).

Additionally, as shown in **Figures 3A, B** (red line), following the internalization of exosomes, both JHH-6 and PLC/PRF/5 Exo EveR showed acquired resistance to EVE treatment as demonstrated by the significantly reduced efficacy in inhibiting

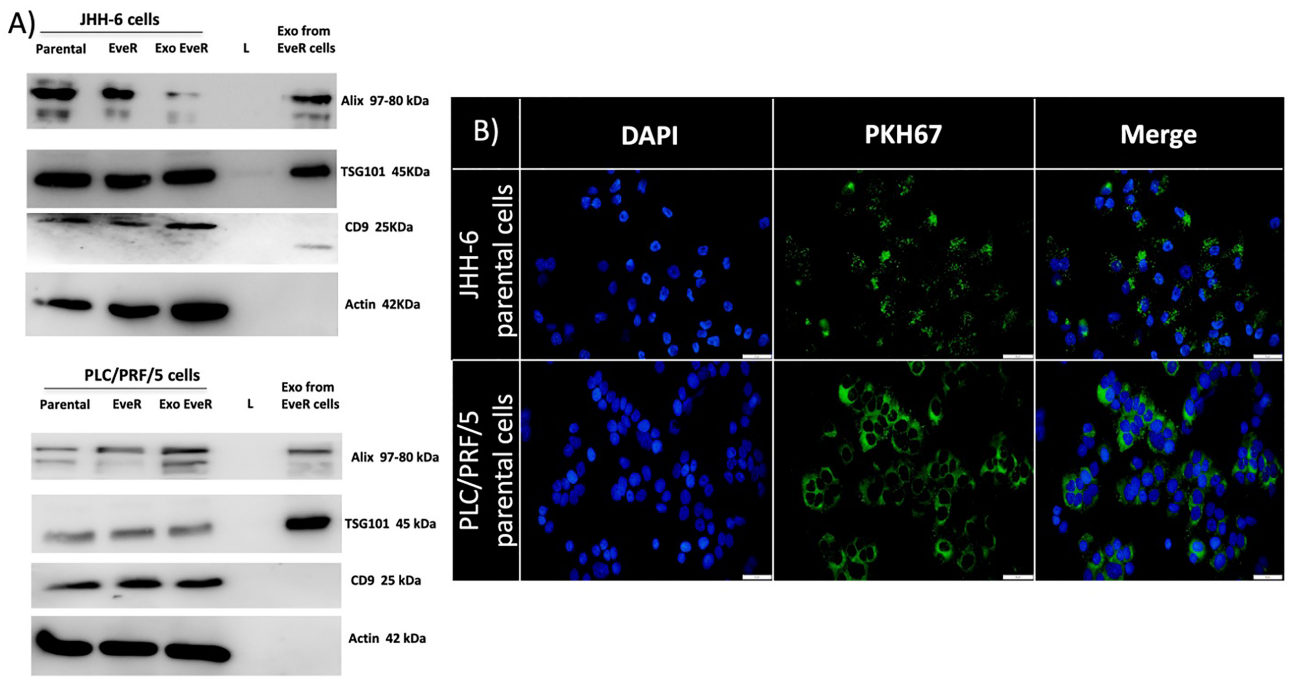

FIGURE 1 | **(A)** Immunoblot analysis of ALIX, TSG101, CD9, and β-actin in whole JHH-6 and PLC/PRF/5 parental cells, EveR, and Exo EveR and in exosome from EveR cell lysates. L, ladder. **(B)** Green fluorescence microscopy showing the uptake of PKH67-labeled exosomes from JHH-6 and PLC/PRF/5 EveR cells to recipient JHH-6 and PLC/PRF/5 parental cells. Blue represents DAPI staining of the nuclei; green represents exosome membrane staining.

the cell proliferation observed at the lower concentrations of EVE (10^{-10} M and 10^{-9} M) tested. Indeed, in JHH-6 parental cells, the EVE 10^{-10} M treatment induced 24.7% of inhibition compared to control, whereas the same treatment no longer induced any inhibition in JHH-6 Exo EveR ($p < 0.0001$ vs. EVE 10^{-10} M in JHH-6 parental cells). Accordingly, even the EVE 10^{-9} M treatment induced 56.5% of inhibition ($p < 0.0001$) in JHH-6 parental cells compared to control, whereas the same treatment in JHH-6 Exo EveR induced only 26.1% of inhibition compared to control, with a reduced percentage of inhibition (30.4%, $p < 0.05$) compared to the effect of the same EVE treatment in JHH-6 parental (**Figure 3A**). Consistently, in PLC/PRF/5 parental cells, the EVE 10^{-10} M treatment induced 16.8% of inhibition ($p < 0.05$) compared to control, whereas the same treatment no longer induced any inhibition in PLC/PRF/5 Exo EveR ($p < 0.01$ vs. EVE 10^{-10} M in PLC/PRF/5 parental cells). Accordingly, even the EVE 10^{-9} M treatment induced 41.7% of inhibition ($p < 0.0001$) in PLC/PRF/5 parental cells compared to control, whereas the same treatment in PLC/PRF/5 Exo EveR induced only 21.8% ($p < 0.001$) of inhibition compared to control, with a reduced percentage of inhibition (19.94%, $p < 0.01$) compared to the effect of the same EVE treatment in PLC/PRF/5 parental (**Figure 3B**).

The percentage of cell proliferation inhibition induced by EVE in PLC/PRF/5 and JHH-6 Exo EveR cells is summarized in **Table 1**.

As shown in **Figure 4**, a colony formation assay, performed with the PLC/PRF/5 cells that in contrast to JHH-6 cells were able to form colonies, demonstrated that the internalization of EveR-derived exosome in parental cells (PLC/PRF/5 Exo EveR) induced the formation of a higher colony number ($p = 0.034$) and higher colony size ($p < 0.0001$) compared to parental cells, suggesting that the internalization of EveR-derived exosome might induce a more aggressive phenotype. Nevertheless, the internalization of EveR-derived exosome does not induce EVE resistance compared to parental cells as observed in colony number formation. Indeed, EVE treatment in PLC/PRF/5 parental cells induces 46.7% ($p = 0.006$) of colony number inhibition and 37.0% ($p = 0.009$) of colony size reduction compared to the same untreated cells whereas EVE treatment in Exo EveR cells induces 35.3% ($p = 0.012$) of colony number inhibition and 52.7% ($p = 0.001$) of colony size reduction compared to the same untreated cells, with a non-significant difference between the effect observed in parental cells treated with EVE and that in Exo-EveR treated with EVE.

As shown in **Figure 5**, according to the immunoblot analysis, the protein content of the different mTOR pathway components reflects the acquired resistance to EVE in JHH-6 and PLC/PRF/5 EveR cells. Indeed, a strong reduction of the activity of mTOR downstream effectors p70S6K and 4eBP1 was detected in both cell lines. Interestingly, the internalization of exosomes from EveR cells into parental cells induces a reduction in protein content of phosphorylated forms of p70S6k in both JHH-6 and PLC/PRF/5 Exo EveR cells and of 4eBP1 in PLC/PRF/5 Exo EveR cells, and concomitantly, a hyperexpression of the phosphorylated form of Akt was observed in JHH-6 Exo EveR cells compared to the parental cells.

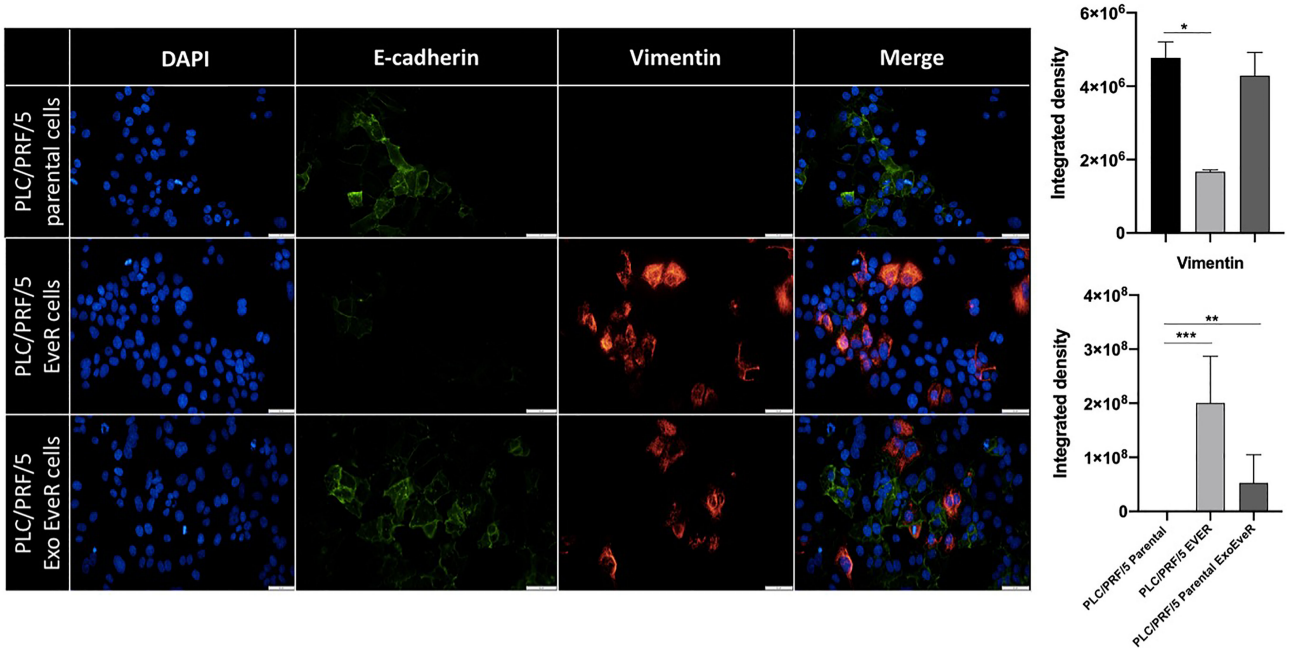

FIGURE 2 | EMT markers in PLC/PRF/5 parental, EveR, and Exo EveR cells. Exosomes from PLC/PRF/5 EveR cells induce EMT in PLC/PRF/5 parental cells. Blue represents DAPI staining of nuclei; green represents FITC staining of E-cadherin protein; red represents TRITC staining of vimentin protein. *$p < 0.05$; **$p < 0.01$; ***$p < 0.001$.

Vitamin D Reduces the Exosome-Mediated Transfer of Cancer Resistance to EVE in HCC Cell Lines

To investigate whether EveR-derived exosome internalization might be reduced by VitD, a cell proliferation assay was performed in both JHH-6 and PLC/PRF/5 Exo EveR, while a colony formation assay was performed only in PLC/PRF/5 Exo EveR, after the exposure to VitD 10^{-7} M, alone and in combination with EVE 10^{-10} M for 6 days, in the proliferation assay, and for 21 days, in the colony formation assay.

As shown in **Figure 6A**, VitD induces 23.4% ($p < 0.01$) of cell proliferation inhibition in JHH-6 Exo EveR, and no further significant inhibition was observed when VitD was combined with EVE compared to control, whereas VitD resensitizes the PLC/PRF/5 Exo EveR to the inhibitory effect of EVE, with 63%

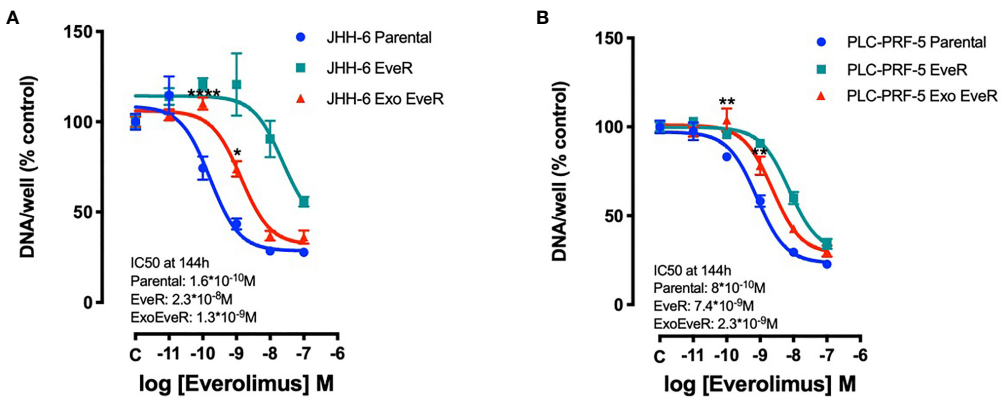

FIGURE 3 | Exosomes are responsible for acquired EVE resistance in HCC cell lines. The graphs represent the proliferation of parental, EveR, and Exo EveR cells in JHH-6 **(A)** and PLC/PRF/5 **(B)** cell lines. Parental cells were exposed for 16 days to exosomes isolated by EveR cells (red lines) and then treated for 6 days at escalating doses of EVE. *$p < 0.05$, **$p < 0.01$, and ****$p < 0.0001$ compared to the effect reached after the same EVE treatment doses in parental cells.

TABLE 1 | PLC/PRF/5 and JHH-6 Exo EveR cells acquired resistance to EVE as demonstrated by a reduced percentage of cell proliferation inhibition.

Cell lines	EVE 10^{-10} M		EVE 10^{-9} M	
	% of inhibition vs. C	*p*	% of inhibition vs. C	*p*
Parental JHH-6	24.6	< 0.0001	56.5	< 0.0001
Exo EveR JHH-6	i.n.i.	n.s.	26.1	n.s.
Parental PLC/PRF/5	16.8	< 0.05	41.7	< 0.0001
Exo EveR PLC/PRF/5	i.n.i.	n.s.	21.8	< 0.001

*Parental and Exo EveR cells were exposed to serial EVE concentrations for 6 days. While parental cells displayed an evident dose–response curve (blue lines in **Figures 3A, B**) even at the lowest EVE concentrations (10^{-10} M and 10^{-9} M), Exo EveR cells showed loss of response to drug treatment at the lowest concentrations. i.n.i., inhibition not induced; n.s., not significant.*

($p < 0.0001$) of inhibition compared to control and with 50% ($p < 0.0001$) of inhibition compared to EVE alone.

Moreover, as shown in **Figure 6B**, when VitD was combined with EVE, a trend of further, although not significant, inhibition in colony number and size was also observed in PLC/PRF/5 Exo EveR compared to the effect induced by the treatment with the EVE alone. Indeed, EVE induced 63% ($p < 0.001$) while the combined treatment induced 80% ($p < 0.0001$) of inhibition of colony number compared to control. Accordingly, EVE induced 47% ($p < 0.01$) while the combined treatment induced 79% ($p < 0.001$) of inhibition of colony size compared to control.

DISCUSSION

The increased number of deaths due to HCC remains a growing concern, although in recent years, great progress has been achieved in diagnosis and therapeutic strategies for the clinical management of HCC (1, 2). Among systemic target therapies recommended for patients who have advanced disease, the multi-kinase inhibitors sorafenib, approved by the Food and Drug Administration (FDA) as a first-line treatment, and regorafenib, approved by FDA as a second-line treatment, have been demonstrated to be safe and effective in increasing survival rate (2). Several additional agents tested for second-line treatment, including the mTOR inhibitor EVE, did not increase the survival rate of advanced HCC (2). The response of a tumor to multi-kinase inhibitors or chemotherapy may be strongly influenced by microenvironmental factors (15). Indeed, solid tumors, including HCC, represent heterogeneous structures composed of cancer, stromal, and immune cells, surrounded by extracellular matrix, and sustained by aberrant vasculature, and exosomes secreted by cancer cells and released in the microenvironment can have an impact on oncogenesis, tumor progression, and drug resistance (15). Increasing evidence demonstrated that exosomes can directly transmit drug-resistant signals by mediating cargo signals including proteins, nucleic acids, and micro-RNA (miRNAs) and affecting EMT or cancer stem cell properties, and by influencing immune response (16–18). It is well known that exosomes have a role in the

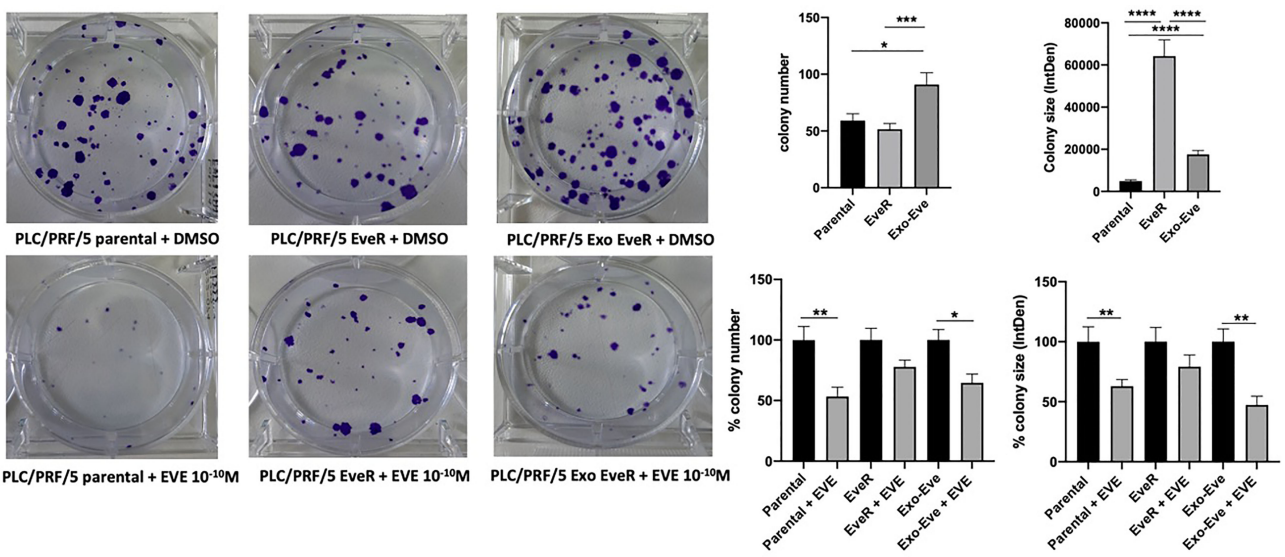

FIGURE 4 | Exosomes are responsible for acquired EVE resistance in HCC cell lines. The images and graphs represent the colony size of parental, EveR, and Exo EveR cells in PLC/PRF/5 before and after EVE treatment. Parental cells were exposed for 16 days to exosomes isolated by EveR cells. All cells were treated for 10 days at EVE 10^{-10} M. *$p < 0.05$; **$p < 0.01$; ***$p < 0.001$; ****$p < 0.0001$.

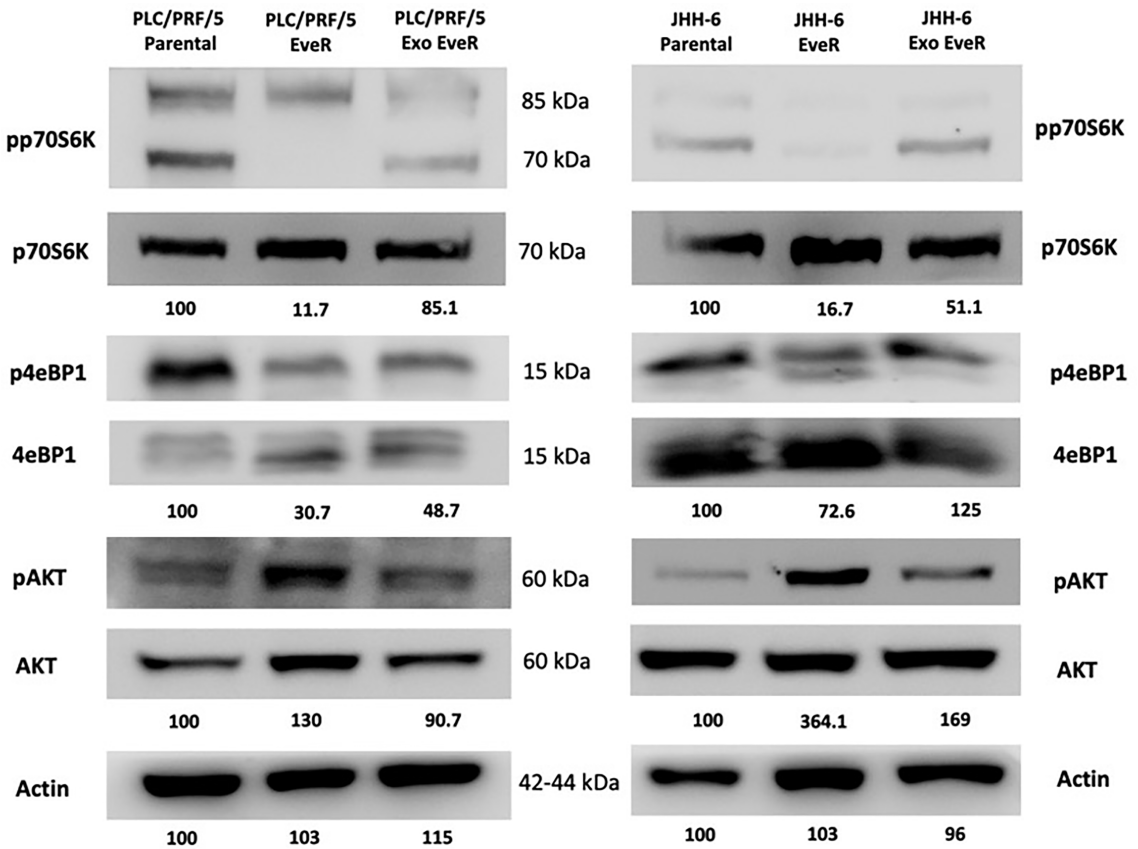

FIGURE 5 | Immunoblot analysis of mTOR components in JHH-6 and PLC/PRF/5 parental, EveR, and Exo EveR cells. Densitometry analysis values represent the ratio of phosphorylated/total proteins and of actin as mean of two independent experiments.

interactions between HCC tumor cells and their surrounding hepatic milieu. Indeed, a large number of pro-tumorigenic RNAs and proteins, such as MET proto-oncogene, S100 family members, and the caveolins, carried by exosomes from metastatic cell lines, can enhance the migratory and invasive abilities of non-motile immortalized hepatocyte cell line, by activating the mTOR and MAPK pathway (19). In the context of cancer, consisting of heterogeneous cell populations, sensitive cancer cells represent the main cell population that can be affected by multi-kinase inhibitor treatment. Using melanoma cell models, it has been proven that drug-sensitive cells can release "secretomes" driving and fostering the outgrowth of drug-resistant cells (20), and exosomes might represent the major part of these "secretomes" as demonstrated in *in vitro* and *in vivo* HCC models where cell-derived exosomes promoted resistance to sorafenib (6). Nevertheless, to the best of our knowledge, it is not clearly demonstrated in HCC models whether the drug-resistant cells can promote and sustain drug resistance in sensitive cancer cells, triggering their cell proliferation progression.

The primary findings of the current study support the hypothesis that exosomes derived from drug-resistant cells mediate tumor cell–cell communications promoting the resistance to EVE and, consequently, inducing tumor progression by the activation of cell proliferation and survival of sensitive HCC cancer cells. Exosomes derived from EVE-resistant cells bestow the mesenchymal phenotype and deregulate the mTOR pathway to sensitive cells, conferring the transmission of an aggressive phenotype. Accordingly, previous studies reported that exosomes derived from highly metastatic HCC cell lines can be taken up by lowly metastatic HCC cell lines undergoing EMT, showing a higher expression of mesenchymal markers and a lower expression of epithelial markers (21, 22). Moreover, previous findings reported by the authors demonstrated that the chronic exposure of HCC cell lines to EVE induces a change in cell phenotype, allowing the cells to acquire more aggressive features as confirmed by the higher expression of vimentin (8). In addition, the results of the current study prove that the "information" of acquired aggressiveness following chronic EVE exposure can be conveyed to sensitive cells through paracrine or endocrine cargo signals by exosomes in HCC *in vitro* models.

Moreover, the present findings reveal that the chronic EVE exposure induces the inhibition of phosphorylation in Thr389 and in Ser65 in both mTOR pathway components, p70S6K and 4eBP1, respectively, and the activation of Akt in Ser473 in both JHH-6 and

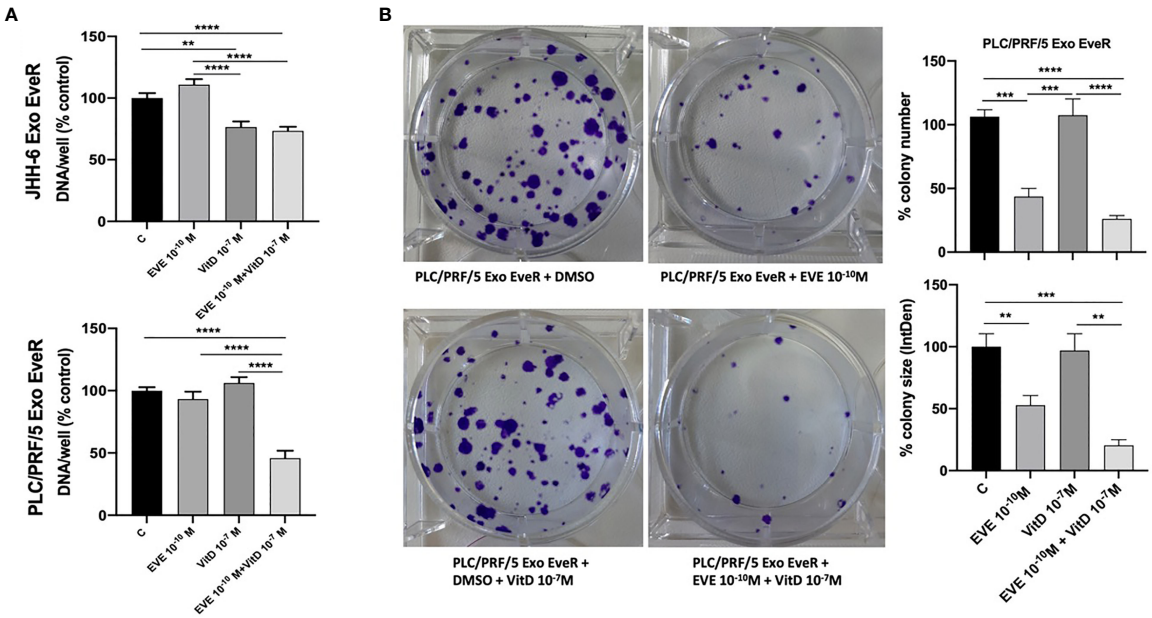

FIGURE 6 | VitD reduces the exosome-mediated transfer of cancer resistance to EVE in the PLC/PRF/5 cell line. **(A)** The graph represents the proliferation of JHH-6 and PLC/PRF/5 Exo EveR cells after 6 days of treatment with EVE 10^{-10} M, VitD 10^{-7} M, and EVE 10^{-10} M + VitD 10^{-7} M. $^{**}p < 0.01$; $^{****}p < 0.0001$. **(B)** The images and graph represent the colony number and size of PLC/PRF/5 Exo EveR treated for 21 days with EVE 10^{-10} M, VitD 10^{-7} M, and EVE 10^{-10} M + VitD 10^{-7} M. $^{**}p < 0.01$; $^{***}p < 0.001$; $^{****}p < 0.0001$.

PLC/PRF/5 cell models. These data are in line with what has been previously reported even in the BON-1 cell line, a model of pancreatic neuroendocrine tumor, in which a long-lasting (8 weeks) exposure to EVE induced mTOR pathway inactivation of pp70S6K on Thr389 and of p4eBP1 on Thr70 (23). Remarkably, the reduction of molecular target activity is one of best-known mechanisms of resistance to target-based agents. Dowling et al. reported that the key proteins of mTOR pathway p70S6K and 4eBP1 regulate cell growth and mediate cell proliferation, respectively, and notably, when 4eBP1 was knocked down, the anti-proliferative effect of EVE was decreased (24). Interestingly, depending on the cell models and solid tumors, EVE can inhibit the phosphorylation of 4eBP1 on several threonine and serine residues, including Thr70 and Ser65 (25–27), and consequently, the reduced 4eBP1 phosphorylation results in the attenuated effect of EVE that chronically induces EVE resistance. On the other hand, phosphorylation of Akt on Ser473 through the mTOR complex 2 tended to be stronger in EVE-treated cells of solid and hematological tumors, causing the insufficient anti-tumor effect of EVE and triggering the resistant properties of these cells (27–29). Accordingly, the results of the current study showed reduced phosphorylation of p70S6K in JHH-6 and PLC/PRF/5 Exo EveR and of 4eBP1 in PLC/PRF/5 Exo EveR, demonstrating that internalization of EveR exosomes transfers cargo signals capable of deregulating the activity of mTOR target molecules and inducing EVE resistance.

The role of VitD as a reversal agent of drug resistance is gaining growing interest in the scientific community as witnessed by the evidence accumulated during these recent years. Indeed, in several cancer models, VitD has been reported to sensitize tumor drug-resistant cells to chemotherapy and multi-kinase drugs acting through several mechanisms (7), mainly inducing the mesenchymal–epithelial transition (8), inhibiting pro-oncogenic pathway in cancer stem cells (30), upregulating miRNAs that reduce oncogene protein expression (8), and downregulating the expression of multi-drug-resistant protein 1 (MRP1) and multi-drug-resistant protein 5 (MRP5), efflux proteins that cause the chemotherapy and multi-kinase drugs to pump out (31, 32). The results of the current study demonstrated for the first time that VitD can resensitize Exo EveR JHH-6 and PLC/PRF/5 to EVE treatment; indeed, VitD when combined with EVE can inhibit cell proliferation and colony forming, overcoming EVE resistance induced by internalization of EveR exosomes. Further studies need to address the underlying mechanisms through which VitD acts in this experimental setting.

In conclusion, the findings of the current study demonstrated that exosomes, released by HCC cell lines induced to be EVE-resistant by drug chronic exposure, may prompt drug resistance in HCC cell lines in terms of cell proliferation and clonal expansion. The exosome-related drug resistance is due at least to the acquired mesenchymal phenotype and to the deregulation of the mTOR pathway through cargo signals. Moreover, the results of the present study proved that VitD may resensitize HCC cells to the exosome-related EVE resistance.

DATA AVAILABILITY STATEMENT

The raw data supporting the conclusions of this article will be made available by the authors, without undue reservation.

AUTHOR CONTRIBUTIONS

MN, FA, AG, RobP, and TM performed experiments, analyzed data, and prepared figures. CdA, CS, and RPir performed literature search, contributed to the interpretation of the data, and provided technical assistance. RA critically revised the manuscript. AC and RPiv provided a significant expert contribution in the scientific content revision process. CP conceived the project, designed the experiments, wrote the manuscript and supervised the manuscript drafting, and critically reviewed and revised it for important intellectual content. All authors contributed to the article and approved the submitted version.

SUPPLEMENTARY MATERIAL

The Supplementary Material for this article can be found online at: https://www.frontiersin.org/articles/10.3389/fonc.2022.874091/full#supplementary-material

Supplementary Figure 1 | Schematic protocol summarizing the sequential steps for the isolation of exosomes from HCC resistant cells and for the internalization in HCC parental cells. On day zero, $1.5x10_6$ JHH-6 EveR, $2x10_6$ PLC/PRF/5 EveR, $0.5x10_6$ JHH-6 and $1x10_6$ PLC/PRF/5 parental cells were seeded in 75 cm_2 flasks in exosome-free medium and grown at 37°C in a humidified atmosphere with 5% CO_2. After 3 days and every 3 days, precisely at the day 6, 9, 12 and 15, exosomes were isolated from EveR exosome-free medium by Cell Culture Exosome Purification Midi Kit, according to the manufacture instructions and inoculated in the flasks containing parental cells to allow the complete cellular internalization of exosomes. On days 6 and 12, after the collection of media for the exosome isolation, EveR cells, that reached the confluence, were trypsinized and $1.5x10_6$ JHH-6 EveR and $2x10_6$ PLC/PRF/5 EveR were seeded again in a new 75 cm_2 flasks in exosome-free medium and grown at 37°C in a humidified atmosphere with 5% CO_2. Alike, on days 8 and 14, parental cells, already exposed to exosomes in the previous days, were trypsinized and $0.5x10_6$ JHH-6 and $1x10_6$ PLC/PRF/5 parental cells were seeded again in a new 75cm2 flasks in exosome-free medium and grown at 37°C in a humidified atmosphere with 5% CO_2.

REFERENCES

1. Villanueva A. Hepatocellular Carcinoma. *N Engl J Med* (2019) 380(15):1450–62. doi: 10.1056/NEJMra1713263
2. Forner A, Reig M, Bruix J. Hepatocellular Carcinoma. *Lancet* (2018) 391 (10127):1301–14. doi: 10.1016/S0140-6736(18)30010-2
3. Shibue T, Weinberg RA. Emt, Cscs, and Drug Resistance: The Mechanistic Link and Clinical Implications. *Nat Rev Clin Oncol* (2017) 14(10):611–29. doi: 10.1038/nrclinonc.2017.44
4. Aleksakhina SN, Kashyap A, Imyanitov EN. Mechanisms of Acquired Tumor Drug Resistance. *Biochim Biophys Acta Rev Cancer* (2019) 1872(2):188310. doi: 10.1016/j.bbcan.2019.188310
5. Kalluri R. The Biology and Function of Exosomes in Cancer. *J Clin Invest* (2016) 126(4):1208–15. doi: 10.1172/JCI81135
6. Qu Z, Wu J, Wu J, Luo D, Jiang C, Ding Y. Exosomes Derived From Hcc Cells Induce Sorafenib Resistance in Hepatocellular Carcinoma Both *In Vivo* and *In Vitro*. *J Exp Clin Cancer Res* (2016) 35(1):159. doi: 10.1186/s13046-016-0430-z
7. Negri M, Gentile A, de Angelis C, Monto T, Patalano R, Colao A, et al. Vitamin D-Induced Molecular Mechanisms to Potentiate Cancer Therapy and to Reverse Drug-Resistance in Cancer Cells. *Nutrients* (2020) 12(6):1798. doi: 10.3390/nu12061798
8. Provvisiero DP, Negri M, de Angelis C, Di Gennaro G, Patalano R, Simeoli C, et al. Vitamin D Reverts Resistance to the Mtor Inhibitor Everolimus in Hepatocellular Carcinoma Through the Activation of a Mir-375/Oncogenes Circuit. *Sci Rep* (2019) 9(1):11695. doi: 10.1038/s41598-019-48081-9
9. Pivonello C, Negri M, De Martino MC, Napolitano M, de Angelis C, Provvisiero DP, et al. The Dual Targeting of Insulin and Insulin-Like Growth Factor 1 Receptor Enhances the Mtor Inhibitor-Mediated Antitumor Efficacy in Hepatocellular Carcinoma. *Oncotarget* (2016) 7 (9):9718–31. doi: 10.18632/oncotarget.6836
10. Pivonello C, Rousaki P, Negri M, Sarnataro M, Napolitano M, Marino FZ, et al. Effects of the Single and Combined Treatment With Dopamine Agonist, Somatostatin Analog and Mtor Inhibitors in a Human Lung Carcinoid Cell Line: An *In Vitro* Study. *Endocrine* (2017) 56(3):603–20. doi: 10.1007/s12020-016-1079-2
11. Hofland LJ, van Koetsveld PM, Lamberts SW. Percoll Density Gradient Centrifugation of Rat Pituitary Tumor Cells: A Study of Functional Heterogeneity Within and Between Tumors With Respect to Growth Rates, Prolactin Production and Responsiveness to the Somatostatin Analog Sms 201-995. *Eur J Cancer* (1990) 26(1):37–44. doi: 10.1016/0277-5379(90)90254-q
12. Franken NA, Rodermond HM, Stap J, Haveman J, van Bree C. Clonogenic Assay of Cells *In Vitro*. *Nat Protoc* (2006) 1(5):2315–9. doi: 10.1038/nprot.2006.339
13. Zhao H, Desai V, Wang J, Epstein DM, Miglarese M, Buck E. Epithelial-Mesenchymal Transition Predicts Sensitivity to the Dual Igf-1r/Ir Inhibitor Osi-906 in Hepatocellular Carcinoma Cell Lines. *Mol Cancer Ther* (2012) 11 (2):503–13. doi: 10.1158/1535-7163.MCT-11-0327
14. Serova M, Tijeras-Raballand A, Dos Santos C, Albuquerque M, Paradis V, Neuzillet C, et al. Effects of Tgf-Beta Signalling Inhibition With Galunisertib (Ly2157299) in Hepatocellular Carcinoma Models and in *Ex Vivo* Whole Tumor Tissue Samples From Patients. *Oncotarget* (2015) 6(25):21614–27. doi: 10.18632/oncotarget.4308
15. Klemm F, Joyce JA. Microenvironmental Regulation of Therapeutic Response in Cancer. *Trends Cell Biol* (2015) 25(4):198–213. doi: 10.1016/j.tcb.2014.11.006
16. Li S, Yi M, Dong B, Jiao Y, Luo S, Wu K. The Roles of Exosomes in Cancer Drug Resistance and Its Therapeutic Application. *Clin Transl Med* (2020) 10 (8):e257. doi: 10.1002/ctm2.257
17. Zhang X, Yuan X, Shi H, Wu L, Qian H, Xu W. Exosomes in Cancer: Small Particle, Big Player. *J Hematol Oncol* (2015) 8:83. doi: 10.1186/s13045-015-0181-x
18. Li I, Nabet BY. Exosomes in the Tumor Microenvironment as Mediators of Cancer Therapy Resistance. *Mol Cancer* (2019) 18(1):32. doi: 10.1186/s12943-019-0975-5
19. He M, Qin H, Poon TC, Sze SC, Ding X, Co NN, et al. Hepatocellular Carcinoma-Derived Exosomes Promote Motility of Immortalized Hepatocyte Through Transfer of Oncogenic Proteins and Rnas. *Carcinogenesis* (2015) 36 (9):1008–18. doi: 10.1093/carcin/bgv081
20. Obenauf AC, Zou Y, Ji AL, Vanharanta S, Shu W, Shi H, et al. Therapy-Induced Tumour Secretomes Promote Resistance and Tumour Progression. *Nature* (2015) 520(7547):368–72. doi: 10.1038/nature14336
21. Chen L, Guo P, He Y, Chen Z, Chen L, Luo Y, et al. Hcc-Derived Exosomes Elicit Hcc Progression and Recurrence by Epithelial-Mesenchymal Transition Through Mapk/Erk Signalling Pathway. *Cell Death Dis* (2018) 9(5):513. doi: 10.1038/s41419-018-0534-9
22. Qu Z, Feng J, Pan H, Jiang Y, Duan Y, Fa Z. Exosomes Derived From Hcc Cells With Different Invasion Characteristics Mediated Emt Through Tgf-Beta/Smad Signaling Pathway. *Onco Targets Ther* (2019) 12:6897–905. doi: 10.2147/OTT.S209413
23. Sciammarella C, Luce A, Riccardi F, Mocerino C, Modica R, Berretta M, et al. Lanreotide Induces Cytokine Modulation in Intestinal Neuroendocrine Tumors and Overcomes Resistance to Everolimus. *Front Oncol* (2020) 10:1047. doi: 10.3389/fonc.2020.01047
24. Dowling RJ, Topisirovic I, Alain T, Bidinosti M, Fonseca BD, Petroulakis E, et al. Mtorc1-Mediated Cell Proliferation, But Not Cell Growth, Controlled by the 4e-Bps. *Science* (2010) 328(5982):1172–6. doi: 10.1126/science.1187532
25. Nishi T, Iwasaki K, Ohashi N, Tanaka C, Kobayashi D, Nakayama G, et al. Phosphorylation of 4e-Bp1 Predicts Sensitivity to Everolimus in Gastric Cancer Cells. *Cancer Lett* (2013) 331(2):220–9. doi: 10.1016/j.canlet.2013.01.004

26. Zhou Q, Wong CH, Lau CP, Hui CW, Lui VW, Chan SL, et al. Enhanced Antitumor Activity With Combining Effect of Mtor Inhibition and Microtubule Stabilization in Hepatocellular Carcinoma. *Int J Hepatol* (2013) 2013:103830. doi: 10.1155/2013/103830
27. Tabernero J, Rojo F, Calvo E, Burris H, Judson I, Hazell K, et al. Dose- and Schedule-Dependent Inhibition of the Mammalian Target of Rapamycin Pathway With Everolimus: A Phase I Tumor Pharmacodynamic Study in Patients With Advanced Solid Tumors. *J Clin Oncol* (2008) 26(10):1603–10. doi: 10.1200/JCO.2007.14.5482
28. Tamburini J, Chapuis N, Bardet V, Park S, Sujobert P, Willems L, et al. Mammalian Target of Rapamycin (Mtor) Inhibition Activates Phosphatidylinositol 3-Kinase/Akt by Up-Regulating Insulin-Like Growth Factor-1 Receptor Signaling in Acute Myeloid Leukemia: Rationale for Therapeutic Inhibition of Both Pathways. *Blood* (2008) 111(1):379–82. doi: 10.1182/blood-2007-03-080796
29. Vilar E, Perez-Garcia J, Tabernero J. Pushing the Envelope in the Mtor Pathway: The Second Generation of Inhibitors. *Mol Cancer Ther* (2011) 10 (3):395–403. doi: 10.1158/1535-7163.MCT-10-0905
30. Zheng W, Duan B, Zhang Q, Ouyang L, Peng W, Qian F, et al. Vitamin D-Induced Vitamin D Receptor Expression Induces Tamoxifen Sensitivity in Mcf-7 Stem Cells *Via* Suppression of Wnt/Beta-Catenin Signaling. *Biosci Rep* (2018) 38(6):BSR20180595. doi: 10.1042/BSR20180595
31. Tan KW, Sampson A, Osa-Andrews B, Iram SH. Calcitriol and Calcipotriol Modulate Transport Activity of Abc Transporters and Exhibit Selective Cytotoxicity in Mrp1-Overexpressing Cells. *Drug Metab Dispos* (2018) 46 (12):1856–66. doi: 10.1124/dmd.118.081612
32. Gilzad-Kohan H, Sani S, Boroujerdi M. Calcitriol Reverses Induced Expression of Efflux Proteins and Potentiates Cytotoxic Activity of Gemcitabine in Capan-2 Pancreatic Cancer Cells. *J Pharm Pharm Sci* (2017) 20(0):295–304. doi: 10.18433/J37W7R

Conflict of Interest: The authors declare that the research was conducted in the absence of any commercial or financial relationships that could be construed as a potential conflict of interest.

frontiers | Frontiers in Pharmacology

SYSTEMATIC REVIEW
published: 09 June 2022
doi: 10.3389/fphar.2022.908079

Role of N6-Methyladenosine Methylation Regulators in the Drug Therapy of Digestive System Tumours

Zhelin Xia[1†], *Fanhua Kong*[2†], *Kunpeng Wang*[3] *and Xin Zhang*[1*]

[1]*Department of Pharmacy, Taizhou Central Hospital (Taizhou University Hospital), Taizhou, China,* [2]*Zhongnan Hospital of Wuhan University, Institute of Hepatobiliary Diseases of Wuhan University, Transplant Center of Wuhan University, National Quality Control Center for Donated Organ Procurement, Hubei Key Laboratory of Medical Technology on Transplantation, Hubei Clinical Research Center for Natural Polymer Biological Liver, Hubei Engineering Center of Natural Polymer-based Medical Materials, Wuhan, China,* [3]*Department of General Surgery Taizhou Central Hospital (Taizhou University, Hospital), Taizhou, China*

Digestive system tumours, including stomach, colon, esophagus, liver and pancreatic tumours, are serious diseases affecting human health. Although surgical treatment and postoperative chemoradiotherapy effectively improve patient survival, current diagnostic and therapeutic strategies for digestive system tumours lack sensitivity and specificity. Moreover, the tumour's tolerance to drug therapy is enhanced owing to tumour cell heterogeneity. Thus, primary or acquired treatment resistance is currently the main hindrance to chemotherapy efficiency. N6-methyladenosine (m6A) has various biological functions in RNA modification. m6A modification, a key regulator of transcription expression, regulates RNA metabolism and biological processes through the interaction of m6A methyltransferase ("writers") and demethylase ("erasers") with the binding protein decoding m6A methylation ("readers"). Additionally, m6A modification regulates the occurrence and development of tumours and is a potential driving factor of tumour drug resistance. This review systematically summarises the regulatory mechanisms of m6A modification in the drug therapy of digestive system malignancies. Furthermore, it clarifies the related mechanisms and therapeutic prospects of m6A modification in the resistence of digestive system malignancies to drug therapy.

Keywords: digestive system tumors, N6-methyladenosine, drug resistance, chemotherapy, immunotherapy

OPEN ACCESS

Edited by:
Leonardo Freire-De-Lima, Federal University of Rio de Janeiro, Brazil

Reviewed by:
Keyang Xu, Zhejiang Chinese Medical University, China
Zhijie Xu, Central South University, China

***Correspondence:**
Xin Zhang
zx1360576@126.com

†These authors have contributed equally to this work and share first authorship

Specialty section:
This article was submitted to Pharmacology of Anti-Cancer Drugs, a section of the journal Frontiers in Pharmacology

Received: *30 March 2022*
Accepted: *17 May 2022*
Published: *09 June 2022*

Citation:
Xia Z, Kong F, Wang K and Zhang X (2022) Role of N6-Methyladenosine Methylation Regulators in the Drug Therapy of Digestive System Tumours. Front. Pharmacol. 13:908079. doi: 10.3389/fphar.2022.908079

INTRODUCTION

Digestive system tumours predominantly include stomach, colon, esophagus, liver and pancreatic tumours. Currently, these tumours have high morbidity and mortality rates. Among patients with digestive system tumours, the elderly account for approximately 68.5% (Sung et al., 2021). Surgery, including open, laparoscopic and endoscopic surgeries, is currently the standard treatment for digestive system tumours (Chesney et al., 2021). To date, several treatment strategies, including chemotherapy and radiation, have enhanced the disease-free and overall survival rates of patients with cancer (Zhang et al., 2020a). However, owing to the heterogeneity of cancer cells, primary or acquired treatment resistance is often observed, leading to treatment failure (Dagogo-Jack and Shaw, 2018). Additionally, the occurrence and development of digestive system tumours are reported to be related to the activation of oncogenes, inactivation of tumour suppressor genes and activation of abnormal cell signalling pathways. Furthermore, epigenetic processes regulate gene expression *via*

DNA methylation, histone modification and RNA modification, thereby affecting the occurrence and development of tumours in the digestive system (Kong et al., 2020a).

Liver cancer is the fourth most common cause of cancer-related death worldwide, with hepatocellular carcinoma (HCC) as the most prevalent form, and the incidence of liver cancer is reported to be increasing globally (Kong et al., 2019; Chen et al., 2021a; Kong et al., 2021). HCC is the second most common cause of cancer-related death, but its current treatment strategies and outcomes are poor (Chen et al., 2021a; Llovet et al., 2021). Several drugs, such as Sorafenib (SOR) and Lenvatinib, have been approved for the first-line systemic therapy of advanced or unresectable patients with HCC (Al-Salama et al., 2019; Kant et al., 2021). Thus, the identification of new drug targets for the treatment of HCC is important, especially in tumour immuno-targeted therapy. Currently, systematic therapies, including immune checkpoint inhibitors (ICIs), tyrosine kinase inhibitors and monoclonal antibodies, have been reporting better outcomes than traditional HCC therapies (Llovet et al., 2021). Over the past five years, significant advances have been made in overall survival and the quality of life (Llovet et al., 2018). However, various challenges continue to exist in the treatment of HCC, such as drug resistance.

Pancreatic cancer, a highly lethal malignancy with a 5-year survival rate of approximately 10% in the United States, is becoming an increasingly common cause of cancer-associated death (Mizrahi et al., 2020). Currently, surgical resection remains the only option to cure pancreatic cancer. However, adjuvant chemotherapy has made significant progress in improving the prognosis of patients with pancreatic cancer (Wang et al., 2021a). Adjuvant chemotherapy regimens include FOLFIRINOX [5-fluorouracil (FU), folate, irinotecan and oxaliplatin (OX)] and gemcitabine combined with sodium protein, sodium and paclitaxel and have been shown to prolong overall survival (Mizrahi et al., 2020). Currently, many clinical trials are evaluating the effectiveness of immunotherapy strategies in pancreatic cancer, including ICIs; cancer vaccines; adoptive cell metastasis; and combinations with other immunotherapy agents, chemoradiotherapy, or other molecule-targeted agents. However, the therapeutic outcomes of these strategies remain poor (Schizas et al., 2020). Therefore, the molecular mechanism of pancreatic cancer requires further exploration.

Colorectal cancer (CRC) is the third most common cancer type and has the third-highest rate of cancer-related deaths in the United States (Kong et al., 2020b). CRC ranks 2nd to 4th in the global incidence of cancer depending on region, cancer type or gender (Sawicki et al., 2021). It remains one of the deadliest diseases worldwide due to the lack of early detection methods and appropriate drug treatment strategies (Pavitra et al., 2021). Surgery remains the preferred treatment method for CRC (Chen et al., 2018). Additionally, chemotherapy has become an effective treatment to prolong the survival of patients with CRC. Currently, the commonly used treatment regimens are FOLFOX (OX + calcium folate and FU), CAPEOX (OX + capecitabine) and FOLFIRI (irinotecan + calcium folate and FU) (Dekker et al., 2019). However, the treatment and prognosis of CRC have been unsatisfactory, especially for patients with metastasis. Therefore, the identification of novel drug targets and the improvement of drug resistance could effectively improve the prognosis and survival rate of patients with CRC.

Gastric cancer is the fifth most common cancer worldwide and the third most common cause of cancer-associated deaths (Smyth et al., 2020). Gastric cancer is a multifactorial disease wherein environmental and genetic factors influence its occurrence and development. It is also a highly invasive and heterogeneous malignant tumour (Machlowska et al., 2020). Presently, surgery is the first-line of treatment for gastric cancer (Johnston and Beckman, 2019). Postoperative adjuvant radiotherapy/chemotherapy and targeted therapy have become a routine course of treatment for gastric cancer. Furthermore, active early screening could effectively aid in the early diagnosis of gastric cancer. However, the early diagnosis of gastric cancer remains a challenge due to the poor specificity of diagnostic markers and the cost of screening (Johnston and Beckman, 2019). Therefore, the development of new diagnostic and therapeutic targets is vital to the treatment of gastric cancer.

N6-methyladenosine (m6A) is considered to be the most common, abundant and conserved internal transcriptional modification, especially in eukaryotic messenger RNA (mRNA) (Huo et al., 2020). m6A modification exists in mRNA and various non-coding RNAs (Ma et al., 2019; Huang et al., 2020). m6A is modified by m6A methyltransferase (writer), removed by m6A methylase (eraser) and recognized by reading proteins (reader). It regulates RNA metabolism, including translation, splicing, export, degradation and microRNA (miRNA) processing. Recently, m6A RNA modification has been proved to play a key role in tumour development (Yan et al., 2021). The alteration of m6A levels regulates the expression of tumour-related genes, such as BRD4, MYC, SOCS2 and epidermal growth factor receptor (EGFR), thereby promoting the pathogenesis and development of tumours (He et al., 2019). Many studies report that the dysregulation of m6A is associated with the progression and drug resistance of various cancers, suggesting that m6A regulatory factors can be used as therapeutic targets in cancer treatment and biomarkers in overcoming drug resistance (Xu et al., 2020a).

MOLECULAR MECHANISMS OF N6-METHYLADENOSINE MODIFICATION

N6-Methyladenosine Writers

m6A writers are composed of KIAA1429 (VIRMA), METTL3, RBM15, WTAP, ZC3H13, METTL16, METTL14, and CBLL1 (Shen et al., 2020). As a heterodimer, METTL3/METTL14 can be catalysed and bound by WTAP, which interacts with METTL3/METTL14 and regulates the translation stability of mRNA (Schöller et al., 2018). KIAA1429 plays a key role in guiding the deposition of regionally selective m6A (Hu et al., 2020) and regulating the expression of sex-lethal genes by the selective splicing of pre-mRNA using WTAP (Bansal et al., 2014). METTL16, a newly discovered RNA m6A methyltransferase, acts as an RNA-binding protein (RBP) and plays a key role in

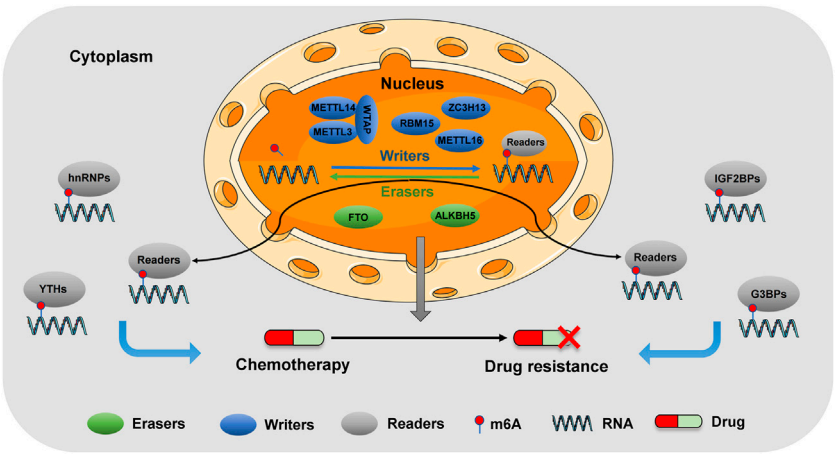

FIGURE 1 | Molecular mechanisms of m6A modification in digestive tumors. m6A modification is a dynamic and reversible process. Methyltransferase complexes (writers) catalyze m6A methylation, demethylase (erasers) reverse m6A methylation, and m6A binding protein (readers) promote its function. m6A methylation is involved in carcinogenesis and chemotherapy resistance of digestive tumors.

SAM homeostasis by regulating SAM synthase MAT2A mRNA (Doxtader et al., 2018). RBM15, an RBP, can regulate Notch, Wnt and other signalling pathways and affect the development of various tumour cells (Wang et al., 2021b). ZC3H13 plays the role of a tumour suppressor, mainly inhibiting tumour occurrence by regulating the Ras–ERK signalling pathway (Zhu et al., 2019a). The mechanism of action of m6A writers in tumours is shown in **Figure 1**.

N6-Methyladenosine Erasers

m6A erasers are predominantly composed of ALKBH5 and FTO (Huo et al., 2020). ALKBH5 regulates RNA metabolism through m6A demethylation, such as pre-mRNA processing and mRNA decay and translation (Qu et al., 2022). It participates in the modification of oncogene or tumour suppressor gene mRNA in an m6A-dependent manner. Moreover, ALKBH5 regulates the transcriptome of tumours, causing changes in cell proliferation, survival, invasion and metastasis; drug sensitivity; tumour stem cell status; and tumour immunity (Qu et al., 2022). Given that ALKBH5 has high substrate specificity in tumours, targeting ALKBH5 has promising potential in cancer treatment (Wang et al., 2020a). On understanding ALKBH5 structure, mediated carcinogenesis and drug reaction mechanism, ALKBH5-targeted therapy could be applied in clinical practice. FTO, a demethylase, was originally identified to be involved in the development of obesity and type 2 diabetes. This gene encodes the FTO protein, which belongs to the ALKB dioxygenase family that is dependent on Fe^{2+} and 2-oxoglutarate (Gerken et al., 2007). The dysregulation of FTO demethylation has been identified as a driver of various diseases, including cancer, metabolic diseases and neuropsychiatric disorders (Annapoorna et al., 2019). Studies have found that the abnormal expression of FTO is increasingly associated with various diseases, especially cancer. Thus, the development of FTO modulators has potential therapeutic applications. Recent studies report that inhibitors that interfere with FTO activity show significant therapeutic effects in different cancers, thus providing a new strategy for identifying drugs that target external transcriptomic RNA methylation in drug discovery (Zhou et al., 2021). The mechanism of action of m6A erasers in tumours is illustrated in **Figure 1**.

N6-Methyladenosine Readers

m6A readers can be divided into three types based on binding m6A-containing transcription: YTH domain (YTH family protein), HNRNP family (hnRNPC, hnRNPG and hnRNPA2B1) and common RNA-binding domain and its flanking regions (IGF2BPs and hnRNPA2B1) (Shi et al., 2021; Huang et al., 2022). Additionally, FXR family, IGF2BP family, eIF family and G3BPs family (44). Heterogeneous nuclear ribonucleoproteins (hnRNPs) are a large family of RBPs that are involved in the many aspects of nucleic acid metabolism, including alternative splicing, mRNA stabilization and transcription and translation regulation (Geuens et al., 2016). hnRNP family proteins are abnormally expressed in most tumours and play a role in promoting tumour occurrence and development. The YTH domain protein family is the main "reader" of m6A modification while the YTH domain can recognize and bind m6A-containing RNA. YTH family proteins have different functions to determine the metabolic fate of m6A-modified RNAs (Shi et al., 2021). YTHDF1 selectively recognises m6A-modified mRNA through the YTH domain, promotes its loading into ribosomes and interacts with initiation factors to promote its translation through the N-terminal domain (Wang et al., 2015). Conversely, YTHDF2 selectively binds m6A-modified RNA and regulates its degradation by recruiting CCR4–NOT complexes to accelerate RNA de-enylation (Zhao et al., 2017). YTHDF3 acts as an assigner, following which YTHDF1 and YTHDF2 competitively interact with YTHDF3, thus determining the fate of the mRNA transcript (Jin et al., 2020). YTHDC1, a widely expressed nuclear protein, is located in YT bodies near nuclear spots and phosphorylated by members of the SRC and

TEC tyrosine kinase families in the cytoplasm, leading to its conversion function in RNA splicing (Rafalska et al., 2004). Like other proteins in the YTH family, YTHDC2 can recognize and bind to the m6A fragment of mRNA to play a regulatory role (Wojtas et al., 2017). YTHDC2 can improve the translation efficiency of its target, thus affecting the occurrence of tumours (Hsu et al., 2017). The mechanism of m6A readers in tumours is shown in **Figure 1**.

IMPLICATIONS OF N6-METHYLADENOSINE IN CANCER CHEMOTHERAPY

The prognosis of digestive tract tumours has been significantly improved in recent years. However, the early diagnosis of digestive tract tumours remains elusive, and the phenomenon of drug resistance persists. Moreover, the underlying aetiology of these malignancies remains unclear, therefore, the epigenetic factors that promote the occurrence and development of digestive malignancies should be elucidated and novel biomarkers or effective therapeutic targets should be simultaneously identified (Seebacher et al., 2019). Numerous studies report that m6A modification promotes the occurrence and development of tumours by regulating oncogene expression and inhibiting genes (Huo et al., 2020). Through epigenetic modification, m6A can promote and inhibit tumorigenesis, playing a "double-edged sword" role (He et al., 2019). Furthermore, the m6A regulatory protein is a therapeutic target for cancer and plays an important biological role in the resistance of malignant tumours to chemotherapy (Yu et al., 2019). Additionally, studies show that the mechanisms of drug resistance in malignant tumours are complex and diverse. m6A-dependent RNA modification has also received extensive attention as a potential determinant of tumour heterogeneity and chemotherapy response.

Presently, the identification of efficient and safe chemical drugs for m6A modification is under study. In particular, few drugs based on natural products are characterised by novel structures, various biological activities and reliable safety (Lu and Wang, 2020). Therefore, an m6A regulator based on natural product discovery is considered the future research direction. Furthermore, modern drug discovery platforms, which are characterized by a combination of web-based pharmacology, chemical databases derived from natural resources, computer-aided design and chemical modifications, have been recognized to aid in the development of new drugs that target m6A regulators (Zhang et al., 2021a). Recently, natural products have been used as the chemical libraries of m6A-targeted anticancer drugs, subsequently becoming potential anti-tumour drugs. For example, curcumin is a natural phenolic compound that down-regulates the expression of ALKBH5 and enhances the expression of m6A modified TRAF4-mRNA (Chen et al., 2021b). Resveratrol is a natural polyphenol with antioxidant, anti-inflammatory, heart-protective and anticancer properties that can be used in combination with curcumin to reduce m6A modifications, thereby effectively improving normal growth performance and intestinal mucosal integrity (Gan et al., 2019). Quercetin, another flavonoid, has various biological functions, including anti-cancer activity. It can inhibit the proliferation, migration and invasion of HeLa and SiHa cells synergistically with cisplatin by inhibiting METTL3 expression (Xu et al., 2021). Recent studies suggest that betaine plays an important role in the methylation of m6A. Zhang et al. found that betaine inhibited the expression of m6A methylases, METTL3 and METTL14, in HepG2 cells, but promoted the expression of demethylases, FTO and ALKBH5 Zhang et al. (2019). In addition to these natural products, other active natural products have also been shown to have anti-M6A bioactivity and anti-cancer activity. Fusarium acid decreases p53 expression in HCC HepG2 cells by down-regulating the m6A methylation of p53-mRNA (Ghazi et al., 2021). Although many studies have shown promising prospects for the development of targeted m6A modification drugs, only a few have potential drug-capabilities and can be used as therapeutic targets for cancer treatment. The currently developed m6A modification inhibitors and activators still have disadvantages, such as poor target specificity, efficacy, safety and pharmacokinetics (Huff et al., 2021). Hence, developing novel drugs is vital to cancer treatment.

Thanks to the rapid development of science and technology, especially artificial intelligence (AI) technology and computer technology, the newly discovered drugs have the advantages of fast speed, easy use and cost-saving. Presently, AI-assisted technology has been widely used in drug candidate discovery and development (Paul et al., 2021). Chen et al. (2012) developed a series of FTO inhibitors using AI techniques. The natural product rhein was identified as the first cell-based FTO inhibitor, which also inhibited ALKBH2 activity. Additionally, they designed and synthesised eight luciferin molecules whose structures were similar to two luciferin molecules. The structure-activity relationship of these fluorescent FTO inhibitors was elucidated by the X-ray crystal structure of FTO/luciferin complexes. These studies demonstrate advancement in identifying novel chemical CLASS FTO inhibitors with strictly defined physicochemical properties by combining structure-based drug design with high-throughput *in vitro* inhibition test systems. Additionally, Huang et al. identified Entacapone as an FTO inhibitor by combining several methods, including structure-based hierarchical virtual screening strategies, biochemical experiments, *in vivo* experiments and transcriptome sequencing analysis (Peng et al., 2019). Chen et al. also found two effective FTO inhibitors CS1 and CS2 using structure-based virtual screening (Su et al., 2020). Using molecular docking, Lan et al. identified a cage-like molecular activator of METTL3/14, the photocured substituent-linked MPCH. The drug activates METTL3/14 and results in m6A hypermethylation under short periods of ultraviolet light exposure (Lan et al., 2021a). Currently, AI has aided in the development of revolutionary approaches to drug discovery, design and development, therefore, targeting m6A modification regulators could be a possibility, thereby proving its therapeutic potential in cancer treatment.

EFFECTS OF N6-METHYLADENOSINE ON DRUGS IN TUMOUR THERAPY

Hepatocellular Carcinoma

Liver cancer is the sixth most common cancer worldwide, including HCC and cholangiocarcinoma (CCA) subtypes. Recent studies have shown that m6A regulatory factor is closely related to the development of HCC and is expected to be a potential therapeutic target for HCC (Xu et al., 2019). Moreover, HCC is often too advanced for surgical treatment by the time it is diagnosed (Kong et al., 2022). SOR, a bisaryl urea multikinase inhibitor, is the first molecularly targeted drug approved by the Food and Drug Administration (FDA) for the clinical treatment of HCC (Kong et al., 2021). SOR has strong antitumour and antiangiogenic effects, effectively improving the survival rate of patients with advanced HCC (Palazzo et al., 2010; Iacovelli et al., 2015). However, during treatment, changes in epigenetic modifications occur due to the heterogeneity of HCC. This phenomenon suggests that acquired or primary SOR resistance is a major obstacle to the survival of patients with HCC (Zhu et al., 2017a). As an important member of RNA modification, m6A modification plays an important role in regulating drug resistance during HCC treatment. As the most famous m6A methyltransferase, METTL3 has been identified as a key regulator in many biological processes, including cell cycle, apoptosis, migration, invasion, differentiation and inflammatory response (Maldonado López and Capell, 2021). Kong et al. (2022) showed that the lncRNA LINC01273 can promote the resistance of HCC to SOR. LINC01273 increases the stability of miR-600 by acting as a "reservoir" and enhances the inhibition of miR-600 on METTL3 mRNA, resulting in the downregulation of METTL3 and drug resistance of HCC cells to SOR. Additionally, METTL3 increases the m6A level of LINC01273 and decreases the stability of LINC01273 in recognizing YTHDF2. Therefore, the dysregulation of the LINC01273/miR-600/METTL3 axis could be a potential cause of SOR resistance in HCC cells. Notably, METTL3 is often reported as an oncogene and is upregulated in most tumours (Zeng et al., 2020). This could be associated with the dual regulatory role of the m6A regulatory factor. Lin et al. (2020) also found that METTL3 expression is significantly downregulated in SOR-resistant HCC cells. The deletion or depletion of METTL3 promotes the expression of SOR drug resistance and angiogenesis genes and activates autophagy-related pathways. The downregulation of METTL3 expression leads to the decreased stability of FOXO3-mRNA, which promotes the resistance of HCC to SOR. This indicates that METTL3 is a negative regulator of SOR resistance and could be related to the bidirectional action of METTL3, and its internal mechanism is worth further study. Additionally, Xu et al. (2020b) showed that m6A modification promotes the drug resistance of HCC to SOR by regulating the expression level of circRNA-SORE, especially *via* an m6A modification site in circRNA-SORE. Furthermore, the m6A level of circRNA-SORE was increased in SOR-resistant HepG2 cells and the level of circRNA-SORE was significantly decreased on METTL3/14 knockout. These results indicated that m6A modification promotes HCC resistance to SOR through the circRNA expression level. Currently, SOR has become the first-line drug for patients with advanced liver cancer. Despite the wide use of SOR, it has certain disadvantages in its clinical application (Llovet et al., 2008; Cervello et al., 2012). Some patients acquire resistance to SOR in the course of treatment, which affects the overall survival time of patients with HCC (Zhu et al., 2017b). Therefore, further studies on the mechanism of drug resistance could improve and overcome this obstacle. The mechanism of m6A regulatory factors in HCC is shown in **Figure 2** and **Table 1**.

Pancreatic Cancer

Pancreatic cancer is one of the leading causes of cancer-related deaths in the Western world, owing to its advanced nature, early metastasis and limited response to chemotherapy or radiation. Adjuvant chemotherapy after surgical resection is the preferred treatment for early pancreatic cancer (Zeng et al., 2019). Although gemcitabine remains a cornerstone in the treatment of early-stage advanced pancreatic cancer, its clinical efficacy is poor due to molecular mechanisms, epigenetic modifications, limitations in cell uptake and activation and chemotherapeutic resistance development within weeks of treatment initiation (Amrutkar and Gladhaug, 2017). Current studies on the mechanism of drug resistance in pancreatic cancer report that m6A modification plays an important role in the drug resistance of pancreatic cancer to chemotherapy drugs. The deletion of METTL3, an m6A writer, enhances the sensitivity of pancreatic cancer cells to gemcitabine, 5-FU, cisplatin and radiotherapy. Furthermore, METTL3 could promote the resistance of pancreatic cancer to gemcitabine, 5-FU and cisplatin via several key pathways, including the MAPK cascade, ubiquitin-dependent processes, RNA splicing and cellular process regulation (Taketo et al., 2018). METTL14, another regulator of m6A writer, forms a functional heterodimer with METTL3, which is further catalysed and stabilised by WTAP, promoting the effect of m6A modification (Schöller et al., 2018). Furthermore, METTL14, one of the key methyltransferases, is an RNA-binding scaffold that recognizes the substrate of the m6A methyltransferase complex and has 20% sequence homology with METTL3. Among m6A methyltransferases, METTL14 is speculated to have a methyltransferase function that aids in RNA binding and METTL3 stabilisation (Wang et al., 2017). Kong et al. (2020a) showed that METTL14 is upregulated in pancreatic cancer tissues, with METTL14 knockdown in pancreatic cancer cells enhancing its sensitivity to cisplatin therapy. METTL14 regulates the sensitivity of pancreatic cancer cells to cisplatin treatment via the AMPKα, ERK1/2, and mTOR signalling pathways and improves autophagy via the mTOR signalling pathway. Additionally, METTL14 expression is closely associated with gemcitabine-resistant treatment and upregulated in gemcitabine-resistant human pancreatic cancer cells. METTL14 increases the expression of cytidine deaminase, an enzyme that inhibits gemcitabine. Therefore, METTL14 knockdown significantly increases the sensitivity of gemcitabine in drug-resistant cells (Zhang et al., 2021b). Although the expression of METTL14 is increased in drug-resistant pancreatic cancer cells, its expression regulation mechanism remains unclear. Therefore, further studies on the mechanism of METTL14 resistance are required.

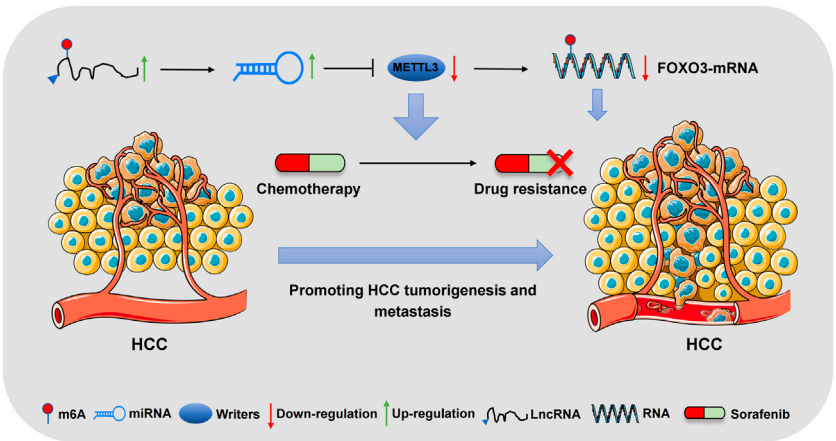

FIGURE 2 | The regulatory mechanism of m6A modification on chemotherapy resistance in HCC. METTL3, as an m6A writer, is down-regulated in HCC and regulated by LncRNA and miRNA. Meanwhile, METTL3 also regulates the stability of FOXO-mRNA and promotes the resistance of HCC to sorafenib.

TABLE 1 | The roles of different m6A regulators in hepatocellular carcinoma.

m6A regulators	Genes/RNAs	Drugs	Mechanism	Function	References
METTL3	LncRNA LINC01273, miR-600	Sorafenib	1. Enhance the inhibitory effect of miR-600 on METTL3 2. Down-regulation of METTL3	Increased resistance to Sorafenib	Kong et al. (2022)
YTHDF2	LncRNA LINC01273	Sorafenib	1. METTL3 increases the m6A level of LINC01273 2. Decreased the stability of LINC01273 in recognizing YTHDF2	Increased resistance to Sorafenib	Kong et al. (2022)
METTL3	FOXO3-mRNA	Sorafenib	1. Down-regulation of METTL3 2. Decreased the stability of FOXO3-mRNA	Increased resistance to Sorafenib	Lin et al. (2020)
METTL3/14	CircRNA-SORE	Sorafenib	m6A modification of circRNA-SORE was increased	Increased resistance to Sorafenib	Xu et al. (2020b)

ALKBH5, an m6A eraser, is downregulated in pancreatic cancer. The overexpression of ALKBH5 can inhibit the proliferation, migration and invasive activities of pancreatic cancer (Guo et al., 2020). Compared with existing tumour markers, ALKBH5 shows good prognostic ability, and its expression level is positively correlated with the prognosis of The Cancer Genome Atlas cohort patients (Cho et al., 2018). In patients with pancreatic cancer treated with gemcitabine, ALKBH5 expression is down regulated, whereas its overexpression induces the pancreatic cancer cells' sensitivity to chemotherapy. The sensitivity of pancreatic cancer cells to gemcitabine is affected by the regulation of Wnt inhibitor 1 and the Wnt pathway (Tang et al., 2020). Unlike readers and writers, only two m6A demethylases, FTO and ALKBH5, are known that rely on Fe (II) and α-ketoglutaric acid (Dai et al., 2018). The downregulation of m6A promotes the resistance of FTO and ALKBH5 to PARPi. Moreover, m6A was confirmed to play an important regulatory role in treatments related to DNA damage response, including radiotherapy, chemotherapy and therapy targeting mutations related to DNA damage repair. Considering that the crystal structures of FTO and ALKBH5 have been determined, the development of drugs targeting FTO and ALKBH5 is a potential research direction (Han et al., 2010; Aik et al., 2014). The mechanism of the m6A regulatory factor in pancreatic cancer is shown in **Figure 3** and **Table 2**.

Colorectal Cancer

Radical surgical resection is the preferred treatment regimen for CRC, and radiotherapy and chemotherapy, as a routine treatment strategy after surgery, can effectively improve the survival of patients (Liu et al., 2019; Kong et al., 2020b). OX, a third-generation platinum drug, is widely used as a first-line chemotherapy agent for CRC. However, repeated long-term dosing induces chemotherapeutic resistance by increasing the expression of multidrug-resistant proteins, glutathione and excision repair cross-complement and promoting cell export and excision repair nucleotides (Allen and Johnston, 2005). Lan et al. (2021b) found that total m6A RNA content and critical methyltransferase METTL3 expression were increased in the CRC tissues of patients with OX resistance. The overexpression of METTL3 enhances the resistance of CRC cells to OX *via* TRAF5-mediated necrosis. Patients with CRC often develop resistance to 5-FU. Studies showed that miRNAs in exosomes secreted by cancer-associated fibroblasts (CAFs) are

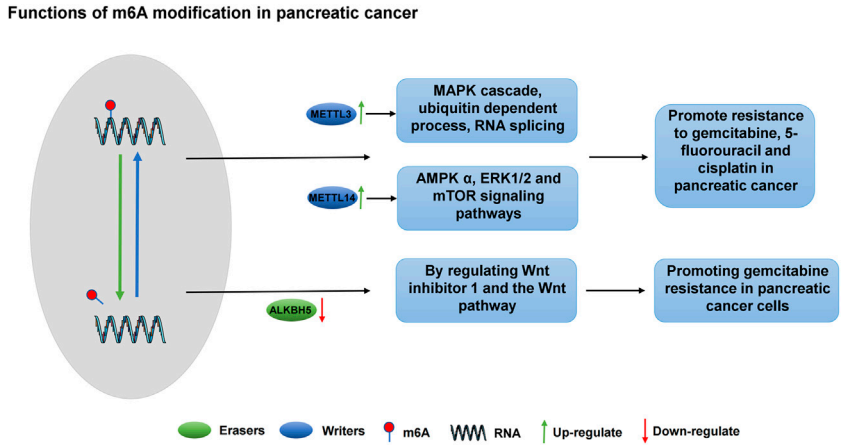

FIGURE 3 | The regulatory mechanism of m6A modification on chemotherapy resistance in pancreatic cancer. METTL3 and METTL14 are up-regulated in pancreatic cancer and promote drug resistance to gemcitabine, 5-fluorouracil and cisplatin through MAPK cascade, ubiquitin-dependent process, RNA splicing, AMPK α, ERK1/2, and mTOR signaling pathways. The down-regulated expression of ALKBH5 in pancreatic cancer affects the sensitivity of pancreatic cancer cells to gemcitabine by regulating Wnt inhibitor 1 and the Wnt pathway.

TABLE 2 | The roles of different m6A regulators in pancreatic cancer.

m6A regulators	Genes/RNAs	Drugs	Mechanism	Function	References
METTL3	MAPK cascades	Gemcitabine 5-fluorouracil Cis-platinum	Up-regulation of METTL3	Increased resistance to gemcitabine, 5-fluorouracil and cis-platinum	Taketo et al. (2018)
METTL14	--	Cis-platinum	1.Up-regulation of METTL14 2. Through AMPK α, ERK1/2 and mTOR signaling pathways	Increased resistance to cis-platinum	Kong et al. (2020a)
METTL14	Cytidine deaminase (CDA)	Gemcitabine	1. Up-regulation of METTL14 2. Increased cytidine deaminase (CDA) expression	Increased resistance to gemcitabine	Zhang et al. (2021b)
ALKBH5	Wnt inhibitory factor 1 (WIF1)	Gemcitabine	1. Down-regulation of ALKBH5 2. Regulation of Wnt inhibitory factor 1 and Wnt pathway	Increased resistance to gemcitabine	Tang et al. (2020)

associated with sensitivity to 5-FU (Hu et al., 2019). METTL3 promotes miR-181d-5p secretion through the DiGeorge Syndrome Critical Region 8 (DGCR8) in CAFs. CAF-derived exosomes enhance 5-FU resistance in CRC cells *via* the METTL3/miR-181d-5p axis. Thus, a novel role of exosome miR-181d-5p secreted by CAFs was revealed. METTL3-dependent m6A methylation is upregulated in CRC, thereby promoting miR-181d-5p processing by DGCR8, resulting in increased miR-181d-5plevels, and inhibiting 5-FU sensitivity by targeting NCALD (Pan et al., 2022). METTL3 also promotes CRC resistance to 5-FU through circ-0000677 (Liu et al., 2022a). Additionally, METTL3 catalyses transition adenosine methylation and promotes pre-mRNA preferential splicing and p53 protein's R273H mutation, leading to acquired drug resistance in colon cancer cells (Uddin et al., 2019).

Cisplatin is a platinum-based chemotherapy drug that has been clinically proven to treat various malignant tumours (Dasari and Tchounwou, 2014). Although cisplatin therapy has achieved good prognosis and survival rates in patients with cancer, problems of drug resistance and considerable side effects remain (Galluzzi et al., 2012). YTHDF1, an m6A "reader", is an important regulator of tumour progression (Chen et al., 2021c). The expression of YTHDF1 is significantly upregulated in CRC, and its overexpression can reduce the sensitivity of colon cancer cells to cisplatin. YTHDF1 promotes the synthesis of GLS1 protein by binding to GLS1 3′UTR, which causes cisplatin resistance in colon cancer cells (Chen et al., 2021d). Yang et al. (2021) analysed CRC cells using proteomic and transcriptomic analyses to identify proteins involved in multidrug resistance in CRC. Results showed that IGF2BP3 expression was upregulated in CRC, whereas IGF2BP3 knockout significantly improved the sensitivity of CRC to adriamycin. Therefore, IGF2BP3 could be a potential biomarker to predict the occurrence of CRC multidrug resistance. Targeting IGF2BP3 could also be a potential chemotherapy strategy to prevent the development of

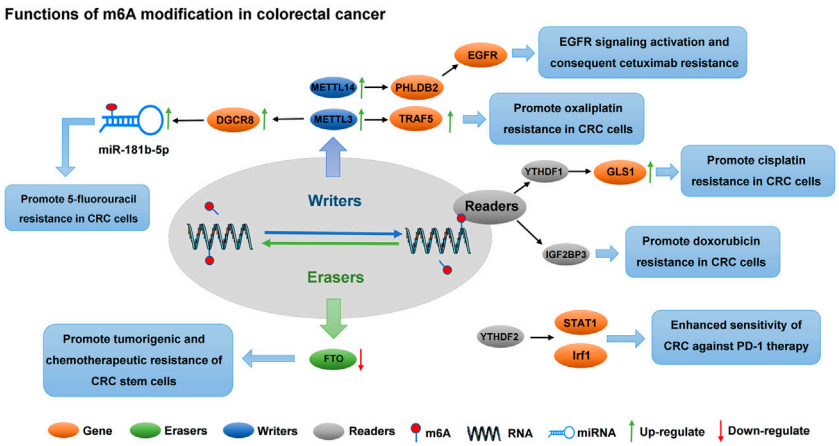

FIGURE 4 | The regulatory mechanism of m6A modification on chemotherapy resistance in CRC. In CRC, m6A Writers, Erasers, and Readers are dysregulated and promote CRC resistance to cisplatin, 5-fluorouracil, oxaliplatin, doxorubicin, and targeted agents by regulating the stability of downstream gene expression.

multidrug resistance in CRC. FTO, an m6A eraser, blocks the ability of cancer stem cells through its N-6,2′-O-dimethyladenosine demethylase activity. The downregulation of FTO expression in CRC enhances the m6A modification level of mRNA, leading to increased tumorigenicity and chemotherapy resistance *in vivo* (Relier et al., 2021).

Immunotherapy and targeted therapy are current strategies for the treatment of CRC. Programmed cell death-1 (PD-1) checkpoint blocking immunotherapy has achieved impressive clinical success in treating various cancers (Lipson et al., 2015). However, limited or nonresponsive to PD-1 antibody therapy remains a challenge (Ganesh et al., 2019). In immunotherapy-resistant CRC, the deletion of METTL3 and METTL14 enhances the response of CRC and melanoma to PD-1 therapy. This could be attributed to the downregulated expression of METTL3 or METTL14, YTHDF2-stabilized STAT1 and Irf1 mRNA, activated IFN-γ–STAT1–IRF1 signalling pathway and enhanced sensitivity of CRC against PD-1 treatment (Wang et al., 2020b). Cetuximab is an FDA-approved monoclonal antibody against EGFR that is recommended for patients with metastatic CRC and wild-type KRAS/NRAS/BRAF tumours; however, its efficacy remains unsatisfactory, especially in patients with potentially metastatic CRC and adjuvant therapy progression (Benson et al., 2021). Additionally, PHLDB2 is upregulated in CRC and promotes the migration and invasion of cancer cells. METTL14 regulates PHLDB2 and promotes its expression, whereas PHLDB2 upregulation stabilises EGFR and promotes its nuclear translocation, leading to EGFR signal transduction activation and cetuximab resistance (Luo et al., 2022). Therefore, PHLDB2 is a potential therapeutic target for CRC. Hao et al. report that MIR100HG expression is closely related to the markers of epithelial–mesenchymal transformation in CRC and can serve as a positive regulator of epithelial–mesenchymal transformation. MIR100HG maintains cetuximab resistance *in vitro* and *in vivo* and promotes the invasion and metastasis of CRC cells. Furthermore, hnRNPA2B1 binds with MIR100HG and maintains the mRNA stability of TCF7L2. hnRNPA2B1 identifies the TCF7L2 mRNA m6A site *via* the MIR100HG hnRNPA2B1/TCF7L2 axis and enhances CRC resistance to cetuximab (Liu et al., 2022b). Therefore, targeted therapy combined with MIR100HG and immune checkpoint blockade could be a potential therapeutic strategy to improve the immunotherapy response of patients with CRC. The mechanism of m6A regulation in CRC is shown in **Figure 4** and **Table 3**.

Gastric Cancer

Endoscopic resection is the standard treatment regimen for early gastric cancer. Non-inchoate operable gastric cancer is treated by surgery while sequential chemotherapy is used for advanced gastric cancer. The first-line treatment also includes platinum drugs and FU double chain (Smyth et al., 2020). OX, a first-line treatment for advanced gastric cancer, has been widely used in clinical settings; however, drug resistance mainly causes treatment failure (Boku et al., 2019; Harada et al., 2021). Li et al. (2022a) showed that CD133+ stem cell-like cells are the main subgroup of OX resistance whereas PARP1 is the central gene mediating OX resistance in gastric cancer. PARP1 can effectively repair the DNA damage caused by OX, leading to the occurrence of drug resistance. Moreover, METTL3 expression is upregulated in CD133+ stem cells. METTL3 recruits YTHDF1 to enhance the stability of PARP1 mRNA, thus playing a role in the repair of PARP1-mediated DNA damage and the development of OX resistance in gastric cancer cells. In addition to OX, cisplatin, either alone or in combination with other chemotherapeutic agents, is a first-line chemotherapy drug for patients with advanced gastric cancer (Kang et al., 2020). However, cisplatin resistance remains a major challenge in the treatment of advanced gastric cancer (Wang et al., 2016). Zhu et al. (2022) found that lncRNA LINC00942 is upregulated in gastric cancer and associated with poor prognosis. LINC00942 upregulates MSI2 expression by blocking the interaction between MSI2 and $SCF^{\beta-TrCP}$ E3 ubiquitin ligase, ultimately inhibiting its

TABLE 3 | The roles of different m6A regulators in colorectal cancer.

m6A regulators	Genes/RNAs	Drugs	Mechanism	Function	References
METTL3	TRAF5-mRNA	Oxaliplatin	1. Up-regulation of METTL3 2. Regulation of TRAF5 expression	Increased resistance to oxaliplatin	Lan et al. (2021b)
METTL3	DGCR8-mRNA miR-181b-5p	5-fluorouracil	METTL3 promotes the secretion of miR-181b-5p by DGCR8	Increased resistance to 5-fluorouracil	Pan et al. (2022)
METTL3	circ_0000677 ABCC1-Mrna	5-fluorouracil	1. METTL3 enhances the m6A level of CIRC_0000677 2. Circ_0000677 regulates ABCC1 and promotes CRC resistance	Increased resistance to 5-fluorouracil	Liu et al. (2022a)
YTHDF1	GLS1-mRNA	Cis-platinum	1. Up-regulation of YTHDF1 2. Promote the synthesis of GLS1 protein	Increased resistance to cis-platinum	Chen et al. (2021d)
IGF2BP3	ABCB1-mRNA	Doxorubicin	1. Up-regulation of IGF2BP3 2. IGF2BP3 promotes ABCB1 expression	Increased resistance to doxorubicin	Yang et al. (2021)
FTO	PCIF1/CAPAM	5-fluorouracil	Down-regulation of FTO	Increased resistance to 5-fluorouracil	Relier et al. (2021)
METTL3/14	STAT1-mRNA Irf1-mRNA	Anti-PD-1 antibody	1.Up-regulation of METTL3/14 2. Activation of IFN-γ -STAT1-IRF1 signaling pathway	Increased resistance to Anti-PD-1 antibody	Wang et al. (2020b)
METTL14	PHLDB2-mRNA	Cetuximab	1. METTL14 promotes PHLDB2 expression PHLDB 2. Activates EGFR signal transduction	Increased resistance to Cetuximab	Luo et al. (2022)
hnRNPA2B1	MIR100HG-mRNA TCF7L2-mRNA	Cetuximab	Activate MIR100HG/hnRNPA2B1/TCF7L2 axis	Increased resistance to Cetuximab	Liu et al. (2022b)

ubiquitination. Subsequently, LINC00942 enhances C-Myc mRNA stability in an m6A-dependent manner and enhances cisplatin resistance in gastric cancer. Therefore, blocking the LINC00942–MSI2–C-Myc axis could be a novel therapeutic strategy for patients with chemotherapy-resistant gastric cancer. Another lncRNA, ARHGAP5-AS1, is upregulated in gastric cancer and associated with poor prognosis. ARHGAP5-AS1 enhances the stability of ARHGAP5 mRNA by recruiting METTL3 and modifying ARHGAP5 mRNA. Therefore, the upregulation of ARHGAP5 could promote cisplatin chemotherapy resistance in gastric cancer (Zhu et al., 2019b). Hence, targeting the ARHGAP5-AS1/ARHGAP5 axis is a promising strategy for overcoming chemotherapy resistance in gastric cancer. Recently, a special relationship between the tumour microenvironment infiltration of immune cells and m6A modification has been revealed, which cannot be explained by the mechanism of RNA degradation. Therefore, a comprehensive understanding of the characteristics of cell infiltration in the tumour microenvironment mediated by multiple m6A regulatory factors could aid in our understanding of the tumour microenvironment immune regulation. Zhang et al. (2020b) comprehensively analysed the m6A landscape associated with immunophenotype in 1,938 gastric cancer samples and constructed an m6A scoring system called the m6Ascore to quantify the m6A characteristics associated with immune cell infiltration in individual patients with GC. When the m6A score was low, the neoantigen load was increased and immune infiltration was high, indicating that the immune checkpoint blockade (PD-1 and PD-L1) has good clinical efficacy. Therefore, m6A modification plays an important role in the diversity and complexity of the tumour microenvironment. Additionally, Feng et al. (2021) speculate that proton pump inhibitors could be a promising therapeutic strategy to further improve the sensitivity of gastric cancer cells to antitumour drugs. For example, omeprazole pre-treatment can enhance the inhibitory effect of 5-FU, DDP and TAX on gastric cancer cells, increase the total m6A level of gastric cancer cells and inhibit autophagy, thereby improving the anti-tumour efficiency of chemotherapy drugs. The mechanism of m6A regulation in gastric cancer is shown in **Table 4**.

Esophageal Cancer

Esophageal cancer is a malignant tumour with a high degree of malignancy and mortality (Jain and Dhingra, 2017; Miller et al., 2020). m6A methylation is an important epigenetic modification involved in the physiological and pathological mechanisms of cancer. However, its role in esophageal cancer remains unclear. Current studies show that m6A modification plays a complex role in the occurrence, development and biological function of esophageal cancer, and it is a research hotspot in epigenetics. m6A modification also has therapeutic potential as an early diagnostic marker and therapeutic target in esophageal cancer. METTL3 has been identified as a decisive inducer of cancer progression, which is up-regulated in esophageal cancer and promotes epithelial-mesenchymal transformation, invasion and migration by regulating miR-20a-5p expression and inhibiting NFIC transcription (Liang et al., 2021). Furthermore, METTL3 was attributed to altered m6A levels in esophageal cancer, and its upregulation was significantly associated with cancer progression. Moreover, the deletion of METTL3 induces the G2/M arrest of esophageal cancer cells via the P21 signalling pathway (Zou et al., 2021). Therefore, METTL3 is a potential target molecule

TABLE 4 | The roles of different m6A regulators in gastric cancer.

m6A regulators	Genes/RNAs	Drugs	Mechanism	Function	References
METTL3 YTHDF1	PARP1- mRNA	Oxaliplatin	1. PARP1 repairs DNA damage caused by oxaliplatin 2. METTL3 recruited YTHDF1 to enhance the stability of PARP1 mRNA	Increased resistance to oxaliplatin	Li et al. (2022a)
METTL3-METTL14-WTAP complex	LncRNA LINC00942 c-Myc-mRNA	Cis-platinum	LINC00942 enhances the stability of c-Myc-mRNA in an m6A dependent manner	Increased resistance to cis-platinum	Zhu et al. (2022)
METTL3	LncRNA ARHGAP5-AS1 ARHGAP5-mRNA	Cis-platinum	Enhance the stability of ARHGAP5-mRNA	Increased resistance to cis-platinum	Zhu et al. (2019b)

in esophageal cancer treatment. ALKBH5, an m6A regulatory factor, is down-regulated in esophageal cancer. The overexpression of ALKBH5 inhibits esophageal cancer cell proliferation and promotes ESCC cell apoptosis (Li et al., 2021a). Liu et al. revealed a METTL14-miR-99a-5p-TRIB2 positive feedback loop in esophageal cancer that enhances tumour stem cell characterisation and drug resistance of ESCC cells. METTL14 has been shown to play an antitumour role through its N6-methyladenosine modification function. In esophageal cancer, METTL14 downregulation eliminated the inhibitory effect of Mir-99a-5p on TRIB2 expression by blocking Mir-99a-5p maturation, which subsequently increased the radiation-resistance of ESCC (Liu et al., 2021). Using METTL14's effect on radiation therapy, Li et al. analysed 15 m6A regulatory factors and identified three new molecular subtypes associated with clinical features and esophageal cancer prognosis. By constructing a protein-protein interaction network for the three novel molecular subtypes and analysing their related genes, eight potential drugs (such as gefitinib, nalatinib, and imatinib) that closely interacted with these genes were identified. This study provides a valuable reference for identifying potential targets and drugs for esophageal cancer treatment (Li et al., 2022b). Currently, studies on m6A modification are limited to the interaction mechanism of esophageal cancer, and there is a lack of research on drug therapy. Therefore, further studies are needed to promote the application of m6A modification in clinical practice, such as the combination of m6A with chemotherapy and immunotherapy.

ROLE OF N6-METHYLADENOSINE MODIFICATION IN TUMOUR CELL APOPTOSIS, AUTOPHAGY AND FERROPTOSIS

m6A is one of the richest modifications that determine the fate of RNA. Currently, m6A modification is closely related to tumorigenesis and plays an important role in the fate of tumour cells, including tumour proliferation and metastasis, tumour cell apoptosis, autophagy and iron death. The abnormal levels of m6A modification during the progression of apoptosis, autophagy, ferroptosis, necrosis and pyroptosis have been detected in gastrointestinal tumours (Zhi et al., 2022). Apoptosis, a type of cell death, is closely related to m6A modification (Zhi et al., 2022), wherein it regulates apoptosis by regulating apoptosis-related gene expression, silencing methylation or demethylase genes and reducing YTHDF2-mediated transcripts (Liu et al., 2022c). For example, METTL3 inhibits the apoptosis of non-small cell lung cancer (NSCLC) cells by promoting miR-1246 maturation and down-regulating PEG3 expression levels (Huang et al., 2021). In a recent study of lncRNAs containing m6A, LNC942 was observed to directly recruit METTL14, a core member of the m6A methyltransferase complex, and associated with increased levels of m6A methylation modification in breast cancer cells. Further, the LNC942-METTL14-CXCR4/CYP1B1 signal axis accelerated cell proliferation and colony formation, and reduced cell apoptosis rate (Sun et al., 2020).

Autophagy is a degradation process involving the lysosomal cytoplasmic content and autophagy-associated (ATG) proteins and transcription factors. It is also closely influenced by different stimulators and inhibitors. Autophagy can promote the resistance of tumour cells to chemotherapy and enable tumour cells to survive (Levy et al., 2017). Various studies have revealed the potential correlation between m6A modification and autophagy mechanism. Kong et al. found that METTL14 expression was higher in pancreatic cancer tissues than in non-tumour tissues, with METTL14 downregulation increasing the sensitivity of pancreatic cancer cells to cisplatin. Compared with the control group, the apoptosis and autophagy of tumour cells were significantly enhanced after METT14 gene knockout (Kong et al., 2020a). YTHDF1 expression is an independent prognostic factor for patients with HCC. Multiple HCC models confirmed that YTHDF1 cannot inhibit the autophagy, growth and metastasis of HCC (Li et al., 2021b). These findings highlight the interaction between autophagy and m6A regulators, but the relationship between m6A and autophagy remains unclear.

Ferroptosis is a novel pro-inflammatory programmed cell death pathway that plays a key role in the clearance of malignant cells. It is caused by the inhibition of the xCT/GSH/GPX4 axis and characterised by iron hyperplasia, lipid peroxidation and the compression of mitochondrial membrane density (Mou et al., 2019). Current studies on ferroptosis modified with m6A have focused on the interference of reader and writer factors on lipid peroxidation or antioxidant enzymes. However, few studies have detected the level of m6A erasers and their correlation with abnormal ferroptosis execution in cancer cells. In NSCLC, METTL3 is involved in cisplatin-mediated ferroptosis *via* m6A enrichment in FSP1 mRNA (Song et al.,

2021). Thus, the relationship between m6A modification and iron death suggests that targeting m6A to induce ferrous iron death could be a promising therapeutic strategy.

CONCLUSION AND PERSPECTIVES

m6A RNA modification has attracted attention in epigenetic research and is involved in many biological processes and disease progressions. From the perspective of epigenetics, m6A modification provides novel insights into the pathogenesis of many diseases, especially tumours. However, further studies are required to understand the dynamic nature of m6A RNA modification in post-transcriptional regulation (Chen and Wong, 2020). m6A RNA modification plays an important role in promoting or inhibiting the growth, proliferation, migration, invasion, specific metastasis, drug resistance and prognosis of digestive tumours through three effector factors, writers, erasers and readers. With increasing studies on the network mechanism of m6A modification regulation, the related mechanism of m6A modification on tumour drug resistance will be clarified (Qiu et al., 2022).

Multiple studies showed that m6A-modified regulatory factors are resistant to SOR in HCC. In CRC, OX, cisplatin and other drug resistance are observed. Resistant to gemcitabine, 5-FU and cisplatin are also observed in pancreatic cancer. Additionally, m6A plays an important role in the regulation of OX and cisplatin resistance in gastric cancer. However, these studies are preliminary, requiring more systematic studies. Furthermore, translational studies are needed to further clarify the use of m6A alone or in combination with other therapies for the treatment of digestive tumours.

Immunotherapy is a new cancer treatment strategy that has been widely used to treat various solid tumours, including various digestive tract tumours and other solid tumours (Kong et al., 2021; Lee et al., 2021). In recent years, promising progress has been made in tumour immunotherapy with m6A modification, among which, ICIs harness the patient's immune system, offering a novel method of cancer treatment. However, immunotherapy, such as ICIs, also presents drug resistance in some patients. For example, from the perspective of an m6A "writer", Wang et al. found that the deletion of methyltransferases METTL3 and METTL14 inhibits m6A modification and enhances pMR-MSI-L response to PD-1 therapy in patients with CRC and melanoma, significantly delaying tumour growth and prolonging patient survival Wang et al. (2020b). However, large-scale basic research is needed to further clarify the specific mechanism of m6A modification in immunotherapy.

m6A plays various roles in different tumour types, suggesting the complexity and diversity of m6A modifications in drug resistance. Recent studies also showed that m6A-modified regulatory factors have potential as therapeutic targets and can enhance the sensitivity of tumour cells to anticancer drugs, providing a new research direction in solving the problem of anticancer drug resistance. This review also highlights the positive prospects of targeted m6A modifications.

DATA AVAILABILITY STATEMENT

The original contributions presented in the study are included in the article/supplementary material, further inquiries can be directed to the corresponding author.

AUTHOR CONTRIBUTIONS

ZX, FK, and XZ contributed to conceive and design the study. ZX and KW performed the systematic searching. ZX and FK extracted the data. ZX and XZ wrote the manuscript. KW and FK supervised the manuscript. All of the authors read and approved the final manuscript.

FUNDING

This project was supported by the grants from Science and Technology Plan Project of Taizhou (Nos. 21ywb36 and 20ywb41).

REFERENCES

Aik, W., Scotti, J. S., Choi, H., Gong, L., Demetriades, M., Schofield, C. J., et al. (2014). Structure of Human RNA N^6-methyladenine Demethylase ALKBH5 Provides Insights into its Mechanisms of Nucleic Acid Recognition and Demethylation. *Nucleic Acids Res.* 42 (7), 4741–4754. doi:10.1093/nar/gku085

Al-Salama, Z. T., Syed, Y. Y., and Scott, L. J. (2019). Lenvatinib: A Review in Hepatocellular Carcinoma. *Drugs* 79 (6), 665–674. doi:10.1007/s40265-019-01116-x

Allen, W. L., and Johnston, P. G. (2005). Role of Genomic Markers in Colorectal Cancer Treatment. *J. Clin. Oncol.* 23 (20), 4545–4552. doi:10.1200/jco.2005.19.752

Amrutkar, M., and Gladhaug, I. P. (2017). Pancreatic Cancer Chemoresistance to Gemcitabine. *Cancers (Basel)* 9 (11). doi:10.3390/cancers9110157

Annapoorna, P. K., Iyer, H., Parnaik, T., Narasimhan, H., Bhattacharya, A., and Kumar, A. (2019). FTO: An Emerging Molecular Player in Neuropsychiatric Diseases. *Neuroscience* 418, 15–24. doi:10.1016/j.neuroscience.2019.08.021

Bansal, H., Yihua, Q., Iyer, S. P., Ganapathy, S., Proia, D. A., Proia, D., et al. (2014). WTAP Is a Novel Oncogenic Protein in Acute Myeloid Leukemia. *Leukemia* 28 (5), 1171–1174. doi:10.1038/leu.2014.16

Benson, A. B., Venook, A. P., Al-Hawary, M. M., Arain, M. A., Chen, Y. J., Ciombor, K. K., et al. (2021). Colon Cancer, Version 2.2021, NCCN Clinical Practice Guidelines in Oncology. *J. Natl. Compr. Canc Netw.* 19 (3), 329–359. doi:10.6004/jnccn.2021.0012

Boku, N., Ryu, M. H., Kato, K., Chung, H. C., Minashi, K., Lee, K. W., et al. (2019). Safety and Efficacy of Nivolumab in Combination with S-1/capecitabine Plus Oxaliplatin in Patients with Previously Untreated, Unresectable, Advanced, or Recurrent Gastric/gastroesophageal Junction Cancer: Interim Results of a Randomized, Phase II Trial (ATTRACTION-4). *Ann. Oncol.* 30 (2), 250–258. doi:10.1093/annonc/mdy540

Cervello, M., McCubrey, J. A., Cusimano, A., Lampiasi, N., Azzolina, A., and Montalto, G. (2012). Targeted Therapy for Hepatocellular Carcinoma: Novel Agents on the Horizon. *Oncotarget* 3 (3), 236–260. doi:10.18632/oncotarget.466

Chen, B., Xiong, L., Chen, W. D., Zhao, X. H., He, J., Zheng, Y. W., et al. (2018). Photodynamic Therapy for Middle-Advanced Stage Upper Gastrointestinal

Carcinomas: A Systematic Review and Meta-Analysis. *World J. Clin. Cases* 6 (13), 650–658. doi:10.12998/wjcc.v6.i13.650

Chen, B., Ye, F., Yu, L., Jia, G., Huang, X., Zhang, X., et al. (2012). Development of Cell-Active N6-Methyladenosine RNA Demethylase FTO Inhibitor. *J. Am. Chem. Soc.* 134 (43), 17963–17971. doi:10.1021/ja3064149

Chen, M., and Wong, C. M. (2020). The Emerging Roles of N6-Methyladenosine (m6A) Deregulation in Liver Carcinogenesis. *Mol. Cancer* 19 (1), 44. doi:10.1186/s12943-020-01172-y

Chen, P., Liu, X. Q., Lin, X., Gao, L. Y., Zhang, S., and Huang, X. (2021). Targeting YTHDF1 Effectively Re-sensitizes Cisplatin-Resistant Colon Cancer Cells by Modulating GLS-Mediated Glutamine Metabolism. *Mol. Ther. Oncolytics* 20, 228–239. doi:10.1016/j.omto.2021.01.001

Chen, W., Zhang, Z., Fang, X., Xiong, L., Wen, Y., Zhou, J., et al. (2021). Prognostic Value of the ALBI Grade Among Patients with Single Hepatocellular Carcinoma without Macrovascular Invasion. *Med. Baltim.* 100 (24), e26265. doi:10.1097/md.0000000000026265

Chen, Y., Wu, R., Chen, W., Liu, Y., Liao, X., Zeng, B., et al. (2021). Curcumin Prevents Obesity by Targeting TRAF4-induced Ubiquitylation in M 6 A-dependent Manner. *EMBO Rep.* 22 (5), e52146. doi:10.15252/embr.202052146

Chen, Z., Zhong, X., Xia, M., and Zhong, J. (2021). The Roles and Mechanisms of the m6A Reader Protein YTHDF1 in Tumor Biology and Human Diseases. *Mol. Ther. Nucleic Acids* 26, 1270–1279. doi:10.1016/j.omtn.2021.10.023

Chesney, T. R., Haas, B., Coburn, N., Mahar, A. L., Davis, L. E., Zuk, V., et al. (2021). Association of Frailty with Long-Term Homecare Utilization in Older Adults Following Cancer Surgery: Retrospective Population-Based Cohort Study. *Eur. J. Surg. Oncol.* 47 (4), 888–895. doi:10.1016/j.ejso.2020.09.009

Cho, S. H., Ha, M., Cho, Y. H., Ryu, J. H., Yang, K., Lee, K. H., et al. (2018). ALKBH5 Gene Is a Novel Biomarker that Predicts the Prognosis of Pancreatic Cancer: A Retrospective Multicohort Study. *Ann. Hepatobiliary Pancreat. Surg.* 22 (4), 305–309. doi:10.14701/ahbps.2018.22.4.305

Dagogo-Jack, I., and Shaw, A. T. (2018). Tumour Heterogeneity and Resistance to Cancer Therapies. *Nat. Rev. Clin. Oncol.* 15 (2), 81–94. doi:10.1038/nrclinonc.2017.166

Dai, D., Wang, H., Zhu, L., Jin, H., and Wang, X. (2018). N6-methyladenosine Links RNA Metabolism to Cancer Progression. *Cell. Death Dis.* 9 (2), 124. doi:10.1038/s41419-017-0129-x

Dasari, S., and Tchounwou, P. B. (2014). Cisplatin in Cancer Therapy: Molecular Mechanisms of Action. *Eur. J. Pharmacol.* 740, 364–378. doi:10.1016/j.ejphar.2014.07.025

Dekker, E., Tanis, P. J., Vleugels, J. L. A., Kasi, P. M., and Wallace, M. B. (2019). Colorectal Cancer. *Lancet* 394 (10207), 1467–1480. doi:10.1016/s0140-6736(19)32319-0

Doxtader, K. A., Wang, P., Scarborough, A. M., Seo, D., Conrad, N. K., and Nam, Y. (2018). Structural Basis for Regulation of METTL16, an S-Adenosylmethionine Homeostasis Factor. *Mol. Cell.* 71 (6), 1001–e4. e4. doi:10.1016/j.molcel.2018.07.025

Feng, S., Qiu, G., Yang, L., Feng, L., Fan, X., Ren, F., et al. (2021). Omeprazole Improves Chemosensitivity of Gastric Cancer Cells by m6A Demethylase FTO-Mediated Activation of mTORC1 and DDIT3 Up-Regulation. *Biosci. Rep.* 41 (1). doi:10.1042/bsr20200842

Galluzzi, L., Senovilla, L., Vitale, I., Michels, J., Martins, I., Kepp, O., et al. (2012). Molecular Mechanisms of Cisplatin Resistance. *Oncogene* 31 (15), 1869–1883. doi:10.1038/onc.2011.384

Gan, Z., Wei, W., Wu, J., Zhao, Y., Zhang, L., Wang, T., et al. (2019). Resveratrol and Curcumin Improve Intestinal Mucosal Integrity and Decrease m6A RNA Methylation in the Intestine of Weaning Piglets. *ACS Omega* 4 (17), 17438–17446. doi:10.1021/acsomega.9b02236

Ganesh, K., Stadler, Z. K., Cercek, A., Mendelsohn, R. B., Shia, J., Segal, N. H., et al. (2019). Immunotherapy in Colorectal Cancer: Rationale, Challenges and Potential. *Nat. Rev. Gastroenterol. Hepatol.* 16 (6), 361–375. doi:10.1038/s41575-019-0126-x

Gerken, T., Girard, C. A., Tung, Y. C., Webby, C. J., Saudek, V., Hewitson, K. S., et al. (2007). The Obesity-Associated FTO Gene Encodes a 2-oxoglutarate-dependent Nucleic Acid Demethylase. *Science* 318 (5855), 1469–1472. doi:10.1126/science.1151710

Geuens, T., Bouhy, D., and Timmerman, V. (2016). The hnRNP Family: Insights into Their Role in Health and Disease. *Hum. Genet.* 135 (8), 851–867. doi:10.1007/s00439-016-1683-5

Ghazi, T., Nagiah, S., and Chuturgoon, A. A. (2021). Fusaric Acid Decreases P53 Expression by Altering Promoter Methylation and m6A RNA Methylation in Human Hepatocellular Carcinoma (HepG2) Cells. *Epigenetics* 16 (1), 79–91. doi:10.1080/15592294.2020.1788324

Guo, X., Li, K., Jiang, W., Hu, Y., Xiao, W., Huang, Y., et al. (2020). RNA Demethylase ALKBH5 Prevents Pancreatic Cancer Progression by Posttranscriptional Activation of PER1 in an m6A-YTHDF2-dependent Manner. *Mol. Cancer* 19 (1), 91. doi:10.1186/s12943-020-01158-w

Han, Z., Niu, T., Chang, J., Lei, X., Zhao, M., Wang, Q., et al. (2010). Crystal Structure of the FTO Protein Reveals Basis for its Substrate Specificity. *Nature* 464 (7292), 1205–1209. doi:10.1038/nature08921

Harada, K., Sakamoto, N., Ukai, S., Yamamoto, Y., Pham, Q. T., Taniyama, D., et al. (2021). Establishment of Oxaliplatin-Resistant Gastric Cancer Organoids: Importance of Myoferlin in the Acquisition of Oxaliplatin Resistance. *Gastric Cancer* 24 (6), 1264–1277. doi:10.1007/s10120-021-01206-4

He, L., Li, H., Wu, A., Peng, Y., Shu, G., and Yin, G. (2019). Functions of N6-Methyladenosine and its Role in Cancer. *Mol. Cancer* 18 (1), 176. doi:10.1186/s12943-019-1109-9

Hsu, P. J., Zhu, Y., Ma, H., Guo, Y., Shi, X., Liu, Y., et al. (2017). Ythdc2 Is an N6-Methyladenosine Binding Protein that Regulates Mammalian Spermatogenesis. *Cell. Res.* 27 (9), 1115–1127. doi:10.1038/cr.2017.99

Hu, J. L., Wang, W., Lan, X. L., Zeng, Z. C., Liang, Y. S., Yan, Y. R., et al. (2019). CAFs Secreted Exosomes Promote Metastasis and Chemotherapy Resistance by Enhancing Cell Stemness and Epithelial-Mesenchymal Transition in Colorectal Cancer. *Mol. Cancer* 18 (1), 91. doi:10.1186/s12943-019-1019-x

Hu, Y., Ouyang, Z., Sui, X., Qi, M., Li, M., He, Y., et al. (2020). Oocyte Competence Is Maintained by m6A Methyltransferase KIAA1429-Mediated RNA Metabolism during Mouse Follicular Development. *Cell. Death Differ.* 27 (8), 2468–2483. doi:10.1038/s41418-020-0516-1

Huang, H., Weng, H., and Chen, J. (2020). The Biogenesis and Precise Control of RNA m6A Methylation. *Trends Genet.* 36 (1), 44–52. doi:10.1016/j.tig.2019.10.011

Huang, S., Luo, S., Gong, C., Liang, L., Xiao, Y., Li, M., et al. (2021). MTTL3 Upregulates microRNA-1246 to Promote Occurrence and Progression of NSCLC via Targeting Paternally Expressed Gene 3. *Mol. Ther. Nucleic Acids* 24, 542–553. doi:10.1016/j.omtn.2021.02.020

Huang, W., Kong, F., Li, R., Chen, X., and Wang, K. (2022). Emerging Roles of m6A RNA Methylation Regulators in Gynecological Cancer. *Front. Oncol.* 12, 827956. doi:10.3389/fonc.2022.827956

Huff, S., Tiwari, S. K., Gonzalez, G. M., Wang, Y., and Rana, T. M. (2021). m6A-RNA Demethylase FTO Inhibitors Impair Self-Renewal in Glioblastoma Stem CellsA-RNA Demethylase FTO Inhibitors Impair Self-Renewal in Glioblastoma Stem Cells. *ACS Chem. Biol.* 16 (2), 324–333. doi:10.1021/acschembio.0c00841

Huo, F. C., Zhu, Z. M., and Pei, D. S. (2020). N6 -methyladenosine (M6 A) RNA Modification in Human Cancer. *Cell. Prolif.* 53 (11), e12921. doi:10.1111/cpr.12921

Iacovelli, R., Sternberg, C. N., Porta, C., Verzoni, E., de Braud, F., Escudier, B., et al. (2015). Inhibition of the VEGF/VEGFR Pathway Improves Survival in Advanced Kidney Cancer: a Systematic Review and Meta-Analysis. *Curr. Drug Targets* 16 (2), 164–170. doi:10.2174/1389450115666141120120145

Jain, S., and Dhingra, S. (2017). Pathology of Esophageal Cancer and Barrett's Esophagus. *Ann. Cardiothorac. Surg.* 6 (2), 99–109. doi:10.21037/acs.2017.03.06

Jin, D., Guo, J., Wu, Y., Yang, L., Wang, X., Du, J., et al. (2020). m6A Demethylase ALKBH5 Inhibits Tumor Growth and Metastasis by Reducing YTHDFs-Mediated YAP Expression and Inhibiting miR-107/lats2-Mediated YAP Activity in NSCLCA Demethylase ALKBH5 Inhibits Tumor Growth and Metastasis by Reducing YTHDFs-Mediated YAP Expression and Inhibiting miR-107/lats2-Mediated YAP Activity in NSCLC. *Mol. Cancer* 19 (1), 40. doi:10.1186/s12943-020-01161-1

Johnston, F. M., and Beckman, M. (2019). Updates on Management of Gastric Cancer. *Curr. Oncol. Rep.* 21 (8), 67. doi:10.1007/s11912-019-0820-4

Kang, Y. K., Chin, K., Chung, H. C., Kadowaki, S., Oh, S. C., Nakayama, N., et al. (2020). S-1 Plus Leucovorin and Oxaliplatin versus S-1 Plus Cisplatin as First-Line Therapy in Patients with Advanced Gastric Cancer (SOLAR): a Randomised, Open-Label, Phase 3 Trial. *Lancet Oncol.* 21 (8), 1045–1056. doi:10.1016/s1470-2045(20)30315-6

Kant, R., Yang, M. H., Tseng, C. H., Yen, C. H., Li, W. Y., Tyan, Y. C., et al. (2021). Discovery of an Orally Efficacious MYC Inhibitor for Liver Cancer Using a GNMT-Based High-Throughput Screening System and Structure-Activity Relationship Analysis. *J. Med. Chem.* 64 (13), 8992–9009. doi:10.1021/acs.jmedchem.1c00093

Kong, F., Liu, X., Zhou, Y., Hou, X., He, J., Li, Q., et al. (2020). Downregulation of METTL14 Increases Apoptosis and Autophagy Induced by Cisplatin in Pancreatic Cancer Cells. *Int. J. Biochem. Cell. Biol.* 122, 105731. doi:10.1016/j.biocel.2020.105731

Kong, F., Zou, H., Liu, X., He, J., Zheng, Y., Xiong, L., et al. (2020). miR-7112-3p Targets PERK to Regulate the Endoplasmic Reticulum Stress Pathway and Apoptosis Induced by Photodynamic Therapy in Colorectal Cancer CX-1 Cells. *Photodiagnosis Photodyn. Ther.* 29, 101663. doi:10.1016/j.pdpdt.2020.101663

Kong, F. H., Miao, X. Y., Zou, H., Xiong, L., Wen, Y., Chen, B., et al. (2019). End-stage Liver Disease Score and Future Liver Remnant Volume Predict Post-hepatectomy Liver Failure in Hepatocellular Carcinoma. *World J. Clin. Cases* 7 (22), 3734–3741. doi:10.12998/wjcc.v7.i22.3734

Kong, F. H., Ye, Q. F., Miao, X. Y., Liu, X., Huang, S. Q., Xiong, L., et al. (2021). Current Status of Sorafenib Nanoparticle Delivery Systems in the Treatment of Hepatocellular Carcinoma. *Theranostics* 11 (11), 5464–5490. doi:10.7150/thno.54822

Kong, H., Sun, J., Zhang, W., Zhang, H., and Li, H. (2022). Long Intergenic Non-protein Coding RNA 1273 Confers Sorafenib Resistance in Hepatocellular Carcinoma via Regulation of Methyltransferase 3. *Bioengineered* 13 (2), 3108–3121. doi:10.1080/21655979.2022.2025701

Lan, H., Liu, Y., Liu, J., Wang, X., Guan, Z., Du, J., et al. (2021). Tumor-Associated Macrophages Promote Oxaliplatin Resistance via METTL3-Mediated m6A of TRAF5 and Necroptosis in Colorectal Cancer. *Mol. Pharm.* 18 (3), 1026–1037. doi:10.1021/acs.molpharmaceut.0c00961

Lan, L., Sun, Y. J., Jin, X. Y., Xie, L. J., Liu, L., and Cheng, L. (2021). A Light-Controllable Chemical Modulation of M6 A RNA Methylation. *Angew. Chem. Int. Ed. Engl.* 60 (33), 18116–18121. doi:10.1002/anie.202103854

Lee, J. C., Green, M. D., Huppert, L. A., Chow, C., Pierce, R. H., and Daud, A. I. (2021). The Liver-Immunity Nexus and Cancer Immunotherapy. *Clin. Cancer Res.* 28, 5–12. doi:10.1158/1078-0432.ccr-21-1193

Levy, J. M. M., Towers, C. G., and Thorburn, A. (2017). Targeting Autophagy in Cancer. *Nat. Rev. Cancer* 17 (9), 528–542. doi:10.1038/nrc.2017.53

Li, H., Wang, C., Lan, L., Yan, L., Li, W., Evans, I., et al. (2022). METTL3 Promotes Oxaliplatin Resistance of Gastric Cancer CD133+ Stem Cells by Promoting PARP1 mRNA Stability. *Cell. Mol. Life Sci.* 79 (3), 135. doi:10.1007/s00018-022-04129-0

Li, J., Liu, H., Dong, S., Zhang, Y., Li, X., and Wang, J. (2021). ALKBH5 Is Lowly Expressed in Esophageal Squamous Cell Carcinoma and Inhibits the Malignant Proliferation and Invasion of Tumor Cells. *Comput. Math. Methods Med.* 2021, 1001446. doi:10.1155/2021/1001446

Li, J., Zhu, H., Yang, Q., Xiao, H., Wu, H., Fang, Z., et al. (2022). Identification of Molecular Subtypes and Potential Small-Molecule Drugs for Esophagus Cancer Treatment Based on m6A Regulators. *J. Oncol.* 2022, 5490461. doi:10.1155/2022/5490461

Li, Q., Ni, Y., Zhang, L., Jiang, R., Xu, J., Yang, H., et al. (2021). HIF-1α-induced Expression of m6A Reader YTHDF1 Drives Hypoxia-Induced Autophagy and Malignancy of Hepatocellular Carcinoma by Promoting ATG2A and ATG14 Translation. *Signal Transduct. Target Ther.* 6 (1), 76. doi:10.1038/s41392-020-00453-8

Liang, X., Zhang, Z., Wang, L., Zhang, S., Ren, L., Li, S., et al. (2021). Mechanism of Methyltransferase like 3 in Epithelial-Mesenchymal Transition Process, Invasion, and Metastasis in Esophageal Cancer. *Bioengineered* 12 (2), 10023–10036. doi:10.1080/21655979.2021.1994721

Lin, Z., Niu, Y., Wan, A., Chen, D., Liang, H., Chen, X., et al. (2020). RNA M6 A Methylation Regulates Sorafenib Resistance in Liver Cancer through FOXO3-Mediated Autophagy. *Embo J.* 39 (12), e103181. doi:10.15252/embj.2019103181

Lipson, E. J., Forde, P. M., Hammers, H. J., Emens, L. A., Taube, J. M., and Topalian, S. L. (2015). Antagonists of PD-1 and PD-L1 in Cancer Treatment. *Semin. Oncol.* 42 (4), 587–600. doi:10.1053/j.seminoncol.2015.05.013

Liu, H., Li, D., Sun, L., Qin, H., Fan, A., Meng, L., et al. (2022). Interaction of lncRNA MIR100HG with hnRNPA2B1 Facilitates m6A-dependent Stabilization of TCF7L2 mRNA and Colorectal Cancer Progression. *Mol. Cancer* 21 (1), 74. doi:10.1186/s12943-022-01555-3

Liu, L., Li, H., Hu, D., Wang, Y., Shao, W., Zhong, J., et al. (2022). Insights into N6-Methyladenosine and Programmed Cell Death in Cancer. *Mol. Cancer* 21 (1), 32. doi:10.1186/s12943-022-01508-w

Liu, Q., Huang, Q., Liu, H., He, F. J., Liu, J. H., Zhou, Y. Y., et al. (2022). SUMOylation of Methyltransferase-like 3 Facilitates Colorectal Cancer Progression by Promoting Circ_0000677 in an M 6 A-dependent Manner. *J Gastro Hepatol* 37, 700–713. doi:10.1111/jgh.15775

Liu, X., Hou, X., Zhou, Y., Li, Q., Kong, F., Yan, S., et al. (2019). Downregulation of the Helicase Lymphoid-specific (HELLS) Gene Impairs Cell Proliferation and Induces Cell Cycle Arrest in Colorectal Cancer Cells. *Onco Targets Ther.* 12, 10153–10163. doi:10.2147/ott.s223668

Liu, Z., Wu, K., Gu, S., Wang, W., Xie, S., Lu, T., et al. (2021). A Methyltransferase-like 14/miR-99a-5p/tribble 2 Positive Feedback Circuit Promotes Cancer Stem Cell Persistence and Radioresistance via Histone Deacetylase 2-mediated Epigenetic Modulation in Esophageal Squamous Cell Carcinoma. *Clin. Transl. Med.* 11 (9), e545. doi:10.1002/ctm2.545

Llovet, J. M., Kelley, R. K., Villanueva, A., Singal, A. G., Pikarsky, E., Roayaie, S., et al. (2021). Hepatocellular Carcinoma. *Nat. Rev. Dis. Prim.* 7 (1), 6. doi:10.1038/s41572-020-00240-3

Llovet, J. M., Montal, R., Sia, D., and Finn, R. S. (2018). Molecular Therapies and Precision Medicine for Hepatocellular Carcinoma. *Nat. Rev. Clin. Oncol.* 15 (10), 599–616. doi:10.1038/s41571-018-0073-4

Llovet, J. M., Ricci, S., Mazzaferro, V., Hilgard, P., Gane, E., Blanc, J. F., et al. (2008). Sorafenib in Advanced Hepatocellular Carcinoma. *N. Engl. J. Med.* 359 (4), 378–390. doi:10.1056/NEJMoa0708857

Lu, J. J., and Wang, Y. T. (2020). Identification of Anti-cancer Compounds from Natural Products. *Chin. J. Nat. Med.* 18 (7), 481–482. doi:10.1016/s1875-5364(20)30057-1

Luo, M., Huang, Z., Yang, X., Chen, Y., Jiang, J., Zhang, L., et al. (2022). PHLDB2 Mediates Cetuximab Resistance via Interacting with EGFR in Latent Metastasis of Colorectal Cancer. *Cell. Mol. Gastroenterol. Hepatol.* 13 (4), 1223–1242. doi:10.1016/j.jcmgh.2021.12.011

Ma, S., Chen, C., Ji, X., Liu, J., Zhou, Q., Wang, G., et al. (2019). The Interplay between m6A RNA Methylation and Noncoding RNA in Cancer. *J. Hematol. Oncol.* 12 (1), 121. doi:10.1186/s13045-019-0805-7

Machlowska, J., Baj, J., Sitarz, M., Maciejewski, R., and Sitarz, R. (2020). Gastric Cancer: Epidemiology, Risk Factors, Classification, Genomic Characteristics and Treatment Strategies. *Int. J. Mol. Sci.* 21 (11). doi:10.3390/ijms21114012

Maldonado López, A., and Capell, B. C. (2021). The METTL3-m6A Epitranscriptome: Dynamic Regulator of Epithelial Development, Differentiation, and Cancer. *Genes.* 12 (7), 1019. doi:10.3390/genes12071019

Miller, K. D., Fidler-Benaoudia, M., Keegan, T. H., Hipp, H. S., Jemal, A., and Siegel, R. L. (2020). Cancer Statistics for Adolescents and Young Adults, 2020. *CA Cancer J. Clin.* 70 (1), 443–459. doi:10.3322/caac.2159010.3322/caac.21637

Mizrahi, J. D., Surana, R., Valle, J. W., and Shroff, R. T. (2020). Pancreatic Cancer. *Lancet* 395 (10242), 2008–2020. doi:10.1016/s0140-6736(20)30974-0

Mou, Y., Wang, J., Wu, J., He, D., Zhang, C., Duan, C., et al. (2019). Ferroptosis, a New Form of Cell Death: Opportunities and Challenges in Cancer. *J. Hematol. Oncol.* 12 (1), 34. doi:10.1186/s13045-019-0720-y

Palazzo, A., Iacovelli, R., and Cortesi, E. (2010). Past, Present and Future of Targeted Therapy in Solid Tumors. *Curr. Cancer Drug Targets* 10 (5), 433–461. doi:10.2174/156800910791517145

Pan, S., Deng, Y., Fu, J., Zhang, Y., Zhang, Z., and Qin, X. (2022). N6-methyladenosine U-pregulates miR-181d-5p in E-xosomes D-erived from C-ancer-associated F-ibroblasts to I-nhibit 5-FU S-ensitivity by T-argeting NCALD in C-olorectal C-ancer. *Int. J. Oncol.* 60 (2). doi:10.3892/ijo.2022.5304

Paul, D., Sanap, G., Shenoy, S., Kalyane, D., Kalia, K., and Tekade, R. K. (2021). Artificial Intelligence in Drug Discovery and Development. *Drug Discov. Today* 26 (1), 80–93. doi:10.1016/j.drudis.2020.10.010

Pavitra, E., Dariya, B., Srivani, G., Kang, S. M., Alam, A., Sudhir, P. R., et al. (2021). Engineered Nanoparticles for Imaging and Drug Delivery in Colorectal Cancer. *Semin. Cancer Biol.* 69, 293–306. doi:10.1016/j.semcancer.2019.06.017

Peng, S., Xiao, W., Ju, D., Sun, B., Hou, N., Liu, Q., et al. (2019). Identification of Entacapone as a Chemical Inhibitor of FTO Mediating Metabolic Regulation through FOXO1. *Sci. Transl. Med.* 11 (488), 11. doi:10.1126/scitranslmed.aau7116

Qiu, X., Li, X., Yan, Y., Cai, Y., Liang, Q., Peng, B., et al. (2022). Identification of m6A-Associated Gene DST as a Prognostic and Immune-Associated

Biomarker in Breast Cancer Patients. *Int. J. Gen. Med.* 15, 523–534. doi:10.2147/ijgm.s344146

Qu, J., Yan, H., Hou, Y., Cao, W., Liu, Y., Zhang, E., et al. (2022). RNA Demethylase ALKBH5 in Cancer: from Mechanisms to Therapeutic Potential. *J. Hematol. Oncol.* 15 (1), 8. doi:10.1186/s13045-022-01224-4

Rafalska, I., Zhang, Z., Benderska, N., Wolff, H., Hartmann, A. M., Brack-Werner, R., et al. (2004). The Intranuclear Localization and Function of YT521-B Is Regulated by Tyrosine Phosphorylation. *Hum. Mol. Genet.* 13 (15), 1535–1549. doi:10.1093/hmg/ddh167

Relier, S., Ripoll, J., Guillorit, H., Amalric, A., Achour, C., Boissière, F., et al. (2021). FTO-mediated Cytoplasmic m6Am Demethylation Adjusts Stem-like Properties in Colorectal Cancer Cell. *Nat. Commun.* 12 (1), 1716. doi:10.1038/s41467-021-21758-4

Sawicki, T., Ruszkowska, M., Danielewicz, A., Niedźwiedzka, E., Arłukowicz, T., and Przybyłowicz, K. E. (2021). A Review of Colorectal Cancer in Terms of Epidemiology, Risk Factors, Development, Symptoms and Diagnosis. *Cancers (Basel)* 13 (9). doi:10.3390/cancers13092025

Schizas, D., Charalampakis, N., Kole, C., Economopoulou, P., Koustas, E., Gkotsis, E., et al. (2020). Immunotherapy for Pancreatic Cancer: A 2020 Update. *Cancer Treat. Rev.* 86, 102016. doi:10.1016/j.ctrv.2020.102016

Schöller, E., Weichmann, F., Treiber, T., Ringle, S., Treiber, N., Flatley, A., et al. (2018). Interactions, Localization, and Phosphorylation of the m6A Generating METTL3-METTL14-WTAP Complex. *Rna* 24 (4), 499–512. doi:10.1261/rna.064063.117

Seebacher, N. A., Stacy, A. E., Porter, G. M., and Merlot, A. M. (2019). Clinical Development of Targeted and Immune Based Anti-cancer Therapies. *J. Exp. Clin. Cancer Res.* 38 (1), 156. doi:10.1186/s13046-019-1094-2

Shen, H., Lan, Y., Zhao, Y., Shi, Y., Jin, J., and Xie, W. (2020). The Emerging Roles of N6-Methyladenosine RNA Methylation in Human Cancers. *Biomark. Res.* 8, 24. doi:10.1186/s40364-020-00203-6

Shi, R., Ying, S., Li, Y., Zhu, L., Wang, X., and Jin, H. (2021). Linking the YTH Domain to Cancer: the Importance of YTH Family Proteins in Epigenetics. *Cell. Death Dis.* 12 (4), 346. doi:10.1038/s41419-021-03625-8

Smyth, E. C., Nilsson, M., Grabsch, H. I., van Grieken, N. C., and Lordick, F. (2020). Gastric Cancer. *Lancet* 396 (10251), 635–648. doi:10.1016/s0140-6736(20)31288-5

Song, Z., Jia, G., Ma, P., and Cang, S. (2021). Exosomal miR-4443 Promotes Cisplatin Resistance in Non-small Cell Lung Carcinoma by Regulating FSP1 m6A Modification-Mediated Ferroptosis. *Life Sci.* 276, 119399. doi:10.1016/j.lfs.2021.119399

Su, R., Dong, L., Li, Y., Gao, M., Han, L., Wunderlich, M., et al. (2020). Targeting FTO Suppresses Cancer Stem Cell Maintenance and Immune Evasion. *Cancer Cell.* 38 (1), 79–e11. e11. doi:10.1016/j.ccell.2020.04.017

Sun, T., Wu, Z., Wang, X., Wang, Y., Hu, X., Qin, W., et al. (2020). LNC942 Promoting METTL14-Mediated m6A Methylation in Breast Cancer Cell Proliferation and Progression. *Oncogene* 39 (31), 5358–5372. doi:10.1038/s41388-020-1338-9

Sung, H., Ferlay, J., Siegel, R. L., Laversanne, M., Soerjomataram, I., Jemal, A., et al. (2021). Global Cancer Statistics 2020: GLOBOCAN Estimates of Incidence and Mortality Worldwide for 36 Cancers in 185 Countries. *CA Cancer J. Clin.* 71 (3), 209–249. doi:10.3322/caac.21660

Taketo, K., Konno, M., Asai, A., Koseki, J., Toratani, M., Satoh, T., et al. (2018). The Epitranscriptome m6A Writer METTL3 Promotes Chemo- and Radioresistance in Pancreatic Cancer Cells. *Int. J. Oncol.* 52 (2), 621–629. doi:10.3892/ijo.2017.4219

Tang, B., Yang, Y., Kang, M., Wang, Y., Wang, Y., Bi, Y., et al. (2020). m6A Demethylase ALKBH5 Inhibits Pancreatic Cancer Tumorigenesis by Decreasing WIF-1 RNA Methylation and Mediating Wnt signalingA Demethylase ALKBH5 Inhibits Pancreatic Cancer Tumorigenesis by Decreasing WIF-1 RNA Methylation and Mediating Wnt Signaling. *Mol. Cancer* 19 (1), 3. doi:10.1186/s12943-019-1128-6

Uddin, M. B., Roy, K. R., Hosain, S. B., Khiste, S. K., Hill, R. A., Jois, S. D., et al. (2019). An N6-Methyladenosine at the Transited Codon 273 of P53 Pre-mRNA Promotes the Expression of R273H Mutant Protein and Drug Resistance of Cancer Cells. *Biochem. Pharmacol.* 160, 134–145. doi:10.1016/j.bcp.2018.12.014

Wang, J., Wang, J., Gu, Q., Ma, Y., Yang, Y., Zhu, J., et al. (2020). The Biological Function of m6A Demethylase ALKBH5 and its Role in Human Disease. *Cancer Cell. Int.* 20, 347. doi:10.1186/s12935-020-01450-1

Wang, J., Xu, R., Li, J., Bai, Y., Liu, T., Jiao, S., et al. (2016). Randomized Multicenter Phase III Study of a Modified Docetaxel and Cisplatin Plus Fluorouracil Regimen Compared with Cisplatin and Fluorouracil as First-Line Therapy for Advanced or Locally Recurrent Gastric Cancer. *Gastric Cancer* 19 (1), 234–244. doi:10.1007/s10120-015-0457-4

Wang, K., Miao, X., Kong, F., Huang, S., Mo, J., Jin, C., et al. (2021). Integrating Network Pharmacology and Experimental Verification to Explore the Mechanism of Effect of Zuojin Pills in Pancreatic Cancer Treatment. *Drug Des. Devel Ther.* 15, 3749–3764. doi:10.2147/dddt.s323360

Wang, L., Hui, H., Agrawal, K., Kang, Y., Li, N., Tang, R., et al. (2020). m6 A RNA Methyltransferases METTL3/14 Regulate Immune Responses to Anti-PD-1 therapyA RNA Methyltransferases METTL3/14 Regulate Immune Responses to Anti-PD-1 Therapy. *Embo J.* 39 (20), e104514. doi:10.15252/embj.2020104514

Wang, X., Huang, J., Zou, T., and Yin, P. (2017). Human m6A Writers: Two Subunits, 2 Roles. *RNA Biol.* 14 (3), 300–304. doi:10.1080/15476286.2017.1282025

Wang, X., Tian, L., Li, Y., Wang, J., Yan, B., Yang, L., et al. (2021). RBM15 Facilitates Laryngeal Squamous Cell Carcinoma Progression by Regulating TMBIM6 Stability through IGF2BP3 Dependent. *J. Exp. Clin. Cancer Res.* 40 (1), 80. doi:10.1186/s13046-021-01871-4

Wang, X., Zhao, B. S., Roundtree, I. A., Lu, Z., Han, D., Ma, H., et al. (2015). N(6)-methyladenosine Modulates Messenger RNA Translation Efficiency. *Cell.* 161 (6), 1388–1399. doi:10.1016/j.cell.2015.05.014

Wojtas, M. N., Pandey, R. R., Mendel, M., Homolka, D., Sachidanandam, R., and Pillai, R. S. (2017). Regulation of m6A Transcripts by the 3'→5' RNA Helicase YTHDC2 Is Essential for a Successful Meiotic Program in the Mammalian Germline. *Mol. Cell.* 68 (2), 374–e12. e12. doi:10.1016/j.molcel.2017.09.021

Xu, J., Wan, Z., Tang, M., Lin, Z., Jiang, S., Ji, L., et al. (2020). N6-methyladenosine-modified CircRNA-SORE Sustains Sorafenib Resistance in Hepatocellular Carcinoma by Regulating β-catenin Signaling. *Mol. Cancer* 19 (1), 163. doi:10.1186/s12943-020-01281-8

Xu, K., Sun, Y., Sheng, B., Zheng, Y., Wu, X., and Xu, K. (2019). Role of Identified RNA N6-Methyladenosine Methylation in Liver. *Anal. Biochem.* 578, 45–50. doi:10.1016/j.ab.2019.05.005

Xu, W., Xie, S., Chen, X., Pan, S., Qian, H., and Zhu, X. (2021). Effects of Quercetin on the Efficacy of Various Chemotherapeutic Drugs in Cervical Cancer Cells. *Drug Des. Devel Ther.* 15, 577–588. doi:10.2147/dddt.s291865

Xu, Z., Peng, B., Cai, Y., Wu, G., Huang, J., Gao, M., et al. (2020). N6-methyladenosine RNA Modification in Cancer Therapeutic Resistance: Current Status and Perspectives. *Biochem. Pharmacol.* 182, 114258. doi:10.1016/j.bcp.2020.114258

Yan, Y., Liang, Q., Xu, Z., and Yi, Q. (2021). Integrative Bioinformatics and Experimental Analysis Revealed Down-Regulated CDC42EP3 as a Novel Prognostic Target for Ovarian Cancer and its Roles in Immune Infiltration. *PeerJ* 9, e12171. doi:10.7717/peerj.12171

Yang, Z., Zhao, F., Gu, X., Feng, L., Xu, M., Li, T., et al. (2021). Binding of RNA m6A by IGF2BP3 Triggers Chemoresistance of HCT8 Cells via Upregulation of ABCB1. *Am. J. Cancer Res.* 11 (4), 1428–1445.

Yu, S., Li, X., Liu, S., Yang, R., Liu, X., and Wu, S. (2019). N6-Methyladenosine: A Novel RNA Imprint in Human Cancer. *Front. Oncol.* 9, 1407. doi:10.3389/fonc.2019.01407

Zeng, C., Huang, W., Li, Y., and Weng, H. (2020). Roles of METTL3 in Cancer: Mechanisms and Therapeutic Targeting. *J. Hematol. Oncol.* 13 (1), 117. doi:10.1186/s13045-020-00951-w

Zeng, S., Pöttler, M., Lan, B., Grützmann, R., Pilarsky, C., and Yang, H. (2019). Chemoresistance in Pancreatic Cancer. *Int. J. Mol. Sci.* 20 (18). doi:10.3390/ijms20184504

Zhang, B., Wu, Q., Li, B., Wang, D., Wang, L., and Zhou, Y. L. (2020). m6A Regulator-Mediated Methylation Modification Patterns and Tumor Microenvironment Infiltration Characterization in Gastric Cancer A Regulator-Mediated Methylation Modification Patterns and Tumor Microenvironment Infiltration Characterization in Gastric Cancer. *Mol. Cancer* 19 (1), 53. doi:10.1186/s12943-020-01170-0

Zhang, C., Ou, S., Zhou, Y., Liu, P., Zhang, P., Li, Z., et al. (2021). m6A Methyltransferase METTL14-Mediated Upregulation of Cytidine Deaminase Promoting Gemcitabine Resistance in Pancreatic CancerA Methyltransferase METTL14-Mediated Upregulation of Cytidine Deaminase Promoting

Gemcitabine Resistance in Pancreatic Cancer. *Front. Oncol.* 11, 696371. doi:10.3389/fonc.2021.696371

Zhang, L., Qi, Y., ALuo, Z., Zhang, Z., and Zhou, L. (2019). Betaine Increases Mitochondrial Content and Improves Hepatic Lipid Metabolism. *Food Funct.* 10 (1), 216–223. doi:10.1039/c8fo02004c

Zhang, R., Li, X., Zhang, X., Qin, H., and Xiao, W. (2021). Machine Learning Approaches for Elucidating the Biological Effects of Natural Products. *Nat. Prod. Rep.* 38 (2), 346–361. doi:10.1039/d0np00043d

Zhang, X., Xie, K., Zhou, H., Wu, Y., Li, C., Liu, Y., et al. (2020). Role of Non-coding RNAs and RNA Modifiers in Cancer Therapy Resistance. *Mol. Cancer* 19 (1), 47. doi:10.1186/s12943-020-01171-z

Zhao, B. S., Wang, X., Beadell, A. V., Lu, Z., Shi, H., Kuuspalu, A., et al. (2017). m6A-dependent Maternal mRNA Clearance Facilitates Zebrafish Maternal-To-Zygotic transitionA-dependent Maternal mRNA Clearance Facilitates Zebrafish Maternal-To-Zygotic Transition. *Nature* 542 (7642), 475–478. doi:10.1038/nature21355

Zheng, F., Du, F., Zhao, J., Wang, X., Si, Y., Jin, P., et al. (2021). The Emerging Role of RNA N6-Methyladenosine Methylation in Breast Cancer. *Biomark. Res.* 9 (1), 39. doi:10.1186/s40364-021-00295-8

Zhi, Y., Zhang, S., Zi, M., Wang, Y., Liu, Y., Zhang, M., et al. (2022). Potential Applications of N 6 -methyladenosine Modification in the Prognosis and Treatment of Cancers via Modulating Apoptosis, Autophagy, and Ferroptosis. *Wiley Interdiscip. Rev. RNA*, e1719. doi:10.1002/wrna.1719

Zhou, L. L., Xu, H., Huang, Y., and Yang, C. G. (2021). Targeting the RNA Demethylase FTO for Cancer Therapy. *RSC Chem. Biol.* 2 (5), 1352–1369. doi:10.1039/d1cb00075f

Zhu, D., Zhou, J., Zhao, J., Jiang, G., Zhang, X., Zhang, Y., et al. (2019). ZC3H13 Suppresses Colorectal Cancer Proliferation and Invasion via Inactivating Ras-ERK Signaling. *J. Cell. Physiol.* 234 (6), 8899–8907. doi:10.1002/jcp.27551

Zhu, L., Zhu, Y., Han, S., Chen, M., Song, P., Dai, D., et al. (2019). Impaired Autophagic Degradation of lncRNA ARHGAP5-AS1 Promotes Chemoresistance in Gastric Cancer. *Cell. Death Dis.* 10 (6), 383. doi:10.1038/s41419-019-1585-2

Zhu, Y. J., Zheng, B., Wang, H. Y., and Chen, L. (2017). New Knowledge of the Mechanisms of Sorafenib Resistance in Liver Cancer. *Acta Pharmacol. Sin.* 38 (5), 614–622. doi:10.1038/aps.2017.5

Zhu, Y. J., Zheng, B., Wang, H. Y., and Chen, L. (2017). New Knowledge of the Mechanisms of Sorafenib Resistance in Liver Cancer. *Acta Pharmacol. Sin.* 38 (5), 614–622. doi:10.1038/aps.2017.5

Zhu, Y., Zhou, B., Hu, X., Ying, S., Zhou, Q., Xu, W., et al. (2022). LncRNA LINC00942 Promotes Chemoresistance in Gastric Cancer by Suppressing MSI2 Degradation to Enhance c-Myc mRNA Stability. *Clin. Transl. Med* 12 (1), e703. doi:10.1002/ctm2.703

Zou, J., Zhong, X., Zhou, X., Xie, Q., Zhao, Z., Guo, X., et al. (2021). The M6A Methyltransferase METTL3 Regulates Proliferation in Esophageal Squamous Cell Carcinoma. *Biochem. Biophys. Res. Commun.* 580, 48–55. doi:10.1016/j.bbrc.2021.05.048

Conflict of Interest: The authors declare that the research was conducted in the absence of any commercial or financial relationships that could be construed as a potential conflict of interest.

Publisher's Note: All claims expressed in this article are solely those of the authors and do not necessarily represent those of their affiliated organizations, or those of the publisher, the editors and the reviewers. Any product that may be evaluated in this article, or claim that may be made by its manufacturer, is not guaranteed or endorsed by the publisher.

frontiers | Frontiers in Oncology

MINI REVIEW
published: 24 June 2022
doi: 10.3389/fonc.2022.931050

Leukemic Stem Cell: A Mini-Review on Clinical Perspectives

Igor Valentim Barreto[1†], Flávia Melo Cunha de Pinho Pessoa[1†], Caio Bezerra Machado[1], Laudreísa da Costa Pantoja[2,3], Rodrigo Monteiro Ribeiro[4], Germison Silva Lopes[5], Maria Elisabete Amaral de Moraes[1], Manoel Odorico de Moraes Filho[1], Lucas Eduardo Botelho de Souza[6], Rommel Mário Rodriguez Burbano[3], André Salim Khayat[3] and Caroline Aquino Moreira-Nunes[1,3,7]*

[1] Department of Medicine, Pharmacogenetics Laboratory, Drug Research and Development Center (NPDM), Federal University of Ceará, Fortaleza, Brazil, [2] Department of Pediatrics, Octávio Lobo Children's Hospital, Belém, Brazil, [3] Department of Biological Sciences, Oncology Research Center, Federal University of Pará, Belém, Brazil, [4] Department of Hematology, Fortaleza General Hospital (HGF), Fortaleza, Brazil, [5] Department of Hematology, César Cals General Hospital, Fortaleza, Brazil, [6] Center for Cell-based Therapy, Regional Blood Center of Ribeirão Preto, University of São Paulo, São Paulo, Brazil, [7] Ceará State University, Northeast Biotechnology Network (RENORBIO), Fortaleza, Brazil

OPEN ACCESS

Edited by:
Leonardo Freire-de-Lima, Federal University of Rio de Janeiro, Brazil

Reviewed by:
Avik Choudhuri, Harvard University, United States

***Correspondence:**
Caroline Aquino Moreira-Nunes
carolfam@gmail.com

†These authors have contributed equally to this work and share first authorship

Specialty section:
This article was submitted to Pharmacology of Anti-Cancer Drugs, a section of the journal Frontiers in Oncology

Received: *28 April 2022*
Accepted: *25 May 2022*
Published: *24 June 2022*

Citation:
Barreto IV, Pessoa FMCP, Machado CB, Pantoja LC, Ribeiro RM, Lopes GS, Amaral de Moraes ME, de Moraes Filho MO, de Souza LEB, Burbano RMR, Khayat AS and Moreira-Nunes CA (2022) Leukemic Stem Cell: A Mini-Review on Clinical Perspectives. Front. Oncol. 12:931050. doi: 10.3389/fonc.2022.931050

Hematopoietic stem cells (HSCs) are known for their ability to proliferate and self-renew, thus being responsible for sustaining the hematopoietic system and residing in the bone marrow (BM). Leukemic stem cells (LSCs) are recognized by their stemness features such as drug resistance, self-renewal, and undifferentiated state. LSCs are also present in BM, being found in only 0.1%, approximately. This makes their identification and even their differentiation difficult since, despite the mutations, they are cells that still have many similarities with HSCs. Although the common characteristics, LSCs are heterogeneous cells and have different phenotypic characteristics, genetic mutations, and metabolic alterations. This whole set of alterations enables the cell to initiate the process of carcinogenesis, in addition to conferring drug resistance and providing relapses. The study of LSCs has been evolving and its application can help patients, where through its count as a biomarker, it can indicate a prognostic factor and reveal treatment results. The selection of a target to LSC therapy is fundamental. Ideally, the target chosen should be highly expressed by LSCs, highly selective, absence of expression on other cells, in particular HSC, and preferentially expressed by high numbers of patients. In view of the large number of similarities between LSCs and HSCs, it is not surprising that current treatment approaches are limited. In this mini review we seek to describe the immunophenotypic characteristics and mechanisms of resistance presented by LSCs, also approaching possible alternatives for the treatment of patients.

Keywords: hematopoietic stem cells, leukemia stem cell, molecular biomarkers, clinical relapse, drug resistance

INTRODUCTION

Hematopoietic stem cells (HSCs) are located in the bone marrow (BM) and are responsible for sustaining and regenerating the hematological system. It is estimated that in a human organism, $1x10^6$ blood cells are produced every second. This feature comes from the ability of self-renewal together with a high proliferative rate and pluripotency of these cells. It is also worth mentioning the

ability to resist apoptosis, necrosis and genotoxicity produced by reactive oxygen species (ROS) that HSCs have (1–9).

Most of the time, the HSCs are quiescent, at G0 phase of the cell cycle, depending on glucose to carry out their metabolic activities. However, these cells, when receiving the stimuli through severe situations, can quickly enter the cell cycle through activation of genetic factors. It begins with a positive control carried out in part by mTORC1 under the action of CDK6, which in the G0 phase is in low expression or accompanied by inhibitors such as p57 or p18 (8, 10–13).

HSCs enters the cell cycle, and therefore, their metabolic activities start to have mitochondrial oxidative phosphorylation as a source of energy due to the increase in energy demand. This metabolic alteration consequently triggers a series of proteins, such as histone and DNA modifying enzymes, which are fundamental for the epigenetic changes carried out by the modulation of key transcription factor activity. After their activation, HSCs generate multipotent progenitors that are then committed to a cell lineage and gradually differentiate until they become mature and specialized cells (8, 10–12, 14–16).

Due to aging, HSCs lose their regenerative ability and may undergo a process called age-related clonal hematopoiesis (ARCH). In this process, mutations acquired over time continue to be transmitted to their successors, giving rise to cells with mutations. Patients with ARCH are more likely to develop leukemias, however not all cells in this process will be related to the leukemic process. It is known that the presence of certain mutations is related to the severity factor of this cell, as mutations in *TP53* and *U2AF1* genes are associated with pre-leukemic stem cells, and mutations in DNMT3A and TET2 genes have a lower risk regarding transformation of malignancy (12, 17–19).

In this study, we investigated clinical trials in extended literature that focused their efforts on the identification of LSCs in different types of leukemia and we discussed their clinical outcome and the perspectives of new therapies.

PRE-LEUKEMIC STEM CELL AND LEUKEMIC STEM CELL

The constant accumulation of mutations occurring in HSCs due to ARCH or other agents can stimulate the transformation of HSC into a pre-leukemic tumor cell (pre-LSCs). Although mutations are present in these cells, it is still possible for them to continue to give rise to healthy cells. However, pre-LSCs continue to accumulate mutations for years as well as significant clonal expansion until, after a long period, this cell acquires malignant characteristics, becoming a leukemic stem cell (LSC) (20–23). Despite the similarities between these two types of cells, it is still possible to make differentiations, mainly genetic differentiations, where it is observed that pre-LSCs do not have mutations associated with leukemia (12, 24, 25).

Mutations that occur in pre-LSCs are related to epigenetic genes that are responsible for histone modification, DNA methylation and chromatin looping. In pre-LSCs mutations can be found in *AML1, ASXL1, CTCF, DNMT3A, E2H2, FOXO1, IDH1, IDH2, IKZF1, JAK2, NPM1, MED12, SMC1A, STAT5B, TET2* and *WT1*. These mutations alone are incapable of inducing leukemia and appear as precursor events to late mutations that transform pre-LSCs into LSCs, which is shown in **Figure 1**. Therefore, the genetic alterations present in LSCs are related to proliferation and active signaling (26–33).

LSCs are recognized by their stemness features such as drug resistance, self-renewal, and undifferentiated state. They were initially pointed out by Lapidot and colleagues in 1994 (34). This rare population of resistant cells is believed to be at the origin of leukemia relapses. Their quiescent state and their self-renewal capacity makes it possible to leukemia repopulating cells, despite their low frequency (35–39).

LSCs are present at low levels in BM, being found in only 0.1%, approximately. This makes their identification and even their differentiation difficult since, despite the mutations, they are cells that still have many similarities with HSCs (20). Although the common characteristics, LSCs are heterogeneous cells and have different phenotypic characteristics, genetic mutations, and metabolic alterations. This whole set of alterations enables the cell to initiate the process of carcinogenesis, in addition to conferring drug resistance and inducing relapses (36, 37, 40).

During tumor progression, cancer cells continuously acquire genetic changes, and the fittest, most proliferative cells are selected for giving rise to distinct tumor subclones, which is known as clonal hematopoiesis (CH) (41–44). The clonal hematopoiesis of indeterminate potential (CHIP) refers to the presence of at least one driver mutation in hematopoietic cells of peripheral blood, without hematological malignancy. It is associated with increased risk of cancers, particularly in myeloid neoplasms, and chronic inflammatory diseases. The phenomenon of CHIP becomes very common in the population of people aged ≥80 years. That is explained by the accumulation of somatic mutations in HSCs, which occurs in an age-dependent manner (45, 46).

Clones evolve through the interaction of selectively advantageous 'driver' lesions, selectively neutral 'passenger' lesions and deleterious lesions. Driver lesions or mutations are the mutations that increase fitness and confer a clonal growth advantage. The neutral mutations, also known as passenger mutations, are accumulated in these cells but do not confer any fitness advantage. Neutral evolution of these passenger mutations can also shape clonal evolution, notably by a phenomenon called genetic drift, in which the allele frequencies of a mutation change over time. In addition, when both driver and passenger mutations occur in the same cell, the passenger mutations increase their allele frequency with the driver mutations, which is a phenomenon called hitchhiking that also participate in clonal evolution (47, 48).

The recognition of the important role of clonal hematopoiesis and clonal evolution in tumor initiation, disease progression and relapse have profound implications for the diagnosis and treatment of these malignancies. Additionally, the advent of new technologies may facilitate the definition of the molecular determinants and underlying mechanisms of clonal evolution in leukemia, which could provide targeted, individualized therapies for leukemia patients (49, 50).

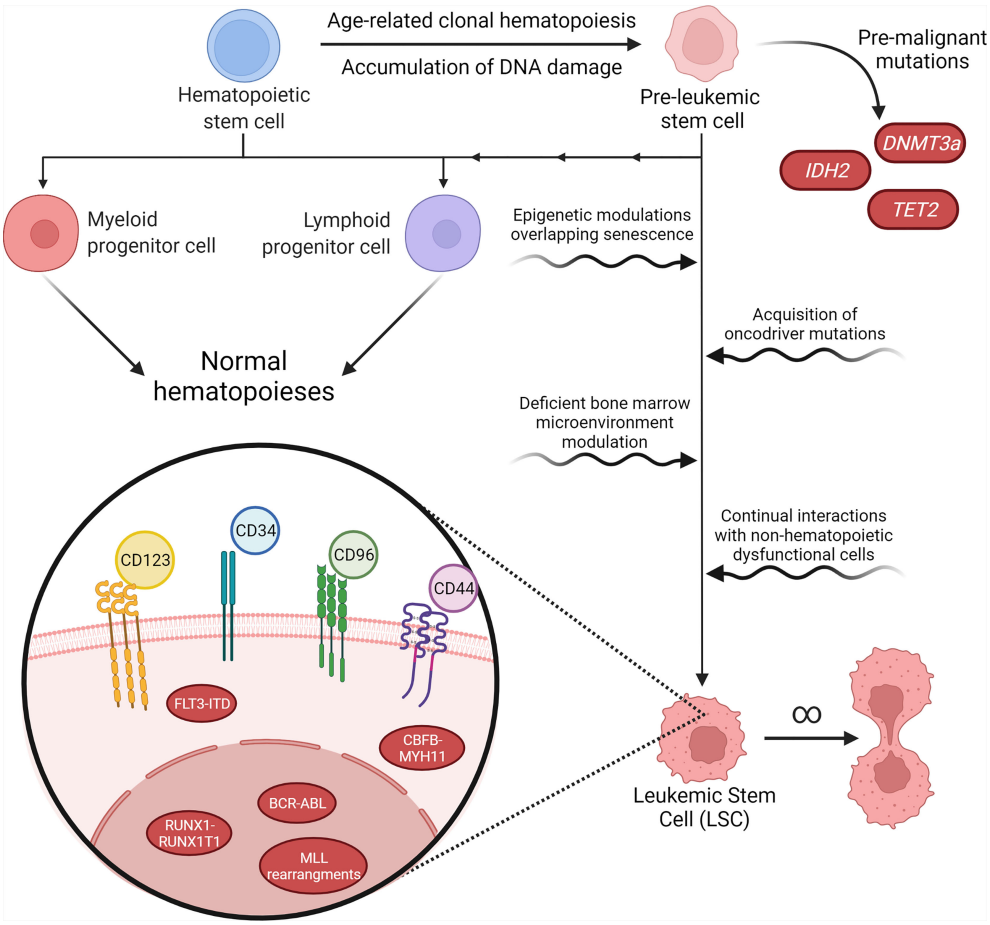

FIGURE 1 | Pathways of malignancy in hematopoiesis and its characteristics. Aging and exposure to hazardous environmental agents lead to accumulation of DNA damage and mutations in hematological precursor cells, inducing a pre-leukemic stem cell (pre-LSC) phenotype. Pre-LSCs acquire proliferation advantages over normal hematopoietic stem cells (HSCs) due to mutations in genes such as DNA methyltransferase 3 alpha (*DNMT3a*), but still retain their capacity to promote normal hematopoiesis. However, further malignant characteristics acquired over the years may tip these cells into a proper leukemic stage. The transformation of pre-LSCs may happen through cell-specific processes, such as epigenetic modulation or new acquired mutations, or through interactions between these cells and their microenvironment, through changes in the normal growth and survival signaling pathways or due to interactions with dysfunctional stromal or mesenchymal cells that are also present in the bone marrow. After malignancy onset, leukemic stem cells (LSC) may present a variety of karyotype rearrangements, such *as BCR-ABL* or *FLT3-ITD*, that determine their malignant characteristics and tend to present immunophenotyping profiles that still resemble normal HSCs, such as $CD34^{+}38^{-}$, while also overexpressing a cohort of cell-surface antigens that are highly variable between patients and even among different cell populations in the same patient.

CHARACTERIZATION OF LEUKEMIC STEM CELLS

A major challenge in studying LSCs is identifying a possible unique cell surface antigen phenotype, from which it would be possible to develop a targeted and much more specific treatment than the treatments currently used. Furthermore, due to the heterogeneity of the different types of leukemias, there is a lot of variation in the antigens found on the surface of these cells, becoming even more difficult to identify a specific marker that is not expressed in normal cells, or has a different expression pattern, density, or distribution (51–54).

Some common stem cell's markers are CD34, CD117 and HLA-DR, which expressions predict lower rate of complete remission (CR). In addition, the principal surface antigens of the myeloid lineage are CD13, CD33, CD14, CD15 and CD11b. Mostly, the expression of these markers have not yet showed any prognostic significance or are associated with a poorer outcome, such as reduction of CR, period of remission and survival. Although, cells that expresses CD15 usually presents a higher CR rate. Another marker found in myeloblasts is CD56, which expression is also reported as a poorer prognostic factor (55)

As an example, we can point out that normal HSC constitutively expresses $CD34^{+}$ and $CD38^{-}$ antigens, in addition to others such as Thy-1^{+}, c-kit^{+} and IL-3Rα. Much of the LSC population immunophenotypically resemble certain normal hematopoietic progenitor populations by also expressing $CD34^{+}$ and $CD38^{-}$ besides others surface markers (56–58)

Despite these difficulties, a great number of cell surface markers have been identified that are upregulated on

$CD34^+CD38^-$ LSCs compared with normal $CD34^+CD38^-$ HSPCs, for example, it has been revealed that CD90 and CD117 are deficient in acute myeloid leukemia (AML) LSCs, while CD123, TIM3, CD47, CD96, CLL-1, and IL-1 receptor accessory protein (IL1RAP), G protein-coupled receptor 56 (GPR56), CD93, CD44 and CD99 are highly expressed in AML LSCs. Targeting these surface markers might be a promising strategy for eradicating AML LSCs (35, 56, 59–62).

Some studies addressing chronic myeloid leukemia (CML) LSCs demonstrated that differentially expressed antigens include CD25, CD26, IL-1RAP, which is associated with the activation of NF-kβ and AKT signaling pathways, increasing proliferation of CML LSCs. In addition, the overexpression of the antigen CD25 is reported to reduce proliferation capacity of CML LSCs. Some data suggest CD25 and IL-1RAP expression are unique to LSCs of this type of leukemia (54, 63, 64).

The presence of LSCs is related to the rates of complete remission (CR) and general survival (OS) of patients, besides that, depending on the remaining amount, they may predispose to relapse of patients with leukemias (65). The identification of certain surface markers and molecular changes in these cells may influence the prognosis of patients, but the results of studies are still somewhat controversial. Bradstock et al. (66) pointed out that patients who expressed CD9, CD14 and CD2 in their CSLs had lower CR rates. The CD9, CD10 and CD11b markers were associated with lower OS rates, and CD11b was also related with a shorter duration of CR.

A study by Béné et al. (67) demonstrated that the expression of CD10, CD14 and CD15 was associated with lower survival rates. Nomdedeu et al. (68) found that patients who expressed CD34, CD45, CD117 and CD123 had worse prognoses with lower OS. Other studies, in turn, pointed out the markers CD2, CD7, CD11b, CD22, CD133, CD135, CD262 and CD120a as markers that confer worse prognosis to patients (69, 70).

The relationship between the molecular alterations observed in patients and their prognosis is also somewhat controversial among studies. Nomdedeu et al. (68) demonstrated that the *FLT3-ITD* mutation had a significant influence on OS, where patients affected by this alteration had lower rates compared to those who did not have the mutation (17.9 vs 41 months). On the other, Béné et al. (67) did not find a difference in survival between patients with and without molecular changes. However, other articles report the relationship of *FLT3-ITD, MLL-PTD, RUNX1-RUNX1T1* and *CBFB-MYH11* mutations with a poor outcome (71, 72).

In addition, studies demonstrated a correlation between white blood cells (WBC) count and poorer prognosis. Patients with a higher WBC count were less likely to achieve CR and presented a shorter survival rate (67, 73). Besides, a higher platelet count was associated with a longer survival time (67). These general findings corroborate with data found in other articles (74–77).

PRESENCE OF LSCS AND RELAPSE

Even with the course of the disease, it is possible to observe that pre-LSCs and LSCs continue to evolve throughout the process, in addition to the fact that treatment often fails to reach these cells. LSCs play a key role from development to disease relapse. Thus, its analysis and quantification can be of great importance as a prognostic factor for patients. Such processes can also assist in choosing a more targeted treatment. The identification of these cells can be performed through immunophenotyping, where it is possible to differentiate HSCs from LSCs. From this differentiation, counting methods are performed (78–80).

Recent studies point to two classifications of relapse related LSCs: the first classification is known as LSCs of committed relapse origin, where these cells are most like the diagnostic cell type and were able to evolve similarly to the diagnostic dominant clone. The second classification is the LSCs of primitive relapse origin, which are rare cells at the diagnosis of the disease and do not usually form blasts. However, these cells may show greater resistance to treatment and later clonal evolutions, causing the patient to relapse, which usually continues with the increase in the amount of LSCs and with greater heterogeneity (81, 82).

Studies reveals that LSCs levels correspond to the clinical and laboratory characteristics of the patient. Due to their insufficient morphological and biochemical characterization, LSCs cannot be reliably measured in patient samples. However, as a consequence of the finite capacity of the joined stem cell niche, HSCs can act as a biomarker for LSCs numbers and help identify patients with an adverse clinical outcome (74, 83, 84).

This is noticeable through the LSCs and the HSCs count, considering that the BM may have a limited number of cells. Therefore, LSCs and HSCs compete for niches, their values being inversely proportional, that is, the more LSCs the less HSCs. Therefore, patients who had a low LSCs load also had lower blast, platelet, and leukocyte counts. In addition to clinical features, the cells count can represent how it might respond molecularly. This is important when evaluating the chosen treatment. Therefore, lower levels of LSCs are associated with a better molecular response to treatment (85, 86).

Still on the quantification of LSCs, its functionality also applies to the assessment of measurable residual disease (MRD) and is considered an effective biomarker for predicting relapses. So, in addition to being used in the diagnosis to choose the treatment, the immunophenotyping test can be used in the post-treatment phase to evaluate its effectiveness and predict the patient's survival. High values of LSCs would be associated with worse survival and low efficacy. This analysis is then performed using molecular methodologies such as quantitative real-time polymerase chain reaction (RT-qPCR) or next-generation sequencing (NGS), and flow cytometry. It is important to remember that all these methodologies for prognostic analysis and MRD are still being carried out in studies and better clarification and standardization are needed for clinical application (83, 84, 87, 88).

INSIGHTS INTO CLINICAL INVESTIGATIONS

Table 1 is comprised of clinical trials from the past 10 years that aimed to identify biomarkers specific to LSCs that could serve as targets for targeted therapies or could be used as prognostic factors (89–98). Most of the reported studies aim at AML

TABLE 1 | Studies of the past 10 years indicating biomarkers for stem cells and "stemness" properties in leukemia and the respective prognostic relevance after treatment.

Leukemia Subtype	Alterations Correlated with LSC Phenotype	Treatment Protocols	Clinical outcomes	Reference
AML	Pre-leukemic phenotype of $CD34^+CD13^+CD33^+$ and increased expression of CD123 and CD117	Intensive and non-intensive induction regimens	Association of pre-leukemic phenotype with persistent clonal hematopoiesis and increased mutation burden	(89)
AML; MDS	Expression of CXCR4/CXCL12	Azacitidine plus DSTAT	ORR of 27% among evaluable patients and major hematologic improvements	(90)
AML	Upregulation of CD70/CD27 interaction	Protocols of cusatuzumab plus azacitidine administration	Strong reduction of LSC viability and proliferation *in vitro*; 100% ORR in 12 analyzed patients with 44% of evaluable patients achieving MRD negativity	(91)
AML	Lower expression of miR-204 increasing the expression of CD34 cell marker	Standard protocols of induction chemotherapy	Low expression of miR-204 is associated with poorer OS and DFS	(92)
AML	High CD123 expression	Standard protocols of induction chemotherapy	Overexpression of CD123 is associated with poor OS and induction therapy failure	(93)
AML	Expression of CD25, CD96 and CD123	Standard protocols of induction chemotherapy	Expression of multiple surface markers is associated with worse OS, PFS and response to chemotherapy	(94)
AML	Presence of $CD34^+CD123^+$ and $CD33^+CD123^+$ cells	CZBG combined with standard chemotherapy regimens	Reduction of $CD34^+CD123^+$ cells in the bone marrow after treatment	(95)
AML	Expression of CD44, CD123 and CD184	Variable protocols of cytotoxic chemotherapy	Increased LSC population is correlated with inability to achieve CR	(96)
CML	*BCR-ABL* translocation in $CD34^+lin^-$ cells	Nilotinib 300mg twice a day	No *BCR-ABL* rearrangement was observed in analyzed $CD34^+lin^-$ cells in the bone marrow at 12 months of treatment	(97)
CML	*BCR-ABL* translocation in $CD34^+CD38^-$ cells	Dasatinib 100mg a day or imatinib 400mg a day	Rapid decrease in LSC and LPC populations after therapy initiation	(98)

LSC, Leukemic Stem Cell; AML, Acute Myeloid Leukemia; NR, Not Reported; MDS, Myelodysplastic Syndrome; DSTAT, Dociparstat Sodium; ORR, Overall Response Rate; MRD, Minimal Residual Disease; OS, Overall Survival; DFS, Disease-free Survival; PFS, Progression-free Survival; CZBG, Compound Zhebei Granule; CR, Complete Response; CML, Chronic Myeloid Leukemia.

treatment since LSC presence and complexity is an established risk factor for disease severity (51, 56).

Studies utilizing standard chemotherapy protocols and induction therapies confirm that identified LSC markers, mainly transmembrane antigens such as CD34 and CD123, correlate with a worse patient prognosis. Increased mutation burden, lower response rates, inability to achieve CR, worst response to chemotherapy and higher incidence of relapse are some of the reported factors associated with increased presence of LSCs (89, 92–94, 96).

Although resistant to most treatment strategies, the use of novel agents targeting specifically LSCs molecular pathways combined with standard treatment protocols showed some promising results for AML patients (90, 91, 95). Huselton et al. (90) combined dociparstat sodium (DSTAT), a drug capable of inhibiting CXCR4/CXCL12 cell adhesion molecules, with hypomethylating agent (HMA) azacitidine in an attempt to disrupt bone marrow niches where LSCs remain in a quiescent state and was able to achieve CR in patients who were previously unresponsive to treatments with HMA alone.

Riether et al. (91) identified WNT pathway as being hyperactivated in AML LSCs due to increased expression and interaction of CD70/CD27 molecules. *In vitro*, the use of monoclonal antibodies targeting CD70 in combination with HMAs was demonstrated to have an additive effect in inhibiting LSC growth since the use of HMAs seem to increase LSCs dependency on CD70/CD27 pathway and concurrent CD70 inhibition was able to further reduce LSCs burden when compared to monotherapies of either agent. In previously untreated AML patients, protocols combining cusatuzumab plus azacitidine induced responses in all treated patients and transcriptome analysis after treatment revealed increased expression of genes involved in pathways of inflammation, differentiation and apoptosis (91).

Lastly, Wang et al. (95) utilized compound zhebei granule (CZBG), a herbal concoction with oncologic uses in traditional Chinese medicine, that acts through mechanism such as apoptosis induction and inhibition of resistance-related drug efflux proteins, combined with standard chemotherapy to treat AML patients and a significant decrease in $CD34^+CD123^+$ cells was observed in bone marrow niches. CZBG was also demonstrated to increase response rates in AML patients in combination with chemotherapy when compared to chemotherapy alone and to be able to reduce LSCs markers in tumor cell xenografts when combined with doxorubicin treatment (95, 99, 100).

In CML patients, *in vitro* studies indicate *BCR-ABL* tyrosine kinase inhibitors (TKIs) to have no efficacy over LSCs and leukemic progenitor cells (LPCs) and, while imatinib initial response rates are overwhelmingly positive, disease recurrence is usually the standard for patients after therapy discontinuation due to remaining Philadelphia-positive (Ph^+) $CD34^+$ cells (101, 102). The use of next-generation TKIs, however, seem to be more effective in reducing stem and progenitor cells in CML than imatinib and may point towards a choice for more intensive treatment options in accordance with increased LSCs and LPCs burden (103).

Pungolino et al. (97) utilized nilotinib, a second-generation BCR-ABL inhibitor, to treat newly diagnosed CML patients and observed a rapid decrease in $CD34^+lin^-Ph^+$ cells in the bone marrow, with total clearance of the analyzed samples at 12

months of treatment. Mustjoki et al. (98) compared imatinib and dasatinib efficiency at decreasing stem and progenitor cell burden and, while both treatments had similar results at LSC inhibition, dasatinib showed increased activity over LPCs levels at 3 months analysis.

TREATMENT PERSPECTIVES

Most conventional treatments for leukemias seek to eradicate blasts, reaching cells that are in their active cycle. However, LSCs are usually in a quiescent state or protected through their molecular resistance mechanisms causing this cell to resist therapy, leading to patient relapse (104–111). One of the major known factors that confer drug resistance is the overexpression of drug efflux pumps, such as the ATP-binding cassette (ABC) transporter family proteins by CSCs. Moreover, drug efflux increase is often combined with the upregulation of enzymes involved in the metabolism of anticancer agents. Therefore, enzymes and efflux transporters expressed by LSCs appear to be crucial not only for their proliferation, but also for their resistance to clinical treatments (108, 112–115).

The selection of a target to LSCs therapy is fundamental. Ideally, the target chosen should be highly expressed by LSCs, highly selective, absence of expression on other cells, in particular HSCs, and preferentially expressed by a high number of patients. In view of the large number of similarities between LSCs and HSCs, it is not surprising that current treatment approaches are limited (20, 81, 116).

Currently, different treatment methodologies have been tested and addressed, such as the use of binding antibodies associated with different toxins to form a specific delivery vehicle for LSCs. Examples of such therapies are the use of Gemtuzumab Ozogamicin for the treatment of AML, a compound that uses an antigen against CD33, associated with a cytotoxic agent; and the inhibition of the SIRP1-α interaction with CD47 that activates innate immunity increasing the death of LSCs. In addition, CD244, CD123, LLC1 or TIM3 targets are also studied and demonstrate antileukemic efficacy in AML patients. However, one of the main difficulties in the treatment of LSCs is due to the low proliferation rate, which makes it difficult to identify the cell to start the therapy (62, 81, 117–119).

Several new strategies are under development to eliminating LSCs, which may result in a better patient response. Many of the studies are associated with the use of TKIs, which to improve their effectiveness can be combined with other agents. TNF-α inhibitors combined with TKIs, for example, have shown positive results in the elimination of LSCs. Blocking of IL-1 signaling may also be a combination with TKIs, as well as blocking of signal pathways such as Wnt/β-catenin, Hedgehog, MAPK/MNK1/2, mTOR, PTEN, PP2A, Alox5 and JAK/STAT. The action of HIF-1 inhibitors associated with TKIs has been shown to reduce the survival and growth of cells in CML in murine models. The *HIF-1* deletion has also been tested in *in vivo* and *in vitro* models and has been shown to inhibit CML proliferation, both without serious effects on HSCs (120–122).

Activations and gene dissections can also be used, as in the case of p53 activation and *EZH2* deletion. Both technologies demonstrate promising results that enhance the eradication of LSCs when combined with TKIs (123, 124). The combination of TKIs with cytarabine was also performed, demonstrating good results in AML patients. Despite the large number of tests involving TKIs, medications and methodologies have also been developing as the case of Bortezomibe. Its function is based on decreasing the expression of CDK6, an important agent in the proliferation of LSCs (120, 125, 126).

Undoubtedly, one of the greatest difficulties in eliminating LSCs is their resistance mechanisms. As a result, studies have specialized in finding drugs and technologies that help to overcome the resistance present in LSCs. In this scenario, research diverges in different areas such as transport proteins and signaling pathways, taking as an example Notch, Hedgehog, and Wnt/β-catenin that are describes also as responsible for drug resistance (104, 127–129). It is also worth mentioning studies focused on the epithelial-mesenchymal transition (EMT), histone acetylation, hypoxia and the BM niche (104, 130, 131).

The tumor microenvironment (TME) creates a niche for itself that influences not only the proliferation and differentiation of LSCs but also the response to drugs. A key factor that modulates the microenvironment and drug resistance is hypoxia, which signaling contributes to chemoresistance of CSCs by increasing the expression of ABC transporters and Aldehyde dehydrogenases, a family of intracellular enzymes, which can be used as molecular markers to identify normal stem cells (NSCs) and CSCs (104, 128, 132–134). An example was demonstrated by Giuntoli et al. (134), when CML cells were grown in low oxygen concentrations and became resistant to Imatinib.

The EMT process is already known in solid tumors and has recently been explored in hematological neoplasms as well as its treatment possibilities (104, 127, 134, 135). Thus, one of the ways is to look for drugs that can act on genes such as *TRPS1, ETS2* and *LSP*, known to belong to this process in AML (136, 137). Competition for the BM niche between LSCs and HSCs has also become a therapeutic target, transforming the environment in a more favorable way for HSCs or increasing their hematopoietic reserve. E-selectin inhibition is an example, being able to promote the displacement of HSCs and LSCs. Regarding hypoxia, the use of hypoxia-activated prodrugs such as TH-302 has already been shown to reduce the population of LSCs in an AML model (138, 139).

In addition to those already mentioned, the combination of Venetoclax with Azacitidine demonstrates potential for the treatment of LSCs in AML, as it suppresses *OXPHOS*. Regarding gene deletion, it was observed that *FOXO1* deletion through genetic or pharmacological pathways is able to inhibit the proliferation of malignant cells, which is present in LSCs and pre-LSCs, becoming a potential target. Studies aimed at the use of microRNAs mimics were also carried out and have potential, such as miR-15a/16-1 acting as a tumor suppressor acting negatively on the *WT1* gene (28, 81, 140, 141).

CONCLUSION

Foremost is important to better define the molecular and cellular biologic features of normal HSCs and LSCs, for improve the

identification of possible therapeutic targets to eradicate the LSCs, that are responsible for treatment resistance and clinical relapse for most patients. It is necessary to carry out studies that correlate the quantification and immunophenotypic characterization of LSCs with clinical data and prognosis presented by patients, regarding the significance of this information pointed in the studies here presented, and due to the lack of this type of study in the literature.

AUTHOR CONTRIBUTIONS

IB, FP and CM wrote the manuscript. All authors contributed to the manuscript and were involved in revisions and proof-reading. All authors contributed to the article and approved the submitted version.

FUNDING

This study was supported by Brazilian funding agencies: Coordination for the Improvement of Higher Education Personnel (CAPES; to CM), National Council of Technological and Scientific Development (CNPq grant number 404213/2021-9 to CM-N; and Productivity in Research PQ Scholarships to MM-F, MM, RB and AK), Cearense Foundation of Scientific and Technological Support (FUNCAP grant number P20-0171-00078.01.00/20 to FP, MM and CM-N) and we also thank PROPESP/UFPA for publication payment.

REFERENCES

1. Wei Q, Frenette PS. Niches for Hematopoietic Stem Cells and Their Progeny. *Immunity* (2018) 48(4):632–648. doi: 10.1016/j.immuni.2018.03.024
2. Yamamoto R, Wilkinson AC, Nakauchi H. Changing Concepts in Hematopoietic Stem Cells. *Sci (1979)* (2018) 362(6417):895–896. doi: 10.1126/science.aat7873
3. Bigas A, Espinosa L. Hematopoietic Stem Cells: To be or Notch to be. *Blood* (2012) 119(14):3226–35. doi: 10.1182/blood-2011-10-355826
4. Ema H, Morita Y, Suda T. Heterogeneity and Hierarchy of Hematopoietic Stem Cells. *Exp Hematol* (2014) 42(2):74–82.e2. doi: 10.1016/j.exphem.2013.11.004
5. Mosaad YM. Hematopoietic Stem Cells: An Overview. *Transfusion Apheresis Sci* (2014) 51(3):68–82. doi: 10.1016/j.transci.2014.10.016
6. Anthony BA, Link DC. Regulation of Hematopoietic Stem Cells by Bone Marrow Stromal Cells. *Trends Immunol* (2014) 35(1):32–7. doi: 10.1016/j.it.2013.10.002
7. Szade K, Gulati GS, Chan CKF, Kao KS, Miyanishi M, Marjon KD, et al. Where Hematopoietic Stem Cells Live: The Bone Marrow Niche. *Antioxidants Redox Signaling* (2018) 29(2):191–204. doi: 10.1089/ars.2017.7419
8. Yamashita M, Dellorusso P v., Olson OC, Passegué E. Dysregulated Haematopoietic Stem Cell Behaviour in Myeloid Leukaemogenesis. *Nat Rev Cancer* (2020) 20(7):365–382. doi: 10.1038/s41568-020-0260-3
9. Nagasawa T. Bone and Stem Cells. Bone Marrow Microenvironment Niches for Hematopoietic Stem and Progenitor Cells. *Clin Calcium* (2014) 24:517–526.
10. Boisset JC, Robin C. On the Origin of Hematopoietic Stem Cells: Progress and Controversy. *Stem Cell Res* (2012) 8(1):1–13. doi: 10.1016/j.scr.2011.07.002
11. Sawai CM, Babovic S, Upadhaya S, Knapp DJHF, Lavin Y, Lau CM, et al. Hematopoietic Stem Cells are the Major Source of Multilineage Hematopoiesis in Adult Animals. *Immunity* (2016) 45(3):597–609. doi: 10.1016/j.immuni.2016.08.007
12. Abelson S, Collord G, Ng SWK, Weissbrod O, Cohen NM, Niemeyer E, et al. Prediction of Acute Myeloid Leukaemia Risk in Healthy Individuals. *Nature* (2018) 559(7714):400–404. doi:–10.1038/s41586-018-0317-6
13. Nakamura-Ishizu A, Takizawa H, Suda T. The Analysis, Roles and Regulation of Quiescence in Hematopoietic Stem Cells. *Dev (Cambridge)* (2014) 141(24):4656–66. doi: 10.1242/dev.106575
14. Bernitz JM, Kim HS, MacArthur B, Sieburg H, Moore K. Hematopoietic Stem Cells Count and Remember Self-Renewal Divisions. *Cell* (2016) 167(5):1296–1309.e10. doi: 10.1016/j.cell.2016.10.022
15. Slukvin II. Hematopoietic Specification From Human Pluripotent Stem Cells: Current Advances and Challenges Toward *De Novo* Generation of Hematopoietic Stem Cells. *Blood* (2013) 122(25):4035–46. doi: 10.1182/blood-2013-07-474825
16. Demirci S, Leonard A, Tisdale JF. Hematopoietic Stem Cells From Pluripotent Stem Cells: Clinical Potential, Challenges, and Future Perspectives. *Stem Cells Trans Med* (2020) 9(12):1549–1557. doi: 10.1002/sctm.20-0247
17. Bowman RL, Busque L, Levine RL. Clonal Hematopoiesis and Evolution to Hematopoietic Malignancies. *Cell Stem Cell* (2018) 22(2):157–170. doi: 10.1016/j.stem.2018.01.011
18. Verovskaya E v., Dellorusso P v., Passegué E. Losing Sense of Self and Surroundings: Hematopoietic Stem Cell Aging and Leukemic Transformation. *Trends Mol Med* (2019) 25(6):494–515. doi: 10.1016/j.molmed.2019.04.006
19. de Haan G, Lazare SS. Aging of Hematopoietic Stem Cells. *Blood* (2018) 131(5):479–487. doi: 10.1182/blood-2017-06-746412
20. Velten L, Story BA, Hernández-Malmierca P, Raffel S, Leonce DR, Milbank J, et al. Identification of Leukemic and Pre-Leukemic Stem Cells by Clonal Tracking From Single-Cell Transcriptomics. *Nat Commun* (2021) 12(1):1366. doi: 10.1038/s41467-021-21650-1
21. Corces MR, Chang HY, Majeti R. Preleukemic Hematopoietic Stem Cells in Human Acute Myeloid Leukemia. *Front Oncol* (2017) 7:263. doi: 10.3389/fonc.2017.00263
22. Pandolfi A, Barreyro L, Steidl U. Concise Review: Preleukemic Stem Cells: Molecular Biology and Clinical Implications of the Precursors to Leukemia Stem Cells. *Stem Cells Trans Med* (2013) 2(2):143–50. doi: 10.5966/sctm.2012-0109
23. Jordan CT, Guzman ML. Mechanisms Controlling Pathogenesis and Survival of Leukemic Stem Cells. *Oncogene* (2004) 23(43):7178–87. doi: 10.1038/sj.onc.1207935
24. Jan M, Snyder TM, Corces-Zimmerman MR, Vyas P, Weissman IL, Quake SR, et al. Clonal Evolution of Preleukemic Hematopoietic Stem Cells Precedes Human Acute Myeloid Leukemia. *Sci Trans Med* (2012) 4(149):149ra118. doi: 10.1126/scitranslmed.3004315
25. Corces-Zimmerman MR, Majeti R. Pre-Leukemic Evolution of Hematopoietic Stem Cells: The Importance of Early Mutations in Leukemogenesis. *Leukemia* (2014) 28(12):2276–82. doi: 10.1038/leu.2014.211
26. Saeed BR, Manta L, Raffel S, Pyl PT, Buss EC, Wang W, et al. Analysis of Nonleukemic Cellular Subcompartments Reconstructs Clonal Evolution of Acute Myeloid Leukemia and Identifies Therapy-Resistant Preleukemic Clones. *Int J Cancer* (2021) 148(11):2825–2838. doi: 10.1002/ijc.33461
27. Corces-Zimmerman MR, Hong WJ, Weissman IL, Medeiros BC, Majeti R. Preleukemic Mutations in Human Acute Myeloid Leukemia Affect Epigenetic Regulators and Persist in Remission. *Proc Natl Acad Sci U.S.A.* (2014) 111(7):2548–53. doi: 10.1073/pnas.1324297111
28. Lin S, Ptasinska A, Chen X, Shrestha M, Assi SA, Chin PS, et al. A FOXO1-Induced Oncogenic Network Defines the AML1-ETO Preleukemic Program. *Blood* (2017) 130(10):1213–1222. doi: 10.1182/blood-2016-11-750976
29. de Bie J, Demeyer S, Alberti-Servera L, Geerdens E, Segers H, Broux M, et al. Single-Cell Sequencing Reveals the Origin and the Order of Mutation

Acquisition in T-Cell Acute Lymphoblastic Leukemia. *Leukemia* (2018) 32 (6):1358–1369. doi: 10.1038/s41375-018-0127-8
30. Shlush LI, Zandi S, Mitchell A, Chen WC, Brandwein JM, Gupta V, et al. Identification of Pre-Leukaemic Haematopoietic Stem Cells in Acute Leukaemia. *Nature* (2014) 506:328–33. doi: 10.1038/nature13038
31. Höllein A, Meggendorfer M, Dicker F, Jeromin S, Nadarajah N, Kern W, et al. NPM1 Mutated AML can Relapse With Wild-Type NPM1: Persistent Clonal Hematopoiesis can Drive Relapse. *Blood Adv* (2018) 2(22):3118–3125. doi: 10.1182/bloodadvances.2018023432
32. Potter N, Miraki-Moud F, Ermini L, Titley I, Vijayaraghavan G, Papaemmanuil E, et al. Single Cell Analysis of Clonal Architecture in Acute Myeloid Leukaemia. *Leukemia* (2019) 33:1113–1123. doi: 10.1038/s41375-018-0319-2
33. Wang X, Hoffman R. What are the Molecular Mechanisms Driving the Switch From Mpns to Leukemia? *Best Pract Res: Clin Haematol* (2021) 34 (1):101254. doi: 10.1016/j.beha.2021.101254
34. Lapidot T, Sirard C, Vormoor J, Murdoch B, Hoang T, Caceres-Cortes J, et al. A Cell Initiating Human Acute Myeloid Leukaemia After Transplantation Into SCID Mice. *Nature* (1994) 367:645–648. doi: 10.1038/367645a0
35. Wang X, Huang S, Chen JL. Understanding of Leukemic Stem Cells and Their Clinical Implications. *Mol Cancer* (2017) 16(1):2. doi: 10.1186/s12943-016-0574-7
36. Touzet L, Dumezy F, Roumier C, Berthon C, Bories C, Quesnel B, et al. CD9 in Acute Myeloid Leukemia: Prognostic Role and Usefulness to Target Leukemic Stem Cells. *Cancer Med* (2019) 8(3):1279–1288. doi: 10.1002/cam4.2007
37. Park SM, Cho H, Thornton AM, Barlowe TS, Chou T, Chhangawala S, et al. IKZF2 Drives Leukemia Stem Cell Self-Renewal and Inhibits Myeloid Differentiation. *Cell Stem Cell* (2019) 24(1):153–165.e7. doi: 10.1016/j.stem.2018.10.016
38. Neering SJ, Bushnell T, Sozer S, Ashton J, Rossi RM, Wang PY, et al. Leukemia Stem Cells in a Genetically Defined Murine Model of Blast-Crisis CML. *Blood* (2007) 110(7):2578–85. doi: 10.1182/blood-2007-02-073031
39. Lane SW, Gilliland DG. Leukemia Stem Cells. *Semin Cancer Biol* (2010) 20 (2):71–6. doi: 10.1016/j.semcancer.2009.12.001
40. Carroll D, St Clair DK. Hematopoietic Stem Cells: Normal Versus Malignant. *Antioxidants Redox Signaling* (2018) 29(16):1612–1632. doi: 10.1089/ars.2017.7326
41. Döhner K, Döhner H. Molecular Characterization of Acute Myeloid Leukemia. *Haematologica* (2008) 93(7):976–82. doi: 10.3324/haematol.13345
42. Desai RH, Zandvakili N, Bohlander SK. Dissecting the Genetic and non-Genetic Heterogeneity of Acute Myeloid Leukemia Using Next-Generation Sequencing and *In Vivo* Models. *Cancers (Basel)* (2022) 14:2182. doi: 10.3390/cancers14092182
43. Ye B, Sheng Y, Zhang M, Hu Y, Huang H. Early Detection and Intervention of Clonal Hematopoiesis for Preventing Hematological Malignancies. *Cancer Lett* (2022) 538:215691. doi: 10.1016/j.canlet.2022.215691
44. Alagpulinsa DA, Toribio MP, Alhallak I, Shmookler Reis RJ. Advances in Understanding the Molecular Basis of Clonal Hematopoiesis. *Trends Mol Med* (2022) 28(5):360–377. doi: 10.1016/j.molmed.2022.03.002
45. Rossi M, Meggendorfer M, Zampini M, Tettamanti M, Riva E, Travaglino E, et al. Clinical Relevance of Clonal Hematopoiesis in Persons Aged ≥80 Years. *Blood* (2021) 138(21):2093–2105. doi: 10.1182/blood.2021011320
46. Asada S, Kitamura T. Clonal Hematopoiesis and Associated Diseases: A Review of Recent Findings. *Cancer Sci* (2021) 112(10):3962–3971. doi: 10.1111/cas.15094
47. Lyne AM, Laplane L, Perié L. To Portray Clonal Evolution in Blood Cancer, Count Your Stem Cells. *Blood* (2021) 137(14):1862–1870. doi: 10.1182/blood.2020008407
48. Greaves M, Maley CC. Clonal Evolution in Cancer. *Nature* (2012) 481:306–13. doi: 10.1038/nature10762
49. Cooper JN, Young NS. Clonality in Context: Hematopoietic Clones in Their Marrow Environment. *Blood* (2017) 130(22):2363–2372. doi: 10.1182/blood-2017-07-794362
50. Ferrando AA, López-Otín C. Clonal Evolution in Leukemia. *Nat Med* (2017) 23(10):1135–1145. doi: 10.1038/nm.4410
51. Chopra M, Bohlander SK. The Cell of Origin and the Leukemia Stem Cell in Acute Myeloid Leukemia. *Genes Chromosomes Cancer* (2019) 58(12):850–858. doi: 10.1002/gcc.22805
52. Mastelaro de Rezende M, Ferreira AT, Paredes-Gamero EJ. Leukemia Stem Cell Immunophenotyping Tool for Diagnostic, Prognosis, and Therapeutics. *J Cell Physiol* (2020) 235(6):4989–4998. doi: 10.1002/jcp.29394
53. Lutz C, Hoang VT, Buss E, Ho AD. Identifying Leukemia Stem Cells - is it Feasible and Does it Matter? *Cancer Lett* (2013) 338(1):10–4. doi: 10.1016/j.canlet.2012.07.014
54. Houshmand M, Simonetti G, Circosta P, Gaidano V, Cignetti A, Martinelli G, et al. Chronic Myeloid Leukemia Stem Cells. *Leukemia* (2019) 33:1543–56. doi: 10.1038/s41375-019-0490-0
55. Mason KD, Juneja SK, Szer J. The Immunophenotype of Acute Myeloid Leukemia: Is There a Relationship With Prognosis? *Blood Rev* (2006) 20 (2):71–82. doi: 10.1016/j.blre.2005.08.002
56. Thomas D, Majeti R. Biology and Relevance of Human Acute Myeloid Leukemia Stem Cells. *Blood* (2017) 129(12):1577–1585. doi: 10.1182/blood-2016-10-696054
57. Wang JCY, Dick JE. Cancer Stem Cells: Lessons From Leukemia. *Trends Cell Biol* (2005) 15:494–501. doi: 10.1016/j.tcb.2005.07.004
58. Roboz GJ, Guzman M. Acute Myeloid Leukemia Stem Cells: Seek and Destroy. *Expert Rev Hematol* (2009) 2(6):663–672. doi: 10.1586/ehm.09.53
59. Horton SJ, Huntly BJP. Recent Advances in Acute Myeloid Leukemia Stem Cell Biology. *Haematologica* (2012) 97(7):966–74. doi: 10.3324/haematol.2011.054734
60. Majeti R. Monoclonal Antibody Therapy Directed Against Human Acute Myeloid Leukemia Stem Cells. *Oncogene* (2011) 30(9):1009–19. doi: 10.1038/onc.2010.511
61. Guzman ML, Allan JN. Concise Review: Leukemia Stem Cells in Personalized Medicine. *Stem Cells* (2014) 32(4):829–843. doi: 10.1002/stem.1597
62. Haubner S, Perna F, Köhnke T, Schmidt C, Berman S, Augsberger C, et al. Coexpression Profile of Leukemic Stem Cell Markers for Combinatorial Targeted Therapy in AML. *Leukemia* (2019) 33:64–74. doi: 10.1038/s41375-018-0180-3
63. Sadovnik I, Hoelbl-Kovacic A, Herrmann H, Eisenwort G, Cerny-Reiterer S, Warsch W, et al. Identification of CD25 as STAT5-Dependent Growth Regulator of Leukemic Stem Cells in Ph+ CML. *Clin Cancer Res* (2016) 22 (8):2051–61. doi: 10.1158/1078-0432.CCR-15-0767
64. Ågerstam H, Hansen N, von Palffy S, Sanden C, Reckzeh K, Karlsson C, et al. IL1RAP Antibodies Block IL-1-Induced Expansion of Candidate CML Stem Cells and Mediate Cell Killing in Xenograft Models. *Blood* (2016) 128 (23):2683–2693. doi: 10.1182/blood-2015-11-679985
65. Shlush LI, Mitchell A, Heisler L, Abelson S, Ng SWK, Trotman-Grant A, et al. Tracing the Origins of Relapse in Acute Myeloid Leukaemia to Stem Cells. *Nature* (2017) 547:104–108. doi: 10.1038/nature22993
66. Bradstock K, Matthews J, Benson E, Page F, Bishop J. Prognostic Value of Immunophenotyping in Acute Myeloid Leukemia. *Blood* (1994) 25(4):367–74. doi: 10.1182/blood.v84.4.1220.1220
67. Béné MC, Bernier M, Casasnovas RO, Castoldi G, Doekharan D, van der Holt B, et al. Acute Myeloid Leukaemia M0: Haematological, Immunophenotypic and Cytogenetic Characteristics and Their Prognostic Significance: An Analysis in 241 Patients. *Br J Haematol* (2001) 113(3):737–45. doi: 10.1046/j.1365-2141.2001.02801.x
68. Nomdedeu J, Bussaglia E, Villamor N, Martinez C, Esteve J, Tormo M, et al. Immunophenotype of Acute Myeloid Leukemia With NPM Mutations: Prognostic Impact of the Leukemic Compartment Size. *Leukemia Res* (2011) 35(2):163–8. doi: 10.1016/j.leukres.2010.05.015
69. Costa AFO, Menezes DL, Pinheiro LHS, Sandes AF, Nunes MAP, Lyra Junior DP, et al. Role of New Immunophenotypic Markers on Prognostic and Overall Survival of Acute Myeloid Leukemia: A Systematic Review and Meta-Analysis. *Sci Rep* (2017) 7(1):4138. doi: 10.1038/s41598-017-00816-2
70. van Solinge TS, Zeijlemaker W, Ossenkoppele GJ, Cloos J, Schuurhuis GJ. The Interference of Genetic Associations in Establishing the Prognostic Value of the Immunophenotype in Acute Myeloid Leukemia. *Cytomet Part B - Clin Cytomet* (2018) 94(1):151–158. doi: 10.1002/cyto.b.21539
71. Patel JP, Gönen M, Figueroa ME, Fernandez H, Sun Z, Racevskis J, et al. Prognostic Relevance of Integrated Genetic Profiling in Acute Myeloid

Leukemia. *New Engl J Med* (2012) 366:1079–89. doi: 10.1056/nejmoa1112304
72. Kihara R, Nagata Y, Kiyoi H, Kato T, Yamamoto E, Suzuki K, et al. Comprehensive Analysis of Genetic Alterations and Their Prognostic Impacts in Adult Acute Myeloid Leukemia Patients. *Leukemia* (2014) 28:1586–1595. doi: 10.1038/leu.2014.55
73. Geller RB, Zahurak M, Hurwitz CA, Burke PJ, Karp JE, Piantadosi S, et al. Prognostic Importance of Immunophenotyping in Adults With Acute Myelocytic Leukaemia: The Significance of the Stem-Cell Glycoprotein CD34 (My 10). *Br J Haematol* (1990) 76:340–347. doi: 10.1111/j.1365-2141.1990.tb06365.x
74. Pfirrmann M, Baccarani M, Saussele S, Guilhot J, Cervantes F, Ossenkoppele G, et al. Prognosis of Long-Term Survival Considering Disease-Specific Death in Patients With Chronic Myeloid Leukemia. *Leukemia* (2016) 30:48–56. doi: 10.1038/leu.2015.261
75. Wattad M, Weber D, Döhner K, Krauter J, Gaidzik VI, Paschka P, et al. Impact of Salvage Regimens on Response and Overall Survival in Acute Myeloid Leukemia With Induction Failure. *Leukemia* (2017) 31:1306–1313. doi: 10.1038/leu.2017.23
76. Padilha SL, Souza EJ dos S, Matos MCC, Domino NR. Acute Myeloid Leukemia: Survival Analysis of Patients at a University Hospital of Paraná. *Rev Bras Hematologia e Hemoterapia* (2013) 37(1):21–7. doi: 10.1016/j.bjhh.2014.11.008
77. Hoyos M, Nomdedeu JF, Esteve J, Duarte R, Ribera JM, Llorente A, et al. Core Binding Factor Acute Myeloid Leukemia: The Impact of Age, Leukocyte Count, Molecular Findings and Minimal Residual Disease. *Eur J Haematol* (2013) 91(3):209–18. doi: 10.1111/ejh.12130
78. Zeijlemaker W, Kelder A, Cloos J, Schuurhuis GJ. Immunophenotypic Detection of Measurable Residual (Stem Cell) Disease Using LAIP Approach in Acute Myeloid Leukemia. *Curr Protoc Cytomet* (2019) 91(1):e66. doi: 10.1002/cpcy.66
79. Heo SK, Noh EK, Ju LJ, Sung JY, Jeong YK, Cheon J, et al. CD45dimCD34+CD38-CD133+ Cells Have the Potential as Leukemic Stem Cells in Acute Myeloid Leukemia. *BMC Cancer* (2020) 20(1):285. doi: 10.1186/s12885-020-06760-1
80. Felipe Rico J, Hassane DC, Guzman ML. Acute Myelogenous Leukemia Stem Cells: From Bench to Bedside. *Cancer Lett* (2013) 338(1):4–9. doi: 10.1016/j.canlet.2012.05.034
81. Pollyea DA, Jordan CT. Therapeutic Targeting of Acute Myeloid Leukemia Stem Cells. *Blood* (2017) 129(12):1627–1635. doi: 10.1182/blood-2016-10-696039
82. Stauber J, Greally JM, Steidl U. Preleukemic and Leukemic Evolution at the Stem Cell Level. *Blood* (2021) 137(8):1013–1018. doi: 10.1182/blood.2019004397
83. Wouters R, Cucchi D, Kaspers GJL, Schuurhuis GJ, Cloos J. Relevance of Leukemic Stem Cells in Acute Myeloid Leukemia: Heterogeneity and Influence on Disease Monitoring, Prognosis and Treatment Design. *Expert Rev Hematol* (2014) 7(6):791–805. doi: 10.1586/17474086.2014.959921
84. Reinisch A, Chan SM, Thomas D, Majeti R. Biology and Clinical Relevance of Acute Myeloid Leukemia Stem Cells. *Semin Hematol* (2015) 52(3):150–64. doi: 10.1053/j.seminhematol.2015.03.008
85. Wang W, Stiehl T, Raffel S, Hoang VT, Hoffmann I, Poisa-Beiro L, et al. Reduced Hematopoietic Stem Cell Frequency Predicts Outcome in Acute Myeloid Leukemia. *Haematologica* (2017) 102(9):1567–1577. doi: 10.3324/haematol.2016.163584
86. Thielen N, Richter J, Baldauf M, Barbany G, Fioretos T, Giles F, et al. Leukemic Stem Cell Quantification in Newly Diagnosed Patients With Chronic Myeloid Leukemia Predicts Response to Nilotinib Therapy. *Clin Cancer Res* (2016) 22(16):4030–8. doi: 10.1158/1078-0432.CCR-15-2791
87. Bruserud Ø, Aasebø E, Hernandez-Valladares M, Tsykunova G, Reikvam H. Therapeutic Targeting of Leukemic Stem Cells in Acute Myeloid Leukemia–the Biological Background for Possible Strategies. *Expert Opin Drug Discovery* (2017) 12(10):1053–1065. doi: 10.1080/17460441.2017.1356818
88. Cloos J, Harris JR, Janssen JJWM, Kelder A, Huang F, Sijm G, et al. Comprehensive Protocol to Sample and Process Bone Marrow for Measuring Measurable Residual Disease and Leukemic Stem Cells in Acute Myeloid Leukemia. *J Visualized Experiments* (2018) 2018 (133):56386. doi: 10.3791/56386
89. Loghavi S, DiNardo CD, Furudate K, Takahashi K, Tanaka T, Short NJ, et al. Flow Cytometric Immunophenotypic Alterations of Persistent Clonal Haematopoiesis in Remission Bone Marrows of Patients With NPM1-Mutated Acute Myeloid Leukaemia. *Br J Haematol* (2021) 192(6):1054–1063. doi: 10.1111/bjh.17347
90. Huselton E, Rettig MP, Campbell K, Cashen AF, DiPersio JF, Gao F, et al. Combination of Dociparstat Sodium (DSTAT), a CXCL12/CXCR4 Inhibitor, With Azacitidine for the Treatment of Hypomethylating Agent Refractory AML and MDS. *Leukemia Res* (2021) 110:106713. doi: 10.1016/j.leukres.2021.106713
91. Riether C, Pabst T, Höpner S, Bacher U, Hinterbrandner M, Banz Y, et al. Targeting CD70 With Cusatuzumab Eliminates Acute Myeloid Leukemia Stem Cells in Patients Treated With Hypomethylating Agents. *Nat Med* (2020) 26(9):1459–1467. doi: 10.1038/s41591-020-0910-8
92. Abdelhafiz AS, Elsayed GM, Saber MM, Gameel A, Hamdy N. Low Expression of Mir-204 is Associated With Expression of CD34 and Poor Performance Status in Denovo AML. *Int J Lab Hematol* (2020) 42(3):263–269. doi: 10.1111/ijlh.13161
93. Arai N, Homma M, Abe M, Baba Y, Murai S, Watanuki M, et al. Impact of CD123 Expression, Analyzed by Immunohistochemistry, on Clinical Outcomes in Patients With Acute Myeloid Leukemia. *Int J Hematol* (2019) 109(5):539–544. doi: 10.1007/s12185-019-02616-y
94. Yabushita T, Satake H, Maruoka H, Morita M, Katoh D, Shimomura Y, et al. Expression of Multiple Leukemic Stem Cell Markers is Associated With Poor Prognosis in *De Novo* Acute Myeloid Leukemia. *Leukemia Lymphoma* (2018) 59(9):2144–2151. doi: 10.1080/10428194.2017.1410888
95. Wang J, Lai Z l, Chen X y, Li D y, Zhang Y y, Ma W, et al. Effect of Compound Zhebei Granule (复方浙贝颗粒) Combined With Chemotherapy on Surface Markers of Leukemia Stem Cell in Patients With Acute Myeloid Leukemia. *Chin J Integr Med* (2016) 22(6):438–44. doi: 10.1007/s11655-015-2117-2
96. Hwang K, Park CJ, Jang S, Chi HS, Kim DY, Lee JH, et al. Flow Cytometric Quantification and Immunophenotyping of Leukemic Stem Cells in Acute Myeloid Leukemia. *Ann Hematol* (2012) 91(10):1541–6. doi: 10.1007/s00277-012-1501-7
97. Pungolino E, D'adda M, de Canal G, Trojani A, Perego A, Elena C, et al. Nilotinib-Induced Bone Marrow CD34+/Lin-Ph+ Cells Early Clearance in Newly Diagnosed CP-Chronic Myeloid Leukemia: Final Report of the Philosophi34 Study. *Eur J Haematol* (2021) 107(4):436–448. doi: 10.1111/ejh.13680
98. Mustjoki S, Richter J, Barbany G, Ehrencrona H, Fioretos T, Gedde-Dahl T, et al. Impact of Malignant Stem Cell Burden on Therapy Outcome in Newly Diagnosed Chronic Myeloid Leukemia Patients. *Leukemia* (2013) 27(7):1520–6. doi: 10.1038/leu.2013.19
99. Zhang Y, Hou L, Chen X y. Effects of Compound Zhebei Granule () Combined With Doxorubicin on Expression of Specific Surface Antigens in Mice With Transplanted KG-1a Cells. *Chin J Integr Med* (2018) 24(3):213–217. doi: 10.1007/s11655-017-2963-1
100. Hou L, Yang S, Yang W, Zhou Y, Liu F, Yang H, et al. Compound Zhebei Granules Combined With Chemotherapy for the Treatment of Refractory Acute Leukemia: A Randomized Clinical Trial. *J Tradit Chin Med* (2016) 36(5):606–12. doi: 10.1016/s0254-6272(16)30079-6
101. Vetrie D, Helgason GV, Copland M. The Leukaemia Stem Cell: Similarities, Differences and Clinical Prospects in CML and AML. *Nat Rev Cancer* (2020) 20(3):158–173. doi: 10.1038/s41568-019-0230-9
102. Bocchia M, Ippoliti M, Gozzetti A, Abruzzese E, Calabrese S, Amabile M, et al. CD34+/Ph+ Cells are Still Detectable in Chronic Myeloid Leukemia Patients With Sustained and Prolonged Complete Cytogenetic Remission During Treatment With Imatinib Mesylate [2]. *Leukemia* (2008) 22(2):426–8. doi: 10.1038/sj.leu.2404893
103. Tusa I, Cheloni G, Poteti M, Silvano A, Tubita A, Lombardi Z, et al. *In Vitro* Comparison of the Effects of Imatinib and Ponatinib on Chronic Myeloid Leukemia Progenitor/Stem Cell Features. *Targeted Oncol* (2020) 15(5):659–671. doi: 10.1007/s11523-020-00741-x
104. Cho Y, Kim YK. Cancer Stem Cells as a Potential Target to Overcome Multidrug Resistance. *Front Oncol* (2020) 10:764. doi: 10.3389/fonc.2020.00764

105. Moitra K. Overcoming Multidrug Resistance in Cancer Stem Cells. *BioMed Res Int* (2015) 2015:635745. doi: 10.1155/2015/635745
106. Zhang Q, Feng Y, Kennedy D. Multidrug-Resistant Cancer Cells and Cancer Stem Cells Hijack Cellular Systems to Circumvent Systemic Therapies, can Natural Products Reverse This? *Cell Mol Life Sci* (2017) 74(5):777–801. doi: 10.1007/s00018-016-2362-3
107. Zhang Z, Zhao Y, Jiang L, Miao X, Zhou H, Jia L. Glycomic Alterations are Associated With Multidrug Resistance in Human Leukemia. *Int J Biochem Cell Biol* (2012) 44(8):1244–53. doi: 10.1016/j.biocel.2012.04.026
108. Dalpiaz A, Paganetto G, Botti G, Pavan B. Cancer Stem Cells and Nanomedicine: New Opportunities to Combat Multidrug Resistance? *Drug Discovery Today* (2020) 25(9):1651–1667. doi: 10.1016/j.drudis.2020.07.023
109. Daflon-Yunes N, Pinto-Silva FE, Vidal RS, Novis BF, Berguetti T, Lopes RRS, et al. Characterization of a Multidrug-Resistant Chronic Myeloid Leukemia Cell Line Presenting Multiple Resistance Mechanisms. *Mol Cell Biochem* (2013) 383(1-2):123–35. doi: 10.1007/s11010-013-1761-0
110. de Moraes ACR, Maranho CK, Rauber GS, Santos-Silva MC. Importance of Detecting Multidrug Resistance Proteins in Acute Leukemia Prognosis and Therapy. *J Clin Lab Anal* (2013) 27(1):62–71. doi: 10.1002/jcla.21563
111. Patel C, Stenke L, Varma S, Lindberg ML, Björkholm M, Sjöberg J, et al. Multidrug Resistance in Relapsed Acute Myeloid Leukemia: Evidence of Biological Heterogeneity. *Cancer* (2013) 119(16):3076–83. doi: 10.1002/cncr.28098
112. Moitra K, Lou H, Dean M. Multidrug Efflux Pumps and Cancer Stem Cells: Insights Into Multidrug Resistance and Therapeutic Development. *Clin Pharmacol Ther* (2011) 89(4):491–502. doi: 10.1038/clpt.2011.14
113. Drewa T, Styczynski J, Szczepanek J. Is the Cancer Stem Cell Population "A Player" in Multi-Drug Resistance? *Acta Poloniae Pharm - Drug Res* (2008) 65.
114. Marques DS, Sandrini JZ, Boyle RT, Marins LF, Trindade GS. Relationships Between Multidrug Resistance (MDR) and Stem Cell Markers in Human Chronic Myeloid Leukemia Cell Lines. *Leukemia Res* (2010) 34(6):757–62. doi: 10.1016/j.leukres.2009.11.004
115. Moreira-Nunes CF, Azevedo TC, Beltrão AC, Francês LT, Sousa RG, Silva IT, et al. Differentially Expressed Genes Responsible for Insensitivity of CD34+ Cells to Kinase Inhibitors in Patients With Chronic Myeloid Leukemia. *BMC Proc* (2013) 7(2):01. doi: 10.1186/1753-6561-7-s2-o1
116. Hanekamp D, Cloos J, Schuurhuis GJ. Leukemic Stem Cells: Identification and Clinical Application. *Int J Hematol* (2017) 105(5):549–557. doi: 10.1007/s12185-017-2221-5
117. Theocharides APA, Jin L, Cheng PY, Prasolava TK, Malko A v, Ho JM, et al. Disruption of Sirpα Signaling in Macrophages Eliminates Human Acute Myeloid Leukemia Stem Cells in Xenografts. *J Exp Med* (2012) 209 (10):1883–99. doi: 10.1084/jem.20120502
118. Walter RB, Appelbaum FR, Estey EH, Bernstein ID. Acute Myeloid Leukemia Stem Cells and CD33-Targeted Immunotherapy. *Blood* (2012) 119(26):6198–208. doi: 10.1182/blood-2011-11-325050
119. Jiang YP, Liu BY, Zheng Q, Panuganti S, Chen R, Zhu J, et al. CLT030, a Leukemic Stem Cell-Targeting CLL1 Antibody-Drug Conjugate for Treatment of Acute Myeloid Leukemia. *Blood Adv* (2018) 2(14):1738–1749. doi: 10.1182/bloodadvances.2018020107
120. Chen Y, Zou J, Cheng F, Li W. Treatment-Free Remission in Chronic Myeloid Leukemia and New Approaches by Targeting Leukemia Stem Cells. *Front Oncol* (2021) 11:769730. doi: 10.3389/fonc.2021.769730
121. Cheloni G, Tanturli M, Tusa I, DeSouza NH, Shan Y, Gozzini A, et al. Targeting Chronic Myeloid Leukemia Stem Cells With the Hypoxia-Inducible Factor Inhibitor Acriflavine. *Blood* (2017) 130(5):655–665. doi: 10.1182/blood-2016-10-745588
122. Zhang H, Li H, Xi HS, Li S. Hif1α is Required for Survival Maintenance of Chronic Myeloid Leukemia Stem Cells. *Blood* (2012) 119(11):2595–607. doi: 10.1182/blood-2011-10-387381
123. Carter BZ, Mak PY, Mak DH, Ruvolo VR, Schober W, McQueen T, et al. Synergistic Effects of P53 Activation *via* MDM2 Inhibition in Combination With Inhibition of Bcl-2 or Bcr-Abl in CD34+ Proliferating and Quiescent Chronic Myeloid Leukemia Blast Crisis Cells. *Oncotarget* (2015) 6 (31):30487–99. doi: 10.18632/oncotarget.5890
124. Xie H, Peng C, Huang J, Li BE, Kim W, Smith EC, et al. Chronic Myelogenous Leukemia-Initiating Cells Require Polycomb Group Protein EZH2. *Cancer Discovery* (2016) 6(11):1237–1247. doi: 10.1158/2159-8290.CD-15-1439
125. Zhou B, Qin Y, Zhou J, Ruan J, Xiong F, Dong J, et al. Bortezomib Suppresses Self-Renewal and Leukemogenesis of Leukemia Stem Cell by NF-κb-Dependent Inhibition of CDK6 in MLL-Rearranged Myeloid Leukemia. *J Cell Mol Med* (2021) 25(6):3124–3135. doi: 10.1111/jcmm.16377
126. Polak A, Bialopiotrowicz E, Krzymieniewska B, Wozniak J, Stojak M, Cybulska M, et al. SYK Inhibition Targets Acute Myeloid Leukemia Stem Cells by Blocking Their Oxidative Metabolism. *Cell Death Dis* (2020) 11 (11):956. doi: 10.1038/s41419-020-03156-8
127. Di C, Zhao Y. Multiple Drug Resistance Due to Resistance to Stem Cells and Stem Cell Treatment Progress in Cancer (Review). *Exp Ther Med* (2015) 9 (2):289–293. doi: 10.3892/etm.2014.2141
128. Misaghian N, Ligresti G, Steelman LS, Bertrand FE, Bäsecke J, Libra M, et al. Targeting the Leukemic Stem Cell: The Holy Grail of Leukemia Therapy. *Leukemia* (2009) 23(1):25–42. doi: 10.1038/leu.2008.246
129. Takebe N, Miele L, Harris PJ, Jeong W, Bando H, Kahn M, et al. Targeting Notch, Hedgehog, and Wnt Pathways in Cancer Stem Cells: Clinical Update. *Nat Rev Clin Oncol* (2015) 12(8):445–64. doi: 10.1038/nrclinonc.2015.61
130. Liesveld J. Targeting Myelogenous Leukemia Stem Cells: Role of the Circulation. *Front Oncol* (2012) 2:86. doi: 10.3389/fonc.2012.00086. 2 AUG.
131. Marchand T, Pinho S. Leukemic Stem Cells: From Leukemic Niche Biology to Treatment Opportunities. *Front Immunol* (2021) 12:775128. doi: 10.3389/fimmu.2021.775128
132. Garcia-Mayea Y, Mir C, Masson F, Paciucci R, LLeonart ME. Insights Into New Mechanisms and Models of Cancer Stem Cell Multidrug Resistance. *Semin Cancer Biol* (2020) 60:166–180. doi: 10.1016/j.semcancer.2019.07.022
133. Bukowski K, Kciuk M, Kontek R. Mechanisms of Multidrug Resistance in Cancer Chemotherapy. *Int J Mol Sci* (2020) 21(9):3233. doi: 10.3390/ijms21093233
134. Giuntoli S, Rovida E, Barbetti V, Cipolleschi MG, Olivotto M, dello Sbarba P. Hypoxia Suppresses BCR/Abl and Selects Imatinib-Insensitive Progenitors Within Clonal CML Populations [2]. *Leukemia* (2006) 20(7):1291–3. doi: 10.1038/sj.leu.2404224
135. Chen SC, Liao TT, Yang MH. Emerging Roles of Epithelial-Mesenchymal Transition in Hematological Malignancies. *J Biomed Sci* (2018) 25(1):37. doi: 10.1186/s12929-018-0440-6
136. Kahlert UD, Joseph J v., Kruyt FAE. EMT- and MET-Related Processes in Nonepithelial Tumors: Importance for Disease Progression, Prognosis, and Therapeutic Opportunities. *Mol Oncol* (2017) 11(7):860–877. doi: 10.1002/1878-0261.12085
137. Stavropoulou V, Kaspar S, Brault L, Sanders MA, Juge S, Morettini S, et al. MLL-AF9 Expression in Hematopoietic Stem Cells Drives a Highly Invasive AML Expressing EMT-Related Genes Linked to Poor Outcome. *Cancer Cell* (2016) 30(1):43–58. doi: 10.1016/j.ccell.2016.05.011
138. Benito J, Ramirez MS, Millward NZ, Velez J, Harutyunyan KG, Lu H, et al. Hypoxia-Activated Prodrug TH-302 Targets Hypoxic Bone Marrow Niches in Preclinical Leukemia Models. *Clin Cancer Res* (2016) 22(7):1687–98. doi: 10.1158/1078-0432.CCR-14-3378
139. Bernasconi P, Borsani O. Targeting Leukemia Stem Cell-Niche Dynamics: A New Challenge in AML Treatment. *J Oncol* (2019) 2019:8323592. doi: 10.1155/2019/8323592
140. Arrigoni E, del Re M, Galimberti S, Restante G, Rofi E, Crucitta S, et al. Concise Review: Chronic Myeloid Leukemia: Stem Cell Niche and Response to Pharmacologic Treatment. *Stem Cells Trans Med* (2018) 7(3):305–314. doi: 10.1002/sctm.17-0175
141. Gao SM, Xing CY, Chen CQ, Lin SS, Dong PH, Yu FJ. MiR-15a and MiR-16-1 Inhibit the Proliferation of Leukemic Cells by Down-Regulating WT1 Protein Level. *J Exp Clin Cancer Res* (2011) 30(1):110. doi: 10.1186/1756-9966-30-110

Conflict of Interest: The authors declare that the research was conducted in the absence of any commercial or financial relationships that could be construed as a potential conflict of interest.

the publisher, the editors and the reviewers. Any product that may be evaluated in this article, or claim that may be made by its manufacturer, is not guaranteed or endorsed by the publisher.

frontiers | Frontiers in Oncology

TYPE Original Research
PUBLISHED 04 August 2022
DOI 10.3389/fonc.2022.949868

OPEN ACCESS

EDITED BY
Takeo Tatsuta,
Tohoku Medical and Pharmaceutical University, Japan

REVIEWED BY
Yousef Nami,
Agricultural Biotechnology Research Institute of Iran, Iran
Lubna Wasim,
All India Institute of Medical Sciences, India

*CORRESPONDENCE
Zhe-Sheng Chen
chenz@stjohns.edu
Feng-Feng Ping
pingfengfeng2017@njmu.edu.cn

SPECIALTY SECTION
This article was submitted to Pharmacology of Anti-Cancer Drugs, a section of the journal Frontiers in Oncology

RECEIVED 21 May 2022
ACCEPTED 27 June 2022
PUBLISHED 04 August 2022

CITATION
Narayanan S, Teng Q-X, Wu Z-X, Nazim U, Karadkhelkar N, Acharekar N, Yoganathan S, Mansoor N, Ping F-F and Chen Z-S (2022) Anticancer effect of Indanone-based thiazolyl hydrazone derivative on p53 mutant colorectal cancer cell lines: An *in vitro* and *in vivo* study.
Front. Oncol. 12:949868.
doi: 10.3389/fonc.2022.949868

Anticancer effect of Indanone-based thiazolyl hydrazone derivative on p53 mutant colorectal cancer cell lines: An *in vitro* and *in vivo* study

Silpa Narayanan[1], Qiu-Xu Teng[1], Zhuo-Xun Wu[1], Urooj Nazim[2], Nishant Karadkhelkar[1], Nikita Acharekar[1], Sabesan Yoganathan[1], Najia Mansoor[2], Feng-Feng Ping[3]* and Zhe-Sheng Chen[1]*

[1]Department of Pharmaceutical Sciences, College of Pharmacy and Health Sciences, St. John's University, Queens, NY, United States, [2]Department of Pharmaceutical Chemistry, University of Karachi, Karachi, Pakistan, [3]Department of Reproductive Medicine, Wuxi People's Hospital Affiliated to Nanjing Medical University, Wu-xi, China

Colorectal cancer is a major health problem, and it is the third most diagnosed cancer in the United States. The current treatment for colorectal cancer includes irinotecan, a topoisomerase I inhibitor, and other targeted drugs, such as bevacizumab and regorafenib. The low response rates and incidence of high toxicity caused by these drugs instigated an evaluation of the anticancer efficacy of a series of 13 thiazolyl hydrazone derivatives of 1-indanone, and four compounds among them show favorable anticancer activity against some of the tested colorectal cancer cell lines with IC_{50} values ranging from 0.41 ± 0.19 to 6.85 ± 1.44 μM. It is noteworthy that one of the indanone-based thiazolyl hydrazone (ITH) derivatives, *N*-Indan-1-ylidene-*N'*-(4-Biphenyl-4-yl-thiazol-2-yl)-hydrazine (ITH-6), has a better cytotoxicity profile against p53 mutant colorectal cancer cells HT-29, COLO 205, and KM 12 than a p53 wild-type colorectal cancer cell line, such as HCT 116. Mechanistic studies show that ITH-6 arrests these three cancer cell lines in the G2/M phase and induces apoptosis. It also causes a rise in the reactive oxygen species level with a remarkable decrease in the glutathione (GSH) level. Moreover, ITH-6 inhibits the expression of NF-κB p65 and Bcl-2, which proves its cytotoxic action. In addition, ITH-6 significantly decreased tumor size, growth rate, and tumor volume in mice bearing HT-29 and KM 12 tumor xenografts. Moreover, CRISPR/Cas9 was applied to establish an NF-κB p65 gene knockout HT-29 cell line model to validate the target of ITH-6. Overall, the results suggest that ITH-6 could be a potential anticancer drug candidate for p53 mutant colorectal cancers.

KEYWORDS

ITH-6, indanone, NF-κB p65, anticancer, tumor xenograft model

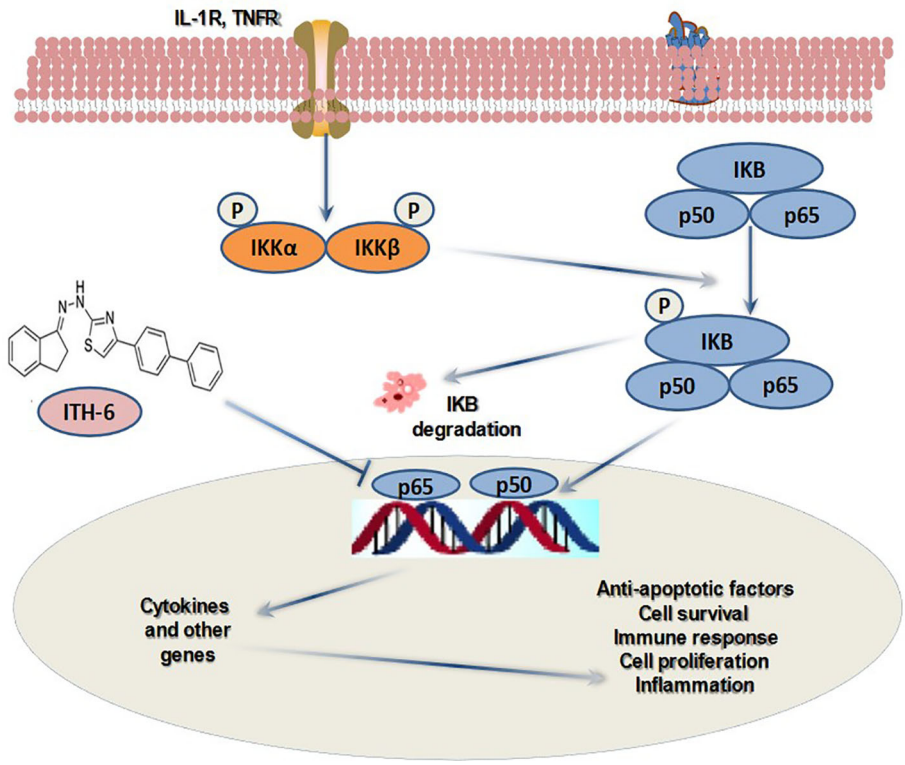

GRAPHICAL ABSTRACT

Introduction

Cancer is the leading disease of human populations regarding the advancement of treatment strategies (1–3). Despite progress in the cancer research field that discovered possible treatments for various cancer types, cancer remains the second leading cause of death after cardiovascular diseases (4–6). In the United States, among malignancies, colorectal cancer (CRC) is the third most common type of cancer, and it consists of a heterogeneous group of tumors, some with gene mutations. According to the data provided by American Cancer Society, there were around 104,610 new CRC cases diagnosed in 2020, and around 53,200 deaths were reported (7). Studies prove that a positive family history increases the risk of occurrence of CRC by approximately 15%–20% (8). The current strategies for the management of primary CRC is the use of a combination of 5-fluorouracil, leucovorin, and either oxaliplatin (FOLFOX protocol) or irinotecan (FOLFIRI protocol) (9–11). These agents exhibit adverse effects, such as vomiting, diarrhea, and other complications, causing a major drawback of the treatment (12, 13). It is reported that the indanone ring exhibits anticancer activity (14–17), and some indanone-related compounds have some crucial bioactivity. Various methods have also been adapted for the synthesis of indanone derivatives as it is a useful moiety. Among the signaling pathways associated with tumorigenesis and inflammation, nuclear factor-kappa B (NF-κB) is a key regulator (18), and the NF-κB family consists of five subunits, RelA (p65), RelB, NF-κB1 (p50 and its precursor p105), NF-κB2 (p52 and its precursor p100), and c-Rel (19). It is established that there is a positive relationship between activation of NF-κB in the intestinal epithelial cells and tumor formation (19), which plays an important role in the occurrence of CRC. NF-κB signaling is associated with a number of responses, including cellular immunity, inflammation, cell differentiation, proliferation, and apoptosis (20–24). This impact on cell proliferation by NF-κB depends on p53 (tumor suppressor gene) status. This is one of the many aspects of the crucial relationship between NF-κB and p53. As studied earlier, wild-type p53 expression opposes NF-κB function and inhibits tumorigenesis, and around half of human cancers exhibit p53 mutations (or have lost the wild-type allele) and, thus, activate the NF-κB pathway during the development of tumors. Moreover, the NF-κB pathway enhances the transcription of mouse double minute 2 (Mdm2), which is a ubiquitin E3 ligase enzyme of p53 and, thus, indirectly helps in regulating the stability of p53 (25). It is established that ITH-6, one of the most active indanone derivatives, arrested the cells at the G2/M phase of the cell cycle and thereby inhibited the proliferation of CRC cells and induced apoptosis by building reactive oxygen species and decreased the intracellular glutathione (GSH) level (26). In the current study, we explore the further mechanism of its anticancer activity by downregulating NF-κB p65 and Bcl-2 expression in *in vitro* and preclinical studies. The current work recognizes the relative part of

the NF-κB pathway in cancer and its activation and its effect on downstream target genes, which is crucial for the design and discovery of novel targeted anticancer agents.

Materials and methods

Chemicals and equipment

The thiazolyl hydrazone derivatives of 1-indanone were synthesized at the University of Karachi, Pakistan (27). Irinotecan hydrochloride was procured from Alfa Aesar (Haverhill, MA). Dulbecco's modified Eagle's medium (DMEM, IX), fetal bovine serum (FBS), phosphate buffered saline (PBS), and trypsin 0.25% were acquired from Hyclone (Waltham, MA). Monoclonal antibodies D97JR (selective against ALDH1A1), E7K2Y (against CD44), D14E12 (against NF-κB p65), E4Z1Q (against topoisomerase I), D3R6Y (against procaspase-3), 44D4 (against IkBα), 16H1 (against GAPDH), D5C9H (against TBP), and secondary anti-rabbit/mouse HRP linked antibody were bought from Cell Signaling (Danvers, MA). A-11005 (alexafluor 594 secondary antibody against NF-κB) and DAPI (catalog # D3571), which stains the nucleus, were purchased from Invitrogen (Waltham, MA). The NF-κB p65, Bcl-2, and 18 S TaqMan gene expression and superscript IV reverse transcription kits were purchased from Fisher Scientific (Waltham, MA).

Cell lines and cell culture

The human CRC parental cell lines SW620 and S1, ABCB1-overexpressing drug-resistant subline, SW620/AD300 and ABCG2-overexpressing drug-resistant cell line, S1-M1-80 were employed for the ABCB1 and ABCG2 reversal studies, respectively. SW620/AD300 cells were maintained in complete medium with 300 ng/ml of doxorubicin (28). S1-M1-80 cells were expanded in the DMEM medium with the anticancer drug mitoxantrone, starting with a low concentration, and the maximum concentration was 80 μg/ml to induce the ABCG2 transporter expression. These cell lines were obtained from Dr. Susan E. Bates (Columbia University, New York). The cell lines were cultured in DMEM medium containing 10% FBS and 1% penicillin/streptomycin at a temperature of 37°C, 5% CO_2.

Experimental animals

Male athymic NCR (nu/nu) nude mice (age 5–7 weeks and weight around 20–25 g) were acquired from Taconic Farms (Albany, NY) for the animal study and remained in polycarbonate cages (four mice/cage) at St. John's University Animal Care Center. They were maintained under light/dark cycles, supplied with food and water, and monitored for tumor growth by measuring the size using Vernier calipers. The protocol was accepted by the St. John's University's Institutional Animal Care & Use Committee (IACUC), protocol #1940. The study was accomplished following the ARRIVE guidelines and Animal Welfare Act and the Guide for the Care and Use of Laboratory Animals.

Cytotoxicity of ITH-6 on ABCB1 and ABCG2 overexpressing cell lines

The cytotoxicity assay was completed using parental (SW620 and S1) and drug-resistant (SW620/AD300 and S1-M1-80) cell lines that were seeded (6×10^3 cells/well) followed by ITH-6 incubation (with a range of 0–100 μM). After 68 h, the absorbance was detected at 570 nm by spectrophotometer as previously described (29, 30) and IC_{50} values were calculated.

Western blot analysis

The Western blot assay was conducted to observe aldehyde dehydrogenase 1 family member A1 (ALDH1A1) expression, a cell surface adhesion receptor protein (CD44), a subunit of nuclear factor kappa light chain enhancer of activated B cells (NF-κB p65) (nuclear and cytoplasmic), procaspase-3, topoisomerase I (TOP 1), and IkBα (nuclear and cytoplasmic) proteins after incubating HT-29, COLO 205, and KM 12 cells with three concentrations of ITH-6, 0.3, 1, and 3 μM for 72 hours by a method (31) and further quantified.

mRNA expression

HT-29, COLO 205, and KM 12 cancer cells were incubated with 0.3, 1, and 3 μM of ITH-6 for 72 hours, and total RNA was extracted using the RNA extraction trizol reagent as previously described (32). The target genes were NF-κB p65 and Bcl-2, and 18S was used as the loading control. The results are represented as relative fold of mRNA expression.

Immunofluorescence

For this experiment, the cells were cultured with ITH-6 (0.3, 1, and 3 μM) for 72 hours and immunofluorescence performed according to the protocol detailed before (33).

Molecular modeling

A Macintosh operating system (OS Sierra) with Mac Pro 6-core Intel Xenon E5 processor system was used to perform docking experiments using the Maestro v12. 3. 012 software (Schrödinger, LLC, New York, NY, USA, 2019) software. Ligprep was used for ITH-6 ligand preparation (34). The heterodimer

protein model was imported from the Protein data bank. "Protein Preparation Wizard" was used for protein preparation. Grid generation was done by selecting residues at 20 Å distance from bound inhibitors in the model protein (1IKN) (35). The residues selected were 26, 28, 29, 30, 49, 50, 181, 222, 224, 225, 236, 237, 238, 239, 241, 258, 259, 260, 261, 275. Extra precision docking was performed with a maximum 10 poses.

Knockout of NF-κB p65 gene in HT-29 cells

A CRISPR/Cas9 system was used to construct the NF-κB p65 gene knockout subline of HT-29 cells. The custom-designed mammalian CRISPR vector was obtained from Vector Builder Inc. (Chicago, IL). The transfection of the NF-κB p65 targeting vector into HT-29 cells was conducted using Fugene 6 transfection reagent (Promega, Madison, WI) according to the manufacturer's instructions. The knockout of the NF-κB p65 gene was further verified by measuring protein expression using Western blotting and by a cell viability study using MTT.

Nude mouse MDR xenograft model

The CRC cells, HT-29, and KM 12 xenograft mouse models were established as previously reported (36, 37). The HT-29 (6×10^{6}) and KM 12 cells (7×10^{6}) were implanted into the mice (right and left sides, respectively), and when the tumors attained a diameter of around 0.5 cm (day 0) after one week, the animals were divided into four groups of six each as follows: (a) polyethylene glycol 300 as the vehicle, given orally (q3d × 7); (b) irinotecan (30 mg/kg, q3d × 7), given intraperitoneally (i.p.), dissolved in normal saline (38); (c) ITH-6 (3 mg/kg) dissolved in PEG 300 and given orally (q3d × 7); and (d) ITH-6 (6 mg/kg) dissolved in PEG 300 and given orally (q3d × 7). The treatment period was 21 days. To determine the drug dosage, the body weights were noted every third day. Tumor volumes (using the two diameters of tumors, termed A and B) were recorded every third day using Vernier calipers using the following formula, $V = \pi/6(A + B/2)^3$ (39, 40). Blood was drawn *via* submandibular puncture on the last treatment day using isoflurane inhalational anesthesia, and white blood cell (WBC) and platelet counts were recorded in all groups.

At the end of the treatment period, the animals were euthanized, and the tumors were removed and weighed.

Collection of plasma and tumor tissues

Mice bearing HT-29 and KM 12 tumors were grouped into three categories: (i) mice receiving 3 mg/kg ITH-6 orally, (ii) 6 mg/kg ITH-6 orally, and (iii) 30 mg/kg i.p. irinotecan. Mice were anesthetized with isoflurane (3%), and 60 μL of blood was taken into heparinized tubes by submandibular puncture at various time points, 5, 30, 60, 120,180, and 240 minutes after the treatment. Moreover, the tumors were removed, weighed, and stored at -80°C for further experiments. The samples were analyzed using high-performance liquid chromatography (HPLC).

Method for Irinotecan: Flow rate: 0.5 ml/min.

Time (min)	Solvent A percentage	Solvent B percentage
0	60	40
10	98	2
12	98	2
15	60	40

Method for ITH-6: Flow rate: 0.5 ml/min.

Time (min)	Solvent A percentage	Solvent B percentage
0	60	40
20	98	2
22	98	2
25	60	40

The t_R (retention time) for irinotecan was 6.2 minutes and t_R for ITH-6 was 17.5 minutes. The standard curve was created based on dosage: Irinotecan (2 mg/ml, 1 mg/ml, 0.5 mg/ml, 0.25 mg/ml, 0.125 mg/ml, and 0.625 mg/ml) and ITH-6 (1 mg/ml, 0.5 mg/ml, 0.25 mg/ml, 0.125 mg/ml, 0.625 mg/ml, and 0.313 mg/ml).

Statistical analysis

The experiments were performed at least three times, and the variations were analyzed using one-way analysis of variance (ANOVA). The statistical significance was determined at $p < .05$. The *post hoc* analysis was carried out using Tukey's test. The data were analyzed using GraphPad Prism, version 6.

Results

ITH-6 is not susceptible to ABCB1- and ABCG2-mediated drug resistance

In order to know if ITH-6 is a substrate of ABC transporters, such as ABCB1 and/or ABCG2, an MTT assay was conducted to determine the susceptibility of ITH-6 to MDR mediated by ABCB1 and ABCG2 transporters. ABCB1 and ABCG2 transporters have established roles in conferring multidrug resistance by lowering intracellular drug accumulation resulting from extrusion of drugs from the tumor cells. Herein, resistance fold (RF) was used to assess if there was any degree of change in the resistance to ITH-6 due to the presence of ABCB1or ABCG2

(41). The results indicate that there was no remarkable difference in the IC_{50} values of ITH-6 in the ABCB1 overexpressing SW620/AD300 cell line (Figure 1A) and ABCG2 overexpressing S1-M1-80 cell line (Figure 1B) relative to their corresponding parental cell lines, hence proving that it is not a substrate of ABCB1 or ABCG2 transporter.

The effect of ITH-6 on the expression level of different targets associated with apoptosis of CRC cells

To figure out the mechanism of the test drug cytotoxicity, we performed Western blotting on various proteins. The proteins selected were ALDH1A1, CD44, NF-κB p65 (nuclear and cytoplasmic), procaspase-3, TOP 1, and IkBα (nuclear and cytoplasm) as they are important prognostic markers in CRC cell lines. At a concentration of 3 μM, ITH-6 downregulated the nuclear NF-κB p65 expression in HT-29 (Figure 2A) and COLO 205 (Figure 2B) cells compared with control, whereas in KM 12 cells, the test compound at concentrations of 0.3, 1, and 3 μM significantly decreased the nuclear NF-κB p65 expression level compared with the positive control; resveratrol (20 μM) and KM 12 cells are more sensitive to NF-κB p65 downregulation following treatment with ITH 6 (Figure 2C). There was no change in the cytoplasmic NF-κB p65 protein expression in all cell lines treated with ITH-6 (Figures 2G–I).

Moreover, there was no change in the expression levels of ALDH1A1 and CD44 (Figures 3A–C), TOP 1 (Figures 4B, G, L), and IkBα (cytoplasmic) levels (Figures 4A, F, K) on these cell lines. There was a concentration-dependent decrease in the procaspase-3 expression in KM 12 (Figures 4G, L) cells cultured with ITH-6 at 3 μM for 72 hours, whereas in COLO 205 and HT-29, there was no change in the expression of procaspase-3 after incubating with ITH-6 (Figures 4B, G). Hence, we can summarize that the possible mechanism behind ITH-6 induced cytotoxicity in these CRC cells results from downregulating nuclear NF-κB p65 protein expression.

The effect of ITH-6 on the mRNA level of NF-κB p65 and Bcl-2 in CRC cell lines

The incubation of these three CRC cell lines with 0.3, 1, and 3 μM of ITH-6 for 72 hours remarkably decreased the NF-κB p65 protein expression compared with the vehicle. Furthermore, quantitative real-time PCR (RT-PCR) experiments prove that the treatment of these cell lines with the ITH-6 for 72 hours remarkably decreased NF-κB p65 mRNA expression (Figures 5A–C).

It was previously indicated that NF-κB p65 transcriptionally regulates Bcl-2, an anti-apoptotic protein (42). Hence, RT-PCR was performed to evaluate the effect of ITH-6 on the Bcl-2 (Figures 5D–F) mRNA level and showed that treatment with ITH-6 downregulated Bcl-2 expression, thereby further proving the role of ITH-6 on the apoptosis of these CRC cell lines.

Immunofluorescence

An immunofluorescence experiment was conducted to find out if ITH-6 can downregulate the expression of nuclear NF-κB p65 in HT-29 (Figure 6A), COLO 205 (Figure 6B), and KM 12 (Figure 6C). Our results confirm that treating these CRC cell lines with ITH-6 decreased NF-κB p65 expression, which is consistent with the Western blot and RT-PCR results.

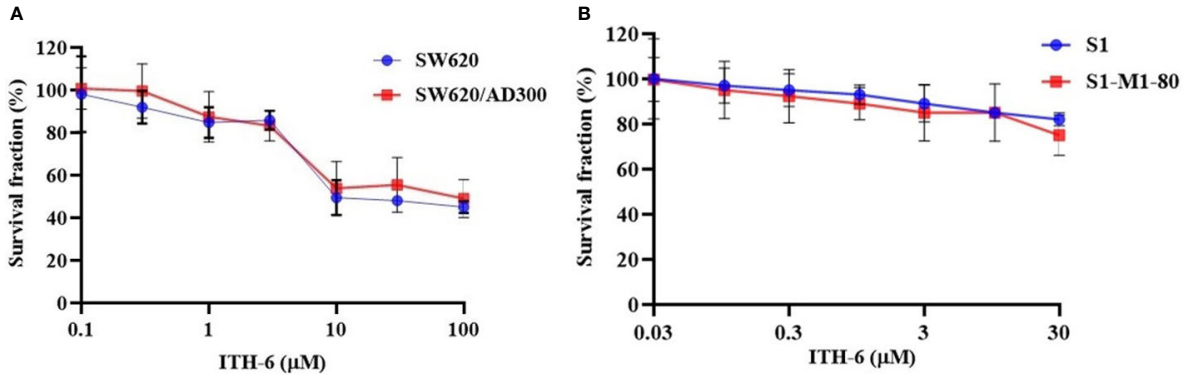

FIGURE 1
Cytotoxicity of ITH-6 on ABCB1- and ABCG2-overexpressing cell lines. Survival fraction (%) was measured after treatment with ITH-6 (μM) for 72 hours on **(A)** SW620, SW620/AD300 and **(B)** S1, S1-M1-80 cell lines. Points with error bars represent the mean ± SD for independent determinations in triplicate. The figures are representative of three independent experiments.

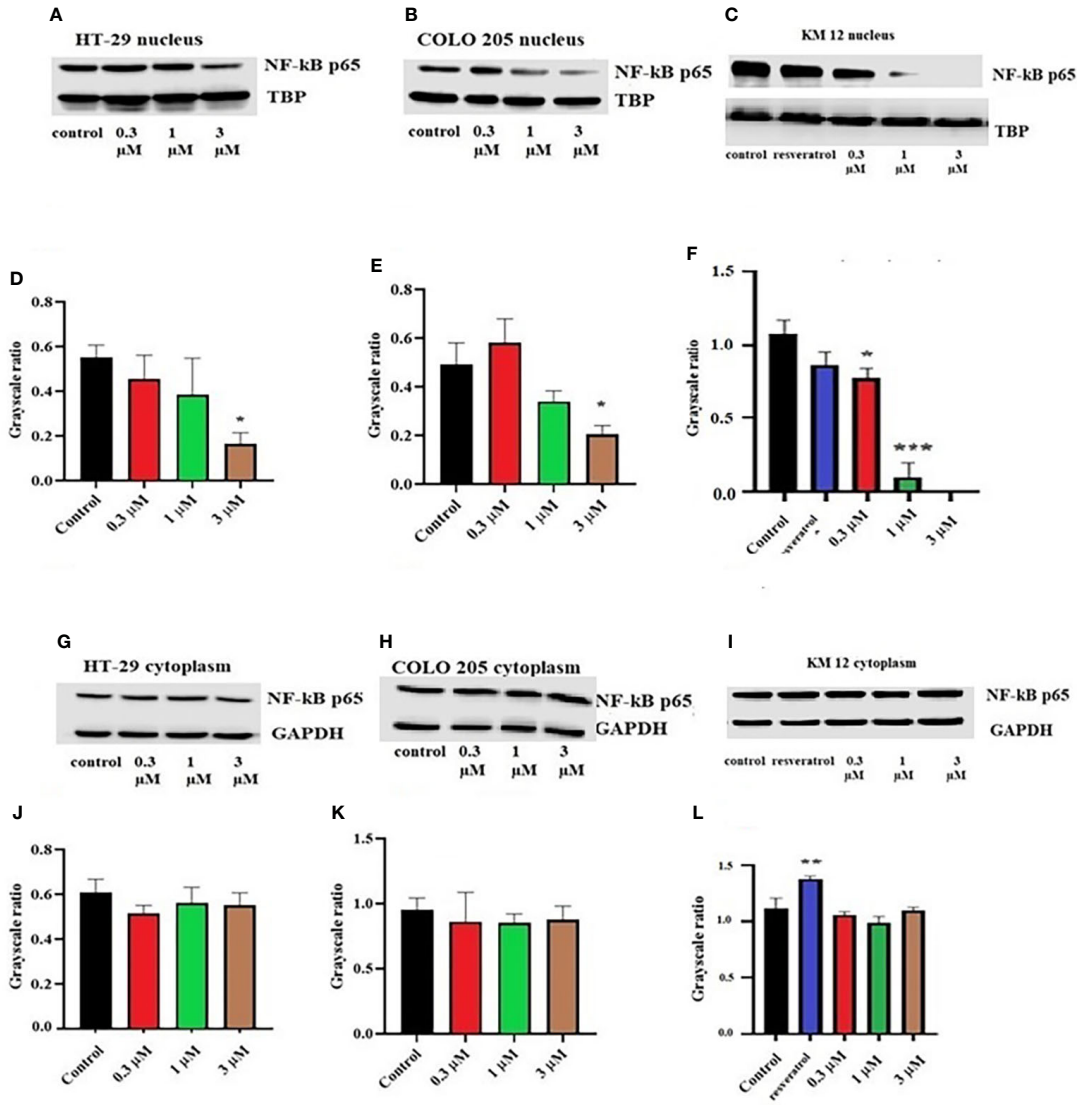

FIGURE 2
Effect of ITH-6 on the expression of the nuclear fraction of NF-kB p65 protein on **(A)** HT-29, **(B)** COLO 205, and **(C)** KM 12 cells and the cytoplasmic fraction on **(G)** HT-29, **(H)** COLO 205, and **(I)** KM 12 cells. The effect of ITH-6 on the expression of the nuclear and cytoplasmic fraction of NF-kB p65 protein was tested after the cells were treated with 0.3, 1, and 3 mM of ITH-6 for 72 hours. Relative quantification of the effect of ITH-6 on **(D–F)** the nuclear and **(J–L)** cytoplasmic fraction of NF-kB p65 in HT-29, COLO 205, and KM 12 cells. The expression level of NF-kB p65 protein was normalized to TBP (nucleus) and GAPDH (cytoplasm). Equal amounts of total cell lysates were used for each sample, and a Western blot analysis was performed. The figures are representative of three independent experiments. * p <.05, ** p <.01 and *** p <.001 compared with the control group.

Interaction analysis of ITH-6-NF-κB p65 docked complex

The previously reported IkBα/NF-κB crystal model (PDB code: 1IKN) was used for docking analysis. Stimulation between ITH-6 and the heterodimer complex was performed using induced fit docking. The docking position of ITH-6 showed an XP docking score of -5.7 kcal mol^{-1}, which shows good binding affinity. Figure 6D depicts the docking pose and interaction between ITH-6 and the IkBα/NF-κB heterodimer protein. Figure 6E shows H-bonding between the thiazolidine hydrogen and the carbonyl oxygen of GLY259. The biphenyl ring resides in the pocket formed by amino acids: GLN 26, LYS 28, GLN 29, ARG 30, whereas the indene ring sits in the pocket made by amino acids: ARG 236, GLY 237, SER 238, PHE 239, GLN 241.

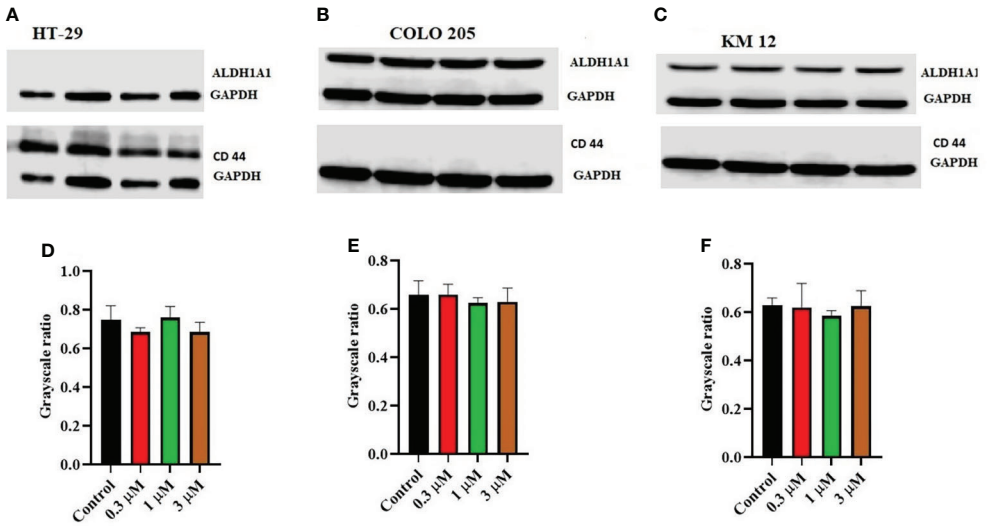

FIGURE 3
Effect of ITH-6 on the expression of ALD1HA1 and CD44: The effect of ITH-6 on the expression of ALDHA1 and CD44 on **(A)** HT-29 **(B)** COLO 205, and **(C)** KM 12 cells were tested after the cells were treated with 0.3, 1, and 3 μM of ITH-6 for 72 hours. Relative quantification of the effect of ITH-6 on **(D)** CD44 in HT-29 and ALDH1A1 in **(E)** COLO 205 and **(F)** KM 12 cells. The expression levels of the target proteins were normalized to GAPDH. Equal amounts of total cell lysates were used for each sample, and a Western blot analysis was performed. The figures are representative of three independent experiments.

Knockout of NF-κB p65 gene in HT-29 cells

The knockout of the NF-κB p65 gene in HT-29-NF-κB p65ko cells was verified by the NF-κB p65 protein expression using Western blotting (Figure 7A). The level of NF-κB p65 in HT-29-NF-κB p65ko cells was remarkably low compared with that of HT-29 cells (Figure 7B).

To further verify the change in gene expression by targeting NF-κB p65 using the CRISPR/Cas9 system in HT-29-NF-κB p65ko cells, MTT assay was performed. RF was used to evaluate if there is any degree of change in the IC_{50} values resulting from the absence of NF-KB p65 expression. Based on the results, the IC_{50} value in HT-29-NF-κB p65ko cells is around 180-fold higher than that of the corresponding HT-29 cell lines (Figure 7C).

The effect of ITH-6 and irinotecan in mice with HT-29 and KM 12 tumor xenografts

We chose irinotecan as a positive control drug because irinotecan is often used for CRC treatment. The two CRC cell lines, HT-29 and KM 12, were implanted, and when the palpable tumors developed, the treatment regimen was started. The mice implanted with HT-29 and KM 12 cells had a significant reduction in volume (Figures 8B, E) and weight (Figures 8C, F) of the tumor after treatment with an oral dose of ITH-6 6 mg/kg compared with the positive control, 30 mg/kg irinotecan, which was given i.p. (Figures 8A, D). The doses that were administered suggest that the drug doses did not produce significant overt toxicity as there was no significant decrease in body weight (Figure 9A) and blood cell count (Figures 9B, C).

Concentration of ITH-6 and irinotecan in the tumor and plasma

The plasma level of irinotecan (i.p.) gradually decreased as time increased (Figure 9E) and for ITH-6 (given orally), plasma concentration was gradually increasing and reached a peak at 60 minutes and then decreased (Figure 9D). However, the tumor concentration of irinotecan (30 mg/kg) was less compared with ITH-6 (6 mg/kg) (Figure 9F).

Discussion

Our previous study found that the drug ITH-**6** has better IC_{50} values on the three CRC cell lines than irinotecan, a clinical-use drug for CRC treatment (26). Indanone-derived compounds have a broader range of different biological activities (43). The IC_{50} values of ITH-6 are 0.44 μM, 0.98 μM, and 0.41 μM on HT-29, COLO 205, and KM 12 cell lines, respectively. Also, the

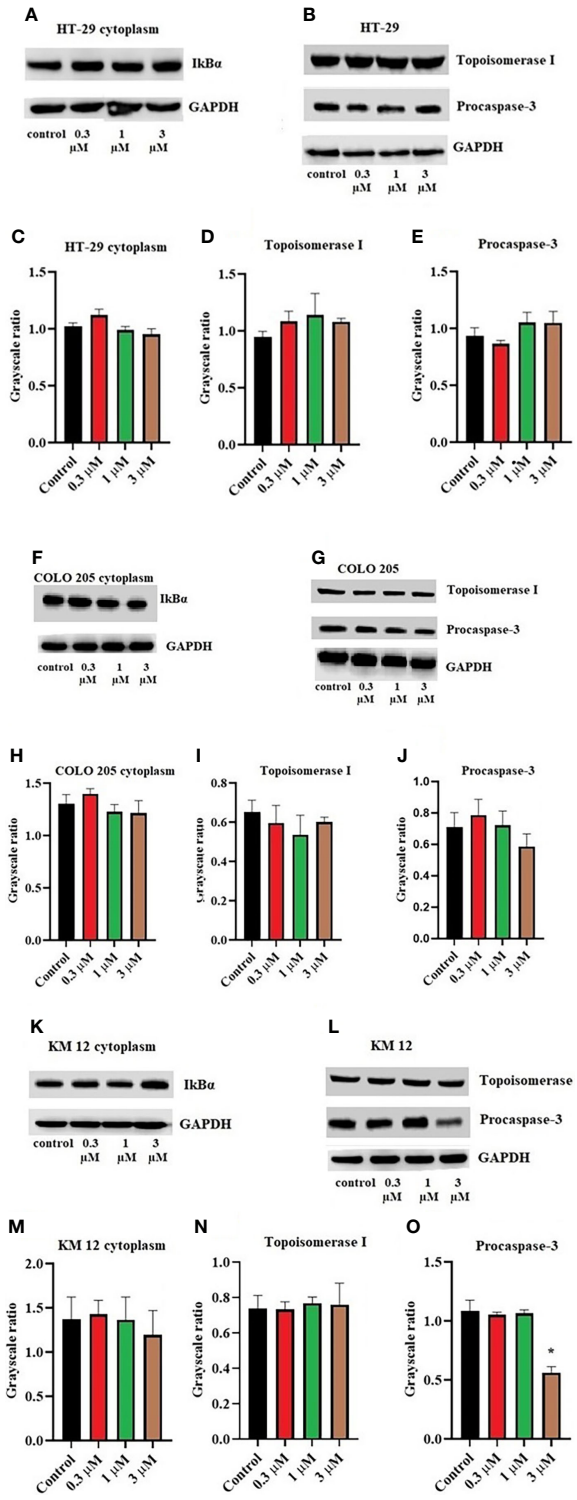

FIGURE 4
Effect of ITH-6 on the expression of cytoplasmic expression of IkBα, Topoisomerase I, and Procaspase-3 on **(A, B)** HT-29, **(F, G)** COLO 205, and **(K, L)** KM 12 cells. The effect of ITH-6 on the expression of Topoisomerase I, Procaspase-3, and IkBα (cytoplasmic) was tested after the cells were treated with 0.3, 1, and 3 μM of ITH-6 for 72 hours. Relative quantification of the effect of ITH-6 on cytoplasmic IkBα on **(C)** HT-29, **(H)** COLO 205, and **(M)** KM 12 cells, Topoisomerase I on **(D)** HT-29, **(I)** COLO 205, and **(N)** KM 12 cells, and Procaspase-3 on **(E)** HT-29, **(J)** COLO 205, and **(O)** KM 12 cells. The expression levels of the target proteins were normalized to GAPDH. Equal amounts of total cell lysates were used for each sample, and a Western blot analysis was performed. The figures are representative of three independent experiments. * p <.05 compared with the control group.

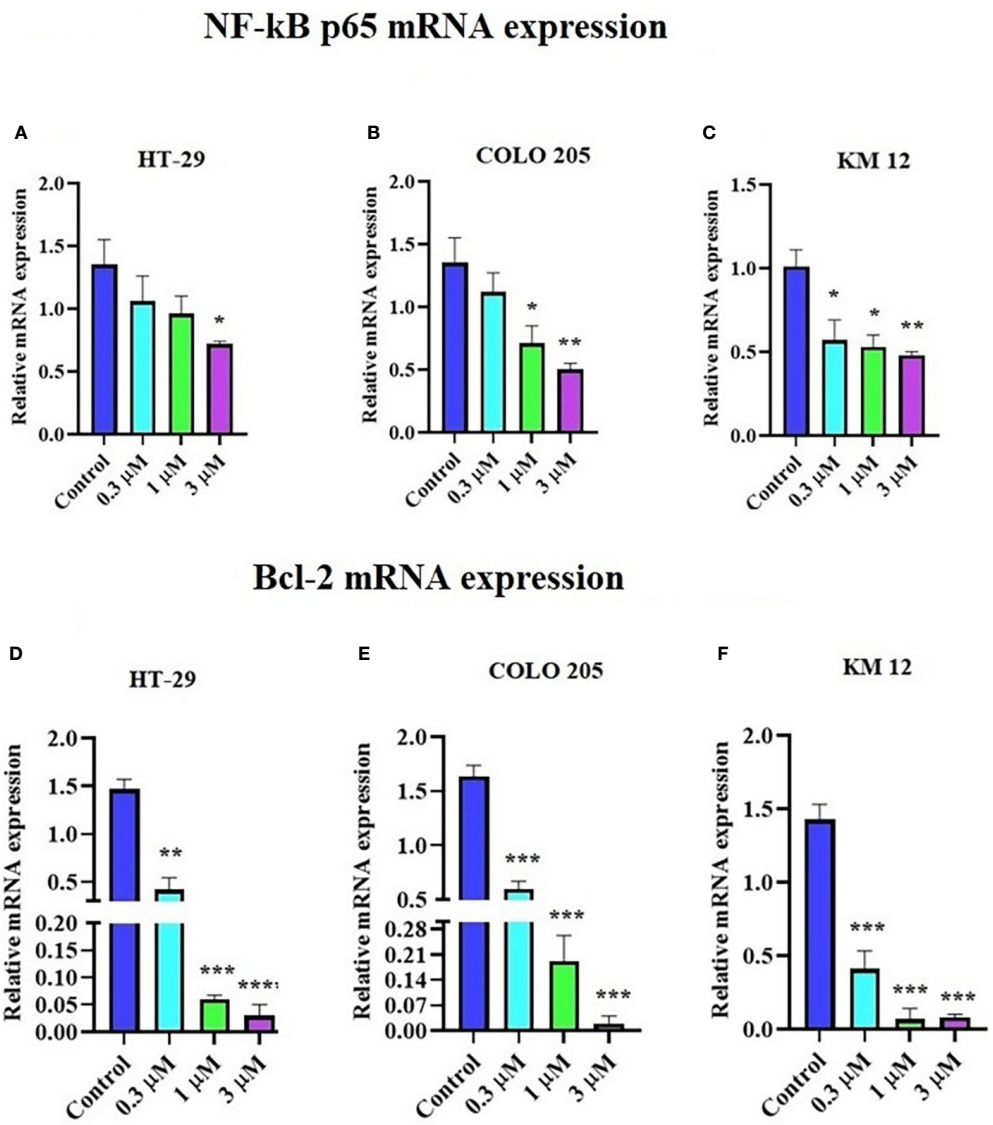

FIGURE 5
Effect of ITH-6 on NF-κB p65 and Bcl-2 expression at mRNA levels on HT-29, COLO 205, and KM 12 cells. The effect of ITH-6 on NF-κB p65 mRNA expression on **(A)** HT-29, **(B)** COLO 205, **(C)** KM 12 cells, and Bcl-2 mRNA expression on **(D)** HT-29, **(E)** COLO 205, and **(F)** KM 12 cells was tested after the cells were treated with 0.3, 1, and 3 μM of ITH-6 different concentrations for 72 hours. Points with error bars represent the mean ± SD for independent determinations in triplicate. The figures are representative of three independent experiments. * p <.05, ** p <.01, *** p <.001 and **** p <.0001 compared with the control group.

previous data showed the mechanism of ITH-6 on the G2/M cell cycle phase with little effect on other phases and caused an increase in apoptosis.

It is already reported that ITH-**6** induces intracellular ROS production and causes a decrease in GSH levels in all three CRC cell lines with the highest impact at 3 μM (26). Given that the cytotoxicity on CRC cells could result from an inhibition of some specific proteins related to the apoptotic pathway, we conducted Western blotting analysis and RT-PCR to figure out the mechanism of ITH-6. Our results indicate that the incubation of these cancer cells with 3 μM of ITH-6 for 72 hours notably decreased the expression of the nuclear fraction of NF-κB p65 protein compared with cells incubated with vehicle, and the downregulation is more predominant compared with 20 μM of the positive control, resveratrol. There was no significant change in the cytoplasmic level of NF-κB p65 protein (an inactive form that is bound to IkBα). ITH-6 acts only on the nuclear fraction of NF-κB p65, thus proving that it is downregulating the active form of NF-κB p65 protein, which is responsible for the cytotoxicity of ITH-6 on these cell lines.

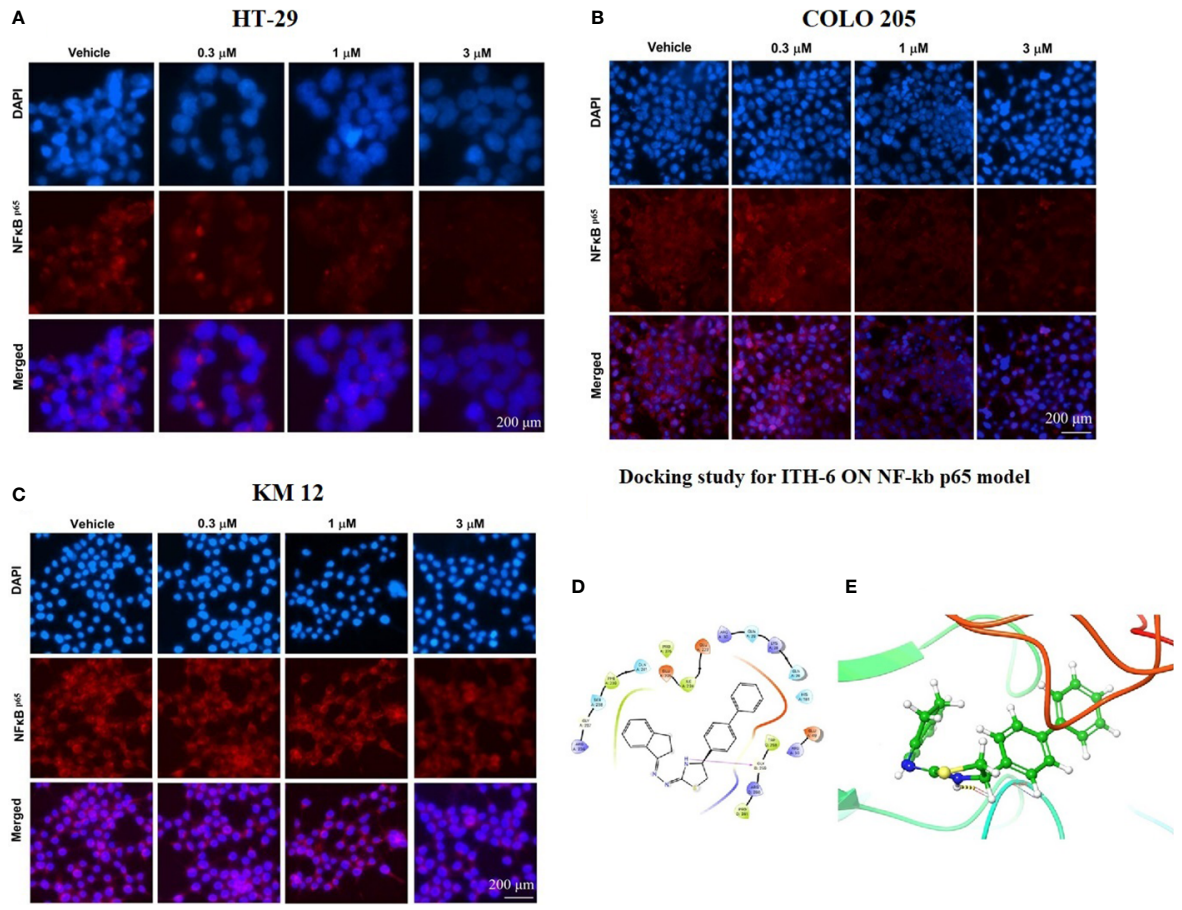

FIGURE 6
The effect of ITH-6 on the expression of NF-κB p65. **(A)** HT-29, **(B)** COLO 205, and **(C)** KM 12 cells were incubated for 72 hours with 0.3, 1, and 3 μM of ITH-6. The red color represents the presence of NF-κB p65, and the blue color represents the nucleus. **(D)** Docking pose of ITH-6 within the binding pocket of IkBα/NF-κB heterodimer. The protein is represented as multicolored ribbons. Amino acid residues are shown as follows: nitrogen in blue, hydrogen in white, carbon in gray, and oxygen in red. The ligand is represented by the ball and stick model with carbon atoms represented as carbon in green, nitrogen in blue, hydrogen in white, and sulfur in yellow. The yellow dashes represent the hydrogen bonding. **(E)** 2-D ligand interaction between ITH-6 and the IkBα/NF-κB heterodimer. Magenta arrow represents hydrogen bonding with amino acid residues within 5 Å of the ligand.

Moreover, there was no significant change in the levels of ALDH1A1, CD44, IkBα (nuclear and cytoplasmic), TOP I protein upon treatment with ITH-6. The expression of ALDH1A1 was absent in HT-29 cells, whereas CD44 was absent in COLO 205 and KM 12 cells. CD44 could be a surface marker in CRC, and some of the CRC cells could be separated into two populations based on CD44 expression, CD44- and CD44+ (44). ALDH1A1, a member of ALD1H1 family **is** a prognostic predictor of many cancers, including CRC. ALDH1A1 in CRC tissues also has a heterogeneous expression pattern with differences in the rate and intensity. This pattern is also observed in a study of 20 cases of normal colorectal mucosa and 65 cases of CRC and their corresponding adjacent tissues in which ALDH1A1 was upregulated in some cases and downregulated in others (45). There are 14 caspases in mammals. The caspases 8, 9, and 10 are activated by apoptotic stimulation, which activates further effector caspases. Moreover, many studies show that active caspase-3 is needed to induce apoptosis in response to chemotherapeutic treatments. Caspase-3 is synthesized as a 32-kDa proenzyme (procasoase-3), which is cleaved into two subunits and reassociated to form the functionally active caspase-3 enzyme (46). The enzyme TOP1 has a specific role in carcinogenesis. Topoisomerase I (TOP1) cuts one strand in the double-stranded DNA, independent of ATP, and topoisomerase II (TOP2) cuts both strands in DNA and is dependent on ATP for its activity. There are two types of topoisomerases, type I and type II topoisomerase inhibitors interfere with the DNA replication. Topotecan and irinotecan are TOP1 inhibitors and currently used in the treatment of cervical and CRC (47). Inhibitors-of-kappaB (IκB) is an inhibitor of NF-κB and includes various

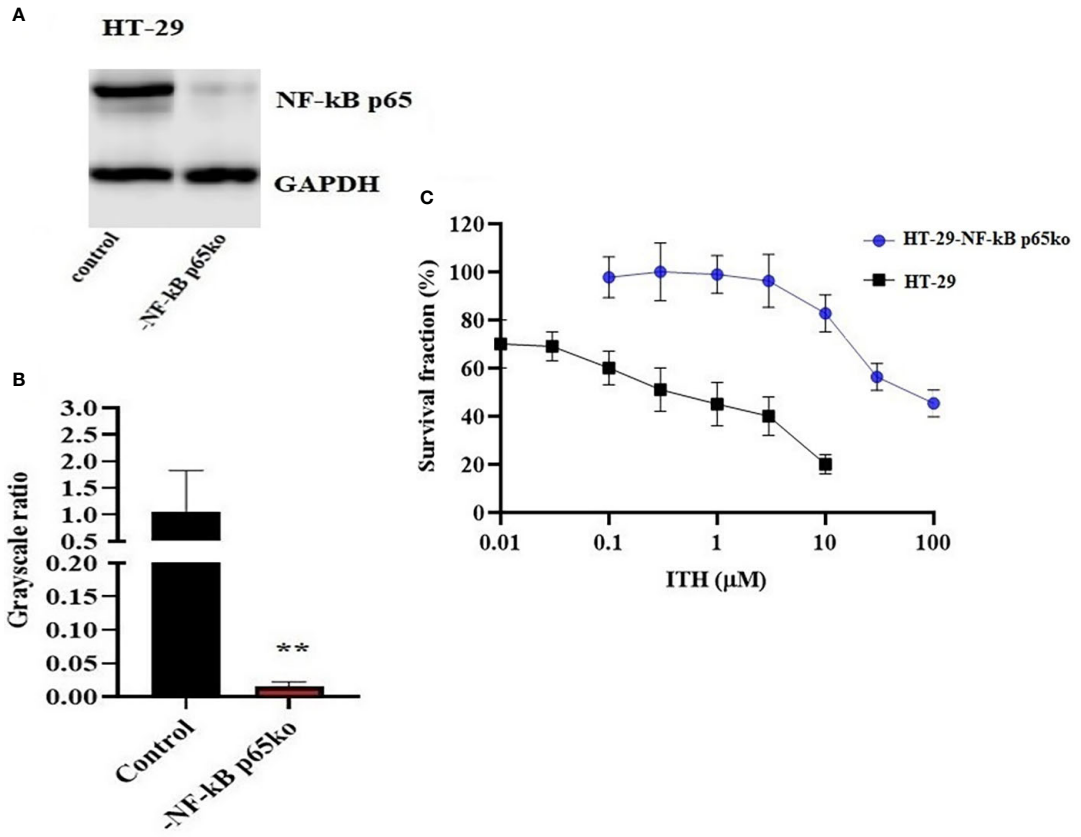

FIGURE 7
Confirmation of NF-κB p65 knockout in HT-29-NF-κB p65ko cells. **(A)** Western blotting result of NF-κB p65 protein expression level and **(B)** relative quantification of NF-κB p65 in HT-29 and HT-29-NF-κB p65ko cells. The expression level of the target protein was normalized to GAPDH. **(C)** Survival fraction (%) was measured after treatment with ITH-6 (μM) for 72 hours on HT-29 and HT-29-NF-κB p65ko cells. Points with error bars represent the mean ± SD for independent determinations in triplicate. The figures are representative of three independent experiments. ** p <.01 compared with the control group.

isoforms, such as IκBα, IκBβ, and IκBε. IκBα binds to NF-κB in the cytoplasm and blocks the nuclear localization and transcriptional activity of p65. It is only degraded if it is phosphorylated, then ubiquitinated, and finally degraded by the proteasome in a ubiquitin-dependent fashion (48).

The effect of ITH-6 may be on either a transcriptional or translational level. The incubation of the abovementioned cancer cells at various concentrations of ITH-6 for 72 hours decreased the mRNA level of NF-κB p65 significantly compared with cells incubated with vehicle. There was a considerable reduction in the mRNA expression of Bcl-2, which is an anti-apoptotic protein and a downstream molecule of the NF-κB pathway and variety of cancers exhibit a higher expression of Bcl-2 and confer resistance to the apoptotic effect of chemo- and radiotherapy (49).

Subsequently, an *in vitro* immunofluorescent experiment showed that incubation with ITH-6 for a time point of 72 hours decreased NF-κB p65 expression, which is consistent with the Western blot and mRNA expression results. Furthermore, cytotoxicity assays on ABCB1- and ABCG2- overexpressing cell lines showed that there was no significant difference in the IC_{50} values of ITH-6, and it proves that it is not a substrate of ABCB1 or ABCG2 transporter. If a drug is a substrate of ABC transporter, it is more likely to extrude from cells, and that affects the bioavailability of the drug. The results from the gene knockout studies suggest that the NF-κB p65 gene knockout in the HT-29-NF-κB p65ko cell line can be useful in investigating whether ITH-6–induced cytotoxicity is related to the downregulation of the target, NF-KB p65, which is highly expressed in p53 mutant CRCs.

Finally, based on our *in vitro* results, preclinical studies in the athymic nude mice models were conducted to determine the effect of the anticancer effect of ITH-6 on tumor growth on mice implanted with HT-29 and KM 12 cells. The oral administration of 6 mg/kg of ITH-6 reduced the tumor growth remarkably compared with mice that received irinotecan (30 mg/kg i.p.). In addition, no marked change in

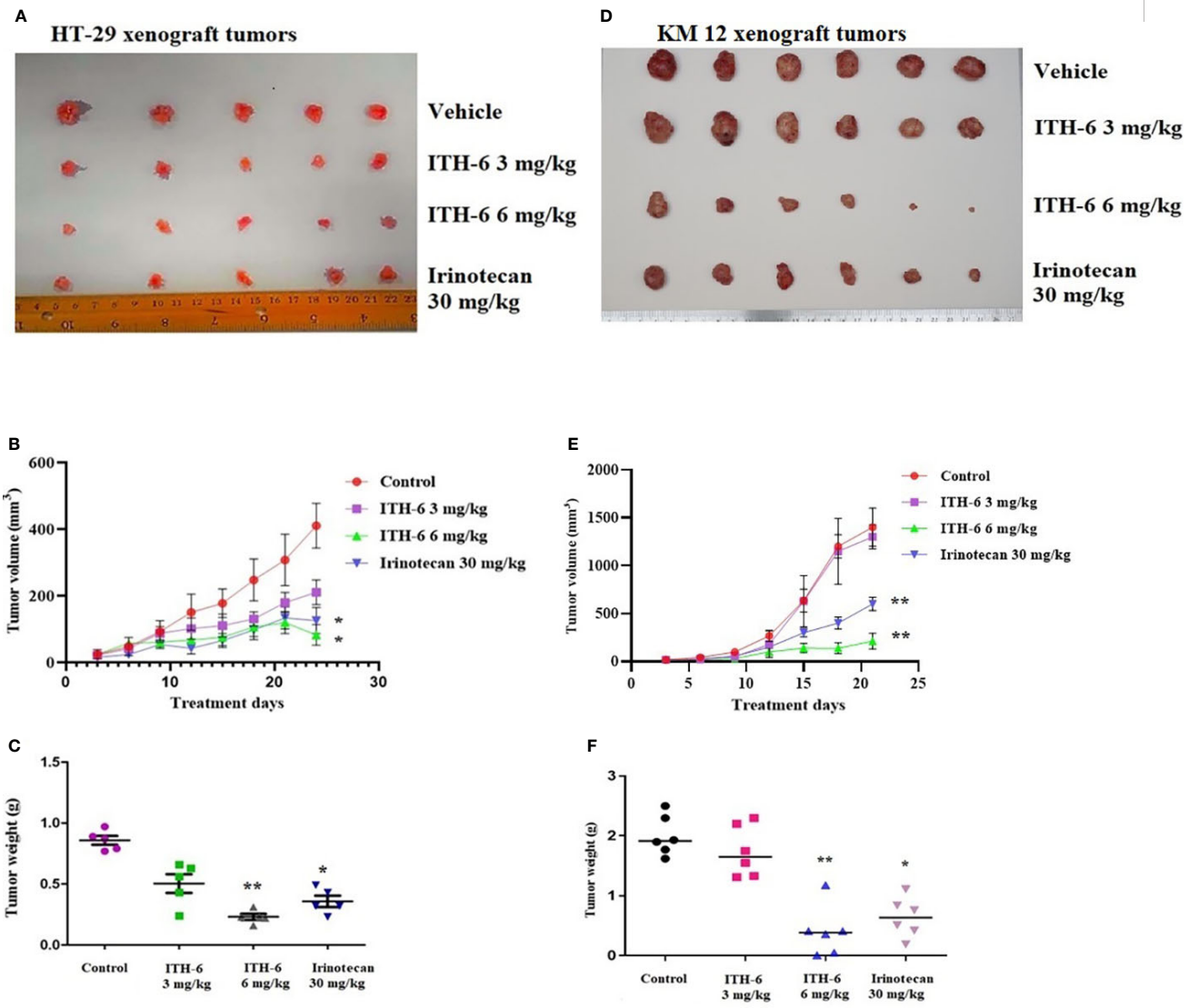

FIGURE 8
ITH-6 inhibits tumor growth, volume, and weight in xenograft mouse model. NCR nude mice were inoculated with subcutaneous implantation of HT-29 and KM 12 cells. During a 21-day treatment period, ITH-6 (6 mg/kg) significantly inhibited the growth, volume, and weight of **(A–C)** HT-29 and **(D–F)** KM 12 tumor xenografts compared with the vehicle control and irinotecan group. Values represent the median ± SD of six animals per group. Similar results were obtained in two independent experiments. * p <.05 and ** p <.01 compared with the control group.

body weight, WBC, and platelet counts were noted, suggesting that ITH-6 can be well-tolerated at this dose and may be a successful drug candidate for treating p53 mutant CRCs. Furthermore, the anticancer efficacy of ITH-6 is better than the positive control, irinotecan, which can be further proved by its increased tumor concentration compared with irinotecan. These data suggest that ITH-6 has a remarkable anticancer activity in mice with HT-29/KM 12 xenografts at a dose that does not produce notable toxic effects.

Anticancer drug discovery and development are one of the great advancements, and in this manuscript, we demonstrate that ITH-6 is a potent cytotoxic agent against p53 mutant CRC cells and has a preferable cytotoxic profile compared with other drugs that are already approved for CRC. ITH-6 acts on the specific cell cycle phase, causing G2/M phase arrest, and induces apoptosis by elevating the intracellular ROS and decreasing the GSH levels. It also inhibits tubulin polymerization and downregulates the expression of the NF-κB p65 and Bcl-2 in these cell lines, which further proves its role in the cytotoxicity of CRC cell lines. ITH-6 at a dose of 6 mg/kg p.o., did not produce any observable toxic effects in the *in vivo* tumor xenografted mice during the treatment period. It significantly decreased tumor size, growth rate, and

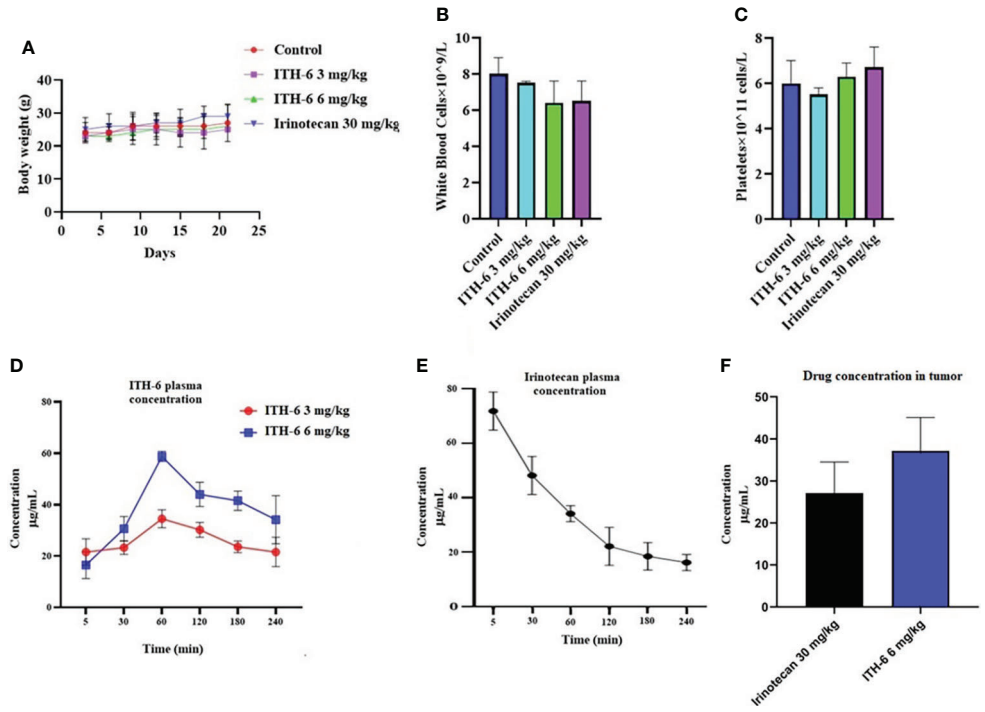

FIGURE 9
(A) Changes in mean body weight before and after treatment for xenograft model are shown. **(B)** The changes in mean white blood cells in nude mice (n = 6) at the end of the 21-day treatment period and **(C)** the changes in mean platelets in nude mice (n = 6) at the end of the 21-day treatment period. Plasma concentrations of **(D)** ITH-6 and **(E)** irinotecan in nude athymic mice at 5, 30, 60, 120, 180, and 240 minutes following administration of ITH-6 (3 and 6 mg/kg) given orally and irinotecan (30 mg/kg) given intraperitoneally. **(F)** Intratumoral concentrations of irinotecan and ITH-6 in KM 12 (n = 6) and HT-29 tumors (n = 6) following administration of these drugs. Points with error bars represent the mean ± SD.

tumor volume in mice bearing HT-29 and KM 12 tumor xenografts compared with irinotecan. Together with its mechanism of action, ITH-**6** could be a potential anticancer drug candidate for p53 mutant CRC treatment.

Data availability statement

The original contributions presented in the study are included in the article/supplementary material. Further inquiries can be directed to the corresponding authors.

Ethics statement

The animal study was reviewed and approved by St. John's University's Institutional Animal Care & Use Committee (IACUC).

Author contributions

SN and Z-SC: Conceptualization, Methodology, and Experimental design. SN, Q-XT NA and Z-XW: Data Curation. UN and NK: Synthesized the compound, SN and F-FP: analyzed the data and SN, SY,NM and Z-SC: Writing-draft preparation, Reviewing and Editing. All authors read and approved the final manuscript.

Funding

This project was supported by St. John's University Research Seed Grant (No. 579-1110-7002), and the Department of Pharmaceutical Sciences at St. John's University. This study was also funded by the National Natural Science Foundation of China (#81874330) and Wuxi Taihu Lake Talent Plan Top Talents Project (BJ 2020001).

Acknowledgments

We are grateful to Dr. Susan E. Bates (Columbia University, NY) for the cell lines. We thank Dr. Mansoor Ahmed (University of Karachi, Pakistan) for providing ITH-6 and other synthetic compounds.

Conflict of interest

The authors declare that the research was conducted in the absence of any commercial or financial relationships that could be construed as a potential conflict of interest.

Publisher's note

References

1. Anreddy N, Patel A, Zhang Y-K, Wang Y-J, Shukla S, Kathawala RJ, et al. A-803467, a tetrodotoxin-resistant sodium channel blocker, modulates ABCG2-mediated MDR *in vitro* and *in vivo*. *Oncotarget* (2015) 6:39276–91. doi: 10.18632/oncotarget.5747

2. Fontana F, Raimondi M, Marzagalli M, Moretti RM, Marelli MM, Limonta P. Tocotrienols and cancer: From the state of the art to promising novel patents. *Recent Pat Anticancer Drug Discovery* (2019) 14:5–18. doi: 10.2174/1574892814666190116111827

3. De Vera AA, Gupta P, Lei Z, Liao D, Narayanan S, Teng Q, et al. Immuno-oncology agent IPI-549 is a modulator of p-glycoprotein (P-gp, MDR1, ABCB1)-mediated multidrug resistance (MDR) in cancer: *In vitro* and *in vivo*. *Cancer Lett* (2019) 442:91–103. doi: 10.1016/j.canlet.2018.10.020

4. Gupta P, Xie M, Narayanan S, Wang Y-J, Wang X-Q, Yuan T, et al. GSK1904529A, a potent IGF-IR inhibitor, reverses MRP1-mediated multidrug resistance. *J Cell Biochem* (2017) 118:3260–7. doi: 10.1002/jcb.25975

5. Wu Z-X, Yang Y, Wang J-Q, Narayanan S, Lei Z-N, Teng Q-X, et al. Overexpression of ABCG2 confers resistance to MLN7243, a ubiquitin-activating enzyme (UAE) inhibitor. *Front Cell Dev Biol* (2021) 9:697927. doi: 10.3389/fcell.2021.697927

6. Narayanan S, Cai C-Y, Assaraf YG, Guo H-Q, Cui Q, Wei L, et al. Targeting the ubiquitin-proteasome pathway to overcome anti-cancer drug resistance. *Drug Resist Update* (2020) 48:100663. doi: 10.1016/j.drup.2019.100663

7. Siegel RL, Miller KD, Jemal A. Cancer statistics, 2020. *CA Cancer J Clin* (2020) 70:7–30. doi: 10.3322/caac.21590

8. Kuipers EJ, Grady WM, Lieberman D, Seufferlein T, Sung JJ, Boelens PG, et al. Colorectal cancer. *Nat Rev Dis Prim* (2015) 1:15065. doi: 10.1038/nrdp.2015.65

9. Barbuti AM, Zhang G-N, Gupta P, Narayanan S, Chen Z-S. Chapter 1 - EGFR and HER2 inhibitors as sensitizing agents for cancer chemotherapy. *Cancer Sensitizing Agents Chemother* (2019) 4:1–11. doi: 10.1016/B978-0-12-816435-8.00001-8

10. Gupta P, Narayanan S, Yang D-H. Chapter 9 - CDK inhibitors as sensitizing agents for cancer chemotherapy. *Cancer Sensitizing Agents Chemother* (2019) 4:125–49. doi: 10.1016/B978-0-12-816435-8.00009-2

11. Van Cutsem E, Cervantes A, Nordlinger B, Arnold D. Metastatic colorectal cancer: ESMO clinical practice guidelines for diagnosis, treatment and follow-up. *Ann Oncol Off J Eur Soc Med Oncol* (2014) 25 Suppl 3:iii1–9. doi: 10.1093/annonc/mdu260

12. Schuell B, Gruenberger T, Kornek GV, Dworan N, Depisch D, Lang F, et al. Side effects during chemotherapy predict tumour response in advanced colorectal cancer. *Br J Cancer* (2015) 93:744–8. doi: 10.1038/sj.bjc.6602783

13. Wiela-Hojeńska A, Kowalska T, Filipczyk-Cisarż E, Łapiński Ł, Nartowski K. Evaluation of the toxicity of anticancer chemotherapy in patients with colon cancer. *Adv Clin Exp Med* (2015) 24:103–11. doi: 10.17219/acem/38154

14. Ganellin C. Indane and indene derivatives of biological interest. *Adv Drug Res* (1967) 4:163–249.

15. Klaus M. Tetrahydronaphthalene and indane compounds useful as anti-tumor agents. *Google Patents* (1983) 1:396–553.

16. Vilums M, Heuberger J, Heitman LH, IJzerman AP. Indanes–properties, preparation, and presence in ligands for G protein coupled receptors. *Med Res Rev* (2015) 35:1097–126. doi: 10.1002/med.21352

17. Yao S-W, Lopes V, Fernández F, Garcıa-Mera X, Morales M, Rodrıguez-Borges J, et al. Synthesis and QSAR study of the anticancer activity of some novel indane carbocyclic nucleosides. *Bioorg Med Chem* (2003) 11:4999–5006. doi: 10.1016/j.bmc.2003.09.005

18. Merga YJ, O'Hara A, Burkitt MD, Duckworth CA, Probert CS, Campbell BJ, et al. Importance of the alternative NF-κB activation pathway in inflammation-associated gastrointestinal carcinogenesis. *Am J Physiol Liver Physiol* (2016) 310:G1081–90. doi: 10.1152/ajpgi.00026.2016

19. Pereira SG, Oakley F. Nuclear factor-kappaB1: regulation and function. *Int J Biochem Cell Biol* (2008) 40:1425–30. doi: 10.1016/j.biocel.2007.05.004

20. Song W, Mazzieri R, Yang T, Gobe GC. Translational significance for tumor metastasis of tumor-associated macrophages and epithelial-mesenchymal transition. *Front Immunol* (2017) 8:1106. doi: 10.3389/fimmu.2017.01106

21. Zhong L, Chen X-F, Wang T, Wang Z, Liao C, Wang Z, et al. Soluble TREM2 induces inflammatory responses and enhances microglial survival. *J Exp Med* (2017) 214:597–607. doi: 10.1084/jem.20160844

22. Vlantis K, Wullaert A, Polykratis A, Kondylis V, Dannappel M, Schwarzer R, et al. NEMO prevents RIP kinase 1-mediated epithelial cell death and chronic intestinal inflammation by NF-κB-Dependent and -independent functions. *Immunity* (2016) 44:553–67. doi: 10.1016/j.immuni.2016.02.020

23. Tosello V, Bordin F, Yu J, Agnusdei V, Indraccolo S, Basso G, et al. Calcineurin and GSK-3 inhibition sensitizes T-cell acute lymphoblastic leukemia cells to apoptosis through X-linked inhibitor of apoptosis protein degradation. *Leukemia* (2016) 30:812–22. doi: 10.1038/leu.2015.335

24. Kwon H-J, Choi G-E, Ryu S, Kwon SJ, Kim SC, Booth C, et al. Stepwise phosphorylation of p65 promotes NF-κB activation and NK cell responses during target cell recognition. *Nat Commun* (2016) 7:11686. doi: 10.1038/ncomms11686

25. Tergaonkar V, Pando M, Vafa O, Wahl G, Verma I. p53 stabilization is decreased upon NFkappaB activation: a role for NFkappaB in acquisition of resistance to chemotherapy. *Cancer Cell* (2002) 1:493–503. doi: 10.1016/s1535-6108(02)00068-5

26. Narayanan S, Gupta P, Nazim U, Ali M, Karadkhelkar N, Ahmad M, et al. Anti-cancer effect of indanone-based thiazolyl hydrazone derivative on colon cancer cell lines. *Int J Biochem Cell Biol* (2019) 110:21–8. doi: 10.1016/j.biocel.2019.02.004

27. Nazim U, Narayanan S, Ali M, Khan K, Ali B, Li J, et al. Synthesis, characterization and cytotoxic effect of some new thiazolyl hydrazone derivatives of 1-indanone. *J Chem Soc Pakistan* (2021) 43:244. doi: 10.52568/000564/JCSP/43.02.2021

28. Lai GM, Chen YN, Mickley LA, Fojo AT, Bates SE. P-glycoprotein expression and schedule dependence of adriamycin cytotoxicity in human colon carcinoma cell lines. *Int J Cancer* (1991) 49:696–703. doi: 10.1002/ijc.2910490512

29. Carmichael J, DeGraff WG, Gazdar AF, Minna JD, Mitchell JB. Evaluation of a tetrazolium-based semiautomated colorimetric assay: Assessment of chemosensitivity testing. *Cancer Res* (1987) 47(4):936–42.

30. Bahuguna A, Khan I, Bajpai VK, Chul S. MTT assay to evaluate the cytotoxic potential of a drug. *Bangladesh J Pharmacol* (2017) 12:8. doi: 10.3329/bjp.v12i2.30892

31. Zhang Y-K, Zhang G-N, Wang Y-J, Patel BA, Talele TT, Yang D-H, et al. Bafetinib (INNO-406) reverses multidrug resistance by inhibiting the efflux

function of ABCB1 and ABCG2 transporters. *Sci Rep* (2016) 6:25694. doi: 10.1038/srep25694

32. Shukla S, Jhamtani R, Dahiya M, Agarwal DR. A novel method to achieve high yield of total RNA from zebrafish for expression studies. *International J. Bioassays* (2017) 6:5383–85. doi: 10.21746/ijbio.2017.05.004

33. Wang Y-J, Zhang Y-K, Zhang G-N, Al Rihani SB, Wei M-N, Gupta P, et al. Regorafenib overcomes chemotherapeutic multidrug resistance mediated by ABCB1 transporter in colorectal cancer: In vitro and in vivo study. *Cancer Lett* (2017) 396:145–54. doi: 10.1016/j.canlet.2017.03.011

34. Patel BA, Abel B, Barbuti AM, Velagapudi UK, Chen Z-S, Ambudkar SV, et al. Comprehensive synthesis of amino acid-derived thiazole peptidomimetic analogues to understand the enigmatic Drug/Substrate-binding site of p-glycoprotein. *J Med Chem* (2018) 61:834–64. doi: 10.1021/acs.jmedchem.7b01340

35. Wu Z-X, Yang Y, Teng Q-X, Wang J-Q, Lei Z-N, Wang J-Q, et al. Tivantinib, a c-met inhibitor in clinical trials, is susceptible to ABCG2-mediated drug resistance. *Cancers (Basel)* (2020) 12:186. doi: 10.3390/cancers12010186

36. Narayanan S, Fan Y-F, Gujarati NA, Teng Q-X, Wang J-Q, Cai C-Y, et al. VKNG-1 antagonizes ABCG2-mediated multidrug resistance *via* p-AKT and bcl-2 pathway in colon cancer: *In vitro* and *In vivo* study. *Cancers (Basel)* (2021) 13:1–22. doi: 10.3390/cancers13184675

37. Bunting KD. ABC Transporters as phenotypic markers and functional regulators of stem cells. *Stem Cells* (2002) 20:274. doi: 10.1634/stemcells.20-3-274

38. Milczarek M, Rosińska S, Psurski M, Maciejewska M, Kutner A, Wietrzyk J. Combined colonic cancer treatment with vitamin d analogs and irinotecan or oxaliplatin. *Anticancer Res* (2013) 33(2):433–44.

39. Dai C, Tiwari AK, Wu C-P, Su X-D, Wang S-R, Liu D, et al. Lapatinib (Tykerb, GW572016) reverses multidrug resistance in cancer cells by inhibiting the activity of ATP-binding cassette subfamily b member 1 and G member 2. *Cancer Res* (2008) 68:7905–14. doi: 10.1158/0008-5472.CAN-08-0499

40. Wang Y-J, Huang Y, Anreddy N, Zhang G-N, Zhang Y-K, Xie M, et al. Tea nanoparticle, a safe and biocompatible nanocarrier, greatly potentiates the anticancer activity of doxorubicin. *Oncotarget* (2016) 7:5877–91. doi: 10.18632/oncotarget.6711

41. Choi C-H. ABC Transporters as multidrug resistance mechanisms and the development of chemosensitizers for their reversal. *Cancer Cell Int* (2005) 5:30. doi: 10.1186/1475-2867-5-30

42. Galante JM, Mortenson MM, Schlieman MG, Virudachalam S, Bold RJ. Targeting NF-kB/BCL-2 pathway increases apoptotic susceptibility to chemotherapy in pancreatic cancer. *J Surg Res* (2004) 121:306–7. doi: 10.1016/j.jss.2004.07.130

43. Leoni LM, Hamel E, Genini D, Shih H, Carrera CJ, Cottam HB, et al. Indanocine, a microtubule-binding indanone and a selective inducer of apoptosis in multidrug-resistant cancer cells. *J Natl Cancer Inst* (2000) 92:217–24. doi: 10.1093/jnci/92.3.217

44. Okuyama H, Nogami W, Sato Y, Yoshida H, Tona Y, Tanaka Y. Characterization of CD44-positive cancer stem-like cells in COLO 201 cells. *Anticancer Res* (2020) 40:169–76. doi: 10.21873/anticanres.13938

45. Xu SL, Zeng DZ, Dong WG, Ding YQ, Rao J, Duan J, et al. Distinct patterns of ALDH1A1 expression predict metastasis and poor outcome of colorectal carcinoma. *Int J Clin Exp Pathol* (2014) 7(6):2976–86.

46. Maurya SK, Tewari M, Sharma B, Shukla HS. Expression of procaspase 3 and activated caspase 3 and its relevance in hormone-responsive gallbladder carcinoma chemotherapy. *Korean J Intern Med* (2013) 28:573–8. doi: 10.3904/kjim.2013.28.5.573

47. Lee S, Ho JY, Liu JJ, Lee H, Park JY, Baik M, et al. CKD-602, a topoisomerase I inhibitor, induces apoptosis and cell-cycle arrest and inhibits invasion in cervical cancer. *Mol Med* (2019) 25:23. doi: 10.1186/s10020-019-0089-y

48. Ferreiro DU, Komives EA. Molecular mechanisms of system control of NF-kappaB signaling by IkappaBalpha. *Biochemistry* (2010) 49:1560–7. doi: 10.1021/bi901948j

49. Mortenson MM, Schlieman MG, Virudalchalam S, Bold RJ. Overexpression of BCL-2 results in activation of the AKT/NF-kB cell survival pathway. *J Surg Res* (2003) 114:302. doi: 10.1016/j.jss.2003.08.103

frontiers | Frontiers in Oncology

TYPE Original Research
PUBLISHED 05 August 2022
DOI 10.3389/fonc.2022.954008

OPEN ACCESS

EDITED BY
Takeo Tatsuta,
Tohoku Medical and Pharmaceutical University, Japan

REVIEWED BY
Olli-Pekka Smolander,
Tallinn University of Technology, Estonia
Nazanin Hosseinkhan,
Iran University of Medical Science, Iran

*CORRESPONDENCE
Marcin Opławski
marcin.oplawski@gmail.com

SPECIALTY SECTION
This article was submitted to Pharmacology of Anti-Cancer Drugs, a section of the journal Frontiers in Oncology

RECEIVED 26 May 2022
ACCEPTED 12 July 2022
PUBLISHED 05 August 2022

CITATION
Opławski M, Średnicka A, Niewiadomska E, Boroń D, Januszyk P and Grabarek BO (2022) Clinical and molecular evaluation of patients with ovarian cancer in the context of drug resistance to chemotherapy. *Front. Oncol.* 12:954008. doi: 10.3389/fonc.2022.954008

Clinical and molecular evaluation of patients with ovarian cancer in the context of drug resistance to chemotherapy

Marcin Opławski[1,2*], Agata Średnicka[1], Ewa Niewiadomska[3], Dariusz Boroń[1,4,5], Piotr Januszyk[6] and Beniamin Oskar Grabarek[1,4,5,7]

[1]Department of Gynecology and Obstetrics with Gynecologic Oncology, Ludwik Rydygier Memorial Specialized Hospital, Kraków, Poland, [2]Department of Gynecology and Obstetrics, Faculty of Medicine and Health Sciences, Andrzej Frycz Modrzewski University in Kraków, Kraków, Poland, [3]Department of Epidemiology and Biostatistics, School of Health Sciences in Bytom, Medical University of Silesia, Katowice, Poland, [4]Department of Histology, Cytophysiology and Embryology, Faculty of Medicine, University of Technology, Academia of Silesia in Katowice, Zabrze, Poland, [5]Department of Gynecology and Obstetrics, Faculty of Medicine, University of Technology, Academia of Silesia in Katowice, Zabrze, Poland, [6]Department of Biochemistry, Faculty of Medicine, University of Technology, Academia of Silesia in Katowice, Zabrze, Poland, [7]GynCentrum, Laboratory of Molecular Biology and Virology, Katowice, Poland

The present study aimed to evaluate changes in the expression patterns at the gene and protein levels associated with drug resistance. The study group included 48 women who had a histopathologically confirmed diagnosis of stage I-IV ovarian cancer, they were divided into two subgroups (groups A and B). In group A, there were 36 patients in whom surgical treatment was supplemented with first-line chemotherapy according to current standards. Within this patient group, 5 had stage I (14%), 5 had stage II (14%), 25 had stage III (69%), and 1 had stage IV ovarian cancer (3%). Drug resistance was found after the third cycle of chemotherapy in 17 patients (71%) and after the sixth cycle in 7 patients (29%). Group B included 12 women with type I ovarian cancer, including 11 with stage I and 1 patient with stage IV ovarian cancer. The oncological treatment required only surgery. The control group (C) included 50 women in whom the uterus and adnexa were surgically removed for non-oncological reasons. Significantly higher levels of carcinoma antigen 125 CA-125 and human epididymis protein 4 HE4 were observed in group A and in menopausal women. Moreover, drug resistance was associated with significantly higher levels of CA-125 ($p < 0.05$). The genes *UBA2*, *GLO1*, *STATH*, and *TUFT1* were differentiated in test samples from control samples. Moreover, drug resistance was associated with significantly higher expression of *GLO1*. The results of these assessments indicated the strong link between *UBA2* and hsa-miR-133a-3p and hsa-miR-133b; *GLO1* and hsa-miR-561-5p; *STATH* and hsa-miR-137-3p and hsa-miR-580-3p; and *TUFT1* and hsa-miR-1233-3p and hsa-miR-2052. Correlation analysis showed a significant correlation between CA-125 and HE4 levels. Moreover, a significant

correlation between TUFT1 mRNA and UBA2, GLO1, STATH (negative correlation), and TUFT1 in relation to CA-125 and HE4 ($p < 0.05$) was noted in all patients. In view of the lack of screening tests for ovarian cancer, the occurrence of the described correlation may be inscribed as an attempt to establish an assay that meets the criteria of a screening test and thus increase the early diagnosis of ovarian cancer.

KEYWORDS

ovarian cancer, CA-125, HE4, mRNA, miRNA

Introduction

The incidence of ovarian cancer during a woman's lifetime is estimated to be approximately 1 in 75 women, and mortality from the disease is nearly 1 in 100 women (1). Worldwide, ovarian cancer ranks fourth in terms of death due to malignancy, and it accounts for 5% of all cancers diagnosed in women and 31% of all cancers of the female reproductive system (2, 3). Unfortunately, it is also associated with the highest mortality rate among all gynecologic cancers (4). According to The American Cancer Society, it is estimated that 19,880 women will be diagnosed with ovarian cancer in 2022 (5). It should be kept in mind that ovarian cancer ranks fifth in all deaths associated with cancer in women and it has the highest risk of death compared with that in all gynecologic cancers (6, 7).

The risk of ovarian cancer increases with age. In the European continent, approximately 80% of ovarian cancers develop in women above the age of 50 years, most commonly between 60 and 64 years of age and after 75 years (8, 9). The risk of developing ovarian cancer increases in women who achieve menopause at a later age compared with those who reach it at an earlier age (10, 11). Important risk factors include infertility (generally no offspring), infertility if treated with ovulation induction, and recurrent inflammatory conditions including endometriosis, overweight/obesity, and smoking (1, 12–15).

According to the World Health Organization classification, primary ovarian cancers are divided into three groups: surface epithelial-stromal tumors, sex cord-stromal tumors, and germ cell tumors. Considering the molecular basis and clinical implications of tumorigenesis, two types of ovarian cancer can be distinguished. The first one develops from benign ovarian tumors or borderline tumors and constitutes approximately one-third of all cases. Type I includes serous carcinoma G1/2, endometroid carcinoma G1/2, mucinous carcinoma, clear cell carcinoma, and Brenner's carcinoma. It is characterized by slow growth and low sensitivity to chemotherapy with a good prognosis (nearly 80% 5-year survival rate) and lower frequency of recurrence. Type II occurs significantly more often (70% of all cases) and is known to have a poor prognosis. It includes serous carcinoma G3, endometroid carcinoma G3, undifferentiated carcinoma G3, and sarcoma. It is most often diagnosed at stages III and IV and is characterized by rapid growth and high sensitivity to chemotherapy but with more frequent recurrence and poor prognosis (nearly 90% of patients die within 5 years of observation) (16–18).

Thus far, annual screening including transvaginal ultrasound and carcinoma antigen (CA-125) evaluation has not been proven to affect population-based detection of ovarian cancer. Additionally, computed tomography (CT), magnetic resonance imaging, and positron emission tomography are used to assess disease progression, monitoring treatment effects, and detecting recurrence (19, 20).

Among useful biochemical markers, CA-125 antigen, which is a glycoprotein that is not present in the epithelial cells of normal ovaries, and human epididymis protein 4 (HE4). The Risk of Ovarian Malignancy Algorithm (ROMA) is calculated based on the determined concentrations of the two tumor markers CA125 and HE4 and considering the woman's menopausal status. On this basis, women can be classified into a high- or low-risk group for developing ovarian cancer. Performing the determinations of both markers simultaneously and calculating the ROMA values increases the diagnostic value of these tests. The role of ROMA in detecting early-stage ovarian cancer is particularly emphasized. The lower limit of normal for laboratory determinations is usually <35 IU/mL. CA-125 levels >35 IU/mL are observed in 50–90% of patients with ovarian cancer. Before surgical treatment, normal levels of CA-125 are found in 50% of women with stage I cancer and 60% women with stage II cancer (21, 22). The HE4 marker, found in the epithelium of the epididymis, trachea, salivary glands, lungs, kidneys, prostate, fallopian tubes, oral mucosa, endometrium, and endocervix, whose normal concentration is <150 pM/L, is also important. Because HE4 does not have such a high tendency for false-positive results, its determination is useful for clinical diagnosis. Elevated levels of HE4 are observed in cases of endometrial cancer, cervical cancer, and benign ovarian

tumors. It should be noted that these markers are not specific and also change in situations not associated with cancer, such as endometriosis, pregnancy, or menstruation (23, 24).

The extent of treatment—surgery and possible supplementation with chemotherapy—depends on the disease stage. Unfortunately, in approximately one-fifth of cases, drug resistance to the platinum compounds (cisplatin) used as first-line chemotherapy is noted (25, 26).

The present study aimed to evaluate the changes in expression patterns at the gene and protein levels associated with the phenomenon of drug resistance, as well as the levels of CA-125 and HE4 markers and the association between them, in patients with stage I-IV ovarian cancer in comparison with control patients.

Patients and methods

The present study was performed in accordance with the guidelines of the 2013 Declaration of Helsinki on human experimentation. It is not possible to identify patients on an individual basis either in this study or in the database. Informed consent was obtained from all patients. Approval from the Bioethical Committee operating at the Regional Medical Chamber in Kraków (approval no. 185/KBL/OIL/2020 and 186/KBL/OIL/2020, dated September 20, 2020) was obtained for this study.

Patients

The study group included 48 women who had a histopathologically confirmed diagnosis of stage I-IV ovarian cancer, from which two subgroups (groups A and B) were identified.

In group A, there were 36 patients in whom surgical treatment was supplemented with first-line chemotherapy according to current standards. Within this patient group, 5 had stage I (14%), 5 had stage II (14%), 25 had stage III (69%), and 1 had stage IV ovarian cancer (3%). Loss of response to chemotherapy in this patient group was assessed on the basis of imaging examinations with CT, performed at intervals compliant with the current recommendations of the Response Evaluation Criteria in Solid Tumors (RECIST) (27, 28). Out of the 36 women in group A, drug resistance was found in 24 patients (67%), after cycle three of chemotherapy 17 patients displayed drug resistance (71%), including 2 women with stage II (12%), 14 women with stage III (82%) and 1 patient with ovarian cancer stage IV (6%) and after cycle six 7 patients displayed drug resistance (29%), including 1 patient with stage II (14%) and 6 patients with ovarian cancer stage III (86%).

Group B included 12 patients with type I ovarian cancer, including 11with stage I and 1 patient with stage IV, whose oncological treatment required only surgery. Chemotherapy was not necessary owing to the low staging of the neoplastic lesions. The control group (C) comprised of 50 women in whom the uterus and adnexa were surgically removed for non-oncological reasons.

Oncological treatment—surgical procedure including removal of the uterus with adnexa, appendix, mesh (non-mesh), pelvic minor lymph nodes, and pelvic and pre-aortic minor lymph nodes, as well as chemotherapy with cisplatin—was performed in the Gynecology and Obstetrics Department with Gynecology Oncology and Clinical Oncology Unit of Ludwik Rydygier Specialist Hospital in Kraków, Poland. Platinum resistance was defined as the recurrence of disease within 6 months after the completion of chemotherapy.

The detailed clinical characteristics of the patients are presented in Table 1. Patients treated with surgery and chemotherapy (group A) were significantly older, and their initial body weight and body mass index (BMI) were significantly lower than those of women in the other groups. Moreover, ascites and menopause were more frequent. A significant decrease in body weight under the influence of treatment was present in all the study groups ($p < 0.05$).

Materials

Tissue material collected during surgery was secured for molecular analyses in Allprotect Tissue Reagent (Qiagen, Wroclaw, Poland, Cat No./ID: 76405) in an Eppendorf tube and stored at -20°C until molecular analyses.

Blood samples were collected from the vein of the ulnar fossa from women in the study and control groups; the samples were collected into tubes designated for clotting, after which the samples were centrifuged for 10 minutes, at 1,500 ×g, at 20°C to obtain serum for further biochemical analyses. The samples were stored at -20°C until the start of the analysis.

Evaluation of CA-125 and HE4 levels

Changes in the concentrations of CA-125 and HE4 markers were assessed from the serum of patients in the pretreatment and control groups by immunohistochemistry analysis involving electroluminescence detection (immunochemical analyzer Cobas e-411 Rack, Roche Diagnostics, Warsaw, Poland). The concentrations of these markers were determined based on a solid phase antigen-antibody reaction. The samples were incubated twice, first with biotinylated monoclonal antibodies specific for CA-125 (SigmaAldrich, Poznan, Poland, Catalog no. RAB0376-1KT) and HE4 (Abcam, Cambridge, MA, USA, Cat. No. ab132299), labelled with ruthenium complexes, and second with streptavidin-labeled microparticles. The reaction mixture was then transferred to the measuring chamber, where the microparticles were magnetically attracted to the electrode surface. Subsequently, unbound substances were removed using ProCell system fluids. The

TABLE 1 Clinical and anthropometric data of patients with histopathologically confirmed diagnosis of stage I-IV ovarian cancer (groups A and B) and control subjects (group C).

Group		Test		Control	Total N=98 (100)	p-value
		A n=36 (36.7)	B n=12 (12.2)	C n=50 (51.0)		
Stage	I	5 (13.9)	11 (91.7)	0 (0)	16 (16.3)	–
	II	5 (13.9)	0 (0)	0 (0)	5 (5.1)	
	III	25 (69.4)	0 (0)	0 (0)	25 (25.5)	
	IV	1 (2.8)	1 (8.3)	0 (0)	2 (2)	
Chemotherapy	No	0 (0)	12 (100)	0 (0)	12 (12.2)	–
	Yes	36 (100)	0 (0)	0 (0)	36 (36.7)	
Chemotherapy resistance	Yes	24 (66.7)	–	–	–	–
Ascites	No	14 (38.9)	11 (91.7)	50 (100)	75 (76.5)	$p<0.001^6$
	Yes	22 (61.1)	1 (8.3)	0 (0)	23 (23.5)	
Menopause	No	6 (16.7)	6 (50)	39 (78)	51 (52)	$p<0.001^6$
	Yes	30 (83.3)	6 (50)	11 (22)	47 (48)	
Age [years]		63 (53-69.5)	47.5 (40-58.5)	46.5 (44-50)	50 (45-60)	$p<0.001^2$ A vs B** A vs C***
Age at menopause [years]		50 (50-54)	51.5 (50-53)	50 (49-52)	50 (50-53)	0.98^2
Height [cm]		160 (155-167)	162.5 (150-166)	158.5 (154-163)	159 (155-165)	0.58^2
Body weight [kg]	before surgery (1)	62.9±10.7	63.5±8.3	69.9±10	66.6±10.6	0.005^1 A vs C**
	after surgery (4 weeks) (2)	60.1±10.3 59 (52-69.5)	61.6±8 60.5 (54-69)	67.7±10 67 (61-76)	64.2±10.5 65 (55-71)	0.002^2 A vs C**
	before chemotherapy (3)	56.6±9.4	–	–	56.6±9.4	–
	p-value	$p<0.001^4$ 1 vs 2*** 2 vs 3*** 1 vs 3***	0.002^3	$p<0.001^3$	$p<0.001^4$ 1 vs 2*** 2 vs 3*** 1 vs 3***	–
BMI [kg/m^2]	before surgery (1)	24.5±4.4	25.1±4	27.6±4.5	26.1±4.7	0.003^1 A vs C**
	after surgery (4 weeks) (2)	23.5±4.4	24.4±4.1	26.8±4.5	25.2±4.7	0.001^1 A vs C**
	before chemotherapy (3)	21.8±4.1	–	–	21.8±4.1	–
	p-value	$p<0.001^4$ 1 vs 2 vs 3*** 1 vs 3***	0.003^3	$p<0.001^3$	$p<0.001^4$ 1 vs 2*** 2 vs 3*** 1 vs 3***	–

(A) ovarian cancer patients treated with surgery and chemotherapy; (B) ovarian cancer patients treated with surgery; (C) control group; BMI, body mass Index
Measurable data are presented as mean ± standard deviation or as media– with quartiles (Q1-Q3) depending on the form of distribution; p-value for groups - significance level with ANOVA[1]/Kruskal-Wallis[2] test; p-value for repeated measures - significance level with Student's t-test[3]/ANOVA[4] For repeated measures. Non-measurable data are presented a' number and percentage. p-value for groups - significance level with Chi-2[5]/Fisher's exact test[6]; ** p < 0.01 determined by the post hoc test; *** p < 0.001 determined by the post hoc test.

voltage that was applied to the electrode induced an electrochemiluminescence reaction and photon emission, which was measured using a photomultiplier. The results were read by constructing a two-point calibration curve.

Extraction of the total RNA

Extraction of total RNA was performed using TRIzol reagent (INvitrogen Life Technologies, Carlsbad, CA, USA, Cat. no. 15596026) according to the manufacturer's protocol. The isolated RNA was then evaluated qualitatively by performing electrophoretic separation of the extracts in 1% agarose gel and quantitatively by performing spectrophotometric analysis (NanoDrop ND, Thermo Fisher Scientific, Waltham, MA, USA). For further molecular analysis, only those RNA extracts that fulfilled the following conditions were qualified: 18S rRNA and 28S rRNA strands visible in the agarose gel, and the absorbance ratio at 260 nm to 280 nm was 1.8-2.0 in the quantitative evaluation.

mRNA microarray analysis

The microarray profile of mRNA expression changes that are associated with drug resistance was determined using the HG-U133A 2_0 microarray (Affymetrix, Santa Clara, CA, USA),

the GeneChip™ 3′ IVT PLUS Reagent Kit, and GeneChip™ HT 3′ IVT PLUS Reagent Kit (Thermo Fisher Scientific, Waltham, MA USA, Cat. no. 902416) according to the manufacturer's recommendations. The mRNA names and their ID number were determined from the Affymetrix NetAffx™ Analysis Center database after entering the phrase "drug resistance" (http://www.affymetrix.com/analysis/index.affx; accessed on February 2, 2022). Data were analyzed using a microarray scanning GeneArray scanner (Agilent Technologies, Santa Clara, CA, USA).

miRNA transcriptome analysis

Changes in the miRNA transcriptome in the test samples in comparison with the control samples were determined using the miRNA microarray technique GeneChip miRNA 2.0 Array (Affymetrix), as described by the manufacturer. Data were analyzed using a microarray scanning GeneArray scanner (Agilent Technologies).

Predictive evaluation of the effect of selected miRNAs on mRNAs were significantly differentiated in test samples from control samples was performed using the TargetScan database (http://www.targetscan.org; accessed on February 15, 2022) (29) and miRanda (http://mirdb.org; accessed on15 February 2022) (30, 31). According to the miRDB database, "This is an online database for miRNA target prediction and functional annotations. All the targets in miRDB were predicted using a bioinformatics tool, MirTarget, which was developed by analyzing thousands of miRNA-target interactions from high-throughput sequencing experiments. Common features associated with miRNA binding and target downregulation have been identified and are used to predict miRNA targets with machine learning methods. A predicted target with a prediction score of >80 is most likely to be real; however, if the score is below 60, then one needs to exercise caution, and it is recommended to have other supporting evidence as well" (30, 31).

Reverse-transcription quantitative polymerase chain reaction assay

To validate the semi-quantitative results of the microarray expression pattern of the mRNAs evaluated, reverse-transcription quantitative polymerase chain reaction (RT-qPCR) was performed using the SensiFast ™ SYBR No-ROX One-Step Kit (Bioline, London, UK), where β-actin was used as the endogenous control.

The thermal profile of the reaction was as follows: reverse transcription (45°C for 10 min); activation of the polymerase (95°C for 2 min); and 40 cycles of denaturation (95°C for5 s), annealing (60°C for 10 s), and elongation (72°C for 5 s). In Table 2 the nucleotide sequence of primers are presented.

Changes in gene expression were evaluated with the relative method for assessing gene transcriptional activity (also known as $2^{-\Delta\Delta CT}$).

Enzyme-linked immunosorbent assay

After rinsing the slides with phosphate-buffered saline (PBS) solution to remove blood residues, the tissue samples were mechanically homogenized in PBS (10 mg tissue per 100 µL PBS) and centrifuged for 15 min at 1,500 ×g. After collecting the supernatant, enzyme-linked immunosorbent assay (ELISA) was immediately performed.

To determine the concentration of the analyzed proteins, we used the UBA2 Elisa kit (Human ubiquitin-like modifier-activating enzyme 2 ELISA Kit, MyBioSource, Inc. San Diego, CA 92195-3308, USA, Cat. no. MBS9317388), Human GLO1 ELISA Kit (MyBioSource, Inc., Inc., San Diego, CA, USA,Cat. no. MBS761164), Human GLO1 ELISA Kit (MyBioSource, Inc., Inc., San Diego, CA, USA, Cat. no. MBS2533426), and TUFT ELISA kit (Human Tuftelin (TUFT) ELISA Kit, MyBioSource, Inc., Inc., San Diego, CA, USA, Cat. no. MBS2104898) in accordance with the manufacturer's recommendation.

Statistical analysis

Statistical analysis of data obtained in the mRNA microarray analysis was performed using the Transcriptome Analysis Console program (Thermo Fisher Scientific, Waltham, MA, USA) which links the CEL file analysis and QC features of Expression Console and the statistical analysis of TAC into a single software application." In the first step, the results were normalized using the Robust Multiarray Average (RMA) method, which consisted in the logarithmic transformation of the fluorescence signal value for each transcript ($\log_2$). Based on the $\log_2$ Fold Change (FC) value, the multiple of the difference between the expression level of mRNA transcriptomes of the

TABLE 2 Nucleotide sequences of primers used to amplify genes differentiated in the study samples (group A and B) from the control samples (group C) by the RT-qPCR.

mRNA	Primer sequence (Forward, reverse)
UBA2	Forward 5'-AAAAAGGGTGTGACCGAGTG-3' Reverse 5'-GCATCTTCTTCCCCAAACAA-3'
GLO1	Forward 5'-GCGTAGTGTGTGACTCCT-3' Reverse 5'-TCACTCGTAGCATGGTCTGC-3'
STATH	Forward 5'-TTTGCCTTCATCTTGGCTCT-3' Reverse 5'-TGTGGTTGGTATGGTTTGG-3'
TUFT1	Forward 5'-TCAGTCATGGCAACTTCAGC-3' Reverse 5'-GGGACAGTCAGGAAGTCAA-3'

UBA2, ubiquitin-like modifier-activating enzyme 2; GLO1, glyoxalase I; STATH, statherin; TUFT1, tuftelin 1; RT-qPCR, reverse-transcription-polymerase chain reaction.

compared groups was assessed, while the statistical strength of the observed difference was assessed based on the *p*-value. The criterion for recognizing a gene as differentiating required that the absolute value of the difference in fluorescence signals between the compared groups (FC) was greater than 1.1 (minimum 1.1-fold decrease or increase in signal intensity) and the *p* value < 0.05.

Data analysis was performed using the Statistica 13.3 program (Stat Soft, Poland) and R, version 4.1.1 (The R Foundation for Statistical Computing).

For non-measurable data, numeric-percentage notation was used and χ^2 or Fisher's exact test of independence was employed. Measurable data were presented as mean ± standard deviation (SD) and median with quartiles (Q1-Q3). Compliance with normal distribution was verified with the Shapiro-Wilk test.

If data were normally distributed, we used Student's t-test (comparison of the two groups) or one-way analysis of variance ANOVA with Bonferroni correction and *post-hoc* Tukey's honestly significant difference test (comparison of more than two groups) to determine the statistically significant differences in mean values. In turn, if data were skewed statistically significant differences in distributions were analyzed using Mann–Whitney U (comparison of the two groups) or Kruskal–Wallis's test with Bonferroni correction (comparison of more than two groups) and *post-hoc* Dunn's test or Scheirer–Ray–Hare test (non-parametric version of two-way ANOVA based on ranks).

Correlation analysis was performed using Spearman's correlation coefficient and its significance test. Moreover, odds ratios (OR) with their confidence intervals (Cis) were determined using univariate logistic regression models. Multivariate analysis did not identify a significant regression model. When interpreting the results, a *p*-value of < 0.05 was considered as indicating statistical significance.

Results

Concentration of the markers CA-125 and HE4

We first evaluated changes in the concentrations of the two biochemical markers currently used in diagnosis: CA-125 and HE4. Significantly higher levels of CA-125 and HE4 were observed in group A and among menopausal women. Moreover, drug resistance was associated with significantly higher CA-125 levels (Table 3; $p < 0.05$).

Microarray analysis

In the first stage of microarray analysis mRNAs that were significantly differentiated in ovarian cancer samples from control samples ($p<0.05$) were selected. Out of the 47 mRNAs associated with drug resistance, 12 mRNAs were significantly differentiated in the study samples (group A and B) from control samples (one-way ANOVA variance analysis; $p<0.05$).

According to the *post-hoc* Tukey's honestly significant difference test, we observed that seven genes, *UBA2*, *GLO1*, *STATH*, *TUFT1*, *RIC8A*, *ABCC5*, and *HPD*, were differentiated in group A vs. C samples. Five genes, *UBA2*, *GLO1*, *STATH*, *TUFT1*, and *GBF1*, were differentiated in group B vs. C samples.

TABLE 3 Concentrations of CA-125 and HE4 in groups of patients with histopathologically confirmed diagnosis of ovarian cancer (groups A and B) and control group (C), including patients undergoing chromotherapy (in A group) and menopause (total and in A group).

Group	Total N=98 (100)	Test		Control	p-value
		A n=36 (36.7)	B n=12 (12.2)	C n=50 (51.0)	
CA-125	5.3 (0.6-144.9)	320 (65-751.2)	21.4 (7.9-79)	0.6 (0.3-1)	p<0.001[2] A vs C*** B vs C***
HE4	72 (44-439)	439 (243-772.5)	83.1 (61.9-302)	44.9 (32.4-54.9)	p<0.001[2] A vs C*** B vs C*
Indicators		Ca-125		HE4	
Chemo-therapy resistance Group A	Yes	563.8 (166.7-1545.2)		485.5 (238.5-772.5)	
	No	75.5 (27.5-320)		298.5 (243.5-662.5)	
p-value		0.04[1]		0.61[1]	
Indicators		Before menopause	Menopause	Before menopause	Menopause
Total		0.9 (0.4-3)	79 (7-588.2)	47.1 (33.8-65.3)	289 (120-637)
p-value		p<0.0001[1]		p<0.0001[1]	
Chemo-therapy resistance Group A	Yes	50.6 (44-397)	588.2 (167-1821.1)	167 (98-332.5)	554.5 (289-838.5)
	No	315 (315-315)	45 (13-325)	1176.5 (482-1871)	264.5 (235-324)
p-value		0.15[3]		0.07[3]	

(A) ovarian cancer patients treated with surgery and chemotherapy; (B) ovarian cancer patients treated with surgery; (C) control group; ANOVA, analysis of variance
Measurable data are presented as mean ± standard deviation or as median with quartiles (Q1-Q3) depending on the form of distribution; p-value for groups - significance level with U Mann-Whitney[1]/Kruskal-Wallis[2] test; p-value in 2-factor analysis - significance level with Scheirer-Ray-Hare[3] test; * p < 0.05 determined by the post hoc test; p < 0.01 determined by the post hoc test.

Four genes, *UBA2*, *GLO1*, *STATH*, and *TUFT1*. were common to group A and B (Figure 1; $p < 0.05$).

RT-qPCR assay

In the next step, we quantified the expression of the four common genes differentiated in ovarian cancer samples from control samples. The same direction of expression changes of the selected transcripts by the RTqPCR technique, as in microarray analysis, was noted. We noted that the mRNA of *UBA2, GLO1, TUFT1, HPD*, and *GBF1* were upregulated in the ovarian cancer samples in comparison to the control samples (Table 4). The mRNA of *STATH*, *RIC8A*, and *ABCC5* levels were downregulated in cancer samples in comparison to the control samples (Table 4). Significantly higher absolute mRNA values, *UBA2, GLO1, STATH*, and *TUFT1*, were observed in group A (Table 4). Moreover, drug resistance was associated with significantly higher *GLO1* expression in group A ($p < 0.05$). Significantly higher mRNA values of *GLO1* were observed among women undergoing chromotherapy (in A group) and menopause (total and in A group) ($p < 0.05$).

Expression pattern of selected miRNAs

Based on the target score value, we observed the strongest link between the following entities: *UBA2* and hsa-miR-133a-3p (target score 98) and hsa-miR-133b (target score 98); *GLO1* and hsa-miR-561-5p (target score 90), *STATH* and hsa-miR-137-3p (target score 97) and has-miR-580-3p (target score 80); *TUFT1* and hsa-miR-1233-3p (target Ire 86), and hsa-miR-2052 (target score 94). It was observed that only one miRNA corresponding to hsa-miR-561-5p was downregulated in ovarian cancer samples in comparison to the control group ($p < 0.05$). For the remaining miRNAs, we found overexpression in the ovarian cancer samples compared to the controls ($p < 0.05$). In addition, we determined the same direction of change in expression in both groups of ovarian cancer samples ($p < 0.05$). Changes in the expression of the indicated miRNAs in individual groups of women with ovarian cancer in comparison with control subjects are shown in Figure 2. Then, with the use of bioinformatics tools, it was shown, which miRNAs are potentially involved in the regulation of the expression of previously selected mRNAs (Figure 3).

ELISA results

Significantly higher absolute levels of UBA2, GLO1, and TUFT1 proteins were observed in group A and among menopausal women (Table 5; $p < 0.0001$). Notably, the *STATH* protein level was significantly higher in group B ($p < 0.0001$) and among premenopausal women ($p < 0.0001$). No

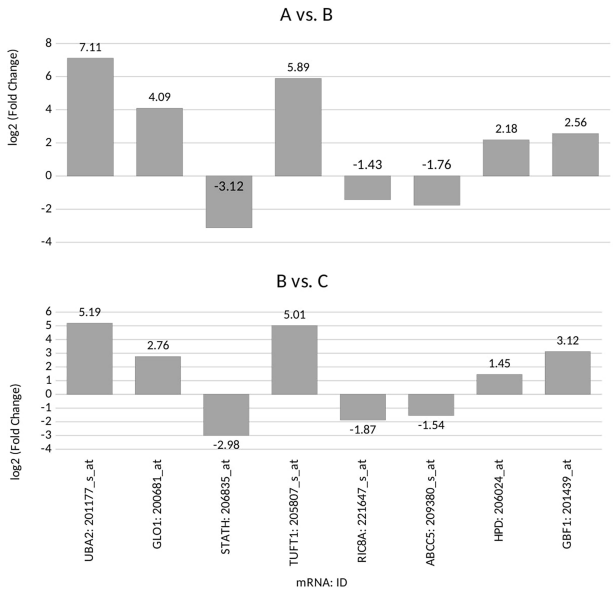

FIGURE 1
Microarray expression profile of genes associated with drug resistance differentiating between the ovarian cancer samples (groups A and B) from control samples (group C) ($p<0.05$) for: *UBA2*, ubiquitin-like modifier-activating enzyme 2; *GLO1*, glyoxalase I; *STATH*, statherin; TUFT1, tuftelin 1; *RIC8A*, RIC8 guanine nucleotide exchange factor B; *ABCC5*, ATP-binding cassette subfamily C member 5; *HPD*, 4-hydroxyphenylpyruvate dioxygenase; *GBF1*, Golgi brefeldin A-resistant guanine nucleotide exchange factor 1; (+), overexpression in comparison with the control (−);, downregulation in comparison with the control.

TABLE 4 Expression pattern of selected genes in the study groups (A and B) in comparison with the control group (C) obtained by RT-qPCR, including patients undergoing chromotherapy (in A group) and menopause (total and in A group).

mRNA	Total N=98 (100)	Comparison group				Control		p-value	
		A vs. C n=36 (36.7)		B vs. C n=12 (12.2)		C n=50 (51.0)			
UBA2	8.9 (6.3-9.4)	9.2 (8.4-9.7)		6.1 (5.9-6.9)		–		0.0002[2]	
GLO1	3.5 (2.8-4)	3.8 (3.2-4.1)		1.9 (1.7-2.1)		–		p<0.0001[2]	
STATH	-3.4±0.7	-3.5±0.6		-2.9±0.6		–		0.004[1]	
TUFT1	5.2 (4.9-7)	6.3 (5.1-7.7)		4.1 (4.1-4.6)		–		p<0.0001[2]	
mRNA		UBA2		GLO1		STATH		TUFT1	
Chemo-therapy resistance Group A	Yes	9.1 (7.6-9.8)		3.9±0.4		-3.5±0.6		6.5±1.6 6.4 (5.2-7.7)	
	No	9.2 (8.9-9.4)		3.5±0.6		-3.4±0.7		6.3±1.9	
p-value		0.99[2]		0.02[1]		0.59[1]		0.83[1]	
mRNA		Before menopause	Menopause	Before menopause	Menopause	Before menopause	Menopause	Before menopause	Menopause
Total		7.6 (6.1-9.1)	9 (6.8-9.7)	2.8±1	3.5±0.8	-3.2±0.8	-3.4±0.6	5.9±2	5.9±1.7
p-value		0.27[2]		0.02[1]		0.37[1]		0.91[1]	
Chemotherapy resistance Group A	Yes	9 (8.5-10.1)	9.2 (7.1-9.8)	4 (3.9-4.1)	3.9 (3.6-4.1)	-3.9 (-4–3.8)	-3.4 (-3.9–3.1)	7.5 (6.6-8)	6.2 (5.2-7.3)
	No	9.1 (9-9.2)	9.3 (8.9-9.5)	3.1 (3.1-3.2)	3.4 (3.1-4.1)	-3.2 (-3.2–3.1)	-3.4 (-4–3)	7.7 (5.1-10.3)	5.8 (5.1-7)
p-value		0.84[3]		0.19[3]		0.12[3]		0.92[3]	

(A) ovarian cancer patients treated with surgery and chemotherapy; (B) ovarian cancer patients treated with surgery; (C) control group; ANOVA, analysis of variance; RT-qPCR, reverse-transcription-polymerase chain reaction
UBA2, ubiquitin-like modifier-activating enzyme 2; GLO1, glyoxalase I; STATH, statherin, TUFT1, tuftelin 1; (+), overexpression in comparison with the control; (-), downregulation in comparison with the control group.
Measurable data are presented as mean ± standard deviation and median with quartiles (Q1-Q3) depending on the form of distribution; p-value for groups - significance level with t-Student[1]/U Mann Whitney[2] test; p-value in 2-factor analysis - significance level with Scheirer-Ray-Hare[3] test

significant difference was found in relation to the existence of drug resistance.

Changes in the expression of the selected mRNA-miRNA-proteins

We assessed the relationship between the expression of mRNA, miRNA regulating each mRNA, and the respective protein coded for by the selected mRNA (Table 6). For *UBA2, GLO1*, and *STATH* in both groups (groups A and B), compared with the control group, we found the same level of expression changes at the mRNA and protein levels (up/up or down/down). However, when comparing the expression between groups B and C for *TUFT1*, a different expression profile at the mRNA and protein levels (up/down) was noted. It can be concluded that overexpression of an miRNA potentially regulating the expression of a given mRNA, only for the *STATH* and (hsa-miR-137-3p or hsa-miR-580-3p) resulted in silencing at the protein level. In turn, silencing the expression of hsa-miR-561-5p, potentially regulating *GLO1* mRNA expression, resulted in its overexpression at the transcript and protein levels in the test group compared to the control.

Correlation analysis

Correlation analysis indicated a significant association between the levels of the CA-125 and HE4 markers (Table 7). Moreover, a significant association of *TUFT1* mRNA, as well as proteins UBA2, GLO1, STATH (negative correlation), and TUFT1 in relation to CA-125 and HE4 ($p < 0.0001$) was evident for all patients.

Risk factors for drug resistance in patients with ovarian cancer and the occurrence of malignancy

Figures 4 and 5 illustrate the influence of selected factors on the occurrence of drug resistance and cancer. A significantly higher risk of drug resistance in group A patients was observed in women with stage III/IV disease due to increased expression of *GLO1* mRNA and protein encoded by this gene. A significantly higher cancer risk was associated with menopause, age, lower BMI, and higher levels of HE4 and UBA2 protein.

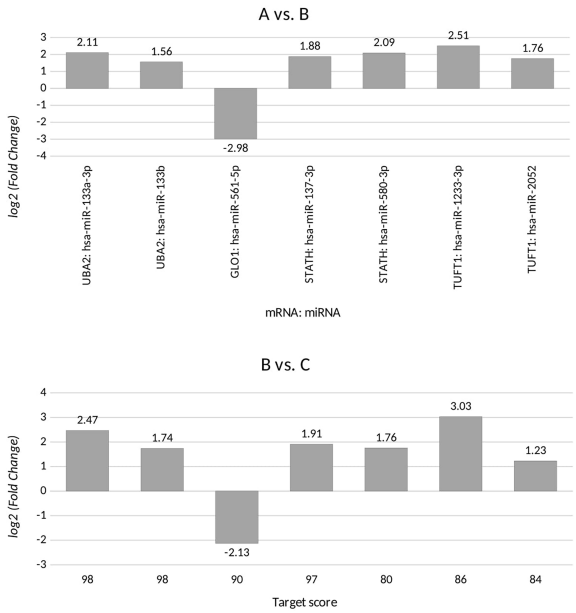

FIGURE 2
Changes in miRNA expression levels for differentiating ovarian cancer samples (groups A and B) from control samples (group C) that are potentially involved in regulating the expression of the selected transcripts, for *UBA2*, ubiquitin-like modifier-activating enzyme 2; *GLO1*, glyoxalase I; *STATH*, statherin, *TUFT1*, tuftelin 1; *RIC8A*, RIC8 guanine nucleotide exchange factor B; *ABCC5*, ATP-binding cassette subfamily C member 5; *HPD*, 4-hydroxyphenylpyruvate dioxygenase; *GBF1*, Golgi brefeldin A-resistant guanine nucleotide exchange factor 1. (+), overexpression in comparison with the control; (-), downregulation in comparison with the control.

FIGURE 3
miRNAs affecting the transcriptional activity of genes differentiating ovarian cancer samples compared to the control samples. *UBA2*, ubiquitin-like modifier-activating enzyme 2; *GLO1*, glyoxalase I; *STATH*, statherin, *TUFT1*, tuftelin 1; *RIC8A*, RIC8 guanine nucleotide exchange factor B; *ABCC5*, ATP-binding cassette subfamily C member 5; *HPD*, 4-hydroxyphenylpyruvate dioxygenase; *GBF1*, Golgi brefeldin A-resistant guanine nucleotide exchange factor 1.

TABLE 5 Differences in the concentration of UBA2, GLO1, TUFT1, and STATH in the study (A and B) and control (C) groups obtained by ELISA assay, and their relationship with chemotherapy resistance including patients undergoing chromotherapy (in A group) and menopause (total and in A group).

Protein	Total N=98 (100)	Test				Control		p-value	
		A n=36 (36.7)		B n=12 (12.2)		C n=50 (51.0)			
UBA2	2 (0.9-4.2)	4.5 (4.1-4.9)		2.2 (2.2-2.6)		0.9 (0.5-1.1)		p<0.0001[3] A vs B* A vs C*** B vs C**	
GLO1	5.3 (3.4-55)	56.6 (55-58.4)		14.2 (12.8-15)		3.4 (3.2-3.9)		p<0.0001[3] A vs B* A vs C*** B vs C**	
STATH	19.1 (12.7-24.6)	12.3 (11.5-12.8)		99.6 (95.1-103.9)		23.6 (19.1-24.6)		p<0.0001[3] A vs B*** A vs C*** B vs C**	
TUFT1	1 (0.6-12.5)	12.9 (11.9-13.9)		7.4 (7.2-7.8)		0.6 (0.6-0.8)		p<0.0001[3] A vs B* A vs C*** B vs C**	
Protein		UBA2		GLO1		STATH		TUFT1	
Chemotherapy resistance Group A	Yes	4.5±0.5		57.4±2.5		12.2±0.9		13.3±1.6	
	No	4.4±0.5		54.9±4		12.2±0.9		12.8±1.1	
p-value		0.73[1]		0.07[1]		0.88[1]		0.32[1]	
Protein		Before menopause	Menopause	Before menopause	Menopause	Before menopause	Menopause	Before menopause	Menopause
Total		1.1 (0.8-2)	4.1 (1.9-4.8)	3.8 (3.2-5.3)	54.5 (12-57.8)	23.6 (18-24.8)	12.8 (11.9-24.5)	0.7 (0.6-1)	11.9 (7-13.5)
p-value		p<0.0001[2]		p<0.0001[2]		p<0.0001[2]		p<0.0001[2]	
Chemotherapy resistance Group A	Yes	4.2 (4-4.6)	4.5 (4.1-4.9)	58.7 (55.9-61.2)	57.3 (55.2-58.8)	12.2 (11.7-12.6)	12.3 (11.5-12.9)	13.8 (12.7-15.5)	12.9 (12-13.8)
	No	3.7 (3.3-4.1)	4.7 (4.2-4.9)	54.5 (54.2-54.9)	54.8 (51.2-57)	13.3 (13-13.6)	12.1 (11.5-12.7)	12.3 (11.8-12.8)	12.8 (11.8-13.8)
p-value		0.21[4]		0.4[4]		0.05[4]		0.24[4]	

(A) ovarian cancer patients treated with surgery and chemotherapy; (B) ovarian cancer patients treated with surgery; (C) control group.
ELISA, enzyme-linked immunosorbent assay; UBA2, ubiquitin-like modifier-activating enzyme 2; GLO1, glyoxalase I; STATH, statherin, TUFT1, tuftelin 1
Measurable data are presented as mean ± standard deviation or as median with quartiles (Q1-Q3) depending on the form of distribution; p-value for groups - significance level with Student's t-test[1]/U Mann-Whitney[2]/Kruskal-Wallis[3] test; p-value in 2-factor analysis - significance level with Scheirer-Ray-Hare[4] test; * $p < 0.05$ determined by the post hoc test; ** $p < 0.01$ determined by the post hoc test; *** $p < 0.001$ determined by the post hoc test.

Discussion

Despite many years of research and the development of modern diagnostic techniques including biochemical and molecular analyses, ovarian cancer is diagnosed at very late stages and the available treatments do not provide the expected outcome, which is attributed to the development of drug resistance during chemotherapy (7, 32).

In our analysis, we evaluated changes in the levels of biochemical markers—CA-125 and HE4—and the expression profile of genes and proteins encoded by them associated with drug resistance in patients with ovarian cancer in comparison to control subjects. Significantly higher concentrations of these markers were found in the serum of patients in the study group, regardless of whether treatment was supplemented with chemotherapy or not. Higher levels of CA-125 and HE4 being

TABLE 6 Summarizing the changes in the expression of the selected mRNA-miRNA-protein for differentiating ovarian cancer samples (groups A and B) from control samples (group C).

Group	A vs. C			B vs. C		
Expression	mRNA	miRNA related to mRNA	Protein	mRNA	miRNA related to mRNA	Protein
UBA2	*up*	*up*	*up*	*up*	*up*	*up*
GLO1	*up*	*down*	*up*	*up*	*down*	*up*
STATH	*down*	*up*	*down*	*up*	*up*	*up*
TUFT	*up*	*up*	*up*	*down*	*up*	*up*

(up), overexpression in comparison with the control; (down), downregulation in comparison with the control; (A) ovarian cancer patients treated with surgery and chemotherapy; (B) ovarian cancer patients treated with surgery; (C) control group.
UBA2, ubiquitin-like modifier-activating enzyme 2; GLO1, glyoxalase I; STATH, statherin, TUFT1, tuftelin 1.

TABLE 7 Correlation between levels of biochemical and molecular markers, as values of Spearman's R coefficients and the significance *p*-value, among women with ovarian cancer (groups A and B) compared with those of women in the control group (C).

Ca-125 vs.		Total N=98 (100)	Test		Control
			A n=36 (36.7)	B n=12 (12.2)	C n=50 (51.0)
HE4		0.84 p<0.001	0.45 p=0.02	0.72 p=0.02	0.34 p=0.055
mRNA	UBA2	0.22 p=0.2	-0.11 p=0.61	0.19 p=0.6	–
	GLO1	0.44 p=0.007	0.03 p=0.89	0.15 p=0.68	–
	STATH	-0.07 p=0.71	0.03 p=0.89	0.49 p=0.15	–
	TUFT1	0.51 p=0.001	0.13 p=0.54	0.44 p=0.2	–
Protein	UBA2	0.76 p<0.0001	0.29 p=0.14	0.07 p=0.85	-0.21 p=0.22
	GLO1	0.83 p<0.0001	-0.09 p=0.65	0.76 p=0.01	0.21 p=0.22
	STATH	-0.49 p<0.0001	-0.26 p=0.2	-0.05 p=0.88	-0.16 p=0.36
	TUFT1	0.8 p<0.0001	-0.13 p=0.52	0.2 p=0.58	-0.0008 p=0.996
Ca-125 vs.		mRNA-UBA2	mRNA-GLO1	mRNA-STATH	mRNA-TUFT1
Chemotherapy resistance	Yes	-0.08 p=0.75	-0.12 p=0.63	-0.3 p=0.23	-0.09 p=0.74
	No	-0.29 p=0.49	-0.4 p=0.32	0.69 p=0.06	0.38 p=0.35
Ca-125 vs.		Protein-UBA2	Protein -GLO1	Protein -STATH	Protein -TUFT1
Chemotherapy resistance	Yes	0.47 p=0.05	-0.27 p=0.28	-0.24 p=0.33	-0.37 p=0.13
	No	0.34 p=0.42	-0.69 p=0.06	-0.3 p=0.47	0.17 p=0.69
HE4 vs.		Total N=98 (100)	Test		Control
A n=36 (36.7)	B n=12 (12.2)	C n=50 (51.0)			
mRNA	UBA2	0,13 p=0,38	-0,12 p=0,48	0,6 p=0,07	–
	GLO1	0,19 p=0,21	-0,14 p=0,43	-0,27 p=0,45	–
	STATH	0,23 p=0,13	0,34 p=0,04	0,72 p=0,02	–
	TUFT1	0,42 p=0,004	0,24 p=0,15	0,26 p=0,47	–
Protein	UBA2 [ng/mL]	0,72 p<0.0001	0,09 p=0,58	0,11 p=0,76	-0,08 p=0,65
	GLO1 [pg/mL]	0,74 p<0.0001	-0,15 p=0,37	0,76 p=0,01	0,04 p=0,79
	STATH [pg/mL]	-0,52 p<0.0001	0,05 p=0,77	-0,08 p=0,83	-0,04 p=0,82
	TUFT1 [pg/mL]	0,7 p<0.0001	-0,08 p=0,65	0,21 p=0,56	-0,24 p=0,15
HE4 vs.		MRNA-UBA2	MRNA-GLO1	MRNA-STATH	MRNA-TUFT1
Chemotherapy resistance	Yes	-0.28 p=0.19	-0.12 p=0.59	0.24 p=0.26	0.28 p=0.19
	No	0.29 p=0.35	-0.29 p=0.35	0.57 p=0.05	0.15 p=0.63
HE4 vs.		Protein-UBA2	Protein -GLO1	Protein STATH	Protein TUFT1
Chemotherapy resistance	Yes	0.14 p=0.53	-0.17 p=0.43	-0.04 p=0.85	-0.18 p=0.4
	No	-0.02 p=0.94	-0.14 p=0.66	0.33 p=0.29	0.09 p=0.78
mRNA vs.		mRNA-UBA2 +	mRNA-GLO1 +	mRNA-STATH -	mRNA-TUFT1 +
Protein	UBA2	0.32 p=0.03	0.57 p<0.0001	-0.35 p=0.01	0.42 p=0.003
	GLO1	0.46 p<0.0001	0.61 p<0.0001	-0.43 p=0.002	0.5 p<0.0001
	STATH	-0.56 p<0.0001	-0.58 p<0.0001	0.39 p=0.01	-0.49 p<0.0001
	TUFT1	0.57 p<0.0001	0.63 p<0.0001	-0.14 p=0.35	0.49 p<0.0001

(A) ovarian cancer patients treated with surgery and chemotherapy; (B) ovarian cancer patients treated with surgery; (C) control group.
UBA2, ubiquitin-like modifier-activating enzyme 2; GLO1, glyoxalase I; STATH, statherin, TYFT1, tuftelin 1.
The results of the analyses are presented as values of Spearman's R coefficients together with the result of the significance test (p-value).

characteristic of patients in group A, in whom resistance to cisplatin was observed, and in premenopausal age.

Potenza et al. evaluated 78 patients diagnosed with epithelial ovarian cancer regarding the utility of CA-125 and HE4 determination in monitoring response to cytotoxic treatment. The authors concluded that both parameters are good markers of loss of adequate response to treatment, as their levels were not recorded after the third cycle of chemotherapy in patients with an initially good response to treatment (33). Nevertheless, Castella et al., who also evaluated changes in CA-125 and HE4 levels among 72 patients with ovarian cancer, reported that an increase in biomarkers corresponded with disease recurrence, confirmed by diagnostic imaging, in most patients, although in some women, there was an upward trend in the CA-125 and HE4 levels not associated with recurrence (34). This leads to the search for new markers, mainly at the molecular level, on the

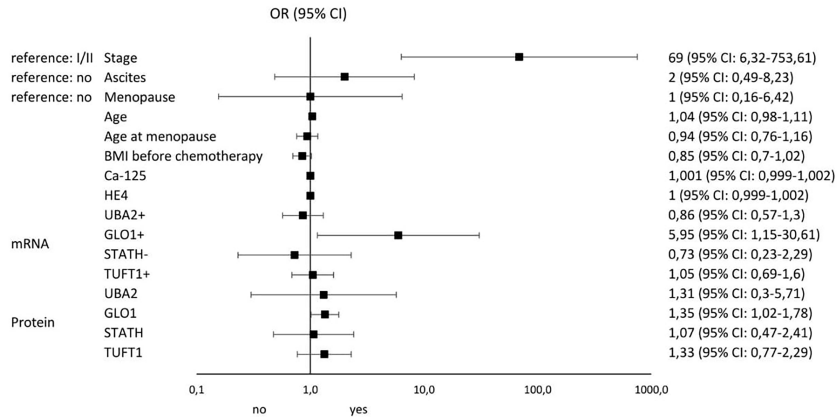

FIGURE 4
Results of univariable logistic regression analysis - odds ratio (OR) and its 95% confidence interval (95% CI) for the relationship between the occurrence of chemotherapy resistance (no/yes) and particular classification variables in group A of patients with histopathologically confirmed diagnosis of stage I-IV ovarian cancer, treated with surgery and supplemented with chemotherapy as per –tandard guidelines.

basis of which the occurrence of drug resistance can be established before its phenotypic manifestation, because molecular changes precede phenotypic changes (35, 36). It is a more reasonable approach as we demonstrated significant correlation between CA-125 and HE4 levels and the four proteins that were differentiated in the test samples in groups A and B from control samples ($p < 0.05$). Studies on a larger population of patients should be performed to determine the usefulness of CA-125 and HE4 analyses and the mentioned proteins in the diagnosis of ovarian cancer and determination of resistance to chemotherapy.

In our study, we found drug resistance in 24 of 36 patients (66.7%) in whom surgery was supplemented with chemotherapy. Therefore, in the second stage of our study, we decided to assess the changes in the expression of genes related to the drug resistance phenomenon that were specifically differentiated in the study group from control samples and the miRNAs that potentially regulate their expression in groups A and B. Based on microarray evaluation of the collected samples, we showed that, in the cases of ovarian cancer, irrespective of the stage and selected treatment option, the expression profile of mRNAs and miRNAs were related to drug resistance changes. mRNAs corresponding to genes *UBA2*, *GLO1*, *STATH*, and *TUFT1*, were differentiated in the study samples, irrespective of the stage of ovarian cancer from the control samples, and we decided to focus on them in further analyses.

He at al. observed a significant increase in the gene and protein expression of *UBA2* in colorectal cancer samples when compared with control samples, identifying overexpression of this gene as an adverse prognostic marker (37). Moreover, UBA2 participates in the processes of tumor progression, invasion, and metastasis through the Wnt-dependent pathway, consequently

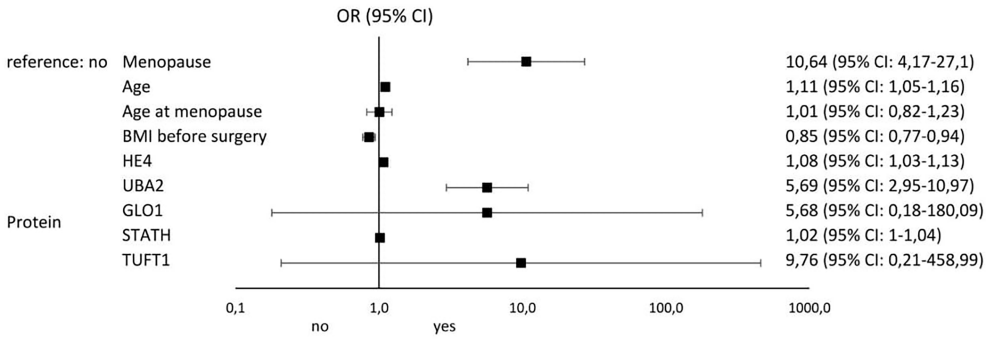

FIGURE 5
Results of univariable logistic regression analysis - odds ratio (OR) and its 95% confidence interval (95% CI) for the relationship between the occurrence of cancer (no/yes) and the particular classification variables of all patients in the study groups (A, B, and C).

promoting epithelial–mesenchymal transition (38). In our analysis, we demonstrated overexpression of *UBA2* mRNA, and the protein coded by it in ovarian cancer samples ($p < 0.05$), it was higher in group A where surgical treatment was complemented by chemotherapy when compared with group B where treatment was terminated by surgery. Nevertheless, we did not identify any relationship between cisplatin drug resistance and UBA2 expression ($p > 0.05$).

Our analysis also showed that *GLO1* mRNA were differentiated in study samples from control samples and is the only transcript among the four mRNAs selected for which we could identify a significant association with the occurrence of cisplatin drug resistance (OR = 5.95; 95% CI 1.15-30.61; $p = 0.02$). Among patients who lost adequate response to treatment, *GLO1* expression was significantly higher than that among women with ovarian cancer responding to chemotherapy ($p < 0.05$). Overexpression of *GLO1*, which encodes for glyoxalase 1, is closely associated with the occurrence of multidrug resistance in the context of not only tumorigenesis (39) but also infections caused by microorganisms (40). It plays a critical role in the development of innate and acquired drug resistance, and in cancer, overexpression of the *GLO1* gene and protein is characteristic of cells with high glycolytic rates (39). Thus, considering the enzymatic activity of glyoxalase 1 catalyzing the conversion of methylglyoxal, a natural antibiotic to glutathione D-lactate, it should be assumed that loss of response to treatment is associated with accumulation of glutathione D-lactate and reduction in glutathione (glyoxalase II) in the cells. This is accompanied by a decrease in the concentration of the substrate methylglyoxal, a cytotoxic byproduct of glycolysis that activates cell apoptosis (41). Sakamoto et al. confirmed significantly higher expression of GLO1 in human monocytic leukemia cell lines, i.e., UK711, K562/ADM, and UK110 cells. These authors indicated that GLO1 inhibits apoptosis of cancer cells by inactivating caspases treated with anticancer drugs, while noting that this may be a reversible effect (42). Interesting in this regard the study of Tamori et al., conducted on a breast cancer model, also confirmed that GLO1 expression is dependent on the histopathological grade of tumor malignancy (χ^2 test, p = 0.002) and was significantly higher in basal cell breast cancer (43). Additionally, our study observed higher *GLO1* expression among patients with drug resistance, which is consistent with the observations of Alhujaly et al. who found that overexpression of this gene and protein reduces the antitumor properties of cisplatin, among others (44).

Moreover, we observed an increase in the mRNA and protein expression of TUFT1 in group A as compared with the control group and group B. However, we did not confirm that changes in the TUFT1 expression profile depend on the occurrence of drug resistance to platinum compounds in ovarian cancer. Thus, we speculate that TUFT1 may serve as a complementary molecular marker in differentiating the clinical stage of ovarian cancer. Such a conclusion seems reasonable taking into account observations made by Yang et al. who found that overexpression of TUFT1 mRNA and protein is characteristic for identifying higher clinical stages of colorectal cancer (stages III and IV) and development of vincristine resistance through the PI3K/AKT pathway (45). Dou et al. confirmed the association between TUFT1 overexpression and unfavorable prognosis among patients with intrahepatic cancer, which is directly related to HIF1-α overexpression and induction of oxidative stress (46).

The last mRNA that was differentiated in the test samples from control samples was the *STATH* gene, for which we noted decreased expression in cancer samples. To the best of our knowledge, this is the first study to report STATH expression in cancer samples. Two studies that evaluated the utility of STATH1 determination in clinical samples have been published thus far. The first one, by Sakurada et al., demonstrated the potential ability to differentiate nasal from vaginal secretions in forensic examinations based on the presence of the STATH1 protein (present only in nasal secretions) (47). The second one, by Gilbert and Stayton, indicated the presence of STATH1 in salivary secretions, where it participates in enamel mineralization and is produced by the human body in natural and recombinant forms (48).

We complemented our analysis of drug resistance-associated mRNA transcriptome by determining the expression pattern of miRNAs that potentially regulate the expression of the selected transcripts and testing this effect by determining the concentration of proteins encoded by the selected genes.

The influence of the selected miRNAs regulating the expression of the indicated mRNAs seems as feasible because for all of them the target score was >80. Thus, considering the results of the predictive analysis of the interaction between mRNA and miRNA and expression at the protein level, it seems correct that miRNAs not only act as negative regulators of expression at the post-transcriptional level but also can enhance expression, resulting in protein overexpression (49–51).

The analysis indicated that hsa-miR-133a-3p and hsa-miR-133b are molecules that regulate *UBA2* expression. The study published by Ukey et al. showed that assessment of hsa-miR-133a-3p levels may be a useful marker of oral squamous cell carcinoma risk (52). Additionally, the observations of Chang et al. are interesting, also showed that overexpression of hsa-miR-133a-3p in the sciatic nerve in rats was associated with more severe pain when compared with control rats. These authors also pointed out to the possibility of using the mentioned miRNA as a promising therapeutic target (53). Asai et al. reported a significant silencing of miR-133a-3p and miR-133b expression in head and neck squamous cell carcinoma samples (54), highlighting that the literature data indicate that miR-133a-3p and miR-133b acted as tumor-suppressive miRNAs (55).

Another miRNA involved in regulating expression of the selected genes is hsa-miR-561-5p, whose decreased expression in

ovarian cancer samples resulted in protein overexpression in groups A and B compared with those in the control group. Our observations are in contrast to those in the reports of Chen et also demonstrated elevated expression of hsa-miR-561-5p in the liver cancer tissue, indicating that, along with miR-137, miR-149-5p is closely associated with the metastatic potential of liver cancer cells and the formation of lung metastases (56). Xi et al. found silencing of miR-561-5p expression in pancreatic ductal adenocarcinoma cell samples. The silencing of its expression resulted in decreased tumor cell proliferative potential, migration, and invasion (57).

This finding is supported by the complex nature of the miRNAs involved, where one miRNA in some tumor types is described as a pro-tumorigenic factor in one tumor lesion and as a tumor growth suppressor in another.

This situation was reported for miR-29, which was silenced in lung cancer and overexpressed in breast cancer samples (58). This may be because the same miRNA participates in different signaling pathways, which translates into the regulation of biological processes. In addition, nearly 60% of all mRNAs are regulated by miRNAs (59).

We observed that overexpression of hsa-miR-137-3p and hsa-miR-580-3p was involved in the regulation of *STATH* expression, with the silencing of STATH protein expression most likely in group A as a result of the aforementioned mRNA-miRNA interaction, while a contradicting outcome was observed in group B when compared with control samples. Considering that STATH expression is different in both groups, it is possible that the expression of the gene itself and the protein encoded by it, as well as miRNAs regulating its expression, depends on the clinical stage of the ovarian cancer lesions. In the case of miR-137-3p and hsa-miR-580-3p, it can be assumed that their expression is tissue specific, as Ding et al. confirmed that the silencing of miR-137-3p expression in colorectal cancer samples (60) and Dong et al. reported reduced expression in non-small cell lung cancer samples (61).

The last miRNAs evaluated are hsa-miR-1233-3p and hsa-miR-2052, whose expression was significantly higher in ovarian cancer samples than in control samples. Overexpression of miR-1233-3p was found among patients with renal cell carcinoma and was considered an adverse prognostic marker. Dias et al. determined the expression of specific miRNAs by using the liquid biopsy technique, which allows the determination of the concentration of selected biomolecules in body fluids, including blood, serum, and lavage. It plays a role in diagnosis and monitoring of therapy (62). miR-2052 has been described in the context of severe acute respiratory syndrome coronavirus 2 infection (63).

Thus, the analysis of drug resistance-associated miRNAs performed in this study indicates that the role of these regulatory molecules in the context of ovarian cancer has been insufficiently described.

In the last stage of our analysis, we summarize the risk factors significantly influencing the occurrence of drug resistance among patients with ovarian cancer. The most important were stage (OR: 69; 95% CI 6.32-753.61), *GLO1* mRNA overexpression (OR: 5.95; 95% CI 1.15-30.51), and ascites (OR: 2; 95% CI 0.49-8.32). The most significant factors predisposing to the development of ovarian cancer include menopause (OR: 10.64; 95% CI 4.17-27.1), TUFT1 protein overexpression (OR: 9.76; 95% CI 0.21-458.99), UBA2 protein overexpression (OR: 5.69; 95% CI 2.95-10.97), and GLO1 protein overexpression (OR: 5.68; 95% CI 0.18-180.09). Thus, it seems that screening diagnosis of ovarian cancer should be supplemented by GLO1, TUFT1, and UBA2 determination and assessment of the risk of loss of adequate response to chemotherapy by *GLO1* mRNA expression pattern determination. Of particular interest to clinicians should be the occurrence of ascites in oncology patients, as it significantly increases the risk of drug resistance to cisplatin.

As recent events surrounding the coronavirus disease pandemic have shown, understanding molecular mechanisms is invariably important and the development and introduction of commercially available diagnostic tests can be simple, effective, and useful.

Our study has both strengths and weaknesses. The strengths include the use of modern techniques to assess changes in mRNA and miRNA transcriptome expression, as well as the association of the observed changes with the concentration of proteins encoded by the selected genes. Although the sample size of the study and control groups may seem relatively small, it should be kept in mind that this is a single-center study, and its duration is short. Therefore, the study, although important, should be extended in the future.

Summary

The analysis showed the greatest association with drug resistance for the following mRNAs and miRNAs: *UBA2* and hsa-miR-133a-3p, and hsa-miR133b; *GLO1* and hsa-miR61-5p; *STATH* and hsa-miR-137-3p, and hsa-miR-580-3p, *TUFT1* and hsa-miR-1233-3p, and hsa-miR-2052. The importance of determination of the biochemical markers CA-125 and HE4 in the diagnosis of ovarian cancer should not be marginalized. Our study suggests supplementing the current diagnostic approach by determining the expression profile of GLO1, TUFT1, and UBA2 and assessing the risk of loss of adequate response to chemotherapy by determining the *GLO1* mRNA expression pattern. Of particular interest to clinicians should be the occurrence of ascites in female cancer patients, which is an unfavorable prognostic factor because it significantly increases the risk of cisplatin resistance. Finally, we confirmed the validity of molecular assessment and the fact that molecular changes

precede phenotypic changes, as we determined changes in gene, miRNA, and protein expression in cancer samples before the finding of cisplatin drug resistance among ovarian cancer patients.

Data availability statement

The datasets presented in this study can be found in online repositories. The names of the repository/repositories and accession number(s) can be found in the article/supplementary material.

Ethics statement

The studies involving human participants were reviewed and approved by Bioethical Committee operating at the Regional Medical Chamber in Kraków, no. 185/KBL/OIL/2020 and 186/KBL/OIL/2020, dated September 20, 2020. Informed consent was obtained from all patients. The patients/participants provided their written informed consent to participate in this study.

Author contributions

Conceptualization, MO and BG; methodology, MO and AŚ; software, EN; investigation, MO, BG, and AŚ; resources, DB; data curation, BG; writing-original draft preparation, PJ, MO, BG; writing-review and editing, RS; supervision, MO and BG; project administration, BG and MO. All authors have read and agreed to the published version of the manuscript.

Acknowledgments

We would like to thank Nikola Zmarzły, PhD for helping with data analysis and improving our paper.

Conflict of interest

The authors declare that the research was conducted in the absence of any commercial or financial relationships that could be construed as a potential conflict of interest.

Publisher's note

References

1. Reid BM, Permuth JB, Sellers TA. Epidemiology of ovarian cancer: A review. *Cancer Biol Med* (2017) 14(1):9–32. doi: 10.20892/j.issn.2095-3941.2016.0084

2. Momenimovahed Z, Tiznobaik A, Taheri S, Salehiniya H. Ovarian cancer in the world: Epidemiology and risk factors. *Int J Womens Health* (2019) 11:287–99. doi: 10.2147/IJWH.S197604

3. Eisenhauer EA. Real-world evidence in the treatment of ovarian cancer. *Ann Oncol* (2017) 28:viii61–5. doi: 10.1093/annonc/mdx443

4. Menon U, Karpinskyj C, Gentry-Maharaj A. Ovarian cancer prevention and screening. *Obstetrics Gynecol* (2018) 131(5):909–27. doi: 10.1097/AOG.0000000000002580

5. Cancer (IARC). *T.I.A. for R. on Global Cancer Observatory*. Available at: https://gco.iarc.fr/.

6. Stewart C, Ralyea C, Lockwood S. Ovarian cancer: An integrated review. *Semin Oncol Nursing* (2019) 35(2):151–6. doi: 10.1016/j.soncn.2019.02.001

7. Torre LA, Trabert B, DeSantis CE, Miller KD, Samimi G, Runowicz CD, et al. Ovarian cancer statistics, 2018. *CA: A Cancer J Clin* (2018) 68(4):284–96. doi: 10.3322/caac.21456

8. Zhang Y, Luo G, Li M, Guo P, Xiao Y, Ji H, et al. Global patterns and trends in ovarian cancer incidence: Age, period and birth cohort analysis. *BMC Cancer* (2019) 19(1):984. doi: 10.1186/s12885-019-6139-6

9. Palmer M, Saito E. Age-specific incidence rates of ovarian cancer worldwide. *Japanese J Clin Oncol* (2020) 50(9):1086–7. doi: 10.1093/jjco/hyaa148

10. Liu Y, Ma L, Yang X, Bie J, Li D, Sun C, et al. Menopausal hormone replacement therapy and the risk of ovarian cancer: A meta-analysis. *Front Endocrinol* (2019) 10:801. doi: 10.3389/fendo.2019.00801

11. Temkin SM, Mallen A, Bellavance E, Rubinsak L, Wenham RM. The role of menopausal hormone therapy in women with or at risk of ovarian and breast cancers: Misconceptions and current directions. *Cancer* (2019) 125(4):499–514. doi: 10.1002/cncr.31911

12. Herreros-Villanueva M, Chen CC, Tsai EM, Er TK. Endometriosis-associated ovarian cancer: What have we learned so far? *Clinica Chimica Acta* (2019) 493:63–72. doi: 10.1016/j.cca.2019.02.016

13. Sumanasekera WK. Epidemiology of ovarian cancer: Risk factors and prevention. *BJSTR* (2018) 11(2):8405–17. doi: 10.26717/BJSTR.2018.11.002076

14. Abdulaziz G, Welc NA, Gąsiorowska E, Nowak-Markwitz E. Assessment of gynecological and lifestyle-related risk factors of ovarian cancer. *Prz Menopauzalny* (2021) 20(4):184–92. doi: 10.5114/pm.2021.109847

15. Xu Y, Jia Y, Zhang Q, Du Y, He Y, Zheng A. Incidence and risk factors for postoperative venous thromboembolism in patients with ovarian cancer: Systematic review and meta-analysis. *Gynecologic Oncol* (2021) 160(2):610–8. doi: 10.1016/j.ygyno.2020.11.010

16. Whitwell HJ, Worthington J, Blyuss O, Gentry-Maharaj A, Ryan A, Gunu R, et al. Improved early detection of ovarian cancer using longitudinal multimarker models. *Br J cancer* (2020) 122(6):847–56. doi: 10.1038/s41416-019-0718-9

17. Yang L, Wang S, Zhang QI, Pan Y, Lv Y, Chen X, et al. Clinical significance of the immune microenvironment in ovarian cancer patients. *Mol omics* (2018) 14(5):341–51. doi: 10.1039/C8MO00128F

18. Kurman RJ, Shih IM. The origin and pathogenesis of epithelial ovarian cancer- a proposed unifying theory. *Am J Surg Pathol* (2010) 34(3):433–43. doi: 10.1097/PAS.0b013e3181cf3d79

19. Forstner R, Meissnitzer M, Cunha TM. Update on imaging of ovarian cancer. *Curr Radiol Rep* (2016) 4(6):31. doi: 10.1007/s40134-016-0157-9

20. Risum S, Høgdall C, Loft A, Berthelsen AK, Høgdall E, Nedergaard L, et al. The diagnostic value of PET/CT for primary ovarian cancer–a prospective study. *Gynecologic Oncol* (2007) 105(1):145–9. doi: 10.1016/j.ygyno.2006.11.022

21. Rustin GJS. Use of CA-125 to assess response to new agents in ovarian cancer trials. *J Clin Oncol* (2003) 2110 Suppl:187s–93s. doi: 10.1200/JCO.2003.01.223

22. Razmi N, Hasanzadeh M. Current advancement on diagnosis of ovarian cancer using biosensing of CA 125 biomarker: Analytical approaches. *TrAC Trends Analytical Chem* (2018) 108:1–12. doi: 10.1016/j.trac.2018.08.017

23. Huang J, Chen J, Huang Q. Diagnostic value of HE4 in ovarian cancer: A meta-analysis. *Eur J Obstetrics Gynecology Reprod Biol* (2018) 231:35–42. doi: 10.1016/j.ejogrb.2018.10.008

24. Dochez V, Caillon H, Vaucel E, Dimet J, Winer N, Ducarme G. Biomarkers and algorithms for diagnosis of ovarian cancer: CA125, HE4, RMI and ROMA, a review. *J Ovarian Res* (2019) 12(1):28. doi: 10.1186/s13048-019-0503-7

25. Elies A, Rivière S, Pouget N, Becette V, Dubot C, Donnadieu A, et al. The role of neoadjuvant chemotherapy in ovarian cancer. *Expert Rev Anticancer Ther* (2018) 18(6):555–66. doi: 10.1080/14737140.2018.1458614

26. Ai Z, Lu Y, Qiu S, Fan Z. Overcoming cisplatin resistance of ovarian cancer cells by targeting HIF-1-Regulated cancer metabolism. *Cancer Letters* (2016) 373 (1):36–44. doi: 10.1016/j.canlet.2016.01.009

27. Basta A, Bidziński M, Bieńkiewicz A, Blecharz P, Bodnar L, Jach R, et al. Rekomendacje polskiego towarzystwa ginekologii onkologicznej dotyczące diagnostyki I leczenia raka jajnika wersja 2015.1. *Onkologia w Praktyce Klinicznej - Edukacja* (2015) 1(2):83–93.

28. Płużański A. Evaluation of response to treatment — criteria RECIST 1.1. nowotwoal. *J Oncol* (2014) 64(4):331–5. doi: 10.5603/NJO.2014.0055

29. Agarwal V, Bell GW, Nam JW, Bartel DP. Predicting effective microRNA target sites in mammalian mRNAs. *eLife* (2015) 4:e05005. doi: 10.7554/eLife.05005

30. Chen Y, Wang X. miRDB: An online database for prediction of functional microRNA targets. *Nucleic Acids Res* (2020) 48(D1):D127–31. doi: 10.1093/nar/gkz757

31. Liu W, Wang X. Prediction of functional microRNA targets by integrative modeling of microRNA binding and target expression data. *Genome Biol* (2019) 20 (1):18. doi: 10.1186/s13059-019-1629-z

32. Armstrong DK, Alvarez RD, Bakkum-Gamez JN, Barroilhet L, Behbakht K, Berchuck A, et al. Ovarian cancer, version 2.2020, NCCN clinical practice guidelines in oncology. *J Natl Compr Cancer Network* (2021) 19(2):191–226. doi: 10.6004/jnccn.2021.0007

33. Potenza E, Parpinel G, Laudani ME, Macchi C, Fuso L, Zola P. Prognostic and predictive value of combined HE-4 and CA-125 biomarkers during chemotherapy in patients with epithelial ovarian cancer. *Int J Biol Markers* (2020) 35(4):20–7. doi: 10.1177/1724600820955195

34. Castella J, Taus Á, Esteban B, Espuelas S, Fabrego B, Rovira EM, et al. 800 the role of Ca-125 and HE-4 in epithelial ovarian cancer follow-up. *Int J Gynecologic Cancer* (2021) 31(Suppl 3):1–395. doi: 10.1136/ijgc-2021-ESGO.474

35. Cheng X, Zhang L, Chen Y, Qing C. Circulating cell-free DNA and circulating tumor cells, the "Liquid biopsies" in ovarian cancer. *J Ovarian Res* (2017) 10(1):75. doi: 10.1186/s13048-017-0369-5

36. Obermayr E, Castillo-Tong DC, Pils D, Speiser P, Braicu I, Van Gorp T, et al. Molecular characterization of circulating tumor cells in patients with ovarian cancer improves their prognostic significance — a study of the OVCAD consortium. *Gynecologic Oncol* (2013) 128(1):15–21. doi: 10.1016/j.ygyno.2012.09.021

37. He P, Sun X, Cheng HJ, Zou YB, Wang Q, Zhou CL, et al. UBA2 promotes proliferation of colorectal cancer. *Mol Med Rep* (2018) 18(6):5552–62. doi: 10.3892/mmr.2018.9613

38. Cheng H, Sun X, Li J, He P, Liu W, Meng X. Knockdown of Uba2 inhibits colorectal cancer cell invasion and migration through downregulation of the wnt/β-catenin signaling pathway. *J Cell Biochem* (2018) 119(8):6914–25. doi: 10.1002/jcb.26890

39. Thornalley PJ, Rabbani N. Glyoxalase in tumourigenesis and multidrug resistance. *Semin Cell Dev Biol* (2011) 22(3):318–25. doi: 10.1016/j.semcdb.2011.02.006

40. Ma H, Lai B, Zan C, Di X, Zhu X, Wang K. GLO1 contributes to the drug resistance of escherichia coli through inducing PER type of extended-spectrum β-lactamases. *Infe©esist* (2022) 15:1573–86. doi: 10.2147/IDR.S358578

41. Kędzia B, Hołderna-Kędzia E. Occurence of methylglyoxal in manuka honey and its influence on human body. *Postępy Fitoterapii* (2015) 3:172–6.

42. Sakamoto H, Mashima T, Kizaki A, Dan S, Hashimoto Y, Naito M, et al. Glyoxalase I is involved in resistance of human leukemia cells to antitumor agent-induced apoptosis. *Blood* (2000) 95(10):3214–8. doi: 10.1182/blood.V95.10.3214

43. Tamori S, Nozaki Y, Motomura H, Nakane H, Katayama R, Onaga C, et al. Glyoxalase 1 gene is highly expressed in basal-like human breast cancers and contributes to survival of ALDH1-positive breast cancer stem cells. *Oncotarget* (2018) 9(92):36515–29. doi: 10.18632/oncotarget.26369

44. Alhujaily M, Abbas H, Xue M, de la Fuente A, Rabbani N, Thornalley PJ. Studies of glyoxalase 1-linked multidrug resistance reveal glycolysis-derived reactive metabolite, methylglyoxal, is a common contributor in cancer chemotherapy targeting the spliceosome. *Front Oncol* (2021) 11:748698. doi: 10.3389/fonc.2021.748698

45. Yang Y, Zhang T, Wu L. TUFT1 facilitates metastasis, stemness, and vincristine resistance in colorectal cancer *via* activation of PI3K/AKT pathway. *Biochem Genet* (2021) 59(4):1018–32. doi: 10.1007/s10528-021-10051-0

46. Zhou Z, Xu Q, Liu Z, Zeng Y, et al. Hypoxia-induced TUFT1 promotes the growth and metastasis of hepatocellular carcinoma by activating the Ca 2+/PI3K/AKT pathway. *Oncogene* (2019) 38(8):1239. doi: 10.1038/s41388-018-0505-8

47. Sakurada K, Akutsu T, Watanabe K, Fujinami Y, Yoshino M. Expression of statherin mRNA and protein in nasal and vaginal secretions. *Leg Med (Tokyo)* (2011) 13(6):309–13. doi: 10.1016/j.legalmed.2011.07.002

48. Gilbert M, Stayton PS. Expression and characterization of human salivary statherin from escherichia coli using two different fusion constructs. *Protein Expression Purification* (1999) 16(2):243–50. doi: 10.1006/prep.1999.1048

49. Xiao M, Li J, Li W, Wang Y, Wu F, Xi Y, et al. MicroRNAs activate gene transcription epigenetically as an enhancer trigger. *RNA Biol* (2017) 14(10):1326–34. doi: 10.1080/15476286.2015.1112487

50. Suzuki HI, Young RA, Sharp PA. Super-Enhancer-Mediated RNA processing revealed by integrative MicroRNA network analysis. *Cell* (2017) 168 (6):1000–1014.e15. doi: 10.1016/j.cell.2017.02.015

51. Liang Y, Xu P, Zou Q, Luo H, Yu W. An epigenetic perspective on tumorigenesis: Loss of cell identity, enhancer switching, and NamiRNA network. *Semin Cancer Biol* (2019) 57:1–9. doi: 10.1016/j.semcancer.2018.09.001

52. Ukey S, Jain A, Dwivedi S, Choudhury C, Vishnoi JR, Chugh A, et al. Study of MicroRNA (miR-221-3p, miR-133a-3p, and miR-9-5p) expressions in oral submucous fibrosis and squamous cell carcinoma. *Ind J Clin Biochem* (2022) 2022:1–10. doi: 10.1007/s12291-022-01035-x

53. Chang LL, Wang HC, Tseng KY, Su MP, Wang JY, Chuang YT, et al. Upregulation of miR-133a-3p in the sciatic nerve contributes to neuropathic pain development. *Mol Neurobiol* (2020) 57(9):3931–42. doi: 10.1007/s12035-020-01999-y

54. Asai S, Koma A, Nohata N, Kinoshita T, Kikkawa N, Kato M, et al. Impact of miR-1/miR-133 clustered miRNAs: PFN2 facilitates malignant phenotypes in head and neck squamous cell carcinoma. *Biomedicines* (2022) 10(3):663. doi: 10.3390/biomedicines10030663

55. Nohata N, Hanazawa T, Kikkawa N, Sakurai D, Sasaki K, Chiyomaru T, et al. Identification of novel molecular targets regulated by tumor suppressive miR-1/miR-133a in maxillary sinus squamous cell carcinoma. *Int J Oncol* (2011) 39 (5):1099–107. doi: 10.3892/ijo.2011.1096

56. Chen EB, Zhou ZJ, Xiao K, Zhu GQ, Yang Y, Wang B, et al. The miR-561-5p/CX3CL1 signaling axis regulates pulmonary metastasis in hepatocellular carcinoma involving CX3CR1+ natural killer cells infiltration. *Theranostics* (2019) 9(16):4779–94. doi: 10.7150/thno.32543

57. Xi B, Lai M, Zhang W, Wang F. MicroRNA-561-5p inhibits cell proliferation and invasion by targeting RAC1 in pancreatic ductal adenocarcinoma. *Ann Clin Lab Sci* (2022) 52(2):213–21.

58. Fabbri M, Garzon R, Cimmino A, Liu Z, Zanesi N, Callegari E MicroRNA-29 family reverts aberrant methylation in lung cancer by targeting DNA methyltransferases 3A and 3B. *PNAS* (2007) 107:15805–10. doi: 10.1073/pnas.0707628104

59. Reddy KB. MicroRNA (miRNA) in cancer. *Cancer Cell Int* (2015) 15(1):38. doi: 10.1186/s12935-015-0185-1

60. Ding X, Zhang J, Feng Z, Tang Q, Zhou X. MiR-137-3p inhibits colorectal cancer cell migration by regulating a KDM1A-dependent epithelial–mesenchymal transition. *Dig Dis Sci* (2021) 66(7):2272–82. doi: 10.1007/s10620-020-06518-6

61. Dong X, Chang M, Song X, Ding S, Xie L, Song X. Plasma miR-1247-5p, miR-301b-3p and miR-105-5p as potential biomarkers for early diagnosis of non-small cell lung cancer. *Thorac Cancer* (2021) 12(4):539–48. doi: 10.1111/1759-7714.13800

62. Dias F, Teixeira AL, Ferreira M, Adem B, Bastos N, Vieira J, et al. Plasmatic miR-210, miR-221 and miR-1233 profile: Potential liquid biopsies candidates for renal cell carcinoma. *Oncotarget* (2017) 8(61):103315–26. doi: 10.18632/oncotarget.21733

63. Banaganapalli B, Al-Rayes N, Awan ZA, Alsulaimany FA, Alamri AS, Elango R, et al. Multilevel systems biology analysis of lung transcriptomics data identifies key miRNAs and potential miRNA target genes for SARS-CoV-2 infection. *Comput Biol Med* (2021) 135:104570. doi: 10.1016/j.compbiomed.2021.104570

frontiers | Frontiers in Oncology

TYPE Review
PUBLISHED 17 August 2022
DOI 10.3389/fonc.2022.951864

OPEN ACCESS

EDITED BY
Takeo Tatsuta,
Tohoku Medical and Pharmaceutical University, Japan

REVIEWED BY
Jayant Maini,
Manav Rachna International Institute of Research and Studies (MRIIRS), India
Hamed Shoorei,
Birjand University of Medical Sciences, Iran

*CORRESPONDENCE
Ying Liu
liuying_hero@163.com

†These authors have contributed equally to this work

SPECIALTY SECTION
This article was submitted to Pharmacology of Anti-Cancer Drugs, a section of the journal Frontiers in Oncology

RECEIVED 24 May 2022
ACCEPTED 02 August 2022
PUBLISHED 17 August 2022

CITATION
Zhou X, Ao X, Jia Z, Li Y, Kuang S, Du C, Zhang J, Wang J and Liu Y (2022) Non-coding RNA in cancer drug resistance: Underlying mechanisms and clinical applications. *Front. Oncol.* 12:951864. doi: 10.3389/fonc.2022.951864

Non-coding RNA in cancer drug resistance: Underlying mechanisms and clinical applications

Xuehao Zhou[1†], Xiang Ao[1†], Zhaojun Jia[2], Yiwen Li[1], Shouxiang Kuang[1], Chengcheng Du[1], Jinyu Zhang[1], Jianxun Wang[1] and Ying Liu[1,3*]

[1]School of Basic Medical Sciences, Qingdao Medical College, Qingdao University, Qingdao, China, [2]College of New Materials and Chemical Engineering, Beijing Key Laboratory of Enze Biomass Fine Chemicals, Beijing Institute of Petrochemical Technology, Beijing, China, [3]Institute for Translational Medicine, The Affiliated Hospital of Qingdao University, Qingdao Medical College, Qingdao University, Qingdao, China

Cancer is one of the most frequently diagnosed malignant diseases worldwide, posing a serious, long-term threat to patients' health and life. Systemic chemotherapy remains the first-line therapeutic approach for recurrent or metastatic cancer patients after surgery, with the potential to effectively extend patient survival. However, the development of drug resistance seriously limits the clinical efficiency of chemotherapy and ultimately results in treatment failure and patient death. A large number of studies have shown that non-coding RNAs (ncRNAs), particularly microRNAs, long non-coding RNAs, and circular RNAs, are widely involved in the regulation of cancer drug resistance. Their dysregulation contributes to the development of cancer drug resistance by modulating the expression of specific target genes involved in cellular apoptosis, autophagy, drug efflux, epithelial-to-mesenchymal transition (EMT), and cancer stem cells (CSCs). Moreover, some ncRNAs also possess great potential as efficient, specific biomarkers in diagnosis and prognosis as well as therapeutic targets in cancer patients. In this review, we summarize the recent findings on the emerging role and underlying mechanisms of ncRNAs involved in cancer drug resistance and focus on their clinical applications as biomarkers and therapeutic targets in cancer treatment. This information will be of great benefit to early diagnosis and prognostic assessments of cancer as well as the development of ncRNA-based therapeutic strategies for cancer patients.

KEYWORDS

non-coding RNA, cancer, drug resistance, biomarker, therapeutic target

Introduction

Cancer is the second leading cause of death after cardiovascular disease globally, representing a serious threat to patients' life and health (1, 2). Based on recent statistics from the International Agency for Research, approximately 19.3 million new cancer cases and more than 10.0 million deaths occurred in 2020 (3). Currently, surgical resection, radiation, endocrine therapy, targeted therapy, and systemic chemotherapy are the main methods of cancer treatment. Among them, systemic chemotherapy is the most effective therapeutic option for all stages of cancer, with the potential to improve patients' prognosis in the short term (4–6). It has been reported that chemotherapy could extend the overall survival (OS) of patients with advanced cancer by 6.7 months compared to patients only treated with best supportive care (7). However, the emergency of drug resistance significantly limits the clinical application of chemotherapeutic agents, ultimately resulting in treatment failure and patient death. Drug resistance has become an immense obstacle in cancer treatment (8). The underlying mechanisms involved in drug resistance are considerably complex and have not been fully elucidated. Therefore, a better understanding of the mechanisms responsible for drug resistance will provide opportunities for the development of precise therapeutic strategies for cancer patients.

Non-coding RNAs (ncRNAs), such as microRNAs (miRNAs), long non-coding RNAs (lncRNAs), and circular RNAs (circRNAs), are a large group of transcripts that have no protein coding potential. They were recognized as by-products of transcription without biological function in the past long period of time (9). In recent years, an increasing amount of evidence has suggested that ncRNAs are crucial regulators in almost all cellular processes, such as transcription, apoptosis, proliferation, and differentiation (10, 11). They play crucial roles in the regulation of a variety of physiological and pathological processes. The dysregulation of ncRNAs has been shown to be closely associated with a variety of diseases, particularly cancer (12–14). For instance, the overexpression of miRNA-200a-3p was found to significantly facilitate cell proliferation, migration, and invasion as well as induce apoptosis in gastric cancer (GC) by directly targeting DLC-1 (15). LncRNA ITGB8-AS1 was found to promote cell proliferation, colony formation, and tumor growth in colorectal cancer (CRC) by upregulating ITGA3 and ITGB3 *via* sponging miR-33b-5p and let-7c-5p/let-7d-5p (16). Furthermore, circRNA C190 overexpression facilitated the proliferation, and migration of non-small cell lung carcinoma (NSCLC) cell lines by targeting CDK1 and CDK6 *via* sequestrating miR-142-5p (17). Notably, ncRNA dysregulation contributes to the development of cancer drug resistance *via* various mechanisms, such as the inhibition of apoptosis, enhancement of epithelial-to-mesenchymal transition (EMT), and induction of autophagy (18–20). In addition, the differential expression patterns of ncRNAs endow them with great potential as biomarkers and therapeutic targets for cancer patients.

In this review, we summarize the recent findings on the regulatory mechanisms of ncRNAs in cancer drug resistance and highlight their clinical applications as promising biomarkers and therapeutic targets for cancer patients. A better understanding of the underlying mechanisms of ncRNAs in drug resistance may offer an opportunity to develop ncRNA-based therapeutic strategies for cancer patients against drug resistance.

Overview of ncRNAs

Classification of ncRNAs

It has been reported that ncRNAs make up about 98% of the human genome (21). With the continuous development of high-throughput sequencing technologies, an increasing number of ncRNAs are being identified in eukaryotic cells. According to distinguished classification standards, ncRNAs can be divided into a variety of categories. For instance, ncRNAs are classified into housekeeping ncRNAs (e.g., rRNAs and tRNAs) and regulatory ncRNAs (e.g., miRNAs, circRNAs and lncRNAs) based on their cellular functions. According to their transcript size, ncRNAs are divided into lncRNAs (> 200 nucleotides) and small ncRNAs (< 200 nucleotides), including miRNAs, small interfering RNAs (siRNAs), and piwi-interacting RNAs (piRNAs) (22, 23). Besides, lncRNAs are sorted into two categories, linear lncRNAs and circular lncRNAs based on their structure (24). Moreover, according to the role of lncRNAs in gene expression regulation, they are classified as cis-lncRNAs or trans-lncRNAs (25). In addition, ncRNAs can also be divided into distinct categories based on their subcellular localization (e.g., small nuclear RNAs and cytoplasm-located siRNAs) and genomic origins (including sense or antisense ncRNAs, bidirectional ncRNAs, intronic ncRNAs, and intergenic ncRNAs) (26). Collectively, scientific and systematic classification will be of great benefit in better understanding the characteristics of ncRNAs.

Biogenesis of ncRNAs

The mechanisms of ncRNA biogenesis are extremely complicated, and individual ncRNA categories possess unique characteristics (Figure 1). For instance, both miRNAs and lncRNAs are transcribed by RNA polymerase II (Pol II) from genomic loci. Primary miRNAs (pri-miRNAs) are subsequently catalyzed by a microprocessor complex consisting of DiGeorge syndrome critical region 8 (DGCR8) and Drosha to generate precursor miRNAs (pre-miRNAs). Pre-miRNAs are translocated from the nucleus to the cytoplasm, and then processed into double-stranded miRNAs by the Dicer/TRBP/PACT complex. Finally, the

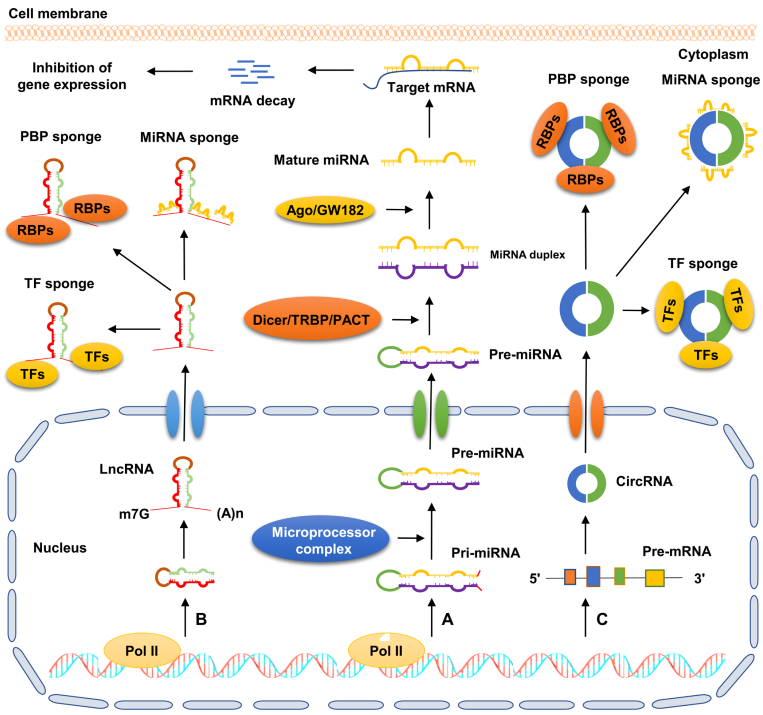

FIGURE 1
Schematic diagram of ncRNA biogenesis and action patterns. **(A)** Pri-miRNA is transcribed by RNA polymerasel II from genomic loci and further processed into pre-miRNA by microprocessor complex. Subsequently, pre-miRNA is exported to the cytoplasm and further processed into double-stranded miRNA *via* the Dicer/TRBP/PACT complex. Next, with the help of Ago/GW182, the double-stranded miRNA is processed into mature miRNA, which directly binds to the 3′-UTR of target mRNA, and then facilitates its degradation. **(B)** LncRNA transcribed by RNA polymerase II is exported to the cytoplasm. Subsequently, lncRNA exerts its biological role by acting as sponges of miRNAs, RBPs, and TFs. **(C)** CircRNA is mainly derived from precursor mRNAs *via* back-splicing reaction, by which the single strand of circRNA forms a covalently closed-loop structure. CircRNA plays crucial roles in cellular processes by serving as sponges of miRNAs, RBPs, and TFs.

double-stranded miRNAs are processed into mature miRNAs by a series of regulators, including helicase and the RNA-induced silencing complex (RISC) (27). Different from miRNAs, lncRNAs contain 5' caps and 3' poly(A) tails. Most lncRNAs undergo a canonical mechanism similar to the biogenesis of mRNAs, by which they are often capped by 7-methyl guanosine at the 5' end of Pol II transcripts, polyadenylated at their 3′ ends, and spliced similarly to mRNAs (28). CircRNAs are a novel type of ncRNAs characterized by the formation of covalently closed-loop structures without 5' caps and 3' tails. CircRNAs are mainly produced from precursor mRNAs *via* a unique mechanism called back-splicing reaction, in which a downstream splice donor site binds to an upstream splice acceptor site to form a single-strand, covalently closed-loop structure (29).

The biogenesis of ncRNAs is widely regulated by various factors, such as trans-acting factors, RNA binding proteins (RBPs), and epigenetic modifications. For instance, the overexpression of poly(A)-binding protein nuclear 1 (PABPN1) was found to facilitate the turnover of non-coding transcripts *via* a polyadenylation-dependent mechanism, indicating its negative role in modulating the processing of certain ncRNAs (30). Alternative splicing factor1/pre-mRNA splicing factor SF2 (ASF/SF2) is a classical RBP encoded by the *SFRS1* gene. Wu et al. showed that SF2/ASF overexpression facilitated the maturation process of a series of miRNAs, including miR-7, miR-29b, miR-221, and miR-222. Consistent with this, the knockdown of SF2/ASF resulted in a decreased level of mature miR-7 (31). N^6-methyladenosine (m^6A) is a well-studied RNA modification that plays crucial roles in distinct processes modulating RNA metabolism, such as the splicing, stability, and translation of mRNA (32). Timoteo et al. revealed that specific m6As promoted circRNA back-splicing reaction in a METTL3- and YTHDC1-dependent manner, whereas the mutation of the m6A sites significantly decreased the circRNA levels, which was paralleled by a strong increase in the precursor RNA (33). Although some progress has been made in recent years, ncRNA biogenesis and its regulatory mechanisms are still not fully understood. Continuous in-depth studies will be beneficial not only in differentiating ncRNAs from protein-coding RNAs but also in deciphering their functional significance.

Patterns of ncRNA action

A large amount of evidence suggests that ncRNAs are involved in almost all physiological and pathological processes, including tissue development, cancer progression, and drug resistance. They play crucial roles in these processes *via* distinct molecular mechanisms, such as regulating the expression of specific target genes, altering the function and activity of proteins, and targeting related signaling pathways (34–36). All these mechanisms are mainly based on the interaction of ncRNAs with DNA, RNA, and proteins (Figure 1). For instance, miRNAs are 19–25 nucleotides in length and play crucial roles in pivotal cellular processes by regulating specific gene expression at the post-transcriptional level (37, 38). They inhibit the expression of specific genes by directly binding to 3′ untranslated regions (UTRs) of their target mRNAs. One single miRNA can simultaneously control the expression of multiple target genes involved in distinct cellular processes (e.g., invasion, metastasis, and cell cycle), while one gene can also be regulated by several miRNAs (39). LncRNAs and circRNAs have been shown to exert their biological functions by acting as sponges or molecular sinks for miRNAs, RBPs, and transcription factors to specifically modulate their target gene expression. These ncRNAs are also called intracellular competitive endogenous RNAs (ceRNAs) (40, 41). For instance, lncRNA SLC25A25-AS1 was found to promote proliferation, migration, and invasion, and induced apoptosis in NSCLC A549 and H460 cells by upregulating integrin α2 *via* sponging miR-195-5p (42). Due to their central role in physiological and pathological processes, the dysregulation of ncRNAs is closely associated with the occurrence and development of many diseases including cancer. In fact, the aberrant expression of ncRNAs has been observed in cancer tissues and cell lines. They are involved in the regulation of cancer progression by serving as oncogenes or tumor suppressors (10). In addition, ncRNAs are also crucial regulators in the development of cancer drug resistance (10). In-depth investigations of the underlying mechanism of ncRNAs in cancer drug resistance could contribute to the precise treatment of cancer patients, particularly those with poor response to chemotherapy.

Mechanisms of ncRNAs in mediating cancer drug resistance

Chemotherapy remains the most effective first-line therapeutic approach for all stages of cancer and can effectively improve the clinical outcomes of patients in the short term. However, its long-term role in extending the OS of cancer patients is extremely restricted due to the emergence of drug resistance (43). Drug resistance is classified into single drug resistance and multidrug resistance (MDR). Of these, MDR is the main cause of mortality for most patients (44). Emerging evidence has shown that ncRNAs are closely associated with cancer drug resistance (Table 1). Their dysregulation contributes to the development of cancer drug resistance *via* distinct mechanisms, including inhibition of apoptosis, activation of protective autophagy, enhancement of drug efflux, induction of EMT, and enhancement of cancer stem cells (CSCs) stemness (Figure 2). However, the exact mechanisms are still not fully clarified. In this section, the involvement of ncRNAs in cancer drug resistance is outlined.

MiRNAs and cancer drug resistance

MiRNAs affect drug-induced apoptosis by targeting apoptosis-related proteins or drug-resistance pathways

The inhibition of drug-induced apoptosis is one of the main mechanisms contributing to cancer drug resistance. Apoptosis can be divided into two categories: the extrinsic pathways mediated by death receptors and intrinsic (mitochondrial) pathways associated with apoptosis-related proteins such as B-cell lymphoma-2 (Bcl-2) (135). MiRNAs have been shown to influence cancer drug resistance by manipulating apoptosis-related proteins (27, 136). For instance, in our previous work, miR-633 was found to be significantly upregulated in GC tissues and cells, and its upregulation in GC samples was closely associated with the downregulation of Fas-associated protein with death domain (FADD), an adaptor involved in the extrinsic pathway of apoptosis. Mechanistic analysis revealed that miR-633 inhibited doxorubicin (DOX)/cisplatin (CDDP)-induced apoptosis in SGC-7901 and AGS cells by downregulating FADD *via* directly targeting its 3′-UTR (137). In another study, Yang et al. found that miR-92a-3p was upregulated in both cervical cancer (CC) tissues and CDDP-resistant CC cell lines HeLa and SiHa. The overexpression of miR-92a-3p inhibited the CDDP-induced apoptosis of HeLa and SiHa cells by targeting the expression of Krüppel-like factor 4 (KLF4), leading to the enhancement of CDDP resistance in CC. Consistent with this, miR-92a-3p knockdown increased the sensitivity of HeLa and SiHa cells to CDDP (138).

The Bcl-2 family consisting of anti-apoptotic proteins (e.g., Bcl-2, Mcl-1, and Bcl-xl) and pro-apoptotic proteins (e.g., Bax, Bim, and Bak) plays crucial roles in the mitochondrial apoptotic pathway (139). It has been reported that the ratio between anti-apoptotic proteins and BH3-only proteins (a subtype of pro-apoptotic proteins) can alter the outer mitochondrial membrane permeability by regulating the activation of pore-forming proteins, thereby inducing apoptosis of the cancer cells (140). Zhong et al. showed that miR-625-3p overexpression significantly inhibited the CDDP-induced apoptosis of high-grade serous ovarian cancer (OC) cells OVCAR3 and OVCAR4

TABLE 1 Roles of ncRNAs in cancers drug resistance.

Cancer types	Chemotherapeutic drugs	ncRNAs	Gene type	Alteration	Effect on Drug Resistance	Reference
OC	CDDP	miR-133a, miR-29c-3p, miR-30a LINC01125, LINC01508 circRNA Cdr1as	Tumor suppressor	Downregulated	Sensitivity to CDDP	(45–50)
		miR-181d, miR-149-3p lncRNA WDFY3-AS2, lncRNA CCAT1 circ-LPAR3, circHIPK2	Oncogene	Upregulated	Resistance to CDDP	(51–56)
	PTX	miR-194-5p, hsa-miR-105 lncRNA SNHG5, lncRNA KB-1471A8.2 circEXOC6B	Tumor suppressor	Downregulated	Sensitivity to PTX	(57–61)
		lncRNA SDHAP1, lncRNA HULC circ_0061140, circ_CELSR1	Oncogene	Upregulated	Resistance to PTX	(62–65)
GC	5-FU	miR-204, miR195, exosomal miR-107	Tumor suppressor	Downregulated	Sensitivity to 5-FU	(66–68)
		miR-149 lncRNA HAGLR, lncRNA HNF1A-AS1 circRNA CPM, circNRIP1	Oncogene	Upregulated	Resistance to 5-FU	(69–73)
	CDDP	microRNA-206 lncRNA ADAMTS9-AS2 circRNA MCTP2, circ_0001017	Tumor suppressor	Downregulated	Sensitivity to CDDP	(74–77)
		miR-193a-3p lncRNA BANCR, lncRNA MCM3AP-AS1 circRNA DONSON	Oncogene	Upregulated	Resistance to CDDP	(78–81)
	OXA	hsa_circ_0001546	Tumor suppressor	Downregulated	Sensitivity to OXA	(82)
		lncRNA DDX11-AS1 circ_0032821	Oncogene	Upregulated	Resistance to OXA	(83, 84)
NSCLC	CDDP	miR-186-5p, miR-101-3p lncRNA SPRY4-IT1 circ_0030998	Tumor suppressor	Downregulated	Sensitivity to CDDP	(85–88)
		microRNA-25-3p lncRNA SNHG1, LINC01224 circRNA_100565	Oncogene	Upregulated	Resistance to CDDP	(89–92)
CRC	5-FU	miR-375-3p lncRNA HAND2-AS1, circDDX17	Tumor suppressor	Downregulated	Sensitivity to 5-FU	(93–95)
		miR-29b-3p lncRNA LBX2-AS1 circ_0007031	Oncogene	Upregulated	Resistance to 5-FU	(96–98)
	OXA	miR-200b-3p circ-FBXW7	Tumor suppressor	Downregulated	Sensitivity to OXA	(99, 100)
		miR-454-3p lncRNA CACS15	Oncogene	Upregulated	Resistance to OXA	(101, 102)
HCC	sorafenib	miR-138-1-3p, miRNA-124-3p.1 lncRNA FOXD2-AS1	Tumor suppressor	Downregulated	Sensitivity to sorafenib	(103–105)
		miR-126-3p lncRNA DANCR circFOXM1	Oncogene	Upregulated	Resistance to sorafenib	(106–108)
	CDDP	miR-27a-3p lncRNA GAS5	Tumor suppressor	Downregulated	Sensitivity to CDDP	(109, 110)
		lncRNA FGD5-AS1 circMRPS35	Oncogene	Upregulated	Resistance to CDDP	(111, 112)

(Continued)

TABLE 1 Continued

Cancer types	Chemotherapeutic drugs	ncRNAs	Gene type	Alteration	Effect on Drug Resistance	Reference
BC	ADR	miR-3609 circKDM4C	Tumor suppressor	Downregulated	Sensitivity to ADR	(113, 114)
		microRNA-221 lnc-LOC645166 circRNA_0044556	Oncogene	Upregulated	Resistance to ADR	(115–117)
	tamoxifen	lncRNA ADAMTS9-AS2 hsa_circ_0025202	Tumor suppressor	Downregulated	Sensitivity to tamoxifen	(118, 119)
		miR-24-3p lncRNA CYTOR	oncogene	Upregulated	Resistance to tamoxifen	(120, 121)
CC	CDDP	miR-144	Tumor suppressor	Downregulated	Sensitivity to CDDP	(122)
		lncRNA OTUD6B-AS1	Oncogene	Upregulated	Resistance to CDDP	(123)
Prostate cancer	docetaxel	circFoxo3	Tumor suppressor	Downregulated	Sensitivity to docetaxel	(124)
		exosomal circ-XIAP	Oncogene	Upregulated	Resistance to docetaxel	(125)
PC	gemcitabine	miRNA-3662 circ_0092367	Tumor suppressor	Downregulated	Sensitivity to gemcitabine	(126, 127)
		miR-93-5p lncRNA PVT1 circHIPK3	Oncogene	Upregulated	Resistance to gemcitabine	(128–130)
Bladder cancer	CDDP	exosomal LINC00355 circ_0058063	Oncogene	Upregulated	Resistance to CDDP	(131, 132)
Renal cancer	sunitinib	miR-130b circSNX6	Oncogene	Upregulated	Resistance to sunitinib	(133, 134)

by targeting Bcl-2 and Bax expression, resulting in the inhibition of CDDP sensitivity in these cells (141). Ashofteh et al. revealed that miRNA-15a promoted cellular apoptosis by downregulating the mRNA levels of Mcl-1 and Bcl-2 in chronic lymphocytic leukemia (CLL), thereby enhancing the sensitivity of CLL-CII leukemia cells to fludarabine (142). In addition, Sun et al. demonstrated that miR-374a was downregulated in A2780 cells by propofol. The overexpression miR-374a suppressed the apoptosis of A2780 cells by decreasing the expression of Bim, p27, and FOXO1, leading to the enhancement of CDDP resistance in OC (143).

The Wnt/β-catenin signaling pathway is involved in the modulation of various cellular processes of cancer cells, such as apoptosis, proliferation, and metastasis. The dysregulation of this pathway has been shown to contribute to the development of cancer drug resistance by influencing the apoptotic pathways (144). For instance, Han et al. found that miR-199b-3p knockdown enhanced the sensitivity of cetuximab-resistant OC cells SW480 and HCT116 to cetuximab by promoting cell apoptosis. Mechanistically, silencing miR-199b-3p could enhance cetuximab-induced apoptosis in cetuximab-resistant SW480 and HCT116 cells by activating the Wnt/β-catenin signaling pathway *via* downregulating CRIM1 (145). Liu et al. showed that miR-217 was significantly reduced in CDDP-resistant OC COC1 cells compared with in CDDP-sensitive COC1 cells. The overexpression of miR-217 in COC1 cells facilitated CDDP-induced apoptosis and enhanced CDDP sensitivity by inhibiting the activation of the Wnt/β-catenin signaling pathway (146). In addition, multiple miRNAs, such as miR-323a-3p, miR-6727-5p, and miRNA-223-3p, have also been found to contribute to the development of cancer drug resistance by regulating apoptotic pathways *via* targeting other drug resistance-related signaling pathways, including the phosphatidylinositol 3-kinase (PI3K)/AKT, mitogen-activated protein kinase (MAPK), and nuclear factor kappa B (NF-κB) signaling pathways (147–149). Collectively, these findings indicate that targeting the apoptotic pathways is a common regulation mechanism for miRNAs in cancer drug resistance. Further investigating the mechanisms of miRNAs in drug-induced apoptosis may provide new insights on therapeutic strategies against cancer drug resistance.

MiRNAs and drug efflux in cancer drug resistance

Excessive drug efflux is considered a critical mechanism contributing to cancer drug resistance, in which the efficiency of anticancer drugs is significantly limited due to the reduction in drug concentration in cancer cells (150). It has been reported that excessive drug efflux is a result of the upregulation of drug efflux pumps, including ATP-binding cassette (ABC) transporters. Several members of the ABC family, such as ABCB1, ABCC2, and ABCG2, have been shown to contribute

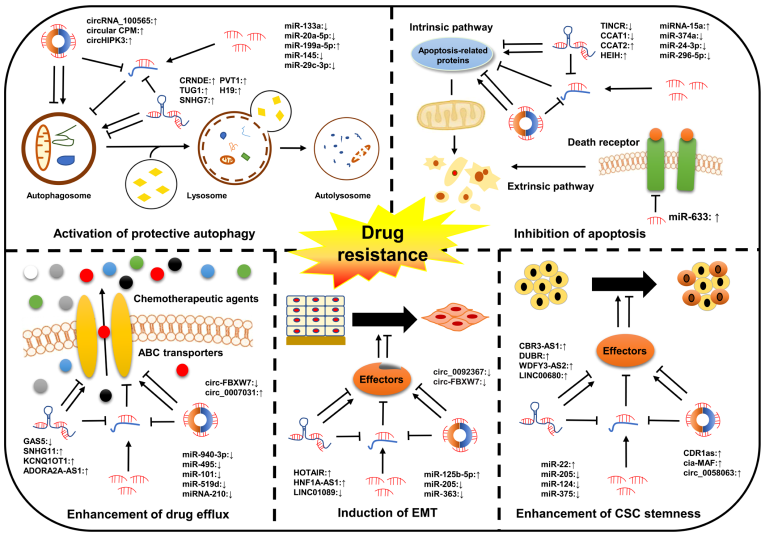

FIGURE 2
Classical mechanisms of ncRNAs in cancer drug resistance. The dysregulation of ncRNAs contributes to the development of cancer drug resistance by modulating multiple cellular processes of cancer cells, such as drug efflux, cell apoptosis, autophagy, and EMT as well as the acquisition of CSC characteristics.

to the development of MDR in a variety of cancers (151). Increasing evidence suggest that miRNAs participate in the modulation of drug efflux in cancer cells by altering the expression ABC transporters (152). For instance, Zou et al. showed that the overexpression of miR-495 significantly reduced the drug efflux in MDR OC cell line A2780DX5 and GC cell line SGC7901R by directly targeting ABCB1, thereby enhancing the sensitivity of cancer cells to DOX and paclitaxel (PTX) (153). ABCB1 is also a target of miR-101 in GC. The overexpression of miR-101 in drug-resistant SGC7901 cells significantly decreased ABCB1 expression at the mRNA and protein levels (154). Tian et al. found that miR-940-3p negatively modulated ABCC2 expression in CDDP-resistant OVCAR3 and SKOV3 cells by directly binding to its 3'-UTR region, leading to the enhancement of CDDP sensitivity in OC (155). Additionally, Tsai et al. revealed that miR-519d was downregulated in human osteosarcoma cells MG-63 and U-2 by CCN family member 2, and its reduction facilitated drug resistance by upregulating the ABCG2 levels (156). Moreover, Amponsah et al. demonstrated that miR-210 overexpression decreased ABCC5 mRNA levels in pancreatic cancer (PC) cell lines (ASAN-PaCa, AsPC-1 and MIA-PaCa2) by targeting its 3'-UTR, leading to the enhancement of gemcitabine sensitivity in PC (157). In addition, several miRNAs, such as miR-34a, miR-7-5p, and miR-325-3p, have also been shown to play a role in cancer drug resistance by influencing drug efflux *via* targeting ABC transporters in a variety of cancers, including colon cancer, glioblastoma, and hepatocellular carcinoma (HCC) (158–160). Taken together, these studies strongly suggest that miRNAs are involved in the development of cancer drug resistance by altering the function of drug efflux pumps. However, the detailed mechanisms are still inconclusive and need to be further elucidated.

MiRNAs are involved in the development of cancer drug resistance by modulating autophagy

Autophagy is a lysosomal degradation process that is essential for cellular survival, differentiation, and homeostasis. Protective autophagy has been recognized as one of the main mechanisms resulting in cancer drug resistance, by which cancer cells eliminate the cytotoxicity of chemotherapeutic drugs (161). Therefore, targeting autophagy may be an effective therapeutic strategy for improving the poor prognosis of cancer patients. MiRNAs have been shown to participate in cancer drug resistance by regulating autophagy-related genes (162). For instance, Zhou et al. found that miR-133a was significantly downregulated in CDDP-resistant OC cell lines A2780 and SKOV3. The overexpression of miR-133a significantly enhanced the CDDP sensitivity in CDDP-resistant A2780 and SKOV3 cells by inhibiting autophagy *via* directly targeting YES1 (45). Li et al. showed that miR-20a-5p inhibited autophagy in CDDP-resistant OC cells. Mechanistically, miR-20a-5p suppressed the expression of RBP1 in CDDP-resistant A2780 and COC1 by promoting DNMT3B-mediated RBP1 methylation, resulting in the inhibition of autophagy and CDDP resistance in OC (163). H446/EP was a MDR small cell lung cancer (SCLC) cell line that was developed from H446. Li

et al. demonstrated that miR-199a-5p was significantly upregulated in H446/EP cells compared to non-drug-resistant H446 cells. MiR-199a-5p overexpression decreased the CDDP sensitivity in H446 cells by enhancing the autophagy activity *via* directly targeting p62 (164). Moreover, Zhao et al. revealed that miR-145 was downregulated in CRC tissues and cell lines (HCT116, SW620, and HCT-8). The overexpression of miR-145 enhanced 5-fluorouracil (5-FU) sensitivity in 5-FU-resistant HCT116, SW620, and HCT-8 cells by enhancing 5-FU-induced apoptosis and reducing autophagy. Mechanistically, miR-145 activated p53 by directly targeting HDAC4, thereby inhibiting 5-FU resistance in CRC (165). Collectively, these studies indicate that protective autophagy induced by miRNA dysregulation is a crucial factor resulting in the occurrence of cancer drug resistance. Moreover, miRNAs may simultaneously target apoptotic pathways and autophagy. Thus, it is a valuable strategy to comprehensively identify miRNAs associated with these death pathways to help patients overcome cancer drug resistance.

MiRNAs alter stemness characteristics and EMT in cancer cells

CSCs, also known as tumor-initiating cells (TICs), are a unique subset of tumor cells exhibiting capabilities of self-renewal, differentiation, and tumor initiation. CSCs have been recognized as the main cause of drug resistance, metastasis, and recurrence of cancer (166, 167). Growing evidence suggests that miRNAs are involved in cancer drug resistance by altering the characteristics of CSCs (168). For instance, Zhang et al. found that miR-132 was upregulated in the $Lrg5^+$ gastric CSCs isolated from MKN45 and MKN28 cells. High miR-132 expression was closely associated with chemo-resistance in GC patients. Mechanistic assays revealed that miR-132 facilitated CDDP resistance in $Lrg5^+$ gastric CSCs by upregulating ABCG2 *via* directly targeting SIRT1 (169). Feng et al. showed that miR-25 was upregulated in liver CSCs (LCSCs) isolated from HepG2, Huh7, and PLC cells compared with the non-CSCs. The knockdown of miR-25 significantly enhanced the sensitivity of the LCSCs to tumor necrosis factor-related apoptosis-inducing ligand (TRAIL)-induced apoptosis by inhibiting Bad phosphorylation *via* upregulating phosphatase and tensin homologue (PTEN), a PI3K inhibitor (170). In addition, Ni et al. revealed that miR-375 suppressed the stemness of GC cells BGC-823 and SGC-7901 by triggering ferroptosis *via* directly targeting SLC7A11 (171). Epithelial mesenchymal transition (EMT) is a morphogenetic process that endows epithelial cells with migratory and invasive characteristics. The aberrant activation of EMT has been shown to facilitate the development of cancer drug resistance by enabling the conversion of non-CSCs into CSCs (172, 173). MiRNAs can participate in the development of cancer drug resistance by targeting the EMT process. For instance, Hirao et al. showed that the overexpression of miR-125b-5p in HCC cell lines (PLC/PRF5-R1/R2) enhanced sorafenib resistance. Mechanistically, miR-125b-5p promoted the EMT process and conferred stemness characteristics in PLC/PRF5-R1/R2 cells by targeting ATXN1, leading to the reduction of sorafenib sensitivity in HCC. Consistent with this, ATXN1 knockdown in HCC cells exhibited a higher CSC population and an EMT phenotype (174). Chaudhary et al. revealed that miR-205 was highly downregulated in gemcitabine-resistant MIA PaCa-2R cells compared to gemcitabine-sensitive MIA PaCa-2 cells. The overexpression of miR-205 resulted in a reduction in EMT, CSCs, and chemo-resistance markers in MIA PaCa-2R cells, suggesting that miR-205 can enhance the sensitivity of gemcitabine-resistant PC cells to gemcitabine (175). In addition, the overexpression of miR-363 in drug-resistant OC cell lines (A2780cp and C13) restores CDDP sensitivity by directly targeting Snail (a mesenchymal marker). Consistent with this, Snail overexpression dramatically suppressed the effect of miR-363 on CDDP resistance of A2780cp and C13 cells, indicating that miR-363 regulates CDDP resistance in OC through Snail-induced EMT (176). In summary, understanding the effect of miRNAs on stemness properties and EMT in the development of cancer drug resistance may provide new insights into the development of therapeutic strategies for patients with a poor response to chemotherapeutic agents.

MiRNAs are involved in the regulation of inflammation by targeting T cells

Chronic inflammation triggered by infections, aberrant immune reactions or environmental factors is an uncontrolled inflammatory response and contributes to cancer progression by influencing various biological behaviors of cancer cells, including cellular proliferation, invasion, angiogenesis, metastasis, and drug resistance (177). T cells are the major effector cells in cellular immunity. They are involved in inflammation by producing cytokines in immune responses (178). The immune evasion and immune tolerance induced by the dysregulation of T cell function have shown to be the main causes of drug resistance development (27). Therefore, targeting T cells is an effective way to improve drug sensitivity for cancer patients. An increasing amount of evidence suggests that miRNAs are crucial regulators of T cell functions. For example, Yan et al. discovered that miR-181a was upregulated in T-cell lymphoblastic lymphoma Jurkat and H9 cells treated with DOX, CDDP, cyclophosphamide, and cytarabine. Knockdown of miR-181a in Jurkat and H9 cells significantly enhanced the sensitivity of these chemotherapeutic drugs (179). Ning et al. demonstrated that miR-208b was upregulated in exosomes from CRC cell lines NCM460, SW480, and oxaliplatin (OXA)-resistant SW480. Exosomal miR-208b facilitated regulatory T cells expansion by targeting programmed cell death factor 4, thereby enhancing OXA resistance in CRC (180). Xu et al. showed that miR-424 (322) reversed drug resistance in OC by activating T cell immune response,

resulting in the inhibition of immune evasion in drug-resistant OC. Mechanistically, miR-424 (322) inhibited IFN-γ-induced apoptosis in PD-L1-associated $CD8^+$ T cells and altered T cell cytokine secretions by downregulating PD-L1, resulting in the enhancement of chemotherapy efficacy in Skov3 (CP) cells (181). In addition, the downregulation of miR-145 by CDDP in A2780 cells increased PD-L1 levels by directly targeting c-Myc, leading to the induction of T cell apoptosis and enhancement of CDDP resistance in OC (182), indicating that miR-145 dysregulation contributes to the development CDDP resistance *via* T cell dysfunction-mediated immune tolerance. All these findings support the hypothesis that miRNAs are involved in the regulation of cancer drug resistance by targeting T cells. Therefore, in-depth investigations are required to clarify the detailed mechanisms of miRNAs in regulating T cells, which may provide new insights into the development of miRNA-based therapeutic strategies for cancer patients, particularly those with a poor response to chemotherapy.

LncRNAs and cancer drug resistance

LncRNAs control the cellular death pathways in cancer drug resistance

The dysregulation of lncRNAs has been shown to participate in the development of cancer drug resistance through interference with cellular apoptosis or proliferation pathways (18, 183). For instance, Li et al. revealed that lncRNA TINCR was significantly increased in CDDP-resistant choroidal melanoma (CM) tissues and cells. TINCR overexpression in OCM-1 cells promoted proliferation and inhibited apoptosis by upregulating ERK-2 *via* sponging miR-19b-3p, leading to the enhancement of CDDP resistance in CM (184). Zhou et al. found that lncRNA CCAT2 was upregulated in breast cancer (BC) tissues and 5-FU-resistant BC cell lines (MDA-MB-231, SKBR-3, MCF-7, and HCC-1937) after chemotherapy. CCAT2 overexpression in 5-FU-resistant MDA-MB-231, MCF-7 cells inhibited apoptosis and increased proliferation by activating the mTOR signaling pathway, resulting in a reduction in 5-FU sensitivity (185). Guo et al. demonstrated that lncRNA HEIH was upregulated in PTX-resistant endometrial cancer Ishikawa and HHUA cells. The overexpression of HEIH in Ishikawa and HHUA cells enhanced PTX resistance by depressing cell apoptosis and enhancing cell proliferation and viability *via* activating the MAPK signaling pathway (186). Zhu et al. showed that LINC00942 was significantly upregulated in drug-resistant GC cell lines SGC7901 and BGC823, and its overexpression in SGC7901 and BGC823 cells facilitated drug resistance by suppressing cellular apoptosis and enhancing their stemness features. Mechanistically, LINC00942 upregulated MSI2 by inhibiting its degradation *via* preventing its interaction with SCFβ-TRCP E3 ubiquitin ligase, thereby stabilizing c-Myc mRNA in an m6A-dependent manner (187). In addition, several oncogenic lncRNAs, such as APOC1P1-3, PRLB, and WDFY3-AS2, have also been reported to promote drug resistance by targeting the apoptotic pathways in distinct cancer types (53, 188, 189).

Recent studies indicate that the activation of autophagy by chemotherapeutic agents can protect cancer cells from drug-induced apoptosis (161, 190). Zhang et al. showed that exosomal lncRNA SNHG7 was highly expressed in docetaxel-resistant lung adenocarcinoma (LUAD) H1299 and SPC-A1 cells. The knockdown of SNHG7 in docetaxel-resistant H1299 and SPC-A1 cells significantly inhibited cell proliferation and autophagy and enhanced docetaxel sensitivity. Mechanistically, SNHG7 upregulation facilitated autophagy of H1299 and SPC-A1 cells by stabilizing autophagy-related genes autophagy related 5 (ATG5) and autophagy related 12 (ATG12) *via* recruiting human antigen R (HuR), resulting in the enhancement of docetaxel resistance in LUAD. Moreover, the transmission of exosomal SNHG7 from docetaxel-resistant H1299 and SPC-A1 cells to parental H1299 and SPC-A1 cells also promoted docetaxel resistance (191). In another study, lncRNA TUG1 was found to be upregulated in CRC tissues. The overexpression of TUG1 in LoVo and HCT15 cells enhanced CDDP resistance. Functional assays revealed that TUG1 promoted the proliferation and autophagy of LoVo and HCT15 cells by activating the HDGF/DDX/β-catenin axis *via* sequestrating miR-195-5p, leading to the enhancement of CDDP resistance in CRC (192). In addition, Chen et al. found that CRNDE triggered autophagy in HepG2 and Hep3B cells by increasing ATG4B levels *via* sponging miR-543. CRNDE silencing enhanced the sorafenib sensitivity of HepG2 and Hep3B cells, indicating that CRNDE may promote sorafenib resistance in HCC by driving ATG4B-mediated autophagy (193). High-mobility group box 1 (HMGB1) is a classical non-histone protein closely associated with autophagy (194). Chen et al. revealed that lncRNA H19 overexpression in CDDP-resistant TU-177 and AMC-HN-8 cells significantly facilitated autophagy by upregulating HMGB1 *via* sequestrating miR-107, resulting in the enhancement of CDDP resistance in laryngeal squamous cell carcinoma (LSCC). Consistent with this, the knockdown of H19 in CDDP-resistant TU-177 cells inhibited autophagy and CDDP resistance (195). Taken together, these findings strongly suggest that lncRNAs are widely involved in the development of cancer drug resistance by targeting cellular death pathways. However, the detailed mechanisms are still not fully understood; additional investigations are required to fully uncover the regulatory role of lncRNAs in cellular death pathways.

LncRNAs modulate ABC transporter-mediated drug efflux in cancer cells

The upregulation of ABC transporters is considered a main cause of MDR development in cancer. An increasing amount of evidence has shown that lncRNAs are involved in cancer drug

resistance by regulating ABC transporter-mediated drug efflux (196). For instance, Chen et al. revealed that lncRNA GAS5 overexpression in BC cells significantly enhanced the adriamycin (ADR) sensitivity by inhibiting ABCB1-mediated drug efflux. Mechanistically, GAS5 suppressed the expression of ABCB1 in ADR-resistant MCF-7 cells by activating the Wnt/β-catenin signaling pathway *via* miR-221-3p/DKK2 axis (197). In another study, lncRNA ADORA2A-AS1 was found to be upregulated in chronic myeloid leukemia (CML). ADORA2A-AS1 knockdown in K562 and KCL22 cells significantly enhanced the imatinib sensitivity of cells. Functional assays showed that ADORA2A-AS1 facilitated ABCC2 expression in K562 and KCL22 cells *via* sponging miR-665, indicating that ADORA2A-AS1 may contribute to the development of imatinib resistance by driving ABCC2-mediated drug efflux in CML (198). Moreover, Wang et al. demonstrated that lncRNA KCNQ1OT1 significantly increased in temozolomide (TMZ)-resistant U251 and U87 cells compared to TMZ-sensitive U251 and U87 cells. KCNQ1OT1 overexpression in TMZ-resistant U251/TMZ and U87/TMZ cells significantly upregulated the expression of ABCB1, c-Myc, and survivin by increasing PIM1 expression *via* sponging miR-761, leading to the enhancement of TMZ resistance (199). Shen et al. found that lncARSR was upregulated in ADR-resistant osteosarcoma U2OS and MG63 cells and accompanied by acquired MDR against PTX and CDDP. Mechanistically, lncARSR overexpression in ADR-resistant U2OS and MG63 cells significantly promoted cell rhodamine 123 efflux, survival, and migration by upregulating ABCB1, survivin, and matrix metalloproteinase-2 (MMP2) *via* activating AKT. Consistent with this, lncARSR knockdown in these ADR-resistant osteosarcoma cells facilitated cell rhodamine 123 retention and apoptosis (200). In addition, Li et al. showed that lncRNA HOTTIP was highly expressed in serum from esophageal cancer (EC) patients. Extracellular vesicles-containing HOTTIP contributed to ADR resistance in EC Eca109 cells by positively activating ABCG2 (201). Collectively, these studies indicate that the dysregulation of lncRNAs contributes to the development of cancer drug resistance by modulating ABC transporter-mediated drug efflux *via* targeting miRNAs. The exact mechanisms of the lncRNA/miRNA axis in drug efflux need to be further elucidated.

LncRNAs manipulate malignant features of cancer cells

LncRNAs have been shown to regulate the stemness of cancer cells, thereby demonstrating their regulatory roles in cancer drug resistance. For instance, Xie et al. found that lncRNA CBR3-AS1 was significantly upregulated in CRC cell lines (HCT116, HT29, SW620, and SW480) compared to normal colon epithelial FHC cells. CBR3-AS1 knockdown in OXA-resistant HCT116 and SW480 cells notably enhanced OXA sensitivity. Mechanistically, CBR3-AS1 knockdown inhibited the stem-like properties of HCT116 and SW480 cells by downregulating Nanog, Sox2, and Oct4 (stem cell markers) *via* sponging miR-145-5p, resulting in the reduction of OXA resistance in CRC (202). Liu et al. showed that lncROPM promoted the drug resistance of breast CSCs (BCSCs) isolated from BT-549, Hs578T, and MCF-7 cells by upregulating PLA2G16 *via* increasing its mRNA stability. Moreover, lncROPM contributed to the maintenance of BCSC stemness by facilitating phospholipid metabolism and the production of free fatty acid (such as arachidonic acid) *via* increasing the PLA2G16 levels (203). Cheng et al. revealed that lncRNA SNHG7 significantly increased in PC cells (PANC-1 and AsPC-1) co-cultured with mesenchymal stem cells (MSCs). The upregulation of SNHG7 induced by the MSCs in PANC-1 and AsPC-1 cells facilitated stemness of cells and Folfirinox resistance by activating the Notch1/Jagged1/Hes-1 signaling pathway *via* increasing Notch1 expression (204). In addition, Liu et al. demonstrated that lncRNA DUBR was highly expressed in HCC tissues and liver CSCs isolated from MHCC-97H, SNU-368 and MIHA, and its high expression was closely associated with poor chemotherapy response. DUBR overexpression in SNU-368 and MHCC-97H cells promoted the stemness of cancer cells and OXA resistance. Functional assays revealed that DUBR activated the Notch1 signaling pathway by upregulating cancerous inhibitor of protein phosphatase 2A (CIP2A) levels *via* sponging miR-520d-5p, leading to the enhancement of the stemness characteristics of the HCC cells and drug resistance (205).

LncRNA dysregulation contributes to the development of cancer drug resistance by altering T cell activity. For instance, KCNQ1OT1 was found to be upregulated in sorafenib-resistant HCC tissues and cells, and its knockdown in sorafenib-resistant SK-HEP-1 and Huh-7 cells co-cultured with T cells significantly inhibited immune escape by enhancing the immune surveillance ability of T cells. Mechanistically, KCNQ1OT1 upregulated PD-L1 levels in sorafenib-resistant SK-HEP-1 and Huh-7 cells by sponging miR-506, thereby reducing the apoptosis of $CD8^+$ T cells (206). In another study, LINC00184 overexpression in docetaxel-resistant DU145 and PC3 cells facilitated cell immune escape by upregulating PD-L1 *via* sponging miR-105-5p, resulting in the enhancement of docetaxel resistance in PCa (207). In addition, HCG18 could inhibit $CD8^+$ T cells activity by increasing PD-L1 levels *via* sponging miR-20b-5p, leading to the promotion of cetuximab resistance in CRC cells (208). LncRNAs can also act as the recruiters of epigenetic modifiers to play a role in cancer drug resistance. For instance, Li et al. found that PCAT-1 was upregulated in CDDP-resistant GC tissues and cell lines. PCAT-1 knockdown resensitized CDDP-resistant BGC823 and SGC790 cells to CDDP. Functional assays revealed that PCAT-1 epigenetically silenced PTEN by increasing H3K27me3 *via* recruiting the histone methyltransferase enhancer of zeste homolog 2 (EZH2), resulting in the enhancement of CDDP resistance in GC (209). Si et al. showed that H19 was highly

expressed in PTX-resistant BC cells. H19 upregulation in PTX-resistant MCF-7 and ZR-75-1 cells facilitated the recruitment of EZH2 to the *BIK* gene promoter, increasing H3K27me3 modification and suppressing *BIK* gene expression (210). In addition, Lin et al. revealed that LINC00261 was downregulated in 5-FU-resistant EC tissues. The overexpression of LINC00261 dramatically inhibited resistance to apoptosis in 5-FU-resistant TE-1 and -5 cells, whereas LINC00261 knockdown observed the opposite effect. Mechanistically, LINC00261 significantly decreased the levels of dihydropyrimidine dehydrogenase by increasing the methylation of its promoter through the recruitment of DNA methyltransferase, thereby enhancing 5-FU sensitivity in EC (211).

LncRNAs are able to govern the EMT process and malignant features of cancer cells to play a role in cancer drug resistance. Li et al. discovered that HOTTIP overexpression in glioma A172 and LN229 cells significantly increased cell proliferation, migration, and metastasis. Further, HOTTIP facilitated the EMT process in TMZ-resistant A172 and LN229 cells by decreasing E-cadherin expression and increasing Zeb1/Zeb2 (mesenchymal markers) *via* upregulating miR-10b, resulting in the enhancement of TMZ resistance in glioma. Consistent with this, miR-10b knockdown in HOTTIP-overexpressing A172 and LN229 cells reversed the EMT with associated TMZ sensitization (212). Zhang et al. demonstrated that HOTAIR facilitated migration, proliferation, and the resistance of HeLa and Siha cells to CDDP, PTX, and docetaxel. Mechanistically, HOTAIR enhanced the EMT process in HeLa and Siha cells by activating the PTEN/PI3K axis *via* sequestrating miR-29b, leading to the enhancement of MDR in CC (213). Jiang et al. revealed that HNF1A-AS1 facilitated 5-FU resistance in GC cells (MKN-45 and HGC-27) by enhancing the EMT process *via* increasing EIF5A2 levels. HNF1A-AS1 served as a sponge of miR-30b-5p to upregulate EIF5A2 (71). Moreover, Zhao et al. showed that DLX6-AS1 promoted proliferation, migration, invasion, and secondary CDDP resistance in LSCC cell lines SK-MES-1 and NCIH226. Mechanistically, DLX6-AS1 increased the expression of CUGBP, Elav-like family member 1 by sponging miR-181a-5p and miR-382-5p, resulting in the secondary CDDP resistance of LSCC cells (214). In addition, multiple lncRNAs, such as LINC01089, CYTOR, and H19, have also been shown to demonstrate their roles in cancer drug resistance by targeting the EMT process and altering malignant characteristics, such as proliferation, invasion, and metastasis (215–217). Altogether, these findings suggest that the underlying mechanisms of lncRNAs in cancer drug resistance involve their modulation of CSC expansion, T cell activity, EMT process, and malignant characteristics. In-depth investigations are required to fully elucidate the exact mechanisms behind lncRNA-mediated cancer drug resistance, which will be of great benefit in the development of lncRNA-based therapeutic strategies for cancer patients exhibiting a poor response to chemotherapy.

CircRNAs and cancer drug resistance

In recent years, the role of circRNAs in cancer progression has become a research hotspot, but the investigation of the contribution of circRNAs to cancer drug resistance is still at an initial stage (20, 218, 219). Emerging evidence indicates that the dysregulation of circRNAs is involved in cancer drug resistance *via* distinct mechanisms, such as drug transportation, cell death, DNA repair, and cancer stemness (220).

CircRNAs mainly act as miRNA sponges to play regulatory roles in cancer drug resistance. For instance, Xu et al. showed that circ-FBXW7 was downregulated in OXA-resistant CRC tissues and cells. Exosomal transfer of circ-FBXW7 enhanced the sensitivity of the OXA-resistant SW480 and HCT116 cells to OXA by inhibiting OXA efflux, elevating the OXA-induced apoptosis, and suppressing OXA-induced EMT *via* sponging miR-18b-5p (100). Another circRNA, circRNA_101277, was found to be highly expressed in CRC tissues and cells, and its overexpression in SW620 and SW480 cells facilitated CDDP resistance by upregulating IL-6 *via* sequestering miR-370 (221). Furthermore, Zhong et al. revealed that circRNA_100565 was upregulated in CDDP-resistant NSCLC tissues and cells. CircRNA_100565 knockdown in the drug-resistant A549 and H1299 cells reduced CDDP resistance by enhancing cell apoptosis and inhibiting proliferation and autophagy. Mechanistically, circRNA_100565 exerted its anti-drug resistant role by upregulating ADAM28 expression *via* sponging miR-377-3p in CDDP-resistant A549 and H1299 cells (92). Additionally, Huang et al. demonstrated that circAKT3 was highly expressed in CDDP-resistant GC tissues and cells compared to CDDP-sensitive samples. The upregulation of circAKT3 was closely associated with aggressive characteristics in GC patients receiving CDDP treatment. Functional assays demonstrated that circAKT3 upregulated PIK3R1 *via* sequestrating miR-198, thereby enhancing CDDP resistance by facilitating DNA damage repair and inhibiting the apoptosis of CDDP-resistant SGC7901 and BGC823 cells (222). CircRNA CDR1as was found to contribute to the development of CDDP resistance in NSCLC by altering the stemness characteristics of NSCLC cells. The overexpression of circRNA CDR1as in CDDP-sensitive NSCLC cells (A549, H1299, and Calu6) significantly increased the expression of stemness signatures (e.g., Sox2, Oct4 and Nanog) by upregulating HOXA9 *via* sponging miR-641, leading to the enhancement of CDDP resistance. Consistent with this, circRNA CDR1as knockdown in CDDP-resistant A549, H1299, and Calu6 cells suppressed the stemness of cancer cells (223). Moreover, Huang et al. demonstrated that circ_0001598 was highly expressed in trastuzumab-resistant BC samples, and its overexpression facilitated immune escape and trastuzumab-resistance of SKBR-3 and BT474 cells by upregulating PD-L1 levels *via* sponging PD-L1 (224). In

addition, Chen et al. showed that high circUSP7 levels are closely associated with $CD8^+$ T cell dysfunction in NSCLC patients. Exosomal circUSP7 inhibited $CD8^+$ T cell activity by upregulating Src homology region 2 (SH2)-containing protein tyrosine phosphatase 2 *via* sponging miR-934, resulting in enhanced resistance to anti-PD1 immunotherapy in NSCLC patients (225). There is no doubt that circRNAs have multifaceted functions in cancer drug resistance due to the broad involvement of miRNAs.

CircRNAs can also participate in cancer drug resistance by combining with other molecules. For instance, Wei et al. found circ0008399 enhanced CDDP resistance in bladder cancer EJ and T24T cells by upregulating TNF alpha-induced protein 3 (TNFAIP3) *via* directly binding to Wilms' tumor 1-associating protein (WTAP). Mechanistically, circ0008399 interacted with WTAP to promote the formation of the WTAP/METTL3/METTL14 m6A methyltransferase complex, thereby upregulating TNFAIP3 expression in an m6A-dependent manner. Consistent with this, targeting the circ0008399/WTAP/TNFAIP3 axis promoted CDDP sensitivity in EJ and T24T cells (226). Hu et al. showed that circFARP1 was involved in the regulation of stemness and gemcitabine resistance in pancreatic ductal adenocarcinoma by altering the ability of cancer-associated fibroblasts *via* leukemia inhibitory factor (LIF). Functional assays revealed that circFARP1 directly interacted with caveolin 1 to inhibit its degradation by blocking the binding of caveolin 1 to its ubiquitin E3 ligase zinc and ring finger 1 (ZNRF1), thereby enhancing LIF secretion (227). In addition, Chen et al. demonstrated that the overexpression of circRNA cia-MAF drove LCSC propagation, self-renewal, and metastasis by facilitating MAFF expression *via* recruiting the TIP60 complex to its promoter, indicating that cia-MAF may contribute to the drug resistance of liver cancer by modulating CSCs (228). Particular circRNAs may participate in cancer drug resistance by altering the key regulators during cancer progression. Further investigations are required to fully understand the detailed mechanisms of circRNAs in cancer drug resistance. In addition, the circRNA/miRNA axis associated with chemotherapeutic responsiveness in cancer should be clarified.

PiRNAs and cancer drug resistance

PiRNAs are a novel class of short chain ncRNAs (26-30 nucleotides) involved in a wide variety of physiological and pathological processes. They can regulate the expression of somatic genes through various mechanisms, including DNA methylation, chromatin modification and transposon silencing (229, 230). An increasing amount of evidence suggests that piRNAs are key regulators in the development of cancer drug resistance (231–233). For instance, Tan et al. discovered that piRNA-36,712 was significantly downregulated in BC tissues. The overexpression of piRNA-36,712 in MCF-7 and ZR75-1 cells significantly enhanced the sensitivity of cells to PTX and DOX. Correspondingly, piRNA-36,712 knockdown obtained the opposite effects. Mechanistically, piRNA-36,712 directly interacted with *SEPW1P* RNA (SEPW1 pseudogene), thereby suppressing SEPW1 expression by facilitating miR-7 and miR-324 to target *SEPW1* RNA, resulting in the enhancement of PTX and DOX sensitivity in BC (231). Mai et al. showed that piRNA-54265 was upregulated in CRC tissues. The overexpression of piRNA-54265 in HCT116 and LoVo cells promoted the formation of PIWIL2/STAT3/p-SRC complex by directly binding to PIWIL2, thereby activating the STAT3 signaling pathway, leading to the resistance of CRC cells to 5-FU and OXA (232). In addition, Wang et al. demonstrated that piR-L-138 was upregulated in CDDP-treated LSCC cells and patient-derived xenograft treated with CDDP. The knockdown of piR-L-138 in H157 and SKMES-1 cells enhanced CDDP sensitivity by directly binding to p60-MDM2 (233). Collectively, these findings indicate that piRNAs play vital roles in the regulation of cancer drug resistance, but the detailed mechanisms remain largely unknown. In-depth investigation may bring great benefits to the development of piRNA-based therapeutic strategies for cancer patients, particularly those with a poor response to chemotherapy.

Clinical implications of ncRNAs in cancer drug resistance

NcRNAs as biomarkers for the diagnosis and prognosis of cancer patients

It has been reported that approximately 50% of cancer patients are diagnosed at an advanced stage, with poor response rates and a low chance of cure (3). This is the main factor leading to the poor survival of cancer patients. Moreover, it is difficult for most cancer patients to obtain accurate individualized therapeutic strategies due to the lack of effective methods for prognostic assessment in clinical practice. In recent years, several protein biomarkers, such as carcinoembryonic antigen, carbohydrate antigen 15-3, and human epidermal growth factor receptor-2, have been applied in the early diagnosis and prognostic assessment of cancer patients. However, the unsatisfactory sensitivity and specificity of these biomarkers restricts their further utilization (234–236). Thus, it is urgent to develop new biomarkers with high sensitivity and specificity for cancer patients, particularly those with a poor response to chemotherapy.

NcRNAs can be secreted in actively packed particles (e.g., exosomes, microvesicles, or apoptotic bodies) and freely circulate in the blood, and their concentrations are almost the same as those in primary tumors (237, 238). Moreover, they also exhibit some unique characteristics, such as differently expressed patterns, high stability, and high detectability (239). These

features strongly suggest that ncRNAs possess great potential as ideal diagnostic and prognostic biomarkers for cancer patients in clinical treatment. In fact, a large number of ncRNAs, particularly miRNAs and lncRNAs, have been identified as diagnostic and/or prognostic biomarkers of cancer (Table 2). For instance, Pan et al. showed that the levels of miR-33a-5p and miR-128-3p in whole blood were significantly downregulated in lung cancer patients or early-stage lung cancer patients compared to healthy controls. Further prospective study revealed that the area under the curve (AUC) value for the combination of miR-33a-5p and miR-128-3p was 0.9511, which was higher than that for CYFR21-1 (0.5856), NSE (0.6189), and CA72-4 (0.5206), indicating that the combination of the two miRNAs can serve as novel biomarkers for the early detection of lung cancer (284). In another study, Lu et al. developed a 21-miRNA-based diagnostic model and a 3-miRNA-based prognostic model that can be used to predict the prognosis of uterus corpus endometrial cancer patients and their response to chemotherapy and immunotherapy. The AUC values for the diagnostic panels were 0.911 in the training set, 0.827 in the test set, and 0.878 in the entire set. The diagnostic panel was closely associated with tumor mutation burden, PDL1 expression, and the infiltration of immune cells. Moreover, the prognostic risk signature of the prognostic panel can be used to predict the response to some commonly used chemotherapy regimens (285).

In a recent study by Xu et al., they found that the plasma levels of ZFAS1, SNHG11, LINC00909 and LINC00654 were significantly downregulated in postoperative CRC patients compared to preoperative CRC patients. The combination of these four lncRNAs exhibited high diagnostic performance for CRC (AUC = 0.937), especially early-stage disease (AUC = 0.935). Moreover, SNHG11 exhibited the greatest diagnostic ability to distinguish precancerous lesions from early-stage tumor formation (286). Besides, Meng et al. showed that lncRNA BCAR4 overexpression was closely associated with lymph node metastasis ($p < 0.001$), high tumor stage ($p < 0.001$), and distant metastasis ($p < 0.001$). Cancer patients with upregulated lncRNA BCAR4 exhibited poor OS ($p < 0.001$), suggesting that lncRNA BCAR4 is a promising prognostic biomarker in cancer patients (287). CircRNAs are also promising biomarker candidates in cancer treatment. Liu et al. revealed that hsa_circRNA_101237 was significantly upregulated in multiple myeloma (MM) cells, bortezomib-resistant MM cells, and the bone marrow tissues of MM patients. The high expression of hsa_circRNA_101237 reduced the sensitivity of the MM patients to bortezomib. Further, the AUC value for hsa_circRNA_101237 was 0.92 ($p < 0.0001$). MM patients with upregulated hsa_circRNA_101237 also demonstrated shorter OS and progression-free survival (PFS). This data indicated that hsa_circRNA_101237 possessed great potential as a diagnostic and prognostic biomarker for MM (288). Collectively, these studies strongly suggest that ncRNAs are valuable biomarkers for diagnosis, prognosis, and predicting drug response in cancer treatment. However, larger patient cohorts are required to further validate their potential as biomarkers in clinical applications.

Therapeutic potential of ncRNAs in cancer drug resistance

The poor response of patients to chemotherapy and the emergence of drug resistance are still the most critical obstacles in clinical cancer treatment. A large number of studies have confirmed the essential roles of ncRNAs in the development of cancer drug resistance (289). They may act as oncogenes or tumor suppressors to play dual roles in cancer progression, depending on their diverse downstream targets (290). These characteristics endow ncRNAs with great potential as promising therapeutic targets or therapeutic agents in cancer treatment. Therapeutic strategies that make use of ncRNAs or directly target ncRNAs may bring great benefits to the precise treatment of cancer patients, particularly those demonstrating a poor response to chemotherapy. The delivery of tumor-suppressive ncRNAs to target cancer cells is considered a promising strategy to improve cancer intervention. For instance, miRNA-3662 was found to be downregulated in pancreatic ductal adenocarcinoma (PDAC) tissues and cell lines. MiRNA-3662 overexpression enhanced gemcitabine sensitivity and inhibited aerobic glycolysis in the PDAC cells by decreasing hypoxia-inducible factor 1α (HIF-1α) expression (126). LncRNA ENSG0000254615 was found to be highly expressed in 5-FU-sensitive CRC cells. ENSG0000254615 overexpression inhibited cell proliferation and 5-FU resistance by upregulating p21 and downregulating Cyclin D1 in CRC (291). Circ-G004213 was significantly upregulated in CDDP-sensitive liver cancer cells and its high expression was positively associated with the prognosis of patients with liver cancer. Further analysis revealed that circ-G004213 suppressed CDDP resistance by upregulating PRPF39 *via* sponging miR-513b-5p (292). Therefore, the upregulation of tumor-suppressive ncRNAs, such as miRNA-3662, ENSG0000254615, and circ-G004213, may represent an effective way to inhibit cancer progression and reverse drug resistance. Targeting oncogenic ncRNAs could be another effective strategy to overcome cancer drug resistance. For instance, miR-192 was significantly increased in CDDP-resistant lung cancer cells compared to non-resistant cancer cells. The overexpression of miR-192 activated the NF-κB signaling pathway by directly targeting NF-κB repressing factor, resulting in the inhibition of apoptosis, promotion of proliferation, and enhancement of CDDP resistance in the lung cancer cells. MiR-192 knockdown obtained the opposite effect (293). In another study, circFBXL5 was found to be highly expressed in BC tissues and 5-FU-resistant BC cells. CircFBXL5 knockdown enhanced the 5-FU sensitivity in the

TABLE 2 NcRNAs as biomarkers diagnostic and prognostic in cancers drug resistance.

Cancer types	Biomarker types	ncRNAs	Potential values	Reference
OC	Diagnosis	miR-138-5p, miR-182-5p LINC01508 circRNA_0000735	Low levels of miR-138-5p, miR-182-5p, LINC01508 and circRNA_0000735 predict poor response to chemotherapy.	(49, 240–242)
		miR-205-5p lncRNA CHRF exosomal circFoxp1	High levels of miR-205-5p, lncRNA CHRF and exosomal circFoxp1 predict poor response to chemotherapy.	(243–245)
	Prognosis	miR-378a-3p, miR-513a-3p LINC00515	Low levels of miR-378a-3p, miR-513a-3p and LINC00515 predict poor prognosis.	(246–248)
		miR-98-5p lncRNA HOTAIR circTNPO3	High levels of miR-98-5p, lncRNA HOTAIR and circTNPO3 predict poor prognosis.	(249–251)
GC	Diagnosis	miR-124-3p lncRNA CASC2 hsa_circ_0000520	Low levels of miR-124-3p, lncRNA CASC2, hsa_circ_0000520 predict poor response to chemotherapy.	(252–254)
		exosomal miR-223 lncRNA MALAT1 circ_0026359	High levels of exosomal miR-223, lncRNA MALAT1, circ_0026359 predict poor response to chemotherapy.	(255–257)
	Prognosis	miR-34a hsa_circ_0001546	Low levels of miR-34a and hsa_circ_0001546 predict poor prognosis.	(82, 258)
		miR-15a-5p lncRNA EIF3J-DT circ_0026359	High levels of miR-15a-5p, LncRNA EIF3J-DT and circ_0026359 predict poor prognosis.	(257, 259, 260)
NSCLC	Diagnosis	miR-519d-3p	Low expression level of miR-519d-3p correlates with a decreased responsiveness to gefitinib.	(261)
		exosomal miR-136-5p lncRNA HOST2	High level of exosomal miR-136-5p and lncRNA HOST2 predict poor response to chemotherapy.	(262, 263)
	Prognosis	miR-133a-3p lncRNA RHPN1-AS1	Low levels of miR-133a-3p and lncRNA RHPN1-AS1 predict poor prognosis.	(264, 265)
		lncRNA EGFR-AS1 circ_0005909	High levels of lncRNA EGFR-AS1 and circ_0005909 predict poor prognosis.	(266, 267)
CRC	Diagnosis	miR-325 lncRNA MEG3	Low levels of miR-325 and lncRNA MEG3 predict poor response to chemotherapy.	(268, 269)
		miR-454-3p	Upregulated miR-454-3p is related to a poor response to OXA-based treatment.	(101)
	Prognosis	miR-302a lncRNA HAND2-AS1	Low levels of miR-302a and lncRNA HAND2-AS1 predict poor prognosis.	(94, 270)
		lncRNA AGAP2-AS1 circHIPK3	High levels of lncRNA AGAP2-AS1 and circHIPK3 predict poor prognosis.	(271, 272)
BC	Diagnosis	miR-24-3p LINC00160	High levels of miR-24-3p and LINC00160 predict poor response to chemotherapy.	(120, 273)
		lncRNA CBR3-AS1 circWAC	High levels of lncRNA CBR3-AS1 and circWAC predict poor prognosis.	(274, 275)
HCC	Diagnosis	LINC00680 circRNA-SORE	High levels of LINC00680 and circRNA-SORE predict poor response to chemotherapy.	(276, 277)
	Prognosis	circRNA_101237	High serum level of circRNA_101237 is related to a poor survival of patients (P<0.001).	(278)

(Continued)

TABLE 2 Continued

Cancer types	Biomarker types	ncRNAs	Potential values	Reference
PC	Diagnosis	miR-20a-5p	MiR-20a-5p level can serve as a predictor of gemcitabine resistance with an AUC of 89% (P<0.0001), for its downregulation correlates with poor response to gemcitabine.	(279)
	Prognosis	microRNA-296-5p lncRNA HCP5	High levels of microRNA-296-5p and lncRNA HCP5 predict poor prognosis.	(280, 281)
Glioma	Prognosis	miR-1246	Overexpression of miR-1246 predict a low OS in high grade glioma patients.	(282)
Multiple Myeloma	Diagnosis	exosomal circMYC	Upregulated expression of circulating exosomal circMYC correlates with decreased sensitivity to bortezomib.	(283)

BC cells by suppressing cell migration and invasion and facilitating apoptosis. Mechanistically, circFBXL5 promoted 5-FU resistance by upregulating HMGA2 *via* sequestrating miR-216b (294). Oncogenic ncRNAs, such as miRNA-3662 and circFBXL5, might be used as ideal candidates for therapeutic targets. These findings strongly suggest that the activation of tumor-suppressive ncRNAs or the inactivation of oncogenic ncRNAs are critical mechanisms that restore cancer drug sensitivity. A better understanding of the molecular mechanism of ncRNAs involved in cancer progression and drug resistance will substantially contribute to the precise treatment of cancer patients. However, there are still some challenges that need to be addressed, such as, low bioavailability, side effects, and off-target effects.

Conclusion and perspective

Cancer is one of the most common and fatal malignant diseases worldwide, with high rates of metastasis and recurrence. Chemotherapy remains the best choice for all stages of cancer, and it can effectively improve patients' prognosis. However, the emergency of drug resistance seriously restricts the clinical efficiency of chemotherapy, and ultimately results in treatment

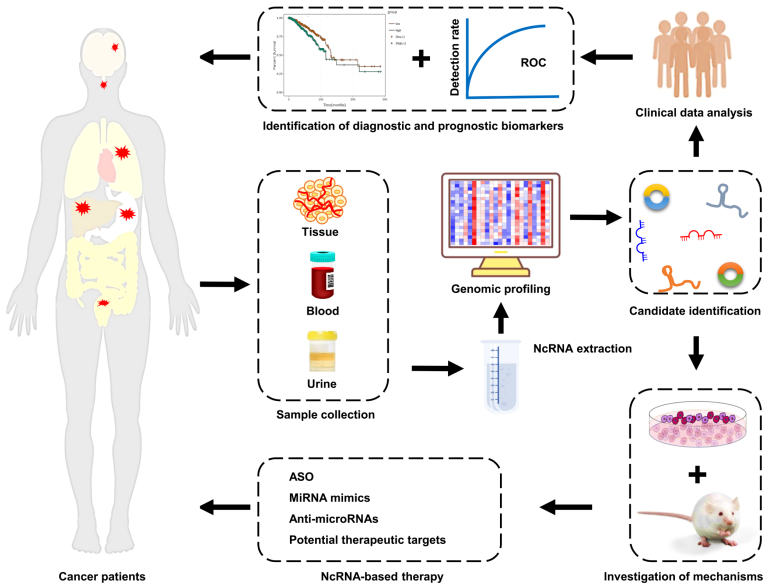

FIGURE 3
Clinical implications of ncRNAs in cancer drug resistance. NcRNAs are enriched in tissue, blood, and urine samples from cancer patients with drug resistance. The expression profiles of ncRNAs are mapped using high-throughput sequencing technologies. Next, the differentially expressed ncRNAs are screened and identified by bioinformatics analysis. Subsequently, the mechanisms of ncRNAs in cancer drug resistance are elucidated using cell and animal models. The aberrantly expressed ncRNAs that possessed great potential as biomarkers and/or therapeutic targets are identified. Finally, cancer patients, particularly those with drug resistance, receive the individualized precision treatment strategies.

failure. Therefore, a better understanding of the mechanisms responsible for cancer drug resistance will be of great benefit to the development of precise therapeutic strategies for cancer patients, particularly those demonstrating a poor response to chemotherapy. With the rapid development of high-throughput sequencing techniques, a large number of ncRNAs, particularly miRNAs, lncRNAs, and circRNAs, have been found to be aberrantly expressed in cancer tissues and cell lines. These aberrantly expressed ncRNAs are closely associated with cancer progression and drug resistance. It is well established that ncRNAs participate in the development of cancer drug resistance *via* distinct mechanisms, including the suppression of cell death pathways, induction of excessive drug efflux, facilitation of autophagy, regulation of CSC features, and enhancement of the EMT. Aberrant levels of ncRNAs have been observed in cancer patients' blood, tissue, and even urine (295). Furthermore, the aberrant expression of ncRNAs was found to be closely associated with some pathological characteristics of cancer patients, including OS and PFS (288). These features endow ncRNAs with great potential as ideal biomarkers for the diagnosis and prognosis of cancer patients. In addition, due to the crucial roles of ncRNAs in cancer progression and drug resistance, they are considered to be promising therapeutic targets or therapeutic agents for cancer patients (Figure 3). The direct delivery of tumor-suppressive ncRNAs to target cancer cells is a promising way to improve cancer intervention. On the other hand, silencing oncogenic ncRNAs is also an effective strategy to overcome cancer drug resistance. Therefore, it is urgent to develop efficient and non-toxic delivery systems and ncRNA silencing technologies. Although some progress has been made in this area, overcoming resistance to chemotherapeutic drugs remains a large challenge. More clinical trials need to be launched to advance the development of ncRNA-based therapeutic strategies to benefit cancer patients.

Author contributions

XZ: original draft preparation and writing—review and editing. XA: data curation and funding acquisition. ZJ: data curation. YiwL: data curation. SK: data curation. CD: data curation. JZ: data curation. JW: data curation. YinL: writing—conceptualization, original draft preparation, and writing—review and editing. All authors contributed to the article and approved the submitted version.

Funding

All authors are supported by Qingdao Medical College, Qingdao University. This work was funded by the China Postdoctoral Science Foundation (2018M642607).

Conflict of interest

The authors declare that the research was conducted in the absence of any commercial or financial relationships that could be construed as a potential conflict of interest.

Publisher's note

References

1. Yin W, Wang J, Jiang L, James Kang Y. Cancer and stem cells. *Exp Biol Med (Maywood)* (2021) 246(16):1791–801. doi: 10.1177/15353702211005390

2. Wang M, Yu F, Zhang Y, Chang W, Zhou M. The effects and mechanisms of flavonoids on cancer prevention and therapy: Focus on gut microbiota. *Int J Biol Sci* (2022) 18(4):1451–75. doi: 10.7150/ijbs.68170

3. Sung H, Ferlay J, Siegel RL, Laversanne M, Soerjomataram I, Jemal A, et al. Global cancer statistics 2020: Globocan estimates of incidence and mortality worldwide for 36 cancers in 185 countries. *CA: Cancer J Clin* (2021) 71(3):209–49. doi: 10.3322/caac.21660

4. Hirsch FR, Walker J, Higgs BW, Cooper ZA, Raja RG, Wistuba II. The combiome hypothesis: Selecting optimal treatment for cancer patients. *Clin Lung Cancer* (2022) 23(1):1–13. doi: 10.1016/j.cllc.2021.08.011

5. Lara-Velazquez M, Mehkri Y, Panther E, Hernandez J, Rao D, Fiester P, et al. Current advances in the management of adult craniopharyngiomas. *Curr Oncol* (2022) 29(3):1645–71. doi: 10.3390/curroncol29030138

6. Zuo YB, Zhang YF, Zhang R, Tian JW, Lv XB, Li R, et al. Ferroptosis in cancer progression: Role of noncoding rnas. *Int J Biol Sci* (2022) 18(5):1829–43. doi: 10.7150/ijbs.66917

7. Wagner AD, Syn NL, Moehler M, Grothe W, Yong WP, Tai BC, et al. Chemotherapy for advanced gastric cancer. *Cochrane Database Syst Rev* (2017) 8: CD004064. doi: 10.1002/14651858.CD004064.pub4

8. Liu Y, Ao X, Zhou X, Du C, Kuang S. The regulation of pbxs and their emerging role in cancer. *J Cell Mol Med* (2022) 26(5):1363–79. doi: 10.1111/jcmm.17196

9. Zhang Y, Wei YJ, Zhang YF, Liu HW, Zhang YF. Emerging functions and clinical applications of exosomal ncrnas in ovarian cancer. *Front Oncol* (2021) 11:765458. doi: 10.3389/fonc.2021.765458

10. Jiang Y, Zhao L, Wu Y, Deng S, Cao P, Lei X, et al. The role of ncrnas to regulate immune checkpoints in cancer. *Front Immunol* (2022) 13:853480. doi: 10.3389/fimmu.2022.853480

11. Wang M, Chen X, Yu F, Ding H, Zhang Y, Wang K. Extrachromosomal circular dnas: Origin, formation and emerging function in cancer. *Int J Biol Sci* (2021) 17(4):1010–25. doi: 10.7150/ijbs.54614

12. Najafi S, Tan SC, Raee P, Rahmati Y, Asemani Y, Lee EHC, et al. Gene regulation by antisense transcription: A focus on neurological and cancer diseases. *Biomed Pharmacother = Biomed Pharmacotherapie* (2022) 145:112265. doi: 10.1016/j.biopha.2021.112265

13. Zhang YF, Shan C, Wang Y, Qian LL, Jia DD, Zhang YF, et al. Cardiovascular toxicity and mechanism of bisphenol a and emerging risk of bisphenol s. *Sci Total Environ* (2020) 723:137952. doi: 10.1016/j.scitotenv.2020.137952

14. Shan P, Yang F, Qi H, Hu Y, Zhu S, Sun Z, et al. Alteration of Mdm2 by the small molecule Yf438 exerts antitumor effects in triple-negative breast cancer. *Cancer Res* (2021) 81(15):4027–40. doi: 10.1158/0008-5472.CAN-20-0922

15. Li Z, Wang Y, Liu S, Li W, Wang Z, Jia Z, et al. Mir-200a-3p promotes gastric cancer progression by targeting dlc-1. *J Mol Histol* (2022) 53(1):39–49. doi: 10.1007/s10735-021-10037-7

16. Lin X, Zhuang S, Chen X, Du J, Zhong L, Ding J, et al. Lncrna Itgb8-As1 functions as a cerna to promote colorectal cancer growth and migration through integrin-mediated focal adhesion signaling. *Mol Ther* (2022) 30(2):688–702. doi: 10.1016/j.ymthe.2021.08.011

17. Ishola AA, Chien CS, Yang YP, Chien Y, Yarmishyn AA, Tsai PH, et al. Oncogenic circrna C190 promotes non-small cell lung cancer *Via* modulation of the Egfr/Erk pathway. *Cancer Res* (2022) 82(1):75–89. doi: 10.1158/0008-5472.CAN-21-1473

18. Chen B, Dragomir MP, Yang C, Li Q, Horst D, Calin GA. Targeting non-coding rnas to overcome cancer therapy resistance. *Signal Transduction Targeted Ther* (2022) 7(1):121. doi: 10.1038/s41392-022-00975-3

19. Yamaguchi K, Yamamoto T, Chikuda J, Shirota T, Yamamoto Y. Impact of non-coding rnas on chemotherapeutic resistance in oral cancer. *Biomolecules* (2022) 12(2):284. doi: 10.3390/biom12020284

20. Wang M, Yu F, Li P, Wang K. Emerging function and clinical significance of exosomal circrnas in cancer. *Mol Ther Nucleic Acids* (2020) 21:367–83. doi: 10.1016/j.omtn.2020.06.008

21. Mattick JS. Non-coding rnas: The architects of eukaryotic complexity. *EMBO Rep* (2001) 2(11):986–91. doi: 10.1093/embo-reports/kve230

22. Nair J, Maheshwari A. Non-coding rnas in necrotizing enterocolitis- a new frontier? *Curr Pediatr Rev* (2022) 18(1):25–32. doi: 10.2174/1573396317666211102093646

23. Liu Y, Ao X, Jia Y, Li X, Wang Y, Wang J. The foxo family of transcription factors: Key molecular players in gastric cancer. *J Mol Med (Berl)* (2022) 100 (7):997–1015. doi: 10.1007/s00109-022-02219-x

24. Dahariya S, Paddibhatla I, Kumar S, Raghuwanshi S, Pallepati A, Gutti RK. Long non-coding rna: Classification, biogenesis and functions in blood cells. *Mol Immunol* (2019) 112:82–92. doi: 10.1016/j.molimm.2019.04.011

25. Ma L, Bajic VB, Zhang Z. On the classification of long non-coding rnas. *RNA Biol* (2013) 10(6):925–33. doi: 10.4161/rna.24604

26. Dozmorov MG, Giles CB, Koelsch KA, Wren JD. Systematic classification of non-coding rnas by epigenomic similarity. *BMC Bioinf* (2013) 14 Suppl 14:S2. doi: 10.1186/1471-2105-14-S14-S2

27. Liu Y, Ao X, Ji G, Zhang Y, Yu W, Wang J. Mechanisms of action and clinical implications of micrornas in the drug resistance of gastric cancer. *Front Oncol* (2021) 11:768918. doi: 10.3389/fonc.2021.768918

28. Liu Y, Ding W, Yu W, Zhang Y, Ao X, Wang J. Long non-coding rnas: Biogenesis, functions, and clinical significance in gastric cancer. *Mol Ther Oncolytics* (2021) 23:458–76. doi: 10.1016/j.omto.2021.11.005

29. Liu Y, Ao X, Yu W, Zhang Y, Wang J. Biogenesis, functions, and clinical implications of circular rnas in non-small cell lung cancer. *Mol Ther Nucleic Acids* (2022) 27:50–72. doi: 10.1016/j.omtn.2021.11.013

30. Hurschler BA, Harris DT, Grosshans H. The type ii poly(a)-binding protein pabp-2 genetically interacts with the let-7 mirna and elicits heterochronic phenotypes in caenorhabditis elegans. *Nucleic Acids Res* (2011) 39(13):5647–57. doi: 10.1093/nar/gkr145

31. Wu H, Sun S, Tu K, Gao Y, Xie B, Krainer AR, et al. A splicing-independent function of Sf2/Asf in microrna processing. *Mol Cell* (2010) 38(1):67–77. doi: 10.1016/j.molcel.2010.02.021

32. Akhtar J, Lugoboni M, Junion G. M(6)a rna modification in transcription regulation. *Transcription* (2021) 12(5):266–76. doi: 10.1080/21541264.2022.2057177

33. Di Timoteo G, Dattilo D, Centron-Broco A, Colantoni A, Guarnacci M, Rossi F, et al. Modulation of circrna metabolism by M(6)a modification. *Cell Rep* (2020) 31(6):107641. doi: 10.1016/j.celrep.2020.107641

34. Galicia J, Khan AA. Non-coding rnas in endodontic disease. *Semin Cell Dev Biol* (2022) 124:82–4. doi: 10.1016/j.semcdb.2021.07.006

35. Chen X, Li X, Wei C, Zhao C, Wang S, Gao J. High expression of Setdb1 mediated by mir-29a-3p associates with poor prognosis and immune invasion in breast invasive carcinoma. *Transl Cancer Res* (2021) 10(12):5065–75. doi: 10.21037/tcr-21-1527

36. Gao XQ, Liu CY, Zhang YH, Wang YH, Zhou LY, Li XM, et al. The circrna cneacr regulates necroptosis of cardiomyocytes through Foxa2 suppression. *Cell Death Differ* (2022) 29(3):527–39. doi: 10.1038/s41418-021-00872-2

37. Zhang L, Zhang Y, Zhao Y, Wang Y, Ding H, Xue S, et al. Circulating mirnas as biomarkers for early diagnosis of coronary artery disease. *Expert Opin Ther Pat* (2018) 28(8):591–601. doi: 10.1080/13543776.2018.1503650

38. Zhang L, Zhang Y, Xue S, Ding H, Wang Y, Qi H, et al. Clinical significance of circulating micrornas as diagnostic biomarkers for coronary artery disease. *J Cell Mol Med* (2020) 24(1):1146–50. doi: 10.1111/jcmm.14802

39. Ghanbarian H, Yildiz MT, Tutar Y. Microrna targeting. *Methods Mol Biol* (2022) 2257:105–30. doi: 10.1007/978-1-0716-1170-8_6

40. Gan J, Gu T, Yang H, Ao Z, Cai G, Hong L, et al. Non-coding rnas regulate spontaneous abortion: A global network and system perspective. *Int J Mol Sci* (2022) 23(8):4214. doi: 10.3390/ijms23084214

41. Zhang L, Wang Y, Yu F, Li X, Gao H, Li P. Circhipk3 plays vital roles in cardiovascular disease. *Front Cardiovasc Med* (2021) 8:733248. doi: 10.3389/fcvm.2021.733248

42. Chen J, Gao C, Zhu W. Long non-coding rna Slc25a25-As1 exhibits oncogenic roles in non-small cell lung cancer by regulating the microrna-195-5p/Itga2 axis. *Oncol Lett* (2021) 22(1):529. doi: 10.3892/ol.2021.12790

43. Bahar E, Han SY, Kim JY, Yoon H. Chemotherapy resistance: Role of mitochondrial and autophagic components. *Cancers* (2022) 14(6):1462. doi: 10.3390/cancers14061462

44. Liu Y, Ao X, Wang Y, Li X, Wang J. Long non-coding rna in gastric cancer: Mechanisms and clinical implications for drug resistance. *Front Oncol* (2022) 12:841411. doi: 10.3389/fonc.2022.841411

45. Zhou Y, Wang C, Ding J, Chen Y, Sun Y, Cheng Z. Mir-133a targets Yes1 to reduce cisplatin resistance in ovarian cancer by regulating cell autophagy. *Cancer Cell Int* (2022) 22(1):15. doi: 10.1186/s12935-021-02412-x

46. Hu Z, Cai M, Zhang Y, Tao L, Guo R. Mir-29c-3p inhibits autophagy and cisplatin resistance in ovarian cancer by regulating Foxp1/Atg14 pathway. *Cell Cycle* (2020) 19(2):193–206. doi: 10.1080/15384101.2019.1704537

47. Cai Y, An B, Yao D, Zhou H, Zhu J. Microrna mir-30a inhibits cisplatin resistance in ovarian cancer cells through autophagy. *Bioengineered* (2021) 12 (2):10713–22. doi: 10.1080/21655979.2021.2001989

48. Guo J, Pan H. Long noncoding rna Linc01125 enhances cisplatin sensitivity of ovarian cancer *Via* mir-1972. *Med Sci Monitor Int Med J Exp Clin Res* (2019) 25:9844–54. doi: 10.12659/MSM.916820

49. Xiao L, Shi XY, Li ZL, Li M, Zhang MM, Yan SJ, et al. Downregulation of Linc01508 contributes to cisplatin resistance in ovarian cancer *Via* the regulation of the hippo-yap pathway. *J Gynecol Oncol* (2021) 32(5):e77. doi: 10.3802/jgo.2021.32.e77

50. Zhao Z, Ji M, Wang Q, He N, Li Y. Circular rna Cdr1as upregulates scai to suppress cisplatin resistance in ovarian cancer *Via* mir-1270 suppression. *Mol Ther Nucleic Acids* (2019) 18:24–33. doi: 10.1016/j.omtn.2019.07.012

51. Huang W, Chen L, Zhu K, Wang D. Oncogenic microrna-181d binding to ogt contributes to resistance of ovarian cancer cells to cisplatin. *Cell Death Discovery* (2021) 7(1):379. doi: 10.1038/s41420-021-00715-6

52. Wang J, Liu L. Mir-149-3p promotes the cisplatin resistance and emt in ovarian cancer through downregulating Timp2 and Cdkn1a. *J Ovarian Res* (2021) 14(1):165. doi: 10.1186/s13048-021-00919-5

53. Wu Y, Wang T, Xia L, Zhang M. Lncrna Wdfy3-As2 promotes cisplatin resistance and the cancer stem cell in ovarian cancer by regulating hsa-Mir-139-5p/Sdc4 axis. *Cancer Cell Int* (2021) 21(1):284. doi: 10.1186/s12935-021-01993-x

54. Wang DY, Li N, Cui YL. Long non-coding rna Ccat1 sponges mir-454 to promote chemoresistance of ovarian cancer cells to cisplatin by regulation of surviving. *Cancer Res Treat* (2020) 52(3):798–814. doi: 10.4143/crt.2019.498

55. Liu X, Yin Z, Wu Y, Zhan Q, Huang H, Fan J. Circular rna lysophosphatidic acid receptor 3 (Circ-Lpar3) enhances the cisplatin resistance of ovarian cancer. *Bioengineered* (2022) 13(2):3739–50. doi: 10.1080/21655979.2022.2029109

56. Cao Y, Xie X, Li M, Gao Y. Circhipk2 contributes to ddp resistance and malignant behaviors of ddp-resistant ovarian cancer cells both *in vitro* and *in vivo* through Circhipk2/Mir-338-3p/Chtop cerna pathway. *Onco Targets Ther* (2021) 14:3151–65. doi: 10.2147/OTT.S291823

57. Nakamura K, Sawada K, Miyamoto M, Kinose Y, Yoshimura A, Ishida K, et al. Downregulation of mir-194-5p induces paclitaxel resistance in ovarian cancer cells by altering Mdm2 expression. *Oncotarget* (2019) 10(6):673–83. doi: 10.18632/oncotarget.26586

58. Li M, Zhang S, Ma Y, Yang Y, An R. Role of Hsamir105 during the pathogenesis of paclitaxel resistance and its clinical implication in ovarian cancer. *Oncol Rep* (2021) 45(5):84. doi: 10.3892/or.2021.8035

59. Lin H, Shen L, Lin Q, Dong C, Maswela B, Illahi GS, et al. Snhg5 enhances paclitaxel sensitivity of ovarian cancer cells through sponging mir-23a. *Biomed Pharmacother = Biomed Pharmacotherapie* (2020) 123:109711. doi: 10.1016/j.biopha.2019.109711

60. Zhang M, Liu S, Fu C, Wang X, Zhang M, Liu G, et al. Lncrna kb-1471a8.2 overexpression suppresses cell proliferation and migration and antagonizes the paclitaxel resistance of ovarian cancer cells. *Cancer Biother Radiopharm* (2019) 34 (5):316–24. doi: 10.1089/cbr.2018.2698

61. Zheng Y, Li Z, Yang S, Wang Y, Luan Z. Circexoc6b suppresses the proliferation and motility and sensitizes ovarian cancer cells to paclitaxel through mir-376c-3p/Foxo3 axis. *Cancer Biother Radiopharm* (2020). doi: 10.1089/cbr.2020.3739

62. Zhao H, Wang A, Zhang Z. Lncrna Sdhap1 confers paclitaxel resistance of ovarian cancer by regulating Eif4g2 expression *Via* mir-4465. *J Biochem* (2020) 168 (2):171–81. doi: 10.1093/jb/mvaa036

63. Huang B, Wei M, Hong L. Long noncoding rna hulc contributes to paclitaxel resistance in ovarian cancer *Via* mir-137/Itgb8 axis. *Open Life Sci* (2021) 16(1):667–81. doi: 10.1515/biol-2021-0058

64. Zhu J, Luo JE, Chen Y, Wu Q. Circ_0061140 knockdown inhibits tumorigenesis and improves ptx sensitivity by regulating mir-136/Cbx2 axis in ovarian cancer. *J Ovarian Res* (2021) 14(1):136. doi: 10.1186/s13048-021-00888-9

65. Wei S, Qi L, Wang L. Overexpression of Circ_Celsr1 facilitates paclitaxel resistance of ovarian cancer by regulating mir-149-5p/Sik2 axis. *Anticancer Drugs* (2021) 32(5):496–507. doi: 10.1097/CAD.0000000000001058

66. Li LQ, Pan D, Chen Q, Zhang SW, Xie DY, Zheng XL, et al. Sensitization of gastric cancer cells to 5-fu by microrna-204 through targeting the Tgfbr2-mediated epithelial to mesenchymal transition. *Cell Physiol Biochem* (2018) 47(4):1533–45. doi: 10.1159/000490871

67. Wang CQ. Mir-195 reverses 5-fu resistance through targeting Hmga1 in gastric cancer cells. *Eur Rev Med Pharmacol Sci* (2019) 23(9):3771–8. doi: 10.26355/eurrev_201905_17803

68. Jiang L, Zhang Y, Guo L, Liu C, Wang P, Ren W. Exosomal microrna-107 reverses chemotherapeutic drug resistance of gastric cancer cells through Hmga2/Mtor/P-gp pathway. *BMC Cancer* (2021) 21(1):1290. doi: 10.1186/s12885-021-09020-y

69. Wang XY, Zhou YC, Wang Y, Liu YY, Wang YX, Chen DD, et al. Mir-149 contributes to resistance of 5-fu in gastric cancer *Via* targeting Trem2 and regulating beta-catenin pathway. *Biochem Biophys Res Commun* (2020) 532 (3):329–35. doi: 10.1016/j.bbrc.2020.05.135

70. Hu J, Huang L, Ding Q, Lv J, Chen Z. Long noncoding rna haglr sponges mir-338-3p to promote 5-fu resistance in gastric cancer through targeting the ldha-glycolysis pathway. *Cell Biol Int* (2022) 46(2):173–84. doi: 10.1002/cbin.11714

71. Jiang L, Zhang Y, Su P, Ma Z, Ye X, Kang W, et al. Long non-coding rna Hnf1a-As1 induces 5-fu resistance of gastric cancer through mir-30b-5p/Eif5a2 pathway. *Transl Oncol* (2022) 18:101351. doi: 10.1016/j.tranon.2022.101351

72. Fang L, Lv J, Xuan Z, Li B, Li Z, He Z, et al. Circular cpm promotes chemoresistance of gastric cancer *Via* activating Prkaa2-mediated autophagy. *Clin Transl Med* (2022) 12(1):e708. doi: 10.1002/ctm2.708

73. Xu G, Li M, Wu J, Qin C, Tao Y, He H. Circular rna Circnrip1 sponges microrna-138-5p to maintain hypoxia-induced resistance to 5-fluorouracil through hif-1alpha-Dependent glucose metabolism in gastric carcinoma. *Cancer Manag Res* (2020) 12:2789–802. doi: 10.2147/CMAR.S246272

74. Chen Z, Gao YJ, Hou RZ, Ding DY, Song DF, Wang DY, et al. Microrna-206 facilitates gastric cancer cell apoptosis and suppresses cisplatin resistance by targeting Mapk2 signaling pathway. *Eur Rev Med Pharmacol Sci* (2019) 23 (1):171–80. doi: 10.26355/eurrev_201901_16761

75. Ren N, Jiang T, Wang C, Xie S, Xing Y, Piao D, et al. Lncrna Adamts9-As2 inhibits gastric cancer (Gc) development and sensitizes chemoresistant gc cells to cisplatin by regulating mir-223-3p/Nlrp3 axis. *Aging* (2020) 12(11):11025–41. doi: 10.18632/aging.103314

76. Sun G, Li Z, He Z, Wang W, Wang S, Zhang X, et al. Circular rna Mctp2 inhibits cisplatin resistance in gastric cancer by mir-99a-5p-Mediated induction of Mtmr3 expression. *J Exp Clin Cancer Res* (2020) 39(1):246. doi: 10.1186/s13046-020-01758-w

77. Zhang J, Zha W, Qian C, Ding A, Mao Z. Circular rna Circ_0001017 sensitizes cisplatin-resistant gastric cancer cells to chemotherapy by the mir-543/Phlpp2 axis. *Biochem Genet* (2022) 60(2):558–75. doi: 10.1007/s10528-021-10110-6

78. Lee SD, Yu D, Lee DY, Shin HS, Jo JH, Lee YC. Upregulated microrna-193a-3p is responsible for cisplatin resistance in Cd44(+) gastric cancer cells. *Cancer Sci* (2019) 110(2):662–73. doi: 10.1111/cas.13894

79. Miao X, Liu Y, Fan Y, Wang G, Zhu H. Lncrna bancr attenuates the killing capacity of cisplatin on gastric cancer cell through the Erk1/2 pathway. *Cancer Manag Res* (2021) 13:287–96. doi: 10.2147/CMAR.S269679

80. Sun H, Wu P, Zhang B, Wu X, Chen W. Mcm3ap-As1 promotes cisplatin resistance in gastric cancer cells *Via* the mir-138/Foxc1 axis. *Oncol Lett* (2021) 21 (3):211. doi: 10.3892/ol.2021.12472

81. Liu Y, Xu J, Jiang M, Ni L, Ling Y. Circrna donson contributes to cisplatin resistance in gastric cancer cells by regulating mir-802/Bmi1 axis. *Cancer Cell Int* (2020) 20:261. doi: 10.1186/s12935-020-01358-w

82. Wu Q, Wang H, Liu L, Zhu K, Yu W, Guo J. Hsa_Circ_0001546 acts as a mirna-421 sponge to inhibit the chemoresistance of gastric cancer cells *Via* Atm/Chk2/P53-dependent pathway. *Biochem Biophys Res Commun* (2020) 521(2):303–9. doi: 10.1016/j.bbrc.2019.10.117

83. Song W, Qian Y, Zhang MH, Wang H, Wen X, Yang XZ, et al. The long non-coding rna Ddx11-As1 facilitates cell progression and oxaliplatin resistance *Via* regulating mir-326/Irs1 axis in gastric cancer. *Eur Rev Med Pharmacol Sci* (2020) 24(6):3049–61. doi: 10.26355/eurrev_202003_20669

84. Zhong Y, Wang D, Ding Y, Tian G, Jiang B. Circular rna Circ_0032821 contributes to oxaliplatin (Oxa) resistance of gastric cancer cells by regulating Sox9 *Via* mir-515-5p. *Biotechnol Lett* (2021) 43(2):339–51. doi: 10.1007/s10529-020-03036-3

85. Liu X, Zhou X, Chen Y, Huang Y, He J, Luo H. Mir-186-5p targeting Six1 inhibits cisplatin resistance in non-Small-Cell lung cancer cells (Nsclcs). *Neoplasma* (2020) 67(1):147–57. doi: 10.4149/neo_2019_190511N420

86. Cui D, Feng Y, Qian R. Up-regulation of microrna mir-101-3p enhances sensitivity to cisplatin *Via* regulation of small interfering rna (Sirna) anti-human Agt4d and autophagy in non-Small-Cell lung carcinoma (Nsclc). *Bioengineered* (2021) 12(1):8435–46. doi: 10.1080/21655979.2021.1982274

87. Ye Y, Gu J, Liu P, Wang H, Jiang L, Lei T, et al. Long non-coding rna Spry4-It1 reverses cisplatin resistance by downregulating mpzl-1 *Via* suppressing emt in nsclc. *Onco Targets Ther* (2020) 13:2783–93. doi: 10.2147/OTT.S232769

88. Zhu C, Jiang X, Xiao H, Guan J. Circ_0030998 restrains cisplatin resistance through mediating mir-1323/Pdcd4 axis in non-small cell lung cancer. *Biochem Genet* (2022). doi: 10.1007/s10528-022-10220-9

89. Sun B, Hu N, Cong D, Chen K, Li J. Microrna-25-3p promotes cisplatin resistance in non-Small-Cell lung carcinoma (Nsclc) through adjusting Pten/Pi3k/Akt route. *Bioengineered* (2021) 12(1):3219–28. doi: 10.1080/21655979.2021.1939577

90. Ge P, Cao L, Zheng M, Yao Y, Wang W, Chen X. Lncrna Snhg1 contributes to the cisplatin resistance and progression of nsclc *Via* mir-330-5p/Dclk1 axis. *Exp Mol Pathol* (2021) 120:104633. doi: 10.1016/j.yexmp.2021.104633

91. Xiao S, Sun L, Ruan B, Li J, Chen J, Xiong J, et al. Long non-coding rna Linc01224 promotes progression and cisplatin resistance in non-small lung cancer by sponging mir-2467. *Pulm Pharmacol Ther* (2021) 70:102070. doi: 10.1016/j.pupt.2021.102070

92. Zhong Y, Lin H, Li Q, Liu C, Shen J. Circrna_100565 contributes to cisplatin resistance of nsclc cells by regulating proliferation, apoptosis and autophagy *Via* mir-337-3p/Adam28 axis. *Cancer biomark* (2021) 30(2):261–73. doi: 10.3233/CBM-201705

93. Xu F, Ye ML, Zhang YP, Li WJ, Li MT, Wang HZ, et al. Microrna-375-3p enhances chemosensitivity to 5-fluorouracil by targeting thymidylate synthase in colorectal cancer. *Cancer Sci* (2020) 111(5):1528–41. doi: 10.1111/cas.14356

94. Jiang Z, Li L, Hou Z, Liu W, Wang H, Zhou T, et al. Lncrna Hand2-As1 inhibits 5-fluorouracil resistance by modulating mir-20a/Pdcd4 axis in colorectal cancer. *Cell Signalling* (2020) 66:109483. doi: 10.1016/j.cellsig.2019.109483

95. Ren TJ, Liu C, Hou JF, Shan FX. Circddx17 reduces 5-fluorouracil resistance and hinders tumorigenesis in colorectal cancer by regulating mir-31-5p/Kank1 axis. *Eur Rev Med Pharmacol Sci* (2020) 24(4):1743–54. doi: 10.26355/eurrev_202002_20351

96. Wu S, Zhou Y, Liu P, Zhang H, Wang W, Fang Y, et al. Microrna-29b-3p promotes 5-fluorouracil resistance <Em>Via</Em> suppressing Traf5-mediated necroptosis in human colorectal cancer. *Eur J Histochem* (2021) 65(2):3247. doi: 10.4081/ejh.2021.3247

97. Ma YN, Hong YG, Yu GY, Jiang SY, Zhao BL, Guo A, et al. Lncrna Lbx2-As1 promotes colorectal cancer progression and 5-fluorouracil resistance. *Cancer Cell Int* (2021) 21(1):501. doi: 10.1186/s12935-021-02209-y

98. He X, Ma J, Zhang M, Cui J, Yang H. Circ_0007031 enhances tumor progression and promotes 5-fluorouracil resistance in colorectal cancer through regulating mir-133b/Abcc5 axis. *Cancer biomark* (2020) 29(4):531–42. doi: 10.3233/CBM-200023

99. Wu YZ, Lin HY, Zhang Y, Chen WF. Mir-200b-3p mitigates oxaliplatin resistance *Via* targeting Tubb3 in colorectal cancer. *J Gene Med* (2020) 22(7):e3178. doi: 10.1002/jgm.3178

100. Xu Y, Qiu A, Peng F, Tan X, Wang J, Gong X. Exosomal transfer of circular rna Fbxw7 ameliorates the chemoresistance to oxaliplatin in colorectal cancer by sponging mir-18b-5p. *Neoplasma* (2021) 68(1):108–18. doi: 10.4149/neo_2020_200417N414

101. Qian XL, Zhou F, Xu S, Jiang J, Chen ZP, Wang SK, et al. Mir-454-3p promotes oxaliplatin resistance by targeting pten in colorectal cancer. *Front Oncol* (2021) 11:638537. doi: 10.3389/fonc.2021.638537

102. Gao R, Fang C, Xu J, Tan H, Li P, Ma L. Lncrna Cacs15 contributes to oxaliplatin resistance in colorectal cancer by positively regulating Abcc1 through sponging mir-145. *Arch Biochem Biophys* (2019) 663:183–91. doi: 10.1016/j.abb.2019.01.005

103. Li TT, Mou J, Pan YJ, Huo FC, Du WQ, Liang J, et al. Microrna-138-1-3p sensitizes sorafenib to hepatocellular carcinoma by targeting Pak5 mediated beta-Catenin/Abcb1 signaling pathway. *J BioMed Sci* (2021) 28(1):56. doi: 10.1186/s12929-021-00752-4

104. Dong ZB, Wu HM, He YC, Huang ZT, Weng YH, Li H, et al. Mirna-124-3p.1 sensitizes hepatocellular carcinoma cells to sorafenib by regulating Foxo3a by targeting Akt2 and Sirt1. *Cell Death Dis* (2022) 13(1):35. doi: 10.1038/s41419-021-04491-0

105. Sui C, Dong Z, Yang C, Zhang M, Dai B, Geng L, et al. Lncrna Foxd2-As1 as a competitive endogenous rna against mir-150-5p reverses resistance to sorafenib in hepatocellular carcinoma. *J Cell Mol Med* (2019) 23(9):6024–33. doi: 10.1111/jcmm.14465

106. Tan W, Lin Z, Chen X, Li W, Zhu S, Wei Y, et al. Mir-126-3p contributes to sorafenib resistance in hepatocellular carcinoma *Via* downregulating Spred1. *Ann Trans Med* (2021) 9(1):38. doi: 10.21037/atm-20-2081

107. Liu Y, Chen L, Yuan H, Guo S, Wu G. Lncrna dancr promotes sorafenib resistance *Via* activation of il-6/Stat3 signaling in hepatocellular carcinoma cells. *Onco Targets Ther* (2020) 13:1145–57. doi: 10.2147/OTT.S229957

108. Weng H, Zeng L, Cao L, Chen T, Li Y, Xu Y, et al. Circfoxm1 contributes to sorafenib resistance of hepatocellular carcinoma cells by regulating Mecp2 *Via* mir-1324. *Mol Ther Nucleic Acids* (2021) 23:811–20. doi: 10.1016/j.omtn.2020.12.019

109. Yang Y, Yang Z, Zhang R, Jia C, Mao R, Mahati S, et al. Mir-27a-3p enhances the cisplatin sensitivity in hepatocellular carcinoma cells through inhibiting Pi3k/Akt pathway. *Biosci Rep* (2021) 41(12):BSR20192007. doi: 10.1042/BSR20192007

110. Zhao P, Cui X, Zhao L, Liu L, Wang D. Overexpression of growth-Arrest-Specific transcript 5 improved cisplatin sensitivity in hepatocellular carcinoma through sponging mir-222. *DNA Cell Biol* (2020) 39(4):724–32. doi: 10.1089/dna.2019.5282

111. Yang Y, Shi L, Zhang D, Wu D, An Y, Zhang Y, et al. Long non-coding rna Fgd5-As1 contributes to cisplatin resistance in hepatocellular carcinoma *Via* sponging microrna-153-3p by upregulating twinfilin actin binding protein 1 (Twf1). *Bioengineered* (2021) 12(1):6713–23. doi: 10.1080/21655979.2021.1971484

112. Li P, Song R, Yin F, Liu M, Liu H, Ma S, et al. Circmrps35 promotes malignant progression and cisplatin resistance in hepatocellular carcinoma. *Mol Ther* (2022) 30(1):431–47. doi: 10.1016/j.ymthe.2021.08.027

113. Li D, Wang X, Yang M, Kan Q, Duan Z. Mir3609 sensitizes breast cancer cells to adriamycin by blocking the programmed death-ligand 1 immune checkpoint. *Exp Cell Res* (2019) 380(1):20–8. doi: 10.1016/j.yexcr.2019.03.025

114. Liang Y, Song X, Li Y, Su P, Han D, Ma T, et al. Circkdm4c suppresses tumor progression and attenuates doxorubicin resistance by regulating mir-548p/Pbld axis in breast cancer. *Oncogene* (2019) 38(42):6850–66. doi: 10.1038/s41388-019-0926-z

115. Yin Y, Wang X, Li T, Ren Q, Li L, Sun X, et al. Microrna-221 promotes breast cancer resistance to adriamycin *Via* modulation of Pten/Akt/Mtor signaling. *Cancer Med* (2020) 9(4):1544–52. doi: 10.1002/cam4.2817

116. Zheng R, Jia J, Guan L, Yuan H, Liu K, Liu C, et al. Long noncoding rna lnc-Loc645166 promotes adriamycin resistance *Via* nf-Kappab/Gata3 axis in breast cancer. *Aging* (2020) 12(10):8893–912. doi: 10.18632/aging.103012

117. Chen J, Shi P, Zhang J, Li Y, Ma J, Zhang Y, et al. Circrna_0044556 diminishes the sensitivity of triplenegative breast cancer cells to adriamycin by sponging Mir145 and regulating nras. *Mol Med Rep* (2022) 25(2):51. doi: 10.3892/mmr.2021.12567

118. Shi YF, Lu H, Wang HB. Downregulated lncrna Adamts9-As2 in breast cancer enhances tamoxifen resistance by activating microrna-130a-5p. *Eur Rev Med Pharmacol Sci* (2019) 23(4):1563–73. doi: 10.26355/eurrev_201902_17115

119. Li H, Li Q, He S. Hsa_Circ_0025202 suppresses cell tumorigenesis and tamoxifen resistance *Via* mir-197-3p/Hipk3 axis in breast cancer. *World J Surg Oncol* (2021) 19(1):39. doi: 10.1186/s12957-021-02149-x

120. Han X, Li Q, Liu C, Wang C, Li Y. Overexpression mir-24-3p repressed bim expression to confer tamoxifen resistance in breast cancer. *J Cell Biochem* (2019) 120(8):12966–76. doi: 10.1002/jcb.28568

121. Liu Y, Li M, Yu H, Piao H. Lncrna cytor promotes tamoxifen resistance in breast cancer cells *Via* sponging Mir125a5p. *Int J Mol Med* (2020) 45(2):497–509. doi: 10.3892/ijmm.2019.4428

122. Shi F, Su J, Liu Z, Wang J, Wang T. Mir-144 reverses cisplatin resistance in cervical cancer *Via* targeting Lhx2. *J Cell Biochem* (2019) 120(9):15018–26. doi: 10.1002/jcb.28763

123. Hou H, Yu R, Zhao H, Yang H, Hu Y, Hu Y, et al. Lncrna Otud6b-As1 induces cisplatin resistance in cervical cancer cells through up-regulating cyclin D2 *Via* mir-206. *Front Oncol* (2021) 11:777220. doi: 10.3389/fonc.2021.777220

124. Shen Z, Zhou L, Zhang C, Xu J. Reduction of circular rna Foxo3 promotes prostate cancer progression and chemoresistance to docetaxel. *Cancer Lett* (2020) 468:88–101. doi: 10.1016/j.canlet.2019.10.006

125. Zhang H, Li M, Zhang J, Shen Y, Gui Q. Exosomal circ-xiap promotes docetaxel resistance in prostate cancer by regulating mir-1182/Tpd52 axis. *Drug Des Devel Ther* (2021) 15:1835–49. doi: 10.2147/DDDT.S300376

126. Liu A, Zhou Y, Zhao T, Tang X, Zhou B, Xu J. Mirna-3662 reverses the gemcitabine resistance in pancreatic cancer through regulating the tumor metabolism. *Cancer Chemother Pharmacol* (2021) 88(2):343–57. doi: 10.1007/s00280-021-04289-z

127. Yu S, Wang M, Zhang H, Guo X, Qin R. Circ_0092367 inhibits emt and gemcitabine resistance in pancreatic cancer *Via* regulating the mir-1206/Esrp1 axis. *Genes* (2021) 12(11):1701. doi: 10.3390/genes12111701

128. Wu Y, Xu W, Yang Y, Zhang Z. Mirna-93-5p promotes gemcitabine resistance in pancreatic cancer cells by targeting the pten-mediated Pi3k/Akt signaling pathway. *Ann Clin Lab Sci* (2021) 51(3):310–20.

129. Zhou C, Yi C, Yi Y, Qin W, Yan Y, Dong X, et al. Lncrna Pvt1 promotes gemcitabine resistance of pancreatic cancer *Via* activating Wnt/Beta-catenin and autophagy pathway through modulating the mir-619-5p/Pygo2 and mir-619-5p/Atg14 axes. *Mol Cancer* (2020) 19(1):118. doi: 10.1186/s12943-020-01237-y

130. Liu Y, Xia L, Dong L, Wang J, Xiao Q, Yu X, et al. Circhipk3 promotes gemcitabine (Gem) resistance in pancreatic cancer cells by sponging mir-330-5p and targets Rassf1. *Cancer Manag Res* (2020) 12:921–9. doi: 10.2147/CMAR.S239326

131. Luo G, Zhang Y, Wu Z, Zhang L, Liang C, Chen X. Exosomal Linc00355 derived from cancer-associated fibroblasts promotes bladder cancer cell resistance to cisplatin by regulating mir-34b-5p/Abcb1 axis. *Acta Biochim Biophys Sin (Shanghai)* (2021) 53(5):558–66. doi: 10.1093/abbs/gmab023

132. Sun M, Liu X, Zhao W, Zhang B, Deng P. Circ_0058063 contributes to cisplatin-resistance of bladder cancer cells by upregulating B2m through acting as rna sponges for mir-335-5p. *BMC Cancer* (2022) 22(1):313. doi: 10.1186/s12885-022-09419-1

133. Sekino Y, Sakamoto N, Sentani K, Oue N, Teishima J, Matsubara A, et al. Mir-130b promotes sunitinib resistance through regulation of pten in renal cell carcinoma. *Oncology* (2019) 97(3):164–72. doi: 10.1159/000500605

134. Huang KB, Pan YH, Shu GN, Yao HH, Liu X, Zhou M, et al. Circular rna Circsnx6 promotes sunitinib resistance in renal cell carcinoma through the mir-1184/Gpcpd1/ lysophosphatidic acid axis. *Cancer Lett* (2021) 523:121–34. doi: 10.1016/j.canlet.2021.10.003

135. Yuan L, Xu ZY, Ruan SM, Mo S, Qin JJ, Cheng XD. Long non-coding rnas towards precision medicine in gastric cancer: Early diagnosis, treatment, and drug resistance. *Mol Cancer* (2020) 19(1):96. doi: 10.1186/s12943-020-01219-0

136. Liu Y, Ao X, Ding W, Ponnusamy M, Wu W, Hao X, et al. Critical role of Foxo3a in carcinogenesis. *Mol Cancer* (2018) 17(1):104. doi: 10.1186/s12943-018-0856-3

137. Pang X, Zhou Z, Yu Z, Han L, Lin Z, Ao X, et al. Foxo3a-dependent mir-633 regulates chemotherapeutic sensitivity in gastric cancer by targeting fas-associated death domain. *RNA Biol* (2019) 16(2):233–48. doi: 10.1080/15476286.2019.1565665

138. Yang J, Hai J, Dong X, Zhang M, Duan S. Microrna-92a-3p enhances cisplatin resistance by regulating kruppel-like factor 4-mediated cell apoptosis and epithelial-to-Mesenchymal transition in cervical cancer. *Front Pharmacol* (2021) 12:783213. doi: 10.3389/fphar.2021.783213

139. Suraweera CD, Banjara S, Hinds MG, Kvansakul M. Metazoans and intrinsic apoptosis: An evolutionary analysis of the bcl-2 family. *Int J Mol Sci* (2022) 23(7):3691. doi: 10.3390/ijms23073691

140. Warren CFA, Wong-Brown MW, Bowden NA. Bcl-2 family isoforms in apoptosis and cancer. *Cell Death Dis* (2019) 10(3):177. doi: 10.1038/s41419-019-1407-6

141. Zhong L, Liu X, Wang L, Liu Y, Zhang D, Zhao Y. Microrna-625-3p improved proliferation and involved chemotherapy resistance *Via* targeting pten in high grade ovarian serous carcinoma. *J Ovarian Res* (2022) 15(1):7. doi: 10.1186/s13048-021-00939-1

142. Ashofteh N, Amini R, Molaee N, Karami H, Baazm M. Mirna-mediated knock-down of bcl-2 and mcl-1 increases fludarabine-sensitivity in cll-cii cells. *Asian Pac J Cancer Prev* (2021) 22(7):2191–8. doi: 10.31557/APJCP.2021.22.7.2191

143. Sun Y, Peng YB, Ye LL, Ma LX, Zou MY, Cheng ZG. Propofol inhibits proliferation and cisplatin resistance in ovarian cancer cells through regulating the Microrna374a/Forkhead box O1 signaling axis. *Mol Med Rep* (2020) 21(3):1471–80. doi: 10.3892/mmr.2020.10943

144. Hiremath IS, Goel A, Warrier S, Kumar AP, Sethi G, Garg M. The multidimensional role of the Wnt/Beta-catenin signaling pathway in human malignancies. *J Cell Physiol* (2022) 237(1):199–238. doi: 10.1002/jcp.30561

145. Han H, Li Y, Qin W, Wang L, Yin H, Su B, et al. Mir-199b-3p contributes to acquired resistance to cetuximab in colorectal cancer by targeting Crim1 *Via* Wnt/Beta-catenin signaling. *Cancer Cell Int* (2022) 22(1):42. doi: 10.1186/s12935-022-02460-x

146. Liu HR, Zhao J. Effect and mechanism of mir-217 on drug resistance, invasion and metastasis of ovarian cancer cells through a regulatory axis of Cul4b gene Silencing/Inhibited Wnt/Beta-catenin signaling pathway activation. *Eur Rev Med Pharmacol Sci* (2021) 25(1):94–107. doi: 10.26355/eurrev_202101_24353

147. Zhang Y, Liang S, Xiao B, Hu J, Pang Y, Liu Y, et al. Mir-323a regulates Erbb3/Egfr and blocks gefitinib resistance acquisition in colorectal cancer. *Cell Death Dis* (2022) 13(3):256. doi: 10.1038/s41419-022-04709-9

148. Liu H, Song M, Sun X, Zhang X, Miao H, Wang Y. T-Box transcription factor Tbx1, targeted by microrna-6727-5p, inhibits cell growth and enhances cisplatin chemosensitivity of cervical cancer cells through akt and mapk pathways. *Bioengineered* (2021) 12(1):565–77. doi: 10.1080/21655979.2021.1880732

149. Yuan J, Zhang Q, Wu S, Yan S, Zhao R, Sun Y, et al. Mirna-223-3p modulates ibrutinib resistance through regulation of the Chuk/Nf-kappab signaling pathway in mantle cell lymphoma. *Exp Hematol* (2021) 103:52–9.e2. doi: 10.1016/j.exphem.2021.08.010

150. Adhikari S, Bhattacharya A, Adhikary S, Singh V, Gadad SS, Roy S, et al. The paradigm of drug resistance in cancer: An epigenetic perspective. *Biosci Rep* (2022) 42(4):BSR20211812. doi: 10.1042/BSR20211812

151. Robey RW, Pluchino KM, Hall MD, Fojo AT, Bates SE, Gottesman MM. Revisiting the role of abc transporters in multidrug-resistant cancer. *Nat Rev Cancer* (2018) 18(7):452–64. doi: 10.1038/s41568-018-0005-8

152. Gomes BC, Rueff J, Rodrigues AS. Micrornas and cancer drug resistance. *Methods Mol Biol* (2016) 1395:137–62. doi: 10.1007/978-1-4939-3347-1_9

153. Zou Z, Zou R, Zong D, Shi Y, Chen J, Huang J, et al. Mir-495 sensitizes mdr cancer cells to the combination of doxorubicin and taxol by inhibiting Mdr1 expression. *J Cell Mol Med* (2017) 21(9):1929–43. doi: 10.1111/jcmm.13114

154. Bao J, Xu Y, Wang Q, Zhang J, Li Z, Li D, et al. Mir-101 alleviates chemoresistance of gastric cancer cells by targeting Anxa2. *Biomed Pharmacother = Biomed Pharmacotherapie* (2017) 92:1030–7. doi: 10.1016/j.biopha.2017.06.011

155. Tian J, Xu YY, Li L, Hao Q. Mir-490-3p sensitizes ovarian cancer cells to cisplatin by directly targeting Abcc2. *Am J Transl Res* (2017) 9(3):1127–38.

156. Tsai HC, Chang AC, Tsai CH, Huang YL, Gan L, Chen CK, et al. Ccn2 promotes drug resistance in osteosarcoma by enhancing Abcg2 expression. *J Cell Physiol* (2019) 234(6):9297–307. doi: 10.1002/jcp.27611

157. Amponsah PS, Fan P, Bauer N, Zhao Z, Gladkich J, Fellenberg J, et al. Microrna-210 overexpression inhibits tumor growth and potentially reverses gemcitabine resistance in pancreatic cancer. *Cancer Lett* (2017) 388:107–17. doi: 10.1016/j.canlet.2016.11.035

158. Li Y, Gong P, Hou JX, Huang W, Ma XP, Wang YL, et al. Mir-34a regulates multidrug resistance *Via* positively modulating Oaz2 signaling in colon cancer cells. *J Immunol Res* (2018) 2018:7498514. doi: 10.1155/2018/7498514

159. Gajda E, Godlewska M, Mariak Z, Nazaruk E, Gawel D. Combinatory treatment with mir-7-5p and drug-loaded cubosomes effectively impairs cancer cells. *Int J Mol Sci* (2020) 21(14):5039. doi: 10.3390/ijms21145039

160. Li R, Xu T, Wang H, Wu N, Liu F, Jia X, et al. Dysregulation of the mir-325-3p/Dpagt1 axis supports hbv-positive hcc chemoresistance. *Biochem Biophys Res Commun* (2019) 519(2):358–65. doi: 10.1016/j.bbrc.2019.08.116

161. Wang M, Yu F, Chen X, Li P, Wang K. The underlying mechanisms of noncoding rnas in the chemoresistance of hepatocellular carcinoma. *Mol Ther Nucleic Acids* (2020) 21:13–27. doi: 10.1016/j.omtn.2020.05.011

162. Shahverdi M, Hajiasgharzadeh K, Sorkhabi AD, Jafarlou M, Shojaee M, Jalili Tabrizi N, et al. The regulatory role of autophagy-related mirnas in lung cancer drug resistance. *Biomed Pharmacother = Biomed Pharmacotherapie* (2022) 148:112735. doi: 10.1016/j.biopha.2022.112735

163. Li H, Lei Y, Li S, Li F, Lei J. Microrna-20a-5p inhibits the autophagy and cisplatin resistance in ovarian cancer *Via* regulating Dnmt3b-mediated DNA methylation of Rbp1. *Reprod Toxicol* (2022) 109:93–100. doi: 10.1016/j.reprotox.2021.12.011

164. Li T, Zhang H, Wang Z, Gao S, Zhang X, Zhu H, et al. The regulation of autophagy by the mir-199a-5p/P62 axis was a potential mechanism of small cell lung cancer cisplatin resistance. *Cancer Cell Int* (2022) 22(1):120. doi: 10.1186/s12935-022-02505-1

165. Zhao L, Chen H, Zhang Q, Ma J, Hu H, Xu L. Atf4-mediated microrna-145/Hdac4/P53 axis affects resistance of colorectal cancer cells to 5-fluorouracil by regulating autophagy. *Cancer Chemother Pharmacol* (2022) 89(5):595–607. doi: 10.1007/s00280-021-04393-0

166. Liu Y. Targeting the non-canonical akt-Foxo3a axis: A potential therapeutic strategy for oral squamous cell carcinoma. *EBioMedicine* (2019) 49:6–8. doi: 10.1016/j.ebiom.2019.10.020

167. Ao X, Ding W, Zhang Y, Ding D, Liu Y. Tcf21: A critical transcription factor in health and cancer. *J Mol Med (Berl)* (2020) 98(8):1055–68. doi: 10.1007/s00109-020-01934-7

168. Saha T, Lukong KE. Breast cancer stem-like cells in drug resistance: A review of mechanisms and novel therapeutic strategies to overcome drug resistance. *Front Oncol* (2022) 12:856974. doi: 10.3389/fonc.2022.856974

169. Zhang L, Guo X, Zhang D, Fan Y, Qin L, Dong S, et al. Upregulated mir-132 in Lgr5(+) gastric cancer stem cell-like cells contributes to cisplatin-resistance *Via* Sirt1/Creb/Abcg2 signaling pathway. *Mol Carcinog* (2017) 56(9):2022–34. doi: 10.1002/mc.22656

170. Feng X, Jiang J, Shi S, Xie H, Zhou L, Zheng S. Knockdown of mir-25 increases the sensitivity of liver cancer stem cells to trail-induced apoptosis *Via* Pten/Pi3k/Akt/Bad signaling pathway. *Int J Oncol* (2016) 49(6):2600–10. doi: 10.3892/ijo.2016.3751

171. Ni H, Qin H, Sun C, Liu Y, Ruan G, Guo Q, et al. Mir-375 reduces the stemness of gastric cancer cells through triggering ferroptosis. *Stem Cell Res Ther* (2021) 12(1):325. doi: 10.1186/s13287-021-02394-7

172. Niu G, Hao J, Sheng S, Wen F. Role of T-box genes in cancer, epithelial-mesenchymal transition, and cancer stem cells. *J Cell Biochem* (2022) 123(2):215–30. doi: 10.1002/jcb.30188

173. Liu Y, Ding W, Ge H, Ponnusamy M, Wang Q, Hao X, et al. Foxk transcription factors: Regulation and critical role in cancer. *Cancer Lett* (2019) 458:1–12. doi: 10.1016/j.canlet.2019.05.030

174. Hirao A, Sato Y, Tanaka H, Nishida K, Tomonari T, Hirata M, et al. Mir-125b-5p is involved in sorafenib resistance through ataxin-1-Mediated epithelial-mesenchymal transition in hepatocellular carcinoma. *Cancers* (2021) 13(19):4917. doi: 10.3390/cancers13194917

175. Chaudhary AK, Mondal G, Kumar V, Kattel K, Mahato RI. Chemosensitization and inhibition of pancreatic cancer stem cell proliferation by overexpression of microrna-205. *Cancer Lett* (2017) 402:1–8. doi: 10.1016/j.canlet.2017.05.007

176. Cao L, Wan Q, Li F, Tang CE. Mir-363 inhibits cisplatin chemoresistance of epithelial ovarian cancer by regulating snail-induced epithelial-mesenchymal transition. *BMB Rep* (2018) 51(9):456–61. doi: 10.5483/BMBRep.2018.51.9.104

177. Singh N, Baby D, Rajguru JP, Patil PB, Thakkannavar SS, Pujari VB. Inflammation and cancer. *Ann Afr Med* (2019) 18(3):121–6. doi: 10.4103/aam.aam_56_18

178. Dong C. Cytokine regulation and function in T cells. *Annu Rev Immunol* (2021) 39:51–76. doi: 10.1146/annurev-immunol-061020-053702

179. Yan ZX, Zheng Z, Xue W, Zhao MZ, Fei XC, Wu LL, et al. Microrna181a is overexpressed in T-cell Leukemia/Lymphoma and related to chemoresistance. *BioMed Res Int* (2015) 2015:197241. doi: 10.1155/2015/197241

180. Ning T, Li J, He Y, Zhang H, Wang X, Deng T, et al. Exosomal mir-208b related with oxaliplatin resistance promotes treg expansion in colorectal cancer. *Mol Ther* (2021) 29(9):2723–36. doi: 10.1016/j.ymthe.2021.04.028

181. Xu S, Tao Z, Hai B, Liang H, Shi Y, Wang T, et al. Mir-424(322) reverses chemoresistance *Via* T-cell immune response activation by blocking the pd-L1 immune checkpoint. *Nat Commun* (2016) 7:11406. doi: 10.1038/ncomms11406

182. Sheng Q, Zhang Y, Wang Z, Ding J, Song Y, Zhao W. Cisplatin-mediated down-regulation of mir-145 contributes to up-regulation of pd-L1 *Via* the c-myc transcription factor in cisplatin-resistant ovarian carcinoma cells. *Clin Exp Immunol* (2020) 200(1):45–52. doi: 10.1111/cei.13406

183. Chae Y, Roh J, Kim W. The roles played by long non-coding rnas in glioma resistance. *Int J Mol Sci* (2021) 22(13):6834. doi: 10.3390/ijms22136834

184. Li W, Nie A, Jin L, Cui Y, Xie N, Liang G. Long non-coding rna terminal differentiation-induced non-coding rna regulates cisplatin resistance of choroidal melanoma by positively modulating extracellular signal-regulated kinase 2 *Via* sponging microrna-19b-3p. *Bioengineered* (2022) 13(2):3422–33. doi: 10.1080/21655979.2021.2014618

185. Zhou D, Gu J, Wang Y, Luo B, Feng M, Wang X. Long noncoding rna Ccat2 reduces chemosensitivity to 5-fluorouracil in breast cancer cells by activating the mtor axis. *J Cell Mol Med* (2022) 26(5):1392–401. doi: 10.1111/jcmm.17041

186. Guo JL, Tang T, Li JH, Yang YH, Zhang L, Quan Y. Lncrna heih enhances paclitaxel-tolerance of endometrial cancer cells *Via* activation of mapk signaling pathway. *Pathol Oncol Res* (2020) 26(3):1757–66. doi: 10.1007/s12253-019-00718-w

187. Zhu Y, Zhou B, Hu X, Ying S, Zhou Q, Xu W, et al. Lncrna Linc00942 promotes chemoresistance in gastric cancer by suppressing Msi2 degradation to enhance c-myc mrna stability. *Clin Transl Med* (2022) 12(1):e703. doi: 10.1002/ctm2.703

188. Lu Q, Wang L, Gao Y, Zhu P, Li L, Wang X, et al. Lncrna Apoc1p1-3 promoting anoikis-resistance of breast cancer cells. *Cancer Cell Int* (2021) 21(1):232. doi: 10.1186/s12935-021-01916-w

189. Zhao Y, Hong L. Lncrna-prlb confers paclitaxel resistance of ovarian cancer cells by regulating Rsf1/Nf-kappab signaling pathway. *Cancer Biother Radiopharm* (2021) 36(2):202–10. doi: 10.1089/cbr.2019.3363

190. He J, Zhu S, Liang X, Zhang Q, Luo X, Liu C, et al. Lncrna as a multifunctional regulator in cancer multi-drug resistance. *Mol Biol Rep* (2021) 48(8):1–15. doi: 10.1007/s11033-021-06603-7

191. Zhang K, Chen J, Li C, Yuan Y, Fang S, Liu W, et al. Exosome-mediated transfer of Snhg7 enhances docetaxel resistance in lung adenocarcinoma. *Cancer Lett* (2022) 526:142–54. doi: 10.1016/j.canlet.2021.10.029

192. Xia C, Li Q, Cheng X, Wu T, Gao P, Gu Y. Insulin-like growth factor 2 mrna-binding protein 2-stabilized long non-coding rna taurine up-regulated gene 1 (Tug1) promotes cisplatin-resistance of colorectal cancer *Via* modulating autophagy. *Bioengineered* (2022) 13(2):2450–69. doi: 10.1080/21655979.2021.2012918

193. Chen L, Sun L, Dai X, Li T, Yan X, Zhang Y, et al. Lncrna crnde promotes Atg4b-mediated autophagy and alleviates the sensitivity of sorafenib in hepatocellular carcinoma cells. *Front Cell Dev Biol* (2021) 9:687524. doi: 10.3389/fcell.2021.687524

194. Xu T, Jiang L, Wang Z. The progression of Hmgb1-induced autophagy in cancer biology. *Onco Targets Ther* (2019) 12:365–77. doi: 10.2147/OTT.S185876

195. Chen L, Xu Z, Zhao J, Zhai X, Li J, Zhang Y, et al. H19/Mir-107/Hmgb1 axis sensitizes laryngeal squamous cell carcinoma to cisplatin by suppressing autophagy *in vitro* and *in vivo*. *Cell Biol Int* (2021) 45(3):674–85. doi: 10.1002/cbin.11520

196. Liu K, Gao L, Ma X, Huang JJ, Chen J, Zeng L, et al. Long non-coding rnas regulate drug resistance in cancer. *Mol Cancer* (2020) 19(1):54. doi: 10.1186/s12943-020-01162-0

197. Chen Z, Pan T, Jiang D, Jin L, Geng Y, Feng X, et al. The lncrna-Gas5/Mir-221-3p/Dkk2 axis modulates Abcb1-mediated adriamycin resistance of breast cancer *Via* the Wnt/Beta-catenin signaling pathway. *Mol Ther Nucleic Acids* (2020) 19:1434–48. doi: 10.1016/j.omtn.2020.01.030

198. Liu Y, Li H, Zhao Y, Li D, Zhang Q, Fu J, et al. Knockdown of Adora2a antisense rna 1 inhibits cell proliferation and enhances imatinib sensitivity in chronic myeloid leukemia. *Bioengineered* (2022) 13(2):2296–307. doi: 10.1080/21655979.2021.2024389

199. Wang W, Han S, Gao W, Feng Y, Li K, Wu D. Long noncoding rna Kcnq1ot1 confers gliomas resistance to temozolomide and enhances cell growth by retrieving Pim1 from mir-761. *Cell Mol Neurobiol* (2022) 42(3):695–708. doi: 10.1007/s10571-020-00958-4

200. Shen P, Cheng Y. Long noncoding rna lncarsr confers resistance to adriamycin and promotes osteosarcoma progression. *Cell Death Dis* (2020) 11(5):362. doi: 10.1038/s41419-020-2573-2

201. Li Y, Liu Y, Chen G, Liu H, Wu Y, Liu J, et al. Hottip is upregulated in esophageal cancer and triggers the drug resistance. *J BUON* (2021) 26(3):1056–61.

202. Xie L, Cui G, Li T. Long noncoding rna Cbr3-As1 promotes stem-like properties and oxaliplatin resistance of colorectal cancer by sponging mir-145-5p. *J Oncol* (2022) 2022:2260211. doi: 10.1155/2022/2260211

203. Liu S, Sun Y, Hou Y, Yang L, Wan X, Qin Y, et al. A novel lncrna ropm-mediated lipid metabolism governs breast cancer stem cell properties. *J Hematol Oncol* (2021) 14(1):178. doi: 10.1186/s13045-021-01194-z

204. Cheng D, Fan J, Qin K, Zhou Y, Yang J, Ma Y, et al. Lncrna Snhg7 regulates mesenchymal stem cell through the Notch1/Jagged1/Hes-1 signaling pathway and influences folfirinox resistance in pancreatic cancer. *Front Oncol* (2021) 11:719855. doi: 10.3389/fonc.2021.719855

205. Liu S, Bu X, Kan A, Luo L, Xu Y, Chen H, et al. Sp1-induced lncrna dubr promotes stemness and oxaliplatin resistance of hepatocellular carcinoma *Via* E2f1-Cip2a feedback. *Cancer Lett* (2022) 528:16–30. doi: 10.1016/j.canlet.2021.12.026

206. Zhang J, Zhao X, Ma X, Yuan Z, Hu M. Kcnq1ot1 contributes to sorafenib resistance and programmed Deathligand1mediated immune escape *Via* sponging Mir506 in hepatocellular carcinoma cells. *Int J Mol Med* (2020) 46(5):1794–804. doi: 10.3892/ijmm.2020.4710

207. Zhang W, Xin J, Lai J, Zhang W. Lncrna Linc00184 promotes docetaxel resistance and immune escape *Via* mir-105-5p/Pd-L1 axis in prostate cancer. *Immunobiology* (2022) 227(1):152163. doi: 10.1016/j.imbio.2021.152163

208. Xu YJ, Zhao JM, Ni XF, Wang W, Hu WW, Wu CP. Lncrna Hcg18 suppresses Cd8(+) T cells to confer resistance to cetuximab in colorectal cancer *Via* mir-20b-5p/Pd-L1 axis. *Epigenomics* (2021) 13(16):1281–97. doi: 10.2217/epi-2021-0130

209. Li H, Ma X, Yang D, Suo Z, Dai R, Liu C. Pcat-1 contributes to cisplatin resistance in gastric cancer through epigenetically silencing pten *Via* recruiting Ezh2. *J Cell Biochem* (2020) 121(2):1353–61. doi: 10.1002/jcb.29370

210. Si X, Zang R, Zhang E, Liu Y, Shi X, Zhang E, et al. Lncrna H19 confers chemoresistance in eralpha-positive breast cancer through epigenetic silencing of the pro-apoptotic gene bik. *Oncotarget* (2016) 7(49):81452–62. doi: 10.18632/oncotarget.13263

211. Lin K, Jiang H, Zhuang SS, Qin YS, Qiu GD, She YQ, et al. Long noncoding rna Linc00261 induces chemosensitization to 5-fluorouracil by mediating methylation-dependent repression of dpyd in human esophageal cancer. *FASEB J* (2019) 33(2):1972–88. doi: 10.1096/fj.201800759R

212. Li Z, Li M, Xia P, Lu Z. Hottip mediated therapy resistance in glioma cells involves regulation of emt-related mir-10b. *Front Oncol* (2022) 12:873561. doi: 10.3389/fonc.2022.873561

213. Zhang W, Wu Q, Liu Y, Wang X, Ma C, Zhu W. Lncrna hotair promotes chemoresistance by facilitating epithelial to mesenchymal transition through mir-29b/Pten/Pi3k signaling in cervical cancer. *Cells Tissues Organs* (2022) 211(1):16–29. doi: 10.1159/000519844

214. Zhao X, Wang J, Zhu R, Zhang J, Zhang Y. Dlx6-As1 activated by H3k4me1 enhanced secondary cisplatin resistance of lung squamous cell carcinoma through modulating mir-181a-5p/Mir-382-5p/Celf1 axis. *Sci Rep* (2021) 11(1):21014. doi: 10.1038/s41598-021-99555-8

215. Sun J, Zheng X, Wang B, Cai Y, Zheng L, Hu L, et al. Lncrna limt (Linc01089) contributes to sorafenib chemoresistance *Via* regulation of mir-665 and epithelial to mesenchymal transition in hepatocellular carcinoma cells. *Acta Biochim Biophys Sin (Shanghai)* (2022) 54(2):261–70. doi: 10.3724/abbs.2021019

216. Yang J, Ma Q, Zhang M, Zhang W. Lncrna cytor drives l-ohp resistance and facilitates the epithelial-mesenchymal transition of colon carcinoma cells *Via* modulating mir-378a-5p/Serpine1. *Cell Cycle* (2021) 20(14):1415–30. doi: 10.1080/15384101.2021.1934626

217. Cai J, Sun H, Zheng B, Xie M, Xu C, Zhang G, et al. Curcumin attenuates lncrna H19induced epithelialmesenchymal transition in Tamoxifenresistant breast cancer cells. *Mol Med Rep* (2021) 23(1):13. doi: 10.3892/mmr.2020.11651

218. Zhang Y, Jia DD, Zhang YF, Cheng MD, Zhu WX, Li PF, et al. The emerging function and clinical significance of circrnas in thyroid cancer and autoimmune thyroid diseases. *Int J Biol Sci* (2021) 17(7):1731–41. doi: 10.7150/ijbs.55381

219. Wen ZJ, Xin H, Wang YC, Liu HW, Gao YY, Zhang YF. Emerging roles of circrnas in the pathological process of myocardial infarction. *Mol Ther Nucleic Acids* (2021) 26:828–48. doi: 10.1016/j.omtn.2021.10.002

220. Cui C, Yang J, Li X, Liu D, Fu L, Wang X. Functions and mechanisms of circular rnas in cancer radiotherapy and chemotherapy resistance. *Mol Cancer* (2020) 19(1):58. doi: 10.1186/s12943-020-01180-y

221. Lv Q, Xia Q, Li A, Wang Z. Circrna_101277 influences cisplatin resistance of colorectal cancer cells by modulating the mir-370/Il-6 axis. *Genet Res (Camb)* (2022) 2022:4237327. doi: 10.1155/2022/4237327

222. Huang X, Li Z, Zhang Q, Wang W, Li B, Wang L, et al. Circular rna Akt3 upregulates Pik3r1 to enhance cisplatin resistance in gastric cancer *Via* mir-198 suppression. *Mol Cancer* (2019) 18(1):71. doi: 10.1186/s12943-019-0969-3

223. Zhao Y, Zheng R, Chen J, Ning D. Circrna Cdr1as/Mir-641/Hoxa9 pathway regulated stemness contributes to cisplatin resistance in non-small cell lung cancer (Nsclc). *Cancer Cell Int* (2020) 20:289. doi: 10.1186/s12935-020-01390-w

224. Huang L, Ma J, Cui M. Circular rna Hsa_Circ_0001598 promotes programmed death-Ligand-1-Mediated immune escape and trastuzumab resistance *Via* sponging mir-1184 in breast cancer cells. *Immunol Res* (2021) 69(6):558–67. doi: 10.1007/s12026-021-09237-w

225. Chen SW, Zhu SQ, Pei X, Qiu BQ, Xiong D, Long X, et al. Cancer cell-derived exosomal Circusp7 induces Cd8(+) T cell dysfunction and anti-Pd1 resistance by regulating the mir-934/Shp2 axis in nsclc. *Mol Cancer* (2021) 20(1):144. doi: 10.1186/s12943-021-01448-x

226. Wei W, Sun J, Zhang H, Xiao X, Huang C, Wang L, et al. Circ0008399 interaction with wtap promotes assembly and activity of the M(6)a methyltransferase complex and promotes cisplatin resistance in bladder cancer. *Cancer Res* (2021) 81(24):6142–56. doi: 10.1158/0008-5472.CAN-21-1518

227. Hu C, Xia R, Zhang X, Li T, Ye Y, Li G, et al. Circfarp1 enables cancer-associated fibroblasts to promote gemcitabine resistance in pancreatic cancer *Via* the Lif/Stat3 axis. *Mol Cancer* (2022) 21(1):24. doi: 10.1186/s12943-022-01501-3

228. Chen Z, Lu T, Huang L, Wang Z, Yan Z, Guan Y, et al. Circular rna cia-maf drives self-renewal and metastasis of liver tumor-initiating cells *Via* transcription factor maff. *J Clin Invest* (2021) 131(19):e148020. doi: 10.1172/JCI148020

229. Jia DD, Jiang H, Zhang YF, Zhang Y, Qian LL, Zhang YF. The regulatory function of Pirna/Piwi complex in cancer and other human diseases: The role of DNA methylation. *Int J Biol Sci* (2022) 18(8):3358–73. doi: 10.7150/ijbs.68221

230. Riquelme I, Perez-Moreno P, Letelier P, Brebi P, Roa JC. The emerging role of piwi-interacting rnas (Pirnas) in gastrointestinal cancers: An updated perspective. *Cancers* (2021) 14(1):202. doi: 10.3390/cancers14010202

231. Tan L, Mai D, Zhang B, Jiang X, Zhang J, Bai R, et al. Piwi-interacting rna-36712 restrains breast cancer progression and chemoresistance by interaction with Sepw1 pseudogene Sepw1p rna. *Mol Cancer* (2019) 18(1):9. doi: 10.1186/s12943-019-0940-3

232. Mai D, Ding P, Tan L, Zhang J, Pan Z, Bai R, et al. Piwi-interacting rna-54265 is oncogenic and a potential therapeutic target in colorectal adenocarcinoma. *Theranostics* (2018) 8(19):5213–30. doi: 10.7150/thno.28001

233. Wang Y, Gable T, Ma MZ, Clark D, Zhao J, Zhang Y, et al. A pirna-like small rna induces chemoresistance to cisplatin-based therapy by inhibiting apoptosis in lung squamous cell carcinoma. *Mol Ther Nucleic Acids* (2017) 6:269–78. doi: 10.1016/j.omtn.2017.01.003

234. Matsuoka T, Yashiro M. Biomarkers of gastric cancer: Current topics and future perspective. *World J Gastroenterol* (2018) 24(26):2818–32. doi: 10.3748/wjg.v24.i26.2818

235. Umelo IA, Costanza B, Castronovo V. Innovative methods for biomarker discovery in the evaluation and development of cancer precision therapies. *Cancer Metastasis Rev* (2018) 37(1):125–45. doi: 10.1007/s10555-017-9710-0

236. Liu Y, Wang Y, Li X, Jia Y, Wang J, Ao X. Foxo3a in cancer drug resistance. *Cancer Lett* (2022) 540:215724. doi: 10.1016/j.canlet.2022.215724

237. Beermann J, Piccoli MT, Viereck J, Thum T. Non-coding rnas in development and disease: Background, mechanisms, and therapeutic approaches. *Physiol Rev* (2016) 96(4):1297–325. doi: 10.1152/physrev.00041.2015

238. Aurilia C, Donati S, Palmini G, Miglietta F, Falsetti I, Iantomasi T, et al. Are non-coding rnas useful biomarkers in parathyroid tumorigenesis? *Int J Mol Sci* (2021) 22(19):10465. doi: 10.3390/ijms221910465

239. Zhang L, Zhang Y, Wang Y, Zhao Y, Ding H, Li P. Circular rnas: Functions and clinical significance in cardiovascular disease. *Front Cell Dev Biol* (2020) 8:584051. doi: 10.3389/fcell.2020.584051

240. Liang M, Li Q, Shi S, Tian YN, Feng Y, Yang Y, et al. Overexpression of mir-138-5p sensitizes taxol-resistant epithelial ovarian cancer cells through targeting cyclin-dependent kinase 6. *Gynecol Obstet Invest* (2021) 86(6):533–41. doi: 10.1159/000518510

241. Duan L, Yan Y, Wang G, Xing YL, Sun J, Wang LL. Muir-182-5p functions as a tumor suppressor to sensitize human ovarian cancer cells to cisplatin through direct targeting the cyclin dependent kinase 6 (Cdk6). *J BUON* (2020) 25(5):2279–86.

242. Chen YY, Tai YC. Hsa_Circ_0006404 and Hsa_Circ_0000735 regulated ovarian cancer response to docetaxel treatment *Via* regulating p-gp expression. *Biochem Genet* (2022) 60(1):395–414. doi: 10.1007/s10528-021-10080-9

243. Shi X, Xiao L, Mao X, He J, Ding Y, Huang J, et al. Mir-205-5p mediated downregulation of pten contributes to cisplatin resistance in C13k human ovarian cancer cells. *Front Genet* (2018) 9:555. doi: 10.3389/fgene.2018.00555

244. Tan WX, Sun G, Shangguan MY, Gui Z, Bao Y, Li YF, et al. Novel role of lncrna chrf in cisplatin resistance of ovarian cancer is mediated by mir-10b induced emt and Stat3 signaling. *Sci Rep* (2020) 10(1):14768. doi: 10.1038/s41598-020-71153-0

245. Luo Y, Gui R. Circulating exosomal Circfoxp1 confers cisplatin resistance in epithelial ovarian cancer cells. *J Gynecol Oncol* (2020) 31(5):e75. doi: 10.3802/jgo.2020.31.e75

246. Xu ZH, Yao TZ, Liu W. Mir-378a-3p sensitizes ovarian cancer cells to cisplatin through targeting Mapk1/Grb2. *Biomed Pharmacother = Biomed Pharmacotherapie* (2018) 107:1410–7. doi: 10.1016/j.biopha.2018.08.132

247. Chen Y, Zhao XH, Zhang DD, Zhao Y. Mir-513a-3p inhibits emt mediated by Hoxb7 and promotes sensitivity to cisplatin in ovarian cancer cells. *Eur Rev Med Pharmacol Sci* (2020) 24(20):10391–402. doi: 10.26355/eurrev_202010_23389

248. Ni MW, Zhou J, Zhang YL, Zhou GM, Zhang SJ, Feng JG, et al. Downregulation of Linc00515 in high-grade serous ovarian cancer and its relationship with platinum resistance. *biomark Med* (2019) 13(7):535–43. doi: 10.2217/bmm-2018-0382

249. Wang Y, Bao W, Liu Y, Wang S, Xu S, Li X, et al. Mir-98-5p contributes to cisplatin resistance in epithelial ovarian cancer by suppressing mir-152 biogenesis *Via* targeting Dicer1. *Cell Death Dis* (2018) 9(5):447. doi: 10.1038/s41419-018-0390-7

250. Jiang J, Wang S, Wang Z, Cai J, Han L, Xie L, et al. Hotair promotes paclitaxel resistance by regulating Chek1 in ovarian cancer. *Cancer Chemother Pharmacol* (2020) 86(2):295–305. doi: 10.1007/s00280-020-04120-1

251. Xia B, Zhao Z, Wu Y, Wang Y, Zhao Y, Wang J. Circular rna Circtnpo3 regulates paclitaxel resistance of ovarian cancer cells by mir-1299/Nek2 signaling pathway. *Mol Ther Nucleic Acids* (2020) 21:780–91. doi: 10.1016/j.omtn.2020.06.002

252. Jin L, Zhang Z. Serum mir-3180-3p and mir-124-3p may function as noninvasive biomarkers of cisplatin resistance in gastric cancer. *Clin Lab* (2020) 66 (12). doi: 10.7754/Clin.Lab.2020.200302

253. Li Y, Lv S, Ning H, Li K, Zhou X, Xv H, et al. Down-regulation of Casc2 contributes to cisplatin resistance in gastric cancer by sponging mir-19a. *Biomed Pharmacother = Biomed Pharmacotherapie* (2018) 108:1775–82. doi: 10.1016/j.biopha.2018.09.181

254. Lv X, Li P, Wang J, Gao H, Hei Y, Zhang J, et al. Hsa_Circ_0000520 influences herceptin resistance in gastric cancer cells through Pi3k-akt signaling pathway. *J Clin Lab Anal* (2020) 34(10):e23449. doi: 10.1002/jcla.23449

255. Gao H, Ma J, Cheng Y, Zheng P. Exosomal transfer of macrophage-derived mir-223 confers doxorubicin resistance in gastric cancer. *Onco Targets Ther* (2020) 13:12169–79. doi: 10.2147/OTT.S283542

256. Zhang Z, Li M, Zhang Z. Lncrna Malat1 modulates oxaliplatin resistance of gastric cancer *Via* sponging mir-22-3p. *Onco Targets Ther* (2020) 13:1343–54. doi: 10.2147/OTT.S196619

257. Zhang Z, Yu X, Zhou B, Zhang J, Chang J. Circular rna Circ_0026359 enhances cisplatin resistance in gastric cancer *Via* targeting mir-1200/Pold4 pathway. *BioMed Res Int* (2020) 2020:5103272. doi: 10.1155/2020/5103272

258. Zhou Y, Ding BZ, Lin YP, Wang HB. Mir-34a, as a suppressor, enhance the susceptibility of gastric cancer cell to luteolin by directly targeting Hk1. *Gene* (2018) 644:56–65. doi: 10.1016/j.gene.2017.10.046

259. Pang K, Song J, Bai Z, Zhang Z. Mir-15a-5p targets Phlpp2 in gastric cancer cells to modulate platinum resistance and is a suitable serum biomarker for oxaliplatin resistance. *Neoplasma* (2020) 67(5):1114–21. doi: 10.4149/neo_2020_190904N861

260. Luo Y, Zheng S, Wu Q, Wu J, Zhou R, Wang C, et al. Long noncoding rna (Lncrna) Eif3j-dt induces chemoresistance of gastric cancer *Via* autophagy activation. *Autophagy* (2021) 17(12):4083–101. doi: 10.1080/15548627.2021.1901204

261. Zhen Q, Zhang Y, Gao L, Wang R, Chu W, Zhao X, et al. Mir-519d-3p enhances the sensitivity of non-Small-Cell lung cancer to tyrosine kinase inhibitors. *Mamm Genome* (2021) 32(6):508–16. doi: 10.1007/s00335-021-09919-8

262. Gu G, Hu C, Hui K, Zhang H, Chen T, Zhang X, et al. Exosomal mir-136-5p derived from anlotinib-resistant nsclc cells confers anlotinib resistance in non-small cell lung cancer through targeting Ppp2r2a. *Int J Nanomed* (2021) 16:6329–43. doi: 10.2147/IJN.S321720

263. Chen ZY, Liu HY, Jiang N, Yuan JM. Lncrna Host2 enhances gefitinib-resistance in non-small cell lung cancer by down-regulating mirna-621. *Eur Rev Med Pharmacol Sci* (2019) 23(22):9939–46. doi: 10.26355/eurrev_201911_19560

264. Li Q, Wang Y, He J. Mir-133a-3p attenuates resistance of non-small cell lung cancer cells to gefitinib by targeting Spag5. *J Clin Lab Anal* (2021) 35(7): e23853. doi: 10.1002/jcla.23853

265. Li X, Zhang X, Yang C, Cui S, Shen Q, Xu S. The lncrna Rhpn1-As1 downregulation promotes gefitinib resistance by targeting mir-299-3p/Tnfsf12 pathway in nsclc. *Cell Cycle* (2018) 17(14):1772–83. doi: 10.1080/15384101.2018.1496745

266. Xu YH, Tu JR, Zhao TT, Xie SG, Tang SB. Overexpression of lncrna Egfras1 is associated with a poor prognosis and promotes chemotherapy resistance in nonsmall cell lung cancer. *Int J Oncol* (2019) 54(1):295–305. doi: 10.3892/ijo.2018.4629

267. Song HM, Meng D, Wang JP, Zhang XY. Circrna Hsa_Circ_0005909 predicts poor prognosis and promotes the growth, metastasis, and drug resistance of non-Small-Cell lung cancer *Via* the mirna-338-3p/Sox4 pathway. *Dis Markers* (2021) 2021:8388512. doi: 10.1155/2021/8388512

268. Zhang L, Chen H, Song Y, Gu Q, Zhang L, Xie Q, et al. Mir-325 promotes oxaliplatin-induced cytotoxicity against colorectal cancer through the Hspa12b/Pi3k/Akt/Bcl-2 pathway. *Dig Dis Sci* (2021) 66(8):2651–60. doi: 10.1007/s10620-020-06579-7

269. Wang H, Li H, Zhang L, Yang D. Overexpression of Meg3 sensitizes colorectal cancer cells to oxaliplatin through regulation of mir-141/Pdcd4 axis. *Biomed Pharmacother = Biomed Pharmacotherapie* (2018) 106:1607–15. doi: 10.1016/j.biopha.2018.07.131

270. Sun L, Fang Y, Wang X, Han Y, Du F, Li C, et al. Mir-302a inhibits metastasis and cetuximab resistance in colorectal cancer by targeting nfib and Cd44. *Theranostics* (2019) 9(26):8409–25. doi: 10.7150/thno.36605

271. Hong S, Yan Z, Song Y, Bi M, Li S. Lncrna Agap2-As1 augments cell viability and mobility, and confers gemcitabine resistance by inhibiting mir-497 in colorectal cancer. *Aging* (2020) 12(6):5183–94. doi: 10.18632/aging.102940

272. Zhang Y, Li C, Liu X, Wang Y, Zhao R, Yang Y, et al. Circhipk3 promotes oxaliplatin-resistance in colorectal cancer through autophagy by sponging mir-637. *EBioMedicine* (2019) 48:277–88. doi: 10.1016/j.ebiom.2019.09.051

273. Wu H, Gu J, Zhou D, Cheng W, Wang Y, Wang Q, et al. Linc00160 mediated paclitaxel-and doxorubicin-resistance in breast cancer cells by regulating Tff3 *Via* transcription factor C/Ebpbeta. *J Cell Mol Med* (2020) 24(15):8589–602. doi: 10.1111/jcmm.15487

274. Zhang M, Wang Y, Jiang L, Song X, Zheng A, Gao H, et al. Lncrna Cbr3-As1 regulates of breast cancer drug sensitivity as a competing endogenous rna through the Jnk1/Mek4-mediated mapk signal pathway. *J Exp Clin Cancer Res* (2021) 40(1):41. doi: 10.1186/s13046-021-01844-7

275. Wang L, Zhou Y, Jiang L, Lu L, Dai T, Li A, et al. Circwac induces chemotherapeutic resistance in triple-negative breast cancer by targeting mir-142, upregulating Wwp1 and activating the Pi3k/Akt pathway. *Mol Cancer* (2021) 20 (1):43. doi: 10.1186/s12943-021-01332-8

276. Shu G, Su H, Wang Z, Lai S, Wang Y, Liu X, et al. Linc00680 enhances hepatocellular carcinoma stemness behavior and chemoresistance by sponging mir-568 to upregulate Akt3. *J Exp Clin Cancer Res* (2021) 40(1):45. doi: 10.1186/s13046-021-01854-5

277. Xu J, Ji L, Liang Y, Wan Z, Zheng W, Song X, et al. Circrna-sore mediates sorafenib resistance in hepatocellular carcinoma by stabilizing Ybx1. *Signal Transduction Targeted Ther* (2020) 5(1):298. doi: 10.1038/s41392-020-00375-5

278. Zhou S, Wei J, Wang Y, Liu X. Cisplatin resistance-associated Circrna_101237 serves as a prognostic biomarker in hepatocellular carcinoma. *Exp Ther Med* (2020) 19(4):2733–40. doi: 10.3892/etm.2020.8526

279. Lu H, Lu S, Yang D, Zhang L, Ye J, Li M, et al. Mir-20a-5p regulates gemcitabine chemosensitivity by targeting Rrm2 in pancreatic cancer cells and serves as a predictor for gemcitabine-based chemotherapy. *Biosci Rep* (2019) 39(5): BSR20181374. doi: 10.1042/BSR20181374

280. Okazaki J, Tanahashi T, Sato Y, Miyoshi J, Nakagawa T, Kimura T, et al. Microrna-296-5p promotes cell invasion and drug resistance by targeting Bcl2-related ovarian killer, leading to a poor prognosis in pancreatic cancer. *Digestion* (2020) 101(6):794–806. doi: 10.1159/000503225

281. Liu Y, Wang J, Dong L, Xia L, Zhu H, Li Z, et al. Long noncoding rna Hcp5 regulates pancreatic cancer gemcitabine (Gem) resistance by sponging hsa-Mir-214-3p to target hdgf. *Onco Targets Ther* (2019) 12:8207–16. doi: 10.2147/OTT.S222703

282. Wang H, Wu B, Wang J, Hu Y, Dai X, Ye L, et al. Methylation associated mir-1246 contributes to poor prognosis in gliomas treated with temozolomide. *Clin Neurol Neurosurg* (2021) 200:106344. doi: 10.1016/j.clineuro.2020.106344

283. Luo Y, Gui R. Circulating exosomal circmyc is associated with recurrence and bortezomib resistance in patients with multiple myeloma. *Turk J Haematol* (2020) 37(4):248–62. doi: 10.4274/tjh.galenos.2020.2020.0243

284. Pan J, Zhou C, Zhao X, He J, Tian H, Shen W, et al. A two-mirna signature (Mir-33a-5p and mir-128-3p) in whole blood as potential biomarker for early diagnosis of lung cancer. *Sci Rep* (2018) 8(1):16699. doi: 10.1038/s41598-018-35139-3

285. Lu N, Liu J, Ji C, Wang Y, Wu Z, Yuan S, et al. Mirna based tumor mutation burden diagnostic and prognostic prediction models for endometrial cancer. *Bioengineered* (2021) 12(1):3603–20. doi: 10.1080/21655979.2021.1947940

286. Xu W, Zhou G, Wang H, Liu Y, Chen B, Chen W, et al. Circulating lncrna Snhg11 as a novel biomarker for early diagnosis and prognosis of colorectal cancer. *Int J Cancer* (2020) 146(10):2901–12. doi: 10.1002/ijc.32747

287. Meng Y, Liu YL, Li K, Fu T. Prognostic value of long non-coding rna breast cancer anti-estrogen resistance 4 in human cancers: A meta-analysis. *Med (Baltimore)* (2019) 98(21):e15793. doi: 10.1097/MD.0000000000015793

288. Liu X, Tang H, Liu J, Wang X. Hsa_Circrna_101237: A novel diagnostic and prognostic biomarker and potential therapeutic target for multiple myeloma. *Cancer Manag Res* (2020) 12:2109–18. doi: 10.2147/CMAR.S241089

289. Zhang X, Xie K, Zhou H, Wu Y, Li C, Liu Y, et al. Role of non-coding rnas and rna modifiers in cancer therapy resistance. *Mol Cancer* (2020) 19(1):47. doi: 10.1186/s12943-020-01171-z

290. Yan H, Bu P. Non-coding rna in cancer. *Essays Biochem* (2021) 65(4):625–39. doi: 10.1042/EBC20200032

291. Fu Y, Huang R, Li J, Xie X, Deng Y. Lncrna Ensg00000254615 modulates proliferation and 5-fu resistance by regulating P21 and cyclin D1 in colorectal cancer. *Cancer Invest* (2021) 39(9):696–710. doi: 10.1080/07357907.2021.1923727

292. Qin L, Zhan Z, Wei C, Li X, Zhang T, Li J. Hsacircrnag004213 promotes cisplatin sensitivity by regulating Mir513b5p/Prpf39 in liver cancer. *Mol Med Rep* (2021) 23(6):421. doi: 10.3892/mmr.2021.12060

293. Li Y, Zu L, Wu H, Zhang F, Fan Y, Pan H, et al. Mir-192/Nkrf axis confers lung cancer cell chemoresistance to cisplatin *Via* the nf-kappab pathway. *Thorac Cancer* (2022) 13(3):430–41. doi: 10.1111/1759-7714.14278

294. Zhu M, Wang Y, Wang F, Li L, Qiu X. Circfbxl5 promotes the 5-fu resistance of breast cancer *Via* modulating mir-216b/Hmga2 axis. *Cancer Cell Int* (2021) 21(1):384. doi: 10.1186/s12935-021-02088-3

295. Slack FJ, Chinnaiyan AM. The role of non-coding rnas in oncology. *Cell* (2019) 179(5):1033–55. doi: 10.1016/j.cell.2019.10.017

frontiers | Frontiers in Oncology

TYPE Review
PUBLISHED 17 August 2022
DOI 10.3389/fonc.2022.960312

OPEN ACCESS

EDITED BY
Takeo Tatsuta,
Tohoku Medical and Pharmaceutical University, Japan

REVIEWED BY
Junfeng Ma,
Georgetown University, United States
Lara Abramowitz,
National Institute of Diabetes and Digestive and Kidney Diseases (NIH), United States

*CORRESPONDENCE
Ikram El Yazidi-Belkoura
ikram.el-yazidi@univ-lille.fr

SPECIALTY SECTION
This article was submitted to Pharmacology of Anti-Cancer Drugs, a section of the journal Frontiers in Oncology

RECEIVED 02 June 2022
ACCEPTED 19 July 2022
PUBLISHED 17 August 2022

CITATION
Very N and El Yazidi-Belkoura I (2022) Targeting *O*-GlcNAcylation to overcome resistance to anti-cancer therapies.
Front. Oncol. 12:960312.
doi: 10.3389/fonc.2022.960312

Targeting *O*-GlcNAcylation to overcome resistance to anti-cancer therapies

Ninon Very[1] and Ikram El Yazidi-Belkoura[2*]

[1]Université de Lille, Inserm, CHU Lille, Institut Pasteur de Lille, U1011-EGID, Lille, France, [2]Université de Lille, CNRS, UMR 8576-UGSF-Unité de Glycobiologie Structurale et Fonctionnelle, Lille, France

In cancer cells, metabolic reprogramming is associated with an alteration of the *O*-GlcNAcylation homeostasis. This post-translational modification (PTM) that attaches *O*-GlcNAc moiety to intracellular proteins is dynamically and finely regulated by the *O*-GlcNAc Transferase (OGT) and the *O*-GlcNAcase (OGA). It is now established that *O*-GlcNAcylation participates in many features of cancer cells including a high rate of cell growth, invasion, and metastasis but little is known about its impact on the response to therapies. The purpose of this review is to highlight the role of *O*-GlcNAc protein modification in cancer resistance to therapies. We summarize the current knowledge about the crosstalk between *O*-GlcNAcylation and molecular mechanisms underlying tumor sensitivity/resistance to targeted therapies, chemotherapies, immunotherapy, and radiotherapy. We also discuss potential benefits and strategies of targeting *O*-GlcNAcylation to overcome cancer resistance.

KEYWORDS

6845/12000 *O*-GlcNAcylation, cancer, therapy resistance, therapeutic strategy, post-translational modifications (PTMs)

Introduction

One of the main hallmarks of cancer cells is energy metabolism reprogramming to support continuous proliferation (1). This mechanism, known as the Warburg effect, shifts energy production from the oxidative phosphorylation that operates in normal cells to the faster aerobic glycolysis. To compensate for the low energy yield of aerobic glycolysis, tumor cells overexpress Glucose Transporters (GLUTs) (2) and increase their glucose uptake by a factor of 10. In addition to glucose, cancer cells excessively consume glutamine as another source of carbon and nitrogen to produce nucleic acids, lipids, and proteins (3). The conversion of glucose into fructose-6-phosphate is a common step in both glycolysis and the hexosamine biosynthetic pathways (HBP), which metabolizes 2 to 3% of total glucose entering the cell (4).

The final product of the HBP is the nucleotide-sugar uridine diphosphate N-acetylglucosamine (UDP-GlcNAc) that requires building blocks produced by glucose, amino acids (mainly glutamine but also glucogenic and ketogenic amino acids), fatty acids (acetyl-coenzyme A, acetyl-CoA) and nucleotides (uridine triphosphate, UTP) metabolisms. UDP-GlcNAc is therefore considered a cellular nutritional sensor. UDP-GlcNAc serves as a substrate of OGT to *O*-GlcNAcylate serine (Ser) and threonine (Thr) residues of cytoplasmic, nuclear, and mitochondrial proteins; the OGA removes it. The activity of both OGT and OGA makes this ubiquitous intracellular post-translational modification highly dynamic as has been widely described (5–7). A fine "Yin-Yang" occupancy competition mechanism between *O*-GlcNAcylation and phosphorylation on the same or adjacent Ser/Thr residues regulates protein's interaction, stability, subcellular localization, and enzymatic activity of their common target proteins (8). Elevated nutrients uptake and metabolism are correlated with increased HBP flow, UDP-GlcNAc level, and global protein *O*-GlcNAcylation in a wide variety of cancers including chronic lymphocytic leukemia (CLL), breast, lung, liver, prostate, endometrium, pancreas, colon, larynx and bladder (9–17). This aberrant hyper-*O*-GlcNAcylation is also the result of an alteration in the expression and activity of HBP enzymes and OGT (18–21). Interestingly, decreased OGA and/or increased OGT and *O*-GlcNAcylation levels are associated with poor cancer grade progression (10, 14, 16, 20, 22, 23).

For the past two decades, a growing body of evidence has demonstrated the crucial role of abnormal *O*-GlcNAcylation of many oncogenes, tumor suppressors, and signaling actors on the growth, adhesion, migration, and invasion of cancer cells. However, while the role of *O*-GlcNAcylation in carcinogenesis and tumor progression remains of high interest in cancer research (24, 25), the impact of this glycosylation in the response of cancer to therapies is poorly investigated. The donor substrate for *O*-GlcNAcylation UDP-GlcNAc can also be epimerized to uridine diphosphate N-acetylgalactosamine (UDP-GalNAc) or modified into cytidine monophosphate-N-acetylneuraminic acid (CMP-Neu5Ac). UDP-GlcNAc, UDP-GalNAc, and CMP-Neu5Ac are nucleotide-sugar substrates for the complex glycosylation of membrane or secretory proteins. In addition to their role in the development and progression of cancer, complex glycosylation alterations have also been correlated with resistance to anti-cancer therapies by interfering with metabolism and modulating tumor cell aggressiveness (26, 27).

In this review, we summarize recent evidence highlighting that cancer therapeutics affect cellular *O*-GlcNAcylation homeostasis and, reciprocally, that *O*-GlcNAcylation modulates the response of cancer cells to therapies. Finally, we discuss the benefits of targeting *O*-GlcNAcylation as a novel promising therapeutic strategy for cancer.

Impact of anti-cancer therapies on *O*-GlcNAcylation levels

Multiple lines of proof demonstrate that cellular stress (including glucose deprivation, chemotherapeutic and DNA-damaging agents) dramatically increases global *O*-GlcNAcylation of protein and that the sugar might be protective (28–30).

Notably, chemotherapeutic drugs (i.e. doxorubicin (DOX), 5-fluorouracil (5-FU), camptothecin (CPT), and cisplatin induce an accumulation of intracellular UDP-GlcNAc levels and global protein *O*-GlcNAcylation in different cancer cell lines (30–33). The increased flux through the HBP is at least partially mediated by the induction of Glutamine : Fructose-6-phosphate Amidotransferase (GFAT) through the AKT/X-Box Binding Protein 1 (XBP1) transcription factor pathway in an unfolded protein response (UPR)-independent manner (30) and by activation of the direct transcriptional activator Forkhead box A2 (FOXA2) (31). Interestingly, cellular UDP-GlcNAc levels are increased in cisplatin-sensitive brain tumor cells (32). Wang et al. (2021) demonstrated that cisplatin enhances UDP-GlcNAc production and global *O*-GlcNAcylation levels *in vitro* and *in vivo* by OGT, GFAT1 activation, and OGA inhibition (33). Conversely, we recently demonstrated that 5-FU decreases intracellular *O*-GlcNAcylation *in vitro* by reducing OGT at both protein and transcriptional levels but also *in vivo* most likely by reducing OGT activity (34). Owing to the fact that OGT enzymatic activity is inhibited by elevated UDP, UTP, and UDP-GlcNAc (35), we suggest that 5-FU metabolites may inhibit OGT by producing fluorinated derivates or uridine compounds (36). Overall, it seems well defined that cellular *O*-GlcNAcylation is increased in response to anti-cancer therapies-induced stress but the molecular structure of some therapeutic agents could also interfere with UDP-GlcNAc metabolism and OGT activity. UDP-GlcNAc could thus be a potential candidate for monitoring patient response to some anti-cancer therapies.

O-GlcNAcylation is considered a DNA damage-induced PTM since OGT relocates to the sites of damaged DNA caused by several agents (*i.e.* ionizing radiation, etoposide, methyl methanesulfonate (MMS), cisplatin, mitomycin C (MMC)) and catalyzes *O*-GlcNAcylation of several proteins of the repair machinery (37). By interfering with the other post-translational modifications of histones defining the "histone code", it is suggested that *O*-GlcNAcylation regulates chromatin compaction and gene transcription in response to stress (38). Histone *O*-GlcNAcylation and DNA condensation are concomitantly increased under heat shock-induced stress (39). Treatment with AUY922 and ganetespib HSP90 inhibitors induces *O*-GlcNAcylation of core histones (Ser^{122} of H2A, Thr^{45} of H3, and Thr^{30} of H4) in bladder carcinoma cells (40). This study outlines the association between histone PTMs and proteomic changes in response to HSP90 inhibitor treatment

in bladder carcinoma cells. Bibliographic analysis of therapies' impact on *O*-GlcNAcylation shows a steady increase in the number of papers demonstrating that global *O*-GlcNAcylation is moderately increased by chemotherapeutic agents in sensitive cells but more significantly in resistant ones. To have a more precise vision, we will detail below the link between *O*-GlcNAcylation and anticancer response by type of therapy.

Impact of *O*-GlcNAcylation on response to anti-cancer therapies

1 Targeted therapies

1.1 Tamoxifen

Breast cancer is the most common cancer in women and the leading cause of cancer-related death. Among different subtypes, luminal breast cancers expressing the Estrogen Receptor alpha (ERα) represent approximately 80% of cases (41). ERα plays a crucial role in cancer initiation and progression by binding to estrogen response elements sequence in promotor of target genes upon association with estradiol, its natural ligand, and other transcription factors and activation of downstream signaling pathways such as Phosphatidylinositol 3-Kinase (PI3K)/AKT and Mitogen-Activated Protein Kinase (MAPK) (42). Hormone therapies are the mainstay of the treatment of hormone receptor positive breast tumors. Since its approval by the U.S. Food and Drug Administration (FDA) in 1977, tamoxifen is one of the most commonly used hormone therapy and acts as a partial antagonist of ERα. However, many breast tumors exhibit *de novo* or acquired resistance to hormone therapies and some potential mechanisms include deregulation of *endoplasmic reticulum* (*ER*) pathway components, modification of cell cycle, and survival regulators or activation of escape signaling pathways (43). Thus, low expression of ERα is generally associated with resistance and poor prognosis (44).

Since cancer initiation and progression are fueled by metabolic reprogramming, the detection of metabolic biomarkers is an emerging approach for the prediction of cancer recurrence (45). In a retrospective study, Kuo et al. (2021) recently revealed that *O*-GlcNAcylation and Pyruvate Kinase M2 (PKM2) served as potentially independent prognostic markers in luminal breast cancers treated with endocrine treatment including tamoxifen. High levels of *O*-GlcNAcylation or PKM2 are positively associated with a high risk of cancer recurrence and poor long-term disease-free survival (46). PKM2 is a PK isoform preferentially expressed in cancer (47) for which hyper-*O*-GlcNAcylation is observed in breast tumors. *O*-GlcNAcylation of Ser^{362}, Thr^{365}, Thr^{405}, and Ser^{406} causes nuclear translocation of PKM2 leading to up-regulation of GLUT1 and Lactate Dehydrogenase A (LDHA) glycolysis components. Thus, the glycosylation by targeting PKM2 would promote the Warburg effect and breast tumor growth (21, 48) (Figure 1).

Beyond being a recurrence biomarker of endocrine-treated breast tumors, *O*-GlcNAcylation could also be an interesting therapeutic target to sensitize anti-estrogen-resistant breast tumors. First, *O*-GlcNAcylation promotes resistance of MCF-7 HR^+ breast cancer cells to tamoxifen by reducing ERα mRNA levels. In these cells, inhibition of OGT by siRNA or OSMI-1 specific inhibitor potentiates the cytotoxic effect of the drug (49, 50). Interestingly, tamoxifen-resistant cells are also dependent on high OGT activity. The OGT inhibition by OSMI-1 treatment sensitizes tamoxifen-resistant MCF-7 more than parental ones by inducing *ERBB Receptor Feedback Inhibitor 1* (*ERRFI1*) expression. ERRFI1 is a tumor-suppressor that inhibits ErbB receptor tyrosine kinase-signaling which is a known driver of tamoxifen resistance (51) (Figure 1). Thus, high expression of *ERRFI1* is associated with extended survival in patients with tamoxifen-treated ERα-positive breast tumors (52). Altogether, therapeutic approach leading to *O*-GlcNAcylation inhibition could improve the sensitivity of $ER\alpha^+$ breast cancer to tamoxifen.

1.2 Bortezomib

The proteasome is a large intracellular protease complex composed of a 20S proteolytic core and two 19S regulatory particles. Proteasome activity is essential for the control of various cellular processes such as cell cycle, DNA repair, signal transduction, and protein quality control. Bortezomib (BTZ) is a peptide boronic acid that reversibly acts on the chymotrypsin-like activity of the 20S particle. BTZ has become a target of choice for the treatment of cancers that present high proteasome activity (53). Since its FDA authorization in 2003, it is used for the treatment of relapsed/refractory mantle cell lymphoma (MCL) and multiple myeloma and is further undergoing clinical evaluation in solid tumors including breast, colorectal, ovarian, pancreatic, prostate, and squamous cell carcinomas. However, innate and acquired resistance to BTZ are frequently observed. Some BTZ resistance mechanisms include mutations or up-regulation of proteasome subunits, alteration of stress response, and cell survival pathways, or multi-drug resistance (54).

Interestingly, OGT is included in the list of BTZ sensitizers in myeloma cells (55). Several pieces of evidence demonstrate that *O*-GlcNAcylation up-regulates the bounce-back response that restores proteasome activity by transcriptional activation of proteasome subunit genes. There is a positive correlation between OGT and proteasome subunits expression in clinical cancer samples including breast invasive carcinoma and colorectal adenocarcinoma. Sekine et al. (2018) firstly demonstrated that *O*-GlcNAcylation is critical for the maintenance of proteasome activity by regulating Nuclear Respiratory Factor 1 (NRF1) transcription factor through its interaction with Host Cell Factor-1 (HCF-1). In response to

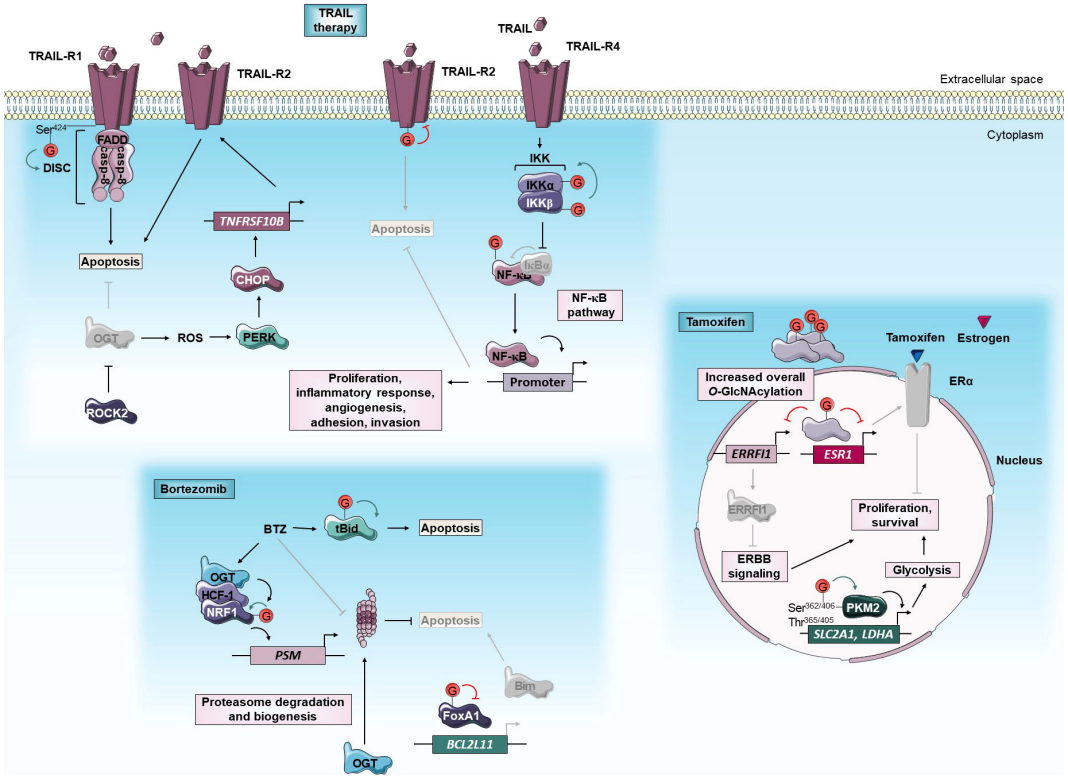

FIGURE 1
O-GlcNAcylation and anti-cancer targeted therapies. *O*-GlcNAcylation modulates sensitivity of cancer cells to TRAIL, bortezomib and tamoxifen targeted therapies. Green and red arrows indicate respectively activation and inhibition of protein targeted by *O*-GlcNAcylation. The gray color indicates that the protein is inactivated/absent or that the cellular mechanism is not taking place.*BCL2L11*, *Bcl-2-Like protein 11*; BTZ, bortezomib; Casp, caspase; CHOP, C/EBP Homologous Protein; DISC, death-inducing signaling complex; ERα, Estrogen receptor α; ERRFI1, ERBB Receptor Feedback Inhibitor 1; *ESR1*, *Estrogen Receptor 1*; FADD, Fas-Associated protein with Death Domain; FoxA1, Forkhead Box A1; HCF-1, Host Cell Factor-1; IKK, Inhibitory κB Kinase; *LDHA*, *Lactate Dehydrogenase A*; NF-κB, Nuclear Factor-Kappa B; NRF1, Nuclear Respiratory Factor 1; OGT, *O*-GlcNAc Transferase; PERK, Protein kinase RNA-like Kinase; PKM2, Pyruvate Kinase M2; *PSM*, *Proteasome subunit*; ROCK2, Rho-associated Coiled-coil forming protein Kinase 2; ROS, reactive oxygen species; Ser, serine; *SLC2A1*, *Solute Carrier family 2 member 1*; tBid, truncated BH3 interacting domain death agonist; *TNFRSF10B*, *Tumor Necrosis Factor (TNF) Receptor Superfamily member 10B*; Thr, threonine; TRAIL, TNF-Related Apoptosis Inducing Ligand; TRAIL-R, TRAIL Receptor.

BTZ, OGT targets and stabilizes NRF1. In turn, HCF-1 promotes the binding of NRF1 at promoter regions of proteasome subunit genes. *OGT* knock-down sensitizes MDA-MB-231 breast and NCI-460 pancreatic cancer cells to BTZ *in vitro* and in xenograft in a mouse model by blocking NRF1-dependent proteasome bounce-back response (56). It was also demonstrated that *O*-GlcNAcylation promotes the bounce-back response in an NRF1-independent-manner by promoting the turnover of the proteasome. Under BTZ-induced proteasome inhibition, *O*-GlcNAcylation enhances both degradation and biogenesis of proteasome allowing the recovery of its activity (Figure 1). The underlying mechanism is not yet clarified but the translation or the stability of proteasome subunits may be improved by *O*-GlcNAcylation since neither the subunit mRNA levels of the proteasome nor its assembly pathway is affected by OGT inhibition (57).

Other studies reveal that *O*-GlcNAcylation could regulate the BTZ-mediated activation of extrinsic and intrinsic apoptosis triggered by the accumulation of pro-apoptotic proteins including BH3 interacting domain death agonist (Bid) and Bim proteins (58). Increased *O*-GlcNAcylation of FOXA1, a forkhead transcription factor that activates Bim expression, is involved in breast cancer resistance to BTZ. There is an association between the elevation of *O*-GlcNAcylation content and resistance to BTZ in mammary cancer samples. BTZ dynamically induces an increase of global *O*-GlcNAcylation levels in intrinsic and extrinsic BTZ resistant breast cell lines but not in sensitive ones. In BTZ resistant cells, *O*-GlcNAcylation targets and reduces the stability of FOXA1 allowing Bim attenuation. OGT silencing or inhibition with L01 small molecule sensitizes resistant cells to BTZ by increasing FOXA1 and Bim protein levels (59). In contrast,

Luanpitpong et al. (2019) demonstrated that *O*-GlcNAcylation of truncated Bid (tBid) pro-apoptotic protein could sensitize MCL to BTZ. The use of pharmacological inhibitors of OGT (alloxan) and OGA (PUGNAc, Thiamet-G, ketoconazole (KCZ)) respectively abrogate and sensitize to BTZ-induced apoptosis in MCL cell lines. *O*-GlcNAcylation targets tBid and interferes with its ubiquitination and its subsequent degradation by the 26S proteasome (60). Glycosylation-mediated stabilization and accumulation of tBid intensify the apoptosis signal induced by BTZ (Figure 1). Thus, OGA inhibition by KCZ treatment increased the sensitivity of patient-derived primary cells and BTZ-resistant MCL cells (61).

Together, these data indicate that, in a cancer type-dependent manner, activation or inhibition of *O*-GlcNAcylation in combination with BTZ proteasome inhibitor is a promising clinical strategy against resistance to therapy.

1.3 Tumor necrosis factor-related apoptosis inducing ligand therapy

Upon Tumor necrosis factor (TNF)-Related Apoptosis Inducing Ligand (TRAIL) cytokine binding, TRAIL-Receptor 1 and 2 (TRAIL-R1 and TRAIL-R2 also known as respectively Death Receptor 4 and 5 (DR4 and DR5)) trigger the assembly of death-inducing signaling complex (DISC). The latter leads to apoptosis by activation of initiator caspases-8/10 and downstream effector caspases such as caspase-3. Unlike TNF-α and FAS extrinsic apoptosis-inducing ligands, TRAIL has an attractive ability to selectively induce apoptosis in tumor cells while sparing normal cells (62). Therefore, several clinical trials are currently underway to assess the efficacy of TRAIL therapy in cancer. Circularly permuted TRAIL (CPT) is tested in myeloma and some antibodies have also been developed: an anti-TRAIL-R (dulanermin) against lymphoma, colorectal and lung cancers, an anti-TRAIL-R1 (mapatumumab) or an anti-TRAIL-R2 (anti-DR5) (tigatuzumab) against several solid tumors (63). However, such clinical trials have failed to achieve a beneficial anticancer activity because a large number of cancers develop intrinsic and acquired resistance to TRAIL. Inhibition of apoptosis can be due to impaired TRAIL-R signaling, reduced caspases function, or disrupted balance between pro-apoptotic and anti-apoptotic proteins (64).

The death domain (DD) of TRAIL-R1 regulates both apoptosis and necrosis upon TRAIL ligand binding. In response to TRAIL, *O*-GlcNAcylation at the Ser^{424} DD residue of TRAIL-R1 facilitates receptors clustering within lipid rafts, DISC assembly, and induction of cell death (Figure 1). Several TRAIL-resistant cancer cell lines display a TRAIL-R1-Ser^{424} mutation and therefore defect of *O*-GlcNAcylation. The mutation at Ser^{424} residue could then be a potential genetic diagnostic marker of patients with cancer to predict TRAIL therapy response (65). *O*-GlcNAcylation of TRAIL-R2 also plays an important role in pancreatic cancer TRAIL resistance (66). Gain- and loss-of-function of OGT respectively render TRAIL-sensitive pancreatic cells more resistant to tigatuzumab TRAIL-R2 agonist and promote tigatuzumab-induced apoptosis in TRAIL-resistant cells *in vitro* and in a mouse model. Since *O*-GlcNAcylation of TRAIL-R2 regulates its trimerization and the activation of apoptotic signals, inhibiting *O*-GlcNAcylation could increase the effectiveness of TRAIL therapy (Figure 1). In addition, the overall level of global *O*-GlcNAcylation or *O*-GlcNAcylated TRAIL-R2 could be a biomarker of pancreatic cancer sensitivity to TRAIL therapy. In addition to activating apoptosis, TRAIL has also been described to induce the Nuclear Factor-Kappa (NF-κB) survival pathway that may promote drug resistance (67). Several studies have already revealed that *O*-GlcNAcylation regulates this pathway (68–72). Recently, Lee et al. (2021) demonstrate that a combination of TRAIL and OSMI-1 (OGT inhibitor) enhances TRAIL-induced apoptosis in colon cancer cells and xenograft tumors by lowering the activity of Inhibitory κB Kinase β (IKKβ) and inhibition of downstream NF-κB pro-survival signaling (73) (Figure 1). Additionally, OGT inhibition by OSMI-1 improves TRAIL-induced apoptosis by a parallel mechanism involving *ER* stress response. Hypo-*O*-GlcNAcylation induces the accumulation of reactive oxygen species (ROS) that leads to *ER* stress and activation of UPR signaling pathways including Protein Kinase RNA (PKR)-like kinase (PERK). Activation of PERK enhances expression of the pro-apoptotic protein C/EBP Homologous Protein (CHOP) that, in turn, up-regulates expression of TRAIL-R2 leading to TRAIL sensitization (73) (Figure 1). Concordantly, *O*-GlcNAcylation prevents activation of CHOP (74). Together, these studies suggest that a combination of TRAIL and OGT inhibition may induce synergistic effects and provide a promising therapeutic strategy for the treatment of various cancers.

Finally, a recent study identifies the GTPase RhoA effector Rho-associated Coiled-coil forming protein Kinase 2 (ROCK2) as a key regulator of *O*-GlcNAcylation and TRAIL sensitivity in osteosarcoma (OS). ROCK2 inhibits TRAIL-mediated apoptosis in OS cells by affecting OGT ubiquitination and degradation, and subsequently increasing protein *O*-GlcNAcylation levels (Figure 1). ROCK2 overexpression is an independent predictor of poor prognosis in OS patients and knock-down of ROCK2 causes a reduction in *O*-GlcNAcylation level and increases the OS cell sensitivity to TRAIL. Based on these data, the authors suggest ROCK2 as a potential biomarker for OS diagnostic and therapeutic tools (75).

2 Chemotherapies

2.1 5-fluorouracil

5-FU is a fluorinated uracil analog that acts as an antimetabolite to disrupt nucleic acid synthesis and repair in highly proliferating cancer cells. It was approved in 1962 by FDA and is widely used in the treatment of solid tumors including

colorectal, breast, anus, esophagus, pancreas, stomach, head, neck, and ovary cancers. The major cytotoxic activity of 5-FU consists of its conversion by Thymidine Kinase (TK) and Thymidine Phosphorylase (TP) into the active metabolite 5-fluorodeoxyuridine monophosphate (FdUMP) which sequesters and inhibits Thymidylate Synthase (TS), a key enzyme involved in the *de novo* synthesis of deoxythymidine monophosphate (dTMP). Cancer resistance to 5-FU can be caused by an alteration in metabolism, TS target level, recognition or repair of DNA damages, and/or inhibition of apoptosis (76).

Several studies have already correlated *OGT* expression with 5-FU sensitivity. Notably, Temmink et al. (2010) showed that H630 colon cancer cells resistant to trifluorothymidine (TFT), a fluorinated thymidine analog that is part of TAS-102 chemotherapy and shares the anabolic pathway of TS inhibition with 5-FU, underexpress OGT, Solute Carrier family 29A (SLC29A), and TK (77). On the contrary, a transcriptomic study on human NCI-60 tumors showed that OGT expression is negatively correlated with FdUMP sensitivity, no correlation with 5-FU sensitivity was established (78). OGT was also identified in a cluster of co-expressed genes associated with 5-FU resistance in colorectal cancer (CRC) (79). Moreover, the 5-FU pathway actors SLC29A1 (80), TP (10), TK (81, 82), and TS (34) are direct targets for *O*-GlcNAcylation (Figure 2). Nevertheless, modified sites and roles of this PTM on these proteins as well as their impacts on 5-FU sensitivity are largely not elucidated yet. Very recently, we demonstrated that TS is stabilized by *O*-GlcNAcylation at Thr^{251} and Thr^{306} residues. *OGT* knock-down decreases 5-FU-induced apoptosis by enhancing TS proteasomal degradation and, by reducing TS level and enzyme activity in HT-29 cell line but not in 5-FU resistant HT-29 counterpart (34) (Figure 2). The latter exhibits *TS* gene amplification and TS overexpression which is a current biomarker of 5-FU resistance in CRC (83). Our data highlight the importance to distinguish *TS* gene overexpression and the corresponding enzyme post-translational stabilization. We have shown that the regulation of 5-FU response by *O*-GlcNAcylation is finely tuned and depends on a proper quantity of TS proteins. In a CRC mouse model, the combination of 5-FU with the OGA inhibitor Thiamet-G had a synergistic inhibitory effect on tumor grade and progression (34). As the *O*-GlcNAcylation homeostasis-TS axis mediates the response to 5-FU, we propose to combine an OGA inhibitor with 5-FU-based therapies to enhance CRC patient response to 5-FU.

Another study showed that, in comparison to parental cells, 5-FU resistant SNUC5 colon cancer cells undergo oxidative stress due to 5-FU-induced accumulation of ROS. These cells overexpressed Tet methylcytosine dioxygenase 1 (TET1) and OGT. Both enzymes interact together at the promoter of Nuclear factor erythroid-2-Related Factor 2 (NRF2), a transcription factor that regulates the expression of antioxidant enzymes such as Heme Oxygenase-1 (HO-1). OGT indirectly activates the transcription of *NRF2* (Figure 2). Since oxaliplatin-resistant SNUC5 cells and cisplatin-resistant ovarian cancer cells express a high level of NRF2, inhibition of *O*-GlcNAcylation may potentiate the 5-FU-induced oxidative stress in these cells by decreasing NRF2 and HO-1 expression (84, 85). Chen et al. (2017) revealed an opposite functional connection between *O*-GlcNAcylation and NRF2 antioxidant pathway. In fact, Kelch-like ECH-Associated Protein 1 (KEAP1), the primary negative regulator of NRF2, *O*-GlcNAcylation at Ser^{104} is required for proteasomal degradation of NRF2. Gene expression signatures of low OGT activity and high NRF2 activation are strongly correlated in several breast tumor datasets and OGT inhibition induces NRF2 and subsequently reduces cysteine-deprivation induced-oxidative stress in breast MDA-MB-231 cells (86). Additionally, the inhibitory effect of *O*-GlcNAcylation on oxidative stress was confirmed as GFAT inhibition with 6-diazo-5-oxo-norleucine (DON) sensitizes cancer cells to oxidative stress-induced apoptosis (83). Of note, oxidative stress-resistant Phosphatase and tensin homolog (Pten) KO-mice tumors show increased GFAT2 and *O*-GlcNAcylation levels compared to wild-type (87).

2.2 Cisplatin

Cisplatin is a platinum-based alkylating agent that, mechanistically, reacts with DNA bases to cross-link adjacent purines, blocks DNA replication and induce apoptosis in rapidly dividing cells. It was firstly approved by FDA in 1978 for the treatment of testicular, ovarian, and bladder cancers. Nowadays, it is an important component of combination therapy for a wide range of solid tumors. The resistance to cisplatin can be caused by decreased drug accumulation, increased drug detoxification, increased DNA repair or DNA damage tolerance, and cell death escape (68). We describe below how *O*-GlcNAcylation interferes with the three last resistance mechanisms.

Autophagy is a self-protection mechanism that occurs as an emergency response and consists of phagocytosis of cytoplasmic proteins or damaged organelles into autophagosomes to meet the basic metabolic needs of cells. This cellular defensive pathway has a pro-survival role but can induce cell death under certain conditions. Autophagy plays a crucial role in the response of cancer cells to chemotherapeutic drugs including cisplatin (69, 70). Zhou et al. (2018) showed that OGT expression is significantly lower in cisplatin chemoresistant ovarian cancerous tissues compared to sensitive tissues. Additionally, *OGT* knock-down increases resistance to cisplatin of ovarian cancer cells and xenografted in mice (71). Reduced OGT expression regulates Synaptosomal Associated Protein 29 (SNAP 29) component of the Soluble N-ethylmaleimide-sensitive-factor Attachment protein Receptor (SNARE) vesicle formation machinery (72) which increases pro-survival autophagic flux that correlates with decreased apoptosis and increased cisplatin resistance (71) (Figure 2). Conversely, Wang et al. (2018) showed that siRNA invalidation of OGT increases autophagic flux and cisplatin-

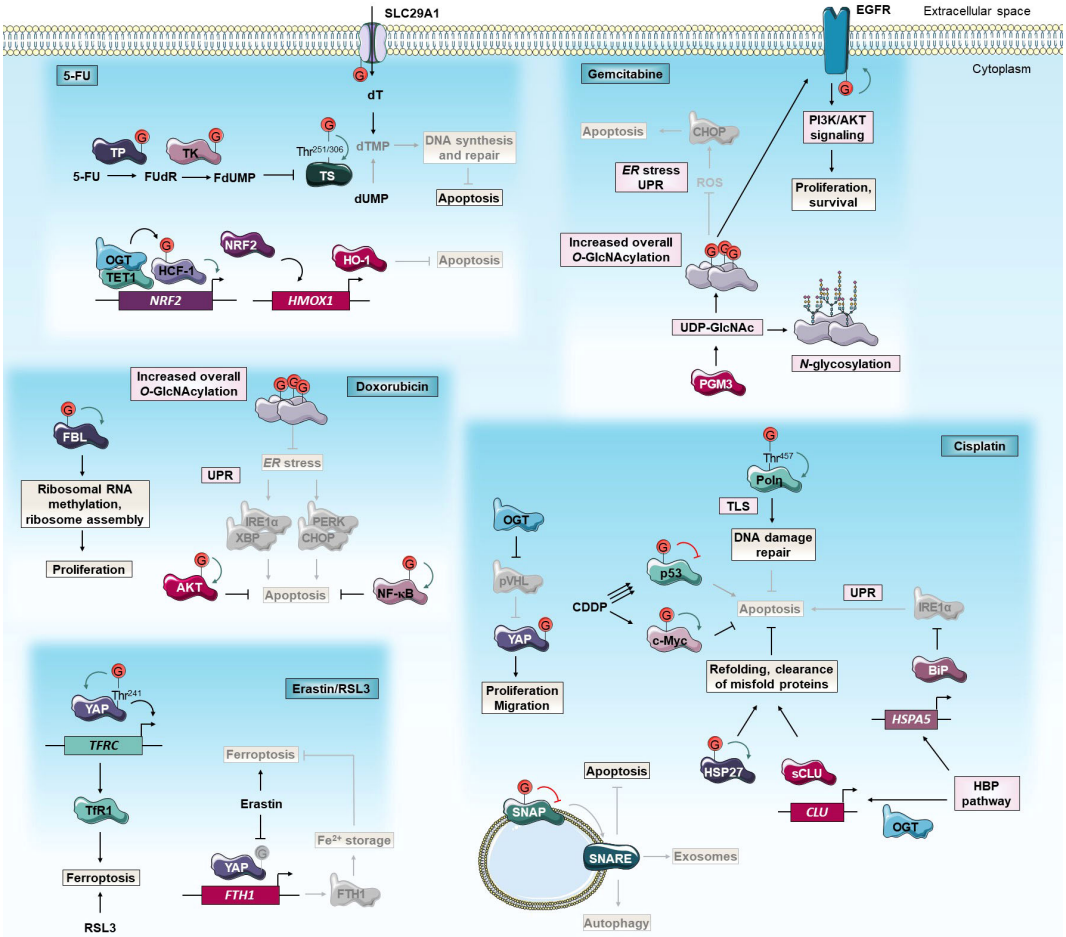

FIGURE 2
O-GlcNAcylation and anti-cancer chemotherapies. *O*-GlcNAcylation modulates cancer cell response to 5-FU, cisplatin, gemcitabine, doxorubicin and erastin/RSL3 chemotherapies. Green and red arrows indicate respectively activation and inhibition of protein targeted by *O*-GlcNAcylation. The gray color indicates that the protein is inactivated/absent or that the cellular mechanism is not taking place.5-FU, 5-fluorouracil; BiP, Binding immunoglobulin Protein; CDDP, cis-diaminedichloroplatinium(II); CHOP, C/EBP Homologous Protein; *CLU*, *Clusterin*; dUMP, deoxyuridine monophosphate; dT, deoxythymidine; dTMP, dT monophosphate; EGFR, Epidermal Growth Factor Receptor; ER, *endoplasmic reticulum*; FBL, Fibrillarin; *FTH1*, Ferritin Heavy chain 1; FdUMP, fluorodUMP; FUdR, fluorodeoxyuridine; HBP, Hexosamine Biosynthetic Pathway; HCF-1, Host Cell Factor-1; *HMOX1*, *Heme Oxygenase-1*; HO-1, Heme Oxygenase-1; HSP27, Heat Shock Protein 27 kD; IRE1α, Inositol-Requiring Enzyme 1α; NF-κB, Nuclear Factor-Kappa B; *NRF2*, Nuclear factor erythroid-2-Related Factor 2; OGT, *O*-GlcNAc Transferase; PERK, Protein kinase RNA-like Kinase; PGM3, Phosphoacetylglucosamine Mutase 3; PI3K, Phosphatidylinositol 3-Kinase; Polη, DNA Polymerase η; pVHL, von Hippel-Lindau protein; ROS, reactive oxygen species; RSL3, Ras-selective lethal small molecule 3; sCLU, secretory CLU; SLC29A1, Solute Carrier family 29 member 1; SNAP, Synaptosomal Associated Protein; SNARE, Soluble N-ethylmaleimide-sensitive-factor Attachment protein Receptor; TET1, Tet methylcytosine dioxygenase 1; TfR1, Transferrin Receptor 1; *TFRC*, Transferrin Receptor; Thr, threonine; TK, Thymidine Kinase; TLS, translesion DNA synthesis; TP, Thymidine Phosphorylase; TS, Thymidylate Synthase; UDP-GlcNAc, uridine disphosphate N-acetylglucosamine; UPR, unfolded protein response; XBP, AKT/X-Box Binding Protein; YAP, Yes-Associated Protein.

induced apoptosis in T24 and UMUC-3 bladder cancer cells (17, 88) (Figure 2). In addition to the degradation of long-lived macromolecules, the autophagy-lysosome system has broader functions and is involved in the selective degradation of other intracellular components including some oncogenes. The transcriptional co-activator Yes-Associated Protein (YAP) is a major effector of the Hippo pathway and its overactivation promotes cancer cell growth and chemoresistance. *O*-GlcNAcylation can block the von Hippel-Lindau protein (pVHL)-mediated lysosomal degradation of YAP and thus enhance cellular proliferation, migration, and cisplatin resistance in lung adenocarcinoma cells (89) (Figure 2). SNARE proteins also regulate the fusion of exosome-containing multivesicular bodies (MVB) to the plasma membrane and their secretion into the extracellular environment. Compared to normal cells, cancer cells secrete an increasing number of exosomes that can facilitate the efflux of intracellular chemotherapeutic drugs, hence promoting

chemoresistance (90). In A2780 and SKOV3 ovarian cancer cells, down-regulation of OGT reduces *O*-GlcNAcylation of SNAP-23 promoting the formation of SNARE complex and exosomes. Thus, this *O*-GlcNAcylation-mediated mechanism causes chemoresistance by increasing the exosome-mediated efflux of intracellular cisplatin (91) (Figure 2).

The tumor suppressor p53 plays a crucial role in cell biology and is considered the "guardian of the genome". In response to DNA damages, caused by chemotherapeutic agents such as cisplatin, p53 is stabilized and activates downstream pathways to arrest the cell cycle, repair the damaged DNA or induce apoptosis. Loss of function of p53 is a common feature in more than 50% of human cancers (92) and drives tumor growth and chemotherapy resistance. Several studies reveal that *O*-GlcNAcylation could regulate cisplatin resistance in a p53-dependent manner. Luanpitpong et al. (2017) showed that, depending on the cellular context and the level of cisplatin-activation of p53, increased *O*-GlcNAcylation could lead to cisplatin resistance in lung cancer cells by distinct molecular mechanisms. Indeed, in NCI-H292 cells, cisplatin weakly induces p53 activation and *O*-GlcNAcylation stabilizes the c-Myc oncoprotein to promote cell survival. In parallel, in NCI-H460 cells in which cisplatin induces strong activation of p53, *O*-GlcNAcylation of p53 increases its ubiquitination and its proteasomal degradation resulting in an enhanced oncogenic and anti-apoptotic phenotype (19) (Figure 2). Of note, literature shows some discrepancy since previous studies showed that *O*-GlcNAcylation stabilizes p53 (93) as in ovarian cancer cells (94). In these cells, the combination of OGA inhibitor Thiamet-G with cisplatin increases the drug sensitivity by inducing cell cycle arrest in wild-type p53 and to a lesser extent in silenced p53 cells. These data suggest that the Thiamet-G and cisplatin synergistic anti-tumoral effect is partially dependent on wild-type p53 pathway activation but also on other unknown growth-related pathways (94). Altogether, these results indicate that the effect of *O*-GlcNAcylation on cisplatin chemotherapy response could depend on the type of cancer and/or induction level, mutation status, and site-specific *O*-GlcNAcylation of p53.

After cisplatin exposure, DNA damage responses are initiated to maintain genome integrity. DNA cross-links are removed by the Nucleotide Excision Repair (NER) pathway or bypassed during replication through translesion DNA synthesis (TLS). TLS is mediated by specialized DNA polymerases (Pol) including Polη characterized by a low fidelity and the ability to replicate damaged DNA on stalled replication forks. TLS process is believed to contribute to the development of cisplatin resistance (95). In response to DNA damage, OGT relocates to DNA lesions and catalyzed *O*-GlcNAcylation of several substrates (37). Notably, Polη undergoes *O*-GlcNAcylation at Thr^{457} which allows its polyubiquitination at Lys^{462} and its subsequent dissociation from replication forks. Thus, cells expressing the *O*-GlcNAc-deficient T457A mutant Polη exhibit a higher sensitivity to cisplatin (96) (Figure 2). Given the key role of Polη in TLS and cisplatin chemoresistance of ovarian cancer stem cells (95), targeting Polη *O*-GlcNAcylation could be a chemotherapy-enhancing strategy in ovarian cancer treatment.

Stress conditions can destabilize the folding of cytoplasmic proteins leading to exposure of hydrophobic regions that interact with each other to form deleterious proteolysis resistant aggregates. In these conditions, molecular chaperones can form multimeric complexes to refold denatured or aggregated proteins. Elevated activity of chaperones allows cancer cells to grow and resist stress conditions including chemotherapy (97). Several studies showed that *O*-GlcNAcylation modulates cisplatin response by targeting directly or indirectly molecular chaperons. Based on the initial observation that higher *O*-GlcNAcylation levels in hepatoblastoma tissues might be associated with the pathogenesis, Song and collaborators (2019) realized a global proteomic analysis using *O*-GlcNAc antibody beads and immobilized metal affinity chromatography (IMAC) enrichments followed by liquid chromatography coupled to tandem mass spectrometry (LC-MS/MS) to identify potential *O*-GlcNAcylated and phosphorylated therapeutic targets. Among them, the anti-apoptotic chaperone Heat Shock Protein 27 kD (HSP27, also known as Heat Shock Protein family Beta-1 (HSPB1)) was identified, and its *O*-GlcNAcylation was further shown to promote cell proliferation and cisplatin resistance in hepatic cancer cell lines (98) (Figure 2). Overexpression of HSP27 is related to tumorigenesis, metastasis, and therapy resistance by acting as an upstream regulator of oncogenic (*i.e.* Hippo pathway, AKT, Glycogen Synthase Kinase 3 Beta (GSK3β), or β-catenin) and anti-apoptotic (i.e. NF-κB, Mothers Against Decapentaplegic homolog 3 (SMAD3), p38/MAPK) pathways. Targeting HSPs to enhance the effects of anti-cancer drugs is a promising approach and several molecules that modulate HSP protein functions are currently investigated in preclinical and clinical trials. For instance, HSP70 client protein inhibitor sorafenib has been approved to treat hepatocellular, renal, and thyroid carcinoma (97, 99). Studies revealed that *O*-GlcNAcylation stimulates aggressiveness and resistance of several cancers to chemotherapies and targeted therapies by modulating levels, activity, or subcellular localization of HSP proteins (100) including HSP27 (101–103). In this way, decreasing *O*-GlcNAcylation of HSPs could be a new anti-cancer therapeutic strategy. Secretory clusterin (sCLU) is a chaperon that facilitates the extracellular clearance of misfolded proteins. Like HSP proteins, this pro-survival factor is involved in cancer cell proliferation and drug resistance. OGT and sCLU expression are elevated in cervical cancer cell lines, and *O*-GlcNAc-induced up-regulation of sCLU leads to cisplatin resistance (Figure 2). sCLU silencing antisense oligonucleotides have been developed and approved for anti-cancer clinical trials. However, there is no drug currently available that completely blocks sCLU expression.

Then, inhibiting OGT in combination with the knock-down of sCLU could be a new therapeutic strategy to overcome cisplatin resistance (104). Binding immunoglobulin Protein (BiP) is a major *ER* HSP70 family chaperone that binds to misfolded or unfolded proteins and releases UPR sensors (Inositol-Requiring Enzyme 1α (IRE1α), PERK, and Activating Transcription Factor 6 (ATF6)) to initiate the UPR pathway. Inhibition of the HBP pathway with the glutamine analog DON enhances cisplatin-induced apoptosis of lung cancer cells by repressing BiP expression and activating IRE1α (Figure 2). Up-regulation of BiP expression by HBP flux is supported by a previous study carried out in hepatoblastoma cells (105). Together, these data suggest that the combination of cisplatin with HBP inhibitors could improve lung cancer platinum-based chemotherapies (106).

2.3 Gemcitabine

Gemcitabine (GEM) acts as an antimetabolite and is a deoxycytidine nucleoside analog. It was approved by FDA in 1996 as chemotherapy for pancreatic cancer and later on for non-small cell lung, ovarian and breast cancers. GEM is metabolized to the active metabolite, 2',2'-difluoro-2'-deoxycytidine triphosphate (dFdCTP) that can incorporate into DNA and RNA leading to the termination of DNA synthesis and faulty translation respectively. However, many cancers resist to GEM and the main involved mechanism consists of an up-regulation of the catabolic enzyme Cytidine Deaminase (CDA), deficiency in the anabolism enzyme Deoxycytidine Kinase (DCK), and alterations in nucleoside influx transporters (107).

Interestingly, increased metabolism of glucose and glutamine, two substrates for the HBP, fuel GEM resistance of pancreatic cancer (108, 109). Moreover, the HBP enzyme Phosphoacetylglucosamine Mutase 3 (PGM3) was shown to be overexpressed in GEM resistant human pancreatic tumors. Upon increasing GEM doses, PGM3 and global protein *O*-GlcNAcylation levels are decreased in sensitive BxPC-3 pancreatic cancer cells but increased in PANC-1 and MIA PaCa-2 resistant ones (110). Based on these observations, Ricchiardiello et al. (2020) recently investigated the effect of HBP flux inhibition in avoiding GEM resistance. Treatment with PGM3 inhibitor FR054 decreases tri-/tetra-antennary complex N-glycosylation of membrane proteins, *O*-GlcNAcylation of intracellular proteins, and enhances GEM efficiency *in vitro* and *in vivo*. Mechanistically, chemical inhibition of PGM3 causes a sustained activation of the pro-apoptotic UPR protein CHOP associated with a reduction in membrane localization of pro-tumorigenic Epidermal Growth Factor Receptor (EGFR) and a strong attenuation of the EGFR-Akt axis (110) (Figure 2). It was recently demonstrated that EGFR is directly *O*-GlcNAcylated and that *OGT* knock-down downregulates EGFR and its downstream PI3K/AKT pathway, and promotes cell cycle arrest and apoptosis in 786-O renal cell carcinoma cells (111). Pending further investigations to determine whether hypo-*O*-GlcNAcylation induced by PGM3 inhibition is directly involved in GEM sensitization mechanism, we speculate that hypo-*O*-GlcNAcylation could activate CHOP by inducing ROS accumulation, *ER* stress, and UPR activation (73, 74) (Figure 2). Therapeutic approaches involving PGM3 inhibition, and possibly inhibition of protein *O*-GlcNAcylation, in combination with GEM could be promising to bypass the drug resistance in pancreatic cancer.

2.4 Doxorubicin

Doxorubicin (DOX) is an anthracycline class medication approved by FDA and routinely applied to the treatment of several cancers such as breast, lung, gastric, ovarian, thyroid, non-Hodgkin's, and Hodgkin's lymphoma, sarcoma and pediatric tumors. This chemotherapeutic agent acts by intercalation with DNA, disruption of Topoisomerase II (Top-II), and production of quinone-type free radicals triggering cell death. Chemoresistance involves alteration of efflux ATP-Binding Cassette (ABC) transporter proteins, epigenetics, and signaling pathways (e.g. MAPK, PI3K/AKT/mammalian Target Of Rapamycin (mTOR), Wnt/β-catenin, Notch and Transforming Growth Factor Beta (TGF-β)) (112).

As previously mentioned, DOX treatment stimulates HBP flux and protein *O*-GlcNAcylation through the XBP1/AKT axis and FOXA2 leading to activation of pro-survival pathways (30, 31). Interestingly, recent studies showed that DOX treatment in combination with OSMI-1 has a synergistic apoptotic effect not only in several cancer types including sensitive and resistant liver (30, 113), prostate (114), and breast cancer cell lines but also in primary cells from newly diagnosed, refractory and relapsed acute myeloid leukemia (AML) patients (30). Hypo-*O*-GlcNAcylation enhances the sensitivity toward DOX by preventing pro-survival NF-κB and AKT activation (30, 113) and promoting *ER* stress response which leads to increased IRE1α-XBP and PERK-CHOP signaling (113) (Figure 2). Conversely, *O*-GlcNAcylation could protect MCF-7 breast cancer cells against DOX by stabilizing box C/D small nucleolar ribonucleoprotein complexes (snoRNPs) core component fibrillarin (FBL) on Ser^{142} and maintaining ribosomal RNA methylation and ribosome assembly (110) (Figure 2). Dysregulation of ribosome biogenesis promotes cancer cell proliferation (115). To note that treatment of HepG2 hepatocarcinoma cells with a low dose of DOX (1 μM) or a suboptimal dose of OSMI-1 (20 μM) alone did not induce apoptosis while the combined treatment did (113). In addition to improve therapeutic efficacy and alleviate DOX resistance in different cancer types, therapy combination with OGT inhibition could allow the use of smaller doses of DOX, hence reducing the associated side effects.

2.5 Erastin/RSL3

Ferroptosis is a newly identified form of programmed cell death that is characterized by an iron-dependent accumulation of lipid peroxides. Induction of ferroptosis emerged as a new strategy to trigger cancer cell death and ferroptosis-inducing compounds have been categorized into two classes based on their inhibition mode of Glutathione Peroxidase 4 (GPX4). The latter detoxifies lipid hyperoxides within biological membranes. The first class (e.g., erastin, Sorafenib) indirectly inhibits GPX4 by blocking the cysteine-glutamate transporter (system X_C^-) and depleting the GPX4 cofactor glutathione (GSH). The second class (e.g., Ras-selective lethal small molecule 3 (RSL3)) directly inhibits GPX4 leading to lipid-ROS accumulation (116). YAP has been reported to play a pivotal role in ferroptosis by upregulating critical modulators including Acyl-CoA Synthetase Long-chain family member 4 (ACSL4), Transferrin Receptor 1 (TfR1) (117), and Ferritin heavy chain 1 (FTH1) (118). *O*-GlcNAcylation of YAP on Thr^{241} residue prevents its degradation and enhances its transcriptional activity (12, 119). Under ferroptotic stress with erastin, system X_C^- inhibition leads indirectly to Thr^{241} hypo-*O*-GlcNAcylation of YAP, FTH1 down-regulation, free iron release, and increased ferroptosis in lung adenocarcinoma cells (118) (Figure 2). In contrast, Zhu et al. (2021) demonstrate that, under high glucose levels, *O*-GlcNAcylation enhances RSL3-mediated ferroptosis by targeting YAP on Thr^{241} and increasing its transcriptional activity on TfR1 in HCC cell lines (120) (Figure 2). Further study of YAP *O*-GlcNAcylation's role in ferroptosis, which seems to depend on the ferroptosis-inducing compound and the type of cancer tissue, would be useful to clarify these discrepancies.

3 Immunotherapy

Programmed cell Death protein 1 (PD-1) is a suppressive receptor expressed in immune T cells upon T cell activation. It is involved in T cell activation, proliferation, survival, and cytotoxic activity. PD-1 is highly selective for Programmed Death-Ligand 1 (PD-L1), an immune-inhibitory ligand overexpressed by cancer cells as an "adaptive immune mechanism" to escape immune responses. A range of monoclonal antibodies specific to the PD-1 and PD-L1 immune checkpoints have been approved for the treatment of a wide variety of human cancers. However, compensatory up-regulation of PD-L1 gradually causes drug resistance in some cancer patients (121).

Shang et al. (2021) recently showed that the embryo- and tumor-specific folate cycle enzyme Methylenetetrahydrofolate Dehydrogenase 2 (MTHFD2) can rescue cancer cells from T cell cytotoxicity by driving the folate cycle and by sustaining sufficient uridine-related metabolites including UDP-GlcNAc substrate donor. Thus, MTHFD2 is highly positively correlated to global *O*-GlcNAcylation levels which, in turn, targets c-Myc at Thr^{58} and promotes its stability and its direct activation of PD-L1 transcription (122). The c-Myc *O*-GlcNAcylation at Thr^{58} prevents its interaction with F-box/wD repeat-containing protein 7 (Fbw7) ubiquitin E3-ligase, increases its stability, and its transcriptional activity on target genes involved in cell proliferation, metabolism, and apoptosis (123). More particularly, *O*-GlcNAcylation mediated-stabilization of c-Myc is involved in renewal, clonal expansion and malignant transformation of T cell progenitors (88). MTHFD2, which is rarely expressed in normal adult tissues, emerges as a potential safe target. Thus, inhibiting the *O*-GlcNAcylation-c-Myc-PD-L1 signaling axis could be a promising therapeutic strategy to stimulate anti-cancer T cell cytotoxicity, hence improving immunotherapy.

4 Radiotherapy

Radiation therapy is given to about 50% of all cancer patients and contributes to 40% of curative anti-cancer treatments. The mode of action is to prevent cancer cells from proliferation by inducing extensive DNA damage. Exposure to radiation leads to DNA double-strand breaks (DSB) and triggers the DNA damage response (DDR), a complex signal transduction pathway that regulates DNA repair, cell cycle checkpoints activation, chromatin remodeling, cell senescence, and apoptosis. One of the key DNA damage-induced epigenetic modifications is the phosphorylation of H2A histone family member X (H2AX, also known as γH2AX) by a group of PI3-like kinases including Ataxia Telangiectasia Mutated (ATM), ATM and Rad3 related protein (ATR) and DNA-dependent Protein Kinase (DNA-PK). Aberrant DDR pathway activation directly confers tumor radioresistance (124).

In non-irradiated cells, OGT functions to suppress genomic instability and reduce cellular stress probably by protecting cells from oxidative stress and/or cell-cycle defects. Thus, under oxidative stress conditions, increased OGT and *O*-GlcNAc levels were required to induce DDR and proliferation of *Drosophila* intestinal stem/progenitor cells. In an autoregulatory feedback loop, Checkpoint Kinase 1 (CHK1)/CHK2 DDR effectors stabilize OGT (125). Moreover, OGT inhibition can induce cellular stress resulting in constitutive activation of DDR (126). *O*-GlcNAcylation can directly target many proteins of the DDR in response to heat-stress-induced DNA damage (*i.e.* DNA-PK, Coactivator-associated Arginine Methyltransferase 1 (CARM1), Ubiquitin-Associated Protein 2-Like (UBAP2L), Nuclear Factor 45 (NF45), NF90, RuvB-Like 1 (RUVBL1)) (127). A quantitative phosphoproteomic study showed that loss of *O*-GlcNAcylation in OGT null cells affects phosphorylation of cell cycle and DDR proteins including ATM and Checkpoint Kinase 1 (CHK1). Notably, hypo-*O*-GlcNAcylation increases activating phosphorylation events on ATM at Ser^{1981} and on its downstream substrates p53, H2AX, and CHK2 (128). In irradiated cells, OGT is essential for DNA

damage repair, recovery from checkpoint arrest, blockage onset of cellular senescence, and cell survival (126, 129, 130). Quantitative proteomic profiling of irradiated MCF-7 breast cancer cells revealed a strong regulation of chromatin modification and organization and DDR-associated factors upon alteration of *O*-GlcNAcylation (126). The H3K27 methyltransferase (HMT) Enhancer of Zeste 2 (EZH2) of Polycomb Related Complex 2 (PRC2) is considered a potential link between *O*-GlcNAcylation levels and irradiation induced DDR. EZH2-mediated histone methylation is found to promote DSB repair (131) and its Ser^{76} and Ser^{84} *O*-GlcNAcylation increases its stability and its HMT activity (132, 133). Irradiated tumor xenografts treated with shOGT or alloxan OGT inhibitor displayed a decreased EZH2 level, persistent DNA damages, a reduced proliferation, and an increased senescence. PUGNAc-induced elevation of *O*-GlcNAcylation or feeding animals with GlcNAc protects tumors against irradiation (126). Moreover, upon irradiation, *O*-GlcNAcylated H2B at Ser^{122} interacts with Nijmegen Breakage Sydrome 1 protein a member of MRE11-RAD50-NBS1 (MRN) complex, and promotes its accumulation at DSB where it normally acts as a bridge spanning the broken ends (129).

Other study showed contradictory results and point out OGT as a negative regulator to limit the expansion of DDR signaling in response to irradiation. Notably, in irradiated HeLa cervical cancer cells, OGT *O*-GlcNAcylates H2AX at Ser^{139} and Mediator of DNA Damage Checkpoint 1 (MDC1), and restrains the expansion of the DSBs-induced phosphorylation from the DNA damage sites. Thus, depletion of OGT in these cells does not affect DSB repair but prolongs the G_2/M checkpoint, delays cell cycle recovery, and reduces cell viability following DNA damages (37).

Conclusion and perspectives: *O*-GlcNAcylation as a therapeutic target to overcome resistance to anti-cancer therapies

Since its discovery in the 1980s (134, 135), the community have extensively proven the implication of *O*-GlcNAcylation in the etiology of chronic human diseases such as metabolic, neurodegenerative, cardiovascular diseases and cancer (6, 136, 137) but the role of the sugar in the resistance to various anti-cancer therapies has arisen more recently. Although many molecular mechanisms remain to be elucidated, targeting *O*-GlcNAcylation emerges as a promising strategy to impede cancer resistance. The current development of metabolic inhibitors, inhibitors of HBP and *O*-GlcNAcylation enzymes, RNA aptamers and nanobodies appear as promising tools and must be investigated in the light of cancer therapies to prevent or obliviate chemoresistance. The reprogramming of glucose and amino acid metabolisms provides energy and metabolites to cancer cells, including substrates for *O*-GlcNAcylation, to support growth, progression, metastasis, and resistance to anti-cancer therapies. Thus, a first level of action is to use metabolic inhibitors to modulate enzymes and transporters involved in nutrient metabolisms. The 2-deoxy-D-glucose (2DG) and dapagliflozin to target glucose metabolism, and GRASPA and ERY001 to target amino acid metabolism are currently under investigation in clinical trials (138). Direct targeting of HBP enzymes could be an alternative strategy. Thus, some inhibitors more or less specific for the rate-limiting GFAT (*i.e.* DON, azaserine and RO0509347), PGM3 (*i.e.* FR054) or UDP-N-Acetylglucosamine Pyrophosphorylase 1 (UAP1) (*i.e.* UTP a,b-methylenebisphosphonate analogue (meUTP) and GAL-012) are currently used (5). Notably, FR054 PGM3 specific inhibitor appears to have an *in vivo* antitumor efficacy by inhibiting the HBP flux (139). A third considered strategy is to use OGT or OGA inhibitors to directly restore the homeostasis of *O*-GlcNAcylation (5). The small molecule OSMI-1 is a highly specific OGT inhibitor of the quinolinone-6-sulfonamide (Q6S) class. Despite being membrane permeable and relatively large, having low aqueous solubility and inducing toxicity limiting its activity *in cellulo* (140), OSMI-1 could still have therapeutic potential since it synergistically enhances some cancer therapies (*i.e.* TRAIL and DOX)-induced apoptosis *in vivo* in tumor xenograft models (73, 113). The aminothiazoline derivative Thiamet-G is the most widely used OGA inhibitor *in vitro* and *in vivo* due to its stability, selectivity, oral bioavailability, and ability to cross the blood-brain barrier (141). Chronic elevation of *O*-GlcNAcylation by prolonged treatment with Thiamet-G (more than 5 months) was shown nontoxic *in vivo* in mice (142). We recently shown the efficiency of Thiamet-G to improve global *O*-GlcNAcylation levels and 5-FU response in murine carcinogen-induced CRC tumors (34). In addition, other selective OGA inhibitors, MK-8719 (143) and ASN120290 (previously known as ASN-561) (144) have obtained the orphan drug designation by the FDA for the treatment of the progressive supranuclear palsy (PSP) in 2016 and 2018 respectively. However, modulating global cellular *O*-GlcNAcylation levels have limits in term of therapeutic strategy. More than 5000 proteins have been identified as *O*-GlcNAcylated to date. Analysis of this *O*-GlcNAcome revealed the diversity of cellular mechanisms in which it is involved (145). In this way, global regulation of *O*-GlcNAcylation levels could affect proteins essential to cell/tissue physiology and induces severe side effects or induces other pathologies (6). To overcome this limitation, tools to implement a fourth strategy are under development which consists on targeting the *O*-GlcNAcylation of specific protein(s) of interest. Several writing and erasing *O*-GlcNAcylation engineering have been developed and some can allow the glycosylation/deglycosylation of a protein without the

need for prior identification of glyco-sites (146). Notably and very recently, a series of modulated RNA aptamers (147) and nanobody-OGT/OGA (148–150) able to direct these enzymes to a specific target protein of interest have been designed and delivered to living cells. These new approaches seem promising but require further studies to prove their efficiency and explore their possible *in vivo* applications.

Author contributions

NV and IEB co-conceived, co-organized and co-wrote the manuscript. NV prepared the figures. All authors have read and approved the final manuscript.

Funding

This work was supported by the "Ligue Contre le Cancer/ Comité du Nord/Comité de la Somme", the University of Lille and the "Center National de la Recherche Scientifique".

Acknowledgments

We thank Dr Stéphan Hardivillé and Dr Isabel Gonzalez Mariscal for proofreading the review.

Conflict of interest

The authors declare that the research was conducted in the absence of any commercial or financial relationships that could be construed as a potential conflict of interest.

Publisher's note

References

1. Hanahan D, Weinberg RA. Hallmarks of cancer: the next generation. *Cell* (2011) 144:646–74. doi: 10.1016/j.cell.2011.02.013

2. Carvalho KC, Cunha IW, Rocha RM, Ayala FR, Cajaíba MM, Begnami MD, et al. GLUT1 expression in malignant tumors and its use as an immunodiagnostic marker. *Clinics (Sao Paulo)* (2011) 66:965–72. doi: 10.1590/s1807-59322011000600008

3. Deberardinis RJ, Sayed N, Ditsworth D, Thompson CB. Brick by brick: metabolism and tumor cell growth. *Curr Opin Genet Dev* (2008) 18:54–61. doi: 10.1016/j.gde.2008.02.003

4. Marshall S, Bacote V, Traxinger RR. Discovery of a metabolic pathway mediating glucose-induced desensitization of the glucose transport system. role of hexosamine biosynthesis in the induction of insulin resistance. *J Biol Chem* (1991) 266:4706–12.

5. Ma J, Wu C, Hart GW. Analytical and biochemical perspectives of protein O-GlcNAcylation. *Chem Rev* (2021) 121:1513–81. doi: 10.1021/acs.chemrev.0c00884

6. Chatham JC, Zhang J, Wende AR. Role of O-linked n-acetylglucosamine protein modification in cellular (patho)physiology. *Physiol Rev* (2021) 101:427–93. doi: 10.1152/physrev.00043.2019

7. Ma J, Hou C, Wu C. Demystifying the O-GlcNAc code: A systems view. *Chem Rev* (2022). doi: 10.1021/acs.chemrev.1c01006

8. van der Laarse SAM, Leney AC, Heck AJR. Crosstalk between phosphorylation and O-GlcNAcylation: friend or foe. *FEBS J* (2018) 285:3152–67. doi: 10.1111/febs.14491

9. Shi Y, Tomic J, Wen F, Shaha S, Bahlo A, Harrison R, et al. Aberrant O-GlcNAcylation characterizes chronic lymphocytic leukemia. *Leukemia* (2010) 24:1588–98. doi: 10.1038/leu.2010.152

10. Champattanachai V, Netsirisawan P, Chaiyawat P, Phueaouan T, Charoenwattanasatien R, Chokchaichamnankit D, et al. Proteomic analysis and abrogated expression of O-GlcNAcylated proteins associated with primary breast cancer. *Proteomics* (2013) 13:2088–99. doi: 10.1002/pmic.201200126

11. Mi W, Gu Y, Han C, Liu H, Fan Q, Zhang X, et al. O-GlcNAcylation is a novel regulator of lung and colon cancer malignancy. *Biochim Biophys Acta* (2011) 1812:514–9. doi: 10.1016/j.bbadis.2011.01.009

12. Zhang X, Qiao Y, Wu Q, Chen Y, Zou S, Liu X, et al. The essential role of YAP O-GlcNAcylation in high-glucose-stimulated liver tumorigenesis. *Nat Commun* (2017) 8:15280. doi: 10.1038/ncomms15280

13. Olivier-Van Stichelen S, Dehennaut V, Buzy A, Zachayus J-L, Guinez C, Mir A-M, et al. O-GlcNAcylation stabilizes β-catenin through direct competition with phosphorylation at threonine 41. *FASEB J* (2014) 28:3325–38. doi: 10.1096/fj.13-243535

14. Krześlak A, Wójcik-Krowiranda K, Forma E, Bieńkiewicz A, Bryś M. Expression of genes encoding for enzymes associated with O-GlcNAcylation in endometrial carcinomas: clinicopathologic correlations. *Ginekol Pol* (2012) 83:22–6.

15. Lynch TP, Ferrer CM, Jackson SR, Shahriari KS, Vosseller K, Reginato MJ. Critical role of O-linked β-n-acetylglucosamine transferase in prostate cancer invasion, angiogenesis, and metastasis. *J Biol Chem* (2012) 287:11070–81. doi: 10.1074/jbc.M111.302547

16. Starska K, Forma E, Brzezińska-Błaszczyk E, Lewy-Trenda I, Bryś M, Jóźwiak P, et al. Gene and protein expression of O-GlcNAc-cycling enzymes in human laryngeal cancer. *Clin Exp Med* (2015) 15:455–68. doi: 10.1007/s10238-014-0318-1

17. Wang L, Chen S, Zhang Z, Zhang J, Mao S, Zheng J, et al. Suppressed OGT expression inhibits cell proliferation while inducing cell apoptosis in bladder cancer. *BMC Cancer* (2018) 18:1141. doi: 10.1186/s12885-018-5033-y

18. Itkonen HM, Minner S, Guldvik IJ, Sandmann MJ, Tsourlakis MC, Berge V, et al. O-GlcNAc transferase integrates metabolic pathways to regulate the stability of c-MYC in human prostate cancer cells. *Cancer Res* (2013) 73:5277–87. doi: 10.1158/0008-5472.CAN-13-0549

19. Luanpitpong S, Angsutararux P, Samart P, Chanthra N, Chanvorachote P, Issaragrisil S. Hyper-O-GlcNAcylation induces cisplatin resistance *via* regulation of p53 and c-myc in human lung carcinoma. *Sci Rep* (2017) 7:10607. doi: 10.1038/s41598-017-10886-x

20. Xu D, Wang W, Bian T, Yang W, Shao M, Yang H. Increased expression of O-GlcNAc transferase (OGT) is a biomarker for poor prognosis and allows tumorigenesis and invasion in colon cancer. *Int J Clin Exp Pathol* (2019) 12:1305–14.

21. Singh JP, Qian K, Lee J-S, Zhou J, Han X, Zhang B, et al. O-GlcNAcase targets pyruvate kinase M2 to regulate tumor growth. *Oncogene* (2020) 39:560–73. doi: 10.1038/s41388-019-0975-3

22. Trinca GM, Goodman ML, Papachristou EK, D'Santos CS, Chalise P, Madan R, et al. O-GlcNAc-Dependent regulation of progesterone receptor function in breast cancer. *Horm Cancer* (2018) 9:12–21. doi: 10.1007/s12672-017-0310-9

23. Gu Y, Mi W, Ge Y, Liu H, Fan Q, Han C, et al. GlcNAcylation plays an essential role in breast cancer metastasis. *Cancer Res* (2010) 70:6344–51. doi: 10.1158/0008-5472.CAN-09-1887

24. Lee JB, Pyo K-H, Kim HR. Role and function of O-GlcNAcylation in cancer. *Cancers (Basel)* (2021) 13:5365. doi: 10.3390/cancers13215365

25. Fardini Y, Dehennaut V, Lefebvre T, Issad T. O-GlcNAcylation: A new cancer hallmark? *Front Endocrinol (Lausanne)* (2013) 4:99. doi: 10.3389/fendo.2013.00099

26. Very N, Lefebvre T, El Yazidi-Belkoura I. Drug resistance related to aberrant glycosylation in colorectal cancer. *Oncotarget* (2017) 9:1380–402. doi: 10.18632/oncotarget.22377

27. Rodrigues JG, Duarte HO, Reis CA, Gomes J. Aberrant protein glycosylation in cancer: implications in targeted therapy. *Biochem Soc Trans* (2021) 49:843–54. doi: 10.1042/BST20200763

28. Zachara NE, O'Donnell N, Cheung WD, Mercer JJ, Marth JD, Hart GW. Dynamic O-GlcNAc modification of nucleocytoplasmic proteins in response to stress. a survival response of mammalian cells. *J Biol Chem* (2004) 279:30133–42. doi: 10.1074/jbc.M403773200

29. Cheung WD, Hart GW. AMP-activated protein kinase and p38 MAPK activate O-GlcNAcylation of neuronal proteins during glucose deprivation. *J Biol Chem* (2008) 283:13009–20. doi: 10.1074/jbc.M801222200

30. Liu Y, Cao Y, Pan X, Shi M, Wu Q, Huang T, et al. O-GlcNAc elevation through activation of the hexosamine biosynthetic pathway enhances cancer cell chemoresistance. *Cell Death Dis* (2018) 9:485. doi: 10.1038/s41419-018-0522-0

31. Huang H, Wang Y, Huang T, Wang L, Liu Y, Wu Q, et al. FOXA2 inhibits doxorubicin-induced apoptosis *via* transcriptionally activating HBP rate-limiting enzyme GFPT1 in HCC cells. *J Physiol Biochem* (2021) 77:625–38. doi: 10.1007/s13105-021-00829-6

32. Pan X, Wilson M, Mirbahai L, McConville C, Arvanitis TN, Griffin JL, et al. *In vitro* metabonomic study detects increases in UDP-GlcNAc and UDP-GalNAc, as early phase markers of cisplatin treatment response in brain tumor cells. *J Proteome Res* (2011) 10:3493–500. doi: 10.1021/pr200114v

33. Wang D, Wu J, Wang D, Huang X, Zhang N, Shi Y. Cisplatin enhances protein O–GlcNAcylation by altering the activity of OGT, OGA and AMPK in human non–small cell lung cancer cells. *Int J Oncol* (2021) 58:27. doi: 10.3892/ijo.2021.5207

34. Very N, Hardivillé S, Decourcelle A, Thévenet J, Djouina M, Page A, et al. Thymidylate synthase O-GlcNAcylation: a molecular mechanism of 5-FU sensitization in colorectal cancer. *Oncogene* (2022) 41:745–56. doi: 10.1038/s41388-021-02121-9

35. Haltiwanger RS, Blomberg MA, Hart GW. Glycosylation of nuclear and cytoplasmic proteins. purification and characterization of a uridine diphospho-n-acetylglucosamine:polypeptide beta-n-acetylglucosaminyltransferase. *J Biol Chem* (1992) 267:9005–13.

36. Pederson NV, Zanghi JA, Miller WM, Knop RH. Discrimination of fluorinated uridine metabolites in n-417 small cell lung cancer cell extracts *via* 19F- and 31P-NMR. *Magn Reson Med* (1994) 31:224–8. doi: 10.1002/mrm.1910310217

37. Chen Q, Yu X. OGT restrains the expansion of DNA damage signaling. *Nucleic Acids Res* (2016) 44:9266–78. doi: 10.1093/nar/gkw663

38. Dehennaut V, Leprince D, Lefebvre T. O-GlcNAcylation, an epigenetic mark. focus on the histone code, TET family proteins, and polycomb group proteins. *Front Endocrinol (Lausanne)* (2014) 5:155. doi: 10.3389/fendo.2014.00155

39. Sakabe K, Wang Z, Hart GW. β-n-acetylglucosamine (O-GlcNAc) is part of the histone code. *Proc Natl Acad Sci U.S.A.* (2010) 107:19915–20. doi: 10.1073/pnas.1009023107

40. Li QQ, Hao J-J, Zhang Z, Krane LS, Hammerich KH, Sanford T, et al. Proteomic analysis of proteome and histone post-translational modifications in heat shock protein 90 inhibition-mediated bladder cancer therapeutics. *Sci Rep* (2017) 7:201. doi: 10.1038/s41598-017-00143-6

41. Harbeck N, Penault-Llorca F, Cortes J, Gnant M, Houssami N, Poortmans P, et al. Breast cancer. *Nat Rev Dis Primers* (2019) 5:66. doi: 10.1038/s41572-019-0111-2

42. Tokunaga E, Hisamatsu Y, Tanaka K, Yamashita N, Saeki H, Oki E, et al. Molecular mechanisms regulating the hormone sensitivity of breast cancer. *Cancer Sci* (2014) 105:1377–83. doi: 10.1111/cas.12521

43. Hartkopf AD, Grischke E-M, Brucker SY. Endocrine-resistant breast cancer: Mechanisms and treatment. *BRC* (2020) 15:347–54. doi: 10.1159/000508675

44. Kim C, Tang G, Pogue-Geile KL, Costantino JP, Baehner FL, Baker J, et al. Estrogen receptor (ESR1) mRNA expression and benefit from tamoxifen in the treatment and prevention of estrogen receptor-positive breast cancer. *J Clin Oncol* (2011) 29:4160–7. doi: 10.1200/JCO.2010.32.9615

45. Gandhi N, Das GM. Metabolic reprogramming in breast cancer and its therapeutic implications. *Cells* (2019) 8:E89. doi: 10.3390/cells8020089

46. Kuo W-L, Tseng L-L, Chang C-C, Chen C-J, Cheng M-L, Cheng H-H, et al. Prognostic significance of O-GlcNAc and PKM2 in hormone receptor-positive and HER2-nonenriched breast cancer. *Diagnostics (Basel)* (2021) 11:1460. doi: 10.3390/diagnostics11081460

47. Yang Y, Wu K, Liu Y, Shi L, Tao K, Wang G. Prognostic significance of metabolic enzyme pyruvate kinase M2 in breast cancer: A meta-analysis. *Med (Baltimore)* (2017) 96:e8690. doi: 10.1097/MD.0000000000008690

48. Wang Y, Liu J, Jin X, Zhang D, Li D, Hao F, et al. O-GlcNAcylation destabilizes the active tetrameric PKM2 to promote the warburg effect. *Proc Natl Acad Sci U.S.A.* (2017) 114:13732–7. doi: 10.1073/pnas.1704145115

49. Kanwal S, Fardini Y, Pagesy P, N'tumba-Byn T, Pierre-Eugène C, Masson E, et al. O-GlcNAcylation-inducing treatments inhibit estrogen receptor α expression and confer resistance to 4-OH-tamoxifen in human breast cancer-derived MCF-7 cells. *PloS One* (2013) 8:e69150. doi: 10.1371/journal.pone.0069150

50. Barkovskaya A, Seip K, Hilmarsdottir B, Maelandsmo GM, Moestue SA, Itkonen HM. O-GlcNAc transferase inhibition differentially affects breast cancer subtypes. *Sci Rep* (2019) 9:5670. doi: 10.1038/s41598-019-42153-6

51. Massarweh S, Osborne CK, Creighton CJ, Qin L, Tsimelzon A, Huang S, et al. Tamoxifen resistance in breast tumors is driven by growth factor receptor signaling with repression of classic estrogen receptor genomic function. *Cancer Res* (2008) 68:826–33. doi: 10.1158/0008-5472.CAN-07-2707

52. Barkovskaya A, Seip K, Prasmickaite L, Mills IG, Moestue SA, Itkonen HM. Inhibition of O-GlcNAc transferase activates tumor-suppressor gene expression in tamoxifen-resistant breast cancer cells. *Sci Rep* (2020) 10:16992. doi: 10.1038/s41598-020-74083-z

53. D'Arcy P, Brnjic S, Olofsson MH, Fryknäs M, Lindsten K, De Cesare M, et al. Inhibition of proteasome deubiquitinating activity as a new cancer therapy. *Nat Med* (2011) 17:1636–40. doi: 10.1038/nm.2536

54. Lü S, Wang J. The resistance mechanisms of proteasome inhibitor bortezomib. *biomark Res* (2013) 1:13. doi: 10.1186/2050-7771-1-13

55. Zhu YX, Tiedemann R, Shi C-X, Yin H, Schmidt JE, Bruins LA, et al. RNAi screen of the druggable genome identifies modulators of proteasome inhibitor sensitivity in myeloma including CDK5. *Blood* (2011) 117:3847–57. doi: 10.1182/blood-2010-08-304022

56. Sekine H, Okazaki K, Kato K, Alam MM, Shima H, Katsuoka F, et al. O-GlcNAcylation signal mediates proteasome inhibitor resistance in cancer cells by stabilizing NRF1. *Mol Cell Biol* (2018) 38:e00252–18. doi: 10.1128/MCB.00252-18

57. Hashimoto E, Okuno S, Hirayama S, Arata Y, Goto T, Kosako H, et al. Enhanced O-GlcNAcylation mediates cytoprotection under proteasome impairment by promoting proteasome turnover in cancer cells. *iScience* (2020) 23:101299. doi: 10.1016/j.isci.2020.101299

58. Chen S, Zhang Y, Zhou L, Leng Y, Lin H, Kmieciak M, et al. A bim-targeting strategy overcomes adaptive bortezomib resistance in myeloma through a novel link between autophagy and apoptosis. *Blood* (2014) 124:2687–97. doi: 10.1182/blood-2014-03-564534

59. Liu Y, Wang X, Zhu T, Zhang N, Wang L, Huang T, et al. Resistance to bortezomib in breast cancer cells that downregulate bim through FOXA1 O-GlcNAcylation. *J Cell Physiol* (2019) 234:17527–37. doi: 10.1002/jcp.28376

60. Azakir BA, Desrochers G, Angers A. The ubiquitin ligase itch mediates the antiapoptotic activity of epidermal growth factor by promoting the ubiquitylation and degradation of the truncated c-terminal portion of bid. *FEBS J* (2010) 277:1319–30. doi: 10.1111/j.1742-4658.2010.07562.x

61. Luanpitpong S, Chanthra N, Janan M, Poohadsuan J, Samart P, U-Pratya Y, et al. Inhibition of O-GlcNAcase sensitizes apoptosis and reverses bortezomib resistance in mantle cell lymphoma through modification of truncated bid. *Mol Cancer Ther* (2018) 17:484–96. doi: 10.1158/1535-7163.MCT-17-0390

62. Holoch PA, Griffith TS. TNF-related apoptosis-inducing ligand (TRAIL): a new path to anti-cancer therapies. *Eur J Pharmacol* (2009) 625:63–72. doi: 10.1016/j.ejphar.2009.06.066

63. Yuan X, Gajan A, Chu Q, Xiong H, Wu K, Wu GS. Developing TRAIL/TRAIL death receptor-based cancer therapies. *Cancer Metastasis Rev* (2018) 37:733–48. doi: 10.1007/s10555-018-9728-y

64. Ching NS, Sonia WHM. Trailing TRAIL resistance for targeted cancer therapy. *Biomed J Sci Tech Res* (2018) 4:3668–71.

65. Lee H, Oh Y, Jeon Y-J, Lee S-Y, Kim H, Lee H-J, et al. DR4-Ser424 O-GlcNAcylation promotes sensitization of TRAIL-tolerant persisters and TRAIL-resistant cancer cells to death. *Cancer Res* (2019) 79:2839–52. doi: 10.1158/0008-5472.CAN-18-1991

66. Yang S, Xu F, Yuan K, Sun Y, Zhou T, Zhao X, et al. Regulation of pancreatic cancer TRAIL resistance by protein O-GlcNAcylation. *Lab Invest* (2020) 100:777–85. doi: 10.1038/s41374-019-0365-z

67. Yang J, LeBlanc FR, Dighe SA, Hamele CE, Olson TL, Feith DJ, et al. TRAIL mediates and sustains constitutive NF-κB activation in LGL leukemia. *Blood* (2018) 131:2803–15. doi: 10.1182/blood-2017-09-808816

68. Chen S-H, Chang J-Y. New insights into mechanisms of cisplatin resistance: From tumor cell to microenvironment. *Int J Mol Sci* (2019) 20:E4136. doi: 10.3390/ijms20174136

69. He J, Yu J-J, Xu Q, Wang L, Zheng JZ, Liu L-Z, et al. Downregulation of ATG14 by EGR1-MIR152 sensitizes ovarian cancer cells to cisplatin-induced apoptosis by inhibiting cyto-protective autophagy. *Autophagy* (2015) 11:373–84. doi: 10.1080/15548627.2015.1009781

70. Kim M, Jung J-Y, Choi S, Lee H, Morales LD, Koh J-T, et al. GFRA1 promotes cisplatin-induced chemoresistance in osteosarcoma by inducing autophagy. *Autophagy* (2016) 13:149–68. doi: 10.1080/15548627.2016.1239676

71. Zhou F, Yang X, Zhao H, Liu Y, Feng Y, An R, et al. Down-regulation of OGT promotes cisplatin resistance by inducing autophagy in ovarian cancer. *Theranostics* (2018) 8:5200–12. doi: 10.7150/thno.27806

72. Guo B, Liang Q, Li L, Hu Z, Wu F, Zhang P, et al. O-GlcNAc-modification of SNAP-29 regulates autophagosome maturation. *Nat Cell Biol* (2014) 16:1215–26. doi: 10.1038/ncb3066

73. Lee S-J, Lee D-E, Choi S-Y, Kwon O-S. OSMI-1 enhances TRAIL-induced apoptosis through ER stress and NF-κB signaling in colon cancer cells. *Int J Mol Sci* (2021) 22:11073. doi: 10.3390/ijms222011073

74. Jang I, Kim HB, Seo H, Kim JY, Choi H, Yoo JS, et al. O-GlcNAcylation of eIF2α regulates the phospho-eIF2α-mediated ER stress response. *Biochim Biophys Acta* (2015) 1853:1860–9. doi: 10.1016/j.bbamcr.2015.04.017

75. Deng X, Yi X, Huang D, Liu P, Chen L, Du Y, et al. ROCK2 mediates osteosarcoma progression and TRAIL resistance by modulating O-GlcNAc transferase degradation. *Am J Cancer Res* (2020) 10:781–98.

76. Ghafouri-Fard S, Abak A, Tondro Anamag F, Shoorei H, Fattahi F, Javadinia SA, et al. 5-fluorouracil: A narrative review on the role of regulatory mechanisms in driving resistance to this chemotherapeutic agent. *Front Oncol* (2021) 11:658636. doi: 10.3389/fonc.2021.658636

77. Temmink OH, Bijnsdorp IV, Prins H-J, Losekoot N, Adema AD, Smid K, et al. Trifluorothymidine resistance is associated with decreased thymidine kinase and equilibrative nucleoside transporter expression or increased secretory phospholipase A2. *Mol Cancer Ther* (2010) 9:1047–57. doi: 10.1158/1535-7163.MCT-09-0932

78. Gmeiner WH, Reinhold WC, Pommier Y. Genome-wide mRNA and microRNA profiling of the NCI 60 cell-line screen and comparison of FdUMP [10] with fluorouracil, floxuridine, and topoisomerase 1 poisons. *Mol Cancer Ther* (2010) 9:3105–14. doi: 10.1158/1535-7163.MCT-10-0674

79. Cao S, Chang W, Wan C, Zang Y, Zhao J, Chen J, et al. Bi-clustering based biological and clinical characterization of colorectal cancer in complementary to CMS classification. *bioRxiv* (2018) 508275. doi: 10.1101/508275

80. Wang Z, Park K, Comer F, Hsieh-Wilson LC, Saudek CD, Hart GW. Site-specific GlcNAcylation of human erythrocyte proteins. *Diabetes* (2009) 58:309–17. doi: 10.2337/db08-0994

81. Jochmann R, Pfannstiel J, Chudasama P, Kuhn E, Konrad A, Stürzl M. O-GlcNAc transferase inhibits KSHV propagation and modifies replication relevant viral proteins as detected by systematic O-GlcNAcylation analysis. *Glycobiology* (2013) 23:1114–30. doi: 10.1093/glycob/cwt028

82. Hahne H, Sobotzki N, Nyberg T, Helm D, Borodkin VS, van Aalten DM, et al. Proteome wide purification and identification of O-GlcNAc modified proteins using click chemistry and mass spectrometry. *J Proteome Res* (2013) 12:927–36. doi: 10.1021/pr300967y

83. Palmirotta R, Carella C, Silvestris E, Cives M, Stucci SL, Tucci M, et al. SNPs in predicting clinical efficacy and toxicity of chemotherapy: walking through the quicksand. *Oncotarget* (2018) 9:25355–82. doi: 10.18632/oncotarget.25256

84. Kang KA, Piao MJ, Kim KC, Kang HK, Chang WY, Park IC, et al. Epigenetic modification of Nrf2 in 5-fluorouracil-resistant colon cancer cells: involvement of TET-dependent DNA demethylation. *Cell Death Dis* (2014) 5:e1183. doi: 10.1038/cddis.2014.149

85. Kang KA, Piao MJ, Ryu YS, Kang HK, Chang WY, Keum YS, et al. Interaction of DNA demethylase and histone methyltransferase upregulates Nrf2 in 5-fluorouracil-resistant colon cancer cells. *Oncotarget* (2016) 7:40594–620. doi: 10.18632/oncotarget.9745

86. Chen P, Smith TJ, Wu J, Siesser PF, Bisnett BJ, Khan F, et al. Glycosylation of KEAP1 links nutrient sensing to redox stress signaling. *EMBO J* (2017) 36:2233–50. doi: 10.15252/embj.201696113

87. Walter LA, Lin YH, Halbrook CJ, Chuh KN, He L, Pedowitz NJ, et al. Inhibiting the hexosamine biosynthetic pathway lowers O-GlcNAcylation levels and sensitizes cancer to environmental stress. *Biochemistry* (2020) 59:3169–79. doi: 10.1021/acs.biochem.9b00560

88. Swamy M, Pathak S, Grzes KM, Damerow S, Sinclair LV, van Aalten DMF, et al. Glucose and glutamine fuel protein O-GlcNAcylation to control T cell self-renewal and malignancy. *Nat Immunol* (2016) 17:712–20. doi: 10.1038/ni.3439

89. Hu L, Wu H, Jiang T, Kuang M, Liu B, Guo X, et al. pVHL promotes lysosomal degradation of YAP in lung adenocarcinoma. *Cell Signal* (2021) 83:110002. doi: 10.1016/j.cellsig.2021.110002

90. Dorayappan KDP, Wanner R, Wallbillich JJ, Saini U, Zingarelli R, Suarez AA, et al. Hypoxia-induced exosomes contribute to a more aggressive and chemoresistant ovarian cancer phenotype: a novel mechanism linking STAT3/Rab proteins. *Oncogene* (2018) 37:3806–21. doi: 10.1038/s41388-018-0189-0

91. Qian L, Yang X, Li S, Zhao H, Gao Y, Zhao S, et al. Reduced O-GlcNAcylation of SNAP-23 promotes cisplatin resistance by inducing exosome secretion in ovarian cancer. *Cell Death Discovery* (2021) 7:112. doi: 10.1038/s41420-021-00489-x

92. Wang X, Simpson ER, Brown KA. p53: Protection against tumor growth beyond effects on cell cycle and apoptosis. *Cancer Res* (2015) 75:5001–7. doi: 10.1158/0008-5472.CAN-15-0563

93. Yang WH, Kim JE, Nam HW, Ju JW, Kim HS, Kim YS, et al. Modification of p53 with O-linked n-acetylglucosamine regulates p53 activity and stability. *Nat Cell Biol* (2006) 8:1074–83. doi: 10.1038/ncb1470

94. de Queiroz RM, Madan R, Chien J, Dias WB, Slawson C. Changes in O-linked n-acetylglucosamine (O-GlcNAc) homeostasis activate the p53 pathway in ovarian cancer cells. *J Biol Chem* (2016) 291:18897–914. doi: 10.1074/jbc.M116.734533

95. Srivastava AK, Han C, Zhao R, Cui T, Dai Y, Mao C, et al. Enhanced expression of DNA polymerase eta contributes to cisplatin resistance of ovarian cancer stem cells. *Proc Natl Acad Sci U.S.A.* (2015) 112:4411–6. doi: 10.1073/pnas.1421365112

96. Ma X, Liu H, Li J, Wang Y, Ding Y-H, Shen H, et al. Polη O-GlcNAcylation governs genome integrity during translesion DNA synthesis. *Nat Commun* (2017) 8:1941. doi: 10.1038/s41467-017-02164-1

97. Yun CW, Kim HJ, Lim JH, Lee SH. Heat shock proteins: Agents of cancer development and therapeutic targets in anti-cancer therapy. *Cells* (2019) 9:E60. doi: 10.3390/cells9010060

98. Song H, Ma J, Bian Z, Chen S, Zhu J, Wang J, et al. Global profiling of O-GlcNAcylated and/or phosphorylated proteins in hepatoblastoma. *Sig Transduct Target Ther* (2019) 4:1–9. doi: 10.1038/s41392-019-0067-4

99. Shevtsov M, Multhoff G, Mikhaylova E, Shibata A, Guzhova I, Margulis B. Combination of anti-cancer drugs with molecular chaperone inhibitors. *Int J Mol Sci* (2019) 20:5284. doi: 10.3390/ijms20215284

100. Wells L, Vosseller K, Hart GW. Glycosylation of nucleocytoplasmic proteins: signal transduction and O-GlcNAc. *Science* (2001) 291:2376–8. doi: 10.1126/science.1058714

101. Guo K, Gan L, Zhang S, Cui FJ, Cun W, Li Y, et al. Translocation of HSP27 into liver cancer cell nucleus may be associated with phosphorylation and O-GlcNAc glycosylation. *Oncol Rep* (2012) 28:494–500. doi: 10.3892/or.2012.1844

102. Netsirisawan P, Chaiyawat P, Chokchaichamnankit D, Lirdprapamongkol K, Srisomsap C, Svasti J, et al. Decreasing O-GlcNAcylation affects the malignant transformation of MCF-7 cells *via* Hsp27 expression and its O-GlcNAc modification. *Oncol Rep* (2018) 40:2193–205. doi: 10.3892/or.2018.6617

103. Balana AT, Levine PM, Craven TW, Mukherjee S, Pedowitz NJ, Moon SP, et al. O-GlcNAc modification of small heat shock proteins enhances their anti-amyloid chaperone activity. *Nat Chem* (2021) 13:441–50. doi: 10.1038/s41557-021-00648-8

104. Kim MJ, Choi MY, Lee DH, Roh GS, Kim HJ, Kang SS, et al. O-Linked n-acetylglucosamine transferase enhances secretory clusterin expression *via* liver X receptors and sterol response element binding protein regulation in cervical cancer. *Oncotarget* (2018) 9:4625–36. doi: 10.18632/oncotarget.23588

105. Sage AT, Walter LA, Shi Y, Khan MI, Kaneto H, Capretta A, et al. Hexosamine biosynthesis pathway flux promotes endoplasmic reticulum stress, lipid accumulation, and inflammatory gene expression in hepatic cells. *Am J Physiology-Endocrinol Metab* (2010) 298:E499–511. doi: 10.1152/ajpendo.00507.2009

106. Chen W, Do KC, Saxton B, Leng S, Filipczak P, Tessema M, et al. Inhibition of the hexosamine biosynthesis pathway potentiates cisplatin cytotoxicity by decreasing BiP expression in non-small-cell lung cancer cells. *Mol Carcinog* (2019) 58:1046–55. doi: 10.1002/mc.22992

107. Han H, Li S, Zhong Y, Huang Y, Wang K, Jin Q, et al. Emerging pro-drug and nano-drug strategies for gemcitabine-based cancer therapy. *Asian J Pharm Sci* (2022) 17:35–52. doi: 10.1016/j.ajps.2021.06.001

108. Chen R, Lai LA, Sullivan Y, Wong M, Wang L, Riddell J, et al. Disrupting glutamine metabolic pathways to sensitize gemcitabine-resistant pancreatic cancer. *Sci Rep* (2017) 7:7950. doi: 10.1038/s41598-017-08436-6

109. Shukla SK, Purohit V, Mehla K, Gunda V, Chaika NV, Vernucci E, et al. MUC1 and HIF-1alpha signaling crosstalk induces anabolic glucose metabolism to impart gemcitabine resistance to pancreatic cancer. *Cancer Cell* (2017) 32:71–87.e7. doi: 10.1016/j.ccell.2017.06.004

110. Ricciardiello F, Gang Y, Palorini R, Li Q, Giampà M, Zhao F, et al. Hexosamine pathway inhibition overcomes pancreatic cancer resistance to gemcitabine through unfolded protein response and EGFR-akt pathway modulation. *Oncogene* (2020) 39:4103–17. doi: 10.1038/s41388-020-1260-1

111. Wang L, Chen S, Zhang J, Mao S, Mao W, Zhang W, et al. Suppressed OGT expression inhibits cell proliferation and modulates EGFR expression in renal cell carcinoma. *Cancer Manag Res* (2019) 11:2215–23. doi: 10.2147/CMAR.S190642

112. Sritharan S, Sivalingam N. A comprehensive review on time-tested anticancer drug doxorubicin. *Life Sci* (2021) 278:119527. doi: 10.1016/j.lfs.2021.119527

113. Lee SJ, Kwon O-S. O-GlcNAc transferase inhibitor synergistically enhances doxorubicin-induced apoptosis in HepG2 cells. *Cancers (Basel)* (2020) 12:E3154. doi: 10.3390/cancers12113154

114. Makwana V, Dukie AS-A, Rudrawar S. Investigating the impact of OGT inhibition on doxorubicin- and docetaxel-induced cytotoxicity in PC-3 and WPMY-1 cells. *Int J Toxicol* (2020) 39:586–93. doi: 10.1177/1091581820948433

115. Qin W, Lv P, Fan X, Quan B, Zhu Y, Qin K, et al. Quantitative time-resolved chemoproteomics reveals that stable O-GlcNAc regulates box C/D snoRNP biogenesis. *Proc Natl Acad Sci U.S.A.* (2017) 114:E6749–58. doi: 10.1073/pnas.1702688114

116. Wang H, Lin D, Yu Q, Li Z, Lenahan C, Dong Y, et al. A promising future of ferroptosis in tumor therapy. *Front Cell Dev Biol* (2021) 9:629150. doi: 10.3389/fcell.2021.629150

117. Wu J, Minikes AM, Gao M, Bian H, Li Y, Stockwell BR, et al. Intercellular interaction dictates cancer cell ferroptosis *via* NF2-YAP signalling. *Nature* (2019) 572:402–6. doi: 10.1038/s41586-019-1426-6

118. Zhang X, Yu K, Ma L, Qian Z, Tian X, Miao Y, et al. Endogenous glutamate determines ferroptosis sensitivity *via* ADCY10-dependent YAP suppression in lung adenocarcinoma. *Theranostics* (2021) 11:5650–74. doi: 10.7150/thno.55482

119. Peng C, Zhu Y, Zhang W, Liao Q, Chen Y, Zhao X, et al. Regulation of the hippo-YAP pathway by glucose sensor O-GlcNAcylation. *Mol Cell* (2017) 68:591–604.e5. doi: 10.1016/j.molcel.2017.10.010

120. Zhu G, Murshed A, Li H, Ma J, Zhen N, Ding M, et al. O-GlcNAcylation enhances sensitivity to RSL3-induced ferroptosis *via* the YAP/TFRC pathway in liver cancer. *Cell Death Discovery* (2021) 7:1–12. doi: 10.1038/s41420-021-00468-2

121. Chocarro de Erauso L, Zuazo M, Arasanz H, Bocanegra A, Hernandez C, Fernandez G, et al. Resistance to PD-L1/PD-1 blockade immunotherapy. a tumor-intrinsic or tumor-extrinsic phenomenon? *Front Pharmacol* (2020) 11:441. doi: 10.3389/fphar.2020.00441

122. Shang M, Yang H, Yang R, Chen T, Fu Y, Li Y, et al. The folate cycle enzyme MTHFD2 induces cancer immune evasion through PD-L1 up-regulation. *Nat Commun* (2021) 12:1940. doi: 10.1038/s41467-021-22173-5

123. Kamemura K, Hayes BK, Comer FI, Hart GW. Dynamic interplay between O-glycosylation and O-phosphorylation of nucleocytoplasmic proteins: alternative glycosylation/phosphorylation of THR-58, a known mutational hot spot of c-myc in lymphomas, is regulated by mitogens. *J Biol Chem* (2002) 277:19229–35. doi: 10.1074/jbc.M201729200

124. Huang R-X, Zhou P-K. And targets for radiotherapy sensitization in cancer. *Sig Transduct Target Ther* (2020) 5:1–27. doi: 10.1038/s41392-020-0150-x

125. Na H, Akan I, Abramowitz LK, Hanover JA. Nutrient-driven O-GlcNAcylation controls DNA damage repair signaling and Stem/Progenitor cell homeostasis. *Cell Rep* (2020) 31(6):107632. doi: 10.1016/j.celrep.2020.107632

126. Efimova EV, Appelbe OK, Ricco N, Lee SS-Y, Liu Y, Wolfgeher DJ, et al. O-GlcNAcylation enhances double-strand break repair, promotes cancer cell proliferation, and prevents therapy-induced senescence in irradiated tumors. *Mol Cancer Res* (2019) 17:1338–50. doi: 10.1158/1541-7786.MCR-18-1025

127. Zachara NE, Molina H, Wong KY, Pandey A, Hart GW. The dynamic stress-induced "O-GlcNAc-ome" highlights functions for O-GlcNAc in regulating DNA damage/repair and other cellular pathways. *Amino Acids* (2011) 40:793–808. doi: 10.1007/s00726-010-0695-z

128. Zhong J, Martinez M, Sengupta S, Lee A, Wu X, Chaerkady R, et al. Quantitative phosphoproteomics reveals crosstalk between phosphorylation and O-GlcNAc in the DNA damage response pathway. *Proteomics* (2015) 15:591–607. doi: 10.1002/pmic.201400339

129. Wang P, Peng C, Liu X, Liu H, Chen Y, Zheng L, et al. OGT mediated histone H2B S112 GlcNAcylation regulates DNA damage response. *J Genet Genomics* (2015) 42:467–75. doi: 10.1016/j.jgg.2015.07.002

130. Efimova EV, Takahashi S, Shamsi NA, Wu D, Labay E, Ulanovskaya OA, et al. Linking cancer metabolism to DNA repair and accelerated senescence. *Mol Cancer Res* (2016) 14:173–84. doi: 10.1158/1541-7786.MCR-15-0263

131. Campbell S, Ismail IH, Young LC, Poirier GG, Hendzel MJ. Polycomb repressive complex 2 contributes to DNA double-strand break repair. *Cell Cycle* (2013) 12:2675–83. doi: 10.4161/cc.25795

132. Lo P-W, Shie J-J, Chen C-H, Wu C-Y, Hsu T-L, Wong C-H. O-GlcNAcylation regulates the stability and enzymatic activity of the histone methyltransferase EZH2. *Proc Natl Acad Sci* (2018) 115:7302–7. doi: 10.1073/pnas.1801850115

133. Chu C-S, Lo P-W, Yeh Y-H, Hsu P-H, Peng S-H, Teng Y-C, et al. O-GlcNAcylation regulates EZH2 protein stability and function. *Proc Natl Acad Sci* (2014) 111:1355–60. doi: 10.1073/pnas.1323226111

134. Torres CR, Hart GW. Topography and polypeptide distribution of terminal n-acetylglucosamine residues on the surfaces of intact lymphocytes. *Evidence O-linked GlcNAc J Biol Chem* (1984) 259:3308–17.

135. Holt GD, Hart GW. The subcellular distribution of terminal n-acetylglucosamine moieties. localization of a novel protein-saccharide linkage, O-linked GlcNAc. *J Biol Chem* (1986) 261:8049–57.

136. Very N, Vercoutter-Edouart A-S, Lefebvre T, Hardivillé S, El Yazidi-Belkoura I. Cross-dysregulation of O-GlcNAcylation and PI3K/AKT/mTOR axis in human chronic diseases. *Front Endocrinol (Lausanne)* (2018) 9:602. doi: 10.3389/fendo.2018.00602

137. Nie H, Yi W. O-GlcNAcylation, a sweet link to the pathology of diseases. *J Zhejiang Univ Sci B* (2019) 20:437–48. doi: 10.1631/jzus.B1900150

138. Tuerhong A, Xu J, Shi S, Tan Z, Meng Q, Hua J, et al. Overcoming chemoresistance by targeting reprogrammed metabolism: the achilles' heel of pancreatic ductal adenocarcinoma. *Cell Mol Life Sci* (2021) 78:5505–26. doi: 10.1007/s00018-021-03866-y

139. Ricciardiello F, Votta G, Palorini R, Raccagni I, Brunelli L, Paiotta A, et al. Inhibition of the hexosamine biosynthetic pathway by targeting PGM3 causes breast cancer growth arrest and apoptosis. *Cell Death Dis* (2018) 9:1–17. doi: 10.1038/s41419-018-0405-4

140. Ortiz-Meoz RF, Jiang J, Lazarus MB, Orman M, Janetzko J, Fan C, et al. A small molecule that inhibits OGT activity in cells. *ACS Chem Biol* (2015) 10:1392–7. doi: 10.1021/acschembio.5b00004

141. Yuzwa SA, Macauley MS, Heinonen JE, Shan X, Dennis RJ, He Y, et al. A potent mechanism-inspired O-GlcNAcase inhibitor that blocks phosphorylation of tau. *vivo Nat Chem Biol* (2008) 4:483–90. doi: 10.1038/nchembio.96

142. Yuzwa SA, Shan X, Macauley MS, Clark T, Skorobogatko Y, Vosseller K, et al. Increasing O-GlcNAc slows neurodegeneration and stabilizes tau against aggregation. *Nat Chem Biol* (2012) 8:393–9. doi: 10.1038/nchembio.797

143. Selnick HG, Hess JF, Tang C, Liu K, Schachter JB, Ballard JE, et al. Discovery of MK-8719, a potent O-GlcNAcase inhibitor as a potential treatment for tauopathies. *J Med Chem* (2019) 62:10062–97. doi: 10.1021/acs.jmedchem.9b01090

144. Permanne B, Quattropani A, Hantson J, Neny M, Ousson S, Sand A, et al. O3-04-04: Pharmacological intervention with the novel o-glcnacase inhibitor ASN-561 reduces pathological tau in transgenic mice. *Alzheimer's Dementia* (2015) 11:P227–7. doi: 10.1016/j.jalz.2015.07.257

145. Love DC, Hanover JA The hexosamine signaling pathway: deciphering the "O-GlcNAc code." *Sci STKE* (2005) 2005:re13. doi: 10.1126/stke.3122005re13

146. Ge Y, Woo CM. Writing and erasing O-GlcNAc from target proteins in cells. *Biochem Soc Trans* (2021) 49:2891–901. doi: 10.1042/BST20210865

147. Zhu Y, Hart G. Targeting the O-GlcNAc transferase to specific proteins using RNA aptamers. *FASEB J* (2019) 33:799.5–5. doi: 10.1096/fasebj.2019.33.1_supplement.799.5

148. Ramirez DH, Ge Y, Woo CM. O-GlcNAc engineering on a target protein in cells with nanobody-OGT and nanobody-splitOGA. *Curr Protoc* (2021) 1:e117. doi: 10.1002/cpz1.117

149. Ramirez DH, Aonbangkhen C, Wu H-Y, Naftaly JA, Tang S, O'Meara TR, et al. Engineering a proximity-directed O-GlcNAc transferase for selective protein O-GlcNAcylation in cells. *ACS Chem Biol* (2020) 15:1059–66. doi: 10.1021/acschembio.0c00074

150. Ge Y, Ramirez DH, Yang B, D'Souza AK, Aonbangkhen C, Wong S, et al. Target protein deglycosylation in living cells by a nanobody-fused split O-GlcNAcase. *Nat Chem Biol* (2021) 17:593–600. doi: 10.1038/s41589-021-00757-y

Glossary

5-FU	5-fluorouracil
ATM	Ataxia Telangiectasia Mutated
Bid	BH3 interacting domain death agonist
BTZ	bortezomib
CHOP	C/EBP Homologous Protein
CRC	colorectal cancer
DDR	DNA damage response
DOX	doxorubicin
DSB	DNA double-strand break
ER	endoplasmic reticulum
ERRFI1	ERBB Receptor Feedback Inhibitor 1
ERa	Estrogen Receptor alpha
EZH2	Enhancer of Zeste 2
FDA	Food and Drug Administration
FOX	Forkhead box
GEM	gemcitabine
GFAT	Glutamine Fructose-6-phosphate Amidotransferase
GPX4	Glutathione Peroxidase 4
H2AX	H2A histone family member X
HBP	hexosamine biosynthetic pathway
HSP	Heat Shock Protein
IR	ionizing radiation
IRE1a	Inositol- Requiring Enzyme 1a
MCL	mantle cell lymphoma
NF-kB	Nuclear Factor-Kappa
NRF1	Nuclear Respiratory Factor 1
NRF2	Nuclear factor erythroid-2-Related Factor 2
OGA	O-GlcNAcase
O-GlcNAc	O-linked b-Nacetylglucosamine
OGT	O-GlcNAc Transferase
OS	osteosarcoma
PD-L1	Programmed Death-Ligand 1
PERK	Protein Kinase RNA-like kinase
PGM3	Phosphoacetylglucosamine Mutase 3
PKM2	Pyruvate Kinase M2
Pol	DNA Polymerase
PTM	post-translational modification
ROCK2	Rhoassociated Coiled-coil forming protein Kinase 2
ROS	reactive oxygen species
sCLU	secretory Clusterin
Ser	serine
Thr	threonine
TRAIL	TNF-elated Apoptosis Inducing Ligand
TRAIL-R	TRAIL Receptor
TS	Thymidylate Synthase
UDP-GlcNAc	uridine disphosphate Nacetylglucosamine
UPR	unfolded protein response
YAP	Yes-Associated Protein

frontiers | Frontiers in Pharmacology

TYPE Review
PUBLISHED 29 August 2022
DOI 10.3389/fphar.2022.910292

OPEN ACCESS

EDITED BY
Seung-Yeol Park,
Pohang University of Science and Technology, South Korea

REVIEWED BY
Amit Krishna De,
Indian Science Congress Association, India
Jinke Wang,
Southeast University, China

*CORRESPONDENCE
Li-Chen Gao,
89206346@qq.com

SPECIALTY SECTION
This article was submitted to Pharmacology of Anti-Cancer Drugs, a section of the journal Frontiers in Pharmacology

RECEIVED 01 April 2022
ACCEPTED 03 August 2022
PUBLISHED 29 August 2022

CITATION
Li F-J, Long H-Z, Zhou Z-W, Luo H-Y, Xu S-G and Gao L-C (2022), System X_c^-/GSH/GPX4 axis: An important antioxidant system for the ferroptosis in drug-resistant solid tumor therapy. *Front. Pharmacol.* 13:910292. doi: 10.3389/fphar.2022.910292

System X_c^-/GSH/GPX4 *axis*: An important antioxidant system for the ferroptosis in drug-resistant solid tumor therapy

Feng-Jiao Li[1,2], Hui-Zhi Long[1,2], Zi-Wei Zhou[1,2], Hong-Yu Luo[1,2], Shuo-Guo Xu[1,2] and Li-Chen Gao[1,2]*

[1]School of Pharmacy, University of South China, Phase I Clinical Trial Centre, The Affiliated Changsha Central Hospital, Hengyang Medical School, University of South China, Changsha, China, [2]Hunan Provincial Key Laboratory of Tumor Microenvironment Responsive Drug Research, Hengyang, China

The activation of ferroptosis is a new effective way to treat drug-resistant solid tumors. Ferroptosis is an iron-mediated form of cell death caused by the accumulation of lipid peroxides. The intracellular imbalance between oxidant and antioxidant due to the abnormal expression of multiple redox active enzymes will promote the produce of reactive oxygen species (ROS). So far, a few pathways and regulators have been discovered to regulate ferroptosis. In particular, the cystine/glutamate antiporter (System X_c^-), glutathione peroxidase 4 (GPX4) and glutathione (GSH) (System X_c^-/GSH/GPX4 axis) plays a key role in preventing lipid peroxidation-mediated ferroptosis, because of which could be inhibited by blocking System X_c^-/GSH/GPX4 axis. This review aims to present the current understanding of the mechanism of ferroptosis based on the System X_c^-/GSH/GPX4 axis in the treatment of drug-resistant solid tumors.

KEYWORDS

system Xc -/GSH/GPX4 axis, ferroptosis, drug resistance, solid tumor, therapy

Introduction

Ferroptosis, as a regulatory cell death (RCD), has been a research hotspot in the past decade (Galluzzi et al., 2018). The concept of ferroptosis was first proposed by Dr. Brent R Stockwell's group in 2012, who discovered this new cell death pattern that differs from apoptosis, necrosis and autophagy (Dixon et al., 2012). Ferroptosis is thought to be driven by the imbalance between oxidative stress and antioxidant systems (Kuang et al., 2020). Furthermore, ferroptosis can be activated through extracellular (e.g., by inhibiting System X_c^-), and intracellular (e.g., by inhibiting GPX4) pathways (Tang D. et al., 2021). The lipid peroxidation is a free radical-driven reaction that primarily affects polyunsaturated fatty acids (PUFAs) in cell membranes, the product of which gradually increases during the ferroptotic cell death, from the initial lipid hydroperoxides (LOOHs) to the later production of malondialdehyde (MDA) and 4-hydroxynenoal (Kagan et al., 2017). Therefore, ferroptosis leads to the cell membrane rupture and finally death mainly by iron overload and disorders of the antioxidant system. Ferrous ion has the effect of

mediating ROS production and enzyme activity during lipid peroxidation, which can produce a large number of ROS through the Fenton reaction (Dixon et al., 2012), and it also increase the activity of lipoxygenase (LOX) or EGLN prolyl hydroxylases, which are responsible for lipid peroxidation and oxygen homeostasis (Chen P. et al., 2020), so excessive accumulation of iron can result in oxidative damage to cells.

The System X_c^-/GSH/GPX4 axis is an important antioxidant system ferroptosis. Most ferroptosis inducers such as Erastin and RSL3, are inhibitors of System X_c^-/GSH/GPX4 axis, which provide a good basis for us to understand the role of different antioxidants in inhibiting ferroptosis (Kuang et al., 2020).

Since tumor cells with certain oncogenic mutations are very sensitive to ferroptosis, triggering ferroptosis may also have significant therapeutic potential for ferroptosis-sensitive tumor cells (Chen P.-H. et al., 2020). Considering the role of ferroptosis in RCD, ferroptosis might play an important role in tumorigenesis and tumor development. Moreover, drug-resistant tumor cells are more sensitive to lipid peroxidation, and inhibitors of the System X_c^-/GSH/GPX4 axis have been shown to be fatal in host cells. Zhang et al. found that inhibiting the GPX4 with RAS-selective lethal small molecule 3 (RSL3) enhances the antitumor effect of cisplatin (Zhang et al., 2020). Other studies have shown that GPX4 inactivation may increase susceptibility to ferroptosis in renal clear cell carcinoma by increasing lipid peroxidation (Zou et al., 2019). More recently, Ubelacker et al. found that GPX4 inhibitors make melanoma difficult to spread through blood vessels (Ubellacker et al., 2020). Therefore, induction of ferroptosis has emerged as a therapeutic strategy to trigger cancer cell death for drug-resistant solid tumors. Considering these advantages, ferroptosis is expected to become a promising therapeutic strategy for drug-resistant tumors in the near future, either alone or in combination. In this review, we summarize the regulation of the System X_c^-/GSH/GPX4 axis, a major antioxidant system in ferroptosis, and its potential role in drug-resistant solid tumors therapy, and also conclude with a summary of drugs, compounds and nanoparticles targeting this axis that have been studied in recent years.

The antioxidation of system X_c^-/GSH/GPX4 *axis* in ferroptosis

System X_c^-: The pivotal upstream node of system Xc^-/GSH/GPX4 *axis*

By far, System X_c^- is studied widely (Lewerenz et al., 2013). It is a chloride-dependent and sodium-independent antiporter of Cys and Glu, consisting of catalytic subunit xCT/Solute Carrier Family 7 Member 11 (SLC7A11) and regulatory subunit 4F2 (4F2hc)/Solute Carrier Family 3 Member 2 (SLC3A2) connected by disulfide bonds (Gochenauer and Robinson, 2001; Patel et al., 2004). Activation of SLC7A11 expression enables cells to restore redox homeostasis and maintain survival under stressful conditions such as oxidative stress, amino acid starvation, metabolic stress, and genotoxic stress (Koppula et al., 2018). System X_c^- is driven by concentrations gradient from extracellular Cys and intracellular Glu, transporting Cys and Glu in a 1:1 ratio (Figure 1). Cys absorbed by System X_c^- is reduced to cysteine by G-SH or thioredoxin reductase 1 (TrxR1), which then is used for GSH biosynthesis (Mandal et al., 2010; Conrad and Sato, 2012). Since cysteine is a speed-limiting substrate for GSH biosynthesis, and GSH is the main antioxidant in mammalian cells, hindering intracellular cysteine and GSH levels can directly affect the activity of GPX4, which can easily induce ferroptosis. There are many compounds that interfere with System X_c^-, such as Erastin and its analogues, that can lead to cysteine deprivation, glutathione depletion, endoplasmic reticulum stress, and cell death (Dixon et al., 2014; Sato et al., 2018). System X_c^- is therefore a pivotal regulatory channel of System X_c^-/GSH/GPX4 axis. Although intracellular Cys is not only provided by System X_c^-, but also by transsulfuration pathway (Hayano et al., 2016) and the neutral amino acid transporter (Conrad and Sato, 2012). If System X_c^- is dysfunctional, it will still lead to intracellular Cys deficiency, and GSH depletion, making the cell highly sensitive to ferroptosis. As an important target for inducing ferroptosis, System X_c^- can provide a new direction for the treatment of drug-resistant solid tumors.

GSH: The main cofactor of system X_c^-/GSH/GPX4 *axis*

GSH is a core antioxidant that is formed by condensation of Glu, Cys, and Gly. GSH, as the main cofactor of GPX4, plays the role of an electron donor or receptor by conversion between G-SH and GS-SG, making it important to fight oxidative stress (Deponte, 2013). The direct effect of GSH on ferroptosis is demonstrated by the use of Erastin, which activates a morphologically identical form of cell death caused by the lack of GPX4 in sensitive cells by lowering GSH levels (Dixon et al., 2012). Inhibiting the synthesis and utilization of GSH is a classic method to induce ferroptosis (Yang et al., 2014). What's more, the role of GSH in ferroptosis depends mainly on GPX4. GPX4 can catalyze the reduction of phospholipid hydroperoxide (PLOOH) to the corresponding hydroxyl derivatives (Imai and Nakagawa, 2003). In the catalytic cycle of GPX4, the -SeH (the main active group of GPX4) is oxidized by the PLOOH to selenic acid (-SeOH), while G-SH can reduce -SeOH and further activates GPX4, releasing GS-SG to prevent GPX4 from being inactivated (Ingold et al., 2018). The GSH depletion induce many cancer cells to ferroptosis, such as pancreatic tumor (Badgley et al., 2020), liver cancer (Chen et al., 2019; Yang Y. et al., 2020), prostate cancer (Qin et al., 2021), breast cancer (Yang J. et al.,

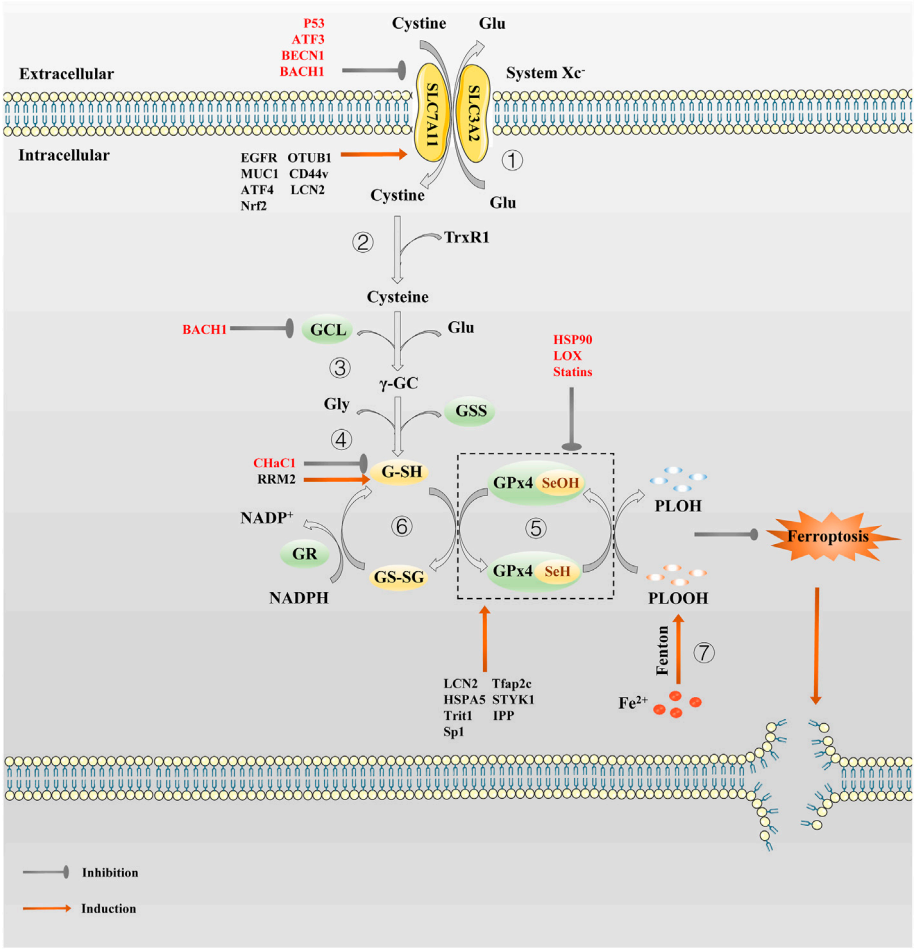

FIGURE 1
The regulation pathway of System Xc^-/GSH/GPx4 in ferroptosis. ① System Xc^- transport cystine into the cell and reverse Glu out of the cell in a 1:1 ratio. ② Cystine absorbed by System Xc^- is reduced to cysteine by G-SH or TrxR1. ③ Then GCL links cysteine and glutamate to produce γ-GC. ④ γ-GC and Gly are catalyzed by GSS to produce G-SH. ⑤In the catalytic cycle of GPx4, the GPx4-SeH is oxidized by the P-LOOH to GPx4-SeOH, while G-SH can reduce -SeOH and further activates GPx4, releasing GS-SG to prevent GPx4 from being inactivated. ⑥GS-SG is reduced to G-SH under the action of GR and Coenzyme NADPH. Since P-LOOH is reduced to PLOH by GPx4-SeH, ferroptosis is inhibited. ⑦Fe^{2+} can produce a large number of PLOOH through the Fenton reaction.

2021) etc. It is also possible to produce an effect similar to GPX4 inactivation by inhibiting the GSH synthesis or antagonizing GSH.

GPX4: The core downstream antioxidant of system X_c^-/GSH/GPX4 *axis*

As the cornerstone of antioxidant defense, GPX4, a phospholipid peroxidation inhibitor, is the only glutathione peroxidase used for intracellular lipid peroxide reduction (Ursini et al., 1982). In the presence of GSH, GPX4 continuously reduce PLOOHs, and if GSH depletion or GPX4 inactivation, intracellular ferrous ions induce ferroptosis by breaking down PLOOHs to cause lipid peroxidation (Ursini and Maiorino, 2020). In early studies, selective knockout of the GPX4 gene in hippocampal neurons promotes neurodegeneration and cell death in a non-apoptotic manner, which provide preliminary evidence for GPX4 as a particular regulator of ferroptosis (Seiler et al., 2008). Subsequently, Stockwell's team demonstrated that GPX4 is a key upstream regulator of ferroptosis in 2014 (Friedmann Angeli et al., 2014; Yang et al., 2014). Well-balanced GSH levels and GPX4 function are significant for maintaining intracellular redox homeostasis. Whether knocking out the GPX4 gene or inhibiting its activity, it can eventually lead to a redox homeostasis imbalance that can have a fatal effect on normal or tumor cells. Photosensitive cells (Ueta et al., 2012), renal tubular cells (Friedmann Angeli et al.,

2014), $CD8^+$ T cells (Matsushita et al., 2015), vascular endothelial cells (Wortmann et al., 2013), hepatocytes (Carlson et al., 2016), sperm cells (Imai et al., 2009), etc. will be highly sensitive to ferroptosis in result of GPX4 inactivation. In addition, inhibiting GPX4 also promote ferroptosis in some malignant tumor cells such as pancreatic ductal adenocarcinoma (Dai et al., 2020) and colorectal cancer cells (Sui et al., 2018), etc. However, as early as the 1996 study by Imai et al. revealed that GPX4 overexpression prevents basophilic leukemia cells in mice from death caused by oxidative damage (Imai et al., 1996), thus, theoretically, GPX4 overexpression could make cells resistant to oxidative stress-induced ferroptosis. Hence, taking GPX4 as a target is of great help for the treatment of drug-resistant tumors.

The regulation of system X_c^-/GSH/GPX4 *axis* in ferroptosis

As the main antioxidant system against ferroptosis, the role of System X_c^-/GSH/GPX4 axis is crucial in the treatment of various types of drug-resistant solid tumors, so an in-depth understanding of the regulatory mechanism of each node on this axis is of great significance for developing effective strategies for System X_c^-/GSH/GPX4 axis targeted treatment of drug-resistant solid tumors (Figure 1).

The regulation of system X_c^- in ferroptosis

As mentioned before, the activity of System X_c^- is mainly determined by SCL7A11 (Sato et al., 1999). The low expression of SCL7A11 reduces System X_c^- activity, resulting in oxidative stress-mediated ferroptosis; conversely, the overexpression of SCL7A11 enhance cell resistance to ferroptosis, which is also one of the reasons for drug resistance in tumor cells (Huang et al., 2005; Dai et al., 2007; Lin et al., 2020). Therefore, the regulation of SCL7A11 is of great importance in ferroptosis resistance. To ensure the proper function of SLC7A11 in maintaining redox homeostasis, the expression and activity of SLC7A11 is strictly regulated by a variety of mechanisms, including transcriptional and epigenetic regulator-mediated transcriptional regulation, as well as post-transcriptional regulatory mechanisms.

Activating transcription factor 4 (ATF4) and nuclear factor erythroid 2-related factor 2 (Nrf2) are the two main transcription factors that mediate stress-induced SLC7A11 transcription. Under various stress conditions, such as amino acid starvation, endoplasmic reticulum stress, hypoxia and virus infection, ATF4 (a member of the ATF/CREB transcription factor family) is mainly induced by mRNA translation (Pakos-Zebrucka et al., 2016). Under the stress of amino acid deprivation, the expression of SLC7A11 is largely mediated by ATF4 (Sato et al., 2004). The translation of ATF4 mRNA increases through the general control non-derepressible-2 (GCN2)-eukaryotic initiation factor 2α (eIF2α) signal axis. Subsequently, ATF4 binds to the amino acid response element (AARE) of gene promoter to further promote the transcription of genes involved in amino acid metabolism and stress response, such as SLC7A11, so that cells can cope with amino acid constraints (Kilberg et al., 2009). SLC7A11 protects cells from ferroptosis caused by cystine starvation (Stockwell and Jiang, 2020). A study has shown that ATF4 can stimulate the transcription of SCLS7A11 and promote tumor angiogenesis (Chen et al., 2017a).Another transcription factor, Nrf2, which promotes SLC7A11 transcription, is a key regulator of antioxidant response. Under non-stress conditions, Nrf2 maintained at a low level via the proteasome degradation mediated by Kelch-like ECH-associated protein 1 (Keap1); instead, Nrf2 dimerizes with members of the small Maf family and binds to the antioxidant response elements (AREs) located in the regulatory region of the cell defense enzyme gene, relieving the inhibition of Keap1 and activating the transcription of cellular protective genes such as SLC7A11 to play an antioxidant role (Ma, 2013). Subsequent studies have proved that activation of Nrf2 and inhibition of Keap1 lead to SLC7A11 upregulation, thereby promoting resistance to ferroptosis (Chen et al., 2017b; Fan et al., 2017).The expression of SLC7A11 can also be inhibited by transcription factors such as Tumor protein p53 (p53) and Activating transcription factor 3 (ATF3). SLC7A11 is a transcription inhibition target of p53 (Jiang et al., 2015; Jennis et al., 2016). Under different ferroptosis induction conditions, p53 promotes ferroptosis partly by inhibiting SLC7A11 expression, while p53 deficiency promotes ferroptosis resistance by SLC7A11 upregulation. ATF3 inhibits SLC7A11 by binding to the SLC7A11 promoter in a p53-independent manner, and promotes Erastin-induced ferroptosis by SLC7A11 downregulation (Wang L. et al., 2020).

Epigenetic regulation of transcription is crucial to control intracellular homeostasis and development. Recent studies have revealed the key role of epigenetic regulation of SLC7A11 transcription in the control of ferroptosis. It was recently pointed out that the anti-oncogene BRCA1-Associated Protein 1 (BAP1) deubiquitinates the H2Aub portion of the SLC7A11 gene promoter and represses SLC7A11 expression, thereby limiting Cys uptake and increasing ferroptosis sensitivity; on the contrary, the lack of BAP1 in cancer cells leads to SLC7A11 upregulation and ferroptosis resistance (Zhang et al., 2018). In addition, p53 promotes nuclear translocation of Ubiquitin Specific peptidase 7 (USP7), and USP7 removes ubiquitin from H2Bub, resulting in a decrease in H2Bub occupation on the SLC7A11 promoter, resulting in SLC7A11 transcriptional inhibition (Wang Y. et al., 2019). Moreover, a histone H3 lysine 9 (H3K9) demethylase KDM3B has been reported to be involved in transcriptional regulation of SLC7A11 (Wang Y. et al., 2020). Overexpression of KDM3B decreased

H3K9 methylation (related to transcriptional inhibition) and upregulated the expression of SLC7A11, thus enhancing resistance to Erastin-induced ferroptosis. Bromodomain-containing protein 4 (BRD4) function as genetic readers of histone acetyl lysine residues to regulate gene transcription. BRD4 inhibitor JQ1 can induce ferroptosis both *in vitro* and in Xenograft model; JQ1 therapy or BRD4 gene knockout can down-regulate ferroptosis regulators including SLC7A11 (Sui et al., 2019). Another key epigenetic mechanism that controls gene transcription involves chromatin remodeling mediated by the SWI/SNF complex, which has been revealed to be related to SLC7A11 transcriptional regulation (Ogiwara et al., 2019). Mechanically, ARID1A is a component of the SWI/SNF complex, which binds to the SLC7A11 promoter and promotes NRF2-mediated SLC7A11 transcriptional activation.

SLC7A11 can be regulated by different post-translation mechanisms. Previous studies have shown that Epidermal Growth Factor Receptor (EGFR), CD44v (an adhesion molecule expressed in cancer stem-like cells) and OTU deubiquitinase, ubiquitin aldehyde-binding 1 (OTUB1), control and stabilize SCL7A11 expression, facilitating Cys uptake by tumor cells (Ishimoto et al., 2011; Tsuchihashi et al., 2016; Liu et al., 2019). Among them, CD44v hastens the interaction of OTUB1-SCL7A11, while inhibition of OTUB1 accelerates the degradation of SLC7A11 (Liu et al., 2019). In addition, transmembrane mucin glycoprotein Mucin 1 (MUC1) binds directly to CD44v, enhancing the stability of SCL7A11 and thus controlling GSH levels (Hasegawa et al., 2016). SLC7A11 can also be inactivated by AMPK-mediated phosphorylation of BECN1, which leads to the formation of BECN1-SLC7A11 complex (Kang et al., 2018; Song et al., 2018). Mechanistic investigation identified SLC7A11 was a direct target of METTL14. Both *in vitro* and *in vivo* assay demonstrated that METTL14 induced N6 -methyladenosine (m^6A) modification at 5′UTR of SLC7A11 mRNA, which promotes SLC7A11 mRNA stability and upregulates its expression by inhibiting the deadenylation process, enhancing ferroptosis resistance (Fan et al., 2021; Liu L. et al., 2022; Hill and Liu, 2022; Peng and Mo, 2022). Additionally, some small molecular inhibitors such as Erastin (Dixon et al., 2014). Piperazine Erastin (PE) and imidazole ketone Erastin (IKE) (Yang et al., 2014; Larraufie et al., 2015), also have good capacity to inactive SLC7A11. In general, interfering with SCL7A11 expression modulates System X_c^- activity during ferroptosis, thereby regulating cancer cell replication, tissue invasion, and metastasis.

The regulation of GSH in ferroptosis

GSH is a key antioxidant against ferroptosis. The synthesis and degradation of GSH play an important part in GSH abundance. Under physiological conditions, GSH synthesis relies on two key enzyme (glutamate cysteine ligase (GCL) and glutathione synthetase (GSS)) and the availability of cysteine (Lu, 2009, 2013). GCL consists of Glutamate-Cysteine ligase Catalytic Subunit (GCLC) and Modifier Subunit (GCLM). Genetic inhibition of GCLC enhances ferroptosis due to metabolic stress, including cystine starvation (Gao et al., 2015).GCL links cysteine and Glu to produce γ-glutamylcysteine (γ-GC) which is catalyzed to G-SH by GSS. Thus, those that inhibit System X_c^- activity are able to inhibit GSH biosynthesis through Cys depletion. Depletion of amino acids other than Cys also lead to GSH depletion (Tan et al., 1998; Sato et al., 2004). Mammals usually rely solely on extracellular uptake as the primary source of Cys, but some mammals also use cystathionine γ-lyase (CGL)-mediated cystathionine-cleavage in the transsulfuration pathway as a surrogate Cys source if System X_c^- is blocked (Shimada and Stockwell, 2016). As an important transcription factor, Nrf2 can not only regulate SLC7A11 transcription, but also up-regulate the expression of GSS and GCLC, which are key rate-limiting enzymes for GSH synthesis (Dodson et al., 2019). Additionally, Nrf2 promotes GSH efflux, which is an unexpected regulator of ferroptosis sensitivity, while Nrf2 inhibition can act synergistically with ferroptosis inducers (Sun et al., 2016a; Sun et al., 2016b; Cao et al., 2019). In addition to inhibiting cellular Cys uptake, ferroptosis can also be achieved by consuming Cys in extracellular. One study demonstrated that an engineered and pharmacologically optimized human cyst(e)inase enzyme that consistently depletes extracellular Cys pools (Cramer et al., 2017). Genome-wide siRNA screening reveals that knockdown of cysteinyl-tRNA synthetase gene activates transulfuration pathway and inhibits ferroptosis induced by System X_c^- inhibitors (e.g. Erastin) (Hayano et al., 2016).

Irreversible inhibitors of GCL, buthionine sulfoxide (BSO) and Cysteine sulfonimide, reduce GSH formation and further inhibit GPX4 activity, promoting ferroptosis alone or enhancing sensitivity to ferroptosis (Yang et al., 2014). Ribonucleotide reductase regulatory subunit M2 (RRM2, a structural unit essential for DNA replication and repair) maintains intracellular GSH by protecting GLC from degradation to exert an anti-ferroptosis effect (Yang Y. et al., 2020). Moreover, ChaC Glutathione Specific Gamma-Glutamylcyclotransferase 1 (CHaC1) also regulates GSH degradation and has been detected to be downregulated in some tumor cells (Hong et al., 2021; Xiao et al., 2022). CHaC1 upregulation promotes GSH degradation and leads to GSH depletion (Chen M.-S. et al., 2017). A recent study indicated that BTB and CNC homology 1 (BACH1, a heme-binding transcription factor required for the regulation of oxidative stress and metabolic pathways associated with heme and iron), suppresses GSH synthesis pathway-related genes such as GCLM and GCLC to reduce GSH and regulate ferroptosis (Igarashi and Watanabe-Matsui, 2014; Nishizawa et al., 2020).

The regulation of GPX4 in ferroptosis

GPX4 is an important arsenic protein in mammals that directly reduces PLOOHs during ferroptosis, and its redox activity depends on the 21st amino acid selenocysteine (Sec) (Ingold et al., 2018). As a key downstream antioxidant enzyme of System X_c^-/GSH/GPX4 axis, GPX4 is often used to develop ferroptosis inducers as an effective target. The activity of GPX4 is regulated by the selenium potency, which is thought to be a constraint on susceptibility to ferroptosis (Hatfield et al., 1991; Cardoso et al., 2017). The mevalonate pathway provides selenium for GPX4 maturation, but statins can block this pathway (Chen and Galluzzi, 2018). Except for selenium, isopentenyl pyrophosphate (IPP) produced by the mevalonate pathway also facilitates GPX4 synthesis (Shimada et al., 2016; Ingold et al., 2018). Additionally, GSH is a main cofactor of GPX4, so GSH regulation can also indirectly modulate GPX4 (Maiorino et al., 2018).

Regulation of GPX4 expression includes multiple mechanisms, such as gene transcription and post-translational modification, which significantly affect the level of lipid peroxidation in tissue damage. The upstream regulation of GPX4 mainly include transcription factors such as Nrf2 (Dodson et al., 2019), MYB (Hao et al., 2017), Tfap2c (Alim et al., 2019), Sp1 (Alim et al., 2019), Lipocalin 2 (LCN2) (Chaudhary et al., 2021), mTORC1 (Saxton and Sabatini, 2017; Zhang Y. et al., 2021), and NUAK2 (Singh et al., 2022). GPX4 is target gene of Nrf2. Nrf2 inhibition reverses resistance to GPX4 inhibitor-induced ferroptosis in head and neck cancer (Shin et al., 2018). Selenium-induced transcription factors Tfap2c and Sp1 upregulate GPX4 to prevent ferroptosis-associated cerebral hemorrhage. While mTORC1 is a key signaling node that integrates multiple environmental signals to modulate protein (e.g., GPX4) synthesis, and its inactivation reduces GPX4 and sensitizes tumor cells to ferroptosis. In contrast, LCN2, a key protein regulating iron homeostasis, inhibit ferroptosis by stimulating GPX4 and SCL7A11 expression. Furthermore, knockdown of tRNA isopentenyltransferase 1 (Trit1, an essential selenoprotein synthesis enzyme) reduces selenoproteins expression (Fradejas et al., 2013). Post-translational modification affects the stability of GPX4 proteins by modulating the degradation of GPX4. The post-translational modifications of GPX4 mainly include succination, ubiquitination and alkylation. Succination is a non-enzymatic, irreversible protein modification mediated by fumaric acid (an intermediate product of Krebs cycle in mitochondria) (Alderson et al., 2006). Fumaric acid binds to the thiol group of cysteine residues in the absence of enzymes to form thioether bonds. It has been found that intracellular fumaric acid aggregation causes succination of GPX4 at cysteine 93, resulting in a decrease in GPX4 activity and sensitizing cancer cells to ferroptosis inducers (Kerins et al., 2018). Ubiquitination is the process by which ubiquitin is added to the lysine residue of the substrate protein by enzymes E1, E2, and E3, which eventually leads to the degradation of the protein by the proteasome. And deubiquitinase (DUB) stabilizes intracellular protein structure by removing ubiquitin chains from ubiquitinated proteins. A recent study by Liu's team demonstrated that the broad-spectrum DUB inhibitor palladium pyrithione complex (PdPT) promote GPX4 degradation, but proteasome inhibitor bortezomib reverses its effect (Yang L. et al., 2020). Another study showed that a bartoldine derivative, DMMOCPTL, binds directly to selenosecysteine 46 of GPX4, resulting in ubiquitination of GPX4 in triple-negative breast cancer cells (Ding et al., 2021). Alkylation is the chemical process of introducing one or more alkyl groups into a protein or compound. Small molecule inhibitors such as RSL3 and ML162 mediate alkylation on GPX4 by binding to the selenium cysteine 46 residue by electrophilic alkyl chloride moieties (Eaton et al., 2020; Vučković et al., 2020). Heat shock protein A family member 5 (HSPA5, a molecular chaperone in the endoplasmic reticulum) binds directly to GPX4 to prevent its degradation (Zhu S. et al., 2017). They also found that LOX catalyzes the covalent inhibition of selenocysteine in GPX4 (Yang et al., 2016).

What's more, There are also some other small molecule regulators that interfere GPX4 such as FIN56 (Shimada et al., 2016), FINO2 (Gaschler et al., 2018), ML210 (Eaton et al., 2020), JKE-1674 (Eaton et al., 2020), JKE-1716 (Eaton et al., 2020), NSC144988 (Stockwell and Jiang, 2020) and PKUMDL-LC-101 series (see in (Li et al., 2019)).

Potential roles of targeting system X_c^-/GSH/GPX4 *axis* in drug-resistant solid tumor

Chemotherapy are by far one of the most commonly used methods to treat malignant tumors, but the continuous overdose of chemotherapeutic drugs has led to varying degrees of resistance and increased aggressiveness of some tumors. Ferroptosis is a RCD caused by intracellular iron accumulation combined with disruption of antioxidant systems, such as GPX4 inactivation and GSH depletion, and subsequent accumulation of toxic lipid peroxides (Dixon et al., 2012; Yang et al., 2014). Importantly, drug-resistant tumor are more sensitive to lipid peroxidation, which undoubtedly makes, the combination of System X_c^-/GSH/GPX4 axis-based ferroptosis inducers with chemotherapeutic agents may become a new strategy for the treatment of drug-resistant solid tumors (Viswanathan et al., 2017). There is also growing evidence that disruption of antioxidant systems in ferroptosis contributes to the anticancer treatment of several forms of drug-resistant solid tumors (Figure 2).

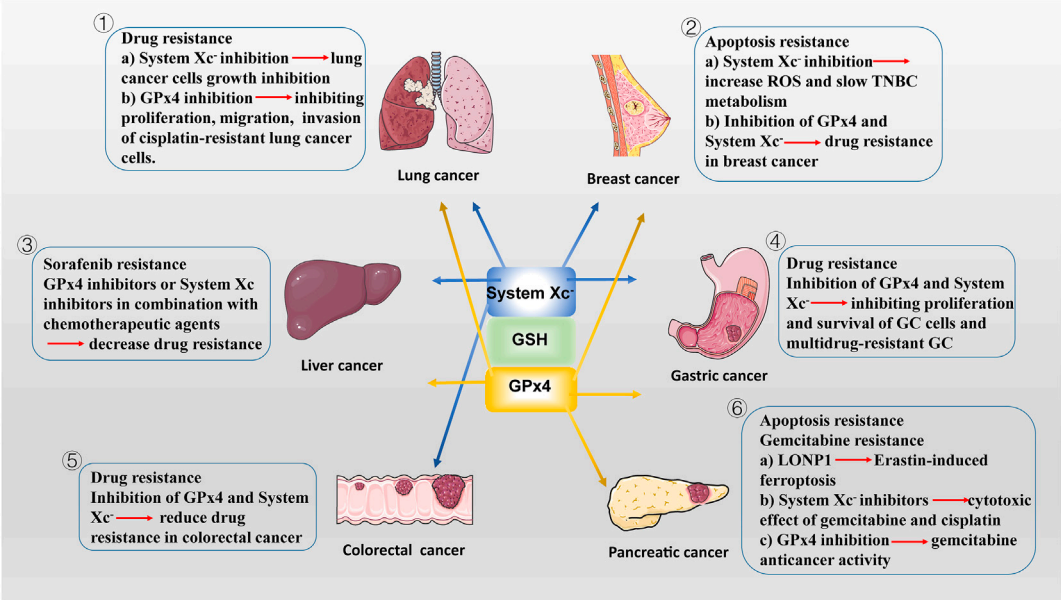

FIGURE 2
The potencial roles of System Xc-/GSH/GPx4 in drug-resistant solid tumor. ① SLC7A11, highly expressed in NSCLC, is a potential target for ferroptosis. SLC7A11 downregulation lead to ferroptosis of lung cancer cells and inhibit their growth. In addition to SLC7A11, lung cancer cell also exhibits high GPx4 expression. GPX4 inhibitor limits proliferation, migration, and invasion of cisplatin-resistant lung cancer cells. ② Drug-resistant breast cancer cells are dependent on GPX4 and SLC7A11. SLC7A11 is upregulated in one-third of TNBC cells *in vivo*, and inhibiting System Xc- activity increases intracellular ROS levels and slows TNBC metabolism. Inhibition of GPX4 and/or System Xc-may be a potential measure to overcome drug resistance in breast cancer. ③ The main regulatory mediators mediating the ferroptotic response in HCC cells have been identified as System Xc-and GPX4. blocking System Xc -/GSH/GPX4 axis in combination with chemotherapeutic agents (e.g., sorafenib) provides new ideas for treatment of drug-resistant HCC. ④ GPx4 is lowly expressed in GC cells, making them more susceptible to ferroptosis than normal intestinal cells. Reducing the expression of GPX4 and System Xc-inhibiting the proliferation of GC cells and multidrug-resistant GC. ⑤ In CSCs, SLC7A11 is extremely expressed, with high GSH levels and low ROS levels, leading to their extreme vulnerability to ferroptosis. Similar to GC cells, targeting the System Xc-/GSH/GPX4 axis is an effective way to inhibit the growth of drug-resistant colorectal cancer. ⑥ LONP1 inhibits Nrf2-mediated GPX4 gene expression, thereby promoting Erastin-induced ferroptosis in human PDAC cells. The use of System Xc-inhibitors enhanced the cytotoxic effect of gemcitabine and cisplatin on PDAC cell lines. Gemcitabine resistance was associated with GPx4 upregulation in PDAC cells. Inhibition of GPX4 activity or induction of GPX4 degradation can restore or enhance the anticancer activity of gemcitabine *in vitro* or in xenogeneic PDAC models.

Lung cancer

SLC7A11, highly expressed in NSCLC, is a potential target for ferroptosis (Baek et al., 2012). SLC7A11 overexpression promote lung cancer cell metastasis and proliferation *in vivo* and *in vitro* by mediating cellular uptake of cysteine and reducing ROS production; conversely, SLC7A11 downregulation lead to ferroptosis (Liu et al., 2020; Chen M. et al., 2021).Meanwhile, lung cancer cell also developed ferroptosis resistance by some mechanisms to enhance the expression of SLC7A11. It has been reported that the RNA-binding protein RBMS1 bridges the 3′ and 5′-UTR of SLC7A11 to enhance its expression by interacting directly with the translation initiation factor eIF3d. And RBMS1 ablation inhibits the translation of SLC7A11, reduces SLC7A11-mediated cystine uptake, and promotes ferroptosis (Zhang W. et al., 2021). In addition, a new miRNA, miR-27a-3p, regulates ferroptosis by directly targeting SLC7A11 in NSCLC cells. miR-27a-3p overexpression leads to SLC7A11 inhibition by direct binding to its 3′-UTR, followed by a reduction of erastin-induced ferroptosis. In contrast, miR-27a-3p inhibiton increases sensitivity of NSCLC cells to erastin (Lu et al., 2021). Moreover, SLC7A11 is also upregulated in lung cancer stem cell-like cells and activated by the cell transcription factor SOX2 (Wang X. et al., 2021). Tumors with higher SOX2 expression are more resistant to ferroptosis, and the expression of SLC7A11 is positively correlated with SOX2 in mouse and human lung cancer tissues (Wang X. et al., 2021).

In addition, Kirsten Rat Sarcoma (KRAS)-mutant lung cancer tumor progression is closely associated with SLC7A11 expression. In several preclinical lung cancer mouse models, treatment of KRAS-mutant lung adenocarcinoma (LUAD) with HG106 (a potent System X_c^- inhibitor), significantly inhibited tumor growth and prolonged survival

TABLE 1 The regulatory small molecule compounds of targeting System X_c^-/GSH/GPX4 axis in ferroptosis.

Target	Compounds	Mechanism	Induce/Inhibit Ferroptosis	References
SLC7A11	Erastin	↓SLC7A11, ↓GSH	Induce	Dixon et al. (2014)
	PE	↓SLC7A11, ↓GSH	Induce	Yang et al. (2014)
	IKE	↓SLC7A11, ↓GSH	Induce	Larraufie et al. (2015)
	HG106	↓SLC7A11, ↓GSH, ↓ΔΨm	Induce	Hu et al. (2020)
GSH	BSO	↓GCL, ↓GSH, ↓GPX4	Induce	Yang et al. (2014)
	Cyst(e)inase	↓extracellular cystine	Induce	Cramer et al. (2017)
GPX4	PdPT	↑GPX4 degradation	Induce	Li Yang et al. (2020)
	FIN56	↑GPX4 degradation	Induce	Shimada et al. (2016)
	Rapamycin	↑GPX4 degradation	Induce	Yang Liu et al. (2021b)
	FINO2	↓GPX4	Induce	Gaschler et al. (2018)
	RSL3	↓GPX4	Induce	Vučković et al. (2020)
	ML210	↓GPX4	Induce	Eaton et al. (2020)
	ML162	↓GPX4	Induce	Shin et al. (2018)
	JKE-1674	↓GPX4	Induce	Eaton et al. (2020)
	JKE-1716	↓GPX4	Induce	Eaton et al. (2020)
	NSC144988	↓GPX4	Induce	Stockwell and Jiang, (2020)
	PKUMDL-LC-101 series	↑GPX4	Inhibit	Li et al. (2019)

Abbreviation. SLC7A11, Solute Carrier Family 7 Member 11; GSH, glutathione; GPX4, glutathione peroxidase 4; PE, piperazine erastin; IKE, imidazole ketone Erastin; ΔΨm, mitochondrial membrane potential; GCL, glutamate cysteine ligase; BSO, buthionine sulfoxide; PdPT, palladium pyrithione complex; RSL3, RAS, selective lethal small molecule 3.

(Hu et al., 2020). The latest researches show that m^6A is associated with regulating sensitivity of LUAD to ferroptosis. The m^6A reader YT521-B homology containing 2 has been identified to inhibit LUAD tumorigenesis by suppressing SLC7A11 and SLC3A2 (Ma et al., 2021). And methyltransferase-like 3, the main catalyst of m^6A, mediate m^6A modification to stabilize SLC7A11 mRNA and promote its translation, which enhances LUAD cell proliferation and inhibits cell ferroptosis (Xu Y. et al., 2022). Additionally, *in vivo*, Circular RNA CircP4HB expression levels are increased in LUAD, which inhibits ferroptosis by regulating miR-1184/SLC7A11-mediated GSH synthesis and, therefore protected LUAD cells from ferroptosis induced by erastin (Pan et al., 2022).

In addition to SLC7A11, lung cancer cell also exhibits high GPX4 expression. GPX4 promotes proliferation and ferroptosis resistance in lung cancer, while GPX4 inhibitor RSL3 limits proliferation, migration, and invasion of cisplatin-resistant A549 cells (Deng et al., 2021). Ni et al. found that GPX4 was upregulated because of enhanced activation of mTORC1 in lapatinib resistant NSCLC cells (Ni J. et al., 2021). Inhibition of mTORC1 leads to the downregulation of GPX4. Further *in vivo* experiments also showed that the silencing of GPX4 enhanced the anti-cancer effect of lapatinib by promoting ferroptosis. A Circular RNA CircDTL acting as an oncogene, was found to be upregulated and exerts its effects via the miR-1287-5p/GPX4 axis in NSCLC (Shanshan et al., 2021). Knockdown of circDTL promoted both apoptosis and ferroptosis of NSCLC cells. Recently, Wang's team discovered that the promoter region of GPX4 binds to cyclic adenosine monophosphate response element binding protein (CREB) and that this binding can be enhanced by E1A binding protein P300 (EP300), promoting tumor proliferation, migration, invasion and angiogenesis. Thus, GPX4 inactivation blocks the CREB/EP300/GPX4 axis, and these findings reveal that SLC7A11 or GPX4 inhibition sensitizes LUAD cells to ferroptosis, providing a potential therapeutic approach for this currently incurable disease (Wang Z. et al., 2021). Moreover, overexpressed serine threonine tyrosine kinase 1 (STYK1) upregulates GPX4, resulting in SW900 cells to be less sensitive to ferroptosis (Lai et al., 2019). Importantly, GPX4 was positively correlated with resistance of lung cancer cells to L-685458, lapatinib, paposilli, and topotecan, suggesting that targeting System X_c^-/GSH/GPX4 axis could overcome drug resistance (Zhang et al., 2020; Ni J. et al., 2021).

A number of studies have proved that some natural compounds (Table 1) such as dihydroartemisinin (Yuan et al., 2020), artesunate (Zhang Q. et al., 2021),sulforaphane (Iida et al., 2021), curcumin (Tang X. et al., 2021), bufotalin (Zhang W. et al., 2022), sanguinarine (Xu R. et al., 2022), sinapine (Shao et al., 2022), solasonine (Zeng et al., 2022), ophiopogonin B (Zhang L. et al., 2022), red ginseng polysaccharide (Zhai et al., 2022) Dihydroisotanshinone I (Wu et al., 2021).inhibits the proliferation, colony formation and induces ferroptosis of lung cancer cells by the interfering mRNA and/or protein expression and/or degradation of SLC7A11 or GPX4. Apart from natural compounds, some drugs that have been marketed (Table 1) such as Vorinostat (Zhang T. et al., 2021), Orlistat (Zhou W. et al.,

2021) have also been found to act as ferroptosis inducers in lung cancer cells via inhibiting System X_c^-/GSH/GPX4 axis. In NSCLC, chemotherapy relies heavily on cisplatin as the first line of clinical treatment (Gridelli et al., 2018). The activation of Nrf2/SLC7A11 pathway is one of the main mechanisms of cisplatin resistance in NSCLC. Erastin or sorafenib combined with small doses of cisplatin can effectively inhibit the growth of cisplatin-resistant NSCLC cells by inhibiting the Nrf2/SLC7A11 pathway (Li et al., 2020). Conversely, SLC7A11 overexpression enhances the resistance of lung cancer cells to cisplatin (Horibe et al., 2018). Gefitinib an EGFR tyrosine kinase inhibitors resistance, was approved for second-line treatment of advanced NSCLC in 2004 and first-line treatment of patients with EGFR mutations in 2010. RSL3 combined with gefitinib inhibits the growth of gefitinib-derived persister lung cancer cells (Ishida et al., 2021). Yan et al. found that gefitinib in combination with betulin (a natural ferroptosis inducer) is a novel therapeutic approach to overcome gefitinib resistance in EGFR wild-type/KRAS-mutant NSCLC cells by inducing ferroptosis *in vitro* and *in vivo* (Yan et al., 2022). Moreover, small molecules activating ferroptosis through System X_c^- inhibition or GPX4 inhibition enhance the antitumor effect of radiotherapy (Ye et al., 2020; Almahi et al., 2022) and photodynamic therapy (Han et al., 2022) in lung cancer.

Breast cancer

Breast cancer is one of the most effective for chemotherapy in solid tumors. More than 80% of breast cancer patients require chemotherapy (Harbeck and Gnant, 2017). But most patients eventually develop drug resistance. Drug-resistant breast cancer cells are dependent on GPX4 and SLC7A11, which means they are vulnerable to ferroptosis caused by GPX4 and SLC7A11 inhibition (Hangauer et al., 2017). Selenium detoxification is critical for breast cancer survival. The micronutrient selenium is incorporated into the rare amino acid selenium cysteine through the selenium cysteine biosynthetic pathway, which is required for GPXs (Burk and Hill, 2015). The selenophosphate synthetase 2 (SEPHS2), an enzyme in the selenocysteine biosynthesis pathway, is required in cancer cells to detoxify selenide, an intermediate that is formed during selenocysteine biosynthesis (Burk and Hill, 2015). Breast and other cancer cells are selenophilic, allowing production of selenoproteins such as GPX4, protects cells against ferroptosis. However, selenide is poisonous and must be processed by SEPHS2. SEPHS2 protein levels are elevated in human breast cancer patient samples and loss of SEPHS2 impairs growth of orthortopic mammary tumor xenografts in mice (Carlisle et al., 2020). Gefitinib-targeted therapy is insufficient to inhibit triple negative breast cancer TNBC cell proliferation (McLaughlin et al., 2019). And GPX4 is increased in gefitinib-resistant cells. Silence or inhibition of GPX4 stimulate ferroptosis and enhance TNBC cell sensitivity to gefitinib (Song et al., 2020).

In 2013, Timmerman et al. identified a subset of TNBC samples as glutamine nutrient deficient by analyzing the functional metabolic profiles of 46 independently sourced breast cell lines, specifically for glutamine uptake and dependence. Tumor cells acquire Cys indirectly via peripheral glutamine using System X_c^- as a carrier, SLC7A11 is upregulated in one-third of TNBC cells *in vivo*, and limiting glutamine uptake or inhibiting System X_c^- activity increases intracellular ROS levels and slows TNBC metabolism (Bannai and Ishii, 1988; Timmerman et al., 2013). Further RNA sequencing analysis showed that SLC7A11 expression was upregulated in breast cancer tissues with brain metastases, suggesting a role for SLC7A11 in breast cancer metastasis (Sato et al., 2017). Yadav et al. demonstrate that miR-5096 is a tumor-suppressive miRNA that can target and downregulate SLC7A11in breast cancer cells (Yadav et al., 2021). Overexpression of miR-5096 reduces mRNA and protein levels of SLC7A11 in breast cancer cells. Virus-like particle immunotherapy or vaccines against SLC7A11 have been developed and shown to reduce the metastatic potential of breast cancer cells (Bolli et al., 2018; Donofrio et al., 2018; Ruiu et al., 2019). Both ferroptosis inducers RSL3 and sulfasalazine (SAS) inhibit GPX4 activity in breast cancer cells (Yu H, et al., 2019). These results suggest that inhibition of GPX4 and/or System X_c^- may be a potential measure to overcome drug resistance in breast cancer. Nrf2 can promote drug resistance of breast cancer cells by regulating System X_c^-/GSH/GPX4 axis. Nrf2 upregulates the expression and activity of SLC7A11 in breast cancer cells during oxidative stress, and promotes the survival of breast cancer cells from drugs and other treatments by antagonizing ROS, while Nrf2 expression is downregulated when ROS levels are reduced (Habib et al., 2015; Mostafavi-Pour et al., 2017).

Monotherapy and combination chemotherapy are commonly used in the treatment of breast cancer. Some drugs commonly used in clinical practice have also been found to have the effect of inducing ferroptosis in breast cancer (Table 2). In addition, Metformin a commonly used hypoglycemic drugs in clinical practice, was found to promote ferroptosis in breast cancer cells by inhibiting the UFMylation of SLC7A11 and the transcription of GPX4 (Yang J. et al., 2021; Hou et al., 2021). Furthermore, one study found that Ketamine inhibit the expression of GPX4 by attenuating KAT5 on the promoter region of GPX4, repressing the enrichment of histone H3 lysine 27 acetylation and RNA polymerase II (Li H. et al., 2021). Some other small molecule compounds (Table 2) such as alloimperatorin (Zhang J. et al., 2022b), tetrandrine citrate (Yin et al., 2022), pyrrolidin-3,2′-oxindoles (Liu S.-J. et al., 2021), Saponin Formosanin C (Chen H.-C. et al., 2022) can also induce ferroptosis in breast cancer cells by

TABLE 2 Drugs and compounds based on System X_c^-/GSH/GPX4 for treatment of drug-resistant solid tumors.

Compounds	Mechanism	Cancer Cell Lines	References
Bufotalin	inhibit the expression of GPX4; facilitate the ubiquitination and degradation of GPX4	A549	Yilei Zhang et al. (2022)
Sanguinarine	Decrease the protein stability of GPX4 through E3 ligase STUB1-mediated ubiquitination and degradation of endogenous GPX4	A549 and H3122	Rongzhong Xu et al. (2022)
Sinapine	Increase intracellular Fe^{2+}, lipid peroxidation, and ROS; upregulate transferrin and transferrin receptor; downregulate the SLC7A11 in a p53 dependent way	A549, SK, H661 and H460	Shao et al. (2022)
Solasonine	Suppress the expression of SLC711 and GPX4; affects mitochondrial function	Calu-1 and A549	Zeng et al. (2022)
		HepG2 and HepRG.	Jin et al. (2020)
		PANC-1 and CFPAC-1	Liang et al. (2022)
Ophiopogonin B	reduce the expression of GPX4 and SLC7A11	AGS and NCI-N87	Liyi Zhang et al. (2022)
Red ginseng polysaccharide	suppress the expression of GPX4	A549 and MDA-MB-231	Zhai et al. (2022)
Atractylodin	inhibit the expression of GPX4 and FTL proteins, and upregulate the expression of ACSL4 and TFR1 proteins	Huh7 and Hccm	Guan-Nan He et al. (2021)
Heteronemin	reduce the expression of GPX4	HA22T and HA59T	Chang et al. (2021)
Alloimperatorin	promote the accumulation of Fe^{2+}, ROS and MDA, and reduce mRNA and protein expression levels of SLC7A11 and GPX4	MCF-10A, MDA-MB-231 and MCF-7	Liyi Zhang et al. (2022)
Tetrandrine citrate	suppress GPX4 expression and activate NCOA4-mediated ferritinophagy	MCF7 and MDA-MB-231	Yin et al. (2022)
Dihydroisotanshinone I	repress the protein expression of GPX4	MCF-7 and MDA-MB-231	Lin et al. (2019)
Saponin formosanin C	Inhibit SLC7A11 and GPX4	MDA-MB-231 and MCF-7	Hsin-Chih Chen et al. (2022)
Lycium barbarum polysaccharide	Inhibit SLC7A11 and GPX4	MDA-MB-231 and MCF-7	Du et al. (2022)
6-Thioguanine	inactivate System X_c^-, block the generation of GSH, downregulate the expression of GPX4, increase the level of lipid ROS	MGC-803 and AGS	Jinping Zhang et al. (2022)
Tanshinone IIA	upregulate p53 expression and downregulate SLC7A11 expression	BGC-823, NCI-H87 and BGC-823	Guan et al. (2020)
			Ni et al. (2022)
Jiyuan oridonin A derivative a2	Decrease GPX4 expression		Ying Liu et al. (2021)
Talaroconvolutin A	Increase ROS, downregulate SLC7A11 and upregulate arachidonate lipoxygenase 3	HCT116, SW480, and SW620	Xia et al. (2020)
Resibufogenin	Inactive GPX4	HT29 and SW480	Shen et al. (2021)
Drugs			
Orlistat	reduce the expression of GPX4 and induce lipid peroxidation	H1299 and A549	Wenjing Zhou et al. (2021)
Ketamine	Decrease the expression of GPX4	HepG2 and Huh7 MCF-7 and T47D	Guan-Nan He et al. (2021)
			Huixin Li et al. (2021)
Sulfasalazine	Increase ROS and decrease GPX4 and System X_c^-	MDA-MB-231 and T47D cells	Haochen Yu et al. (2019)
Metformin	reduce the protein stability of SLC7A11 by inhibiting its UFMylation process; downregulate GPX4 by targeting the miR-324-3p/GPX4 axis	MCF-7, T47D, HCC 1937, Bcap37, NHFB and HBL-100 MDA-MB-231	Jingjing Yang et al. (2021)
			Hou et al. (2021)
Actinidia chinensis Planch	inhibit the GPx4 and SLC7A11 proteins	HGC-27	Gao et al. (2020)
Cisplatin	Reduce GSH and inactive GPX4	A549 and HCT116	Guo et al. (2018)

interfering with the System X_c^-/GSH/GPX4 axis. A polymer carbohydrates *Lycium barbarum* polysaccharide effectively prevents breast cancer cell proliferation and promotes ferroptosis via the System X_c^-/GPX4 pathway (Du et al., 2022).

Combination chemotherapy can significantly improve the efficacy and does not increase toxicity. SAS, an anti-inflammatory drug clinically used in ulcerative colitis, was found to activate ferroptosis in different breast cancer cells, especially in

cells with low estrogen receptor expression (Yu H. et al., 2019). This results of the present study revealed that SAS could inhibit breast cancer cell viability, which was accompanied by an abnormal increase in ROS and a depletion of GPX4 and System X_c^-. Interestingly, in xenograft model, Polyphyllin III, a major saponin extracted from *Paris polyphylla* rhizomes, which induces Kruppel Like Factor 4-mediated protective upregulation of SLC7A11, in combination with the System X_c^- inhibitor SAS, may have a co-induction in MDA-MB-231 breast cancer cells by enhancing intracellular lipid peroxidation and ferroptosis (Zhou Y. et al., 2021). Vorinostat, as mentioned before, is a histone deacetylase inhibitor (HDACI) has limited efficacy against solid tumors because of r the development of resistant cells (Fantin and Richon, 2007). SLC7A11 expressions positively correlate with insensitivity to HDACIs in many types of cancer cell lines (Fantin and Richon, 2007). Watanabe' group demonstrated that the inhibition of SLC7A11 including SAS treatment may overcome resistance to vorinostat by accumulating ROS and inducing ferroptosis in human breast cancer cell and colon cancer cell (Miyamoto et al., 2020). Propofol is a short-acting intravenous anesthetic used for the induction and maintenance of general anesthesia. However, Propofol showed anti-proliferation effects on TNBC cells and could be a potential adjuvant to enhance the chemotherapeutic sensitivity of TNBC cells to doxorubicin and paclitaxel partly by promoting cell ferroptosis via p53-SLC7A11-GPX4 pathway (Sun et al., 2022). Additionally, siramesine, a lysosome disrupting agent, and lapatinib, an EGFR inhibitor, elicit ferroptosis in a synergistic manner in breast and lung cancer by altering iron regulation (Ma et al., 2016; Ma et al., 2017; Villalpando-Rodriguez et al., 2019).

Liver cancer

To date, the main regulatory mediators mediating the ferroptotic response in Hepatocellular Carcinoma (HCC) cells have been identified as System X_c^- and GPX4 (Zhang et al., 2020). The multikinase inhibitor Sorafenib is the conventional first-line chemotherapy drug used to treat advanced HCC. As a System X_c^- inhibitor, Sorafenib is the only anticancer drug that causes ferroptosis in patients with HCC (Louandre et al., 2013). Although drug resistance limits its efficacy, it can still improve patient survival rates (Zhu Y.-J. et al., 2017). Interestingly, inhibition of ferroptosis can usually be detected once upon sorafenib resistance occurs. The resistance of hepatocellular carcinoma cells to chemotherapeutic agents such as sorafenib involves the abnormal expression of multiple transcription factors such as Nrf2, retinoblastoma (Rb) protein, hepatocyte nuclear factor 4α(HNF4α), HIC ZBTB Transcriptional Repressor 1 (HIC1), O-GlcNAcylated c-Jun, YAP/TAZ.

Nrf2 functions by blocking GSH depletion-mediated lipid peroxidation in HCC cells and plays a central role in protecting them from sorafenib-induced ferroptosis (Sun et al., 2016b). The status of Nrf2 is a key determinant of the effect of System X_c^-GSH/GPX4 axis-targeted therapy in HCC, and therefore it is necessary to improve efficacy by inhibiting Nrf2 expression. Nrf2 also counteracts sorafenib-induced ferroptosis by upregulating the iron and reactive oxygen metabolism-related genes HO-1 via the P62-Keap1-Nrf2 pathway (Sun et al., 2016b). Metallothionein-1G (MT-1G), a pivotal negative ferroptosis regulator, is a key regulator and promising therapeutic target for sorafenib resistance in human HCC cells. Sorafenib significantly induces exspression of MT-1G messenger RNA and proteins, and activation of Nrf2 is critical for MT-1G expression induced after sorafenib treatment (Houessinon et al., 2016). Importantly, the genetic and pharmacological inhibition of MT-1G enhances the anticancer activity of sorafenib *in vitro* and tumor xenograft models (Sun et al., 2016a). Sigma-1 receptor (S1R) is an oxidative stress-related protein, which regulates ROS accumulation via Nrf2. (Ha et al., 2011; Pal et al., 2012). Sorafenib significantly upregulated S1R protein expression in HCC cells. Studies have confirmed that the inhibition of S1R strengthen the anticancer effects of sorafenib in HCC cells *in vitro* and *in vivo* by inhibiting the expression of GPX4 (Bai et al., 2019). Overcoming the compensatory elevation of Nrf2 renders hepatocellular carcinoma cells more vulnerable to disulfiram/copper-induced ferroptosis (Ren et al., 2021). Meanwhile, the expression of Nrf2 is suppressed by Glutathione S-transferase zeta 1 (GSTZ1), which ia an enzyme in the catabolism of phenylalanine significantly downregulated in sorafenib-resistant hepatoma cells (Wang Q. et al., 2021a). Mechanistically, GSTZ1 depletion enhanced the activation of the Nrf2 pathway and increased the GPX4 level, thereby suppressing sorafenib-induced ferroptosis (Wang Q. et al., 2021a). But the combination of sorafenib and RSL3 significantly inhibited GSTZ1-deficient cell viability and promoted ferroptosis and increased ectopic iron and lipid peroxides *in vitro* and *in vivo* (Wang Q. et al., 2021a), The loss of function of the Rb protein (a tumor suppressor protein) is an important event during liver carcinogenesis, yet the mechanisms involved are complex. The high expression of RB protein in tumor cells inhibits ferroptosis by interfering mitochondrial ROS production, while also inhibiting the efficacy of sorafinib. Inhibiting RB protein *in vivo* promotes the efficacy of sorafenib, and RB protein can be used as an indicator of sorafenib sensitivity (Louandre et al., 2015). HNF4α has been identified as suppressing ferroptosis, and HIC1 identified as stimulating ferroptosis in liver cancer. HNF4A is critical for liver development (Parviz et al., 2003), and is up-regulated in liver cancer (Dill et al., 2013). By contrast, HIC1 acts as a tumor suppressor, which inhibits cell growth, migration and survival (Ubaid et al., 2018). Wang'group are the first to reveal that HNF4α and HIC1 oppositely regulate production of GSH via PSAT1, a

key enzyme in GSH synthesis (Zhang et al., 2019). Increasing the concentration of GSH by targeting HNF4α and HIC1 might improve soferanib resistance for liver cancer treatment (Zhang et al., 2019). c-Jun is a regulator of glucose metabolism. Activation of c-Jun is associated with resistance to sorafenib and poor overall survival and inhibits sorafenib-induced cell death (Chen et al., 2016; Haga et al., 2017). Moreover, Chen et al. found that O-GlcNAcylated c-Jun stimulated GSH synthesis via increasing PSAT1 and CBS transcription to inhibit ferroptosis in HCC cells (Chen et al., 2019). YAP/TAZ are well-characterized transcriptional effectors of Hippo signaling involved in a variety of physio-pathological processes, including tumorigenesis and tissue regeneration (Harvey et al., 2013). Previous studies have suggested the Hippo-YAP/TAZ pathway is a key driver of ferroptosis in epithelial tumors (Harvey et al., 2013; Yang et al., 2019). However, Gao et al. revealed that YAP/TAZ as key drivers of Sorafenib resistance in HCC by repressing Sorafenib-induced ferroptosis (Gao et al., 2021). Mechanistically, YAP/TAZ induce the expression of SLC7A11 in a TEAD-dependent manner, and sustain the protein stability, nuclear localization, and transcriptional activity of ATF4 which in turn cooperates to induce SLC7A11 expression.

In addition to transcription factors mentioned above, there are also some other mechanisms involved in sorafenib resistance. Branched-chain amino acid aminotransferase 2 (BCAT2) is a novel suppressor of ferroptosis. Mechanistically, BCAT2 as the key enzyme mediating the metabolism of sulfur amino acid, regulated intracellular glutamate level, whose activation by ectopic expression specifically antagonize System X_c^- inhibition and protected liver and pancreatic cancer cells from ferroptosis inducers (erastin, sorafenib, and SAS)-induced ferroptosis *in vitro* and *in vivo* (Wang K. et al., 2021). Besides, ATP-binding Cassette Subfamily C Member 5 (ABCC5), an important membrane transporter, is a universal glutamate conjugate that affects the efflux of endogenous metabolites, toxins, drugs, and intracellular ions (Jansen et al., 2015). The expression of ABCC5 was dramatically induced in sorafenib-resistant HCC cells and was remarkably associated with poor clinical prognoses (Huang et al., 2021). ABCC5 increased intracellular GSH and attenuated lipid peroxidation accumulation by stabilizing SLC7A11 protein, which inhibited ferroptosis (Huang et al., 2021). Additionally, the inhibition of ABCC5 enhanced the anti-cancer activity of sorafenib *in vitro* and *in vivo* (Huang et al., 2021).

DAZ Associated Protein 1 (DAZAP1) is an RNA-binding protein whose relative expression is significantly upregulated in HCC and is positively correlated with several key malignant features and poor postoperative survival in patients. Furthermore, DAZAP1 significantly reduced cellular sensitivity to sorafenib because DAZAP1 interacts with the 3′UTR (untranslated region) of SLC7A11 mRNA and positively regulated its stability (Wang Q. et al., 2021b). Protocadherin Beta 14 (PCDHB14), a member of the cadherin superfamily, is inactivated by aberrant methylation of its promoter in HCC patients and that PCDHB14 ablation inhibit cell cycle arrest, cell proliferation and ferroptosis (Liu Y. et al., 2022). Mechanistically, PCDHB14 is induced by p53, and increased PCDHB14 downregulates the expression of SLC7A11, which is mediated by accelerated p65 protein degradation resulting from PCDHB14 promoting E3 ubiquitin ligase RNF182-mediated ubiquitination of p65 to block p65 binding to the promoter of SLC7A11 (Liu Y. et al., 2022). Transforming growth factor β1 (TGF-β1) is a dichotomous cytokine that acts as a tumor suppressor in low-grade carcinoma cells but as a promotor of metastasis in advanced carcinoma cells (Dituri et al., 2019). Kim' study was the first to show that TGF-β1 repressed the protein and mRNA levels of SLC7A11 in liver cancer cell lines with an early TGF-β1 gene signature but not in those with a late TGF-β1 gene signature (Kim et al., 2020). Macropinocytosis and transsulfuration pathway are important nutrient-scavenging pathway in certain cancer cells, allowing cells to compensate for intracellular amino acid deficiency under nutrient-poor conditions. Sorafenib increased macropinocytosis in human HCC specimens and xenografted HCC tissues, which prevented sorafenib-induced ferroptosis by replenishing intracellular cysteine that was depleted by sorafenib treatment; this rendered HCC cells resistant to sorafenib (Byun et al., 2022). Primary hepatocytes are able to survive for several days in the absence of Cys or cysteine in the culture medium, which thanks to the protective effect of transsulfuration pathway (Lee et al., 2017).

Some natural compouds that induce ferroptosis in liver cancer cells are summarized in Table 2. Some of them also have synergistic effects with sorafenib such as artesunate (Li Z.-J. et al., 2021), Dihydroartemisinin (Cui et al., 2022), Ursolic acid (Li H. et al., 2022), enhancing the anti-cancer effects of sorafenib. Moreover, The depletion of Phosphoseryl-tRNA kinase (PSTK) results in the inactivation of GPX4 and the disruption of GSH metabolism (Chen Y. et al., 2022a). Punicalin, an agent used to treat hepatitis B virus (HBV), was identified as a possible PSTK inhibitor that exhibited synergistic efficacy when applied together with Sorafenib to treat HCC *in vitro* and *in vivo* (Chen Y. et al., 2022a). Taken together, these results support the idea that blocking System X_c^-/GSH/GPX4 axis in combination with chemotherapeutic agents (e.g., sorafenib) provides new ideas for treatment of drug-resistant HCC.

Gastrointestinal cancers

Gastric cancer is the fourth most common cancer worldwide and the second leading cause of cancer-related death after lung

cancer (2020b). GPX4 is lowly expressed in gastric cancer (GC) cells, making them more susceptible to ferroptosis than normal intestinal cells. Cysteine dioxygenase 1 (CDO1) plays an important role in Erastin-induced ferroptosis in GC cells (Hao et al., 2017). CDO1 is a non–heme iron metalloenzyme, transforming cysteine to taurine by catalyzing the oxidation of cysteine to its sulfinic acid, which prevents cytotoxicity from elevated cysteine levels (Stipanuk et al., 2009). Suppression of CDO1 upregulates GPX4 expression, restores cellular GSH levels, prevents ROS generation (Hao et al., 2017). Zhao et al. reported that apatinib reduced the expression of GPX4, thereby inhibiting the proliferation of GC cells and multidrug-resistant GC (Zhao et al., 2021). Previous study showed that miR-375 can inhibit *Helicobacter* pylori-induced gastric carcinogenesis (Miao et al., 2014). MiR-375 reduced the stemness of GC cells *in vitro* and *in vivo* by directly targeting SLC7A11 (Miao et al., 2014). Elevated Growth/differentiation factor 15 (GDF15) level in serum and increased GDF15 expression in cancer tissues are reported in patients with various cancers, and associated with the poor prognosis of the patients (Welsh et al., 2001; Welsh et al., 2003). Recent research has showed that GDF15 regulate SLC7A11 expression, and GDF15 knockdown promote erastin-induced ferroptosis by repressing SLC7A11 expression and suppressing the function of System X_c^- (Chen L. et al., 2020). The inhibition of Sirtuins 6 (SIRT6), a member of the Sirtuin family of NAD (+)-dependent enzymes, lead to the inactivation of the Keap1/Nrf2 signalling pathway and downregulation of GPX4, which overcomes sorafenib resistance by promoting ferroptosis in gastric cancer (Cai et al., 2021).

Another therapeutic target that regulates GC ferroptosis, SLC7A11, its inhibitor Erastin hampers the survival of GC (Sun et al., 2020). Some miRNAs, such as miR-489-3p and miR-375, can directly target SLC7A11 and trigger ferroptosis (Ni H. et al., 2021). Levobupivacaine, an amide-based local anesthetic, inhibits GC by upregulating miR-489-3p (Mao et al., 2021). A study showed that induction of ferroptosis by blocking Nrf2-Keap1 pathway also sensitizes cisplatin-resistant GC cells to cisplatin (Fu et al., 2021). The latest study suggests that Signal transducer and activator of Transcription 3 (STAT3)-mediated ferroptosis is associated with chemoresistance in gastric cancer (Ouyang et al., 2022). STAT3 a key oncogene with dual functions of signal transduction and transcriptional activation, which is hyperactivated in the formation of most human cancers and plays a critical role in cell proliferation, angiogenesis, metastasis, and immunosuppression (El-Tanani et al., 2022). Ouyang et al. demonstrates that STAT3 binds to consensus DNA response elements in the promoters of the GPX4, SLC7A11, and regulates their expression, thereby establishing a negative STAT3-ferroptosis regulatory axis in gastric cancer (Ouyang et al., 2022). However, additional important molecular mechanisms by which STAT3 regulates ferroptosis deserve further exploration.

Similar to GC cells, targeting the System X_c^-/GSH/GPX4 axis is an effective way to inhibit the growth of drug-resistant colorectal cancer (CRC). In colorectal cancer stem cells (CSCs), SLC7A11 is extremely expressed, with high GSH levels and low ROS levels, leading to their extreme vulnerability to ferroptosis (Zeuner et al., 2014). FAM98A (Family with Sequence Similarity 98 Member A), a microtubule-associated protein, plays a critical role in promoting resistance to 5-fluorouracil (5-FU) in CRC. The Enhanced expression of FAM98A recover 5-FU suppressed CRC cell proliferation both *in vitro* and *in vivo* by activating the translation of SLC7A11 in stress granules (He et al., 2022). However, In the xenograft model, the inhibition of GPX4 restrain tumor regrowth after discontinuation of 5-FU treatment (Zhang X. et al., 2022). Yang et al. found that high expression of KIF20A in CRC cells was associated with oxaliplatin resistance, and that resistance to oxaliplatin in CRC could be overcome by disrupting the KIF20A/NUAK1/PP1β/GPX4 pathway (Yang C. et al., 2021). In addition, Serine and arginine rich splicing factor 9 (SFRS9) can upregulate the expression of GPX4 by binding to GPX4 mRNA, which promote the growth of CRC, while SFRS9 knockdown significantly inhibited tumor growth in nude mice (Wang R. et al., 2021). Thus, GPX4 and/or SLC7A11 inhibition combined with chemotherapy or targeted therapy may be a promising therapy for CRC. *In vitro*, β-elemene (a ferroptosis inducer) in combination with cetuximab was shown to induce iron-dependent ROS accumulation, GSH depletion, lipid peroxidation, upregulation of HO-1 and transferrin, and downregulation of GPX4, SLC7A11 and other negative regulatory proteins in KRAS mutant CRC cells (Chen P. et al., 2020). *In vivo*, co-treatment with β-elemene and cetuximab inhibited KRAS mutant tumor growth and lymph nodes metastases (Chen P. et al., 2020).

Pancreatic cancers

The main reason for the poor prognosis of PDAC is the late diagnosis of the disease and resistance to drugs that induce apoptosis (Chen X. et al., 2021b). Therefore, ferroptosis may provide an alternative strategy for killing PDAC cells and overcoming apoptosis resistance (Chen X. et al., 2021a; Yang G. et al., 2021). Gemcitabine (a nucleoside analogue of deoxycytoside) has been at the forefront of the past few decades as a cornerstone of PDAC treatment, despite its poor clinical efficacy.

Gemcitabine induces NF-κB activation and NOX-mediated ROS accumulation in PDAC cells. As a feedback mechanism, elevated ROS levels lead to Nrf2 activation and increased intracellular GSH, which resists treatment with gemcitabine (Manea et al., 2007; Lister et al., 2011). SLC7A11 disruption in PDAC cell lines strongly affects their amino acid and redox balance, and thus suppresses *in vitro* and delays *in vivo* their proliferative phenotype (Daher et al., 2019). Importantly, unlike disruption of other essential amino acid transporters, genetic

ablation of SLC7A11 enhance susceptibility to cell death via ferroptosis (Daher et al., 2019). However, *in vivo* SLC7A11 knock out PDAC cells grew normally. Their further study showed that the presence of a cysteine/cystine shuttle between neighboring cells is the mechanism that provides redox and nutrient balance, and thus ferroptotic resistance in SLC7A11 knock out PDAC cells (Meira et al., 2021). Cysteine is required for preventing ferroptosis in pancreatic cancer (2020a), While the raw material for the synthesis of cysteine is mainly provided by System X_c^-.

Gemcitabine resistance was also associated with GPX4 in PDAC cells. Recent reports elucidated that HSPA5 upregulation negatively regulates ferroptosis in pancreatic cancer, while ATF4 activation upregulates HSPA5, thus the HSPA5-GPX4 pathway is one of the causes of gemcitabine resistance (Zhu S. et al., 2017). When gemcitabine was combined with HSPA5 inhibitor for PDAC, its anticancer activity was significantly enhanced (Zhu S. et al., 2017). Both rapamycin (classical autophagy inducer) and RSL3 can block mechanistic target of rapamycin kinase (MTOR) activation and cause GPX4 protein degradation in human pancreatic cancer cells, which can restore or enhance the anticancer activity of gemcitabine *in vitro* or in xenogeneic PDAC models (Liu Y. et al., 2021b). In addition, mitochondrial protease Lon peptidase 1 (LONP1) inhibits Nrf2-mediated GPX4 gene expression, thereby promoting Erastin-induced ferroptosis in human PDAC cells (Wang H. et al., 2020). However, the high-iron diets or depletion of GPX4 promotes Hydroxyguanosine 8 (8-OHG) release and thus activates the TMEM173/STING-dependent DNA sensor pathway, which results in macrophage infiltration and activation during Kras-driven PDAC in mice (Dai et al., 2020).

An emerging oncoprotein, Myoferlin, controls mitochondria structure and respiratory functions, has been associated with a low survival in several cancer types including PDAC. The pharmacological inhibitor of myoferlin can reduce the abundance of System $X_c^-$and GPX4 which trigger mitophagy and ROS accumulation culminating with lipid peroxidation and ferroptosis (Rademaker et al., 2022). The latest research shows that mitochondrial calcium uniporter (MCU) promotes PDAC cell migration, invasion, metastasis, and metabolic stress resistance by activating the Keap1-Nrf2 antioxidant program (Wang et al., 2022). SLC7A11 was identified as a druggable target downstream of the MCU-Nrf2 axis (Wang et al., 2022). But MCU overexpression makes PDAC cells hypersensitive to cystine deprivation-induced ferroptosis (Wang et al., 2022). Pharmacologic inhibitors of SLC7A11 effectively induce tumor regression and abrogate MCU-driven metastasis in PDAC (Wang et al., 2022). Natural compounds such as piperlongumine and cotylenin A exhibit synergistic therapeutic efficacy with SAS, which suggest that the triple combined treatment with piperlongumine, piperlongumine and SAS is highly effective against pancreatic cancer (Kasukabe et al., 2016; Yamaguchi et al., 2018).

In summary, System X_c^-/GSH/GPX4 axis-based ferroptosis may be a research direction for reversing drug resistance and may provide a rational basis for the development of new therapies for drug resistant solid tumors.

Ferroptosis resistance in tumor cells

In addition to System X_c^-/GSH/GPX4 axis, an antioxidant system that protect tumor cells from ferroptosis, a number of new mechanisms of ferroptosis resistance have been found in *vivo* and *in vitro* studies of drug-resistant solid tumors mentioned above, which are associated with a variety of metabolic enzymes. Metabolic reprogramming is required for both malignant transformation and tumor development, including invasion and metastasis.

Lung adenocarcinomas select for expression of a pathway related to NFS1 that confers resistance to high oxygen tension and protects cells from undergoing ferroptosis in response to oxidative damage (Alvarez et al., 2017). NFS1 is an essential enzyme in eukaryotes that harvests sulfur from cysteine for the biosynthesis of iron–sulfur clusters, is particularly important for maintaining the iron-sulfur co-factors present in multiple cell-essential proteins upon exposure to oxygen compared to other forms of oxidative damage (Stehling et al., 2014). However, the specific mechanism is not yet clear. The latest *in vitro* and *in vivo* research results show that oxaliplatin-based oxidative stress enhance the phosphorylation level of serine residues of NFS1, which protect CRC cells in an S293 phosphorylation-dependent manner during oxaliplatin treatment (Lin et al., 2022). While NFS1 deficiency synergizing with oxaliplatin by increasing the intracellular levels of ROS (Lin et al., 2022).

Nuclear Protein 1 (NUPR1), a stress-inducible transcription factor, was identified as a driver of ferroptosis resistance through regulating Lipocalin 2 (LCN2) (Liu J. et al., 2021). LCN2, a secreted glycoprotein, forms a complex with bacterial and human siderophores, thereby inhibiting bacterial growth and regulating iron homeostasis that maintains the integrity of the gastrointestinal mucosa (Xiao et al., 2017). LCN2 expression is elevated in multiple tumor type. The overexpression of LCN 2 leads to resistance to 5-FU in CRC cell lines *in vitro* and *in vivo* by decreasing intracellular iron levels and stimulating the expression of GPX4 and SLC7A11 (Chaudhary et al., 2021).

Lymphoid-specific helicase (LSH) is involved in ferroptosis and is a potential therapeutic target in cancer because of its crucial role in ferroptosis. LSH, a member of the chromatin remodeling ATPase SNF2 family, establishes the correct levels and patterns of DNA methylation, maintains the stability of the genome in mammalian somatic cells, and is essential for normal development (Fan et al., 2003; Myant et al., 2011; Yu et al., 2014; Jia et al., 2017). One study showed that LSH lower the concentration of lipid ROS and iron by interacting with WDR76, activating lipid metabolic genes, including SCD1 and FADS2, which inhibit the accumulation of lipid ROS and intracellular iron (Jiang et al., 2017a). They further demonstrated that EGLN1 and c-Myc directly activated the expression of LSH by inhibiting HIF-1α (Jiang et al., 2017b). In addition, LSH promotes the expression of long non-coding RNAs LINC00336 in lung cancer tissues. LINC00336 acts as an oncogene that promotes tumor cell proliferation, inhibits ferroptosis, and induces tumor formation in an ELAVL1-dependent manner (Wang M. et al., 2019).

TABLE 3 Novel nano drug delivery systems inducing ferroptosis in solid tumors via System Xc-/GSH/GPX4 axis.

Nanoparticles	Loaded Drugs	Delivery Systems	Mechanism of Drug Release	Mechanism of Action	Cancer Cell Lines	Reference
mPEG-*b*-P (DPA-r-GC)	RSL3	intracellular-acidity-ionizable poly (ethylene glycol)-block-poly (2- (diisopropylamino) ethyl methacrylate) diblock copolymer and acid-liable phenylboronate ester dynamic covalent bonds	At neutral pH of 7.4, the nanoparticles can stably encapsulate RSL-3 inside the hydrophobic PDPA core via π–π stacking interaction with the phenylboronate ester groups; pH = 5.8–6.2, RSL3 release through acid-triggered cleavage of the phenylboronate ester dynamic covalent bonds and protonation of the hydrophobic core	Deplete system X_c^-	B16-F10 and 4T1	Song et al. (2021)
AMSNs/DOX	Doxorubicin	biocompatible arginine-rich manganese silicate nanobubbles	The positively charged drug binds to the negatively charged nanocarrier by electrostatic interaction, while the N atoms in the drug bind to the Mn atoms in the carrier by covalent bonding. At high GSH concentrations and low pH values, drug release is accelerated	Deplete GSH and inactive GPX4; release Mn ions and loaded drugs, resulting in enhanced T1-weighted magnetic resonance imaging contrast	Huh7 and L02	Wang et al. (2018)
MMSNs@SO	Sorafenib	manganese doped mesoporous silica nanoparticles	Manganese-oxidation bonds of nanocarrier could break in high GSH concentration, on-demand drug release is achieved due to the degradation of nanocarriers	consume intracellular GSH and inhibit system X_c^-	HepG2 and LO2	Tang et al. (2019)
FaPEG-MnMSN@SFB	sorafenib	manganese doped silica nanoparticle modified with folate grafted PEG	-Mn-O- bond in nanocarrier is sensitive to acidic and reductive environments and GSH can reduce the -Mn-O- bonds to Mn^{2+}	consume intracellular GSH and inhibit system X_c^-	L02, HUVEC, HepG2, A549 and 4T1	Tang et al. (2020)
MIL-101(Fe)@sor	sorafenib	Fe-metal organic framework [MIL-101 (Fe)]	sorafenib gradually release in a time- and pH-dependent manner without an obvious burst-release effect. Drug release reached approximately 35% at pH 5.5 and only 10% at pH 7.4 after 60 h	consume GSH, decrease GPX4 levels, enhance lipid peroxidation generation, and simultaneously supply iron ions	HepG2	Xianchuang Liu et al. (2021)
AAAF@Cur	Curcumin	the hydrophilic end astragalus polysaccharides connect the ferrocene with azobenzene linker to construct the amphiphilic a hypoxia-responsive liver targeting carrier material AA/ASP-AZO-Fc (AAAF)	The azobenzene linker can be easily broken relying on the reduction reaction in a low oxygen environment, and then triggers the release of the drug	inhibit GSH content	HepG2	Xue Liu et al. (2022)
RSL3@O2-ICG NBs	RSL3	a 2-in-1 nanoplatform connected with nanobubbles (NBs) and sonosensitizer Indocyanine green	NBs could be used as cavitation nuclei, which may expand, compress and destroy under ultrasound stimulation. In cavitation, destruction generates microjets that create shear stress on cells and leads to reversible pore formation in the cell membranes, which could enhance cell membrane permeability transiently without deterring the cell viability and promote the drug into cells	consume GSH, inhibit GPX4 and cause ROS accumulation	HepG2 and Huh7	Yichi Chen et al. (2022b)

(Continued on following page)

TABLE 3 (*Continued*) Novel nano drug delivery systems inducing ferroptosis in solid tumors via System Xc-/GSH/GPX4 axis.

Nanoparticles	Loaded Drugs	Delivery Systems	Mechanism of Drug Release	Mechanism of Action	Cancer Cell Lines	Reference
Erastin@FA-exo	Erastin	exosomes labeled with folate	Exosomes interact with cellular membranes and deliver drugs to cells	deplete GSH over generate ROS, suppress expression of GPX4 and upregulate expression of cysteine dioxygenase	MDA-MB-231	Mengyu Yu et al. (2019)
CSO-SS-Cy7-Hex/SPION/Srfn	sorafenib	Mitochondrial membrane anchored oxidation/reduction response and Fenton-Reaction-Accelerable magnetic nanophotosensitizer complex self-assemblies	The nano-device enrich the tumor sites by magnetic targeting of enhanced permeability and retention effects, which were disassembled by the redox response under high levels of ROS and GSH in ferroptosis therapy cells. Superparamagnetic iron oxide nanoparticles released Fe^{2+} and Fe^{3+} in the acidic environment of lysosomes, and the NIR photosensitizer Cy7-Hex anchored to the mitochondrial membrane, combined sorafenib leading to lipid peroxidation burst	deplete GSH over generate ROS, suppress system X_c^- and enhance Fenton reaction	4T1, MCF-7, and MDA-MB-231	Sang et al. (2019b)
CSO-BHQ-IR780-Hex/MIONPs/Sor	sorafenib	Black Hole Quencher-cyanine conjugates based fluorescence "off–on" NIR nanophotosensitizer self-assembly chitosan with loaded magnetic iron oxide nanoparticles	Black Hole Quencher and IR780 are covalent binding via an ether bond, which is reduced by GSH. Subsequently, the IR780-Hex anchored the mitochondrial membrane nanoparticles and produce a large amount of ROS under a near-infrared laser. magnetic iron oxide nanoparticles release Fe^{2+} under an acid environment	suppress the SLC7A11, GPX4 system and lead to lipid peroxidation burst	4T1 and MCF-7	Sang et al. (2019a)
SRF@Hb-Ce6	sorafenib	a 2-in-1 nanoplatform connected with hemoglobin, the photosensitizer chlorin e6 and the amphiphilic matrix metalloproteinases 2-responsive peptide	Drug release is generally caused by matrix metalloproteinases 2-triggered cleavage, degradation, and/or dissociation of the nanomaterials	Reduce the expression of SLC7A11 and SLC3A2; downregulate GPX4	4T1, HepG2 and A549	Xu et al. (2020)
FPBC@SN	sorafenib and NLG919	The benzimidazole-cyclodextrin-switch-containing polymer vehicle	In weakly acidic solutions suchas tumor cells, protonated benzimidazole was transferred from hydrophobicity to hydrophilicity, and escaped from benzimidazole chambers to lead to nanoparticles disassembly	upregulate nuclear receptor coactivator 4, promote ferritinophagy, enhance Fenton reaction and immunotherapy, block glutathione synthesis and downregulate GPX4	4T1	Zuo et al. (2021)
HMTBF	Bleomycin and ML210	the metal-phenolic network formed by tannic acid, bleomycin, and Fe^{3+} with GPX4 inhibitor (ML210) loaded hollow mesoporous Prussian blue (HMPB) nanocubes	The nanoparticles degrade intracellularly to release drugs	Inactive GPX4, enhance Fenton reaction and apoptosis	4T1	Lulu Zhou et al. (2021)
Cu-TCPP(Fe) MOF	RSL3	Cu-tetra(4-carboxyphenyl) porphyrin chloride metal organic framework-based nanosystem modified with polyethylene glycol and iRGD	The nanosheet system release the supramolecular attached RSL3 in the acidic lysosomes	lead to the simultaneous inhibition of the GPX4/GSH and FSP1/CoQ10H2 pathways	4T1	Ke Li et al. (2022)

(Continued on following page)

TABLE 3 (*Continued*) Novel nano drug delivery systems inducing ferroptosis in solid tumors via System Xc-/GSH/GPX4 axis.

Nanoparticles	Loaded Drugs	Delivery Systems	Mechanism of Drug Release	Mechanism of Action	Cancer Cell Lines	Reference
CDC@SRF	sorafenib	lipid-like dimersomes fabricated by cinnamaldehyde dimers	After reaching the tumor, the nanoparticles quickly underwent breakage in the cytosol owing to the conjugation of hydrophilic GSH on cinnamaldehyde dimers by Michael addition, which not only triggered the drug release	deplete intracellular GSH and inhibit system X_c^-	4T1	Zhou et al. (2022)

A cell-autonomous mechanisms have been identified that account for the resistance of cells to ferroptosis. The FSP1-CoQ10-NAD(P)H pathway exists as a stand-alone parallel system, which co-operates with System X_c^-/GSH/GPX4 axis to suppress phospholipid peroxidation and ferroptosis (Doll et al., 2019). Ferroptosis suppressor protein 1 (FSP1) previously called apoptosis-inducing factor mitochondria-associated 2 (AIFM2) confers protection against ferroptosis by complement the loss of GPX4. Furthermore, the suppression of ferroptosis by FSP1 is mediated by coenzyme Q10 (CoQ10), whose reduced form traps lipid peroxyl radicals that mediate lipid peroxidation, whereas FSP1 catalyses the regeneration of CoQ10 using NAD(P)H (Bersuker et al., 2019). Circular RNA circGFRA1 is remarkably upregulated in HER-2-positive breast cancer, which can bind to miR-1228 and alleviate inhibitory activity of miR-1228 on targeted gene AIFM2 (Bazhabayi et al., 2021). Knockdown of circGFRA1 could attenuate HER-2-positive breast cancer progression by inhibiting the proliferation, infiltration and migratory ability of HER-2-positive breast cancer cells. In addition, plasma-activated medium induces ferroptosis by depleting FSP1 in human lung cancer cells (Jo et al., 2022). Meanwhile, CoQ10-FSP1 axis is a key downstream effector of Keap1-Nrf2 pathway (Koppula et al., 2022). Keap1 is mutated in around 16% of NSCLCs (2012). Keap1 mutation or deficiency in lung cancer cells upregulates FSP1 expression through Nrf2, leading to ferroptosis- and radiation-resistance (Koppula et al., 2022). Furthermore, targeting the CoQ10-FSP1 axis sensitizes Keap1 mutant lung cancer cells or tumors to radiation by inducing ferroptosis (Koppula et al., 2022).

Nanoparticles based on system X_c^-/GSH/GPX4 *axis* for treatment of drug-resistant solid tumors

The current ferroptosis inducers are mainly small molecules targeting the different targets in the System X_c^-/GSH/GPX4 axis. In mechanism, these inducers may have no cancer cell selectivity. Direct intravenous administration of these ferroptosis inducers of small molecules may lead new damage to normal cells and deteriorate the side effects of the current anti-tumor drugs. However, advances in nanomaterial sciences make it possible to improve the properties of drugs, prolong circulation times *in vivo*, and promote tumor-specific drug targeting to improve the therapeutic effect and reduce the incidence of adverse reactions (Amreddy et al., 2018). The nanoparticles developed in recent years that act on the five drug-resistant solid tumors discussed above are summarized in Table 3.

Discussion and prospects

Ferroptosis is an iron-mediated form of cell death caused by the accumulation of lipid peroxides. The intracellular imbalance between oxidant and antioxidant due to the abnormal expression of multiple redox active enzymes will promote the produce ROS. Since the discovery of ferroptosis, much solid evidence has been obtained in experimental tumor models that ferroptosis has good anti-cancer effects. Many aggressive and drug-resistant cancer cells are sensitive to ferroptosis, so ferroptosis is indicated for those tumor cells that are less sensitive to chemotherapy. There is also growing evidence that the activation of ferroptosis contributes to the anticancer treatment of several forms of drug-resistant solid tumors, such as liver cancer, lung cancer, breast cancer, pancreatic cancer, gastrointestinal cancers, which undoubtedly makes that the combination of System X_c^-/GSH/GPX4 axis-based ferroptosis inducers with chemotherapeutic agents may become a new strategy for the treatment of drug-resistant solid tumors. The process of ferroptosis is a pharmacologically modifiable pathway, and there are many easy-to-treat targets on the System X_c^-/GSH/GPX4 axis.

The recognition of many natural products, and some drugs that have been marketed or used in the clinic were found to have the effect of inhibiting System X_c^-/GSH/GPX4 axis, thereby

inducing ferroptosis. Many tumor cells develop chemoresistance through different mechanisms, including primary and acquired resistance. Acquired drug resistance is the most common cause of tumor recurrence. With the passage of time of drug treatment, spontaneous mutations from the tumor itself will lead to an increase in resistant clones. Because of the high heterogeneity of tumors, according to Darwinian evolutionary principles, drug-resistant mutants are selected, or subpopulations of primary resistant tumor stem cells in the dormant phase can cause tumors to regrow or spread. These drug resistant tumor cells protect themselves from death threats including ferroptosis inducers through many mechanisms including System X_c^-/GSH/GPX4 axis. GPX4 and GSH, as important intracellular antioxidants, protect cells from ferroptosis; therefore, GSH deprivation and GPX4 inactivation lead to ferroptosis. By inhibiting this system helps to promote tumor ferroptosis and alleviate drug resistance, which has also been confirmed in data from several studies. These drug-resistant solid tumors can be treated by the combination of ferroptosis inducers and other pathways. However, the induction of ferroptosis has a dual role in tumor growth. Some medicines induce ferroptosis to slow tumor growth, but ferroptosis itself can cause immunosuppression to accelerate tumorigenesis. So deeper mechanisms need to be explored. Also, considering that iron deficiency and iron overload may affect antitumor activity, the appropriate iron concentration and optimal dose of ferroptosis inducer medicines to reduce tumor progression deserves in-depth study. Furthermore, at present, all small molecules used in cancer targeting treatment finally produce drug resistance. The ferroptosis inducers of small molecules are no exception. Some cancer cells evolve specific mechanisms to resist ferroptosis, so discovering and inhibiting these mechanisms combined with ferroptosis is effective in alleviating drug resistance. Importantly, not all ferroptosis inducers are highly tumor-selective, so more research is needed to develop ways to improve drug targeting. Thorough studies are necessary to reveal effective multimodal therapies. Overall, inhibition of key molecules in System X_c^-/GSH/GPX4 axis is a promising therapeutic strategy for the treatment of tumors, especially drug-resistant tumors.

Author contributions

F-JL completed the manuscript. H-ZL, Z-WZ, H-YL, and S-GX helped in searching for related articles. The revision of the manuscript was collaboratively finished by F-JL, H-ZL, Z-WZ, H-YL, S-GX, and L-CG. All authors contributed to the article and finally the submitted version is approved by L-CG.

Funding

This work was supported by Science and Technology Key Program of Hunan Province Grants (2016SK2066), Key Projects of Hunan Health Committee (B2017207), Hunan Province Chinese Medicine Research Program Grants (201940), Changsha City Science and Technology Program Grants (kq1801144), Changsha Central Hospital Affiliated to University of South China Foundation of key Program (YNKY201901), Hunan Province Foundation of High-level Health Talent (225 Program), and Science and Technology Key Program of Hunan Provincial Health Committee (20201904).

Conflict of interest

The authors declare that the research was conducted in the absence of any commercial or financial relationships that could be construed as a potential conflict of interest.

Publisher's note

References

Alderson, N. L., Wang, Y., Blatnik, M., Frizzell, N., Walla, M. D., Lyons, T. J., et al. (2006). S-(2-Succinyl)cysteine: A novel chemical modification of tissue proteins by a Krebs cycle intermediate. *Arch. Biochem. Biophys.* 450 (1), 1–8. doi:10.1016/j.abb.2006.03.005

Alim, I., Caulfield, J. T., Chen, Y., Swarup, V., Geschwind, D. H., Ivanova, E., et al. (2019). Selenium drives a transcriptional adaptive program to block ferroptosis and treat stroke. *Cell.* 177 (5), 1262–1279. e1225. doi:10.1016/j.cell.2019.03.032

Almahi, W. A., Yu, K. N., Mohammed, F., Kong, P., and Han, W. (2022). Hemin enhances radiosensitivity of lung cancer cells through ferroptosis. *Exp. Cell. Res.* 410 (1), 112946. doi:10.1016/j.yexcr.2021.112946

Alvarez, S. W., Sviderskiy, V. O., Terzi, E. M., Papagiannakopoulos, T., Moreira, A. L., Adams, S., et al. (2017). NFS1 undergoes positive selection in lung tumours and protects cells from ferroptosis. *Nature* 551 (7682), 639–643. doi:10.1038/nature24637

Amreddy, N., Babu, A., Muralidharan, R., Panneerselvam, J., Srivastava, A., Ahmed, R., et al. (2018). Recent advances in nanoparticle-based cancer drug and gene delivery. *Adv. Cancer Res.* 137, 115–170. doi:10.1016/bs.acr.2017.11.003

Badgley, M. A., Kremer, D. M., Maurer, H. C., DelGiorno, K. E., Lee, H.-J., Purohit, V., et al. (2020). Cysteine depletion induces pancreatic tumor ferroptosis in mice. *Sci. (New York, N.Y.)* 368 (6486), 85–89. doi:10.1126/science.aaw9872

Baek, S., Choi, C.-M., Ahn, S. H., Lee, J. W., Gong, G., Ryu, J.-S., et al. (2012). Exploratory clinical trial of (4S)-4-(3-[18F]fluoropropyl)-L-glutamate for imaging xC- transporter using positron emission tomography in patients with non-small cell

lung or breast cancer. *Clin. Cancer Res.* 18 (19), 5427–5437. doi:10.1158/1078-0432.CCR-12-0214

Bai, T., Lei, P., Zhou, H., Liang, R., Zhu, R., Wang, W., et al. (2019). Sigma-1 receptor protects against ferroptosis in hepatocellular carcinoma cells. *J. Cell. Mol. Med.* 23 (11), 7349–7359. doi:10.1111/jcmm.14594

Bannai, S., and Ishii, T. (1988). A novel function of glutamine in cell culture: Utilization of glutamine for the uptake of cystine in human fibroblasts. *J. Cell. Physiol.* 137 (2), 360–366. doi:10.1002/jcp.1041370221

Bazhabayi, M., Qiu, X., Li, X., Yang, A., Wen, W., Zhang, X., et al. (2021). CircGFRA1 facilitates the malignant progression of HER-2-positive breast cancer via acting as a sponge of miR-1228 and enhancing AIFM2 expression. *J. Cell. Mol. Med.* 25 (21), 10248–10256. doi:10.1111/jcmm.16963

Bersuker, K., Hendricks, J. M., Li, Z., Magtanong, L., Ford, B., Tang, P. H., et al. (2019). The CoQ oxidoreductase FSP1 acts parallel to GPX4 to inhibit ferroptosis. *Nature* 575 (7784), 688–692. doi:10.1038/s41586-019-1705-2

Bolli, E., O'Rourke, J. P., Conti, L., Lanzardo, S., Rolih, V., Christen, J. M., et al. (2018). A Virus-Like-Particle immunotherapy targeting Epitope-Specific anti-xCT expressed on cancer stem cell inhibits the progression of metastatic cancer *in vivo*. *Oncoimmunology* 7 (3), e1408746. doi:10.1080/2162402X.2017.1408746

Burk, R. F., and Hill, K. E. (2015). Regulation of selenium metabolism and transport. *Annu. Rev. Nutr.* 35, 109–134. doi:10.1146/annurev-nutr-071714-034250

Byun, J.-K., Lee, S., Kang, G. W., Lee, Y. R., Park, S. Y., Song, I.-S., et al. (2022). Macropinocytosis is an alternative pathway of cysteine acquisition and mitigates sorafenib-induced ferroptosis in hepatocellular carcinoma. *J. Exp. Clin. Cancer Res.* 41 (1), 98. doi:10.1186/s13046-022-02296-3

Cai, S., Fu, S., Zhang, W., Yuan, X., Cheng, Y., and Fang, J. (2021). SIRT6 silencing overcomes resistance to sorafenib by promoting ferroptosis in gastric cancer. *Biochem. Biophys. Res. Commun.* 577, 158–164. doi:10.1016/j.bbrc.2021.08.080

Cao, J. Y., Poddar, A., Magtanong, L., Lumb, J. H., Mileur, T. R., Reid, M. A., et al. (2019). A genome-wide haploid genetic screen identifies regulators of glutathione abundance and ferroptosis sensitivity. *Cell. Rep.* 26 (6), 1544–1556. doi:10.1016/j.celrep.2019.01.043

Cardoso, B. R., Hare, D. J., Bush, A. I., and Roberts, B. R. (2017). Glutathione peroxidase 4: A new player in neurodegeneration? *Mol. Psychiatry* 22 (3), 328–335. doi:10.1038/mp.2016.196

Carlisle, A. E., Lee, N., Matthew-Onabanjo, A. N., Spears, M. E., Park, S. J., Youkana, D., et al. (2020). Selenium detoxification is required for cancer-cell survival. *Nat. Metab.* 2 (7), 603–611. doi:10.1038/s42255-020-0224-7

Carlson, B. A., Tobe, R., Yefremova, E., Tsuji, P. A., Hoffmann, V. J., Schweizer, U., et al. (2016). Glutathione peroxidase 4 and vitamin E cooperatively prevent hepatocellular degeneration. *Redox Biol.* 9, 22–31. doi:10.1016/j.redox.2016.05.003

Chang, W.-T., Bow, Y.-D., Fu, P.-J., Li, C.-Y., Wu, C.-Y., Chang, Y.-H., et al. (2021). A marine terpenoid, heteronemin, induces both the apoptosis and ferroptosis of hepatocellular carcinoma cells and involves the ROS and MAPK pathways. *Oxid. Med. Cell. Longev.* 2021, 7689045. doi:10.1155/2021/7689045

Chaudhary, N., Choudhary, B., Shah, S., Khapare, N., Dwivedi, N., Gaikwad, A., et al. (2021). Lipocalin 2 expression promotes tumor progression and therapy resistance by inhibiting ferroptosis in colorectal cancer. *Int. J. Cancer* 149 (7), 1495–1511. doi:10.1002/ijc.33711

Chen, D., Fan, Z., Rauh, M., Buchfelder, M., Eyupoglu, I. Y., and Savaskan, N. (2017a). ATF4 promotes angiogenesis and neuronal cell death and confers ferroptosis in a xCT-dependent manner. *Oncogene* 36 (40), 5593–5608. doi:10.1038/onc.2017.146

Chen, D., Tavana, O., Chu, B., Erber, L., Chen, Y., Baer, R., et al. (2017b). NRF2 is a major target of ARF in p53-independent tumor suppression. *Mol. Cell.* 68 (1), 224–232. doi:10.1016/j.molcel.2017.09.009

Chen, H.-C., Tang, H.-H., Hsu, W.-H., Wu, S.-Y., Cheng, W.-H., Wang, B.-Y., et al. (2022). Vulnerability of triple-negative breast cancer to saponin Formosanin C-induced ferroptosis. *Antioxidants* 11 (2), 298. doi:10.3390/antiox11020298

Chen, J., and Galluzzi, L. (2018). Fighting resilient cancers with iron. *Trends Cell. Biol.* 28 (2), 77–78. doi:10.1016/j.tcb.2017.11.007

Chen, L., Qiao, L., Bian, Y., and Sun, X. (2020). GDF15 knockdown promotes erastin-induced ferroptosis by decreasing SLC7A11 expression. *Biochem. Biophys. Res. Commun.* 526 (2), 293–299. doi:10.1016/j.bbrc.2020.03.079

Chen, M.-S., Wang, S.-F., Hsu, C.-Y., Yin, P.-H., Yeh, T.-S., Lee, H.-C., et al. (2017c). CHAC1 degradation of glutathione enhances cystine-starvation-induced necroptosis and ferroptosis in human triple negative breast cancer cells via the GCN2-eIF2α-ATF4 pathway. *Oncotarget* 8 (70), 114588–114602. doi:10.18632/oncotarget.23055

Chen, M., Jiang, Y., and Sun, Y. (2021). KDM4A-mediated histone demethylation of SLC7A11 inhibits cell ferroptosis in osteosarcoma. *Biochem. Biophys. Res. Commun.* 550, 77–83. doi:10.1016/j.bbrc.2021.02.137

Chen, P.-H., Wu, J., Ding, C.-K. C., Lin, C.-C., Pan, S., Bossa, N., et al. (2020). Kinome screen of ferroptosis reveals a novel role of ATM in regulating iron metabolism. *Cell. Death Differ.* 27 (3), 1008–1022. doi:10.1038/s41418-019-0393-7

Chen, P., Li, X., Zhang, R., Liu, S., Xiang, Y., Zhang, M., et al. (2020). Combinative treatment of β-elemene and cetuximab is sensitive to KRAS mutant colorectal cancer cells by inducing ferroptosis and inhibiting epithelial-mesenchymal transformation. *Theranostics* 10 (11), 5107–5119. doi:10.7150/thno.44705

Chen, W., Xiao, W., Zhang, K., Yin, X., Lai, J., Liang, L., et al. (2016). Activation of c-Jun predicts a poor response to sorafenib in hepatocellular carcinoma: Preliminary Clinical Evidence. *Sci. Rep.* 6, 22976. doi:10.1038/srep22976

Chen, X., Kang, R., Kroemer, G., and Tang, D. (2021a). Broadening horizons: The role of ferroptosis in cancer. *Nat. Rev. Clin. Oncol.* 18 (5), 280–296. doi:10.1038/s41571-020-00462-0

Chen, X., Zeh, H. J., Kang, R., Kroemer, G., and Tang, D. (2021b). Cell death in pancreatic cancer: From pathogenesis to therapy. *Nat. Rev. Gastroenterol. Hepatol.* 18 (11), 804–823. doi:10.1038/s41575-021-00486-6

Chen, Y., Li, L., Lan, J., Cui, Y., Rao, X., Zhao, J., et al. (2022a). CRISPR screens uncover protective effect of PSTK as a regulator of chemotherapy-induced ferroptosis in hepatocellular carcinoma. *Mol. Cancer* 21 (1), 11. doi:10.1186/s12943-021-01466-9

Chen, Y., Shang, H., Wang, C., Zeng, J., Zhang, S., Wu, B., et al. (2022b). RNA-seq explores the mechanism of oxygen-boosted sonodynamic therapy based on all-in-one nanobubbles to enhance ferroptosis for the treatment of HCC. *Int. J. Nanomedicine* 17, 105–123. doi:10.2147/IJN.S343361

Chen, Y., Zhu, G., Liu, Y., Wu, Q., Zhang, X., Bian, Z., et al. (2019). O-GlcNAcylated c-Jun antagonizes ferroptosis via inhibiting GSH synthesis in liver cancer. *Cell. Signal.* 63, 109384. doi:10.1016/j.cellsig.2019.109384

Conrad, M., and Sato, H. (2012). The oxidative stress-inducible cystine/glutamate antiporter, system x (c) (-) : Cystine supplier and beyond. *Amino acids* 42 (1), 231–246. doi:10.1007/s00726-011-0867-5

Cramer, S. L., Saha, A., Liu, J., Tadi, S., Tiziani, S., Yan, W., et al. (2017). Systemic depletion of L-cyst(e)ine with cyst(e)inase increases reactive oxygen species and suppresses tumor growth. *Nat. Med.* 23 (1), 120–127. doi:10.1038/nm.4232

Cui, Z., Wang, H., Li, S., Qin, T., Shi, H., Ma, J., et al. (2022). Dihydroartemisinin enhances the inhibitory effect of sorafenib on HepG2 cells by inducing ferroptosis and inhibiting energy metabolism. *J. Pharmacol. Sci.* 148 (1), 73–85. doi:10.1016/j.jphs.2021.09.008

Daher, B., Parks, S. K., Durivault, J., Cormerais, Y., Baidarjad, H., Tambutte, E., et al. (2019). Genetic ablation of the cystine transporter xCT in PDAC cells inhibits mTORC1, growth, survival, and tumor formation via nutrient and oxidative stresses. *Cancer Res.* 79 (15), 3877–3890. doi:10.1158/0008-5472.CAN-18-3855

Dai, E., Han, L., Liu, J., Xie, Y., Zeh, H. J., Kang, R., et al. (2020). Ferroptotic damage promotes pancreatic tumorigenesis through a TMEM173/STING-dependent DNA sensor pathway. *Nat. Commun.* 11 (1), 6339. doi:10.1038/s41467-020-20154-8

Dai, Z., Huang, Y., Sadee, W., and Blower, P. (2007). Chemoinformatics analysis identifies cytotoxic compounds susceptible to chemoresistance mediated by glutathione and cystine/glutamate transport system xc. *J. Med. Chem.* 50 (8), 1896–1906. doi:10.1021/jm060960h

Deng, S.-H., Wu, D.-M., Li, L., Liu, T., Zhang, T., Li, J., et al. (2021). miR-324-3p reverses cisplatin resistance by inducing GPX4-mediated ferroptosis in lung adenocarcinoma cell line A549. *Biochem. Biophys. Res. Commun.* 549, 54–60. doi:10.1016/j.bbrc.2021.02.077

Deponte, M. (2013). Glutathione catalysis and the reaction mechanisms of glutathione-dependent enzymes. *Biochim. Biophys. Acta* 1830 (5), 3217–3266. doi:10.1016/j.bbagen.2012.09.018

Dill, M. T., Tornillo, L., Fritzius, T., Terracciano, L., Semela, D., Bettler, B., et al. (2013). Constitutive Notch2 signaling induces hepatic tumors in mice. *Hepatology* 57 (4), 1607–1619. doi:10.1002/hep.26165

Ding, Y., Chen, X., Liu, C., Ge, W., Wang, Q., Hao, X., et al. (2021). Identification of a small molecule as inducer of ferroptosis and apoptosis through ubiquitination of GPX4 in triple negative breast cancer cells. *J. Hematol. Oncol.* 14 (1), 19. doi:10.1186/s13045-020-01016-8

Dituri, F., Mancarella, S., Cigliano, A., Chieti, A., and Giannelli, G. (2019). TGF-B as multifaceted orchestrator in HCC progression: Signaling, EMT, immune microenvironment, and novel therapeutic perspectives. *Semin. Liver Dis.* 39 (1), 53–69. doi:10.1055/s-0038-1676121

Dixon, S. J., Lemberg, K. M., Lamprecht, M. R., Skouta, R., Zaitsev, E. M., Gleason, C. E., et al. (2012). Ferroptosis: An iron-dependent form of nonapoptotic cell death. *Cell.* 149 (5), 1060–1072. doi:10.1016/j.cell.2012.03.042

Dixon, S. J., Patel, D. N., Welsch, M., Skouta, R., Lee, E. D., Hayano, M., et al. (2014). Pharmacological inhibition of cystine-glutamate exchange induces endoplasmic reticulum stress and ferroptosis. *eLife* 3, e02523. doi:10.7554/eLife.02523

Dodson, M., Castro-Portuguez, R., and Zhang, D. D. (2019). NRF2 plays a critical role in mitigating lipid peroxidation and ferroptosis. *Redox Biol.* 23, 101107. doi:10.1016/j.redox.2019.101107

Doll, S., Freitas, F. P., Shah, R., Aldrovandi, M., da Silva, M. C., Ingold, I., et al. (2019). FSP1 is a glutathione-independent ferroptosis suppressor. *Nature* 575 (7784), 693–698. doi:10.1038/s41586-019-1707-0

Donofrio, G., Tebaldi, G., Lanzardo, S., Ruiu, R., Bolli, E., Ballatore, A., et al. (2018). Bovine herpesvirus 4-based vector delivering the full length xCT DNA efficiently protects mice from mammary cancer metastases by targeting cancer stem cells. *Oncoimmunology* 7 (12), e1494108. doi:10.1080/2162402X.2018.1494108

Du, X., Zhang, J., Liu, L., Xu, B., Han, H., Dai, W., et al. (2022). A novel anticancer property of *Lycium barbarum* polysaccharide in triggering ferroptosis of breast cancer cells. *J. Zhejiang Univ. Sci. B* 23 (4), 286–299. doi:10.1631/jzus.B2100748

Eaton, J. K., Furst, L., Ruberto, R. A., Moosmayer, D., Hilpmann, A., Ryan, M. J., et al. (2020). Selective covalent targeting of GPX4 using masked nitrile-oxide electrophiles. *Nat. Chem. Biol.* 16 (5), 497–506. doi:10.1038/s41589-020-0501-5

El-Tanani, M., Al Khatib, A. O., Aladwan, S. M., Abuelhana, A., McCarron, P. A., and Tambuwala, M. M. (2022). Importance of STAT3 signalling in cancer, metastasis and therapeutic interventions. *Cell. Signal.* 92, 110275. doi:10.1016/j.cellsig.2022.110275

Fan, T., Yan, Q., Huang, J., Austin, S., Cho, E., Ferris, D., et al. (2003). Lsh-deficient murine embryonal fibroblasts show reduced proliferation with signs of abnormal mitosis. *Cancer Res.* 63 (15), 4677–4683.

Fan, Z., Wirth, A. K., Chen, D., Wruck, C. J., Rauh, M., Buchfelder, M., et al. (2017). Nrf2-Keap1 pathway promotes cell proliferation and diminishes ferroptosis. *Oncogenesis* 6 (8), e371. doi:10.1038/oncsis.2017.65

Fan, Z., Yang, G., Zhang, W., Liu, Q., Liu, G., Liu, P., et al. (2021). Hypoxia blocks ferroptosis of hepatocellular carcinoma via suppression of METTL14 triggered YTHDF2-dependent silencing of SLC7A11. *J. Cell. Mol. Med.* 25 (21), 10197–10212. doi:10.1111/jcmm.16957

Fantin, V. R., and Richon, V. M. (2007). Mechanisms of resistance to histone deacetylase inhibitors and their therapeutic implications. *Clin. Cancer Res.* 13 (24), 7237–7242. doi:10.1158/1078-0432.CCR-07-2114

Fradejas, N., Carlson, B. A., Rijntjes, E., Becker, N.-P., Tobe, R., and Schweizer, U. (2013). Mammalian Trit1 is a tRNA([Ser]Sec)-isopentenyl transferase required for full selenoprotein expression. *Biochem. J.* 450 (2), 427–432. doi:10.1042/BJ20121713

Friedmann Angeli, J. P., Schneider, M., Proneth, B., Tyurina, Y. Y., Tyurin, V. A., Hammond, V. J., et al. (2014). Inactivation of the ferroptosis regulator Gpx4 triggers acute renal failure in mice. *Nat. Cell. Biol.* 16 (12), 1180–1191. doi:10.1038/ncb3064

Fu, D., Wang, C., Yu, L., and Yu, R. (2021). Induction of ferroptosis by ATF3 elevation alleviates cisplatin resistance in gastric cancer by restraining Nrf2/Keap1/xCT signaling. *Cell. Mol. Biol. Lett.* 26 (1), 26. doi:10.1186/s11658-021-00271-y

Galluzzi, L., Vitale, I., Aaronson, S. A., Abrams, J. M., Adam, D., Agostinis, P., et al. (2018). Molecular mechanisms of cell death: Recommendations of the nomenclature committee on cell death 2018. *Cell. Death Differ.* 25 (3), 486–541. doi:10.1038/s41418-017-0012-4

Gao, M., Monian, P., Quadri, N., Ramasamy, R., and Jiang, X. (2015). Glutaminolysis and transferrin regulate ferroptosis. *Mol. Cell.* 59 (2), 298–308. doi:10.1016/j.molcel.2015.06.011

Gao, R., Kalathur, R. K. R., Coto-Llerena, M., Ercan, C., Buechel, D., Shuang, S., et al. (2021). YAP/TAZ and ATF4 drive resistance to Sorafenib in hepatocellular carcinoma by preventing ferroptosis. *EMBO Mol. Med.* 13 (12), e14351. doi:10.15252/emmm.202114351

Gao, Z., Deng, G., Li, Y., Huang, H., Sun, X., Shi, H., et al. (2020). Actinidia chinensis Planch prevents proliferation and migration of gastric cancer associated with apoptosis, ferroptosis activation and mesenchymal phenotype suppression. *Biomed. Pharmacother. = Biomedecine Pharmacother.* 126, 110092. doi:10.1016/j.biopha.2020.110092

Gaschler, M. M., Andia, A. A., Liu, H., Csuka, J. M., Hurlocker, B., Vaiana, C. A., et al. (2018). FINO2 initiates ferroptosis through GPX4 inactivation and iron oxidation. *Nat. Chem. Biol.* 14 (5), 507–515. doi:10.1038/s41589-018-0031-6

Gochenauer, G. E., and Robinson, M. B. (2001). Dibutyryl-cAMP (dbcAMP) up-regulates astrocytic chloride-dependent L-[3H]glutamate transport and expression of both system xc(-) subunits. *J. Neurochem.* 78 (2), 276–286. doi:10.1046/j.1471-4159.2001.00385.x

Gridelli, C., Morabito, A., Cavanna, L., Luciani, A., Maione, P., Bonanno, L., et al. (2018). Cisplatin-based first-line treatment of elderly patients with advanced non-small-cell lung cancer: Joint analysis of MILES-3 and MILES-4 phase III trials. *J. Clin. Oncol.* 36 (25), 2585–2592. doi:10.1200/JCO.2017.76.8390

Guan, Z., Chen, J., Li, X., and Dong, N. (2020). Tanshinone IIA induces ferroptosis in gastric cancer cells through p53-mediated SLC7A11 down-regulation. *Biosci. Rep.* 40 (8), BSR20201807. doi:10.1042/BSR20201807

Guo, J., Xu, B., Han, Q., Zhou, H., Xia, Y., Gong, C., et al. (2018). Ferroptosis: A novel anti-tumor action for cisplatin. *Cancer Res. Treat.* 50 (2), 445–460. doi:10.4143/crt.2016.572

Ha, Y., Dun, Y., Thangaraju, M., Duplantier, J., Dong, Z., Liu, K., et al. (2011). Sigma receptor 1 modulates endoplasmic reticulum stress in retinal neurons. *Invest. Ophthalmol. Vis. Sci.* 52 (1), 527–540. doi:10.1167/iovs.10-5731

Habib, E., Linher-Melville, K., Lin, H. X., and Singh, G. (2015). Expression of xCT and activity of system xc(-) are regulated by NRF2 in human breast cancer cells in response to oxidative stress. *Redox Biol.* 5, 33–42. doi:10.1016/j.redox.2015.03.003

Haga, Y., Kanda, T., Nakamura, M., Nakamoto, S., Sasaki, R., Takahashi, K., et al. (2017). Overexpression of c-Jun contributes to sorafenib resistance in human hepatoma cell lines. *PloS One* 12 (3), e0174153. doi:10.1371/journal.pone.0174153

Han, N., Li, L.-G., Peng, X.-C., Ma, Q.-L., Yang, Z.-Y., Wang, X.-Y., et al. (2022). Ferroptosis triggered by dihydroartemisinin facilitates chlorin e6 induced photodynamic therapy against lung cancerthrough inhibiting GPX4 and enhancing ROS. *Eur. J. Pharmacol.* 919, 174797. doi:10.1016/j.ejphar.2022.174797

Hangauer, M. J., Viswanathan, V. S., Ryan, M. J., Bole, D., Eaton, J. K., Matov, A., et al. (2017). Drug-tolerant persister cancer cells are vulnerable to GPX4 inhibition. *Nature* 551 (7679), 247–250. doi:10.1038/nature24297

Hao, S., Yu, J., He, W., Huang, Q., Zhao, Y., Liang, B., et al. (2017). Cysteine dioxygenase 1 mediates erastin-induced ferroptosis in human gastric cancer cells. *Neoplasia (New York, N.Y.)* 19 (12), 1022–1032. doi:10.1016/j.neo.2017.10.005

Harbeck, N., and Gnant, M. (2017). Breast cancer. *Lancet (London, Engl.* 389 (10074), 1134–1150. doi:10.1016/S0140-6736(16)31891-8

Harvey, K. F., Zhang, X., and Thomas, D. M. (2013). The Hippo pathway and human cancer. *Nat. Rev. Cancer* 13 (4), 246–257. doi:10.1038/nrc3458

Hasegawa, M., Takahashi, H., Rajabi, H., Alam, M., Suzuki, Y., Yin, L., et al. (2016). Functional interactions of the cystine/glutamate antiporter, CD44v and MUC1-C oncoprotein in triple-negative breast cancer cells. *Oncotarget* 7 (11), 11756–11769. doi:10.18632/oncotarget.7598

Hatfield, D., Lee, B. J., Hampton, L., and Diamond, A. M. (1991). Selenium induces changes in the selenocysteine tRNA[Ser]Sec population in mammalian cells. *Nucleic Acids Res.* 19 (4), 939–943. doi:10.1093/nar/19.4.939

Hayano, M., Yang, W. S., Corn, C. K., Pagano, N. C., and Stockwell, B. R. (2016). Loss of cysteinyl-tRNA synthetase (CARS) induces the transsulfuration pathway and inhibits ferroptosis induced by cystine deprivation. *Cell. Death Differ.* 23 (2), 270–278. doi:10.1038/cdd.2015.93

He, G.-N., Bao, N.-R., Wang, S., Xi, M., Zhang, T.-H., and Chen, F.-S. (2021a). Ketamine induces ferroptosis of liver cancer cells by targeting lncRNA PVT1/miR-214-3p/GPX4. *Drug Des. devel. Ther.* 15, 3965–3978. doi:10.2147/DDDT.S332847

He, Y., Fang, D., Liang, T., Pang, H., Nong, Y., Tang, L., et al. (2021b). Atractylodin may induce ferroptosis of human hepatocellular carcinoma cells. *Ann. Transl. Med.* 9 (20), 1535. doi:10.21037/atm-21-4386

He, Z., Yang, J., Sui, C., Zhang, P., Wang, T., Mou, T., et al. (2022). FAM98A promotes resistance to 5-fluorouracil in colorectal cancer by suppressing ferroptosis. *Arch. Biochem. Biophys.* 722, 109216. doi:10.1016/j.abb.2022.109216

Hill, R. A., and Liu, Y.-Y. (2022). N^6 -methyladenosine-RNA methylation promotes expression of solute carrier family 7 member 11, an uptake transporter of cystine for lipid reactive oxygen species scavenger glutathione synthesis, leading to hepatoblastoma ferroptosis resistance. *Clin. Transl. Med.* 12 (5), e889. doi:10.1002/ctm2.889

Hong, Z., Tang, P., Liu, B., Ran, C., Yuan, C., Zhang, Y., et al. (2021). Ferroptosis-related genes for overall survival prediction in patients with colorectal cancer can be inhibited by gallic acid. *Int. J. Biol. Sci.* 17 (4), 942–956. doi:10.7150/ijbs.57164

Horibe, S., Kawauchi, S., Tanahashi, T., Sasaki, N., Mizuno, S., and Rikitake, Y. (2018). CD44v-dependent upregulation of xCT is involved in the acquisition of cisplatin-resistance in human lung cancer A549 cells. *Biochem. Biophys. Res. Commun.* 507 (1-4), 426–432. doi:10.1016/j.bbrc.2018.11.055

Hou, Y., Cai, S., Yu, S., and Lin, H. (2021). Metformin induces ferroptosis by targeting miR-324-3p/GPX4 axis in breast cancer. *Acta Biochim. Biophys. Sin.* 53 (3), 333–341. doi:10.1093/abbs/gmaa180

Houessinon, A., François, C., Sauzay, C., Louandre, C., Mongelard, G., Godin, C., et al. (2016). Metallothionein-1 as a biomarker of altered redox metabolism in hepatocellular carcinoma cells exposed to sorafenib. *Mol. Cancer* 15 (1), 38. doi:10.1186/s12943-016-0526-2

Hu, K., Li, K., Lv, J., Feng, J., Chen, J., Wu, H., et al. (2020). Suppression of the SLC7A11/glutathione axis causes synthetic lethality in KRAS-mutant lung adenocarcinoma. *J. Clin. Invest.* 130 (4), 1752–1766. doi:10.1172/JCI124049

Huang, W., Chen, K., Lu, Y., Zhang, D., Cheng, Y., Li, L., et al. (2021). ABCC5 facilitates the acquired resistance of sorafenib through the inhibition of SLC7A11-induced ferroptosis in hepatocellular carcinoma. *Neoplasia (New York, N.Y.)* 23 (12), 1227–1239. doi:10.1016/j.neo.2021.11.002

Huang, Y., Dai, Z., Barbacioru, C., and Sadée, W. (2005). Cystine-glutamate transporter SLC7A11 in cancer chemosensitivity and chemoresistance. *Cancer Res.* 65 (16), 7446–7454. doi:10.1158/0008-5472.CAN-04-4267

Igarashi, K., and Watanabe-Matsui, M. (2014). Wearing red for signaling: The heme-bach axis in heme metabolism, oxidative stress response and iron immunology. *Tohoku J. Exp. Med.* 232 (4), 229–253. doi:10.1620/tjem.232.229

Iida, Y., Okamoto-Katsuyama, M., Maruoka, S., Mizumura, K., Shimizu, T., Shikano, S., et al. (2021). Effective ferroptotic small-cell lung cancer cell death from SLC7A11 inhibition by sulforaphane. *Oncol. Lett.* 21 (1), 71. doi:10.3892/ol.2020.12332

Imai, H., Hakkaku, N., Iwamoto, R., Suzuki, J., Suzuki, T., Tajima, Y., et al. (2009). Depletion of selenoprotein GPx4 in spermatocytes causes male infertility in mice. *J. Biol. Chem.* 284 (47), 32522–32532. doi:10.1074/jbc.M109.016139

Imai, H., and Nakagawa, Y. (2003). Biological significance of phospholipid hydroperoxide glutathione peroxidase (PHGPx, GPx4) in mammalian cells. *Free Radic. Biol. Med.* 34 (2), 145–169. doi:10.1016/s0891-5849(02)01197-8

Ingold, I., Berndt, C., Schmitt, S., Doll, S., Poschmann, G., Buday, K., et al. (2018). Selenium utilization by GPX4 is required to prevent hydroperoxide-induced ferroptosis. *Cell.* 172 (3), 409–422. doi:10.1016/j.cell.2017.11.048

Imai, H., Sumi, D., Sakamoto, H., Hanamoto, A., Arai, M., Chiba, N., et al. (2018). Overexpression of phospholipid hydroperoxide glutathione peroxidase suppressed cell death due to oxidative damage in rat basophile leukemia cells (RBL-2H3). *Biochem. Biophys. Res. Commun.* 222 (2), 432–438. doi:10.1006/bbrc.1996.0762

Ishida, T., Takahashi, T., Kurokawa, Y., Nishida, T., Hirota, S., Serada, S., et al. (2021). Targeted therapy for drug-tolerant persister cells after imatinib treatment for gastrointestinal stromal tumours. *Br. J. Cancer* 125 (11), 1511–1522. doi:10.1038/s41416-021-01566-9

Ishimoto, T., Nagano, O., Yae, T., Tamada, M., Motohara, T., Oshima, H., et al. (2011). CD44 variant regulates redox status in cancer cells by stabilizing the xCT subunit of system xc(-) and thereby promotes tumor growth. *Cancer Cell.* 19 (3), 387–400. doi:10.1016/j.ccr.2011.01.038

Jansen, R. S., Mahakena, S., de Haas, M., Borst, P., and van de Wetering, K. (2015). ATP-Binding cassette subfamily C member 5 (ABCC5) functions as an efflux transporter of glutamate conjugates and analogs. *J. Biol. Chem.* 290 (51), 30429–30440. doi:10.1074/jbc.M115.692103

Jennis, M., Kung, C.-P., Basu, S., Budina-Kolomets, A., Leu, J. I. J., Khaku, S., et al. (2016). An African-specific polymorphism in the TP53 gene impairs p53 tumor suppressor function in a mouse model. *Genes. Dev.* 30 (8), 918–930. doi:10.1101/gad.275891.115

Jia, J., Shi, Y., Chen, L., Lai, W., Yan, B., Jiang, Y., et al. (2017). Decrease in lymphoid specific helicase and 5-hydroxymethylcytosine is associated with metastasis and genome instability. *Theranostics* 7 (16), 3920–3932. doi:10.7150/thno.21389

Jiang, L., Kon, N., Li, T., Wang, S.-J., Su, T., Hibshoosh, H., et al. (2015). Ferroptosis as a p53-mediated activity during tumour suppression. *Nature* 520 (7545), 57–62. doi:10.1038/nature14344

Jiang, Y., He, Y., Liu, S., and Tao, Y. (2017a). Chromatin remodeling factor lymphoid-specific helicase inhibits ferroptosis through lipid metabolic genes in lung cancer progression. *Chin. J. Cancer* 36 (1), 82. doi:10.1186/s40880-017-0248-x

Jiang, Y., Mao, C., Yang, R., Yan, B., Shi, Y., Liu, X., et al. (2017b). EGLN1/c-Myc induced lymphoid-specific helicase inhibits ferroptosis through lipid metabolic gene expression changes. *Theranostics* 7 (13), 3293–3305. doi:10.7150/thno.19988

Jin, M., Shi, C., Li, T., Wu, Y., Hu, C., and Huang, G. (2020). Solasonine promotes ferroptosis of hepatoma carcinoma cells via glutathione peroxidase 4-induced destruction of the glutathione redox system. *Biomed. Pharmacother. = Biomedecine Pharmacother.* 129, 110282. doi:10.1016/j.biopha.2020.110282

Jo, A., Bae, J. H., Yoon, Y. J., Chung, T. H., Lee, E.-W., Kim, Y.-H., et al. (2022). Plasma-activated medium induces ferroptosis by depleting FSP1 in human lung cancer cells. *Cell. Death Dis.* 13 (3), 212. doi:10.1038/s41419-022-04660-9

Kagan, V. E., Mao, G., Qu, F., Angeli, J. P. F., Doll, S., Croix, C. S., et al. (2017). Oxidized arachidonic and adrenic PEs navigate cells to ferroptosis. *Nat. Chem. Biol.* 13 (1), 81–90. doi:10.1038/nchembio.2238

Kang, R., Zhu, S., Zeh, H. J., Klionsky, D. J., and Tang, D. (2018). BECN1 is a new driver of ferroptosis. *Autophagy* 14 (12), 2173–2175. doi:10.1080/15548627.2018.1513758

Kasukabe, T., Honma, Y., Okabe-Kado, J., Higuchi, Y., Kato, N., and Kumakura, S. (2016). Combined treatment with cotylenin A and phenethyl isothiocyanate induces strong antitumor activity mainly through the induction of ferroptotic cell death in human pancreatic cancer cells. *Oncol. Rep.* 36 (2), 968–976. doi:10.3892/or.2016.4867

Kerins, M. J., Milligan, J., Wohlschlegel, J. A., and Ooi, A. (2018). Fumarate hydratase inactivation in hereditary leiomyomatosis and renal cell cancer is synthetic lethal with ferroptosis induction. *Cancer Sci.* 109 (9), 2757–2766. doi:10.1111/cas.13701

Kilberg, M. S., Shan, J., and Su, N. (2009). ATF4-dependent transcription mediates signaling of amino acid limitation. *Trends Endocrinol. Metab.* 20 (9), 436–443. doi:10.1016/j.tem.2009.05.008

Kim, D. H., Kim, W. D., Kim, S. K., Moon, D. H., and Lee, S. J. (2020). TGF-β1-mediated repression of SLC7A11 drives vulnerability to GPX4 inhibition in hepatocellular carcinoma cells. *Cell. Death Dis.* 11 (5), 406. doi:10.1038/s41419-020-2618-6

Koppula, P., Lei, G., Zhang, Y., Yan, Y., Mao, C., Kondiparthi, L., et al. (2022). A targetable CoQ-FSP1 axis drives ferroptosis- and radiation-resistance in KEAP1 inactive lung cancers. *Nat. Commun.* 13 (1), 2206. doi:10.1038/s41467-022-29905-1

Koppula, P., Zhang, Y., Zhuang, L., and Gan, B. (2018). Amino acid transporter SLC7A11/xCT at the crossroads of regulating redox homeostasis and nutrient dependency of cancer. *Cancer Commun.* 38 (1), 12. doi:10.1186/s40880-018-0288-x

Kuang, F., Liu, J., Tang, D., and Kang, R. (2020). Oxidative damage and antioxidant defense in ferroptosis. *Front. Cell. Dev. Biol.* 8, 586578. doi:10.3389/fcell.2020.586578

Lai, Y., Zhang, Z., Li, J., Li, W., Huang, Z., Zhang, C., et al. (2019). STYK1/NOK correlates with ferroptosis in non-small cell lung carcinoma. *Biochem. Biophys. Res. Commun.* 519 (4), 659–666. doi:10.1016/j.bbrc.2019.09.032

Larraufie, M.-H., Yang, W. S., Jiang, E., Thomas, A. G., Slusher, B. S., and Stockwell, B. R. (2015). Incorporation of metabolically stable ketones into a small molecule probe to increase potency and water solubility. *Bioorg. Med. Chem. Lett.* 25 (21), 4787–4792. doi:10.1016/j.bmcl.2015.07.018

Lee, J., Kang, E. S., Kobayashi, S., Homma, T., Sato, H., Seo, H. G., et al. (2017). The viability of primary hepatocytes is maintained under a low cysteine-glutathione redox state with a marked elevation in ophthalmic acid production. *Exp. Cell. Res.* 361 (1), 178–191. doi:10.1016/j.yexcr.2017.10.017

Lewerenz, J., Hewett, S. J., Huang, Y., Lambros, M., Gout, P. W., Kalivas, P. W., et al. (2013). The cystine/glutamate antiporter system x(c)(-) in health and disease: From molecular mechanisms to novel therapeutic opportunities. *Antioxid. Redox Signal.* 18 (5), 522–555. doi:10.1089/ars.2011.4391

Li, C., Deng, X., Zhang, W., Xie, X., Conrad, M., Liu, Y., et al. (2019). Novel allosteric activators for ferroptosis regulator glutathione peroxidase 4. *J. Med. Chem.* 62 (1), 266–275. doi:10.1021/acs.jmedchem.8b00315

Li, H., Liu, W., Zhang, X., Wu, F., Sun, D., and Wang, Z. (2021). Ketamine suppresses proliferation and induces ferroptosis and apoptosis of breast cancer cells by targeting KAT5/GPX4 axis. *Biochem. Biophys. Res. Commun.* 585, 111–116. doi:10.1016/j.bbrc.2021.11.029

Li, H., Yu, Y., Liu, Y., Luo, Z., Law, B. Y. K., Zheng, Y., et al. (2022). Ursolic acid enhances the antitumor effects of sorafenib associated with Mcl-1-related apoptosis and SLC7A11-dependent ferroptosis in human cancer. *Pharmacol. Res.* 182, 106306. doi:10.1016/j.phrs.2022.106306

Li, K., Lin, C., Li, M., Xu, K., He, Y., Mao, Y., et al. (2022). Multienzyme-like reactivity cooperatively impairs glutathione peroxidase 4 and ferroptosis suppressor protein 1 pathways in triple-negative breast cancer for sensitized ferroptosis therapy. *ACS Nano* 16 (2), 2381–2398. doi:10.1021/acsnano.1c08664

Li, Y., Yan, H., Xu, X., Liu, H., Wu, C., and Zhao, L. (2020). Erastin/sorafenib induces cisplatin-resistant non-small cell lung cancer cell ferroptosis through inhibition of the Nrf2/xCT pathway. *Oncol. Lett.* 19 (1), 323–333. doi:10.3892/ol.2019.11066

Li, Z.-J., Dai, H.-Q., Huang, X.-W., Feng, J., Deng, J.-H., Wang, Z.-X., et al. (2021). Artesunate synergizes with sorafenib to induce ferroptosis in hepatocellular carcinoma. *Acta Pharmacol. Sin.* 42 (2), 301–310. doi:10.1038/s41401-020-0478-3

Liang, X., Hu, C., Han, M., Liu, C., Sun, X., Yu, K., et al. (2022). Solasonine inhibits pancreatic cancer progression with involvement of ferroptosis induction. *Front. Oncol.* 12, 834729. doi:10.3389/fonc.2022.834729

Lin, J.-F., Hu, P.-S., Wang, Y.-Y., Tan, Y.-T., Yu, K., Liao, K., et al. (2022). Phosphorylated NFS1 weakens oxaliplatin-based chemosensitivity of colorectal cancer by preventing PANoptosis. *Signal Transduct. Target. Ther.* 7 (1), 54. doi:10.1038/s41392-022-00889-0

Lin, W., Wang, C., Liu, G., Bi, C., Wang, X., Zhou, Q., et al. (2020). SLC7A11/xCT in cancer: Biological functions and therapeutic implications. *Am. J. Cancer Res.* 10 (10), 3106–3126.

Lin, Y.-S., Shen, Y.-C., Wu, C.-Y., Tsai, Y.-Y., Yang, Y.-H., Lin, Y.-Y., et al. (2019). Danshen improves survival of patients with breast cancer and Dihydroisotanshinone I induces ferroptosis and apoptosis of breast cancer cells. *Front. Pharmacol.* 10, 1226. doi:10.3389/fphar.2019.01226

Lister, A., Nedjadi, T., Kitteringham, N. R., Campbell, F., Costello, E., Lloyd, B., et al. (2011). Nrf2 is overexpressed in pancreatic cancer: Implications for cell proliferation and therapy. *Mol. Cancer* 10, 37. doi:10.1186/1476-4598-10-37

Liu, J., Song, X., Kuang, F., Zhang, Q., Xie, Y., Kang, R., et al. (2021). NUPR1 is a critical repressor of ferroptosis. *Nat. Commun.* 12 (1), 647. doi:10.1038/s41467-021-20904-2

Liu, L., He, J., Sun, G., Huang, N., Bian, Z., Xu, C., et al. (2022). The N6-methyladenosine modification enhances ferroptosis resistance through inhibiting SLC7A11 mRNA deadenylation in hepatoblastoma. *Clin. Transl. Med.* 12 (5), e778. doi:10.1002/ctm2.778

Liu, S.-J., Zhao, Q., Peng, C., Mao, Q., Wu, F., Zhang, F.-H., et al. (2021). Design, synthesis, and biological evaluation of nitroisoxazole-containing spiro[pyrrolidin-oxindole] derivatives as novel glutathione peroxidase 4/mouse double minute 2 dual inhibitors that inhibit breast adenocarcinoma cell proliferation. *Eur. J. Med. Chem.* 217, 113359. doi:10.1016/j.ejmech.2021.113359

Liu, T., Jiang, L., Tavana, O., and Gu, W. (2019). The deubiquitylase OTUB1 mediates ferroptosis via stabilization of SLC7A11. *Cancer Res.* 79 (8), 1913–1924. doi:10.1158/0008-5472.CAN-18-3037

Liu, X., Wu, Z., Guo, C., Guo, H., Su, Y., Chen, Q., et al. (2022). Hypoxia responsive nano-drug delivery system based on angelica polysaccharide for liver cancer therapy. *Drug Deliv.* 29 (1), 138–148. doi:10.1080/10717544.2021.2021324

Liu, X., Zhu, X., Qi, X., Meng, X., and Xu, K. (2021). Co-administration of iRGD with sorafenib-loaded iron-based metal-organic framework as a targeted ferroptosis agent for liver cancer therapy. *Int. J. Nanomedicine* 16, 1037–1050. doi:10.2147/IJN.S292528

Liu, Y., Fan, X., Zhao, Z., and Shan, X. (2020). LncRNA slc7a11-AS1 contributes to lung cancer progression through facilitating TRAIP expression by inhibiting miR-4775. *Onco. Targets. Ther.* 13, 6295–6302. doi:10.2147/OTT.S253082

Liu, Y., Ouyang, L., Mao, C., Chen, Y., Li, T., Liu, N., et al. (2022). PCDHB14 promotes ferroptosis and is a novel tumor suppressor in hepatocellular carcinoma. *Oncogene* 41, 3570–3583. doi:10.1038/s41388-022-02370-2

Liu, Y., Song, Z., Liu, Y., Ma, X., Wang, W., Ke, Y., et al. (2021a). Identification of ferroptosis as a novel mechanism for antitumor activity of natural product derivative a2 in gastric cancer. *Acta Pharm. Sin. B* 11 (6), 1513–1525. doi:10.1016/j.apsb.2021.05.006

Liu, Y., Wang, Y., Liu, J., Kang, R., and Tang, D. (2021b). Interplay between MTOR and GPX4 signaling modulates autophagy-dependent ferroptotic cancer cell death. *Cancer Gene Ther.* 28 (1-2), 55–63. doi:10.1038/s41417-020-0182-y

Louandre, C., Ezzoukhry, Z., Godin, C., Barbare, J.-C., Mazière, J.-C., Chauffert, B., et al. (2013). Iron-dependent cell death of hepatocellular carcinoma cells exposed to sorafenib. *Int. J. Cancer* 133 (7), 1732–1742. doi:10.1002/ijc.28159

Louandre, C., Marcq, I., Bouhlal, H., Lachaier, E., Godin, C., Saidak, Z., et al. (2015). The retinoblastoma (Rb) protein regulates ferroptosis induced by sorafenib in human hepatocellular carcinoma cells. *Cancer Lett.* 356, 971–977. doi:10.1016/j.canlet.2014.11.014

Lu, S. C. (2013). Glutathione synthesis. *Biochim. Biophys. Acta* 1830 (5), 3143–3153. doi:10.1016/j.bbagen.2012.09.008

Lu, S. C. (2009). Regulation of glutathione synthesis. *Mol. Asp. Med.* 30 (1-2), 42–59. doi:10.1016/j.mam.2008.05.005

Lu, X., Kang, N., Ling, X., Pan, M., Du, W., and Gao, S. (2021). MiR-27a-3p promotes non-small cell lung cancer through slc7a11-mediated-ferroptosis. *Front. Oncol.* 11, 759346. doi:10.3389/fonc.2021.759346

Ma, L., Zhang, X., Yu, K., Xu, X., Chen, T., Shi, Y., et al. (2021). Targeting SLC3A2 subunit of system X_C^- is essential for m^6A reader YTHDC2 to be an endogenous ferroptosis inducer in lung adenocarcinoma. *Free Radic. Biol. Med.* 168, 25–43. doi:10.1016/j.freeradbiomed.2021.03.023

Ma, Q. (2013). Role of nrf2 in oxidative stress and toxicity. *Annu. Rev. Pharmacol. Toxicol.* 53, 401–426. doi:10.1146/annurev-pharmtox-011112-140320

Ma, S., Dielschneider, R. F., Henson, E. S., Xiao, W., Choquette, T. R., Blankstein, A. R., et al. (2017). Ferroptosis and autophagy induced cell death occur independently after siramesine and lapatinib treatment in breast cancer cells. *PloS One* 12 (8), e0182921. doi:10.1371/journal.pone.0182921

Ma, S., Henson, E. S., Chen, Y., and Gibson, S. B. (2016). Ferroptosis is induced following siramesine and lapatinib treatment of breast cancer cells. *Cell. Death Dis.* 7, e2307. doi:10.1038/cddis.2016.208

Maiorino, M., Conrad, M., and Ursini, F. (2018). GPx4, lipid peroxidation, and cell death: Discoveries, rediscoveries, and open issues. *Antioxid. Redox Signal.* 29 (1), 61–74. doi:10.1089/ars.2017.7115

Mandal, P. K., Seiler, A., Perisic, T., Kölle, P., Banjac Canak, A., Förster, H., et al. (2010). System x(c)- and thioredoxin reductase 1 cooperatively rescue glutathione deficiency. *J. Biol. Chem.* 285 (29), 22244–22253. doi:10.1074/jbc.M110.121327

Manea, A., Manea, S. A., Gafencu, A. V., and Raicu, M. (2007). Regulation of NADPH oxidase subunit p22(phox) by NF-kB in human aortic smooth muscle cells. *Arch. Physiol. Biochem.* 113 (4-5), 163–172. doi:10.1080/13813450701531235

Mao, S., Zhu, C., Nie, Y., Yu, J., and Wang, L. (2021). Levobupivacaine induces ferroptosis by miR-489-3p/slc7a11 signaling in gastric cancer. *Front. Pharmacol.* 12, 681338. doi:10.3389/fphar.2021.681338

Matsushita, M., Freigang, S., Schneider, C., Conrad, M., Bornkamm, G. W., and Kopf, M. (2015). T cell lipid peroxidation induces ferroptosis and prevents immunity to infection. *J. Exp. Med.* 212 (4), 555–568. doi:10.1084/jem.20140857

McLaughlin, R. P., He, J., van der Noord, V. E., Redel, J., Foekens, J. A., Martens, J. W. M., et al. (2019). A kinase inhibitor screen identifies a dual cdc7/CDK9 inhibitor to sensitise triple-negative breast cancer to EGFR-targeted therapy. *Breast Cancer Res.* 21 (1), 77. doi:10.1186/s13058-019-1161-9

Meira, W., Daher, B., Parks, S. K., Cormerais, Y., Durivault, J., Tambutte, E., et al. (2021). A cystine-cysteine intercellular shuttle prevents ferroptosis in xCT^{KO} pancreatic ductal adenocarcinoma cells. *Cancers* 13 (6), 1434. doi:10.3390/cancers13061434

Miao, L., Liu, K., Xie, M., Xing, Y., and Xi, T. (2014). miR-375 inhibits Helicobacter pylori-induced gastric carcinogenesis by blocking JAK2-STAT3 signaling. *Cancer Immunol. Immunother.* 63 (7), 699–711. doi:10.1007/s00262-014-1550-y

Miyamoto, K., Watanabe, M., Boku, S., Sukeno, M., Morita, M., Kondo, H., et al. (2020). xCT inhibition increases sensitivity to vorinostat in a ROS-dependent manner. *Cancers* 12 (4), E827. doi:10.3390/cancers12040827

Mostafavi-Pour, Z., Ramezani, F., Keshavarzi, F., and Samadi, N. (2017). The role of quercetin and vitamin C in Nrf2-dependent oxidative stress production in breast cancer cells. *Oncol. Lett.* 13 (3), 1965–1973. doi:10.3892/ol.2017.5619

Myant, K., Termanis, A., Sundaram, A. Y. M., Boe, T., Li, C., Merusi, C., et al. (2011). LSH and G9a/GLP complex are required for developmentally programmed DNA methylation. *Genome Res.* 21 (1), 83–94. doi:10.1101/gr.108498.110

Ni, H., Qin, H., Sun, C., Liu, Y., Ruan, G., Guo, Q., et al. (2021). MiR-375 reduces the stemness of gastric cancer cells through triggering ferroptosis. *Stem Cell. Res. Ther.* 12 (1), 325. doi:10.1186/s13287-021-02394-7

Ni, H., Ruan, G., Sun, C., Yang, X., Miao, Z., Li, J., et al. (2022). Tanshinone IIA inhibits gastric cancer cell stemness through inducing ferroptosis. *Environ. Toxicol.* 37 (2), 192–200. doi:10.1002/tox.23388

Ni, J., Chen, K., Zhang, J., and Zhang, X. (2021). Inhibition of GPX4 or mTOR overcomes resistance to Lapatinib via promoting ferroptosis in NSCLC cells. *Biochem. Biophys. Res. Commun.* 567, 154–160. doi:10.1016/j.bbrc.2021.06.051

Nishizawa, H., Matsumoto, M., Shindo, T., Saigusa, D., Kato, H., Suzuki, K., et al. (2020). Ferroptosis is controlled by the coordinated transcriptional regulation of glutathione and labile iron metabolism by the transcription factor BACH1. *J. Biol. Chem.* 295 (1), 69–82. doi:10.1074/jbc.RA119.009548

Ogiwara, H., Takahashi, K., Sasaki, M., Kuroda, T., Yoshida, H., Watanabe, R., et al. (2019). Targeting the vulnerability of glutathione metabolism in arid1a-deficient cancers. *Cancer Cell.* 35 (2), 177–190. doi:10.1016/j.ccell.2018.12.009

Ouyang, S., Li, H., Lou, L., Huang, Q., Zhang, Z., Mo, J., et al. (2022). Inhibition of STAT3-ferroptosis negative regulatory axis suppresses tumor growth and alleviates chemoresistance in gastric cancer. *Redox Biol.* 52, 102317. doi:10.1016/j.redox.2022.102317

Pakos-Zebrucka, K., Koryga, I., Mnich, K., Ljujic, M., Samali, A., and Gorman, A. M. (2016). The integrated stress response. *EMBO Rep.* 17 (10), 1374–1395. doi:10.15252/embr.201642195

Pal, A., Fontanilla, D., Gopalakrishnan, A., Chae, Y.-K., Markley, J. L., and Ruoho, A. E. (2012). The sigma-1 receptor protects against cellular oxidative stress and activates antioxidant response elements. *Eur. J. Pharmacol.* 682 (1-3), 12–20. doi:10.1016/j.ejphar.2012.01.030

Pan, C.-F., Wei, K., Ma, Z.-J., He, Y.-Z., Huang, J.-J., Guo, Z.-Z., et al. (2022). CircP4HB regulates ferroptosis via SLC7A11-mediated glutathione synthesis in lung adenocarcinoma. *Transl. Lung Cancer Res.* 11 (3), 366–380. doi:10.21037/tlcr-22-138

Parviz, F., Matullo, C., Garrison, W. D., Savatski, L., Adamson, J. W., Ning, G., et al. (2003). Hepatocyte nuclear factor 4alpha controls the development of a hepatic epithelium and liver morphogenesis. *Nat. Genet.* 34 (3), 292–296. doi:10.1038/ng1175

Patel, S. A., Warren, B. A., Rhoderick, J. F., and Bridges, R. J. (2004). Differentiation of substrate and non-substrate inhibitors of transport system xc(-): An obligate exchanger of L-glutamate and L-cystine. *Neuropharmacology* 46 (2), 273–284. doi:10.1016/j.neuropharm.2003.08.006

Peng, W.-X., and Mo, Y.-Y. (2022). Connecting N6-methyladenosine modification to ferroptosis resistance in hepatoblastoma. *Clin. Transl. Med.* 12 (4), e820. doi:10.1002/ctm2.820

Qin, Z., Ou, S., Xu, L., Sorensen, K., Zhang, Y., Hu, D.-P., et al. (2021). Design and synthesis of isothiocyanate-containing hybrid androgen receptor (AR) antagonist to downregulate AR and induce ferroptosis in GSH-Deficient prostate cancer cells. *Chem. Biol. Drug Des.* 97 (5), 1059–1078. doi:10.1111/cbdd.13826

Rademaker, G., Boumahd, Y., Peiffer, R., Anania, S., Wissocq, T., Liégeois, M., et al. (2022). Myoferlin targeting triggers mitophagy and primes ferroptosis in pancreatic cancer cells. *Redox Biol.* 53, 102324. doi:10.1016/j.redox.2022.102324

Ren, X., Li, Y., Zhou, Y., Hu, W., Yang, C., Jing, Q., et al. (2021). Overcoming the compensatory elevation of NRF2 renders hepatocellular carcinoma cells more vulnerable to disulfiram/copper-induced ferroptosis. *Redox Biol.* 46, 102122. doi:10.1016/j.redox.2021.102122

Ruiu, R., Rolih, V., Bolli, E., Barutello, G., Riccardo, F., Quaglino, E., et al. (2019). Fighting breast cancer stem cells through the immune-targeting of the xCT cystine-glutamate antiporter. *Cancer Immunol. Immunother.* 68 (1), 131–141. doi:10.1007/s00262-018-2185-1

Sang, M., Luo, R., Bai, Y., Dou, J., Zhang, Z., Liu, F., et al. (2019a). BHQ-cyanine-based "Off-On" long-circulating assembly as a ferroptosis amplifier for cancer treatment: A lipid-peroxidation burst device. *ACS Appl. Mat. Interfaces* 11 (46), 42873–42884. doi:10.1021/acsami.9b12469

Sang, M., Luo, R., Bai, Y., Dou, J., Zhang, Z., Liu, F., et al. (2019b). Mitochondrial membrane anchored photosensitive nano-device for lipid hydroperoxides burst and inducing ferroptosis to surmount therapy-resistant cancer. *Theranostics* 9 (21), 6209–6223. doi:10.7150/thno.36283

Sato, H., Nomura, S., Maebara, K., Sato, K., Tamba, M., and Bannai, S. (2004). Transcriptional control of cystine/glutamate transporter gene by amino acid deprivation. *Biochem. Biophys. Res. Commun.* 325 (1), 109–116. doi:10.1016/j.bbrc.2004.10.009

Sato, H., Tamba, M., Ishii, T., and Bannai, S. (1999). Cloning and expression of a plasma membrane cystine/glutamate exchange transporter composed of two distinct proteins. *J. Biol. Chem.* 274 (17), 11455–11458. doi:10.1074/jbc.274.17.11455

Sato, M., Kusumi, R., Hamashima, S., Kobayashi, S., Sasaki, S., Komiyama, Y., et al. (2018). The ferroptosis inducer erastin irreversibly inhibits system xc- and synergizes with cisplatin to increase cisplatin's cytotoxicity in cancer cells. *Sci. Rep.* 8 (1), 968. doi:10.1038/s41598-018-19213-4

Sato, R., Nakano, T., Hosonaga, M., Sampetrean, O., Harigai, R., Sasaki, T., et al. (2017). RNA sequencing analysis reveals interactions between breast cancer or melanoma cells and the tissue microenvironment during brain metastasis. *Biomed. Res. Int.* 2017, 8032910. doi:10.1155/2017/8032910

Saxton, R. A., and Sabatini, D. M. (2017). mTOR signaling in growth, metabolism, and disease. *Cell.* 169 (2), 361–371. doi:10.1016/j.cell.2017.03.035

Seiler, A., Schneider, M., Förster, H., Roth, S., Wirth, E. K., Culmsee, C., et al. (2008). Glutathione peroxidase 4 senses and translates oxidative stress into 12/15-lipoxygenase dependent- and AIF-mediated cell death. *Cell. Metab.* 8 (3), 237–248. doi:10.1016/j.cmet.2008.07.005

Shanshan, W., Hongying, M., Jingjing, F., Yiming, Y., Yu, R., and Rui, Y. (2021). CircDTL functions as an oncogene and regulates both apoptosis and ferroptosis in non-small cell lung cancer cells. *Front. Genet.* 12, 743505. doi:10.3389/fgene.2021.743505

Shao, M., Jiang, Q., Shen, C., Liu, Z., and Qiu, L. (2022). Sinapine induced ferroptosis in non-small cell lung cancer cells by upregulating transferrin/transferrin receptor and downregulating SLC7A11. *Gene* 827, 146460. doi:10.1016/j.gene.2022.146460

Shen, L.-D., Qi, W.-H., Bai, J.-J., Zuo, C.-Y., Bai, D.-L., Gao, W.-D., et al. (2021). Resibufogenin inhibited colorectal cancer cell growth and tumorigenesis through triggering ferroptosis and ROS production mediated by GPX4 inactivation. *Anat. Rec.* 304 (2), 313–322. doi:10.1002/ar.24378

Shimada, K., Skouta, R., Kaplan, A., Yang, W. S., Hayano, M., Dixon, S. J., et al. (2016). Global survey of cell death mechanisms reveals metabolic regulation of ferroptosis. *Nat. Chem. Biol.* 12 (7), 497–503. doi:10.1038/nchembio.2079

Shimada, K., and Stockwell, B. R. (2016). tRNA synthase suppression activates de novo cysteine synthesis to compensate for cystine and glutathione deprivation during ferroptosis. *Mol. Cell. Oncol.* 3 (2), e1091059. doi:10.1080/23723556.2015.1091059

Shin, D., Kim, E. H., Lee, J., and Roh, J.-L. (2018). Nrf2 inhibition reverses resistance to GPX4 inhibitor-induced ferroptosis in head and neck cancer. *Free Radic. Biol. Med.* 129, 454–462. doi:10.1016/j.freeradbiomed.2018.10.426

Singh, T., Beatty, A., and Peterson, J. R. (2022). The AMPK-related kinase NUAK2 suppresses glutathione peroxidase 4 expression and promotes ferroptotic cell death in breast cancer cells. *Cell. Death Discov.* 8 (1), 253. doi:10.1038/s41420-022-01044-y

Song, R., Li, T., Ye, J., Sun, F., Hou, B., Saeed, M., et al. (2021). Acidity-activatable dynamic nanoparticles boosting ferroptotic cell death for immunotherapy of cancer. *Adv. Mat.* 33 (31), e2101155. doi:10.1002/adma.202101155

Song, X., Wang, X., Liu, Z., and Yu, Z. (2020). Role of GPX4-mediated ferroptosis in the sensitivity of triple negative breast cancer cells to gefitinib. *Front. Oncol.* 10, 597434. doi:10.3389/fonc.2020.597434

Song, X., Zhu, S., Chen, P., Hou, W., Wen, Q., Liu, J., et al. (2018). AMPK-mediated BECN1 phosphorylation promotes ferroptosis by directly blocking system xc- activity. *Curr. Biol.* 28 (15), 2388–2399. doi:10.1016/j.cub.2018.05.094

Stehling, O., Wilbrecht, C., and Lill, R. (2014). Mitochondrial iron-sulfur protein biogenesis and human disease. *Biochimie* 100, 61–77. doi:10.1016/j.biochi.2014.01.010

Stipanuk, M. H., Ueki, I., Dominy, J. E., Simmons, C. R., and Hirschberger, L. L. (2009). Cysteine dioxygenase: A robust system for regulation of cellular cysteine levels. *Amino Acids* 37 (1), 55–63. doi:10.1007/s00726-008-0202-y

Stockwell, B. R., and Jiang, X. (2020). The chemistry and biology of ferroptosis. *Cell. Chem. Biol.* 27 (4), 365–375. doi:10.1016/j.chembiol.2020.03.013

Sui, S., Zhang, J., Xu, S., Wang, Q., Wang, P., and Pang, D. (2019). Ferritinophagy is required for the induction of ferroptosis by the bromodomain protein BRD4 inhibitor (+)-JQ1 in cancer cells. *Cell. Death Dis.* 10 (5), 331. doi:10.1038/s41419-019-1564-7

Sui, X., Zhang, R., Liu, S., Duan, T., Zhai, L., Zhang, M., et al. (2018). RSL3 drives ferroptosis through GPX4 inactivation and ROS production in colorectal cancer. *Front. Pharmacol.* 9, 1371. doi:10.3389/fphar.2018.01371

Sun, C., Liu, P., Pei, L., Zhao, M., and Huang, Y. (2022). Propofol inhibits proliferation and augments the anti-tumor effect of doxorubicin and paclitaxel partly through promoting ferroptosis in triple-negative breast cancer cells. *Front. Oncol.* 12, 837974. doi:10.3389/fonc.2022.837974

Sun, X., Niu, X., Chen, R., He, W., Chen, D., Kang, R., et al. (2016a). Metallothionein-1G facilitates sorafenib resistance through inhibition of ferroptosis. *Hepatology* 64 (2), 488–500. doi:10.1002/hep.28574

Sun, X., Ou, Z., Chen, R., Niu, X., Chen, D., Kang, R., et al. (2016b). Activation of the p62-Keap1-NRF2 pathway protects against ferroptosis in hepatocellular carcinoma cells. *Hepatology* 63 (1), 173–184. doi:10.1002/hep.28251

Sun, Y., Deng, R., and Zhang, C. (2020). Erastin induces apoptotic and ferroptotic cell death by inducing ROS accumulation by causing mitochondrial dysfunction in gastric cancer cell HGC27. *Mol. Med. Rep.* 22 (4), 2826–2832. doi:10.3892/mmr.2020.11376

Tan, S., Sagara, Y., Liu, Y., Maher, P., and Schubert, D. (1998). The regulation of reactive oxygen species production during programmed cell death. *J. Cell. Biol.* 141 (6), 1423–1432. doi:10.1083/jcb.141.6.1423

Tang, D., Chen, X., Kang, R., and Kroemer, G. (2021). Ferroptosis: Molecular mechanisms and health implications. *Cell. Res.* 31 (2), 107–125. doi:10.1038/s41422-020-00441-1

Tang, H., Chen, D., Li, C., Zheng, C., Wu, X., Zhang, Y., et al. (2019). Dual GSH-exhausting sorafenib loaded manganese-silica nanodrugs for inducing the ferroptosis of hepatocellular carcinoma cells. *Int. J. Pharm.* 572, 118782. doi:10.1016/j.ijpharm.2019.118782

Tang, H., Li, C., Zhang, Y., Zheng, H., Cheng, Y., Zhu, J., et al. (2020). Targeted Manganese doped silica nano GSH-cleaner for treatment of Liver Cancer by destroying the intracellular redox homeostasis. *Theranostics* 10 (21), 9865–9887. doi:10.7150/thno.46771

Tang, X., Ding, H., Liang, M., Chen, X., Yan, Y., Wan, N., et al. (2021). Curcumin induces ferroptosis in non-small-cell lung cancer via activating autophagy. *Thorac. Cancer* 12 (8), 1219–1230. doi:10.1111/1759-7714.13904

Timmerman, L. A., Holton, T., Yuneva, M., Louie, R. J., Padro, M., Daemen, A., et al. (2013). Glutamine sensitivity analysis identifies the xCT antiporter as a common triple-negative breast tumor therapeutic target. *Cancer Cell.* 24 (4), 450–465. doi:10.1016/j.ccr.2013.08.020

Tsuchihashi, K., Okazaki, S., Ohmura, M., Ishikawa, M., Sampetrean, O., Onishi, N., et al. (2016). The EGF receptor promotes the malignant potential of glioma by regulating amino acid transport system xc(-). *Cancer Res.* 76 (10), 2954–2963. doi:10.1158/0008-5472.CAN-15-2121

Ubaid, U., Andrabi, S. B. A., Tripathi, S. K., Dirasantha, O., Kanduri, K., Rautio, S., et al. (2018). Transcriptional repressor HIC1 contributes to suppressive function

of human induced regulatory T cells. *Cell. Rep.* 22 (8), 2094–2106. doi:10.1016/j.celrep.2018.01.070

Ubellacker, J. M., Tasdogan, A., Ramesh, V., Shen, B., Mitchell, E. C., Martin-Sandoval, M. S., et al. (2020). Lymph protects metastasizing melanoma cells from ferroptosis. *Nature* 585 (7823), 113–118. doi:10.1038/s41586-020-2623-z

Ueta, T., Inoue, T., Furukawa, T., Tamaki, Y., Nakagawa, Y., Imai, H., et al. (2012). Glutathione peroxidase 4 is required for maturation of photoreceptor cells. *J. Biol. Chem.* 287 (10), 7675–7682. doi:10.1074/jbc.M111.335174

Ursini, F., and Maiorino, M. (2020). Lipid peroxidation and ferroptosis: The role of GSH and GPx4. *Free Radic. Biol. Med.* 152, 175–185. doi:10.1016/j.freeradbiomed.2020.02.027

Ursini, F., Maiorino, M., Valente, M., Ferri, L., and Gregolin, C. (1982). Purification from pig liver of a protein which protects liposomes and biomembranes from peroxidative degradation and exhibits glutathione peroxidase activity on phosphatidylcholine hydroperoxides. *Biochim. Biophys. Acta* 710 (2), 197–211. doi:10.1016/0005-2760(82)90150-3

Villalpando-Rodriguez, G. E., Blankstein, A. R., Konzelman, C., and Gibson, S. B. (2019). Lysosomal destabilizing drug siramesine and the dual tyrosine kinase inhibitor lapatinib induce a synergistic ferroptosis through reduced heme oxygenase-1 (HO-1) levels. *Oxid. Med. Cell. Longev.* 2019, 9561281. doi:10.1155/2019/9561281

Viswanathan, V. S., Ryan, M. J., Dhruv, H. D., Gill, S., Eichhoff, O. M., Seashore-Ludlow, B., et al. (2017). Dependency of a therapy-resistant state of cancer cells on a lipid peroxidase pathway. *Nature* 547 (7664), 453–457. doi:10.1038/nature23007

Vučković, A.-M., Bosello Travain, V., Bordin, L., Cozza, G., Miotto, G., Rossetto, M., et al. (2020). Inactivation of the glutathione peroxidase GPx4 by the ferroptosis-inducing molecule RSL3 requires the adaptor protein 14-3-3ε. *FEBS Lett.* 594 (4), 611–624. doi:10.1002/1873-3468.13631

Wang, H., Liu, C., Zhao, Y., Zhang, W., Xu, K., Li, D., et al. (2020a). Inhibition of LONP1 protects against erastin-induced ferroptosis in Pancreatic ductal adenocarcinoma PANC1 cells. *Biochem. Biophys. Res. Commun.* 522 (4), 1063–1068. doi:10.1016/j.bbrc.2019.11.187

Wang, K., Zhang, Z., Tsai, H.-I., Liu, Y., Gao, J., Wang, M., et al. (2021a). Branched-chain amino acid aminotransferase 2 regulates ferroptotic cell death in cancer cells. *Cell. Death Differ.* 28 (4), 1222–1236. doi:10.1038/s41418-020-00644-4

Wang, L., Liu, Y., Du, T., Yang, H., Lei, L., Guo, M., et al. (2020b). ATF3 promotes erastin-induced ferroptosis by suppressing system Xc(.). *Cell. Death Differ.* 27 (2), 662–675. doi:10.1038/s41418-019-0380-z

Wang, M., Mao, C., Ouyang, L., Liu, Y., Lai, W., Liu, N., et al. (2019). Long noncoding RNA LINC00336 inhibits ferroptosis in lung cancer by functioning as a competing endogenous RNA. *Cell. Death Differ.* 26 (11), 2329–2343. doi:10.1038/s41418-019-0304-y

Wang, Q., Bin, C., Xue, Q., Gao, Q., Huang, A., Wang, K., et al. (2021a). GSTZ1 sensitizes hepatocellular carcinoma cells to sorafenib-induced ferroptosis via inhibition of NRF2/GPX4 axis. *Cell. Death Dis.* 12 (5), 426. doi:10.1038/s41419-021-03718-4

Wang, Q., Guo, Y., Wang, W., Liu, B., Yang, G., Xu, Z., et al. (2021b). RNA binding protein DAZAP1 promotes HCC progression and regulates ferroptosis by interacting with SLC7A11 mRNA. *Exp. Cell. Res.* 399 (1), 112453. doi:10.1016/j.yexcr.2020.112453

Wang, R., Xing, R., Su, Q., Yin, H., Wu, D., Lv, C., et al. (2021). Knockdown of SFRS9 inhibits progression of colorectal cancer through triggering ferroptosis mediated by GPX4 reduction. *Front. Oncol.* 11, 683589. doi:10.3389/fonc.2021.683589

Wang, S., Li, F., Qiao, R., Hu, X., Liao, H., Chen, L., et al. (2018). Arginine-rich manganese silicate nanobubbles as a ferroptosis-inducing agent for tumor-targeted theranostics. *ACS Nano* 12 (12), 12380–12392. doi:10.1021/acsnano.8b06399

Wang, X., Chen, Y., Wang, X., Tian, H., Wang, Y., Jin, J., et al. (2021). Stem cell factor SOX2 confers ferroptosis resistance in lung cancer via upregulation of SLC7A11. *Cancer Res.* 81 (20), 5217–5229. doi:10.1158/0008-5472.CAN-21-0567

Wang, X., Li, Y., Li, Z., Lin, S., Wang, H., Sun, J., et al. (2022). Mitochondrial calcium uniporter drives metastasis and confers a targetable cystine dependency in pancreatic cancer. *Cancer Res.* 82 (12), 2254–2268. doi:10.1158/0008-5472.CAN-21-3230

Wang, Y., Yang, L., Zhang, X., Cui, W., Liu, Y., Sun, Q.-R., et al. (2019b). Epigenetic regulation of ferroptosis by H2B monoubiquitination and p53. *EMBO Rep.* 20 (7), e47563. doi:10.15252/embr.201847563

Wang, Y., Zhao, Y., Wang, H., Zhang, C., Wang, M., Yang, Y., et al. (2020c). Histone demethylase KDM3B protects against ferroptosis by upregulating SLC7A11. *FEBS Open Bio* 10 (4), 637–643. doi:10.1002/2211-5463.12823

Wang, Z., Zhang, X., Tian, X., Yang, Y., Ma, L., Wang, J., et al. (2021). CREB stimulates GPX4 transcription to inhibit ferroptosis in lung adenocarcinoma. *Oncol. Rep.* 45 (6), 88. doi:10.3892/or.2021.8039

Welsh, J. B., Sapinoso, L. M., Kern, S. G., Brown, D. A., Liu, T., Bauskin, A. R., et al. (2003). Large-scale delineation of secreted protein biomarkers overexpressed in cancer tissue and serum. *Proc. Natl. Acad. Sci. U. S. A.* 100 (6), 3410–3415. doi:10.1073/pnas.0530278100

Welsh, J. B., Sapinoso, L. M., Su, A. I., Kern, S. G., Wang-Rodriguez, J., Moskaluk, C. A., et al. (2001). Analysis of gene expression identifies candidate markers and pharmacological targets in prostate cancer. *Cancer Res.* 61 (16), 5974–5978.

Wortmann, M., Schneider, M., Pircher, J., Hellfritsch, J., Aichler, M., Vegi, N., et al. (2013). Combined deficiency in glutathione peroxidase 4 and vitamin E causes multiorgan thrombus formation and early death in mice. *Circ. Res.* 113 (4), 408–417. doi:10.1161/CIRCRESAHA.113.279984

Wu, C.-Y., Yang, Y.-H., Lin, Y.-S., Chang, G.-H., Tsai, M.-S., Hsu, C.-M., et al. (2021). Dihydroisotanshinone I induced ferroptosis and apoptosis of lung cancer cells. *Biomed. Pharmacother. = Biomedecine Pharmacother.* 139, 111585. doi:10.1016/j.biopha.2021.111585

Xia, Y., Liu, S., Li, C., Ai, Z., Shen, W., Ren, W., et al. (2020). Discovery of a novel ferroptosis inducer-talaroconvolutin A-killing colorectal cancer cells *in vitro* and *in vivo*. *Cell. Death Dis.* 11 (11), 988. doi:10.1038/s41419-020-03194-2

Xiao, R., Wang, S., Guo, J., Liu, S., Ding, A., Wang, G., et al. (2022). Ferroptosis-related gene NOX4, CHAC1 and HIF1A are valid biomarkers for stomach adenocarcinoma. *J. Cell. Mol. Med.* 26 (4), 1183–1193. doi:10.1111/jcmm.17171

Xiao, X., Yeoh, B. S., and Vijay-Kumar, M. (2017). Lipocalin 2: An emerging player in iron homeostasis and inflammation. *Annu. Rev. Nutr.* 37, 103–130. doi:10.1146/annurev-nutr-071816-064559

Xu, R., Wu, J., Luo, Y., Wang, Y., Tian, J., Teng, W., et al. (2022). Sanguinarine represses the growth and metastasis of non-small cell lung cancer by facilitating ferroptosis. *Curr. Pharm. Des.* 28 (9), 760–768. doi:10.2174/1381612828666220217124542

Xu, T., Ma, Y., Yuan, Q., Hu, H., Hu, X., Qian, Z., et al. (2020). Enhanced ferroptosis by oxygen-boosted phototherapy based on a 2-in-1 nanoplatform of ferrous hemoglobin for tumor synergistic therapy. *ACS Nano* 14 (3), 3414–3425. doi:10.1021/acsnano.9b09426

Xu, Y., Lv, D., Yan, C., Su, H., Zhang, X., Shi, Y., et al. (2022). METTL3 promotes lung adenocarcinoma tumor growth and inhibits ferroptosis by stabilizing SLC7A11 m^6A modification. *Cancer Cell. Int.* 22 (1), 11. doi:10.1186/s12935-021-02433-6

Yadav, P., Sharma, P., Sundaram, S., Venkatraman, G., Bera, A. K., and Karunagaran, D. (2021). SLC7A11/xCT is a target of miR-5096 and its restoration partially rescues miR-5096-mediated ferroptosis and anti-tumor effects in human breast cancer cells. *Cancer Lett.* 522, 211–224. doi:10.1016/j.canlet.2021.09.033

Yamaguchi, Y., Kasukabe, T., and Kumakura, S. (2018). Piperlongumine rapidly induces the death of human pancreatic cancer cells mainly through the induction of ferroptosis. *Int. J. Oncol.* 52 (3), 1011–1022. doi:10.3892/ijo.2018.4259

Yan, W.-Y., Cai, J., Wang, J.-N., Gong, Y.-S., and Ding, X.-B. (2022). Co-treatment of betulin and gefitinib is effective against EGFR wild-type/KRAS-mutant non-small cell lung cancer by inducing ferroptosis. *Neoplasma* 69 (3), 648–656. doi:10.4149/neo_2022_211103N1568

Yang, C., Zhang, Y., Lin, S., Liu, Y., and Li, W. (2021). Suppressing the KIF20A/NUAK1/Nrf2/GPX4 signaling pathway induces ferroptosis and enhances the sensitivity of colorectal cancer to oxaliplatin. *Aging* 13 (10), 13515–13534. doi:10.18632/aging.202774

Yang, G., Guan, W., Cao, Z., Guo, W., Xiong, G., Zhao, F., et al. (2021). Integrative genomic analysis of gemcitabine resistance in pancreatic cancer by patient-derived xenograft models. *Clin. Cancer Res.* 27 (12), 3383–3396. doi:10.1158/1078-0432.CCR-19-3975

Yang, J., Zhou, Y., Xie, S., Wang, J., Li, Z., Chen, L., et al. (2021). Metformin induces Ferroptosis by inhibiting UFMylation of SLC7A11 in breast cancer. *J. Exp. Clin. Cancer Res.* 40 (1), 206. doi:10.1186/s13046-021-02012-7

Yang, L., Chen, X., Yang, Q., Chen, J., Huang, Q., Yao, L., et al. (2020). Broad spectrum deubiquitinase inhibition induces both apoptosis and ferroptosis in cancer cells. *Front. Oncol.* 10, 949. doi:10.3389/fonc.2020.00949

Yang, W.-H., Ding, C.-K. C., Sun, T., Rupprecht, G., Lin, C.-C., Hsu, D., et al. (2019). The Hippo pathway effector TAZ regulates ferroptosis in renal cell carcinoma. *Cell. Rep.* 28 (10), 2501–2508. doi:10.1016/j.celrep.2019.07.107

Yang, W. S., Kim, K. J., Gaschler, M. M., Patel, M., Shchepinov, M. S., and Stockwell, B. R. (2016). Peroxidation of polyunsaturated fatty acids by lipoxygenases drives ferroptosis. *Proc. Natl. Acad. Sci. U. S. A.* 113 (34), E4966–E4975. doi:10.1073/pnas.1603244113

Yang, W. S., SriRamaratnam, R., Welsch, M. E., Shimada, K., Skouta, R., Viswanathan, V. S., et al. (2014). Regulation of ferroptotic cancer cell death by GPX4. *Cell.* 156 (1-2), 317–331. doi:10.1016/j.cell.2013.12.010

Yang, Y., Lin, J., Guo, S., Xue, X., Wang, Y., Qiu, S., et al. (2020). RRM2 protects against ferroptosis and is a tumor biomarker for liver cancer. *Cancer Cell. Int.* 20 (1), 587. doi:10.1186/s12935-020-01689-8

Ye, L. F., Chaudhary, K. R., Zandkarimi, F., Harken, A. D., Kinslow, C. J., Upadhyayula, P. S., et al. (2020). Radiation-induced lipid peroxidation triggers ferroptosis and synergizes with ferroptosis inducers. *ACS Chem. Biol.* 15 (2), 469–484. doi:10.1021/acschembio.9b00939

Yin, J., Lin, Y., Fang, W., Zhang, X., Wei, J., Hu, G., et al. (2022). Tetrandrine citrate suppresses breast cancer *via* depletion of glutathione peroxidase 4 and activation of nuclear receptor coactivator 4-mediated ferritinophagy. *Front. Pharmacol.* 13, 820593. doi:10.3389/fphar.2022.820593

Yu, H., Yang, C., Jian, L., Guo, S., Chen, R., Li, K., et al. (2019). Sulfasalazine-induced ferroptosis in breast cancer cells is reduced by the inhibitory effect of estrogen receptor on the transferrin receptor. *Oncol. Rep.* 42 (2), 826–838. doi:10.3892/or.2019.7189

Yu, M., Gai, C., Li, Z., Ding, D., Zheng, J., Zhang, W., et al. (2019). Targeted exosome-encapsulated erastin induced ferroptosis in triple negative breast cancer cells. *Cancer Sci.* 110 (10), 3173–3182. doi:10.1111/cas.14181

Yu, W., McIntosh, C., Lister, R., Zhu, I., Han, Y., Ren, J., et al. (2014). Genome-wide DNA methylation patterns in LSH mutant reveals de-repression of repeat elements and redundant epigenetic silencing pathways. *Genome Res.* 24 (10), 1613–1623. doi:10.1101/gr.172015.114

Yuan, B., Liao, F., Shi, Z.-Z., Ren, Y., Deng, X.-L., Yang, T.-T., et al. (2020). Dihydroartemisinin inhibits the proliferation, colony formation and induces ferroptosis of lung cancer cells by inhibiting PRIM2/slc7a11 Axis. *Onco. Targets. Ther.* 13, 10829–10840. doi:10.2147/OTT.S248492

Zeng, Y.-Y., Luo, Y.-B., Ju, X.-D., Zhang, B., Cui, Y.-J., Pan, Y.-B., et al. (2022). Solasonine causes redox imbalance and mitochondrial oxidative stress of ferroptosis in lung adenocarcinoma. *Front. Oncol.* 12, 874900. doi:10.3389/fonc.2022.874900

Zeuner, A., Todaro, M., Stassi, G., and De Maria, R. (2014). Colorectal cancer stem cells: From the crypt to the clinic. *Cell. Stem Cell.* 15 (6), 692–705. doi:10.1016/j.stem.2014.11.012

Zhai, F.-G., Liang, Q.-C., Wu, Y.-Y., Liu, J.-Q., and Liu, J.-W. (2022). Red ginseng polysaccharide exhibits anticancer activity through GPX4 downregulation-induced ferroptosis. *Pharm. Biol.* 60 (1), 909–914. doi:10.1080/13880209.2022.2066139

Zhang, J., Gao, M., Niu, Y., and Sun, J. (2022a). From DNMT1 degrader to ferroptosis promoter: Drug repositioning of 6-Thioguanine as a ferroptosis inducer in gastric cancer. *Biochem. Biophys. Res. Commun.* 603, 75–81. doi:10.1016/j.bbrc.2022.03.026

Zhang, J., Gao, R.-F., Li, J., Yu, K.-d., and Bi, K.-X. (2022b). Alloimperatorin activates apoptosis, ferroptosis and oxeiptosis to inhibit the growth and invasion of breast cancer cells *in vitro*. *Biochem. Cell. Biol.* 100 (3), 213–222. doi:10.1139/bcb-2021-0399

Zhang, L., Li, C., Zhang, Y., Zhang, J., and Yang, X. (2022). Ophiopogonin B induces gastric cancer cell death by blocking the GPX4/xCT-dependent ferroptosis pathway. *Oncol. Lett.* 23 (3), 104. doi:10.3892/ol.2022.13224

Zhang, Q., Yi, H., Yao, H., Lu, L., He, G., Wu, M., et al. (2021). Artemisinin derivatives inhibit non-small cell lung cancer cells through induction of ROS-dependent apoptosis/ferroptosis. *J. Cancer* 12 (13), 4075–4085. doi:10.7150/jca.57054

Zhang, T., Sun, B., Zhong, C., Xu, K., Wang, Z., Hofman, P., et al. (2021). Targeting histone deacetylase enhances the therapeutic effect of Erastin-induced ferroptosis in *EGFR*-activating mutant lung adenocarcinoma. *Transl. Lung Cancer Res.* 10 (4), 1857–1872. doi:10.21037/tlcr-21-303

Zhang, W., Jiang, B., Liu, Y., Xu, L., and Wan, M. (2022). Bufotalin induces ferroptosis in non-small cell lung cancer cells by facilitating the ubiquitination and degradation of GPX4. *Free Radic. Biol. Med.* 180, 75–84. doi:10.1016/j.freeradbiomed.2022.01.009

Zhang, W., Sun, Y., Bai, L., Zhi, L., Yang, Y., Zhao, Q., et al. (2021). RBMS1 regulates lung cancer ferroptosis through translational control of SLC7A11. *J. Clin. Invest.* 131 (22), e152067. doi:10.1172/JCI152067

Zhang, X., Du, L., Qiao, Y., Zhang, X., Zheng, W., Wu, Q., et al. (2019). Ferroptosis is governed by differential regulation of transcription in liver cancer. *Redox Biol.* 24, 101211. doi:10.1016/j.redox.2019.101211

Zhang, X., Ma, Y., Ma, J., Yang, L., Song, Q., Wang, H., et al. (2022). Glutathione peroxidase 4 as a therapeutic target for anti-colorectal cancer drug-tolerant persister cells. *Front. Oncol.* 12, 913669. doi:10.3389/fonc.2022.913669

Zhang, X., Sui, S., Wang, L., Li, H., Zhang, L., Xu, S., et al. (2020). Inhibition of tumor propellant glutathione peroxidase 4 induces ferroptosis in cancer cells and enhances anticancer effect of cisplatin. *J. Cell. Physiol.* 235 (4), 3425–3437. doi:10.1002/jcp.29232

Zhang, Y., Shi, J., Liu, X., Feng, L., Gong, Z., Koppula, P., et al. (2018). BAP1 links metabolic regulation of ferroptosis to tumour suppression. *Nat. Cell. Biol.* 20 (10), 1181–1192. doi:10.1038/s41556-018-0178-0

Zhang, Y., Swanda, R. V., Nie, L., Liu, X., Wang, C., Lee, H., et al. (2021). mTORC1 couples cyst(e)ine availability with GPX4 protein synthesis and ferroptosis regulation. *Nat. Commun.* 12 (1), 1589. doi:10.1038/s41467-021-21841-w

Zhao, L., Peng, Y., He, S., Li, R., Wang, Z., Huang, J., et al. (2021). Apatinib induced ferroptosis by lipid peroxidation in gastric cancer. *Gastric Cancer* 24 (3), 642–654. doi:10.1007/s10120-021-01159-8

Zhou, L., Chen, J., Li, R., Wei, L., Xiong, H., Wang, C., et al. (2021). Metal-polyphenol-network coated prussian blue nanoparticles for synergistic ferroptosis and apoptosis via triggered GPX4 inhibition and concurrent *in situ* bleomycin toxification. *Small (Weinheim Der Bergstrasse, Ger.* 17 (47), e2103919. doi:10.1002/smll.202103919

Zhou, W., Zhang, J., Yan, M., Wu, J., Lian, S., Sun, K., et al. (2021). Orlistat induces ferroptosis-like cell death of lung cancer cells. *Front. Med.* 15 (6), 922–932. doi:10.1007/s11684-020-0804-7

Zhou, Y., Yang, J., Chen, C., Li, Z., Chen, Y., Zhang, X., et al. (2021). Polyphyllin Ⅲ-Induced ferroptosis in MDA-MB-231 triple-negative breast cancer cells can Be protected against by KLF4-mediated upregulation of xCT. *Front. Pharmacol.* 12, 670224. doi:10.3389/fphar.2021.670224

Zhou, Z., Liang, H., Yang, R., Yang, Y., Dong, J., Di, Y., et al. (2022). Glutathione depletion-induced activation of dimersomes for potentiating the ferroptosis and immunotherapy of "cold" tumor. *Angew. Chem. Int. Ed. Engl.* 61 (22), e202202843. doi:10.1002/anie.202202843

Zhu, S., Zhang, Q., Sun, X., Zeh, H. J., Lotze, M. T., Kang, R., et al. (2017). HSPA5 regulates ferroptotic cell death in cancer cells. *Cancer Res.* 77 (8), 2064–2077. doi:10.1158/0008-5472.CAN-16-1979

Zhu, Y.-J., Zheng, B., Wang, H.-Y., and Chen, L. (2017). New knowledge of the mechanisms of sorafenib resistance in liver cancer. *Acta Pharmacol. Sin.* 38 (5), 614–622. doi:10.1038/aps.2017.5

Zou, Y., Palte, M. J., Deik, A. A., Li, H., Eaton, J. K., Wang, W., et al. (2019). A GPX4-dependent cancer cell state underlies the clear-cell morphology and confers sensitivity to ferroptosis. *Nat. Commun.* 10 (1), 1617. doi:10.1038/s41467-019-09277-9

Zuo, T., Fang, T., Zhang, J., Yang, J., Xu, R., Wang, Z., et al. (2021). pH-sensitive molecular-switch-containing polymer nanoparticle for breast cancer therapy with ferritinophagy-cascade ferroptosis and tumor immune activation. *Adv. Healthc. Mat.* 10 (21), e2100683. doi:10.1002/adhm.202100683

Glossary

AREs antioxidant response elements
AARE amino acid response element
ATF3 Activating transcription factor 3
ATF4 Activating transcription factor 4
ABCC5 ATP-binding Cassette Subfamily C Member 5
AIFM2 apoptosis-inducing factor mitochondria-associated 2
BRD4 Bromodomain-containing protein 4
BSO buthionine sulfoxide
BACH1 BTB and CNC homology 1
CGL cystathionine γ-lyase
BCAT2 Branched-chain amino acid aminotransferase 2
CREB cyclic adenosine monophosphate response element binding protein
CHaC1 Gamma-Glutamylcyclotransferase 1
CDO1 Cysteine dioxygenase 1
CRC colorectal cancer
CSCs colorectal cancer stem cells
CoQ10 coenzyme Q10
DUB deubiquitinase
DAZAP1 DAZ Associated Protein 1
EGFR Epidermal Growth Factor Receptor
EP300 E1A binding protein P300
GSH glutathione
FSP1 Ferroptosis suppressor protein 1
GPX4 glutathione peroxidase 4
GCL glutamate cysteine ligase
GSS glutathione synthetase
GCLC Glutamate-Cysteine ligase Catalytic Subunit
GCLM Glutamate-Cysteine ligase Modifier Subunit
GC gastric cancer
GSTZ1 Glutathione S-transferase zeta 1
GDF15 Growth/differentiation factor 15
H3K9 H3 lysine 9
HSPA5 Heat shock protein A family member 5
HDACI histone deacetylase inhibitor
HCC Hepatocellular Carcinoma
HNF4α hepatocyte nuclear factor 4α
HIC1 HIC ZBTB Transcriptional Repressor 1
HBV hepatitis B virus
IKE imidazole ketone Erastin
IPP isopentenyl pyrophosphate
Keap1 Kelch-like ECH-associated protein 1
KRAS Kirsten Rat Sarcoma
LOX lipoxygenase
LOOHs lipid hydroperoxides
LCN2 Lipocalin 2Lipocalin 2
LUAD lung adenocarcinoma
LONP1 Lon peptidase 1
LCN2 Lipocalin 2Lipocalin 2
LSH Lymphoid-specific helicase
MDA malondialdehyde
MUC1 mucin glycoprotein Mucin 1
m6A N6 -methyladenosine
MT-1G Metallothionein-1G
MTOR mechanistic target of rapamycin kinase
MCU mitochondrial calcium uniporter
Nrf2 nuclear factor erythroid 2-related factor 2
NUPR1 Nuclear Protein 1
OTUB1 OTU deubiquitinase, ubiquitin aldehyde-binding 1
PE Piperazine Erastin
p53 Tumor protein p53
PLOOH phospholipid hydroperoxide
PUFAs polyunsaturated fatty acids
PdPT palladium pyrithione complex
PCDHB14 Protocadherin Beta 14
PSTK Phosphoseryl-tRNA kinase
RSL3 RAS-selective lethal small molecule 3
RCD regulatory cell death
ROS reactive oxygen species
RRM2 Ribonucleotide reductase regulatory subunit M2
Rb retinoblastoma; System Xc-, cystine/glutamate antiporter
SLC7A11 Solute Carrier Family 7 Member 11
SLC3A2 Solute Carrier Family 3 Member 2
STYK1 serine threonine tyrosine kinase 1
SEPHS2 selenophosphate synthetase 2
S1R Sigma-1 receptor
SIRT6 Sirtuins 6
STAT3 Signal transducer and activator of Transcription 3
SFRS9 Serine and arginine rich splicing factor 9
TrxR1 thioredoxin reductase 1
Trit1, tRNA isopentenyltransferase 1
TGF-β1 Transforming growth factor β1
USP7 Ubiquitin Specific peptidase 7
γ-GC γ-glutamylcysteine
5-FU 5-fluorouracil
8-OHG Hydroxyguanosine 8

frontiers | Frontiers in Pharmacology

TYPE Original Research
PUBLISHED 31 August 2022
DOI 10.3389/fphar.2022.952980

OPEN ACCESS

EDITED BY
Takeo Tatsuta,
Tohoku Medical and Pharmaceutical University, Japan

REVIEWED BY
Zi-Ning Lei,
Sun Yat-sen University, China
Imran Shair Mohammad,
University of North Carolina at Chapel Hill, United States
Marjana Novič,
National Institute of Chemistry (Slovenia), Slovenia

*CORRESPONDENCE
Chenhui Zhou,
chenhuizh6@126.com
Daohua Xu,
daohuax108@163.com

†These authors have contributed equally to this work

SPECIALTY SECTION
This article was submitted to Pharmacology of Anti-Cancer Drugs, a section of the journal Frontiers in Pharmacology

RECEIVED 25 May 2022
ACCEPTED 05 August 2022
PUBLISHED 31 August 2022

CITATION
Zeng Z, Liao S, Zhou H, Liu H, Lin J, Huang Y, Zhou C and Xu D (2022), Novel Sigma-2 receptor ligand A011 overcomes MDR in adriamycin-resistant human breast cancer cells by modulating ABCB1 and ABCG2 transporter function. *Front. Pharmacol.* 13:952980. doi: 10.3389/fphar.2022.952980

Novel Sigma-2 receptor ligand A011 overcomes MDR in adriamycin-resistant human breast cancer cells by modulating ABCB1 and ABCG2 transporter function

Zhanwei Zeng[1,2†], Shiyi Liao[1,3†], Huan Zhou[1,3†], Hongyu Liu[1,3], Jiantao Lin[1,3], Yunsheng Huang[1,3], Chenhui Zhou[4*] and Daohua Xu[1,3*]

[1]Guangdong Key Laboratory for Research and Development of Natural Drugs, School of Pharmacy, Guangdong Medical University, Zhanjiang, China, [2]Department of Pharmacy, Qingyuan People's Hospital, The Sixth Affiliated Hospital of Guangzhou Medical University, Qingyuan, China, [3]Key Laboratory of Traditional Chinese Medicine and New Pharmaceutical Development, Department of Pharmacology, Guangdong Medical University, Dongguan, China, [4]School of Nursing, Guangdong Medical University, Dongguan, China

Multidrug resistance (MDR) is thought to be one of the main reasons for the failure of chemotherapy in cancers. ATP-binding cassette subfamily B member 1 (ABCB1) or P-glycoprotein (P-gp) and ATP-binding cassette subfamily G member 2 (ABCG2) play indispensable roles in cancer cell MDR. Sigma-2 (σ_2) receptor is considered to be a cancer biomarker and a potential therapeutic target due to its high expression in various proliferative tumors. Recently, σ_2 receptor ligands have been shown to have promising cytotoxic effects against cancer cells and to modulate the activity of P-glycoprotein (ABCB1) *in vitro* experiments, but their specific effects and mechanisms remain to be elucidated. We found that A011, a σ_2 receptor ligand with the structure of 6,7-dimethoxy-1,2,3,4-tetrahydroisoquinoline, showed promising cytotoxicity against breast cancer MCF-7 and adriamycin-resistant MCF-7 (MCF-7/ADR), induced apoptosis, and reversed adriamycin (ADR) and paclitaxel resistance in MCF-7/ADR cells. Furthermore, we demonstrated that A011 increased the accumulation of rhodamine 123 and mitoxantrone in MCF-7/ADR cells. A011 significantly decreased the ATPase activity of the ABCB1 and down-regulated ABCG2 protein expression. In addition, A011, administered alone or in combination with ADR, significantly inhibited tumor growth in the MCF-7/ADR tumor-bearing nude mouse model. A011 may be a potential therapeutic agent for the treatment of tumor resistance.

KEYWORDS

multidrug resistance, MCF-7/ADR, sigma-2 receptor, ABCB1, ABCG2

Introduction

Female breast cancer is one of the most common malignancies in the world. Breast cancer surpassed lung cancer to become the most prevalent cancer in 2020, with an estimated 2.3 million new cases (Sung et al., 2021). Over the past decades, tremendous progress has been made in the development of chemotherapeutic drugs. However, tumor recurrence and metastasis remain one of the major challenges in cancer treatment during the long-term course of chemotherapy (Warren, 2009). Most anti-tumor drugs inevitably show reduced drug efficacy and tumors exhibit multidrug resistance (MDR) to chemotherapeutic drugs during long-term chemotherapy, leading to tumor recurrence in patients. It has been reported that over 90% deaths in the chemotherapy population are associated with MDR (Bukowski et al., 2020). Various mechanisms have been reported to be involved in the development of MDR in tumor cells, including ATP-binding cassette (ABC) transporter family-mediated drug efflux, apoptosis down-regulation and epigenetic regulation, etc., of which the ABC transporter family is the most widely studied (Abraham et al., 2009; Rocha et al., 2018; Assaraf et al., 2019; Bukowski et al., 2020).

The ABC transporter superfamily is one of the largest families of transmembrane proteins, consisting of 49 ABC transporter members (Asif et al., 2020). Structurally, ABC transporters are characterized by a common structure: two nucleotide-binding domains (NBDs), which can bind and hydrolyze ATP, and two transmembrane domains (TMDs), which utilize the energy provided by ATP hydrolysis to transport substrates outside the cell. Functionally, most ABC transporters can transport the substrates produced during cellular metabolism (e.g., sugars, lipids, ions, peptides, amino acids and toxic components) from the cytoplasm to outside the cell membrane, and thus play an important role in maintaining normal physiological and pathological processes in the organism (Borst and Elferink, 2002; Theodoulou and Kerr, 2015). Dysregulated ABC transporters are associated with tumor resistance (Dean et al., 2001; Amawi et al., 2019). More importantly, several ABC transporters have been frequently found to be overexpressed in a variety of tumor resistant cells, such as P-glycoprotein (P-gp, ABCB1) and breast cancer resistance protein (BCRP, ABCG2). It has been found that the ABC transporters could bind and transport chemotherapeutic drugs outside the cell by utilizing the energy provided by ATP hydrolysis, resulting in lowering the concentration of intracellular drug accumulation, reducing the efficacy of chemotherapeutic drugs and the failure of tumor treatment (Amawi et al., 2019; Liu, 2019; Eckenstaler and Benndorf, 2020). Therefore, there is an urgent need to seek small molecule inhibitors targeting ABC transporters to restore the efficacy of chemotherapeutic drugs.

A lot of studies have shown that σ_2 receptor may be a potential therapeutic target for tumors (Zeng and Mach, 2017; Oyer et al., 2019; Schmidt and Kruse, 2019; Chen et al., 2021). The σ_2 receptor was found to be overexpressed in rapidly proliferating tumors such as lung, breast and pancreatic cancers and was identified as an important biomarker of tumor cell proliferation (Zeng et al., 2020). And σ_2 receptor ligands have been found to be potential agents for tumor therapy, with the capacity to inhibit proliferation and induce apoptosis in tumor cells (Nicholson et al., 2015; Cantonero et al., 2020). In addition, the σ_2 receptor ligands exhibited promising anti-tumor proliferative activity against breast cancer MCF-7/ADR cells and could inhibit the activity of ABCB1, suggesting that σ_2 receptor ligands may be potential therapeutic agent in anti-tumor MDR (Azzariti et al., 2006; Abate et al., 2011).

It was reported that σ_2 receptor ligands with a 6,7-dimethoxy-1,2,3,4-tetrahydroisoquinoline structure were capable of modulating the activity of ABCB1 (Pati et al., 2018). Recently, we synthesized a series of σ_2 ligands with 6,7-dimethoxy-1,2,3,4-tetrahydroisoquinoline structural derivatives, and found many of them showed high affinity for the σ_2 receptor (Sun et al., 2018). Our previous study revealed that σ_2 ligand A011 with a 6,7-dimethoxy-1,2,3,4-tetrahydroisoquinoline structure had high affinity for σ_2 receptor and showed good antitumor activity against a variety of tumor cells, including breast cancer MCF-7, MDA-MB-231 and lung cancer A549 cells (Li et al., 2022). However, its role and mechanism in tumor resistance remains to be further investigated.

Materials and methods

Chemicals and reagents

The σ_2 receptor ligand A011 was prepared as previously reported (Feng et al., 2019). KO143 was purchased from MedChemExpress (Monmouth Junction, NJ, United States). Cisplatin (DDP), adriamycin (ADR), paclitaxel, verapamil, mitoxantrone and rhodamine 123 (Rh123) were acquired from Solarbio (Beijing, China). Cell Counting Kit-8 (CCK-8) was bought from Dojindo Laboratories (Japan). Pgp-Glo™ Assay Systems were purchased from Promega (Madison, USA). Anti-P Glycoprotein antibody, ABCG2, GAPDH, Goat Anti-Rabbit IgG H&L Secondary Antibody (Alexa Fluor 488), Goat Anti-Rabbit IgG H&L Secondary Antibody and Goat Anti-Mouse IgG H&L Secondary Antibody were purchased from Abcam (Cambridge, United Kingdom). SlowFade™ Gold antifade reagent was purchased from Thermo Fisher (MA, United States).

Cell lines

ADR-resistant MCF-7 cells (MCF-7/ADR) and DDP-resistant A549 cells (A549/DDP) were purchased from Shanghai GuYan Biotech Co., Ltd. (Shanghai, China). DDP-resistant HepG2 cells (HepG2/DDP) were preserved in our

laboratory. Their parental cells were originally imported from American Type Culture Collection (ATCC, Manassas, United States) and cultured with adriamycin or cisplatin to form MCF-7/ADR cells, A549/DDP and HepG2/DDP. Cells were grown in Minimum Eagle's medium (for MCF-7/ADR), Dulbecco's Modified Eagle Medium (for MCF-7) and RPMI 1640 (for A549, A549/DDP, HepG2, and HepG2/DDP), respectively, containing 10% fetal bovine serum (FBS), 100 U/ml penicillin, 100 μg/ml streptomycin at 37°C, 5% CO_2. MCF-7/ADR cells were maintained using 2 μM ADR. A549/DDP and HepG2/DDP cells were maintained using 2 μg/ml cisplatin. All resistant cells were grown in drug-free medium 2 weeks before experiment.

Cytotoxicity assay

The CCK-8 kit was used to determine the cytotoxicity of chemotherapeutic agents in MCF-7/ADR, A549/DDP, HepG2/DDP and their parental cells. In brief, 5×10^3 cells per well were seeded into 96-well plates with 100 μl medium overnight. Subsequently, cells were cultured with different concentrations of A011, adriamycin, cisplatin, paclitaxel and combination, respectively. After 24, 48, and 72 h incubation, 10 μl CCK-8 was added into each well and incubated for 90 min at 37°C. The absorbance was then measured at 450 nm using a microplate reader. IC_{50} value was calculated as previously described. Survival rate = $(OD_{treatment}—OD_{blank})/(OD_{control}—OD_{blank}) \times 100\%$, Resistant Fold (RF) = $IC_{50\ resistant\ cells}/IC_{50\ parental\ cells}$, Reversal Fold (FR) = $IC_{50\ Monotherapy}/IC_{50\ Combination\ therapy}$.

Colony formation assay

MCF-7 and MCF-7/ADR cells (5×10^3 cells/well) were seeded into 6-well plates overnight. After 24 h incubation, cells were treated with A011 (0.3125, 0.625, 1.25, 2.5, 5 μM) for 24 h and cultured in drug-free medium for 10 days. During this period, cells were washed twice every other day with phosphate buffered saline (PBS) and cultured with fresh medium. Cells were then fixed with 4% paraformaldehyde for 15 min. Crystal violet was used to stain cells for 15 min. The numbers of colonies (cells >50) were counted.

Apoptosis assay

Annexin V-FITC and propidium iodide (PI) kits were used to determine the apoptotic cells induced by A011 in MCF-7/ADR and parental cells. In short, 2×10^5 cells per well were seeded into 6-well plates overnight. Different concentrations of A011 (5, 10, 20, 40 μM) was then added and incubated for 48 h. Subsequently, cells were harvested and washed twice with cold PBS before the addition of Annexin V-FITC and PI for 15 min at room temperature. Flow cytometry was used to detect the apoptotic cells.

Hoechst 33,258 fluorescent reagent was used to detect the effect of A011 on apoptosis in MCF-7/ADR and its parental cells. 2×10^5 cells per well were seeded into 6-well plates. After 24 h incubation, cells were treated with A011 (5, 10, 20 μM) for 48 h. The cells were then washed with PBS and fixed, Hoechst 33,258 was added to stain for 15 min, followed by washing with PBS and photographed under the fluorescence microscope.

Rh123 and mitoxantrone accumulation assay

Flow cytometry was used to detect the intracellular accumulation of Rh123 or mitoxantrone in MCF-7/ADR and its parental cells, with Rh123 and mitoxantrone being the fluorescent substrates for the ABCB1 and ABCG2 transporters, respectively. Briefly, 2×10^5 cells were seeded into 6-well plates. After 24 h incubation, different concentration of A011 (1.25, 2.5, 5, 10 μM), verapamil (10 μM) or KO143 (10 μM) was separately added to each well and incubated for 2 h at 37°C. Subsequently, each well was washed 3 times with PBS and incubated with Rh123 (5 μg/ml) or mitoxantrone (5 μmol/L) for 2 h at 37°C. Finally, all cells were collected and resuspended with cold PBS. Flow cytometry was applied to measure the fluorescence intensity of intracellular Rh123 and mitoxantrone. Verapamil and KO143 were used as positive agent of ABCB1 and ABCG2, respectively.

Rh123 and mitoxantrone efflux assay

Rh123 and mitoxantrone efflux were performed as previously described literature (Gao et al., 2020). In short, cells were seeded into 6-well plates (2×10^5 cells per well) overnight. Cells were then incubated with Rh123 (5 μg/ml) or mitoxantrone (5 μmol/L) for 2 h at 37°C. After 2 h incubation, cells were washed 3 times with PBS and cultured with different concentration of A011 (1.25, 2.5, 5, 10 μM), verapamil (10 μM) or KO143 (10 μM) for 0, 30, 60, 90, 120 min, respectively. Subsequently, cells were collected and washed 3 times with cold PBS. Flow cytometry was used to measure the fluorescence intensity of intracellular Rh123 and mitoxantrone, respectively.

ATPase activity of ABCB1 assay

The impact of A011 on ABCB1-mediated ATP hydrolysis was measured by the Pgp-Glo™ Assay kits. In brief, ABCB1 membranes were thawed and diluted at 4°C. Membranes were treated with various concentrations of A011 for 5 min at 37°C Mg^{2+} and ATP reagent was added into

TABLE 1 IC_{50} values and resistant folds (RF) of A011, adriamycin (ADR), cisplatin (DDP) and paclitaxel on MCF-7/ADR, A549/DDP, HepG2/DDP and their parental cells after 48 h administration.

	IC_{50}(μM)		RF	IC_{50}(μM)		RF	IC_{50}(μM)		RF
	MCF-7	MCF-7/ADR		A549	A549/DDP		HepG2	HepG2/DDP	
A011	3.79± 0.13	5.35± 0.42	1.41	4.59± 0.35	7.74± 0.32	1.69	4.07± 0.25	8.29± 0.04	2.04
ADR	0.61± 0.02	27.19± 0.28	44.57	0.21± 0.01	0.20± 0.06	0.95	0.13± 0.12	48.31± 3.10	371.61
cisplatin	8.26± 0.40	45.83± 1.58	5.55	11.55± 0.36	72.67± 2.93	6.29	11.65± 0.60	52.90± 0.63	4.54
paclitaxel	0.75± 0.03	18.85± 0.45	25.13	0.42± 0.05	23.04± 0.92	54.86	0.55± 0.09	20.86± 0.43	37.92

Resistant Fold (RF) = IC_{50} value of drug in drug-resistant cells/IC_{50} value of drug in parental cells.

each well to trigger the reaction. After 40 min incubation, plates were removed to room temperature and ATP detection reagent was added to initiate luminescence for 20 min at room temperature. Subsequently, luminescence was read on a plate-reading luminometer.

Immunofluorescence assay

Immunofluorescence assay was performed to detect the influence of A011 on the intracellular localization of ABCB1 and ABCG2 in MCF-7/ADR cells. In brief, 2×10^4 cells per well were seed into 6-well plates overnight and treated with A011 (1.25, 2.5 μM). After 48 h incubation, cells were washed twice with cold PBS and fixed by 4% paraformaldehyde for 15 min. Bovine serum albumin (BSA) (2 mg/ml) was added to block proteins for 1 h, primary antibodies ABCB1 (1:200) or ABCG2 (1:200) were used to incubate proteins for 4 h at 4°C, which were subsequently blocked by second antibodies for 1 h. SlowFade™ Gold antifade reagent was used to incubate proteins for 5 min. The fluorescence microscope was performed to collect the images.

Western blot assay

Western blot assays were applied to detect the protein expression of ABCB1 and ABCG2 after A011 treatment in MCF-7/ADR cells. Briefly, cells were cultured with or without A011 (1.25, 2.5, 5 μM) for 48 h. Radio-immune precipitation assay (RIPA) cell lysis buffer was then used to lysis cells for 30 min on the ice. The total protein concentrations were normalized using the BCA protein assay kit. Subsequently, proteins were load and separated by SDS-PAGE kits, following transferred into polyvinylidene difluoride (PVDF) membrane and blocked by non-fat milk. Primary antibodies (ABCB1 1:1,000, ABCG2 1:1,000) were incubated for overnight at 4°C. Horseradish peroxidase (HRP)-conjugated Mouse or Rabbit antibody was used to co-incubate with PVDF membrane for 1 h at room temperature. The protein bands were visualized by Immobilon Western HRP Substrate Kits and the relative protein expression level was analysis by ImageJ software.

Mouse xenograft assay

The MCF-7/ADR cells inoculated nude mice xenograft model was used for *in vivo* studies. The BALB/c female nude mice (4–6 weeks old, weighting 16–18 g) were bought from Guangdong Medical Laboratory Animal Centre (Guangdong, China). 1×10^7 cells were injected subcutaneously into the right flank of each nude mouse. When the tumor volume reached 100 mm^3, nude mice were randomly divided into five groups (6 mice in each group):(1) Control (saline), 2) A011 (1 mg/kg), 3) ADR (5 mg/kg), 4) A011 (5 mg/kg), 5) A011 (1 mg/kg) plus ADR (5 mg/kg) (A011 + ADR). The drugs were administered intraperitoneally every 3 days for 21 days and the body weight and tumor volume (V) of nude mice were measured according to the following formula: $V = 0.5a \times b^2$ ["a" is the length (mm) and "b" is the width (mm)]. The nude mice were killed by spinal dislocation and the tumor tissues were dissected and weighed. The liver, kidney and tumor samples from nude mice were fixed and preserved. All animal experiments complied with the China Animal Welfare Guide. The protocol was reviewed and approved by the Experimental Animal Research Committee of Guangdong Medical University.

Histological analysis

The above tissue samples were dehydrated in ethanol, embedded in paraffin and sectioned with a microtome (4 μm). Sections were stained with hematoxylin and eosin for

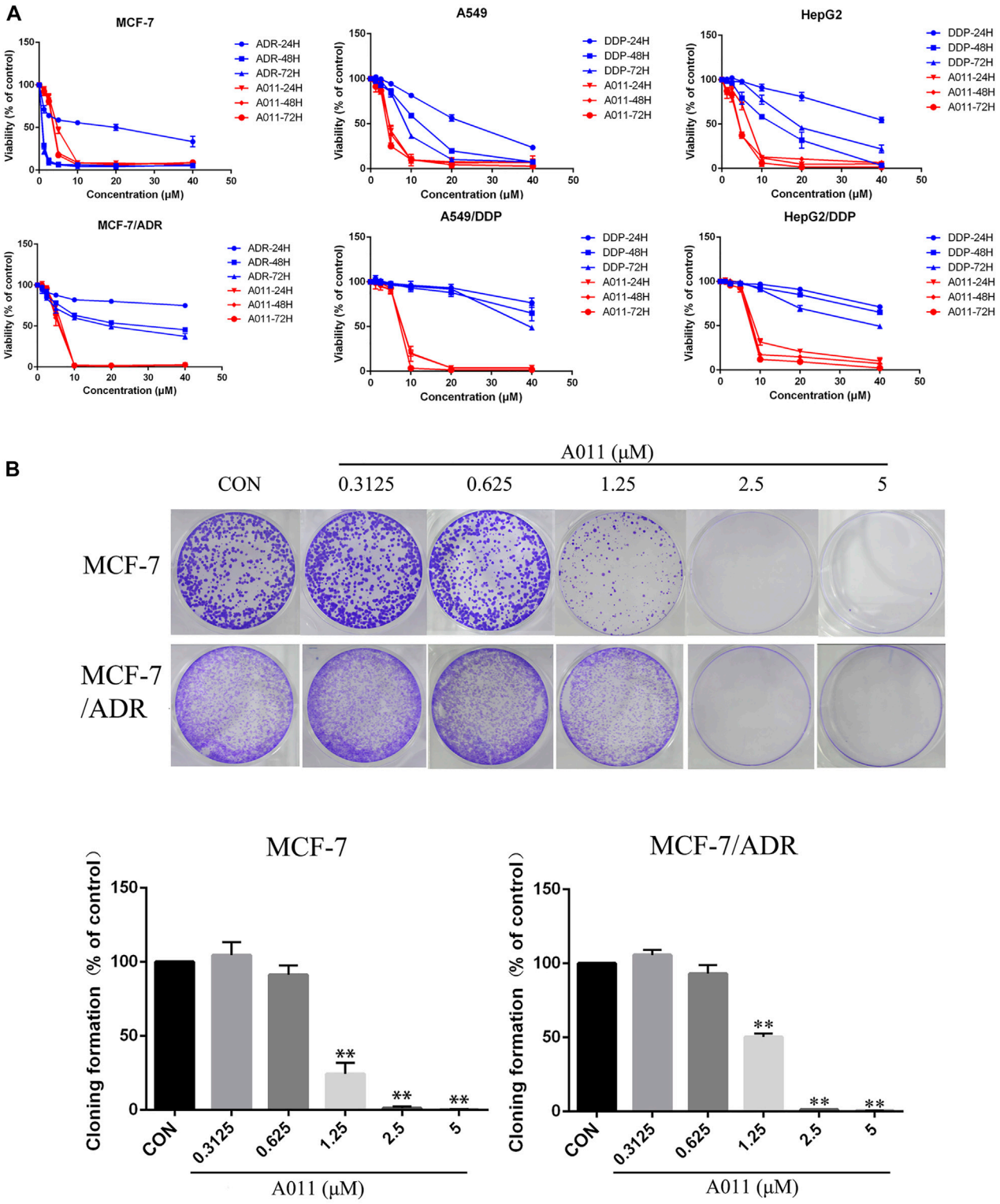

FIGURE 1
Effect of A011 on the viability of three drug-resistant cells MCF-7/ADR, A549/DDP, HepG2/DDP and their parental cells. **(A)** The cytotoxic effects of A011 on MCF-7/ADR, A549/DDP, HepG2/DDP and their parental cells, respectively. Cells were treated with a range of concentrations of A011, adriamycin (ADR) or cisplatin (DDP) for 24, 48 and 72 h. **(B)** Effect of A011 on the inhibition of clonogenic capacity of MCF-7 and MCF-7/ADR cells. Data represent mean ± SD of three different experiments. *$p < 0.05$, **$p < 0.01$ vs. Control.

TABLE 2 Reversal of A011 on resistance of adriamycin (ADR), cisplatin and paclitaxel in MCF-7/ADR and MCF-7 cells.

Group	MCF-7		MCF-7/ADR	
	IC_{50}(μM)	FR	IC_{50}(μM)	FR
ADR	0.61 ± 0.02	1.00	27.19 ± 0.28	1.00
A011 (1.25 μM)+ADR	0.55 ± 0.08	1.11	2.89 ± 0.40	9.41**
A011 (2.5 μM)+ADR	0.48 ± 0.07	1.27	1.18 ± 0.26	23.04**##
verapamil (5 μM)+ADR	0.53 ± 0.07	1.15	4.87 ± 0.61	5.58
KO143 (5 μM)+ADR	0.51 ± 0.10	1.19	18.23 ± 1.20	1.49
cisplatin	8.26 ± 0.40	1.00	45.83 ± 1.58	1.00
A011 (1.25 μM)+cisplatin	8.38 ± 0.56	0.99	34.17 ± 2.57	1.34
A011 (2.5 μM)+cisplatin	7.57 ± 0.39	1.09	17.57 ± 1.58	2.61
verapamil (5 μM)+cisplatin	5.95 ± 0.55	1.39	21.80 ± 2.21	2.10
KO143 (5 μM)+cisplatin	7.16 ± 0.29	1.15	35.42 ± 3.86	1.29
paclitaxel	0.75 ± 0.026	1.00	18.85 ± 0.45	1.00
A011 (1.25 μM)+paclitaxel	0.70 ± 0.01	1.07	4.11 ± 0.27	4.59
A011 (2.5 μM)+paclitaxel	0.59 ± 0.02	1.27	0.91 ± 0.13	20.71*##
verapamil (5 μM)+paclitaxel	0.63 ± 0.01	1.19	1.79 ± 0.45	10.53
KO143 (5 μM)+paclitaxel	0.58 ± 0.03	1.29	2.21 ± 0.22	8.53

Reversal Fold (FR) = $IC_{50\ Monotherapy}/IC_{50\ Combination\ therapy}$. Verapamil as positive control group, *$p < 0.05$, **$p < 0.01$, vs. Verapamil group, ##$p < 0.01$, vs. KO143 group.

hematoxylin-eosin (HE) staining and terminal deoxynucleotidyl transferase-mediated dUTP-biotin nick end labelling (TUNEL) staining, respectively. The immunohistochemistry (IHC) staining was performed with anti-ABCG2 or anti-ABCB1 antibody. The treated samples were observed under a microscope and photographed and the images were analyzed.

Statistical analysis

All experiments were conducted in at least three independent experiments. All data were analyzed using GraphPad Prism's one-way ANOVA and shown as mean ± SD. Differences were considered statistically significant when the p value was less than 0.05.

Results

Cytotoxicity, resistance fold and reversal effect of A011

We determined the cytotoxicity of A011 and positive drugs ADR, cisplatin and paclitaxel on three drug-resistant cells MCF-7/ADR, A549/DDP and HepG2/DDP and their parental cells by CCK-8 kits. ADR, cisplatin and paclitaxel showed good antitumor effects on MCF-7, A549, and HepG2 cells, with significantly decreased cytotoxic effects in MCF-7/ADR, A549/DDP, and HepG2/DDP cells, with RF value mostly >5, indicating that the 3 cell lines were multidrug resistant. In contrast, the IC_{50} values of A011 were 3.79 ± 0.13 μM, 5.35 ± 0.42 μM, RF value 1.41, 4.59 ± 0.35 μM, 7.74 ± 0.32 μM, RF value 1.69, 4.07 ± 0.25 μM, 8.29 ± 0.04 μM, RF value 2.04 for MCF-7, MCF-7/ADR, A549, A549/DDP, HepG2 and HepG2/DDP cells, respectively (Table 1). A011 showed similar anti-proliferative effects on drug-resistant cells and their parental cells, indicating that A011 had excellent anti-tumor MDR effects (Figure 1A).

Based on the results of the CCK-8 assay, A011 had a stronger anti-proliferative effect in MCF-7/ADR cells relative to A549/DDP and HepG2/DDP cells, and therefore MCF-7/ADR cells were used as the subsequent experimental cell line. Moreover, A011 showed >90% survival of MCF-7/ADR cells at 1.25 and 2.5 μM concentrations and were therefore selected as the concentration for combination treatment. The results showed that A011 at 1.25 and 2.5 μM concentrations significantly increased the cytotoxicity of ADR, cisplatin and paclitaxel in MCF-7/ADR cells. No sensitization was observed in parental cells. And the inhibition effect of A011 combined with ADR was superior compared with that of ABCB1 inhibitor verapamil and ABCG2 inhibitor KO143 combined with ADR ($p < 0.05$) (Table 2). In addition, A011 significantly inhibited the clonogenic ability of MCF-7/ADR cells and their parental cells (Figure 1B). These results suggested that A011 has excellent anti-tumor MDR activity and could enhance the sensitivity of MCF-7/ADR cells to ADR, cisplatin and paclitaxel.

A011 induced apoptosis in MCF-7/ADR and its parental cells.

Hoechst 33,258 staining showed that MCF-7/ADR and MCF-7 cells exhibited increased cytoplasmic density, nuclear consolidation, nuclear membrane nucleolus fragmentation and increased apoptotic vesicles in a dose-dependent manner after A011 treatment compared to cells from control group with intact cell structure (Figure 2A). Furthermore, the flow cytometry results showed that A011 (5, 10, 20, and 40 μM) significantly induced apoptosis in MCF-7/ADR and MCF-7 cells, with apoptosis rate of 5.20% ± 0.55%, 25.15% ± 9.99%, 95.6% ± 6.35%, 99.47% ± 0.15% for MCF-7/ADR cells and 9.47% ± 1.25%, 11.87% ± 1.84%, 43.19% ± 8.81% and 87.51% ± 2.70% for MCF-7 cells (Figure 2B). The results indicated A011 could inhibit tumor cells growth by inducing cell apoptosis in MCF-7 and MCF-7/ADR.

A011 significantly increased the accumulation and decreased the efflux of Rh123 and mitoxantrone in MCF-7/ADR cells

To investigate the mechanism by which A011 reversed drug resistance in tumor cells, we determined the effect of A011 on the

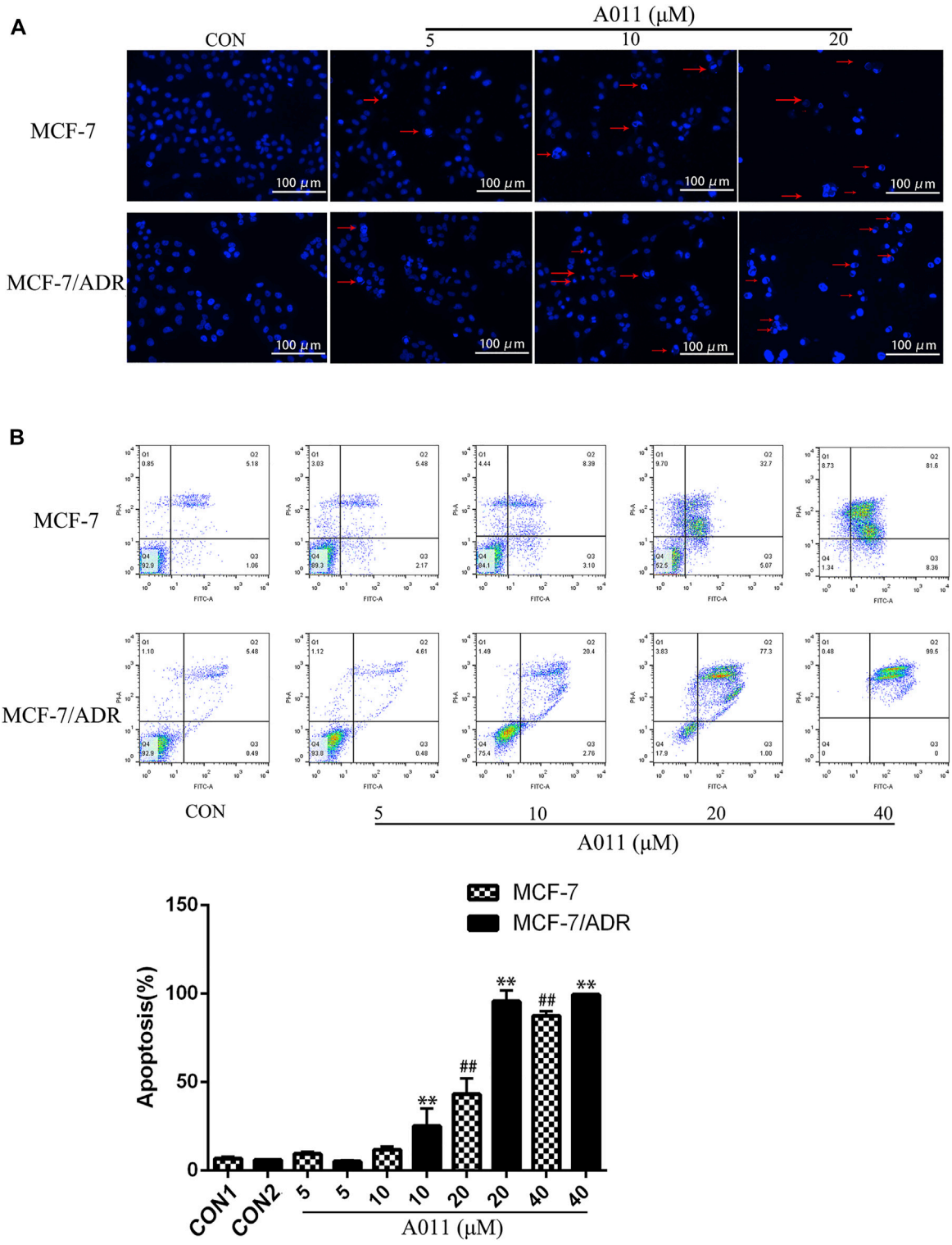

FIGURE 2
Effect of A011 on MCF-7/ADR and MCF-7 cell apoptosis. **(A)** Results of Hoechst 33,258 staining of MCF-7/ADR cells and their parental cells after A011 intervention. The red arrows indicated apoptotic vesicles. **(B)** Flow cytometry results of A011 on MCF-7/ADR cells and their parental cell apoptosis. Data represent mean ± SD of three different experiments. ##$p < 0.01$ vs. CON1; **$p < 0.01$ vs. CON2.

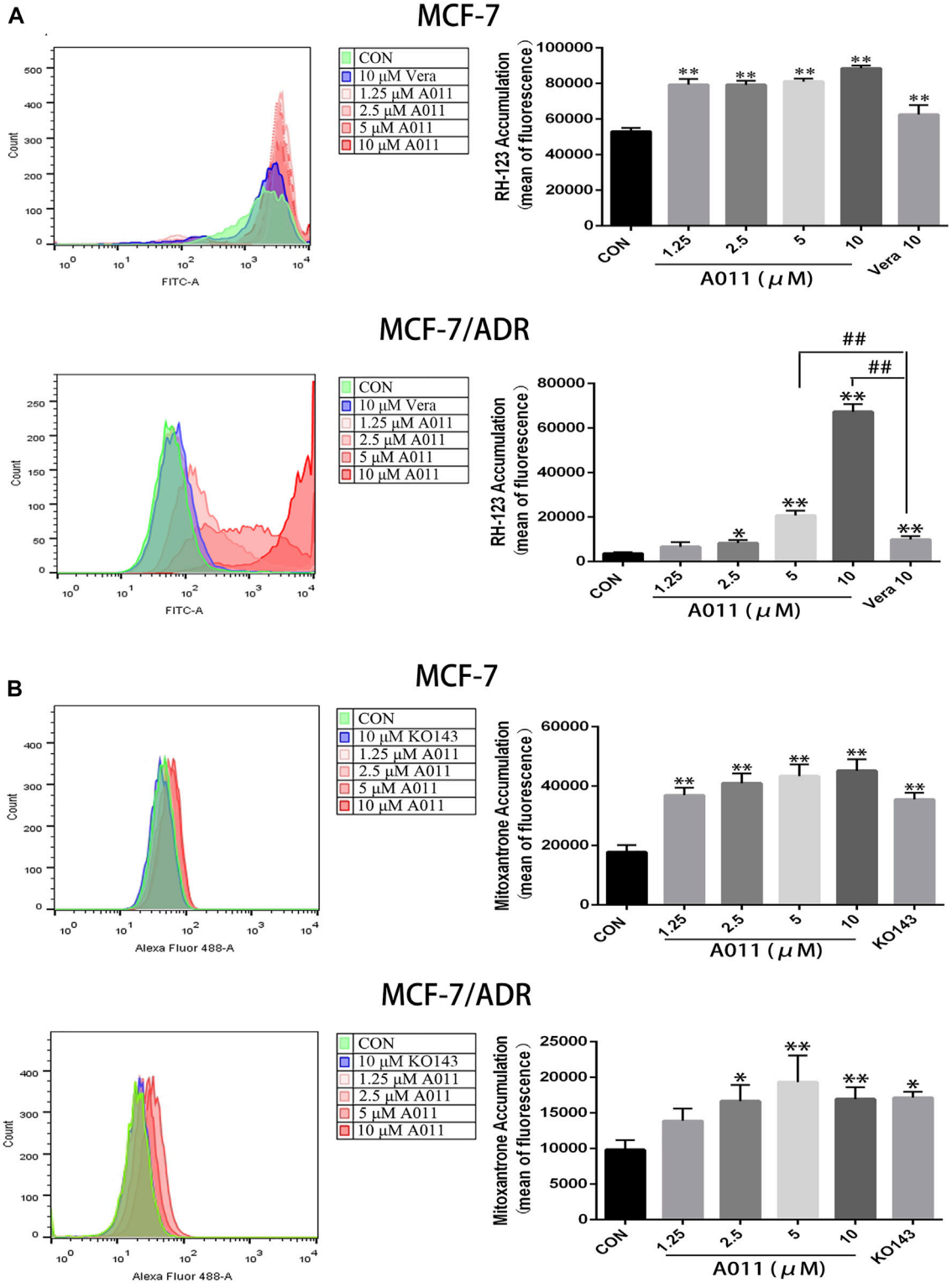

FIGURE 3
Effect of A011 on the transport function of ABCB1 and ABCG2 transporters. **(A)** A011 increased the accumulation of Rh123 in MCF-7/ADR and parental cells. **(B)** A011 increased the accumulation of mitoxantrone in MCF-7/ADR and parental cells. Verapamil (vera) and KO143 as a positive control group. Data represent mean ± SD of three different experiments. *p < 0.05, **p < 0.01 vs. CON.

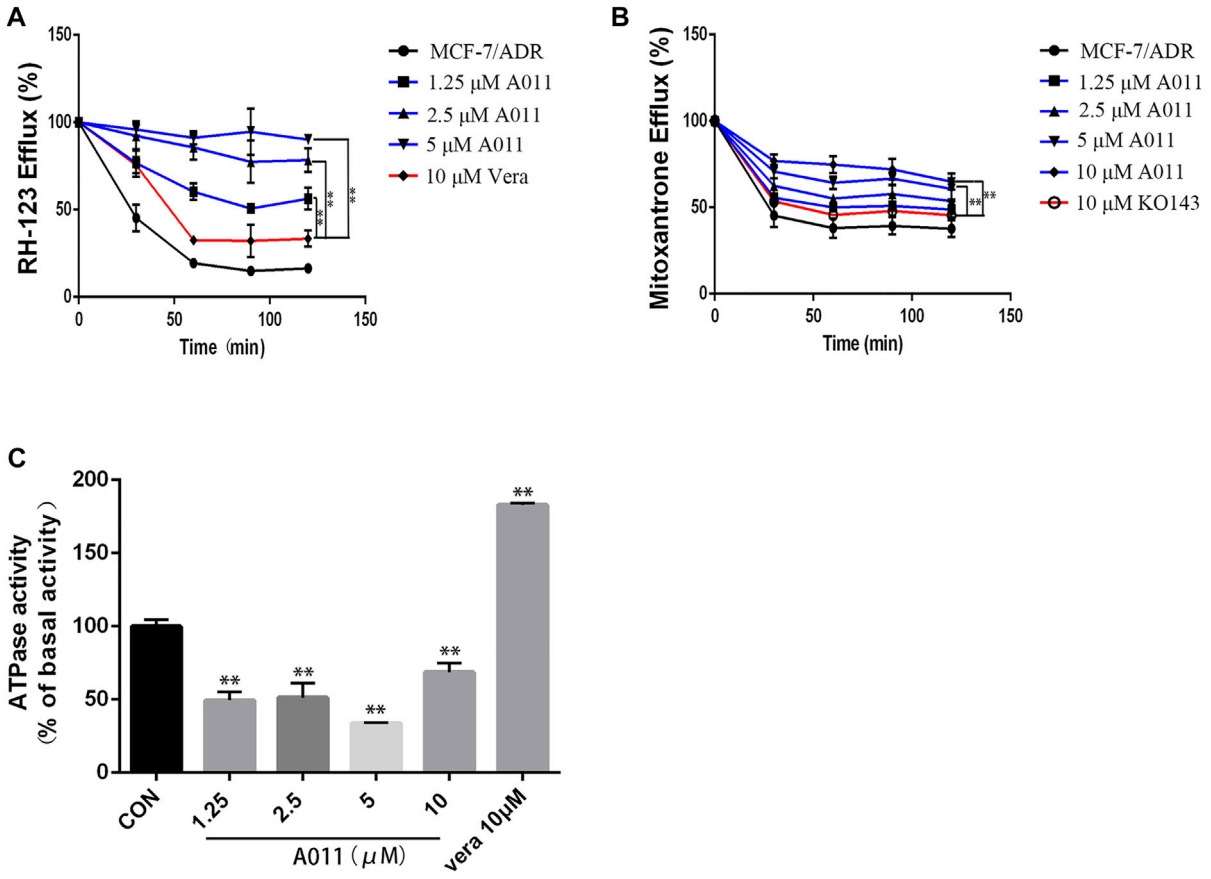

FIGURE 4
Effect of A011 on the transport function of ABCB1 and ABGC2 transporters. **(A)** A011 decreased the efflux of Rh123 in MCF-7/ADR cells. **(B)** A011 decreased the efflux of mitoxantrone in MCF-7/ADR cells. **(C)** A011 decreased the ATPase activity of the ABCB1 transporter. Verapamil (vera) and KO143 as a positive control group. Data represent mean ± SD of three different experiments. **p < 0.01 vs. CON.

function of ABCB1 and ABCG2 transporters. Verapamil and KO143 were inhibitors of the ABCB1 and ABCG2 transporters respectively, and were able to inhibit the transport of substrates outside the cell membrane by the ABCB1 and ABCG2 transporters, so they were used as positive control. In addition, Rh123 and mitoxantrone were fluorescent substrates for the ABCB1 and ABCG2 transporters respectively, and were able to be quantified by flow cytometry. The results showed that the accumulation of Rh123 or mitoxantrone in MCF-7/ADR cells was significantly lower than their accumulation in parental cells. A011 significantly increased the accumulation of Rh123 and mitoxantrone in MCF-7/ADR cells. Moreover, the intracellular accumulation of Rh123 was higher in the A011 group compared to the verapamil group (Figures 3A,B). In addition, efflux experiments showed that the amount of Rh123 or mitoxantrone in MCF-7/ADR cells was significantly reduced during the time course, whereas the addition of A011 significantly inhibited the efflux of Rh123 or mitoxantrone, suggesting that the increased accumulation of Rh123 and mitoxantrone in MCF-7/ADR cells was due to inhibition of their efflux (Figures 4A,B). These results indicated that A011 could inhibit the transport function of ABCB1 and ABCG2 transporters.

A011 significantly decreased the ATPase activity of the ABCB1 transporter

To further investigate the role of A011 on the function of the ABCB1 transporter, we measured the effect of A011 on the ATPase activity of the ABCB1 transporter. The results showed that verapamil increased the activity of ABCB1 transporter ATPase, which was in agreement with the description of previous studies (Ledwitch et al., 2016). In contrast, A011 could significantly decrease the activity of ABCB1 transporter ATPase compared to the control group, indicating that A011 could inhibit the transport function of ABCB1 transporter by inhibiting the activity of ABCB1 transporter ATPase (Figure 4C).

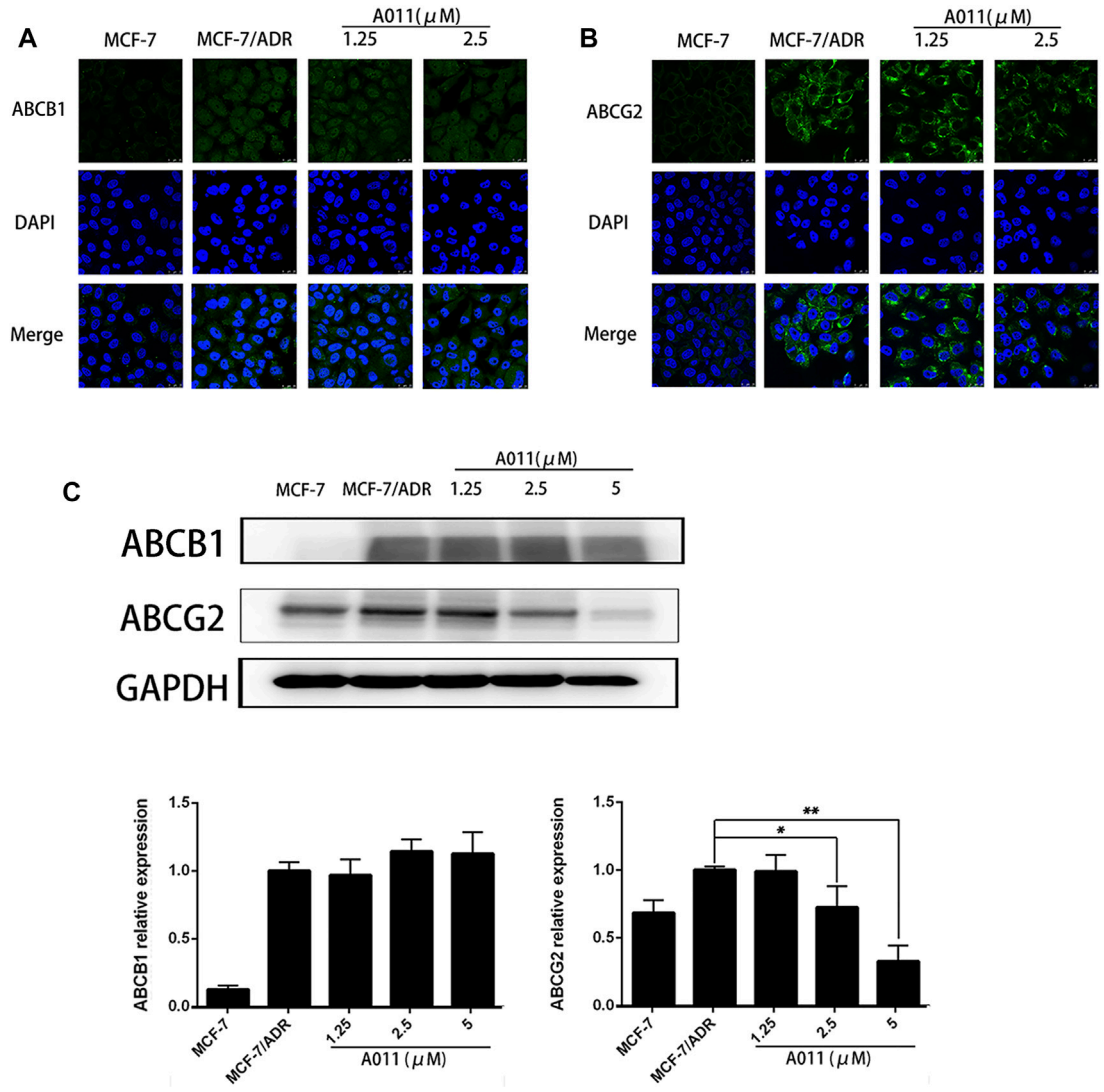

FIGURE 5
Effect of A011 on the expression and intracellular localization of ABCB1 and ABCG2 proteins. **(A)** A011 did not alter the localization of ABCB1 protein in MCF-7/ADR cells. Cells were treated with A011 for 48 h and then detected by immunofluorescence assay. **(B)** A011 did not alter the localization of ABCG2 protein in MCF-7/ADR cells. **(C)** A011 decreased ABCG2 protein expression in MCF-7/ADR cells without altering ABCB1 protein expression. Cells were treated with A011 for 48 h and then detected by western blot assay. Data represent mean ± SD of three different experiments. *$p < 0.05$, **$p < 0.01$ vs. Control. A011 Inhibited the Growth of MCF-7/ADR Xenograft Model in vivo.

A011 Decreased ABCG2 Protein Expression without Altering ABCB1 Protein Expression and Localization of ABCG2 and ABCB1 Proteins in MCF-7/ADR Cells

Given reducing the expression of transporter proteins and altering their localization in cells is one of the mechanisms to overcome MDR, we further investigated the effect of A011 on ABCB1 and ABCG2 proteins in MCF-7/ADR cells by immunofluorescence and western blot. Immunofluorescence assay showed that A011 did not alter the localization of ABCB1 and ABCG2 proteins in MCF-7/ADR cells (Figures 5A,B). And western blot showed that A011 down-regulated ABCG2 protein expression and did not alter ABCB1 protein expression (Figure 5C).

To evaluate the anti-tumor MDR activity of A011 *in vivo*, we established a xenograft model with MCF-7/ADR cells in nude mice. A011 (1 mg/kg) or ADR (5 mg/kg) alone showed low growth inhibitory activity against MCF-7/ADR tumors, with growth inhibition rates of 6.94% and 22.58%, respectively. However, when ADR (5 mg/kg) was co-administered with

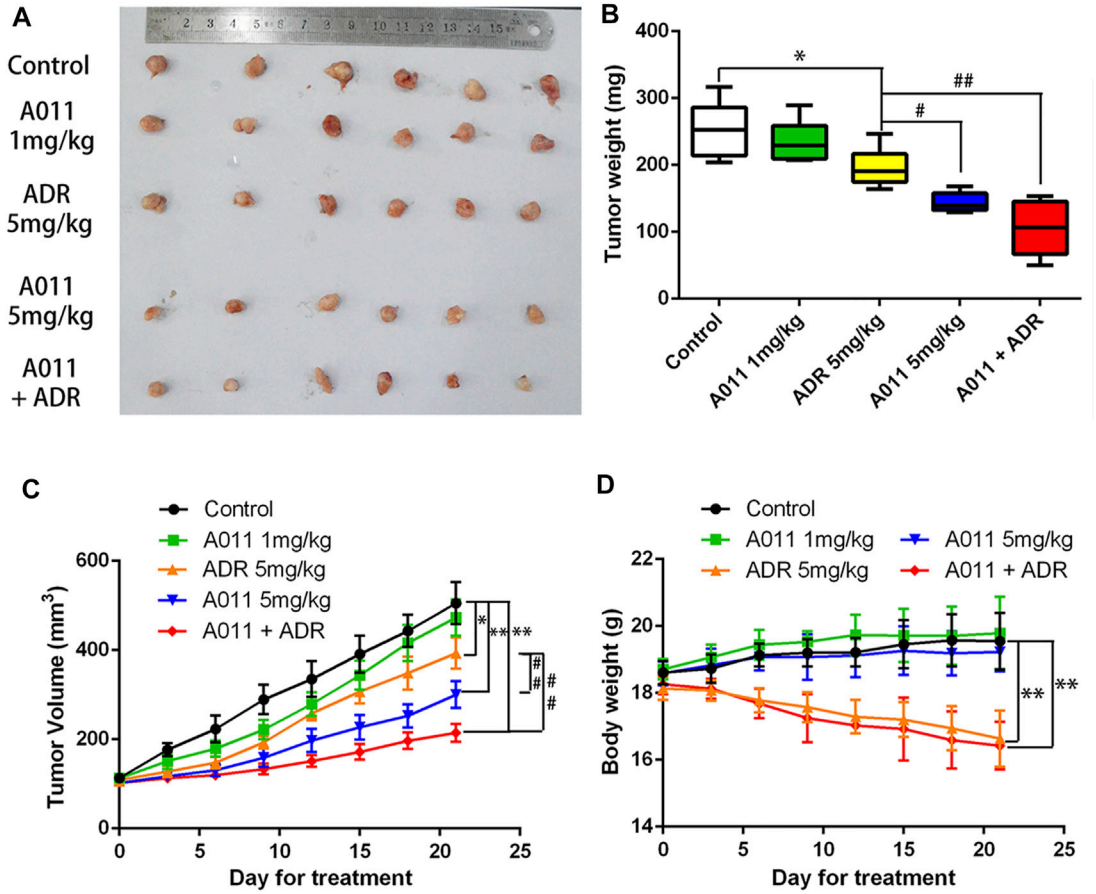

FIGURE 6
A011 inhibited the growth of MCF-7/ADR xenograft model in vivo. MCF-7/ADR cells were injected subcutaneously into the right flank of BALB/c-nu/nu nude mice. **(A)** Photographs of tumors. **(B)** Mean tumor weight was calculated for each group of tumors after dissection of nude mice. **(C)** Change in tumor volume over the 21 days treatment period. **(D)** Change in body weight of nude mice during the 21-days treatment period. Nude mice in Control group treated with saline. Nude mice in the A011 + ADR group were treated with A011 (1 mg/kg) in combination with ADR (adriamycin) (5 mg/kg), while the other groups were treated as depicted above. ADR: adriamycin. Data represent mean ± SD of three different experiments. *$p < 0.05$, **$p < 0.01$ vs. Control. #$p < 0.05$, ##$p < 0.01$ vs. ADR (5 mg/kg). A011 Induced Apoptosis and Downregulated ABCG2 Protein Expression in MCF-7/ADR Tumor Cells without Significant Toxicity to Liver and Kidney

A011 (1 mg/kg), the anti-tumor activity of ADR was significantly enhanced with the growth inhibition rate of 58.43%. A011 (5 mg/kg) alone showed good anti-tumor activity against MCF-7/ADR tumors with the growth inhibition rate of 43.13% (Figures 6A–C). In addition, there was no significant change in body weight in the A011 group compared to the saline group (Figure 6D). These results suggested that A011 alone or in combination had promising anti-tumor MDR activity and was well tolerated *in vivo*.

To evaluate the effects of A011 in liver, kidney and tumor tissues in nude mice, we performed HE tissue staining, TUNEL staining and immunohistochemistry experiments respectively. HE staining of the liver and kidney showed that there was no difference between all treatment groups and control group, except for a small amount of inflammatory cell infiltration in the ADR (5 mg/kg) and A011 combined with ADR groups. In HE staining of tumor tissue, approximately 60% and 70% of tumor cells were necrotic in A011 (5 mg/kg) and A011 combined with ADR respectively, compared to 40% in the control group (Figure 7A). TUNEL staining showed that administration of A011 (5 mg/kg) alone or A011 (1 mg/kg) in combination with ADR (5 mg/kg) significantly induced an increase in MCF-7/ADR tumor apoptosis (Figure 7B). Immunohistochemistry of ABCG2 showed dark brown staining of ABCG2 protein in the saline and ADR (5 mg/kg) groups. As the concentration of A011 increased, the expression of ABCG2 was down-regulated (Figure 7C). A011 did not alter the expression of ABCB1 (Supplementary Figure S1). Above results suggest that A011 could induce apoptosis and down-regulate ABCG2 protein expression in MCF-/ADR tumor cells *in vivo*, without significant toxicity to liver and kidney tissues.

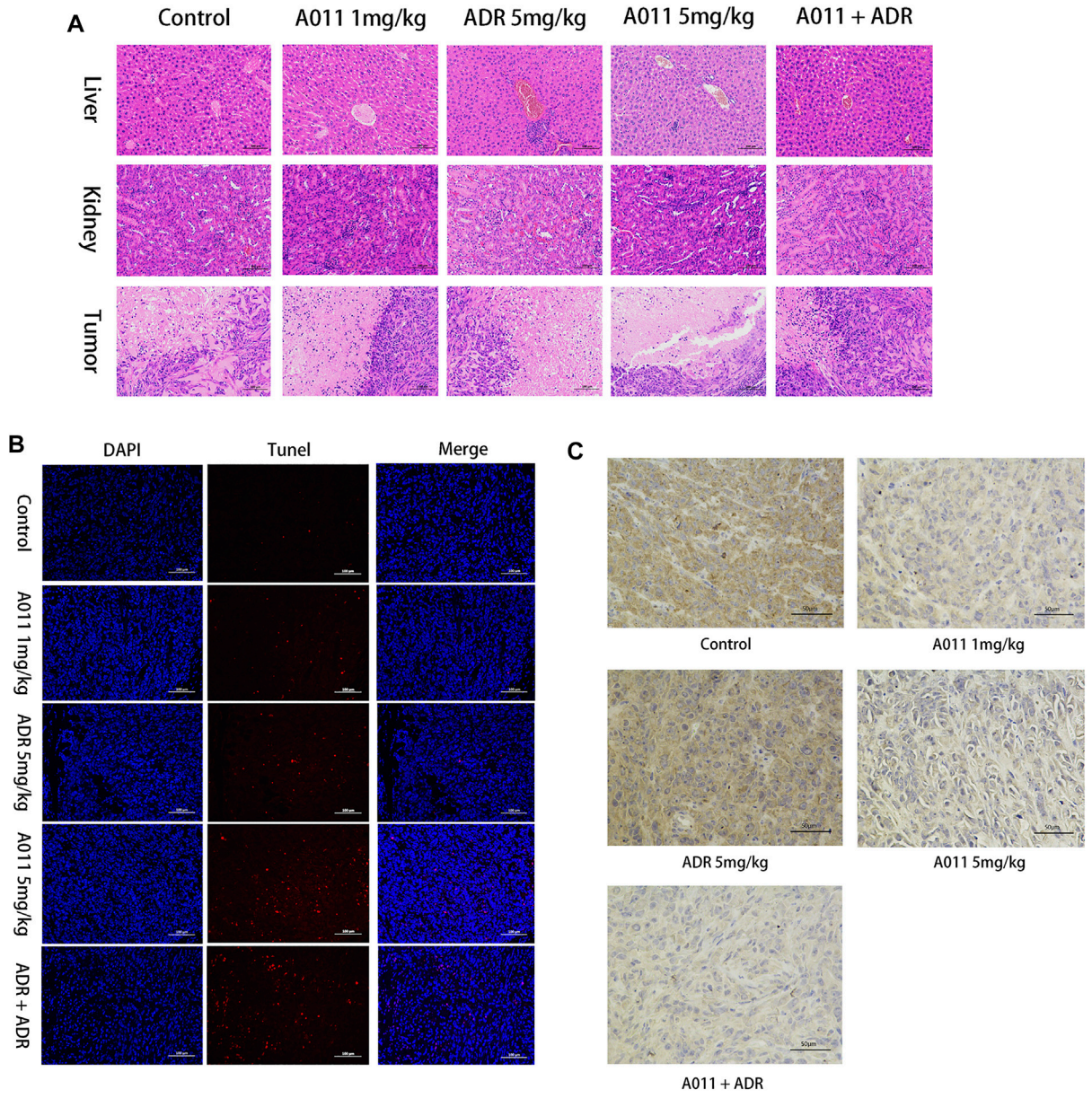

FIGURE 7
Histological analysis results. **(A)** HE staining of liver, kidney and tumor tissue (200×). **(B)** TUNEL staining of each group of tumor tissue. **(C)** Immunohistochemistry of ABCG2 protein in each group of tumor tissues. ADR: adriamycin. Scale bar = 100 μm or 50 μm.

Discussion

Intrinsic MDR and acquired MDR are two of the major barriers to tumor treatment, seriously threatening the survival and affecting the lives of cancer patients (Zheng, 2017; Al-Akra et al., 2019). Due to the narrow therapeutic window of most chemotherapeutic agents, the emergence of tumor MDR has greatly limited the clinical use of chemotherapeutic agents, therefore it is particularly important for cancer treatment to overcome tumor MDR.

The σ_2 receptor has been found to be highly expressed in rapidly proliferating tumors such as breast cancer and is considered to be one of the potential targets for the treatment of tumors (Huang et al., 2014). Most of the σ_2 ligands not only show high affinity for the σ_2 receptor but also exhibit excellent anti-tumor activity (Georgiadis et al., 2017; Sun et al., 2018; Liu et al., 2019), and those with a 6,7-dimethoxy-1,2,3,4-tetrahydroisoquinoline structure could also interact with ABCB1 (Pati et al., 2015). Moreover, a few σ_2 receptor agonists were found to be collateral sensitive and their anti-

proliferative activity was stronger in cells with high P-gp expression than in P-gp negative cells, suggesting that σ_2 receptor ligands may have promising activity in drug-resistant tumors (Niso et al., 2013; Abatematteo et al., 2021). In this study, we found that σ_2 ligand A011 showed significant cytotoxic activity in three tumor cell lines MCF-7, A549 and HepG2 cells and generally showed no decrease in cytotoxic activity in drug-resistant cell lines MCF-7/ADR, A549/DDP and HepG2/DDP cells. In addition, A011 significantly increased the sensitivity of MCF-7/ADR cells to ADR at concentrations of 1.25 and 2.5 μM. And *in vivo* experiments, A011 (5 mg/kg) alone or A011 (1 mg/kg) co-administered with ADR showed promising anti-tumor activity, significantly inhibiting the growth of MCF-7/ADR tumors without significant toxicity, suggesting that A011 has the potential to overcome MDR.

Apoptosis is a form of programmed cell death that is co-regulated by multiple genes with important roles in maintaining the homeostasis of the internal environment and controlling cell proliferation (Goldar et al., 2015). Dysregulation of apoptosis is one of the hallmarks of cancer and is associated not only with tumorigenesis and progression, but also with tumor resistance to chemotherapeutic agents (Pistritto et al., 2016). We found that A011 could dose-dependently induce apoptosis in MCF-7/ADR and its parental cells, and the apoptosis induction of A011 was better in MCF-7/ADR than MCF-7 cells. In a MCF-7/ADR xenograft model, A011 (5 mg/kg) was able to induce an increased apoptosis relative to the control group, suggesting that A011 may also promote cell death by inducing MCF-7/ADR apoptosis.

ABC transporters have been found to be relatively highly expressed in drug-resistant tumors and able to transport intracellular chemotherapeutic agents to the extracellular compartment by relying on the energy provided by ATP hydrolysis, thereby mediating the resistance of tumor cells to chemotherapeutic agents (Choi and Yu, 2014; Beis, 2015). To elucidate the mechanism that A011 overcame MDR in MCF-7/ADR cells, we examined the activity and protein expression of the ABCB1 and ABCG2 transporters. Our results showed that A011 could inhibit ABCB1 transport function and ATPase activity, but had no effect on its protein expression. In addition, it was first discovered that A011 also inhibited the transport function and protein expression of ABCG2, which was further validated in ABCG2 protein immunohistochemical assay *in vivo*. Besides inhibiting ABC transporter activity and protein expression, ABC transporters as transmembrane proteins, altering their localization in cells is also part of the strategy to inhibit ABC transporter-mediated MDR (Zhao et al., 2019). However, A011 did not affect the localization of the ABCB1 and ABCG2 transporters in MCF-7/ADR cells. These results suggested that A011 could inhibit the function of ABCB1 and ABCG2 transporters and reduce the expression of ABCG2 protein, thereby overcoming MDR. However, the mechanisms of A011 inhibiting ATPase activity and expression of ABCG2 protein remain to be clarified.

A variety of σ_2 ligands are currently being developed for clinical diagnosis and cancer treatment with PET imaging of tumors. Phase I clinical trial results for the σ_2 radioligand [^{18}F] ISO-1 showed that [^{18}F]ISO-1 uptake values correlated with tumor Ki-67 (a gold standard proliferation biomarker) and are expected to be used for *in vivo* measurement of tumor proliferation status (Dehdashti et al., 2013). Studies have shown that a lot of selective σ_2 receptor ligands displayed cytotoxic effects on a variety of human cancer cells, and inhibited tumor growth (Asong et al., 2019; Liu et al., 2019). We previously found that A011 was able to increase intracellular ROS and Ca^{2+} levels in MCF-7 cells and induced endoplasmic reticulum stress and autophagy (Li et al., 2022). In addition, the study showed that A011 was well tolerated and had no significant toxicity to liver and kidney tissues. These results provided further insight into the pharmacological role of the σ_2 receptor and A011 may be a candidate for cancer treatment either alone or in combination with other anticancer agents.

Conclusion

In this study, we elucidated that the σ_2 ligand A011, containing a 6,7-dimethoxy-1,2,3,4-tetrahydroisoquinoline structure, exhibited excellent anti-breast cancer MDR activity both *in vivo* and *in vitro*, either alone or in combination with ADR. A011 demonstrated anti-MDR activity by inhibiting the transporting function of ABCB1 and ABCG2 transporters and thus was a potential therapeutic agent for the treatment of tumor resistance.

Data availability statement

The original contributions presented in the study are included in the article/Supplementary Materials, further inquiries can be directed to the corresponding authors.

Ethics statement

The animal study was reviewed and approved by the Experimental Animal Research Committee of Guangdong Medical University.

Author contributions

DX, ZZ, YH, and CZ designed the research. ZZ, SL, HZ, HL, CZ, and JL carried out the experiments and performed data

analysis. DX, ZZ, YH, and CZ wrote and revised the manuscript. All of the authors have read and approved the final manuscript.

Funding

The work was supported by Discipline Construction Project of Guangdong Medical University (4SG22002G); Key Projects of Universities in Guangdong Province (2019KZDXM056).

Conflict of interest

The authors declare that the research was conducted in the absence of any commercial or financial relationships that could be construed as a potential conflict of interest.

Publisher's note

Supplementary material

The Supplementary Material for this article can be found online at: https://www.frontiersin.org/articles/10.3389/fphar.2022.952980/full#supplementary-material

References

Abate, C., Niso, M., Contino, M., Colabufo, N. A., Ferorelli, S., Perrone, R., et al. (2011). 1-Cyclohexyl-4-(4-arylcyclohexyl)piperazines: Mixed σ and human Δ(8)-Δ(7) sterol isomerase ligands with antiproliferative and P-glycoprotein inhibitory activity. *ChemMedChem* 6, 73–80. doi:10.1002/cmdc.201000371

Abatematteo, F. S., Niso, M., Lacivita, E., and Abate, C. (2021). σ_2 receptor and its role in cancer with focus on a MultiTarget directed ligand (MTDL) approach. *Molecules* 26, 3743. doi:10.3390/molecules26123743

Abraham, J., Edgerly, M., Wilson, R., Chen, C., Rutt, A., Bakke, S., et al. (2009). A phase I study of the P-glycoprotein antagonist tariquidar in combination with vinorelbine. *Clin. Cancer Res.* 15, 3574–3582. doi:10.1158/1078-0432.CCR-08-0938

Al-Akra, L., Bae, D. H., Leck, L. Y. W., Richardson, D. R., and Jansson, P. J. (2019). The biochemical and molecular mechanisms involved in the role of tumor microenvironment stress in development of drug resistance. *Biochim. Biophys. Acta. Gen. Subj.* 1863, 1390–1397. doi:10.1016/j.bbagen.2019.06.007

Amawi, H., Sim, H. M., Tiwari, A. K., Ambudkar, S. V., and Shukla, S. (2019). ABC transporter-mediated multidrug-resistant cancer. *Adv. Exp. Med. Biol.* 1141, 549–580. doi:10.1007/978-981-13-7647-4_12

Asif, M., Usman, M., Ayub, S., Farhat, S., Huma, Z., Ahmed, J., et al. (2020). Role of ATP-binding cassette transporter proteins in CNS tumors: Resistance- based perspectives and clinical updates. *Curr. Pharm. Des.* 26, 4747–4763. doi:10.2174/1381612826666200224112141

Asong, G., Zhu, X. Y., Bricker, B., Andey, T., Amissah, F., Lamango, N., et al. (2019). New analogs of SYA013 as sigma-2 ligands with anticancer activity. *Bioorg. Med. Chem.* 27, 2629–2636. doi:10.1016/j.bmc.2019.04.012

Assaraf, Y. G., Brozovic, A., Gonçalves, A. C., Jurkovicova, D., Line, A., Machuqueiro, M., et al. (2019). The multi-factorial nature of clinical multidrug resistance in cancer. *Drug resist. updat.* 46, 100645. doi:10.1016/j.drup.2019.100645

Azzariti, A., Colabufo, N. A., Berardi, F., Porcelli, L., Niso, M., Simone, G. M., et al. (2006). Cyclohexylpiperazine derivative PB28, a Sigma2 agonist and Sigma1 antagonist receptor, inhibits cell growth, modulates P-glycoprotein, and synergizes with anthracyclines in breast cancer. *Mol. Cancer Ther.* 5, 1807–1816. doi:10.1158/1535-7163.MCT-05-0402

Beis, K. (2015). Structural basis for the mechanism of ABC transporters. *Biochem. Soc. Trans.* 43, 889–893. doi:10.1042/BST20150047

Borst, P., and Elferink, R. O. (2002). Mammalian ABC transporters in health and disease. *Annu. Rev. Biochem.* 71, 537–592. doi:10.1146/annurev.biochem.71.102301.093055

Bukowski, K., Kciuk, M., and Kontek, R. (2020). Mechanisms of multidrug resistance in cancer chemotherapy. *Int. J. Mol. Sci.* 21, 3233. doi:10.3390/ijms21093233

Cantonero, C., Camello, P. J., Abate, C., Berardi, F., Salido, G. M., Rosado, J. A., et al. (2020). NO1, a new Sigma 2 receptor/TMEM97 fluorescent ligand, downregulates SOCE and promotes apoptosis in the triple negative breast cancer cell lines. *Cancers* 12, 257. doi:10.3390/cancers12020257

Chen, A. F., Ma, W. H., Xie, X. Y., and Huang, Y. S. (2021). Sigma-2 receptor as a potential drug target. *Curr. Med. Chem.* 28, 4172–4189. doi:10.2174/0929867327666200902172615

Choi, Y. H., and Yu, A. M. (2014). ABC transporters in multidrug resistance and pharmacokinetics, and strategies for drug development. *Curr. Pharm. Des.* 20, 793–807. doi:10.2174/13816128200514021416521 2

Dean, M., Hamon, Y., and Chimini, G. (2001). The human ATP-binding cassette (ABC) transporter superfamily. *J. Lipid Res.* 42, 1007–1017. doi:10.1016/s0022-2275(20)31588-1

Dehdashti, F., Laforest, R., Gao, F., Shoghi, K. I., Aft, R. L., Nussenbaum, B., et al. (2013). Assessment of cellular proliferation in tumors by PET using 18F-ISO-1. *J. Nucl. Med.* 54, 350–357. doi:10.2967/jnumed.112.111948

Eckenstaler, R., and Benndorf, R. A. (2020). 3D Structure of the Transporter ABCG2-What's new? *Br. J. Pharmacol.* 177, 1485–1496. doi:10.1111/bph.14991

Feng, Y., Xie, X. Y., Yang, Y. Q., Sun, Y. T., Ma, W. H., Zhou, P. J., et al. (2019). Synthesis and evaluation of pyrimidoindole analogs in umbilical cord blood *ex vivo* expansion. *Eur. J. Med. Chem.* 174, 181–197. doi:10.1016/j.ejmech.2019.04.042

Gao, L., Zhao, P., Li, Y., Yang, D., Hu, P., Li, L., et al. (2020). Reversal of P-Glycoprotein-Mediated multidrug resistance by novel curcumin analogues in paclitaxel-resistant human breast cancer cells. *Biochem. Cell Biol.* 98, 484–491. doi:10.1139/bcb-2019-0377

Georgiadis, M. O., Karoutzou, O., Foscolos, A. S., and Papanastasiou, I. (2017). Sigma receptor (σR) ligands with antiproliferative and anticancer activity. *Molecules* 22, 1408. doi:10.3390/molecules22091408

Goldar, S., Khaniani, M. S., Derakhshan, S. M., and Baradaran, B. (2015). Molecular mechanisms of apoptosis and roles in cancer development and treatment. *Asian pac. J. Cancer Prev.* 16, 2129–2144. doi:10.7314/apjcp.2015.16.6.2129

Huang, Y. S., Lu, H. L., Zhang, L. J., and Wu, Z. (2014). Sigma-2 receptor ligands and their perspectives in cancer diagnosis and therapy. *Med. Res. Rev.* 34, 532–566. doi:10.1002/med.21297

Ledwitch, K. V., Gibbs, M. E., Barnes, R. W., and Roberts, A. G. (2016). Cooperativity between verapamil and ATP bound to the efflux transporter P-glycoprotein. *Biochem. Pharmacol.* 118, 96–108. doi:10.1016/j.bcp.2016.08.013

Li, Y., Xie, X., Liao, S., Zeng, Z., Li, S., Xie, B., et al. (2022). A011, a novel small-molecule ligand of σ2 receptor, potently suppresses breast cancer progression via endoplasmic reticulum stress and autophagy. *Biomed. Pharmacother.* 152, 113232. doi:10.1016/j.biopha.2022.113232

Liu, C. C., Yu, C. F., Wang, S. C., Li, H. Y., Lin, C. M., Wang, H. H., et al. (2019). Sigma-2 receptor/TMEM97 agonist PB221 as an alternative drug for brain tumor. *BMC Cancer* 19, 473. doi:10.1186/s12885-019-5700-7

Liu, X. (2019). Transporter-mediated drug-drug interactions and their significance. *Adv. Exp. Med. Biol.* 1141, 241–291. doi:10.1007/978-981-13-7647-4_5

Nicholson, H., Comeau, A., Mesangeau, C., McCurdy, C. R., and Bowen, W. D. (2015). Characterization of CM572, a selective irreversible partial agonist of the sigma-2 receptor with antitumor activity. *J. Pharmacol. Exp. Ther.* 354, 203–212. doi:10.1124/jpet.115.224105

Niso, M., Abate, C., Contino, M., Ferorelli, S., Azzariti, A., Perrone, R., et al. (2013). Sigma-2 receptor agonists as possible antitumor agents in resistant tumors: Hints for collateral sensitivity. *ChemMedChem* 8, 2026–2035. doi:10.1002/cmdc.201300291

Oyer, H. M., Sanders, C. M., and Kim, F, J. (2019). Small-molecule modulators of Sigma1 and sigma2/TMEM97 in the context of cancer: Foundational concepts and emerging themes. *Front. Pharmacol.* 10, 1141. doi:10.3389/fphar.2019.01141

Pati, M. L., Abate, C., Contino, M., Ferorelli, S., Luisi, R., Carroccia, L., et al. (2015). Deconstruction of 6, 7-dimethoxy-1, 2, 3, 4-tetrahydroisoquinoline moiety to separate P-glycoprotein (P-gp) activity from σ2 receptor affinity in mixed P-gp/σ2 receptor agents. *Eur. J. Med. Chem.* 89, 691–700. doi:10.1016/j.ejmech.2014.11.001

Pati, M. L., Niso, M., Spitzer, D., Berardi, F., Contino, M., Riganti, C., et al. (2018). Multifunctional thiosemicarbazones and deconstructed analogues as a strategy to study the involvement of metal chelation, sigma-2 (σ_2) receptor and P-gp protein in the cytotoxic action: *In vitro* and *in vivo* activity in pancreatic tumors. *Eur. J. Med. Chem.* 144, 359–371. doi:10.1016/j.ejmech.2017.12.024

Pistritto, G., Trisciuoglio, D., Ceci, C., Garufi, A., and D'Orazi, G. (2016). Apoptosis as anticancer mechanism: Function and dysfunction of its modulators and targeted therapeutic strategies. *Aging (Albany NY)* 8, 603–619. doi:10.18632/aging.100934

Rocha, C. R. R., Silva, M. M., Quinet, A., Cabral-Neto, J. B., and Menck, C. F. M. (2018). DNA repair pathways and cisplatin resistance: an intimate relationship. *Clinics* 73, e478s. doi:10.6061/clinics/2018/e478s

Schmidt, H. R., and Kruse, A. C. (2019). The molecular function of σ receptors: Past, present, and future. *Trends Pharmacol. Sci.* 40, 636–654. doi:10.1016/j.tips.2019.07.006

Sun, Y. T., Wang, G. F., Yang, Y. Q., Jin, F., Wang, Y., Xie, X. Y., et al. (2018). Synthesis and pharmacological evaluation of 6, 7-dimethoxy-1, 2, 3, 4-tetrahydroisoquinoline derivatives as sigma-2 receptor ligands. *Eur. J. Med. Chem.* 147, 227–237. doi:10.1016/j.ejmech.2017.11.016

Sung, H., Ferlay, J., Siegel, R. L., Laversanne, M., Soerjomataram, I., Jemal, A., et al. (2021). Global cancer statistics 2020: GLOBOCAN estimates of incidence and mortality worldwide for 36 cancers in 185 countries. *Ca. Cancer J. Clin.* 71, 209–249. doi:10.3322/caac.21660

Theodoulou, F. L., and Kerr, I. D. (2015). ABC transporter research: Going strong 40 Years on. *Biochem. Soc. Trans.* 43, 1033–1040. doi:10.1042/bst20150139

Warren, M. (2009). Metastatic breast cancer recurrence: a literature review of themes and issues arising from diagnosis. *Int. J. Palliat. Nurs.* 15, 222–225. doi:10.12968/ijpn.2009.15.5.42347

Zeng, C., and Mach, R. H. (2017). The evolution of the sigma-2 (σ_2) receptor from obscure binding site to bona fide therapeutic target. *Adv. Exp. Med. Biol.* 964, 49–61. doi:10.1007/978-3-319-50174-1_5

Zeng, C., Riad, A., and Mach, R. H. (2020). The biological function of sigma-2 receptor/TMEM97 and its utility in PET imaging studies in cancer. *Cancers* 12, 1877. doi:10.3390/cancers12071877

Zhao, R. Q., Wen, Y., Gupta, P., Lei, Z. N., Cai, C. Y., Liang, G., et al. (2019). Y(6), an epigallocatechin gallate derivative, reverses ABCG2-mediated mitoxantrone resistance. *Front. Pharmacol.* 9, 1545. doi:10.3389/fphar.2018.01545

Zheng, H. C. (2017). The molecular mechanisms of chemoresistance in cancers. *Oncotarget* 8, 59950–59964. doi:10.18632/oncotarget.19048

frontiers | Frontiers in Oncology

TYPE Mini Review
PUBLISHED 05 September 2022
DOI 10.3389/fonc.2022.955163

OPEN ACCESS

EDITED BY
Takeo Tatsuta,
Tohoku Medical and Pharmaceutical University, Japan

REVIEWED BY
Ming Yi,
Zhejiang University, China

*CORRESPONDENCE
Yong Yuan
yongyuan@scu.edu.cn

†Those authors have contributed equally to this work

SPECIALTY SECTION
This article was submitted to Pharmacology of Anti-Cancer Drugs, a section of the journal Frontiers in Oncology

RECEIVED 28 May 2022
ACCEPTED 17 August 2022
PUBLISHED 05 September 2022

CITATION
Cheng C, Zhuge L, Xiao X, Luan S and Yuan Y (2022) Overcoming resistance to PD-1/PD-L1 inhibitors in esophageal cancer.
Front. Oncol. 12:955163.
doi: 10.3389/fonc.2022.955163

Overcoming resistance to PD-1/PD-L1 inhibitors in esophageal cancer

Chao Cheng[1†], Lingdun Zhuge[2†], Xin Xiao[1], Siyuan Luan[1] and Yong Yuan[1*]

[1]Department of Thoracic Surgery, West China Hospital of Sichuan University, Chengdu, China, [2]Department of Head and Neck Surgery, National Cancer Center/National Clinical Research Center for Cancer/Cancer Hospital, Chinese Academy of Medical Sciences and Peking Union Medical College, Beijing, China

As the predominant treatment option of the immunotherapy for advanced esophageal cancer (EC), the application of programmed death 1 (PD-1) and programmed death-ligand 1 (PD-L1) inhibitors brings new hope to clinical practice. However, a considerable portion of patients do not response to this therapy, meanwhile most patients sensitive to PD-1 or PD-L1 antibody initially will develop resistance to the treatment eventually. To break through the limits of clinical effect, it is of critical importance to make a profound understanding of the mechanisms of so called primary resistance and acquired resistance. Subsequently, exploring potent predictors to identify suitable patients for anti-PD-1/PD-L1 treatment and investigating efficient strategies to overcome drug resistance will be helpful to expend the benefit of immunotherapy. In the present view, we summarized the potential predictive factors for anti-PD-1/PD-L1 immunotherapy in EC, and demonstrated the plausible mechanisms of resistance to PD-1/PD-L1 blockade as well as its feasible solutions.

KEYWORDS

esophageal cancer, immunotherapy, resistance, immune checkpoint inhibitors, programmed death 1, programmed death-ligand 1

Introduction

Esophageal cancer (EC) is the 6th leading cause of cancer related death worldwide (1). The treatment for EC mainly depends on surgery, chemotherapy and radiotherapy, but the prognosis remains unfavorable (2). Recently, with a deeper understanding of cancer related immune mechanisms, immunotherapy has been widely studied and has brought promising therapeutic outcomes (3–5). Programmed death-1 (PD-1) and programmed death-ligand 1 (PD-L1) are regarded as a pair of critical immune checkpoints, by which cancer cells can suppress the activity of effective immune cells, allowing the immune escape of cancer (6). PD-1/PD-L1 blockade, one of the most

efficient immune checkpoint inhibitors (ICIs), is designed to inhibit the interaction between PD-1 and PD-L1, helping to restore the anti-cancer immune response, which was approved by USFDA as a first-line treatment for advanced EC. Despite the compelling outcomes of anti-PD-1/PD-L1 therapy, drug resistance is regarded as a major problem of this treatment, since a majority of patients do not have a response to ICIs at the beginning of the therapy (7, 8), and those who are sensitive to ICIs will eventually develop therapeutic resistance (9, 10). Thus, a profound understanding of resistance to PD–1/PD–L1 blockade is of necessity to enhance the therapeutic effect of ICIs for patients with EC. In this review, we summarized the main mechanisms of resistance to anti-PD–1/PD–L1 treatment and provided some reliable predictors for the treatment, hoping to find out directions to overcome drug resistance.

Mechanisms of resistance to PD–1/PD–L1 blockade

The interaction of PD-1 with its corresponding ligand PD-L1 leads to the disability of effective T cells, by which cancer cells manage to evade the surveillance and attack from immune system (6). PD–1/PD–L1 inhibitor immunotherapy aims to block PD-1 or PD-L1 expressed on cell surface in order to activate T cells. However, a majority of cancer patients have no significant response to PD–1/PD–L1 targeted treatment (7–10), since cancer cells develop diverse mechanisms to resist ICIs. (Figure 1 and Table 1)

Aberrant expression of PD-L1

Blocking the interaction between PD-1 and PD- L1 is the aim of anti-PD-1/PD-L1 immunotherapy, therefore its therapeutic effect depends on the expression of PD-1 or PD-L1 in cancer microenvironment (11, 12). The abundance of PD-L1 was reported to be related to the genetic signature of cancer cells. For instance, in the experiments based on melanoma cell lines, JAK1/2-inactivating mutations resulting in the lack of reactive PD-L1 expression, lead to the primary resistance to PD–1/PD–L1 inhibitors (13). In addition, in lung cancer, drug resistance of cancer cells was found to be induced after anti-PD-1 therapy by down-regulation of PD-L1 expression and methylation of PD-L1 promoter (14). A series of studies have revealed plausible explanations for the mechanisms of PD-L1 regulation in EC, such as the alteration of PD-L1 level by c-Myc expression (15), and the changeable PD-L1 expression caused by various immune microenvironment (16), helping to explore solutions to overcome the resistance to PD–1/PD–L1 inhibitors for EC patients.

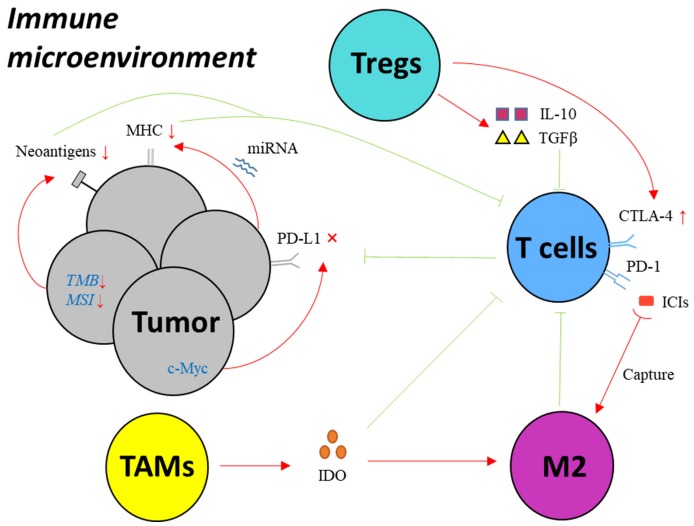

FIGURE 1
Key mechanisms of drug resistance to PD-1/PD-L1 inhibitors in EC. MHC: major histocompatibility complex; PD-1, programmed cell death protein 1; PD-L1, programmed death-ligand 1; IFN-γ, interferon gamma; CTLA-4, cytotoxic T-lymphocyte-associated protein 4; Treg, regulatory T cell; IDO, indoleamine 2,3-dioxygenase; TAM, tumor associated macrophage; M2, macrophages with M2 phenotype; ICI, immune checkpoint inhibitor; miRNA, microRNA; TMB, tumor mutation burden; MSI, microsatellite instability; TGF-β, transforming growth factor-β; IL-10, interleukin-10.

TABLE 1 The common mechanisms of resistance to PD-1/PD-L1 inhibitors in EC and other cancers.

	Common causes	EC specific
Aberrant PD-L1expression	JAK1/2-inactivating mutations Down-regulation of PD-L1 expression Methylation of PD-L1 promoter	Alteration of c-Myc expression PD-L1 expression altered by various microenvironment
Aberrant neoantigen expression	low TMB, low MSI, MMR	
Aberrant neoantigen presentation	Decreased expression of β2M Loss of functional β2M	MHC regulated by miRNAs
Suppressive microenvironment	Immunosuppressive chemokines and cytokines Immune cells: Tregs, TAMs, etc	

Attenuated expression and presentation of tumor neoantigens

Neoantigens produced by cancer cells are indispensable factors for the proliferation and activation of T lymphocytes. The absence of neoantigens disables the recognition of cancer cells by $CD8^+$ T cells, leading to impaired anti-cancer immunity (17). A straightforward way to elude the recognition from immune cells is that cancer cells evolve to lose its neoantigens on the surface. The expression of neoantigens is considered to be related with tumor mutation burden (TMB), since the accumulation of gene mutation creates tumor productions differentiated enough from normal tissue, triggering the response of T cells (18). Base mismatches during the DNA replication process are routinely fixed by some gene components, known as mismatch repair (MMR) genes. But in cancer cells, the deficient MMR results in the occurrence of microsatellite instability (MSI), allowing the accumulation of gene mutations (19, 20). In another word, low TMB level, MSI-low and MMR represent diminished immunogenicity and poor effect of anti-cancer immunotherapy, and are considered to promote primary resistance.

The presentation of tumor neoantigens, another key factor for immunological recognition, mainly relies on the major histocompatibility complex (MHC). Cancer develops an immune escape strategy by down-regulation of MHC class I expression which induces the dysfunction of $CD8^+$ T cells. Beta-2-microglobulin (β2M) as an essential component of MHC class I molecule, helps to present tumor antigens on cell membrane. Cancer cells interfere the synthesis of MHC class I molecule through decreased expression of β2M and loss of functional β2M as a response to immunotherapy, contributing to the acquired resistance (21, 22), which was illustrated by several studies of melanoma. New evidence of MHC-I regulation process has been uncovered by recent studies. For instance, it was reported that reduced expression of MHC-I in esophageal adenocarcinoma (EAC) can be caused by the increased levels of MIR125a-5p and MIR148a-3p, which influenced therapeutic effect (23).

Immune suppressive microenvironment

Immune microenvironment is significantly correlated with prognosis of cancer patient. The interaction among cancer cells, immune cells and immune molecules presents distinctively different immune phenotypes of cancer, having a conspicuous influence on the outcomes of anti-cancer treatment including anti-PD-1/PD-L1 immunotherapy.

Regulatory T cells (Tregs), a typical type of immunosuppressive cells, play a role in immune tolerance maintenance and preventing anti-cancer immune responses through suppressing activation of T cells and APCs, which consequently reduces the effect of ICIs (24). The relevant mechanisms are complex, such as up-regulation of CTLA-4 and increasing expression of PD-L1 on cell surface (25). Additionally, a variety of suppressive cytokines produced by Tregs like IL-10 and TGFβ, act on T lymphocytes as well as other immune cells and then hinder their activation (26).

The function of tumor-associated macrophages (TAMs) polarizes into either anti-tumoral or pro-tumoral effect, known as M1 and M2 subtype (27). Latest studies have demonstrated the roles of TAMs in tumor resistance to PD−1/PD−L1 blockade as follow. TAMs secret a certain type of molecules with immunosuppressive effect, named indoleamine 2,3-dioxygenase (IDO), deactivating effective T cells and inducing polarization of TAMs towards M2 subtype (28). More interestingly, TAMs were found to sabotage the combination of ICI with its target by capturing PD−1 antibody from T cell surface, preventing reactivation of dysfunctional T cells (29).

Immunosuppressive chemokines and cytokines also promote the resistance to anti-PD-1/PD-L1 immunotherapy. TGF-β, a pivotal molecule maintaining immune tolerance, has been reported to shape the microenvironment and restrain the effect of PD-L1 blockade by restricting T-cell infiltration (26).

Others like CCL2, CCL22, CCL5, CCL7 and CXCL8, also take part in limiting the efficacy of ICIs.

Predictors for PD-1/PD-L1 inhibitor effect

The response to ICI treatment varies according to different condition of each individual. Therefore, it is critical to identify reliable indicators for accurate prediction of ICI efficacy and precise identification of suitable patients for immunotherapy. At present, widely used predictors include PD-L1 expression level, TMB, MSI and so forth. With the further understanding of immune mechanisms, more effective biomarkers can be identified for ICI treatment (Figure 2).

PD-L1 expression level

PD-L1 expression level in tumor tissue is widely used in clinical practice as an indicator for the therapeutic effect of anti-PD-1/PD-L1 treatment. Patients with high expression of PD-L1 are supposed to have better prognosis after receiving anti-PD-1/PD-L1 treatment (11, 12). In EAC, according to outcomes of several well-known clinical trials, the lack of benefit of ICIs was observed in the low PD-L1-expressing subgroup (30). However, its predictive efficacy is not that satisfactory, since some patients with low expression of PD-L1 have a positive response to ICIs (31), and vice versa. Additionally, the expression level of PD-L1 does not remain constant. It can be altered during the therapeutic course. A recent study demonstrated the profound influence on the expression of PD-L1 and PD-L2 by chemotherapeutic agents in esophageal squamous cell carcinoma (ESCC) (32), which implied one-time evaluation of PD-L1 might not be sufficient to predict the efficacy of ICIs.

TMB and MSI

The predictive value of TMB and MSI for anti-PD-1/PD-L1 treatment has been verified (33–35). In many malignancies, including EC, high level of TMB or MSI is positively correlated with the prognosis of patients receiving ICIs. The predictive role of TMB is found to be independent of PD-L1 expression level by recent studies (36). Therefore, the approved indications of the application of ICIs include TMB-high or MSI-high EC.

Non-coding RNAs

It is widely acknowledged that non-coding RNAs, such as microRNAs, long non-coding RNAs, and circular RNAs, are involved in multiple cellular functions. Their predictive value for effect of ICIs is gradually revealed by a growing number of studies.

New evidence showed that a group of MDSC-relevant microRNAs indicating MDSC activity closely relates with resistance to treatment with ICIs. A recent study suggested that these RNAs might be potential blood biomarkers predicting immunotherapy outcomes in melanoma (37). A recent study based on a phase II clinical trial investigated the value of microRNAs as predictive makers, and found that serum microRNAs, including miR-1233-5p, miR-6885-5p, miR-4698 and miR-128-2-5p, capable of predicting the response to nivolumab in patients with advanced EC (38).

Immune features

The immune characteristics of cancer patients are significantly related with the outcomes of ICI treatment. T cell

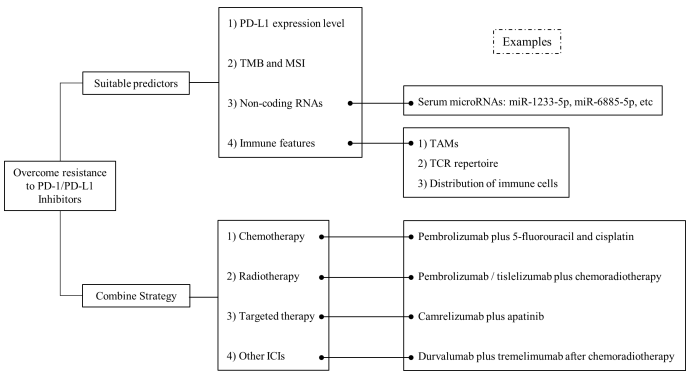

FIGURE 2
Overview on the strategies to overcome drug resistance to PD-1/PD-L1 inhibitors in EC. Strategies including suitable predictors and combined therapy, have been proposed to improve the effect of PD-1/PD-L1 inhibitors in EC.

receptor (TCR) repertoire has been widely studied as a predictor for immunotherapy efficiency. In EC, researchers found the peripheral $CD8^+$ TCR diversity at baseline and dynamic alteration of intratumoral TCRs showed significant correlation with the prognosis of radiotherapy combined with immunotherapy (39). More interestingly, the spatial distribution patterns of immune cells were recently identified as prognostic factors for the therapeutic effect of ICIs in EC, since the spatial distance between cancer cells and various subtypes of immune cells, such as dendritic cells and macrophages, is correlated with PFS and OS (40). The infiltration of macrophages in cancer microenvironment is recognized as an indicator of poor prognosis of EC. Previous studies have identified the role of TAMs in increasing PD-L1 expression in EC (41). Given the close correlation between TAMs and PD-L1, a clinical trial was launched to investigate the therapeutic efficacy of combination of CSF-1R blockade (TAM-targeting therapy) with PD-1/PD-L1 inhibitor in several advanced solid tumors, such as lung cancer, and pancreatic cancer (42).

Strategies to overcome drug resistance and future directions

To enhance the efficacy of ICIs, combination strategy is adopted (Figure 2). Immunotherapy combined with chemotherapy is the most widely used method to improve therapeutic effect for EC patients, since the outcomes of KEYNOTE-590 showed significantly improved survival in ESCC patients when pembrolizumab was added to chemotherapy (43). The plausible explanations for the improved outcomes of the combination might involve several mechanisms, such as increased sensitivity of cancer cells to immunotherapy *via* increase of mutation burden, upregulation of PD-L1 expression, and restoration of exhausted immune cells by chemotherapeutic agents (44, 45). Recently, the value of radiotherapy in addition to ICIs has attracted some attention. Previous study has revealed the immune-related effects of radiotherapy in cancer treatment, including EC (46, 47). For instance, the death of cancer cells allows more exposure of tumor specific antigens, activating antigen-presenting cells (48). A series studies such as KEYNOTE-975 and RATIONALE 311, have been designed to explore the therapeutic effect of ICIs plus chemoradiotherapy in EC treatment (49, 50). Anti-PD-1/PD-L1 treatment added to targeted therapy is regarded as a promising direction. Clinical trials have been launched to evaluate the integration of ICIs and targeted therapy. In patients with advanced ESCC, a single-arm, phase II study analyzing the safety and the efficacy of camrelizumab plus apatinib as second-line treatment showed 34.6% of patients had an objective response, and 44% of patients had grade 3 or worse adverse events (51). The promising activity and manageable toxicity of the combination treatment indicated it might be an option for patients with advanced ESCC. The effective combination of PD-1/PD-L1 blockade with other type of ICIs is under exploration in several malignancies including EC. A latest research reported that additional application of durvalumab and tremelimumab after chemoradiotherapy significantly improved survival in patients with locally advanced ESCC, especially in those with PD-L1 positive tumors (52). Additionally, some studies have found the combination of anti-PD-1/PD-L1 inhibitors with some chemokine or cytokine blockades might bring new solutions to overcome drug resistance. For instance, a novel type of antibody, named YM101, was developed to enhance the effect of ICIs by blocking PD-1/PD-L1 and TGF-β simultaneously, which was found to have a superior anti-tumor effect compared to the monotherapies (53). Some new emerging combination strategies exhibited potent antitumor efficacy (54), which might be future direction for cancer immunotherapy. For example, combining Mn^{2+} with YM101 has a synergistic antitumor effect, effectively controlling tumor growth and prolonging the survival of tumor-bearing mice (55). This novel cocktail strategy has the potential to be a universal regimen for inflamed and non-inflamed tumors.

Discussion

Drug resistance hinders the applicability of PD-1/PD-L1 inhibitors in the treatment of EC. Although the mechanisms are complicated and multifactorial, a systematic investigation and understanding will undoubtedly contribute to establish new strategies to improve efficacy and outcomes of anti-PD-1/PD-L1 treatment in patients with EC.

Given the evidence that we have gathered, one rational option to avoid resistance against PD-L/PD-1 blockade is to identify the suitable population before the application of the therapy. A thorough and accurate profile of immunological status seems to be necessary for each patient, which is also supposed to be a non-invasive or minimal invasive procedure. The modern technologies, such as new generation sequencing and flow cytometry, facilitate the analysis of immunological profile, providing the feasibility to achieve this goal. Some recent studies illustrated the method to depict the status of immune activities using peripheral blood by flow cemetery. For example, in lung cancer, researchers found this method was a reliable and efficient way to identify candidates who might have a better chance of responding to PD-1/PD-L1 inhibitors (56). Another key point of evaluating the appropriateness of anti-PD-1/PD-L1 treatment is a dynamic monitor of immunological profile for patients, since the fluctuations or changes of immune status can significantly influence the effect of immunotherapy, as well as can help to distinguish the response groups of patients.

For instance, some researchers compared the changes of different immune variables in blood samples derived from cancer patients before and after anti-PD-1 treatment, and confirmed these alterations as useful markers to identify eligible patients for anti-PD-1 therapy (57). Of course, the definition of immunological profile is not confined to immune cells or molecules. As aforementioned, the genetic characteristics of cancer cells are also correlated with the anti-cancer immune activities, and therefore have an influence on the outcomes of immunotherapy. With the widely use of new generation sequencing in clinical oncology, it is reasonable to assume this will be a promising approach to screening appropriate candidates for ICI treatment. However, our current knowledge of the correlation between genetic features and outcomes of anti-PD-1/PD-L1 therapies is limited. Hence, identification and construction of gene panels affecting the pathways of immune checkpoints and the outcomes of ICI treatment will play an indispensable role as a critical research subject in oncology in the near future.

In cancer microenvironment, there is an equilibrium between conditions that promote and suppress anti-cancer immunity, which is described as a conceptual framework named "cancer-immune set point" (58). It works as a presumption helping to interpret changeable response to ICI therapies. From this perspective, the purpose of current combination therapies adopted to overcome drug resistance against PD-1/PD-L1 inhibitors can be considered as strategies to enhance the factors contributing to anti-cancer immunity by increasing the expression of neoantigens and further activation of T cells, as well as to diminish unfavorable factors by regulating suppressive immune cells and chemokines. Take the combination of chemotherapy and anti-PD-1/PD-L1 inhibitors as an example. Chemotherapy can cause the up-regulation of antigen expression by triggering DNA damage of cancer cells on one hand, on the other hand it was reported that chemotherapeutic agents are able to alter immune microenvironment of EC through various methods, such as upregulation of cell surface PD-L1 expression (59). And this type of combination showed promising clinical outcomes. Other proposal of combination strategies can be inspired and designed following this thread of thought. Some studies have demonstrated the role of HER2 antibody in promoting anti-cancer immune activities (60), leading to the logical attempt to add anti-HER2 treatment to ICI in EC, which brings us the well-known clinical trials such as KEYNOTE-811 and MAHOGANY studies. With new findings of immune pathways and mechanisms, there is no doubt that more and more efficacious combination strategies will be developed to improve the therapeutic effect of PD-1/PD-L1 inhibitors in EC.

Conclusions

A clear understanding of the mechanisms of drug resistance and identification of reliable predictors help to develop feasible strategies to overcome resistance to anti-PD-1/PD-L1 treatment, and to improve the therapeutic effects of ICIs in EC.

Author contributions

CC and LZ have contributed equally. CC, conception, manuscript preparation, data collection, manuscript editing and manuscript review. LZ, conception, manuscript editing and manuscript review. XX, manuscript editing and manuscript review. SL, manuscript review. YY, conception, manuscript editing and manuscript review. All authors contributed to the article and approved the submitted version.

Funding

This study was supported by the National Natural Science Foundation of China (81802273,81970481), 1.3.5 project for disciplines of excellence, West China Hospital, Sichuan University (Grant No. 2020HXFH047 and 20HXJS005) and Sichuan Science and Technology Program (2022YFS0048).

Conflict of interest

The authors declare that the research was conducted in the absence of any commercial or financial relationships that could be construed as a potential conflict of interest.

Publisher's note

References

1. Bray F, Ferlay J, Soerjomataram I, Siegel RL, Torre LA, Jemal A, et al. Global cancer statistics 2018: GLOBOCAN estimates of incidence and mortality worldwide for 36 cancers in 185 countries. *CA Cancer J Clin* (2018) 68:394–424. doi: 10.3322/caac.21492

2. Baba Y, Yoshida N, Kinoshita K, Iwatsuki M, Yamashita YI, Chikamoto A, et al. Clinical and prognostic features of patients with esophageal cancer and multiple primary cancers: a retrospective single-institution study. *Ann Surg* (2018) 267:478–83. doi: 10.1097/SLA.0000000000002118

3. Shah MA, Kojima T, Hochhauser D, Enzinger P, Raimbourg J, Hollebecque A, et al. Efficacy and safety of pembrolizumab for heavily pretreated patients with advanced, metastatic adenocarcinoma or squamous cell carcinoma of the esophagus: The phase 2 KEYNOTE-180 study. *JAMA Oncol* (2019) 5:546–50. doi: 10.1001/jamaoncol.2018.5441

4. Kojima T, Shah MA, Muro K, Francois E, Adenis A, Hsu CH, et al. Randomized phase III KEYNOTE-181 study of pembrolizumab versus chemotherapy in advanced esophageal cancer. *J Clin Oncol* (2020) 38:4138–48. doi: 10.1200/JCO.20.01888

5. Kato K, Sun J, Shah MA, Enzinger P, Adenis A, Doi T, et al. LBA8_PR - pembrolizumab plus chemotherapy versus chemotherapy as first-line therapy in patients with advanced esophageal cancer: The phase 3 KEYNOTE-590 study. *Ann Oncol* (2020) 31:S1142–215. doi: 10.1016/j.annonc.2020.08.2298

6. Kim JM, Chen DS. Immune escape to PD-L1/PD-1 blockade: Seven steps to success (or failure). *Ann Oncol: Off J Eur Soc Med Oncol* (2016) 27(8):1492–504. doi: 10.1093/annonc/mdw217

7. O'Donnell JS, Smyth MJ, Teng MWL. Acquired resistance to anti-PD1 therapy: Checkmate to checkpoint blockade? *Genome Med* (2016) 8:111. doi: 10.1186/s13073-016-0365-1

8. Jiang X, Zhou J, Giobbie-Hurder A, Wargo J, Hodi FS. The activation of MAPK in melanoma cells resistant to BRAF inhibition promotes PD-L1 expression that is reversible by MEK and PI3K inhibition. *Clin Cancer Res* (2013) 19:598–609. doi: 10.1158/1078-0432.CCR-12-2731

9. Jenkins RW, Barbie D. A, Flaherty KT. Mechanisms of resistance to immune checkpoint inhibitors. *Br J Cancer* (2018) 118:9–16. doi: 10.1038/bjc.2017.434

10. Syn NL, Teng MWL, Mok TSK, Soo RA. *De-novo* and acquired resistance to immune checkpoint targeting. *Lancet Oncol* (2017) 18:e731–41. doi: 10.1016/S1470-2045(17)30607-1

11. Yu H, Boyle TA, Zhou C, Rimm DL, Hirsch FR.. PD-L1 expression in lung cancer. *J Thorac Oncol* (2016) 11(7):964–75. doi: 10.1016/j.jtho.2016.04.014

12. Zhang J, Dang F, Ren J, Wei W. Biochemical aspects of PD-L1 regulation in cancer immunotherapy. *Trends Biochem Sci* (2018) 43(12):1014–32. doi: 10.1016/j.tibs.2018.09.004

13. Shin DS, Zaretsky JM, Escuin-Ordinas H, Garcia-Diaz A, Hu-Lieskovan S, Kalbasi A, et al. Primary resistance to PD-1 blockade mediated by JAK1/2 mutations. *Cancer Discovery* (2017) 7(2):188–201. doi: 10.1158/2159-8290.CD-16-1223

14. Zhang Y, Xiang C, Wang Y, Duan Y, Liu C, Zhang Y, et al. PD-L1 promoter methylation mediates the resistance response to anti-PD-1 therapy in NSCLC patients with EGFR-TKI resistance. *Oncotarget* (2017) 8:101535–44. doi: 10.18632/oncotarget.21328

15. Liang MQ, Yu FQ, Chen C. C-myc regulates PD-L1 expression in esophageal squamous cell carcinoma. *Am J Transl Res* (2020) 12(2):379–88.

16. Zheng S, Shen T, Liu Q, Liu T, Tuerxun A, Zhang Q, et al. CXCL6 fuels the growth and metastases of esophageal squamous cell carcinoma cells both *in vitro* and *in vivo* through upregulation of PD-L1 *via* activation of STAT3 pathway. *J Cell Physiol* (2021) 236(7):5373–86. doi: 10.1002/jcp.30236

17. Chandran SS, Klebanoff CA. T Cell receptor-based cancer immunotherapy: Emerging efficacy and pathways of resistance. *Immunol Rev* (2019) 290(1):127–47. doi: 10.1111/imr.12772

18. Rizvi NA, Hellmann MD, Snyder A, Kvistborg P, Makarov V, Havel JJ, et al. Cancer immunology. mutational landscape determines sensitivity to PD-1 blockade in non-small cell lung cancer. *Science* (2015) 348(6230):124–8. doi: 10.1126/science.aaa1348

19. Baretti M, Le DT. DNA Mismatch repair in cancer. *Pharmacol Ther* (2018) 189:45–62. doi: 10.1016/j.pharmthera.2018.04.004

20. Dudley JC, Lin MT, Le DT, Eshleman JR. Microsatellite instability as a biomarker for PD-1 blockade. *Clin Cancer Res* (2016) 22:813–20. doi: 10.1158/1078-0432.CCR-15-1678

21. Zaretsky JM, Garcia-Diaz A, Shin DS, Escuin-Ordinas H, Hugo W, Hu-Lieskovan S, et al. Mutations associated with acquired resistance to PD-1 blockade in melanoma. *N Engl J Med* (2016) 375:819–29. doi: 10.1056/NEJMoa1604958

22. Sade-Feldman M, Jiao YJ, Chen JH, Rooney MS, Barzily-Rokni M, Eliane JP, et al. Resistance to checkpoint blockade therapy through inactivation of antigen presentation. *Nat Commun* (2017) 8:1–11. doi: 10.1038/s41467-017-01062-w

23. Mari L, Hoefnagel SJM, Zito D, van de Meent M, van Endert P, Calpe S, et al. microRNA 125a regulates MHC-I expression on esophageal adenocarcinoma cells, associated with suppression of antitumor immune response and poor outcomes of patients. *Gastroenterology* (2018) 155(3):784–98. doi: 10.1053/j.gastro.2018.06.030

24. Principe DR, Chiec L, Mohindra NA, Munshi HG. Regulatory T-cells as an emerging barrier to immune checkpoint inhibition in lung cancer. *Front Oncol* (2021) 11:684098. doi: 10.3389/fonc.2021.684098

25. Schmidt A, Oberle N, Krammer PH. Molecular mechanisms of treg-mediated T cell suppression. *Front Immunol* (2012) 3:51. doi: 10.3389/fimmu.2012.00051

26. Mariathasan S, Turley SJ, Nickles D, Castiglioni A, Yuen K, Wang Y, et al. TGFβ attenuates tumour response to PD-L1 blockade by contributing to exclusion of T cells. *Nature* (2018) 554(7693):544–8. doi: 10.1038/nature25501

27. Chanmee T, Ontong P, Konno K, Itano N. Tumor-associated macrophages as major players in the tumor microenvironment. *Cancers (Basel)* (2014) 6:1670–90. doi: 10.3390/cancers6031670

28. Katz JB, Muller AJ, Prendergast GC. Indoleamine 2,3-dioxygenase in T-cell tolerance and tumoral immune escape. *Immunol Rev* (2008) 222:206–21. doi: 10.1111/j.1600-065X.2008.00610.x

29. Arlauckas SP, Garris CS, Kohler RH, Kitaoka M, Cuccarese MF, Yang KS, et al. *In vivo* imaging reveals a tumor-associated macrophage-mediated resistance pathway in anti-PD-1 therapy. *Sci Transl Med* (2017) 9(389):eaal3604. doi: 10.1126/scitranslmed.aal3604

30. Zhao JJ, Yap DWT, Chan YH, Tan BKJ, Teo CB, Syn NL, et al. Low programmed death-ligand 1-expressing subgroup outcomes of first-line immune checkpoint inhibitors in gastric or esophageal adenocarcinoma. *J Clin Oncol* (2022) 40(4):392–402. doi: 10.1200/JCO.21.01862

31. Patel SP, Kurzrock R. PD-L1 expression as a predictive biomarker in cancer immunotherapy. *Mol Cancer Ther* (2015) 14(4):847–56. doi: 10.1158/1535-7163.MCT-14-0983

32. Okadome K, Baba Y, Yasuda-Yoshihara N, Nomoto D, Yagi T, Toihata T, et al. PD-L1 and PD-L2 expression status in relation to chemotherapy in primary and metastatic esophageal squamous cell carcinoma. *Cancer Sci* (2022) 113(2):399–410. doi: 10.1111/cas.15198

33. Carbone DP, Reck M, Paz-Ares L, Creelan B, Horn L, Steins M, et al. First-line nivolumab in stage IV or recurrent non-Small-Cell lung cancer. *N Engl J Med* (2017) 376(25):2415–26. doi: 10.1056/NEJMoa1613493

34. Hellmann MD, Ciuleanu TE, Pluzanski A, Lee JS, Otterson GA, Audigier-Valette C, et al. Nivolumab plus ipilimumab in lung cancer with a high tumor mutational burden. *N Engl J Med* (2018) 378(22):2093–104. doi: 10.1056/NEJMoa1801946

35. Hause RJ, Pritchard CC, Shendure J, Salipante SJ. Classification and characterization of microsatellite instability across 18 cancer types. *Nat Med* (2016) 22(11):1342–50. doi: 10.1038/nm.4191

36. Chan TA, Yarchoan M, Jaffee E, Swanton C, Quezada SA, Stenzinger A, et al. Development of tumor mutation burden as an immunotherapy biomarker: Utility for the oncology clinic. *Ann Oncol* (2019) 30(1):44–56. doi: 10.1093/annonc/mdy495

37. Huber V, Vallacchi V, Fleming V, Hu X, Cova A, Dugo M, et al. Tumor-derived microRNAs induce myeloid suppressor cells and predict immunotherapy resistance in melanoma. *J Clin Invest* (2018) 128(12):5505–16. doi: 10.1172/JCI98060

38. Sudo K, Kato K, Matsuzaki J, Takizawa S, Aoki Y, Shoji H, et al. Identification of serum microRNAs predicting the response of esophageal squamous-cell carcinoma to nivolumab. *Jpn J Clin Oncol* (2020) 50(2):114–21. doi: 10.1093/jjco/hyz146

39. Yan C, Ma X, Guo Z, Wei X, Han D, Zhang T, et al. Time-spatial analysis of T cell receptor repertoire in esophageal squamous cell carcinoma patients treated with combined radiotherapy and PD-1 blockade. *Oncoimmunology* (2022) 11(1):2025668. doi: 10.1080/2162402X.2022.2025668

40. Ma X, Guo Z, Wei X, Zhao G, Han D, Zhang T, et al. Spatial distribution and predictive significance of dendritic cells and macrophages in esophageal cancer treated with combined chemoradiotherapy and PD-1 blockade. *Front Immunol* (2022) 12:786429. doi: 10.3389/fimmu.2021.786429

41. Yagi T, Baba Y, Okadome K, Kiyozumi Y, Hiyoshi Y, Ishimoto T, et al. Tumour-associated macrophages are associated with poor prognosis and programmed death ligand 1 expression in oesophageal cancer. *Eur J Cancer* (2019) 111:38–49. doi: 10.1016/j.ejca.2019.01.018

42. Razak AR, Cleary JM, Moreno V, Boyer M, Calvo Aller E, Edenfield W, et al. Safety and efficacy of AMG 820, an anti-colony-stimulating factor 1 receptor antibody, in combination with pembrolizumab in adults with advanced solid tumors. *J Immunother Cancer* (2020) 8(2):e001006. doi: 10.1136/jitc-2020-001006

43. Sun JM, Shen L, Shah MA, Enzinger P, Adenis A, Doi T, et al. Pembrolizumab plus chemotherapy versus chemotherapy alone for first-line treatment of advanced oesophageal cancer (KEYNOTE-590): a randomised, placebo-controlled, phase 3 study. *Lancet* (2021) 398(10302):759–71. doi: 10.1016/S0140-6736(21)01234-4

44. Zitvogel L, Galluzzi L, Smyth MJ, Kroemer G., et al. Mechanism of action of conventional and targeted anticancer therapies: reinstating immunosurveillance. *Immunity* (2013) 39(1):74–88. doi: 10.1016/j.immuni.2013.06.014

45. Galluzzi L, Buqué A, Kepp O, Kroemer G.. Immunological effects of conventional chemotherapy and targeted anticancer agents. *Cancer Cell* (2015) 28(6):690–714. doi: 10.1016/j.ccell.2015.10.012

46. Yoshimoto Y, Kono K, Suzuki Y. Anti-tumor immune responses induced by radiotherapy: A review. *Fukushima J Med Sci* (2015) 61:13. doi: 10.5387/fms.2015-6

47. Kojima T, Doi T. Immunotherapy for esophageal squamous cell carcinoma. *Curr Oncol Rep* (2017) 19:33. doi: 10.1007/s11912-017-0590-9

48. Gaur P, Hunt CR, Pandita TK. Emerging therapeutic targets in esophageal adenocarcinoma. *Oncotarget* (2016) 7:48644. doi: 10.18632/oncotarget.8777

49. Shah MA, Bennouna J, Doi T, Shen L, Kato K, Adenis A, et al. KEYNOTE-975 study design: A phase III study of definitive chemoradiotherapy plus pembrolizumab in patients with esophageal carcinoma. *Future Oncol* (2021) 17 (10):1143–53. doi: 10.2217/fon-2020-0969

50. Yu R, Wang W, Li T, Li J, Zhao K, Wang W, et al. RATIONALE 311: tislelizumab plus concurrent chemoradiotherapy for localized esophageal squamous cell carcinoma. *Future Oncol* (2021) 17(31):4081–9. doi: 10.2217/fon-2021-0632

51. Meng X, Wu T, Hong Y, Fan Q, Ren Z, Guo Y, et al. Camrelizumab plus apatinib as second-line treatment for advanced oesophageal squamous cell carcinoma (CAP 02): A single-arm, open-label, phase 2 trial. *Lancet Gastroenterol Hepatol* (2022) 7(3):245–53. doi: 10.1016/S2468-1253(21)00378-2

52. Park S, Oh D, Choi YL, Chi SA, Kim K, Ahn MJ, et al. Durvalumab and tremelimumab with definitive chemoradiotherapy for locally advanced esophageal squamous cell carcinoma. *Cancer* (2022) 128(11):2148–58. doi: 10.1002/cncr.34176

53. Yi M, Zhang J, Li A, Niu M, Yan Y, Jiao Y, et al. The construction, expression, and enhanced anti-tumor activity of YM101: A bispecific antibody simultaneously targeting TGF-β and PD-L1. *J Hematol Oncol* (2021) 14(1):27. doi: 10.1186/s13045-021-01045-x

54. Yi M, Zheng X, Niu M, Zhu S, Ge H, Wu K, et al. Combination strategies with PD-1/PD-L1 blockade: current advances and future directions. *Mol Cancer* (2022) 21(1):28. doi: 10.1186/s12943-021-01489-2

55. Yi M, Niu M, Zhang J, Li S, Zhu S, Yan Y, et al. Combine and conquer: manganese synergizing anti-TGF-β/PD-L1 bispecific antibody YM101 to overcome immunotherapy resistance in non-inflamed cancers. *J Hematol Oncol* (2021) 14(1):146. doi: 10.1186/s13045-021-01155-6

56. Zuazo M, Arasanz H, Fernández-Hinojal G, García-Granda MJ, Gato M, Bocanegra A, et al. Functional systemic CD4 immunity is required for clinical responses to PD-L1/PD-1 blockade therapy. *EMBO Mol Med* (2019) 11(7):e10293. doi: 10.1093/annonc/mdz253.058

57. Juliá EP, Mandó P, Rizzo MM, Cueto GR, Tsou F, Luca R, et al. Peripheral changes in immune cell populations and soluble mediators after anti-PD-1 therapy in non-small cell lung cancer and renal cell carcinoma patients. *Cancer Immunol Immunother* (2019) 68(10):1585–96. doi: 10.1007/s00262-019-02391-z

58. Power R, Lowery MA, Reynolds JV, Dunne MR. The cancer-immune set point in oesophageal cancer. *Front Oncol* (2020) 10:891. doi: 10.3389/fonc.2020.00891

59. Van Der Kraak L, Goel G, Ramanan K, Kaltenmeier C, Zhang L, Normolle DP, et al. 5-fluorouracil upregulates cell surface B7-H1 (PD-L1) expression in gastrointestinal cancers. *J Immunother Cancer* (2016) 4:65. doi: 10.1186/s40425-016-0163-8

60. Arnould L, Gelly M, Penault-Llorca F, Benoit L, Bonnetain F, Migeon C, et al. Trastuzumab-based treatment of HER2-positive breast cancer: an antibody-dependent cellular cytotoxicity mechanism? *Br J Cancer* (2006) 94:259–67. doi: 10.1038/sj.bjc.6602930

frontiers | Frontiers in Pharmacology

TYPE Original Research
PUBLISHED 03 October 2022
DOI 10.3389/fphar.2022.931772

OPEN ACCESS

EDITED BY
Takeo Tatsuta,
Tohoku Medical and Pharmaceutical University, Japan

REVIEWED BY
Mohamed A Yassin,
Hamad Medical Corporation, Qatar
Thomas Lion,
St. Anna Children's Cancer Research Institute (CCRI), Austria

*CORRESPONDENCE
Yuping Gong,
gongyuping2010@aliyun.com

†These authors share first authorship

SPECIALTY SECTION
This article was submitted to Pharmacology of Anti-Cancer Drugs, a section of the journal Frontiers in Pharmacology

RECEIVED 29 April 2022
ACCEPTED 23 August 2022
PUBLISHED 03 October 2022

CITATION
Ye W, Wu X, Wang X, Wei X, Tang Y, Ouyang X and Gong Y (2022), The proteolysis targeting chimera GMB-475 combined with dasatinib for the treatment of chronic myeloid leukemia with BCR::ABL1 mutants.
Front. Pharmacol. 13:931772.
doi: 10.3389/fphar.2022.931772

The proteolysis targeting chimera GMB-475 combined with dasatinib for the treatment of chronic myeloid leukemia with BCR::ABL1 mutants

Wu Ye†, Xia Wu†, Xiaojia Wang, Xiaoyu Wei, Yuqian Tang, Xianfeng Ouyang and Yuping Gong*

Department of Hematology, West China Hospital, Sichuan University, Chengdu, Sichuan, China

Patients with chronic myeloid leukemia (CML) show resistance to tyrosine kinase inhibitors (TKIs) targeting ABL1 due to the emergence of BCR::ABL1 mutants, especially compound mutants during the treatment, which brings great challenges to clinical practice. Combination therapy is an effective strategy for drug resistance. GMB-475, a proteolysis targeting chimera (PROTAC) targeting the myristoyl pocket of ABL1 in an allosteric manner, degrades the BCR::ABL1 through the ubiquitin–proteasome pathway. In this study, we combined GMB-475 with orthosteric TKIs targeting ABL1 to overcome resistance. We constructed Ba/F3 cells carrying BCR::ABL1 mutants by gene cloning technology and compared the effects of combination therapy with those of monotherapy on the biological characteristics and signaling pathways in CML cells. We found that the effects of ABL1 inhibitors, including imatinib, dasatinib, ponatinib, and ABL001, on growth inhibition and promoting apoptosis of Ba/F3 cells with BCR::ABL1 mutants, especially compound mutants, were weakened. GMB-475 combined with TKIs, especially dasatinib, synergistically inhibited growth, promoted apoptosis, and blocked the cell cycle of Ba/F3 cells carrying BCR::ABL1 mutants and synergistically blocked multiple molecules in the JAK-STAT pathway. In conclusion, dasatinib enhanced the antitumor effect of GMB-475; that is, the combination of PROTAC targeting ABL1 in an allosteric manner and orthosteric TKIs, especially dasatinib, provides a novel idea for the treatment of CML patients with BCR::ABL1 mutants in clinical practice.

KEYWORDS

chronic myeloid leukemia, GMB-475, dasatinib, combination therapy, BCR::ABL1 mutants

Abbreviations: CML, chronic myeloid leukemia; PROTAC, proteolysis targeting chimera; DAS, dasatinib; WT, wild type; TKIs, tyrosine kinase inhibitors; MTT, thiazolyl blue tetrazolium bromide; CCK8, cell counting kit-8; CI, combination index; qPCR, quantitative real-time PCR; CTR, control.

Introduction

Chronic myeloid leukemia (CML) is a bone marrow proliferative hematopoietic cell malignancy (Eden and Coviello 2021) characterized by the *BCR::ABL1* fusion gene that is formed by genetic translocation between chromosome 9 and chromosome 22 (Haider and Anwer 2021). The BCR::ABL1 fusion oncoprotein, which has tyrosine kinase activity (Cetin et al., 2021) and activates different downstream signal pathways, such as *JAK-STAT, MAPK/ERK*, and *PI3K/Akt/mTOR*, promotes the occurrence and development of leukemia (Singh et al., 2021). In the United States, there are approximately 8000 newly diagnosed cases of CML per year (Patel et al., 2017). Imatinib, the first-generation tyrosine kinase inhibitor (TKI), significantly improved the prognosis of CML patients (Milojkovic et al., 2021; Morita and Sasaki 2021), but approximately 40% of chronic phase patients with CML had to stop imatinib due to failure and/or drug intolerance (Özgür and Eşkazan 2020; Koyama et al., 2021). The mechanisms of CML patients resistant to TKIs can be divided into BCR::ABL1-dependent and BCR::ABL1-independent resistance; the former includes BCR::ABL1 mutation and amplification, and the latter includes abnormal energy metabolism and the persistence of leukemia stem cells (Lei et al., 2021) due to bypass activation (Talati and Pinilla-Ibarz 2018). Second- and third-generation TKIs, such as dasatinib, nilotinib, bosutinib, and ponatinib, provide effective control of drug resistance caused by point mutations in the BCR::ABL1 kinase region (Liu et al., 2021), but these TKIs cannot control drug resistance caused by all site mutations. Compared with imatinib, the second-generation TKI can achieve a faster and deeper molecular response but does not prolong the survival of patients (Morita and Sasaki 2021). Moreover, some serious adverse events, such as cardiovascular toxicity of ponatinib (Singh et al., 2019) and pulmonary hypertension of dasatinib (Guignabert et al., 2016), have limited the application of these agents; meanwhile, the emergence of compound mutations in the BCR::ABL1 kinase region is resistant to all approved TKIs targeting BCR::ABL1 (Khorashad et al., 2013). ABL001, an allosteric inhibitor targeting ABL1, induces the formation of the inactive kinase conformation (Wylie et al., 2017) by binding to the myristoyl pocket of ABL1 (Breccia et al., 2021). ABL001 is effective for most single mutations in the BCR::ABL1 kinase region, but not for compound mutations, mutations in the myristoyl pocket, and the F359V mutation that affects its binding (Eide et al., 2019).

Proteolysis targeting chimera (PROTAC) has been a novel drug development technology since 2000 (Mukhamejanova et al., 2021), and it consists of three parts: ligand binding to the protein of interest, E3 ubiquitination ligase ligand (including Von Hippel–Lindau and cereblon) (Ishida and Ciulli 2021), and linker connecting the two parts (Coll-Martínez et al., 2020; Ghidini et al., 2021). PPOTAC, binding to the target protein and recruiting E3 ubiquitination ligase, ubiquitinates the target protein and then degrades it by the proteasome, which achieves an antitumor effect (Qi et al., 2021). Being widely applied as a biological tool and drug molecule, PROTAC has a potential clinical application value (Zeng et al., 2021) and is considered a novel strategy for the treatment of various diseases (Mukhamejanova et al., 2021). At present, many PROTAC molecules with high degradation efficiency have been reported, including those targeting the androgen receptor (Lee et al., 2021), estrogen receptor (Jiang et al., 2018; Hu et al., 2019; Li et al., 2019), ALK (Yan et al., 2021), BTK (Buhimschi et al., 2018; Sun et al., 2018; Zhao et al., 2021), and many others. The first batch of oral PROTACs has been included in clinical trials achieving exciting results (Protein Degradation, 2020; Qin et al., 2021). Unlike traditional small molecule inhibitors needing stable binding with the target protein, as long as PROTAC binds to the target protein briefly, it would degrade it in a catalytic manner (Martín-Acosta and Xiao 2021). GMB-475 (Burslem et al., 2019), targeting the myristoyl pocket of ABL1 via an allosteric way, degrades the BCR::ABL1 fusion protein through the ubiquitin–proteasome pathway; however, it inhibited proliferation and promoted apoptosis in CML cell lines only at high concentrations. Thus, we combined GMB-475 with orthosteric TKIs targeting ABL1 to reduce the effective concentration of the two drugs. Therefore, this study investigated the combination of GMB-475 and TKIs to overcome drug resistance in CML caused by BCR::ABL1 mutations.

Materials and methods

The sources of the main experimental reagents are shown in Supplementary Table S1.

Cell lines

Using the MSCV-IRES-GFP-p210 (MIG-p210) wild-type plasmid as a template, we constructed MIG-p210 plasmids with BCR::ABL1 single mutations (including E255K, T315I, L387M, F359V, and F486S) by PCR, overlapping PCR, enzyme digestion and enzyme connection, gel purification, and recovery. Then, using MIG-p210 plasmids with BCR::ABL1 single mutations as a template and repeating the above process, we constructed MIG-p210 plasmids with BCR::ABL1 compound mutations (including T315I + E255K, T315I + L387M, and T315I + F486S). After sequencing the MIG-p210 plasmids with BCR::ABL1 mutations, we confirmed that the mutations were successfully introduced at the expected design sites. We obtained MIG-p210 retrovirus that was used to infect Ba/F3 cells via calcium phosphate and then screened Ba/F3 cells stably expressing BCR-ABL1 mutants (Ba/F3-MIG-p210). The cell lines used in this study are shown in Table 1.

TABLE 1 The source of cell lines and the required culture medium.

Cell lines	Sources	Culture medium
Ba/F3	Institute of Hematology, West China Hospital	RPMI 1640 (1 ng/ml IL3)
K562	Institute of Hematology, West China Hospital	RPMI 1640
Ba/F3-MIG-p210^{WT}	This study	RPMI 1640
Ba/F3-MIG-p210^{E255K}	This study	RPMI 1640
Ba/F3-MIG-p210^{T315I}	This study	RPMI 1640
Ba/F3-MIG-p210^{F359V}	This study	RPMI 1640
Ba/F3-MIG-p210^{L387M}	This study	RPMI 1640
Ba/F3-MIG-p210^{F486S}	This study	RPMI 1640
Ba/F3-MIG-p210$^{T315I+E255K}$	This study	RPMI 1640
Ba/F3-MIG-p210$^{T315I+L387M}$	This study	RPMI 1640
Ba/F3-MIG-p210$^{T315I+F486S}$	This study	RPMI 1640
Ba/F3-MIG- p210-Luc	This study	RPMI 1640

Ba/F3-MIG-p210 cells: Ba/F3 cells were transfected with MSCV-IRES-GFP-P210 (MIG-P210) retrovirus to make them express BCR::ABL1 fusion protein with the molecular weight of 210 kDa.

Cell viability analysis

We inoculated Ba/F3-MIG-p210 cells into 96-well plates with 8000 or 3000 cells per well and added different concentrations of TKIs (0–2 μM) (to better distinguish the different effects of ABL1 inhibitors against BCR::ABL1 compound mutations, single-point mutation, and WT, we used drug concentrations less than 2 μM), ABL001 (0–5 μM), or GMB-475 (0–5 μM) (to observe the therapeutic effect of GMB-475 on mutant cells, the maximum concentration was increased to 5 μM); the total volume of each well was 100 μl, and the cells were placed in an incubator at 37 °C and 5% CO_2 for 24/48 h. There were two ways to detect cell viability afterward: 1) After adding 20 μl of 5 mg/ml thiazolyl blue tetrazolium bromide (MTT) per well and waiting for 4–6 h, we added 100 μl of MTT-dissolved solution per well and dissolved it in an incubator at 37°C overnight and measured the absorbance value of each well at 570 nm with a spectrometer the next day; 2) after adding 10 μl of Cell Counting Kit-8 (CCK8) per well and waiting for 3 h, we detected the absorbance value of each well at 450 nm with a spectrometer. The curve of cell viability was drawn with GraphPad Prism 8.0, and CompuSyn software was used to calculate the drug combination index (CI) of GMB-475 with dasatinib or ponatinib. A CI value less than 1 indicates a synergistic effect (a smaller CI indicates a better synergistic effect), while a CI value equal to 1 indicates an additive effect, and a CI value greater than 1 indicates an antagonistic effect.

Cell apoptosis

We inoculated Ba/F3-MIG-p210 cells into six-well plates with 1×10^5 cells per well and added different concentrations of TKIs (0–2 μM), ABL001 (0–5 μM), or GMB-475 (0–5 μM); the total volume of each well was 2 ml, and the cells were placed in an incubator at 37 °C and 5% CO_2 for 24–48 h. Cell apoptosis was detected by annexin V-647 and 7-aminoactinomycin D (7-AAD) double staining. The results were statistically analyzed by GraphPad Prism 8.0 software.

CML mouse model study

Ba/F3-MIG-p210 cells were transfected with HBLV-luciferase-blasticidin virus to construct a cell line expressing luciferase (Ba/F3-MIG-p210-Luc cell line). Four to 6 hours after 3.8 Gy X-ray irradiation, each 8-week-old Balb/c mouse was injected with 3×10^5 Ba/F3-MIG-p210-Luc cells via the tail vein. The mice were administered intraperitoneally with the drug after 72 h. The experimental group was treated with 5 mg/kg GMB-475 once every 2 days (from days 4 to 14), and the control group was injected with the corresponding volume of drug solvent (4% DMSO + 30% PEG300 + 5% Tween 80 + ddH_2O). There were 12 mice in the experimental group and the control group, with 6 mice in each group. The tumor burden of the mice was observed by luminescence imaging, and the survival of the mice was recorded throughout the process.

Cell cycle

We inoculated Ba/F3-MIG-p210 cells into six-well plates with 2×10^5 cells per well and added different concentrations of dasatinib (1 μM or 2 μM) or GMB-475 (1 μM or 2 μM) (to avoid too many dead cells during the experiment, we used the

TABLE 2 The IC50 of GMB-475 in Ba/F3 cells with BCR::ABL1 mutants.

	IC50 of GMB-475 (μM)	IC50 of GMB-475[δ] combined with dasatinib (μM)
Ba/F3-MIG-p210^{T315I}	3.69	0.44
Ba/F3-MIG-p210$^{T315I+E255K}$	8.29	2.57
Ba/F3-MIG-p210$^{T315I+L387M}$	3.70	0.31
Ba/F3-MIG-p210$^{T315I+F486S}$	4.49	0.77

[δ]The IC50 of GMB-475 against Ba/F3-MIG-p210 cells when GMB-475 combined with dasatinib.

drug concentration lower than or equal to 2 μM); the total volume of each well was 2 ml, and the cells were placed in an incubator at 37°C and 5% CO_2 for 48 h. The cells were collected and fixed with 70% ethanol solution overnight, digested with RNase, and stained with propidium iodide (PI). The cell cycle was detected using flow cytometry and analyzed with Modfit software.

Real-time fluorescence quantitative PCR

The changes of mRNA levels induced by the corresponding drugs were detected by real-time fluorescence quantitative PCR (qPCR), and the primer sequences of the genes used for qPCR are shown in Supplementary Table S2.

Western blot

We inoculated Ba/F3-MIG-p210 cells into 6-cm Petri dishes and added different concentrations of drugs; the total volume of each dish was 5 ml, and the cells were placed in an incubator at 37°C and 5% CO_2 for 24/48 h. Then, the proteins of cells were extracted, and the levels of BCR::ABL1 protein and related signal pathway proteins were detected by Western blot.

Statistical analysis

We adopted Kaplan–Meier analysis and the log-rank test to compare the survival of the CML mouse model between the experimental group and the control group. In the Cell Experiments section, the results represent the mean ± standard error of two or three independent experiments. The unpaired *t*-test was used to compare the differences between the two groups, and *p* values less than 0.05 showed significant differences.

Results

The effects of inhibitors targeting ABL1 on the growth inhibition of Ba/F3-MIG-p210 cells with BCR::ABL1 compound mutations were significantly weakened

The viability of Ba/F3-MIG-p210 cells treated with different concentrations of ABL1 inhibitor for 48 h was detected via the MTT assay. The results showed that Ba/F3-MIG-p210 cells with different BCR::ABL1 mutations were generally resistant to imatinib, especially compound mutations, and imatinib did not inhibit cell growth when the concentration reached 2000 nM (Figure 1A). In contrast, dasatinib significantly inhibited the growth of Ba/F3-MIG-p210 cells with the BCR::ABL1 single-point mutation but weakly inhibited the growth of those with compound mutations (Figure 1C). Ponatinib and ABL001 also performed more effectively on Ba/F3-MIG-p210 cells with BCR::ABL1 single-point mutations than those with compound mutations in terms of growth inhibition (Figures 1B,D).

The effects of ABL1 inhibitors on promoting apoptosis of Ba/F3-MIG-p210 cells with BCR::ABL1 mutants were weakened

The apoptosis of Ba/F3-MIG-p210 cells treated with different ABL1 inhibitors for 48 h was detected via annexin V-647 and 7-AAD double staining. The results showed that compared with BCR::ABL1 wild-type, the effects of imatinib, dasatinib, and ABL001 on promoting apoptosis in Ba/F3-MIG-p210 cells with T315I or T315I-including compound mutations, were significantly reduced under the same concentrations and treatment times of agents (Figure 2A). Compared with BCR::ABL1 wild-type or T315I single-point mutation, the effects of promoting apoptosis of ponatinib on cells with BCR::ABL1 compound mutations were also significantly weakened (Figure 2B).

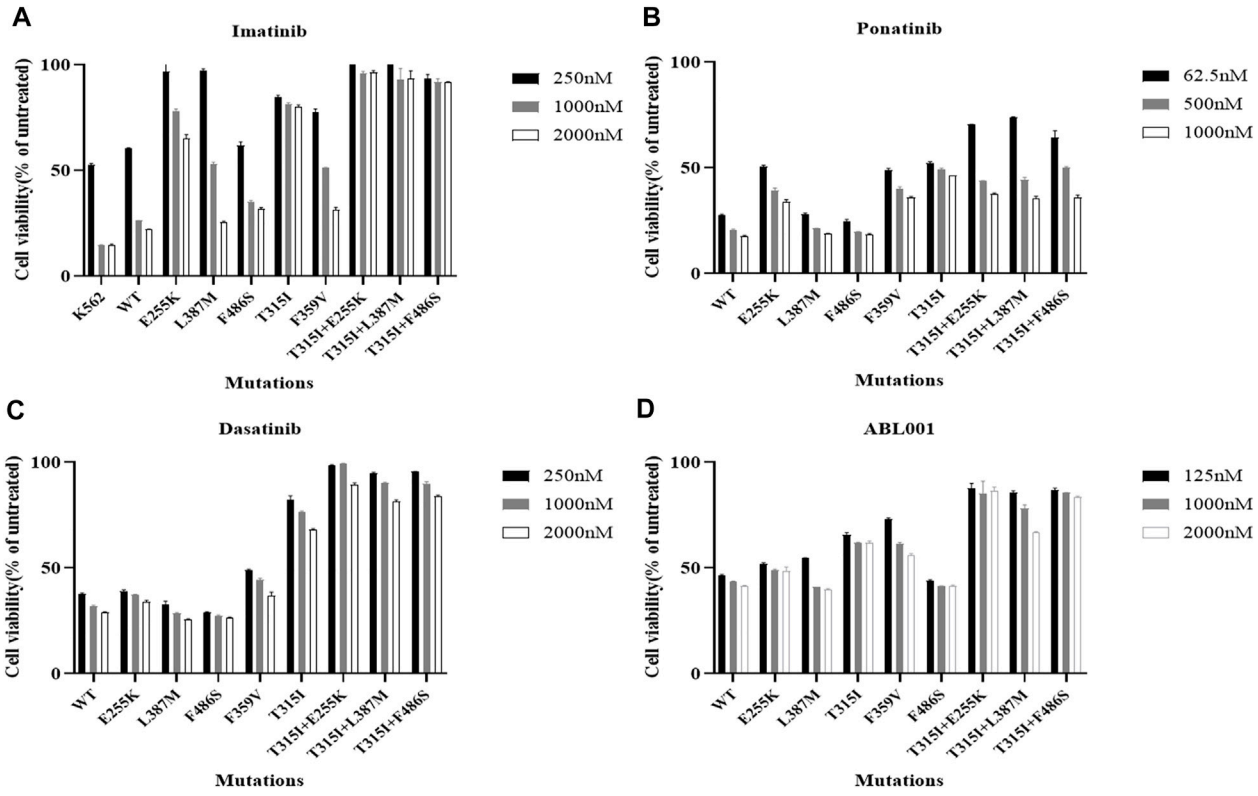

FIGURE 1
Effects of inhibitors targeting ABL1 on the growth inhibition of Ba/F3-MIG-p210 cells with BCR::ABL1 compound mutations were significantly weakened. The viability of Ba/F3-MIG-p210 cells treated with different concentrations of ABL1 inhibitor for 48 h was detected via the MTT assay: **(A)** imatinib, **(B)** ponatinib, **(C)** dasatinib, and **(D)** ABL001.

GMB-475 exhibited a growth inhibition effect on Ba/F3-MIG-p210 cells with BCR::ABL1$^{T315I+F486S}$ mutations but no significant improvement of prognosis in chronic myeloid leukemia mouse models constructed by this cell line

Ba/F3-MIG-p210 cells carrying BCR::ABL1$^{T315I+F486S}$ mutations were treated with different concentrations of GMB-475 for 48 h, and cell viability was detected using the CCK8 assay. The results showed that GMB-475 exhibited a growth inhibition effect on Ba/F3-MIG-p210 cells carrying BCR::ABL1$^{T315I+F486S}$ mutations, and the half inhibitory concentration (IC50) was 4.49 μM (Figure 3A). Twelve 8-week-old Balb/c mice were randomly divided into two groups with six mice in each group: the control group and the GMB-475 administration group. Four to 6 hours after 3.8 Gy X-ray irradiation, each mouse was injected with 3×10^5 Ba/F3-MIG-p210-Luc cells carrying BCR::ABL1$^{T315I+F486S}$ mutations via the tail vein. The mice were administered drugs intraperitoneally after 72 h. The experimental group was treated with 5 mg/kg GMB-475 once every 2 days (from days 4 to 14), and the control group was injected with the corresponding volume of drug solvent. The tumor burden of mice was observed by luminescence imaging at day 9, and the survival of mice was recorded throughout the process. The results showed that although GMB-475 showed a trend of reducing the tumor burden (Figure 3C,D) and prolonging the survival of the CML mouse model (Figure 3B), its effect was limited and not statistically significant. In view of the results, we considered the combination of GMB-475 and TKIs to improve the antitumor effect.

GMB-475 combined with tyrosine kinase inhibitors showed synergistic effects of growth inhibition on Ba/F3-MIG-p210 cells with BCR::ABL1 mutants

The distinct effects of growth inhibition between GMB-475 combined with TKIs and single agents on Ba/F3-MIG-p210 cells were detected using the CCK8 assay. We found that the overall combination index (CI) of GMB-475 and dasatinib in Ba/F3-

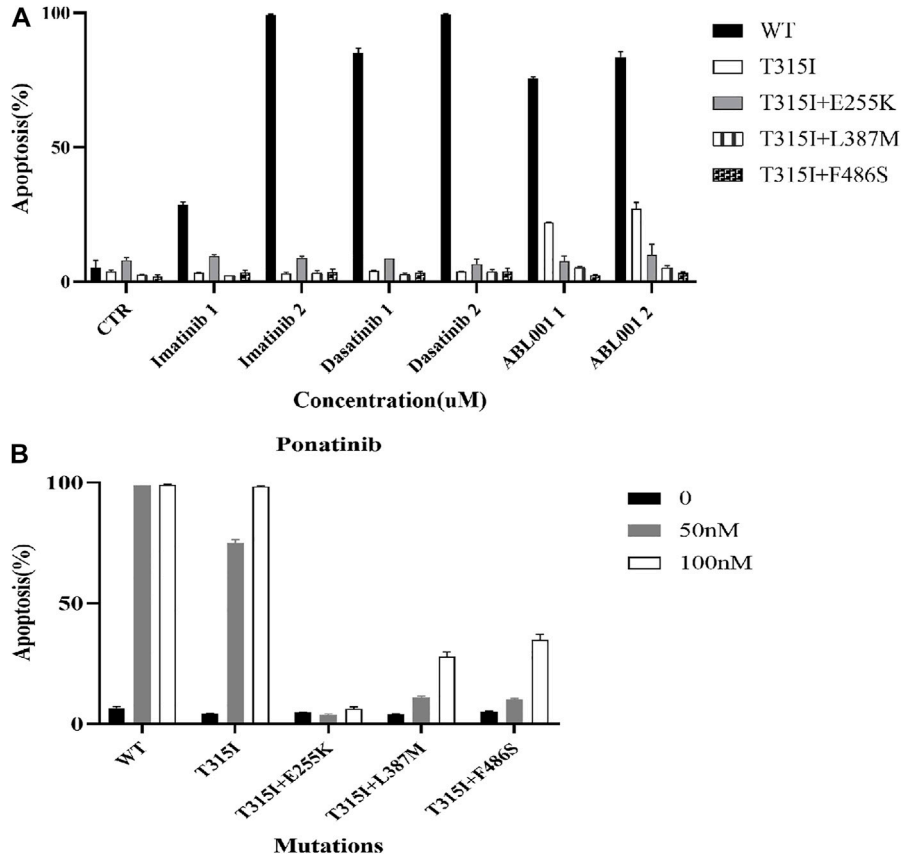

FIGURE 2
Effects of ABL1 inhibitors on promoting apoptosis of Ba/F3-MIG-p210 cells with BCR::ABL1 mutants were weakened. The apoptosis of Ba/F3-MIG-p210 cells treated with different ABL1 inhibitors for 48 h was detected via annexin V-647 and 7-AAD double staining: **(A)** Imatinib, dasatinib, and ABL001; the abscissa marks the names and concentrations of agents, and the ordinate is the apoptosis rate; the colors of the bar graph represent the BCR::ABL1$^{\text{wild type}}$ (WT) or different mutants carried by Ba/F3-MIG-p210 cells, including BCR::ABL1^{T315I}, BCR::ABL1$^{T315I+E255K}$, BCR::ABL1$^{T315I+L387M}$, and BCR::ABL1$^{T315I+F486S}$. **(B)** Ponatinib; the abscissa marks the BCR::ABL1^{WT}, or different mutants carried by Ba/F3-MIG-p210 cells, and the ordinate is the apoptosis rate; the colors of the bar graph represent different concentrations of ponatinib.

MIG-p210 cells with BCR::ABL1^{WT} was 6.96, and the two drugs showed no synergistic effect of growth inhibition on cells (Figures 4A,B). In Ba/F3-MIG-p210 cells with BCR::ABL1^{T315I} or BCR::ABL1$^{T315I+E255K}$ mutations, the overall CIs of GMB-475 and dasatinib were 0.25 and 0.29, respectively, and the two drugs exhibited significant synergistic effects of growth inhibition on cells (Figures 4C–F). When the concentration of dasatinib was fixed at 2 μM and GMB-475 was set at different concentrations, the combination of the two drugs also showed significant synergistic effects of growth inhibition on Ba/F3-MIG-p210 cells with BCR::ABL1$^{T315I+L387M}$ or BCR::ABL1$^{T315I+F486S}$ mutations (the CIs of each concentration were less than 0.54, Figures 4G–J). Meanwhile, dasatinib significantly reduced the IC50 of GMB-475 in Ba/F3-MIG-p210 cells with BCR::ABL1^{T315I}, BCR::ABL1$^{T315I+E255K}$, BCR::ABL1$^{T315I+L387M}$, and BCR::ABL1$^{T315I+F486S}$ mutations (Table 2). Moreover, we also found that GMB-475 combined with ponatinib also showed synergistic effects of growth inhibition on Ba/F3-MIG-p210 with BCR::ABL1$^{T315I+E255K}$ or BCR::ABL1$^{T315I+F486S}$ mutations; the overall CIs were 0.67 and 0.61, and the highest CIs at different concentrations were 0.98 and 1.02, respectively (Supplementary Figures S1A–D). The synergistic effect of GMB-475 combined with ponatinib was weaker than that with dasatinib.

GMB-475 combined with tyrosine kinase inhibitors synergistically promoted the apoptosis of Ba/F3-MIG-p210 cells

The apoptosis of Ba/F3-MIG-p210 cells with BCR::ABL1 wild-type or mutants induced by GMB-475 combined

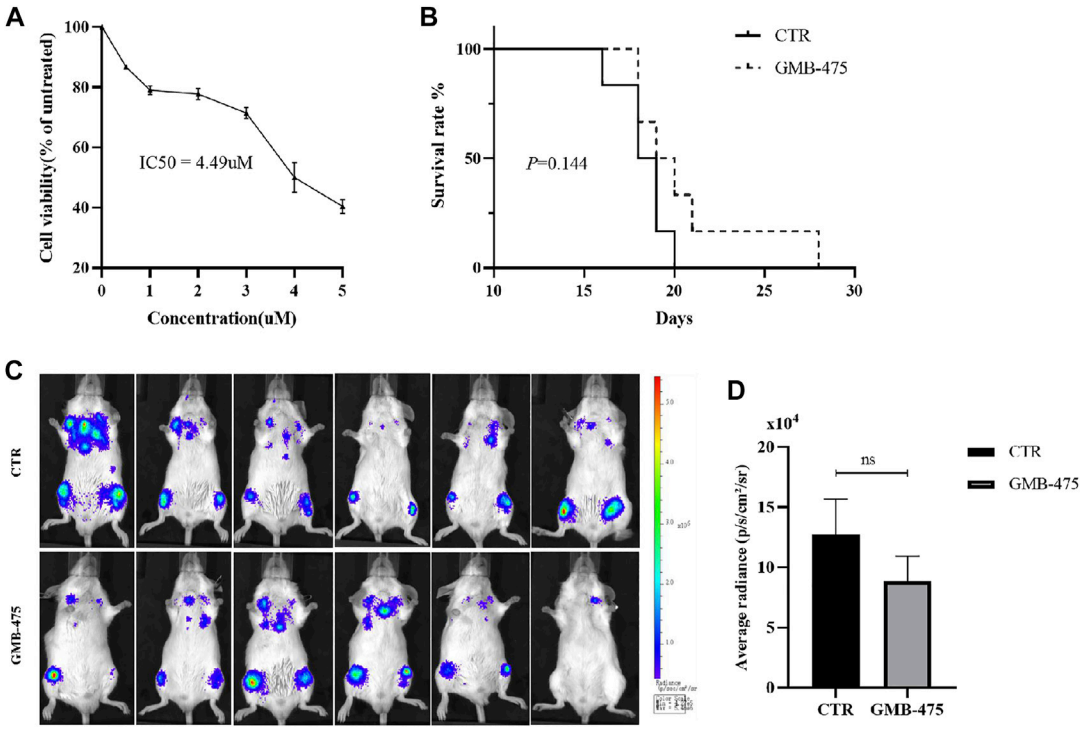

FIGURE 3
GMB-475 exhibited a growth inhibition effect on Ba/F3-MIG-p210 cells carrying BCR::ABL1$^{T315I+F486S}$ mutations but no significant improvement of prognosis in the CML mouse model constructed by this cell line. **(A)** Ba/F3-MIG-p210 cells carrying BCR::ABL1$^{T315I+F486S}$ mutations were treated with different concentrations of GMB-475 for 48 h, and cell viability was detected using the CCK8 assay. **(B)** Survival curve of the CML mouse model for the control group and the GMB-475 administration group. **(C)** Fluorescence imaging of CML mouse model was implemented at day 9. **(D)** Quantitative analysis of the fluorescence signal was performed to measure the tumor burden in the CML mouse model. Abbreviations: CTR, control.

with TKIs was detected by flow cytometry. The results showed that GMB-475 combined with dasatinib synergistically promoted the apoptosis of Ba/F3-MIG-p210 cells (Figure 5). Meanwhile, GMB-475 combined with ponatinib synergistically promoted the apoptosis of Ba/F3-MIG-p210 cells with BCR::ABL1$^{T315I+E255K}$ and BCR::ABL1$^{T315I+F486S}$ mutations (Supplementary Figure S2).

GMB-475 combined with dasatinib exhibited a better synergistic effect on Ba/F3-MIG-p210 cells carrying BCR::ABL1$^{T315I+F486S}$ mutations compared with ABL001

Ba/F3-MIG-p210 cells were treated with different concentrations of ABL001 for 48 h, and cell viability was detected using the CCK8 assay. The IC50 of ABL001 was 9.487 μM (Figure 6A); in contrast, the IC50 of GMB-475 was 4.49 μM. The viability of Ba/F3-MIG-p210 cells treated with different agents for 24 h was detected using the CCK8 assay. The results showed that GMB-475 alone or in combination with dasatinib showed more significant growth inhibition on Ba/F3-MIG-p210 cells carrying BCR::ABL1$^{T315I+F486S}$ mutations than ABL001 alone or in combination with dasatinib, respectively (Figure 6B). The apoptosis of Ba/F3-MIG-p210 cells treated with different agents for 24 h was detected by annexin V and 7-AAD double staining. The results showed that there was no difference between GMB-475 and ABL001 in promoting apoptosis of cells; however, the apoptosis rate of cells treated with GMB-475 combined with dasatinib was significantly higher than that treated with ABL001 combined with dasatinib (Figure 6C). Ba/F3-MIG-p210 cells were treated with different agents for 24 h and continued to be cultured in a complete medium without drugs for 18 h; then the apoptosis of those cells was detected. The results showed that there was no difference between GMB-475 and ABL001 in promoting apoptosis of cells, and the apoptosis rate of cells treated with GMB-475 combined with dasatinib was higher than that treated with ABL001 combined with dasatinib (Figure 6D). GMB-475 combined with dasatinib exhibited a better synergistic effect compared with ABL001 combined with dasatinib.

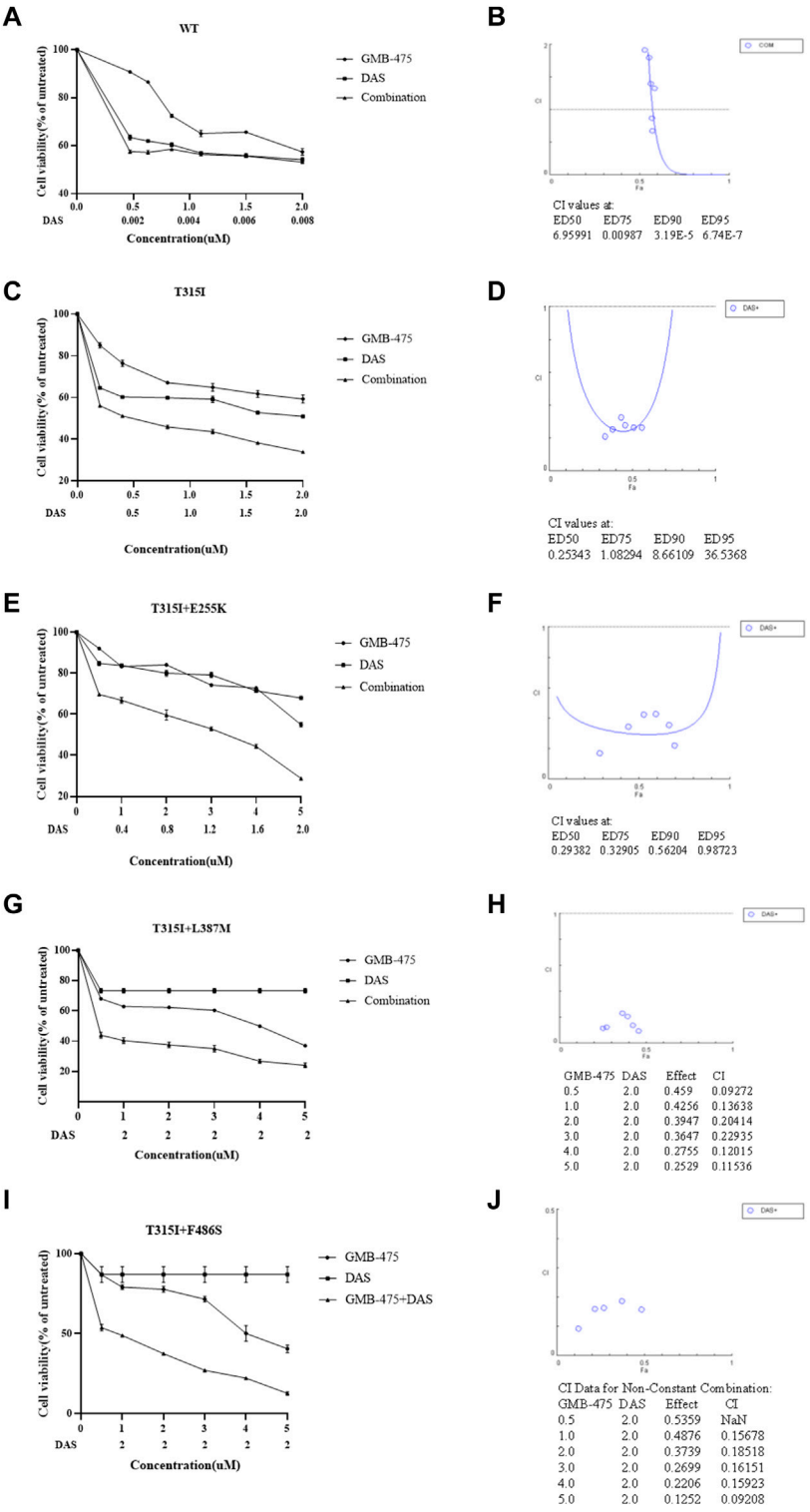

FIGURE 4
GMB-475 combined with dasatinib (DAS) had synergistic effects on the growth inhibition of Ba/F3-MIG-p210 cells with BCR::ABL1 mutants but no synergistic effect on that with BCR::ABL1^{WT}. **(A,C,E,G,I)** The viability of Ba/F3-MIG-p210 cells carrying BCR::ABL1^{WT}, BCR::ABL1^{T315I}, BCR::ABL1$^{T315I+E255K}$, BCR::ABL1$^{T315I+L387M}$, or BCR::ABL1 $^{T315I+F486S}$ mutations treated with different concentrations of GMB-475, dasatinib, or GMB-475 plus dasatinib for 48 h was detected using the CCK8 assay. The abscissa represents the concentrations of GMB-475, and the corresponding concentrations of dasatinib are marked below the abscissa; the ordinate is the cell survival rate. **(B,D,F,H,G)** The curve figures of combination indexes (CIs); the CIs of GMB-475 combined with dasatinib at ED50, ED75, ED90, and ED95, or the CIs for different concentrations of GMB-475 combined with 2-μM dasatinib are shown below the figures; the CI at ED50 was the overall CI.

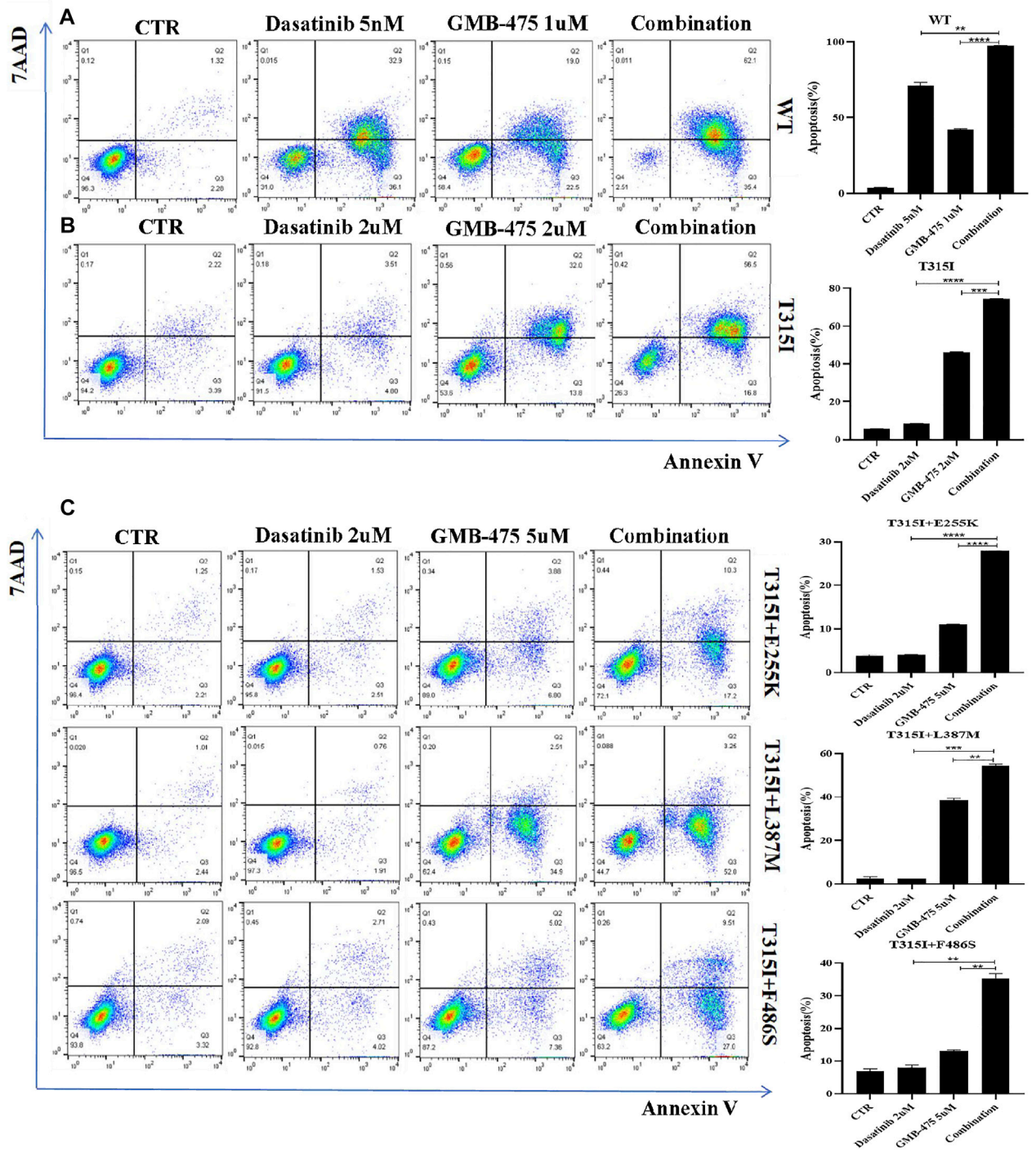

FIGURE 5
GMB-475 combined with dasatinib synergistically promoted the apoptosis of Ba/F3-MIG-p210 cells. The apoptosis of Ba/F3-MIG-p210 cells treated with control medium (CTR), GMB-475, dasatinib, or GMB-475 plus dasatinib for 48 h was detected via annexin V and 7-AAD double staining: **(A)** Ba/F3-MIG-p210 cells with BCR::ABL1^{WT} were treated with CTR, dasatinib 5nM, GMB-475 1 μM, and GMB-475 1 μM plus dasatinib 5 nM. **(B)** Ba/F3-MIG-p210 cells carrying BCR::ABL1^{T315I} were treated with CTR, dasatinib 2 μM, GMB-475 2 μM, and GMB-475 2 μM plus dasatinib 2 μM. **(C)** Ba/F3-MIG-p210 cells carrying BCR::ABL1$^{T315I+E255K}$, BCR::ABL1$^{T315I+L387M}$, or BCR::ABL1 $^{T315I+F486S}$ compound mutations were treated with CTR, dasatinib 2 μM, GMB-475 5 μM, and GMB-475 5 μM plus dasatinib 2 μM, respectively. $^{**}p < 0.01$, $^{***}p < 0.001$, $^{****}p < 0.0001$.

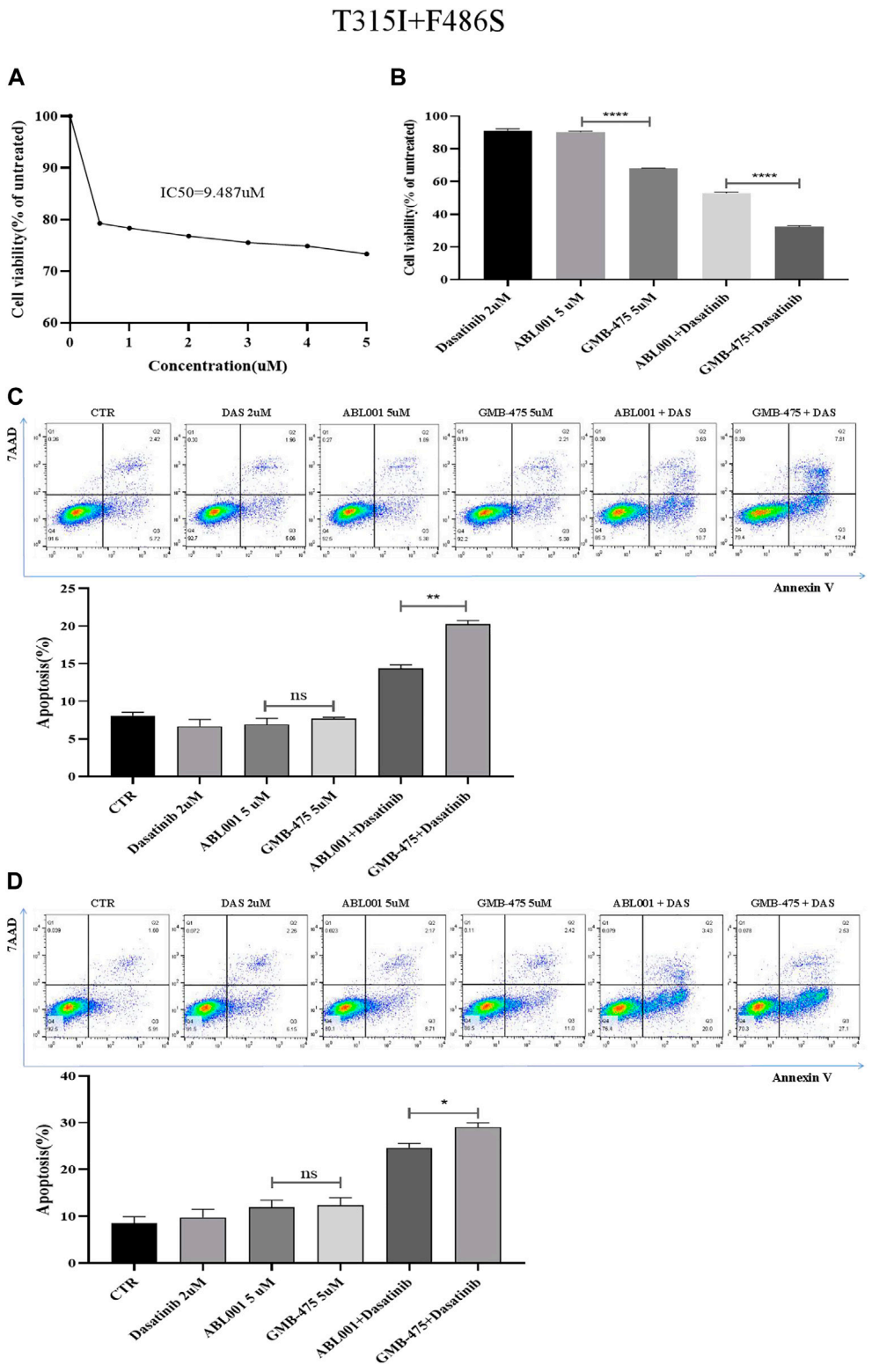

FIGURE 6
GMB-475 combined with dasatinib exhibited a better synergistic effect on Ba/F3-MIG-p210 cells carrying BCR::ABL1$^{T315I+F486S}$ mutations compared with ABL001. **(A)** Ba/F3-MIG-p210 cells were treated with different concentrations of ABL001 for 48 h, and cell viability was detected using the CCK8 assay. **(B)** The viability of Ba/F3-MIG-p210 cells treated with dasatinib 2 μM, ABL001 5 μM, GMB-475 5 μM, ABL001 5 μM plus dasatinib 2 μM, and GMB-475 5 μM plus dasatinib 2 μM for 24 h was detected using the CCK8 assay. **(C)** The apoptosis of Ba/F3-MIG-p210 cells
(*Continued*)

FIGURE 6 (Continued)
treated with control medium (CTR), dasatinib 2 μM, ABL001 5 μM, GMB-475 5 μM, ABL001 5 μM plus dasatinib 2 μM, and GMB-475 5 μM plus dasatinib 2 μM for 24 h was detected via annexin V and 7-AAD double staining. **(D)** Ba/F3-MIG-p210 cells were treated with CTR, dasatinib 2 μM, ABL001 5 μM, GMB-475 5 μM, ABL001 5 μM plus dasatinib 2 μM, and GMB-475 5 μM plus dasatinib 2 μM for 24 h and continued to be cultured in complete medium without drugs for 18 h; then the apoptosis of those cells was detected. $^{ns}p \geq 0.05$, $^{*}p < 0.05$, $^{**}p < 0.01$, $^{****}p < 0.0001$.

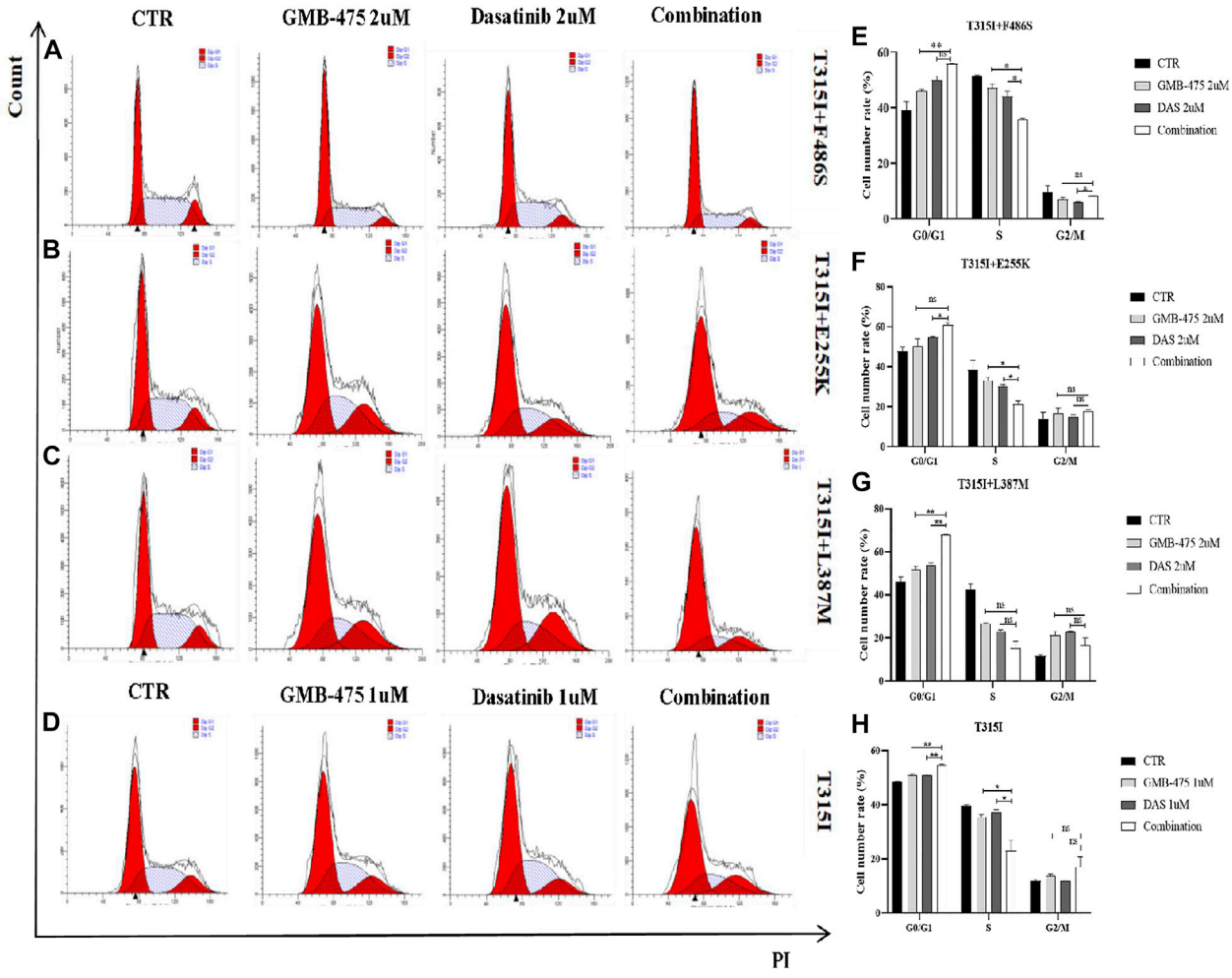

FIGURE 7
GMB-475 combined with dasatinib synergistically blocked the cell cycle of Ba/F3-MIG-p210 cells with BCR::ABL1 mutants. The cell cycle of Ba/F3-MIG-p210 cells treated with the control medium (CTR), GMB-475, dasatinib (DAS), or GMB-475 plus dasatinib for 48 h was detected by PI staining: **(A–C)** Ba/F3-MIG-p210 cells carrying BCR::ABL1$^{T315I+F486S}$, BCR::ABL1$^{T315I+E255K}$, or BCR::ABL1$^{T315I+L387M}$ compound mutations were treated with CTR, dasatinib 2 μM, GMB-475 2 μM, and GMB-475 2 μM plus dasatinib 2 μM, respectively. **(D)** Ba/F3-MIG-p210 cells carrying BCR::ABL1^{T315I} were treated with CTR, dasatinib 1 μM, GMB-475 1 μM, and GMB-475 1 μM plus dasatinib 1 μM. **(E–H)** Statistical analysis results of the cell cycle. $^{ns}p \geq 0.05$, $^{*}p < 0.05$, $^{**}p < 0.01$.

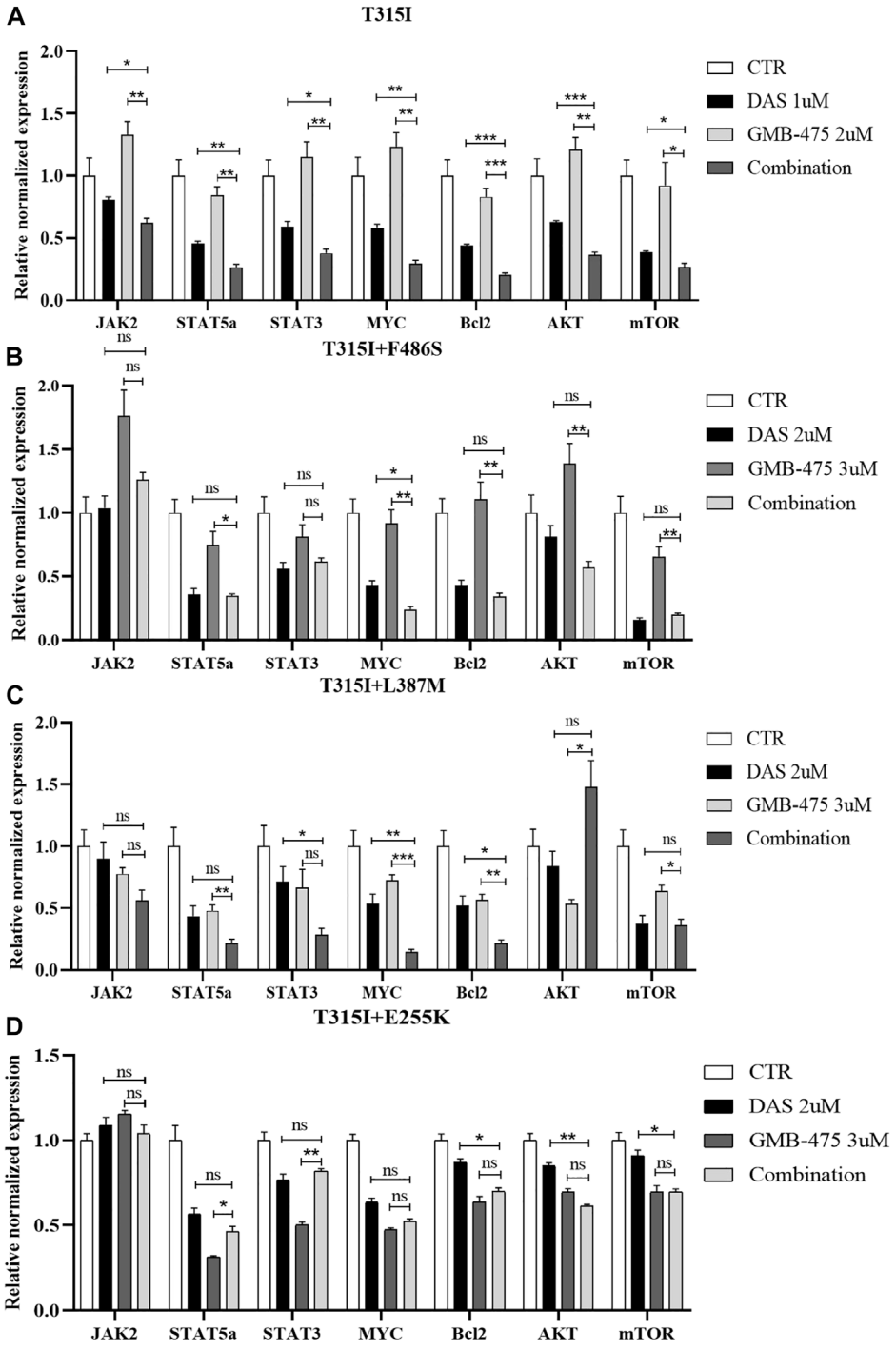

FIGURE 8
GMB-475 combined with dasatinib synergistically downregulated the mRNA levels of the *JAK-STAT* axis, *AKT*, and *mTOR* in Ba/F3-MIG-p210 cells with BCR::ABL1 mutants. The mRNA levels of genes in Ba/F3-MIG-p210 cells treated with control medium (CTR), GMB-475, dasatinib (DAS), or GMB-475 plus dasatinib for 48 h were detected by qPCR: **(A)** Ba/F3-MIG-p210 cells carrying BCR::ABL1^{T315I} mutation were treated with CTR, dasatinib 1 μM, GMB-475 2 μM, and GMB-475 2 μM plus dasatinib 1 μM. **(B–D)** Ba/F3-MIG-p210 cells carrying BCR::ABL1$^{T315I+F486S}$, BCR::ABL1$^{T315I+L387M}$, or BCR::ABL1$^{T315I+E255K}$ compound mutations were treated with CTR, dasatinib 2μM, GMB-475 3 μM, and GMB-475 3 μM plus dasatinib 2 μM, respectively. The types of BCR::ABL1 mutants carried by Ba/F3-MIG-p210 cells are marked at the top of the figures. $^{ns}p \geq 0.05$, $^{*}p < 0.05$, $^{**}p < 0.01$, $^{***}p < 0.001$.

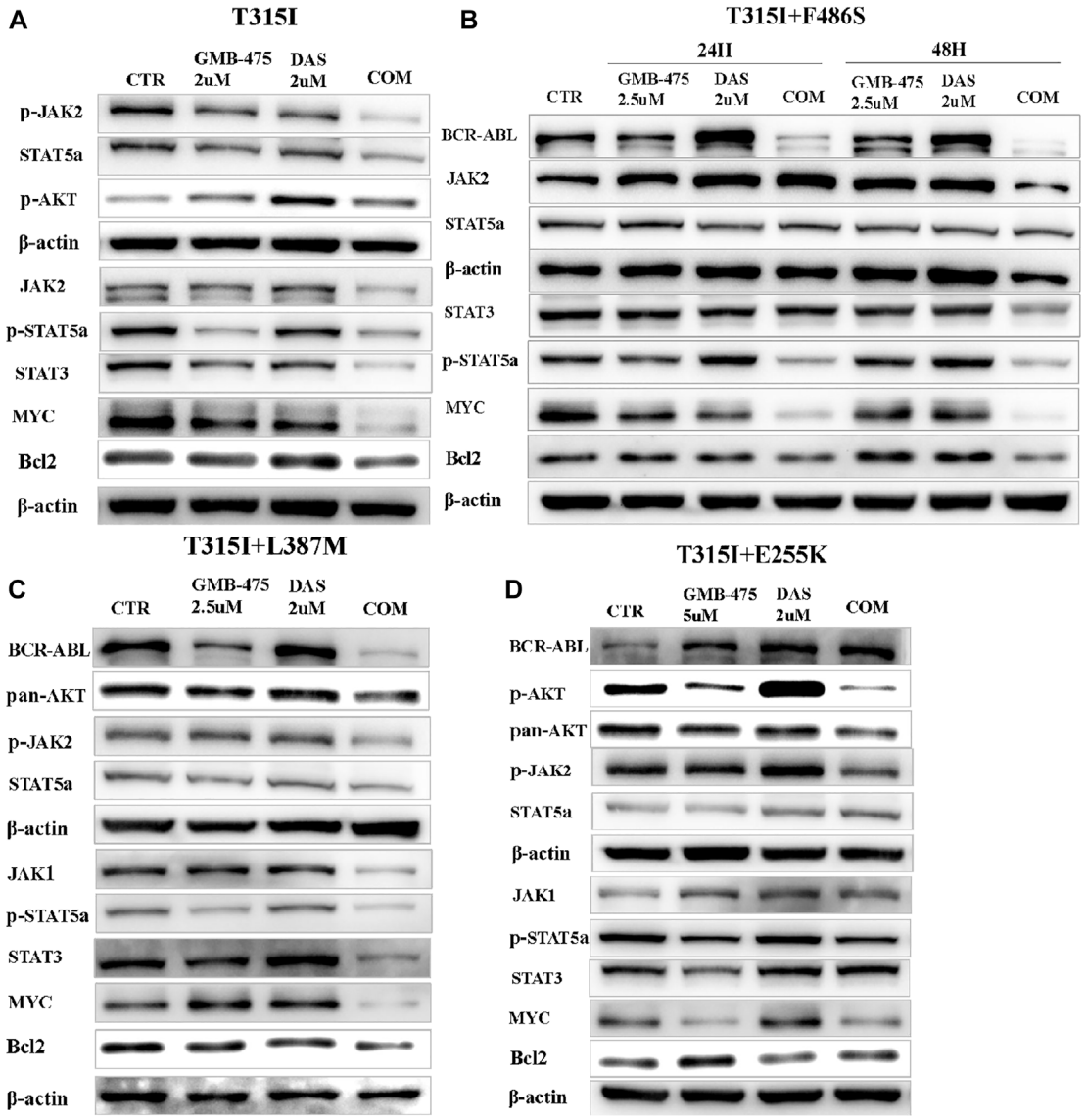

FIGURE 9
GMB-475 combined with dasatinib synergistically downregulated the protein levels of the JAK-STAT axis or AKT in Ba/F3-MIG-p210 cells with BCR::ABL1 mutants. The protein levels of genes in Ba/F3-MIG-p210 cells treated with the control medium (CTR), GMB-475, dasatinib (DAS), or GMB-475 plus dasatinib were detected by western blot: **(A)** Ba/F3-MIG-p210 cells carrying BCR::ABL1^{T315I} were treated with CTR, GMB-475 2 μM, dasatinib 2 μM, and GMB-475 2 μM plus dasatinib 2 μM for 48 h. **(B,C)** Ba/F3-MIG-p210 cells carrying BCR::ABL1 $^{T315I+F486S}$ and BCR::ABL1$^{T315I+L387M}$ compound mutations were treated with CTR, GMB-475 2.5 μM, dasatinib 2 μM, and GMB-475 2.5 μM plus dasatinib 2 μM for 48 h, respectively (Ba/F3-MIG-p210 cells with BCR::ABL1$^{T315I+F486S}$ were treated for 24 and 48 h). **(D)** Ba/F3-MIG-p210 cells carrying BCR::ABL1$^{T315I+E255K}$ were treated with CTR, GMB-475 5 μM, dasatinib 2 μM, and GMB-475 5 μM plus dasatinib 2 μM for 48 h. The types of BCR::ABL1 mutants carried by Ba/F3-MIG-p210 cells are marked at the top of the figures.

GMB-475 combined with dasatinib synergistically blocked the cell cycle of Ba/F3-MIG-p210 cells with BCR::ABL1 mutants

The effects of blocking the cell cycle for GMB-475 combined with dasatinib on Ba/F3-MIG-p210 cells with BCR::ABL1 mutants were detected by PI staining. The results showed that compared with single agents, the proportion of cells in the G0/G1 phase increased but that in the S phase (DNA synthesis phase) decreased under combination therapy; in other words, the effect of blocking the cell cycle of combination therapy was more obvious than that of single agents (Figure 7).

GMB-475 combined with dasatinib synergistically downregulated the mRNA levels of the *JAK-STAT* axis, *AKT*, and *mTOR* in Ba/F3-MIG-p210 cells with BCR::ABL1 mutants

The distinct mRNA levels of genes induced by GMB-475 combined with dasatinib and single agents were detected by qPCR. Compared with the BCR::ABL1^{T315I} single-point mutation, Ba/F3-MIG-p210 cells carrying compound mutations are more resistant to the agents. To observe the change in mRNA levels, the concentrations of the agents were increased when we treated Ba/F3-MIG-p210 cells carrying compound mutations. The results showed that combination therapy downregulated the expression of the *JAK-STAT* pathway in cells compared with the single drugs. In Ba/F3-MIG-p210 cells with the BCR::ABL1^{T315I} mutation, the mRNA levels of *JAK2*, *STAT5a*, *STAT3*, *MYC*, and *BCL2* of the *JAK-STAT* pathway, and *AKT* and *mTOR* that are downstream genes of *JAK*, were downregulated (Figure 8A). The mRNA levels of *MYC* and *MYC* plus *BCL2* were also significantly downregulated in the two Ba/F3-MIG-p210 cell lines with BCR::ABL1$^{T315I+F486S}$ and BCR::ABL1$^{T315I+L387M}$ mutations, respectively. The changes in the mRNA levels of other genes were not statistically significant under the induction of combination therapy, including *JAK2*, *STAT5a*, *STAT3*, *AKT*, and *mTOR* (Figures 8B,C). However, in Ba/F3-MIG-p210 cells with BCR::ABL1$^{T315I+E255K}$ compound mutations, there was no significant distinction in the mRNA levels of genes induced by combination therapy and single drugs (Figure 8D).

GMB-475 combined with dasatinib synergistically downregulated the levels of some proteins in the JAK-STAT axis or AKT in Ba/F3-MIG-p210 cells with BCR::ABL1 mutants

The levels of protein expression of genes in cells induced by agents were detected by WB. The results showed that GMB-475 combined with dasatinib downregulated the protein levels of the JAK-STAT pathway in cells compared with single agents. In Ba/F3-MIG-p210 cells with the BCR::ABL1^{T315I} mutation, the levels of JAK2, p-JAK2, STAT5a, STAT3, and MYC decreased significantly under combination therapy compared with single agents (Figure 9A). In Ba/F3-MIG-p210 cells with BCR::ABL1$^{T315I+F486S}$ compound mutations, the levels of BCR::ABL1, p-STAT5a, STAT3, MYC, and Bcl2 decreased significantly, but JAK2 increased at 24 h under combination therapy compared with single agents (Figure 9B). Similarly, the levels of BCR::ABL1, JAK1, p-JAK2, p-STAT5a, STAT3, MYC, and Bcl2 decreased in Ba/F3-MIG-p210 cells with BCR::ABL1$^{T315I+L387M}$ compound mutations under combination therapy compared with single agents (Figure 9C). However, in Ba/F3-MIG-p210 cells with BCR::ABL1$^{T315I+E255K}$ compound mutations, the levels of BCR::ABL1, STAT3, STAT5, and p-STAT5a were upregulated, MYC and Bcl2 remained unchanged, but p-JAK2, pan AKT, and p-AKT decreased under combination therapy compared with single agents (Figure 9D).

Discussion

CML is characterized by the BCR::ABL1 fusion gene, which is formed by a genetic translocation between chromosome 9 and chromosome 22 (Rinke et al., 2020). ABL1 is a proto oncogene encoding tyrosine kinase protein that is involved in a variety of cellular processes in humans, including cell division, adhesion, differentiation, and stress response. Normally, the tyrosine kinase protein encoded by ABL1 is negatively regulated by its N-terminal myristoyl peptide (Radi et al., 2013), the sequence encoding which is deleted due to the fusion of BCR and ABL1 genes, resulting in the breaking of this self-inhibition balance and the continuous activation of tyrosine kinase. ATP-competitive inhibitors targeting ABL1 have greatly improved the prognosis of CML patients, but drug resistance (Devos et al., 2021), disease progression (Kakiuchi et al., 2021), or some serious adverse events occurring during treatment bring challenges to clinical practices (Castagnetti et al., 2021; Clapper et al., 2021), especially drug resistance caused by BCR::ABL1 mutations (Mian et al., 2021). In the construction of cell lines carrying BCR::ABL1 mutants, we selected 1–2 common mutant sites in four regions including the ATP-binding loop (248–256 amino acids), TKI-binding site, catalytic domain (350–363 amino acids), and activation loop, which are the E255, T315, F359, L387, F486, and including T315 compound mutations. Imatinib, dasatinib, and ponatinib showed the weakened effect of growth inhibition and promoted apoptosis in cells with BCR::ABL1 compound mutations, which further verified the limitations of existing ATP-competitive TKIs targeting ABL1 for the treatment of CML patients with BCR::ABL1 compound mutations. ABL001, also named asciminib, targets the myristoyl pocket of ABL1 in an allosteric manner and simulates the natural N-terminal myristoyl peptide of ABL1, which restores the self-inhibitory conformation of tyrosine kinase and realizes the treatment effect of CML (Jones et al., 2020). ABL001 is effective for the treatment of CML patients with BCR::ABL1 single mutations but has a limited effect on those with BCR::ABL1 compound mutations (Eide et al., 2019), which has been further verified at the cellular level in this study.

GMB-475 is composed of an ABL1-binding element, a ligand targeting the E3 ligase Von Hippel–Lindau (VHL), and an intermediate linker. The BCR::ABL1-binding element binds to the target protein BCR::ABL1; the ligand targeting VHL recruits the E3 ubiquitin ligase VHL, and the intermediate linker "pulls the BCR::ABL1 protein closer to the E3 ubiquitin ligase,"

resulting in the degradation of the BCR::ABL1 protein realized by the ubiquitin–proteasome system (Burslem et al., 2019). GMB-475 has unique advantages even if its binding mode is similar to ABL001. ATP-competitive TKIs and ABL001 inhibit the target protein by occupying the key site of ABL1, that is, the occupancy-driven pharmacological mode of traditional small molecule inhibitors, while PROTAC molecules including GMB-475, adopt the event-driven mode that is relatively less stringent for drug-binding sites, have the opportunity to realize degradation as long as they can bind to the target protein briefly, so that they have better compatibility with the target protein carrying mutations (Pettersson and Crews 2019; Xia et al., 2019; Kastl et al., 2021). We found that the IC50 value of ABL001 to Ba/F3-MIG-p210 cells carrying BCR::ABL1$^{T315I+F486S}$ mutations was more than double that of GMB-475. GMB-475 can be recycled in theory after degrading BCR::ABL1, so its action time is longer than that of ABL1 inhibitors. However, GMB-475 showed significant effects of growth inhibition and promoted apoptosis in CML cell lines carrying BCR::ABL1 mutants only at high drug concentrations and performed a poor treatment effect on the CML mouse model. Combination therapy is an effective strategy for drug resistance. Afterward, we found that GMB-475 combined with dasatinib synergistically inhibited growth, promoted apoptosis, and blocked the cell cycle of Ba/F3 cells carrying BCR::ABL1 mutants, which reduced the effective concentration of the two drugs. For patients treated with dasatinib, the plasma concentration of dasatinib is relevant to efficacy and tolerability outcomes (García-Ferrer et al., 2019). It was recommended that the maximum plasma concentration of dasatinib was greater than 50 ng/ml to achieve clinical efficiency and that the plasma trough concentration was lower than 2.5 ng/ml to avoid adverse events such as pleural effusion (Miura 2015). The combination of GMB-475 and dasatinib can improve the therapeutic effect of dasatinib and may reduce its adverse effects. Due to the similar effects of ABL001 and GMB-475 on the ABL1 kinase and combination therapies of ABL001 with different TKIs being studied in the clinical setting already, we compared the synergistic effects between GMB-475 and ABL001 when in combination with dasatinib. The results indicated that GMB-475 combined with dasatinib showed more significant growth inhibition on Ba/F3-MIG-p210 cells than ABL001 combined with dasatinib, and the apoptosis rate of Ba/F3-MIG-p210 cells treated with GMB-475 plus dasatinib was higher than that treated with ABL001 plus dasatinib whether the drugs continued to act or were removed. GMB-475 combined with dasatinib exhibited a better synergistic effect compared with ABL001 combined with dasatinib. In addition to our study, there have been many studies concerning combination therapy to overcome TKI resistance, such as imatinib combined with farnesyl transferase inhibitors (Radujkovic et al., 2006) or mTOR inhibitors (Alves et al., 2019), dasatinib combined with decitabine (Abaza et al., 2020) or interferon-α2b (Hjorth-Hansen et al., 2016), and ABL001 combined with ponatinib (Gleixner et al., 2021), which is probably the one we are most interested in but did not provide a specific combination index, resulting in losing the opportunity to compare the synergistic effect with this study.

We detected the changes in intracellular signaling pathways induced by GMB-475, dasatinib, and GMB-475 plus dasatinib to explore the synergistic mechanism. Due to the inconsistent sensitivity of different BCR::ABL1 mutations to GMB-475 (the IC50 values of GMB-475 to Ba/F3-MIG-p210 cells with BCR::ABL1^{T315I}, BCR::ABL1$^{T315I+E255K}$, BCR::ABL1 $^{T315I+L387M}$, and BCR::ABL1$^{T315I+F486S}$ at 48 h were 3.69, 8.29, 3.70, and 4.49 μM, respectively), we used distinct treatment concentrations for different mutations in order to avoid the influence of too many dead cells on the experimental results. GMB-475 and dasatinib synergistically downregulated the expression of BCR::ABL1 and some proteins of the JAK-STAT axis in Ba/F3 cells carrying BCR::ABL1 mutants, such as p-JAK2, p-STAT5a, STAT3, MYC, and Bcl2. The JAK-STAT pathway is widely involved in important biological processes, such as cell proliferation, differentiation, apoptosis, and immune regulation (Xin et al., 2020), and GMB-475 combined with dasatinib synergistically regulated the expression levels of some genes in this pathway, which may be the significant mechanism for the synergistic antitumor effect of the two drugs.

In conclusion, the combination of PROTAC molecules targeting ABL1 in an allosteric manner and ATP-competitive TKIs provides a novel idea for the treatment of CML patients with highly resistant BCR::ABL1 mutations in clinical practice. GMB-475 as a single therapy may have great limitations; however, combination therapy based on that has a potential treatment value for CML patients, but further clinical studies are needed for verification.

Data availability statement

The original contributions presented in the study are included in the article/Supplementary Material; further inquiries can be directed to the corresponding author.

Ethics statement

The animal study was reviewed and approved by the Animal Ethics Committee of West China Hospital of Sichuan University.

Author contributions

WY and YG contributed to the study conception and design. The experiments of the study were performed by WY, XW, XW, YT, XO, and YG. The first draft of the manuscript was written by

WY, and all authors commented on previous versions of the manuscript. All authors read and approved the final manuscript.

Funding

This work was supported by the Foundation of the Science and Technology Department of Sichuan Province (NO. 2019YFS0026).

Conflict of interest

The authors declare that the research was conducted in the absence of any commercial or financial relationships that could be construed as a potential conflict of interest.

Publisher's note

Supplementary material

The Supplementary Material for this article can be found online at: https://www.frontiersin.org/articles/10.3389/fphar.2022.931772/full#supplementary-material

References

Abaza, Y., Kantarjian, H., Alwash, Y., Borthakur, G., Champlin, R., Kadia, T., et al. (2020). Phase I/II study of dasatinib in combination with decitabine in patients with accelerated or blast phase chronic myeloid leukemia. *Am. J. Hematol.* 95 (11), 1288–1295. doi:10.1002/ajh.25939

Alves, R., Gonçalves, A. C., Jorge, J., Alves, J., Alves, D. S. A., Freitas-Tavares, P., et al. (2019). Everolimus in combination with Imatinib overcomes resistance in Chronic myeloid leukaemia. *Med. Oncol.* 36 (3), 30. doi:10.1007/s12032-019-1253-5

Breccia, M., Colafigli, G., Scalzulli, E., and Martelli, M. (2021). Asciminib: An investigational agent for the treatment of chronic myeloid leukemia. *Expert Opin. Investig. Drugs* 30, 803–811. doi:10.1080/13543784.2021.1941863

Buhimschi, A. D., Armstrong, H. A., Toure, M., Jaime-Figueroa, S., Chen, T. L., Lehman, A. M., et al. (2018). Targeting the C481S ibrutinib-resistance mutation in bruton's tyrosine kinase using PROTAC-mediated degradation. *BIOCHEMISTRY* 57 (26), 3564–3575. doi:10.1021/acs.biochem.8b00391

Burslem, G. M., Schultz, A. R., Bondeson, D. P., Eide, C. A., Savage, S. S., Druker, B. J., et al. (2019). Targeting BCR-ABL1 in chronic myeloid leukemia by PROTAC-mediated targeted protein Degradation.Research support. *Cancer Res.CANCER Res.* 79 (18), 4744–4753. doi:10.1158/0008-5472.CAN-19-1236

Castagnetti, F., Pane, F., Rosti, G., Saglio, G., and Breccia, M. (2021). Dosing strategies for improving the risk-benefit profile of ponatinib in patients with chronic myeloid leukemia in chronic phase. *Front. Oncol.* 11, 642005. doi:10.3389/fonc.2021.642005

Cetin, Z., Ilker, S. E., and Yilmaz, M. (2021). Crosstalk between CML cells with HUVECS and BMSCs through CML derived exosomes. *Front. Biosci.* 26, 444–467. doi:10.2741/4901

Clapper, E., Di Trapani, G., and Tonissen, K. F. (2021). The regulation of bcr-abl in hypoxia is through the mTOR pathway. *Leuk. Lymphoma* 62 (4), 967–978. doi:10.1080/10428194.2020.1849679

Coll-Martínez, B., Delgado, A., and Crosas, B. (2020). The potential of proteolytic chimeras as pharmacological tools and therapeutic agents. *Molecules* 25 (24), E5956. doi:10.3390/molecules25245956

Devos, T., Havelange, V., Theunissen, K., Meers, S., Benghiat, F. S., Gadisseur, A., et al. (2021). Clinical outcomes in patients with Philadelphia chromosome-positive leukemia treated with ponatinib in routine clinical practice-data from a Belgian registry. *Ann. Hematol.* 100 (7), 1723–1732. doi:10.1007/s00277-021-04507-x

Eden, R. E., and Coviello, J. M. (2021). *Chronic myelogenous leukemia*. National Cancer Institute.

Eide, C. A., Zabriskie, M. S., Savage, S. S., Antelope, O., Vellore, N. A., Extramural, N. I. H., et al. (2019). Combining the allosteric inhibitor asciminib with ponatinib suppresses emergence of and restores efficacy against highly resistant BCR-ABL1 mutants.Combining the allosteric inhibitor asciminib with ponatinib suppresses emergence of and restores efficacy against highly resistant BCR-ABL1 mutants. [journal article; research support. *CANCER Cell* 36 (4), 431–443. doi:10.1016/j.ccell.2019.08.004

García-Ferrer, M., Wojnicz, A., Mejía, G., Koller, D., Zubiaur, P., and Abad-Santos, F. (2019). Utility of therapeutic drug monitoring of imatinib, nilotinib, and dasatinib in chronic myeloid leukemia: A systematic review and meta-analysis. *Clin. Ther.* 41 (12), 2558–2570. doi:10.1016/j.clinthera.2019.10.009

Ghidini, A., Cléry, A., Halloy, F., Allain, F., and Hall, J. (2021). RNA-PROTACs: Degraders of RNA-binding proteins. *Angew. Chem. Int. Ed. Engl.* 60 (6), 3163–3169. doi:10.1002/anie.202012330

Gleixner, K. V., Filik, Y., Berger, D., Schewzik, C., Stefanzl, G., Sadovnik, I., et al. (2021). Asciminib and ponatinib exert synergistic anti-neoplastic effects on CML cells expressing *BCR-ABL1*^{T315I}-compound mutations. *Am. J. Cancer Res.* 11 (9), 4470–4484.

Guignabert, C., Phan, C., Seferian, A., Huertas, A., Tu, L., Thuillet, R., et al. (2016). Dasatinib induces lung vascular toxicity and predisposes to pulmonary hypertension. *J. Clin. Invest.* 126 (9), 3207–3218. doi:10.1172/JCI86249

Haider, M. Z., and Anwer, F. (2021). *Genetics, Philadelphia Chromosome*. Treasure Island (FL): StatPearls Publishing..

Hjorth-Hansen, H., Stentoft, J., Richter, J., Koskenvesa, P., Höglund, M., Dreimane, A., et al. (2016). Safety and efficacy of the combination of pegylated interferon-α2b and dasatinib in newly diagnosed chronic-phase chronic myeloid leukemia patients. *LEUKEMIA* 30 (9), 1853–1860. doi:10.1038/leu.2016.121

Hu, J., Hu, B., Wang, M., Xu, F., Miao, B., Yang, C. Y., et al. (2019). Discovery of ERD-308 as a highly potent proteolysis targeting chimera (PROTAC) degrader of estrogen receptor (ER). *J. Med. Chem.* 62 (3), 1420–1442. doi:10.1021/acs.jmedchem.8b01572

Ishida, T., and Ciulli, A. (2021). E3 ligase ligands for PROTACs: How they were found and how to discover new ones. *SLAS Discov.* 26 (4), 484–502. doi:10.1177/2472555220965528

Jiang, Y., Deng, Q., Zhao, H., Xie, M., Chen, L., Yin, F., et al. (2018). Development of stabilized peptide-based PROTACs against estrogen receptor α. *ACS Chem. Biol.* 13 (3), 628–635. doi:10.1021/acschembio.7b00985

Jones, J. K., Thompson, E. M., and Extramural, N. I. H. (2020). Allosteric inhibition of ABL kinases: Therapeutic potential in Cancer.Review]. *Mol. Cancer Ther.* 19 (9), 1763–1769. doi:10.1158/1535-7163.MCT-20-0069

Kakiuchi, S., Rikitake, J., Kitazawa, H., Harima, I., Nakajima, R., Akiyama, H., et al. (2021). [Successful treatment with ponatinib in combination with hyper-CVAD for chronic myeloid leukemia in the lymphoid blastic phase]. *Rinsho. Ketsueki.* 62 (1), 47–50. doi:10.11406/rinketsu.62.47

Kastl, J. M., Davies, G., Godsman, E., and Holdgate, G. A. (2021). Small-molecule degraders beyond PROTACs-challenges and opportunities. *SLAS Discov.* 26 (4), 524–533. doi:10.1177/2472555221991104

Khorashad, J. S., Kelley, T. W., Szankasi, P., Mason, C. C., Soverini, S., Adrian, L. T., et al. (2013). BCR-ABL1 compound mutations in tyrosine kinase inhibitor-resistant CML: Frequency and clonal relationships. *BLOOD* 121 (3), 489–498. doi:10.1182/blood-2012-05-431379

Koyama, D., Kikuchi, J., Kuroda, Y., Ohta, M., and Furukawa, Y. (2021). AMP-activated protein kinase activation primes cytoplasmic translocation and autophagic degradation of the BCR-ABL protein in CML cells. *Cancer Sci.* 112 (1), 194–204. doi:10.1111/cas.14698

Lee, G. T., Nagaya, N., Desantis, J., Madura, K., Sabaawy, H. E., Kim, W. J., et al. (2021). Effects of MTX-23, a novel PROTAC of androgen receptor splice variant-7 and androgen receptor, on CRPC resistant to second-line antiandrogen therapy. *Mol. Cancer Ther.* 20 (3), 490–499. doi:10.1158/1535-7163.MCT-20-0417

Lei, H., Xu, H. Z., Shan, H. Z., Liu, M., Lu, Y., Fang, Z. X., et al. (2021). Targeting USP47 overcomes tyrosine kinase inhibitor resistance and eradicates leukemia stem/progenitor cells in chronic myelogenous leukemia.Research Support, Non-U.S. Gov't]. *Nat. Commun.Nature Commun.* 12 (1), 51. doi:10.1038/s41467-020-20259-0

Li, Y., Zhang, S., Zhang, J., Hu, Z., Xiao, Y., Huang, J., et al. (2019). Exploring the PROTAC degron candidates: OBHSA with different side chains as novel selective estrogen receptor degraders (SERDs). *Eur. J. Med. Chem.* 172, 48–61. doi:10.1016/j.ejmech.2019.03.058

Liu, J., Zhang, Y., Huang, H., Lei, X., Tang, G., Cao, X., et al. (2021). Recent advances in Bcr-Abl tyrosine kinase inhibitors for overriding T315I mutation. *Chem. Biol. Drug Des.* 97 (3), 649–664. doi:10.1111/cbdd.13801

Martín-Acosta, P., and Xiao, X. (2021). PROTACs to address the challenges facing small molecule inhibitors. *Eur. J. Med. Chem.* 210, 112993. doi:10.1016/j.ejmech.2020.112993

Mian, A. A., Haberbosch, I., Khamaisie, H., Agbarya, A., Pietsch, L., Eshel, E., et al. (2021). Crizotinib acts as ABL1 inhibitor combining ATP-binding with allosteric inhibition and is active against native BCR-ABL1 and its resistance and compound mutants BCR-ABL1^{T315I} and BCR-ABL1$^{T315I\text{-}E255K}$. *Ann. Hematol.* 100, 2023–2029. doi:10.1007/s00277-020-04357-z

Milojkovic, D., Cross, N., Ali, S., Byrne, J., Campbell, G., Dignan, F. L., et al. (2021). Real-world tyrosine kinase inhibitor treatment pathways, monitoring patterns and responses in patients with chronic myeloid leukaemia in the United Kingdom: The UK TARGET CML study. *Br. J. Haematol.* 192 (1), 62–74. doi:10.1111/bjh.16733

Miura, M. (2015). Therapeutic drug monitoring of imatinib, nilotinib, and dasatinib for patients with chronic myeloid leukemia. *Biol. Pharm. Bull.* 38 (5), 645–654. doi:10.1248/bpb.b15-00103

Morita, K., and Sasaki, K. (2021). Current status and novel strategy of CML. *Int. J. Hematol.* 113 (5), 624–631. doi:10.1007/s12185-021-03127-5

Mukhamejanova, Z., Tong, Y., Xiang, Q., Xu, F., and Pang, J. (2021). Recent advances in the design and development of anticancer molecules based on PROTAC technology. *Curr. Med. Chem.* 28 (7), 1304–1327. doi:10.2174/0929867327666200312112412

Özgür, Y. N., and Eşkazan, A. E. (2020). Novel therapeutic approaches in chronic myeloid leukemia. *Leuk. Res.* 91, 106337. doi:10.1016/j.leukres.2020.106337

Patel, A. B., O'Hare, T., and Deininger, M. W. (2017). Mechanisms of resistance to ABL kinase inhibition in chronic myeloid leukemia and the development of next generation ABL kinase inhibitors. *Hematol. Oncol. Clin. North Am.* 31 (4), 589–612. doi:10.1016/j.hoc.2017.04.007

Pettersson, M., and Crews, C. M. (2019). PROteolysis TArgeting Chimeras (PROTACs) - past, present and future. *Drug Discov. Today. Technol.* 31, 15–27. doi:10.1016/j.ddtec.2019.01.002

Protein Degradation (2020). Proof-of-Concept with PROTACs in prostate cancer. *Cancer Discov.* 10 (8), 1084. doi:10.1158/2159-8290.CD-NB2020-054

Qi, S. M., Dong, J., Xu, Z. Y., Cheng, X. D., Zhang, W. D., and Qin, J. J. (2021). Protac: An effective targeted protein degradation strategy for cancer therapy. *Front. Pharmacol.* 12, 692574. doi:10.3389/fphar.2021.692574

Qin, H., Zhang, Y., Lou, Y., Pan, Z., Song, F., Liu, Y., et al. (2021). Overview of PROTACs targeting the estrogen receptor: Achievements for biological and drug discovery. *Curr. Med. Chem.* 29, 3922–3944. doi:10.2174/0929867328666211110101018

Radi, M., Schenone, S., and Botta, M. (2013). Allosteric inhibitors of bcr-abl: Towards novel myristate-pocket binders. *Curr. Pharm. Biotechnol.* 14 (5), 477–487. doi:10.2174/13892010140513111111103750

Radujkovic, A., Topaly, J., Fruehauf, S., and Zeller, W. J. (2006). Combination treatment of imatinib-sensitive and -resistant BCR-ABL-positive CML cells with imatinib and farnesyltransferase inhibitors. *Anticancer Res.* 26 (3A), 2169–2177.

Rinke, J., Hochhaus, A., and Ernst, T. (2020). Cml - not only BCR-ABL1 matters. *Best. Pract. Res. Clin. Haematol.* 33 (3), 101194. doi:10.1016/j.beha.2020.101194

Singh, A. P., Glennon, M. S., Umbarkar, P., Gupte, M., Galindo, C. L., Zhang, Q., et al. (2019). Ponatinib-induced cardiotoxicity: Delineating the signalling mechanisms and potential rescue strategies. *Cardiovasc. Res.* 115 (5), 966–977. doi:10.1093/cvr/cvz006

Singh, P., Kumar, V., Gupta, S. K., Kumari, G., and Verma, M. (2021). Combating TKI resistance in CML by inhibiting the PI3K/Akt/mTOR pathway in combination with TKIs: A review. *Med. Oncol.* 38 (1), 10. doi:10.1007/s12032-021-01462-5

Sun, Y., Zhao, X., Ding, N., Gao, H., Wu, Y., Yang, Y., et al. (2018). PROTAC-induced BTK degradation as a novel therapy for mutated BTK C481S induced ibrutinib-resistant B-cell malignancies. *Cell Res.* 28 (7), 779–781. doi:10.1038/s41422-018-0055-1

Talati, C., and Pinilla-Ibarz, J. (2018). Resistance in chronic myeloid leukemia: Definitions and novel therapeutic agents. *Curr. Opin. Hematol.* 25 (2), 154–161. doi:10.1097/MOH.0000000000000403

Wylie, A. A., Schoepfer, J., Jahnke, W., Cowan-Jacob, S. W., Loo, A., Furet, P., et al. (2017). The allosteric inhibitor ABL001 enables dual targeting of BCR-ABL1. *NATURE* 543 (7647), 733–737. doi:10.1038/nature21702

Xia, L. W., Ba, M. Y., Liu, W., Cheng, W., Hu, C. P., Zhao, Q., et al. (2019). Triazol: A privileged scaffold for proteolysis targeting chimeras. *Future Med. Chem.* 11 (22), 2919–2973. doi:10.4155/fmc-2019-0159

Xin, P., Xu, X., Deng, C., Liu, S., Wang, Y., Zhou, X., et al. (2020). The role of JAK/STAT signaling pathway and its inhibitors in diseases. *Int. Immunopharmacol.* 80, 106210. doi:10.1016/j.intimp.2020.106210

Yan, G., Zhong, X., Yue, L., Pu, C., Shan, H., Lan, S., et al. (2021). Discovery of a PROTAC targeting ALK with *in vivo* activity. *Eur. J. Med. Chem.* 212, 113150. doi:10.1016/j.ejmech.2020.113150

Zeng, S., Huang, W., Zheng, X., Liyan, C., Zhang, Z., Wang, J., et al. (2021). Proteolysis targeting chimera (PROTAC) in drug discovery paradigm: Recent progress and future challenges. *Eur. J. Med. Chem.* 210, 112981. doi:10.1016/j.ejmech.2020.112981

Zhao, Y., Shu, Y., Lin, J., Chen, Z., Xie, Q., Bao, Y., et al. (2021). Discovery of novel BTK PROTACs for B-Cell lymphomas. *Eur. J. Med. Chem.* 225, 113820. doi:10.1016/j.ejmech.2021.113820

frontiers | Frontiers in Oncology

TYPE Original Research
PUBLISHED 06 October 2022
DOI 10.3389/fonc.2022.1011762

OPEN ACCESS

EDITED BY
Sungpil Yoon,
Sungkyunkwan University, South Korea

REVIEWED BY
Ming-Ju Hsieh,
Changhua Christian Hospital, Taiwan
Arianna Giacomini,
University of Brescia, Italy

*CORRESPONDENCE
Malgorzata Zakrzewska
malgorzata.zakrzewska@uwr.edu.pl

SPECIALTY SECTION
This article was submitted to Pharmacology of Anti-Cancer Drugs, a section of the journal Frontiers in Oncology

RECEIVED 04 August 2022
ACCEPTED 20 September 2022
PUBLISHED 06 October 2022

CITATION
Szymczyk J, Sochacka M, Chudy P, Opalinski L, Otlewski J and Zakrzewska M (2022) FGF1 protects FGFR1-overexpressing cancer cells against drugs targeting tubulin polymerization by activating AKT *via* two independent mechanisms. *Front. Oncol.* 12:1011762. doi: 10.3389/fonc.2022.1011762

FGF1 protects FGFR1-overexpressing cancer cells against drugs targeting tubulin polymerization by activating AKT *via* two independent mechanisms

Jakub Szymczyk, Martyna Sochacka, Patryk Chudy, Lukasz Opalinski, Jacek Otlewski and Malgorzata Zakrzewska*

Department of Protein Engineering, Faculty of Biotechnology, University of Wroclaw, Wroclaw, Poland

Cancer drug resistance is a common, unpredictable phenomenon that develops in many types of tumors, resulting in the poor efficacy of current anticancer therapies. One of the most common, and yet the most complex causes of drug resistance is a mechanism related to dysregulation of tumor cell signaling. Abnormal signal transduction in a cancer cell is often stimulated by growth factors and their receptors, including fibroblast growth factors (FGFs) and FGF receptors (FGFRs). Here, we investigated the effect of FGF1 and FGFR1 activity on the action of drugs that disrupt tubulin polymerization (taltobulin, paclitaxel, vincristine) in FGFR1-positive cell lines, U2OS stably transfected with FGFR1 (U2OSR1) and DMS114 cells. We observed that U2OSR1 cells exhibited reduced sensitivity to the tubulin-targeting drugs, compared to U2OS cells expressing a negligible level of FGFRs. This effect was dependent on receptor activation, as inhibition of FGFR1 by a specific small-molecule inhibitor (PD173074) increased the cells' sensitivity to these drugs. Expression of functional FGFR1 in U2OS cells resulted in increased AKT phosphorylation, with no change in total AKT level. U2OSR1 cells also exhibited an elevated MDR1 and blocking MDR1 activity with cyclosporin A increased the toxicity of paclitaxel and vincristine, but not taltobulin. Analysis of tubulin polymerization pattern using fluorescence microscopy revealed that FGF1 in U2OSR1 cells partially reverses the drug-altered phenotype in paclitaxel- and vincristine-treated cells, but not in taltobulin-treated cells. Furthermore, we showed that FGF1, through activation of FGFR1, reduces caspase 3/7 activity and PARP cleavage, preventing apoptosis induced by tubulin-targeting drugs. Next, using specific kinase inhibitors, we investigated which signaling pathways are responsible for the FGF1-mediated reduction of taltobulin cytotoxicity. We found that AKT kinase is a key factor in FGF1-induced cell protection against taltobulin in U2OSR1 and DMS114 cells. Interestingly, only direct inhibition of AKT or dual-inhibition of PI3K and mTOR abolished this effect for cells treated

with taltobulin. This suggests that both canonical (PI3K-dependent) and alternative (PI3K-independent) AKT-activating pathways may regulate FGF1/FGFR1-driven cancer cell survival. Our findings may contribute to the development of more effective therapies and may facilitate the prevention of drug resistance in FGFR1-positive cancer cells.

KEYWORDS

cancer, FGF1, FGFR1, drug resistance, anticancer drugs, taltobulin, AKT

1 Introduction

Due to the complexity of both genetic and epigenetic factors underlying the initiation and progression of tumorigenesis, contemporary anticancer therapies are still not very effective (1). A common feature of cancer cells is their rapid and uncontrolled proliferation, often caused by overexpression of mitogenic proteins such as growth factors, or their receptors (2). Microtubules and their dynamics, involved in all phases of mitosis, are an important element in efficient cell division. Targeting tubulin, a single unit of microtubules, is one of the most common strategies used in anticancer treatment. There is a large group of drugs that act by inhibiting tubulin polymerization (e.g. vincristine) or by stabilizing the resulting microtubules and preventing their depolymerization (e.g. paclitaxel). In both cases, deregulation of tubulin polymerization leads to inhibition of cell division and tumor growth, and ultimately activates apoptosis leading to tumor cell death (3).

One of the most serious problems facing modern cancer-focused medicine is the development of drug resistance to current therapies. Mechanisms underlying chemoresistance include inhibition of apoptosis, drug inactivation, increased drug export, enhancement of DNA repair mechanisms and mutations at drug target sites (4, 5). The aforementioned growth factors, whose enhanced activity can lead to metabolic dysfunction and tumor formation, have also been implicated in the desensitization of cancer cells to drugs (6). Recently increasing attention is being paid to the fibroblast growth factors and their receptors, whose involvement in neoplasia has been demonstrated in many types of cancer (7).

The FGF family consists of 22 proteins that interact with four specific receptors (FGFR1-4) belonging to a group of receptor tyrosine kinases (RTKs). The interaction of FGFs with FGFRs leads to receptor dimerization and activation, which in turn activates signaling cascades, such as AKT/PI3K, MAPKs, PLCγ/PKC, and STATs (8). FGFR-dependent downstream signaling regulates cell differentiation, migration, apoptosis and the cell cycle, so dysregulation of the FGFR axis often leads to various systemic disorders, including cancers and the development of its drug resistance (9). The action of FGFs, particularly FGF1 and FGF2, has been correlated with chemoresistance in many types of cancer, but the exact mechanisms have not been fully described (10). Only a few studies have demonstrated an effect of FGF2 and FGFRs on paclitaxel resistance, but without clearly identifying the specific signaling pathway responsible for this phenomenon (11–13).

In the present study, by investigating the effect of drugs that interfere with tubulin polymerization in FGFR1-positive cell lines, we observed that FGF1 prevents drug-induced apoptosis. We determined that AKT kinase is a key factor in FGF1/FGFR1-dependent cell protection against tubulin-targeting drugs in U2OSR1 and DMS114 cells. This finding may be crucial in the development of more effective combination therapies for the treatment of FGFR1-positive cancers.

2 Materials and methods

2.1 Antibodies and reagents

Primary antibodies: anti-phospho-FGFR (Tyr653/Tyr654) (p-FGFR) (#06-1433) were from Merck (Darmstadt, Germany); anti-phospho-mTOR (Ser2448) (p-mTOR) (#2971), anti-FGFR1 (FGFR1) (#9740), anti-phospho-EGFR (Y1173) (p-EGFR) (#4407), anti-phospho-AKT (Ser473) (p-AKT p-S473) (#9271), anti-phospho-AKT (Thr308) (p-AKT p-T308) (#9275), anti-AKT1/2/3 (AKT) (#9272), anti-phospho-p44/42 (Thr202/Tyr204) MAP kinase (p-ERK1/2) (#9101), anti-p44/42 MAP kinase (ERK1/2) (#9102), anti-MDR1/ABCB1 (MDR1) (#12683), and anti-poly-[ADP-ribose] polymerase (PARP) (#9542) were from Cell Signaling Technology (Danvers, MA, USA); anti-mTOR (mTOR) (#T2949), anti-γ-tubulin (tubulin) (#T6557) and anti-acetylated-α-tubulin (ac-tubulin) (#T7451) were from Sigma Aldrich (St Louis, MO, USA). Horseradish peroxidase-conjugated secondary antibodies were from Jackson Immuno-Research Laboratories (Cambridge, UK) and a chemiluminescent substrate was used to visualize them in the ChemiDoc station (BioRad, Hercules, CA, USA).

AlexaFluor®594-conjugated secondary antibodies were from Abcam (Cambridge, UK). NucBlue Live ReadyProbes Reagent was from Thermo Fisher (Waltham, MA, USA). Geneticin (G-418) was from BioShop (Puck, Poland). Penicillin-Streptomycin Solution was from Biowest (Nuaille, France). Heparin came from Sigma-Aldrich.

2.2 Anticancer drugs and inhibitors

Taltobulin (HTI-286) and Dactolisib (BEZ235) were from MedChem Express (Monmouth Junction, NJ, USA). Vincristine and API-2 came from Selleckchem (Houston, TX, USA). Paclitaxel, PD173074, Gefitinib, LY294002, and UO126 were purchased from Sigma-Aldrich. Torin-2 was from Cell Signaling Technology (Danvers, MA, USA), SB203580 from Calbiochem (San Diego, CA, USA), and Cyclosporin A from Carbosynth (Compton, UK).

2.3 Recombinant proteins

Recombinant FGF1 and FGF2 proteins were produced as previously described (14, 15). Recombinant EGF protein was obtained from M.C.Biotec.Inc (Nanjing, China).

2.4 Cell lines

The human osteosarcoma cell line (U2OS), and the small cell lung cancer (SCLC) cell line (DMS114) were obtained from the American Type Culture Collection (ATCC). The non-small lung cancer cell line (HCC15) was supplied by the Leibniz Institute DSMZ-German Collection of Microorganisms and Cell Cultures (DSMZ). U2OS cell lines stably transfected with pcDNA3.1 vector containing the sequence encoding the full-length FGFR1 (U2OSR1) or empty pcDNA3.1 vector (U2OS) were prepared as described previously (16). The U2OS cell line stably transfected with FGFR1-IIIc_K514R (U2OSR1-K514R) was kindly provided by Dr. Ellen M. Haugsten from the Department of Molecular Cell Biology, Institute for Cancer Research (Oslo University Hospital). U2OS, U2OSR1, and U2OSR1-K514R cells were cultured in DMEM (Biowest) supplemented with 10% fetal bovine serum (Thermo Fisher Scientific) and antibiotics (100 U/ml penicillin, 100 µg/ml streptomycin and 1 mg/ml geneticin). DMS114 cells grew in Waymouth's MB 752/1 medium (ATCC) supplemented with 10% fetal bovine serum (Thermo Fisher Scientific) and antibiotics (100 U/mL penicillin, 100 µg/mL streptomycin). HCC15 cells were cultured in RPMI 1640 Medium (Biowest) supplemented with 10% fetal bovine serum (Thermo Fisher Scientific) and antibiotics (100 U/mL penicillin, 100 µg/mL streptomycin). All cancer cell lines were kept at 37 °C in a 5% CO_2 incubator.

2.5 Cell cytotoxicity assay

Cancer cells were seeded in 96-well plates at a density of 1×10^4 cells/well (U2OS, HCC15) or 4×10^4 (DMS114). When comparing all three U2OS sublines for response to cytotoxic drugs, cells were kept without the addition of geneticin during the experiments. After 24 h anticancer drugs were added in various concentration (0.5 - 10 nM taltobulin (TLT), 1 - 50 nM paclitaxel (PTX) or 1 - 50 nM vincristine (VCR)) in the presence or absence of 10 ng/mL of FGF1, FGF2 or EGF and 10 U/mL heparin. When chemical inhibitors were used, they were first added to the cells for 15 min (100 nM PD174074, 20 µM UO126, 20 µM LY294002, 5 µM SB203580, 1 µM API-2, 100 nM BEZ235, 10 µM Cyclosporin A) or 60 min (100 nM Torin-2), followed by administration of the indicated drugs and/or growth factors. After 48 h of incubation, alamarBlue Cell Viability Reagent (Thermo Fisher Scientific) was added to each well according to the manufacturer's protocol. The emission of the fluorescent reduced form of the dye was recorded at 590 nm upon excitation at 560 nm using an Infinite M1000 PRO plate reader (Tecan). The cytotoxic effect of the drugs was normalized and expressed as a percentage of cell viability of untreated cells. All experiments were performed 3 times (n=3) with at least three replicates in each experiment.

2.6 FGFR1 activation and downstream signaling

For the comparison of protein level and protein phosphorylation in the selected cancer cell lines, cells were seeded in 6-well plates at the density of 2×10^5 cells/well for 24 h. Cells were lysed with sample buffer (8% SDS, 2% β-ME), and then cell lysates were sonicated, heated, and subjected to SDS-PAGE and western blotting.

For the examination of growth factors' activity in receptor and downstream signaling activation, serum-starved (6 h) cancer cells were treated for 15 min with 100 ng/mL of FGF1, FGF2, or EGF in the presence of heparin (10 U/ml) with or without the indicated inhibitors. Inhibitors were added 15 min or 60 min (for Torin-2) before stimulation. Cells were then lysed with sample buffer (8% SDS, 2% β-ME), followed by sonication, heating, SDS-PAGE and western blotting.

2.7 Fluorescence microscopy

U2OSR1 cells were treated with indicated drugs with the presence or absence of 10 ng/mL FGF1 and 10 U/mL heparin for

24 h. Cells were then fixed with 4% paraformaldehyde, permeabilized with 0.1% Triton in PBS, and blocked with blocking buffer (2% BSA, 0.1 M glycine in PBS). Primary antibodies (1:500) targeted against acetylated α-tubulin were added to the cells to visualize changes in tubulin polymerization under drug conditions. Next, secondary antibodies (1:500) conjugated with AlexaFluor594 were added, followed by staining of cell nuclei with NucBlue Live ReadyProbes Reagent. Fluorescence microscopy was performed using a Zeiss Axio Observer Z1 fluorescence microscope (Zeiss, Oberkochen, Germany).

2.8 Cell apoptosis assays

2.8.1 Caspase-3/7 activity

Cancer cells were seeded in 96-well plates at a cell density of 1×10^4 cells/well (U2OSR1) or 4×10^4 (DMS114). After 24 h cells were treated with indicated drugs (5 nM TLT, 20 nM PTX, or 10 nM VCR) in the presence or absence of 10 ng/mL of FGF1 and 10 U/mL heparin. 24 h later, caspases 3/7 activity was measured using the ApoLive-Glo Multiplex Assay (Promega, WI, USA) according to the manufacturer's protocol. The ratio of caspase-3/7 activity to cell viability was normalized towards untreated cells and denoted as a relative caspase-3/7 activity. All experiments were performed three times (n=3) with at least three replicates in each experiment.

2.8.2 Flow cytometry

U2OSR1 cells were seeded in 12-well plates at a cell density of 1×10^5. After 24 h cells were treated with 5 nM TLT in the presence or absence of 10 ng/mL of FGF1 and 10 U/mL heparin. After 24 h of incubation, cells were harvested and washed with PBS. Drug-induced cell apoptosis was monitored using eBioscience™ Annexin V-FITC Apoptosis Kit (Thermo Fisher Scientific) according to the manufacturer's protocol. Briefly, cells were first washed with binding buffer and then incubated sequentially with the indicated concentration of Annexin V-FITC and PI. Finally, all samples were analyzed using a NovoCyte 2060R Flow Cytometer (ACEA Biosciences, CA, USA), and 10,000 events were recorded for each analysis.

2.9 Statistical analysis

For statistical analysis, a one-tailed t-test was applied using GraphPad Prism 5 (GraphPad Software, CA, USA); $p < 0.05$ was considered statistically significant. The results are expressed as means ± SD.

3 Results

3.1 FGFR1 overexpression attenuates drug cytotoxicity in U2OS cells

To investigate whether overproduction of FGFR1 can make cancer cells less sensitive to drugs that interfere with tubulin polymerization, we measured the viability of cells in the U2OS sublines: a control cell line, transfected with empty pcDNA3.1 vector (U2OS), cells stably transfected with FGFR1 wild-type (U2OSR1) and the kinase-dead mutant of FGFR1 (U2OSR1-K514R) after 48 h of treatment with 5 nM taltobulin (TLT), 20 nM paclitaxel (PTX), and 10 nM vincristine (VCR), using the alamarBlue Cell Viability Reagent (Figure 1A). For all three drugs, U2OS cells overexpressing FGFR1 (U2OSR1) show a reduced response to drug toxicity compering to U2OS cells lacking FGFR1 (U2OS). For U2OS cells overexpressing the inactive (kinase-dead) mutant of FGFR1 (U2OSR1-K514R), PTX and VCR toxicity was similar to that in control U2OS cells, and even higher for TLT.

We compared the levels and phosphorylation of major FGFR-dependent downstream signaling molecules between U2OS sublines. U2OSR1 cells showed increased phosphorylation of AKT at Ser473 and Thr308 residues without an increase in total AKT level compared to control cells or the U2OSR1-K514R line (Figure 1B). No differences in mTOR or ERKs activation were observed in all sublines of U2OS cells.

Next, to be able to verify the response of U2OSR1 cells treated with drugs targeting tubulin polymerization to different growth factors, we used a range of concentrations of taltobulin, paclitaxel and vincristine, estimating the drug doses at which the effect of FGF1 is most effective (Figure 1C). For selected concentrations (5 nM TLT, 20 nM PTX and 10 nM VCR), we analyzed the effect of stimulation of U2OSR1 cells by FGF1, FGF2 or EGF (10 ng/mL with 10 U/mL heparin). Both FGF1 and FGF2 reduced cells sensitivity to all drugs tested, while EGF stimulation had no effect on cell viability (Figure 1D). We observed that FGF1 protection was concentration-dependent (Supplementary Figure 1A). As a control, we used U2O2R1-K514R cells, in which FGF1 stimulation had no protective effect against all three drugs tested (Supplementary Figure 1B).

3.2 FGF1 and FGF2 stimulation reduces drug-induced cytotoxicity in DMS114 cancer cells

Next, we investigated the protective effect of FGF1 and FGF2 in other FGFR1-positive cancer cell lines, DMS114, and FGFR1-negative cell line, HCC15 (17, 18). Cells were treated with different concentration of the drugs (TLT, PTX and VCR) in

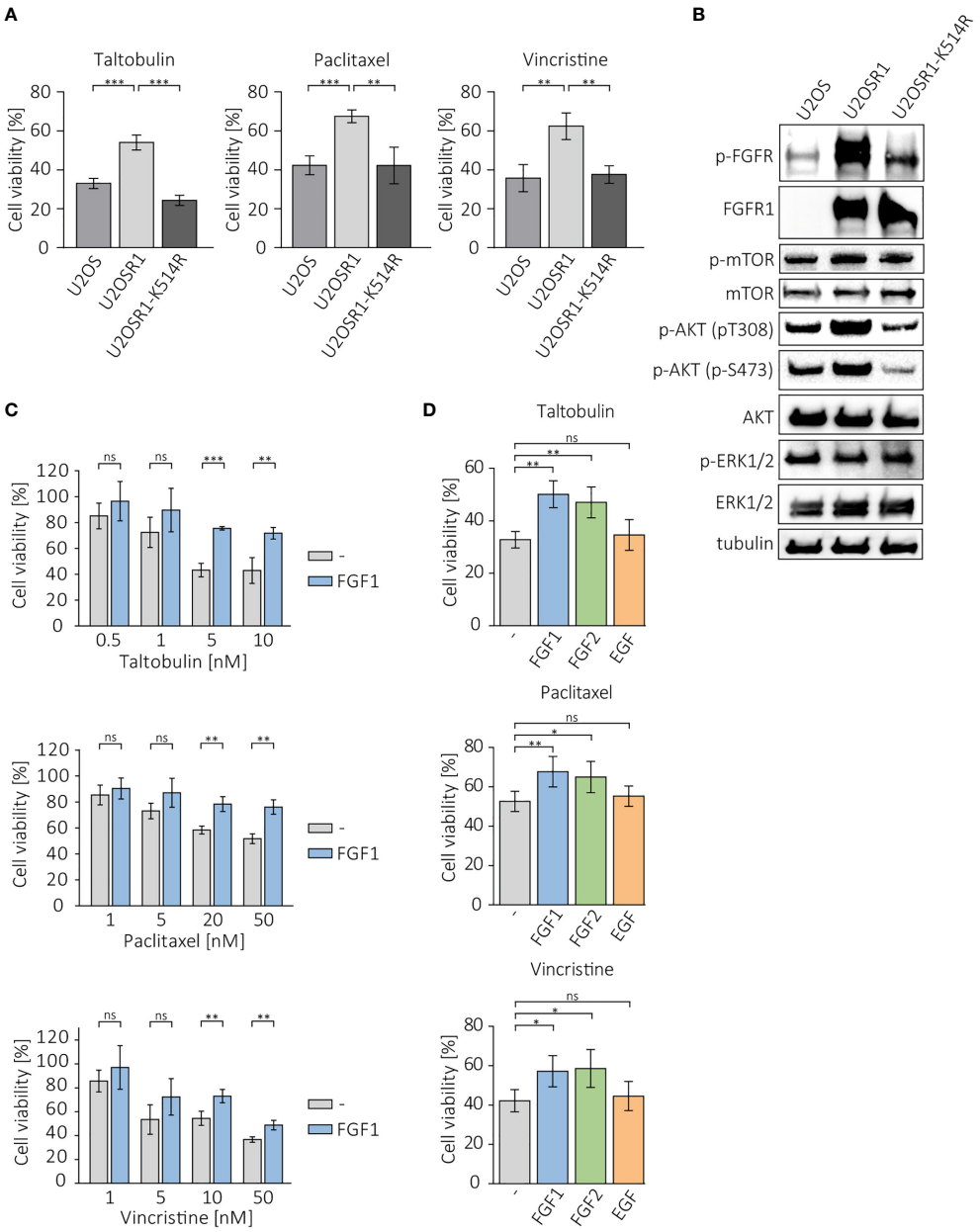

FIGURE 1
Protective effect of FGFR1 activity against cytotoxicity of taltobulin (TLT), paclitaxel (PTX) and vincristine (VCR). **(A)** Comparison of cytotoxicity of 5 nM TLT, 20 nM PTX, and 10 nM VCR in U2OS sublines. **(B)** Western blotting analysis of protein level and activation in U2OS sublines performed using the indicated primary antibodies directed to major FGFR-dependent signaling proteins. Anti-tubulin antibody served as an equal loading control. **(C)** Effect of FGF1 stimulation (10 ng/mL) in U2OSR1 cells treated with different concentration of the indicated drugs. **(D)** Effect of FGF1, FGF2, and EGF stimulation (10 ng/mL) on drug cytotoxicity in U2OSR1 cells. Cell viability in all experiments was monitored using the alamarBlue assay. Results represent the mean ± SD of at least three independent experiments and are normalized to untreated cells; statistical significance: *p<0.05, **p<0.01, ***p<0.001, no significant differences are marked as 'ns'.

the presence of 10 ng/mL FGF1 and 10 U/mL heparin, and cell viability was assessed after 48 h using alamarBlue assay. In DMS114 cells, the presence of FGF1 reduced the cytotoxicity of all three drugs (Figure 2A), while it had no in HCC15 cells (Figure 2B). Next, we tested the effect of FGF2 and EGF stimulation (10 ng/mL with 10 U/mL heparin) in DMS114 and HCC15 cells against the indicated drugs. FGF2 protected DMS114 cells in the same manner as FGF1 (Figure 2A), whereas it did not in HCC15 (Figure 2B). Furthermore, EGF had no effect on drugs cytotoxicity in both cancer cell lines, even in EGFR-

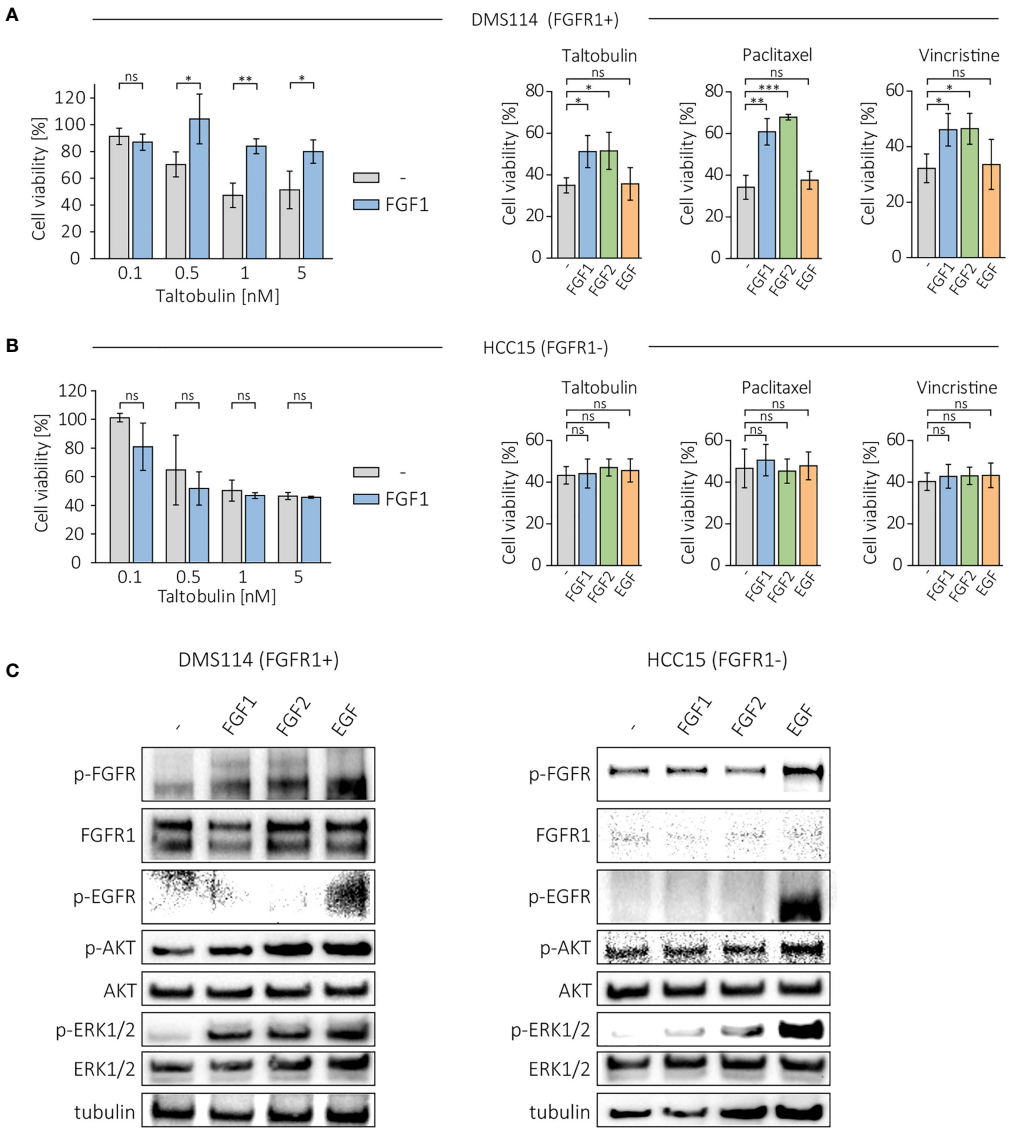

FIGURE 2
Effect of FGF1, FGF2 and EGF in DMS114 and HCC15 cells treated with the indicated drugs. Viability of **(A)** DMS114 and **(B)** HCC15 cells treated with different concentrations of TLT in the presence of 10 ng/mL FGF1 for 48 h (left panels) and comparison of the effect of FGF1, FGF2 and EGF (10 ng/mL) in cells treated for 48 h with 5 nM TLT, 20 nM PTX and 10 nM VCR (right panels). Cell viability was monitored using the alamarBlue assay. Results represent the mean ± SD of at least three independent experiments and are normalized to untreated cells; statistical significance: *p<0.05, **p<0.01, ***p<0.001, no significant differences are marked as 'ns'. **(C)** Western blotting analysis of FGF1, FGF2 and EGF (10 ng/mL) activity in DMS114 and HCC15 cells using anti-phospho-FGFR, anti-FGFR1, anti-phospho-EGFR, anti-phospho-AKT, anti-AKT, anti-phospho-ERK1/2 and anti-ERK1/2 antibodies. Anti-tubulin antibody served as an equal loading control.

positive HCC15 cells (Figures 2A, B). We also verified the short-term cell response to FGF1, FGF2 or EGF (10 ng/mL with 10 U/mL heparin) in DMS114 and HCC15 cells, by administering growth factors to serum-starved cells for 15 min and monitoring FGFR, EGFR, ERK1/2 and AKT activation by western blotting analysis (Figure 2C). Both FGF1 and FGF2, but not EGF, activate FGFR (upper band) in DMS114 cells. We observed a non-specific signal (lower band) detected by anti-phospho-FGFR in EGF-stimulated DMS114 cells (slightly stronger than in untreated cells) and in all HCC15 cell samples. To confirm that is not an effect of FGFR activation, we performed the experiment in both cell lines in the presence of a specific FGFR inhibitor, PD173074, and observed exactly the same pattern. However, after treatment with an EGFR inhibitor (Gefitinib), the signal was much weaker (Supplementary Figure 2), suggesting that the anti-phospho-FGFR antibody non-specifically recognizes some phosphorylation of EGFR. Due to the presence of both FGFR and EGFR in DMS114 cells

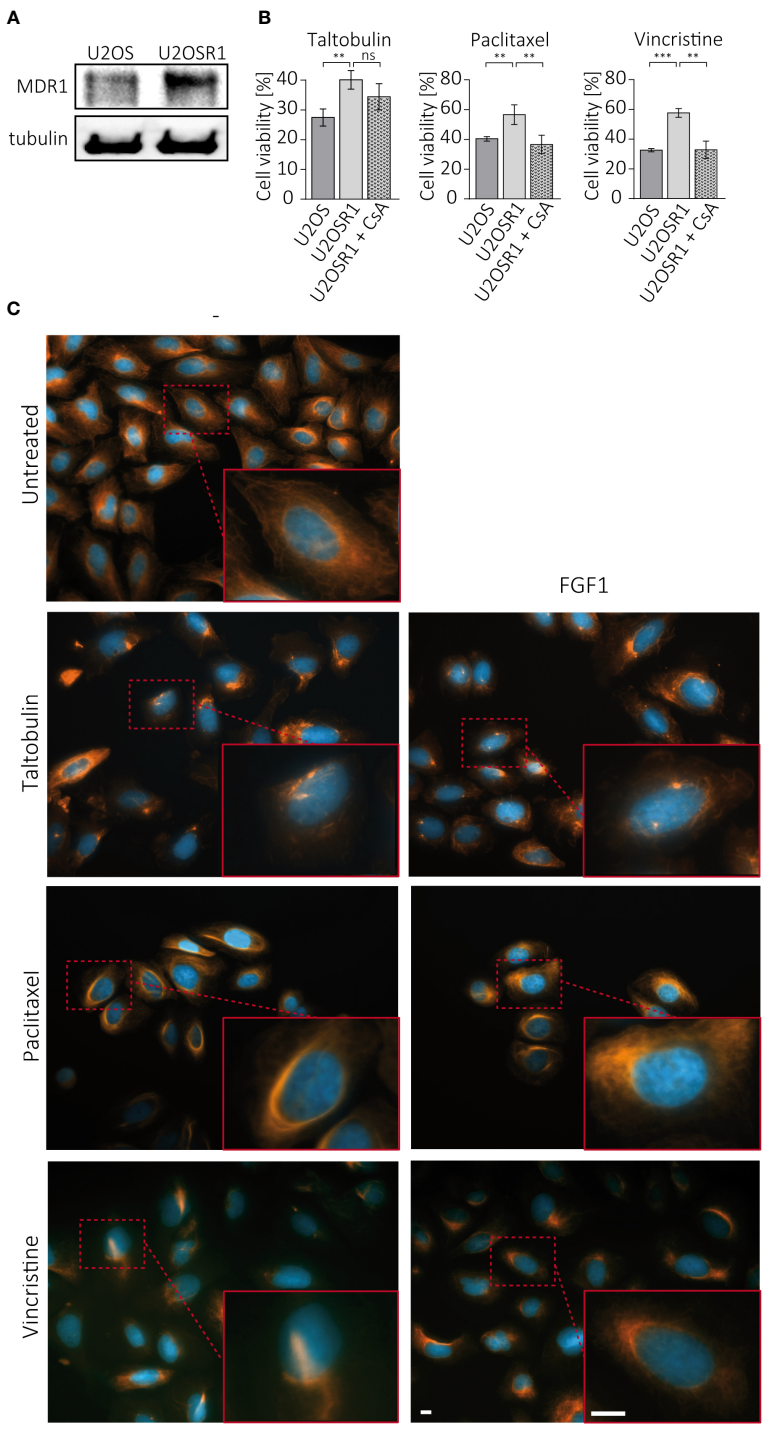

FIGURE 3
Effect of cell membrane transporters on the FGFR1-dependent protective effect against TLT, PTX and VCR. **(A)** MDR1 levels in U2OS and U2OS-R1 cells were analyzed by western blotting using anti-MDR1 antibody. **(B)** The effect of MDR1 inhibition with 10 μM cyclosporine A (CsA) on drug sensitivity in U2OSR1 cells was checked by monitoring cell viability 48 h after drug administration with the alamarBlue assay. Results represent the mean ± SD of at least three independent experiments and are normalized to untreated cells (w/o drug and CsA); statistical significance: **p<0.01, ***p<0.001, no significant differences are marked as 'ns'. **(C)** Changes in microtubules structures after 24-h treatment with drugs (5 nM TLT, 20 nM PTX, 10 nM VCR) and the effect of FGF1 (10 ng/mL) on this process were visualized by fluorescence microscopy using antibodies against acetylated-tubulin. Scale bar represents 10 μm.

for all growth factors, we observed ERKs phosphorylation. We observed only a slight increase in AKT phosphorylation, as even in untreated cells the level of phosphorylated AKT was relatively high. As expected, in HCC15 (FGFR-negative) cells, only EGF activated ERK1/2 and increased the level of phospho-AKT.

3.3 Protection against taltobulin in FGFR1-positive cells does not depend on the activity of the drug efflux proteins

Drug resistance in cancer cells often depends on the activity of ABC transporters, which can reduce drug cytotoxicity by actively pumping toxic molecules out of the cell (2). U2OSR1 cells used in the study show high level of MDR1, one of the main efflux transporters involved in drug resistance (Figure 3A). To test the importance of MDR1 activity in FGFR1-dependent protection, U2OSR1 cells were treated for 1 h with cyclosporine A (CsA), an MDR1 inhibitor, and then with the indicated drugs. After 48 h, cell viability was measured in the alamarBlue assay. Figure 3B shows that U2OSR1 cells both untreated and treated with cyclosporine A, exhibit reduced taltobulin-induced cytotoxicity compared to U2OS control cells. However, cyclosporine A significantly lowered the protective effect of FGFR1 in U2OSR1 against paclitaxel and vincristine. We next investigated whether the FGF1 stimulation could reverse the drug-altered phenotype of tubulin polymerization in U2OSR1 cells treated with TLT, PTX or VCR. Cells were treated with the indicated drug for 24 h in the presence of 10 ng/mL FGF1 and 10 U/mL heparin. After incubation, cells were fixed and changes in tubulin polymerization were visualized with anti-acetylated-tubulin antibodies by fluorescence microscopy (Figure 3C). All tested drugs, according to their mechanism of action, induced changes in microtubule structure in U2OSR1 cells. However, FGF1 partially reversed the drug-altered phenotype in PTX- and VCR-treated cells, but not in TLT-treated cells. In addition, we analyzed changes in acetylated tubulin levels during incubation of U2OSR1 cells with taltobulin by western blotting. As expected, ac-tubulin levels decreased over time, but we did not observe differences due to the presence of FGF1 (Supplementary Figure 3). These data suggest that FGFR1-dependent signaling protects U2OSR1 cells from TLT independently of drug release from the cell, in contrast to cell protection from PTX and VCR, which is at least partially dependent on the activity of cell-membrane transporters, which may prevent drug-accumulation in cells.

3.4 FGF1 inhibits drug-induced apoptosis *via* activation of FGFR1

We further investigated whether FGF1 stimulation could suppress drug-induced apoptosis in cancer cells expressing FGFR1. U2OSR1 cells were treated with 5 nM TLT, 10 ng/mL FGF1 and 10 U/mL heparin in the presence or absence of the potent FGFR1 inhibitor, 100 nM PD173074. After 24-h incubation, we monitored drug-induced apoptosis by measuring caspase 3/7 activity using ApoLive-Glo Multiplex Assay. FGF1 stimulation decreased relative caspase 3/7 activity in TLT-treated U2OSR1 (Figure 4A), and this effect was dependent on FGFR1 activation, as inhibition of the receptor kinase by PD173074 abolished it. To confirm our results, we compared the number of apoptotic and dead TLT-treated cells in the presence or absence of FGF1 by flow cytometry analysis using the eBioscience Annexin V-FITC Apoptosis Kit (Supplementary Figure 4A). For all three drugs (5 nM TLT, 20 nM PTX or 10 nM VCR), we also performed western blotting analysis with an anti-PARP antibody to detect PARP cleavage (Figure 4B). In all cases, we observed that FGF1 stimulation reduced PARP processing, demonstrating that FGF1 acts as an inhibitor of apoptosis in cancer cells treated with anticancer drugs targeting tubulin polymerization. We also confirmed the anti-apoptotic activity of FGF1 in DMS114 cells treated with TLT, PTX and VCR (Supplementary Figure 4B).

3.5 Only direct AKT inhibition abrogates the protective effect of FGF1

Following on from our previous results, in which we showed that cells resistant to the drugs tested had an elevated level of phosphorylated AKT, we investigated the effect of inhibiting AKT and other FGFR-dependent kinases on the protective effect of FGF1. U2OS-R1 and DMS114 cells were treated with specific chemical inhibitors that block major FGFR-dependent signaling pathways (PI3K/AKT and MAPKs) known to be the main culprits of drug resistance (19–21). Cells were then treated with 5 nM TLT in the presence of 10 ng/mL FGF1 and 10 U/mL heparin. After 48 h of incubation, cell viability was monitored with alamarBlue assay. Inhibition of PI3K (upstream activator of AKT) by LY294002 or MAPK kinases by UO126 (MEK/ERKs) or by SB203580 (p38) had no effect on FGF1 action in both U2OSR1 (Figure 5A) and DMS114 cells (Supplementary Figure 5A). In contrast, inhibition of mTOR by Torin-2 partially reduced the protective effect of FGF1, especially in DMS114 cells (Figure 5A, Supplementary Figure 5A).

We next examined whether direct AKT inhibition or simultaneous blockage of both PI3K and mTOR (as an alternative activator of AKT under stress conditions) could affect the effect of FGF1 in protecting against TLT, as direct inhibition of FGFR does. Again, we confirmed that the protective effect of FGF1 stimulation was dependent on FGFR1 activation, as FGF1 did not reduce the sensitivity to TLT when FGFR was inhibited by PD173074 (Figure 5B). Direct inhibition of AKT with API-2 inhibitor completely abolished the protective effect of FGF1 in both U2OSR1 and DMS114 cells (Figure 5B, Supplementary Figure 5B). Moreover, the combination of

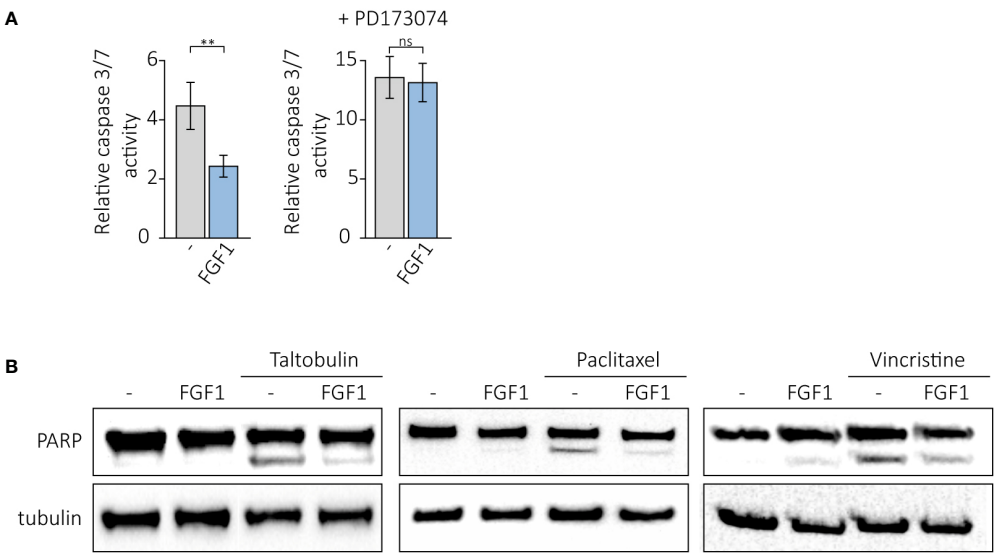

FIGURE 4
Anti-apoptotic effect of FGF1 stimulation in U2OSR1 cells treated with drugs targeting tubulin polymerization. **(A)** Relative caspase 3/7 activity induced by 5 nM TLT in U2OSR1 cells was measured using ApoLive-Glo Multiplex Assay 24 h after drug administration in the presence or absence of 10 ng/mL FGF1 and 100 nM PD173074. Results represent the mean ± SD of at least three independent experiments and are normalized to untreated cells; statistical significance: **p<0.01, no significant difference is marked as 'ns'. **(B)** Protective effect of FGF1 against drug-induced apoptosis in U2OSR1 cells assessed by PARP cleavage. Western blotting was performed with anti-PARP antibodies 24 h after administration of 5 nM TLT, 20 nM PTX or 10 nM VCR in the presence or absence of 10 ng/mL FGF1.

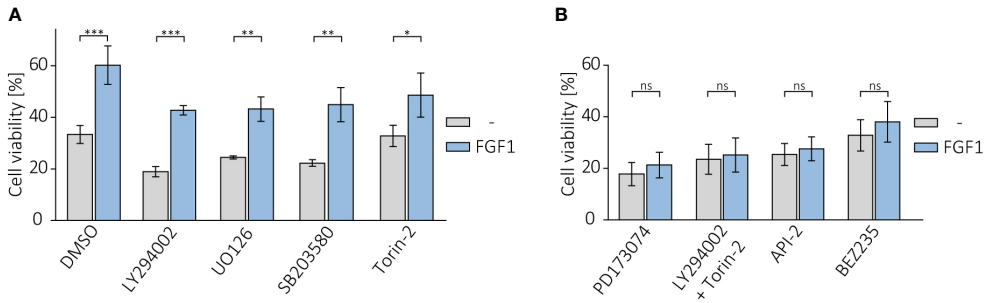

FIGURE 5
Effect of AKT inhibition on protective effect of FGF1 against TLT. Viability of U2OSR1 cells treated with 5 nM TLT and **(A)** different chemical inhibitors of major FGF-induced signaling pathways (20 μM LY294002 (PI3K), 20 μM UO126 (MEK1/2), 5 μM SB203580 (p38), 100 nM Torin-2 (mTOR)) or **(B)** FGFR inhibitor (100 nM PD173074), a direct AKT inhibitor (1 μM API-2), a dual mixture of PI3K and mTOR inhibitors (20 μM LY294002 + 100 nM Torin-2) or an inhibitor of both kinases, PI3K and mTOR (100 nM BEZ235) for 48 h in the presence or absence of 10 ng/mL FGF1, monitored by the alamarBlue assay. Results represent the mean ± SD of at least three independent experiments and are normalized to cells untreated with TLT; statistical significance: *p<0.05, **p<0.01, ***p<0.001, no significant differences are marked as 'ns'.

PI3K and mTOR inhibitors (LY294002 and Torin-2) or a dual inhibitor of both kinases (BEZ235) also fully inhibited FGF1-induced TLT resistance (Figure 5B, Supplementary Figure 5B). This result suggests that in drug-induced cellular stress AKT can also be activated *via* a PI3K-independent pathway. Taken together, our data demonstrate that the mechanism of FGFR1's protective effect against taltobulin cytotoxicity is directly related to AKT activation.

4 Discussion

The acquisition of drug resistance by cancer cells, a consequence of the enormous diversity and complexity of the molecular processes occurring in the tumor-affected tissues, results in a significant reduction in the efficacy of current anticancer therapies (1). This phenomenon affects biological drugs (such as antibodies and antibody-drug conjugates) as well

as cytotoxic drugs and small-molecule inhibitors, including protein kinase inhibitors (4, 22). The two main mechanisms involved are: (i) the development of alternative pathways that transmit mitogenic signals in tumor cells bypassing the blocked molecules (23) and (ii) the overexpression of specific membrane ABC- transporters (ATP-dependent drug efflux pumps) that actively pump drugs out of the cell before they affect cell function (24, 25).

The latter mechanism is commonly observed for drugs that disrupt microtubule function and ultimately inhibit cell division, such as vinca alkaloids and taxanes (3), often leading to multidrug resistance (MDR). Other mechanisms inducing chemoresistance to tubulin-targeting drugs include mutations in the drug-binding region of β-tubulin or alterations in actin regulations (26, 27). Current knowledge of the involvement of FGFs and FGFRs in the development of cancer cell resistance to this broad group of anticancer agents is limited to a few studies describing a correlation between FGF2/FGFR1 activity and the acquisition of insensitivity to paclitaxel (12, 28, 29), most likely through stimulation of the PI3K/AKT pathway (29). There are also reports showing that inhibition of FGFRs by chemical inhibitors (such as PD173074 or BGJ398) in cancer cells increased the cytotoxicity of paclitaxel or vincristine (30–32). Undoubtedly, the actions of FGFs/FGFRs leading to cancer cell resistance include avoidance of apoptosis, EMT, stimulation of angiogenesis, and excessive cell proliferation (10). However, despite increased research into chemoresistance, the exact mechanisms activated by FGF/FGFR complexes remain unclear.

Here, we demonstrate that overexpression of FGFR1 in U2OS cells leads to reduced cytotoxicity of paclitaxel, vincristine and taltobulin compered to U2OS cells with negligibly level of FGFR1. This effect was dependent on FGFR1 activation, as it was enhanced with additional FGF1 or FGF2 stimulation and inhibited in the presence of an FGFR inhibitor. A similar effect was observed in other FGFR1-positive cells, DMS114, the small cell lung cancer cell line. In contrast, as in U2OS cells, in HCC15, an FGFR1-negative non-small lung cancer cell line, FGF1 and FGF2 did not reduce drug toxicity. Interestingly, in HCC15 cells expressing the EGF receptor, its natural ligand, EGF, did not prevent drug-induced cytotoxicity.

U2OSR1 cells showed elevated level of MDR1 protein (multidrug resistance protein 1 or P-gp), one of the most common ABC transporters involved in multidrug resistance. Blockage of MDR1 by cyclosporine A (CsA) increased sensitivity to paclitaxel and vincristine in U2OSR1 cells to the level of U2OS cells. These data suggest that overexpression of FGFR1 may affect ABC transporter levels, which in turn leads to MDR. It has already been observed that FGF2 activity correlates with increased level of MDR1 in resistant tumors (12), but to our knowledge there have been no previous unequivocal reports that FGFRs may be involved. Only two studies to date have shown that an FGFR inhibitor reverses ABC transporter-mediated MDR and restores sensitivity to paclitaxel and vincristine (31, 33). We have also demonstrated that FGF1 partially reversed the PTX- and VCR-induced alternations in microtubules structure in U2OSR1 cells, which may confirm FGFR-induced drug efflux pumps activity and reduced drug accumulation inside the treated cells.

Surprisingly, completely different results were obtained for taltobulin, a drug that inhibits tubulin polymerase very effectively (at much lower concentrations than similar drugs (34)). Firstly, cyclosporin A did not significantly affect the sensitivity of U2OSR1 cells treated with taltobulin. This may be due to the fact that taltobulin has a low affinity for ABC transporters (35), a promising feature that has led to the use of taltobulin in clinical trials for the treatment of non-small-cell lung cancer (36). Unfortunately, the phase II clinical trial was suspended before completion, and the data from this study have not been published. It has been shown that tumors can develop resistance to taltobulin trough mutations in α- or β-tubulin and through reduced accumulation of the drug in the cell regardless of the presence of MDR1 (35, 37). In agreement with these studies, we observed no differences in TLT-induced changes in microtubule structure in FGF1-stimulated cells compared to unstimulated cells, as well as in acetylated α-tubulin levels. These data suggest that the action of the FGF1/FGFR1 axis protects U2OSR1 cells independently of drug accumulation in the cells and its effect on microtubule structure. Since one mechanism of chemoresistance is apoptosis avoidance, we investigated the effect of FGF1 on drug-dependent apoptosis in U2OSR1 cells. We observed reduced caspase 3/7 activity and PARP cleavage in the presence of FGF1 in TLT-treated cells. In addition, we confirmed that FGF1 reduces PARP cleavage in U2OSR1 cells treated with PTX and VCR in the same manner as TLT. There are two main mechanisms for the anti-apoptotic action of FGF1: (i) extracellular, through activation of the receptor and initiation of downstream signaling (7), and (ii) intracellular, while FGF1, independently of receptor activation, crosses the cell membrane and interacts with apoptosis-related proteins inside the cell (38). In the case of anticancer drug resistance, the vast majority of studies describe the first mechanism as the main cause of drug insensitivity (10). However, there are reports that FGF1 can also protect cells from the effects of cisplatin and etoposide action in a receptor activation-independent manner (39, 40). In our hands, for taltobulin, this effect was completely dependent on receptor activation, as PD173074 treatment fully inhibited the anti-apoptotic activity of FGF1.

Finally, we wanted to clarify which signaling pathway(s) is responsible for the protective effect of FGF1 in cancer cells treated with taltobulin. In the last two decades of cancer drug resistance research, it has been shown that, depending on the tumor as well as the drug, different signaling pathways activated by growth factors can be crucial for reducing the efficacy of anticancer drugs (41). Thus, for example, the MAPKs pathway is responsible for tamoxifen resistance in ER-positive breast cancer

(42), and the AKT pathway plays role in desensitizing EGFR-overexpressing lung cancer to gefitinib (43). Some studies have also indicated the involvement of more than one pathway in the resistance of cancer cells to drugs, suggesting the acquisition of molecular cross-talks between them (44). We therefore performed experiments using specific inhibitors of FGF/FGFR-activated major kinases in U2OSR1 and DMS114 cells treated with taltobulin. After inhibition of each of the three major signaling pathways (PI3K/AKT, ERK1/2 and p38), we observed no significant changes in the protective effect of FGF1. Inhibition of mTOR only partially reduced this effect, especially in DMS114 cells. As a next step, we decided to block AKT kinase directly, using API-2 inhibitor. In both U2OSR1 and DMS114 cells, direct AKT inhibition completely abolished the protective effect of FGF1.

Since only direct AKT inhibition affected FGF1 action in TLT-treated cells, while inhibition of the activator of this kinase (PI3K) did not, we next tested dual inhibition of PI3K and mTOR. PI3K phosphorylates AKT on the T308 residue, but further phosphorylation by mTOR on the S473 residue is required for full AKT activation (45). Only after treatment with a mixture of PI3K and mTOR inhibitors (LY294002 and Torin-2) or a dual inhibitor of both kinases (BEZ235) did we observe abrogation of the protective effect of FGF1 in TLT-treated U2OSR1 and DMS114 cells. Our observation is consistent with previous reports by Sathe and colleagues, who indicated that only simultaneous inhibition of PI3K and mTOR inhibits bladder cancer cell proliferation (46).

Interestingly, the mechanism of dual AKT activation in taltobulin protection is entirely dependent on FGFR1. No EGF-induced protective effect was observed in DMS114 or HCC15 cells, although this factor is well described as an activator of the PI3K/AKT pathway (47) and MDR gene expression (48). We suggest that AKT activation by FGFR-dependent pathway(s) in cancer cells exposed to anticancer drugs may be more complex and requires further research to fully understand it.

Conclusions

We demonstrate for the first time that the protection of FGFR-positive cancer cells against drugs affecting tubulin polymerization is directly dependent on the action of AKT, which is activated by two alternative pathways. Only dual inhibition of PI3K and mTOR or direct blockade of AKT completely abolishes the protective effect of FGF1 against taltobulin. Our data may have important implications for understanding the mechanisms of chemoresistance and developing new combination therapy for drug-resistant tumors.

Data availability statement

The original contributions presented in the study are included in the article/Supplementary Material. Further inquiries can be directed to the corresponding author.

Author contributions

MZ designed and supervised the project. JS, LO, and MZ designed the experiments. JS, MS, PC, and LO performed the experiments. JS, MS, PC, LO, and MZ analyzed data. JS, MS, LO, and MZ prepared the figures. JS and MZ wrote the first draft of the manuscript. All authors contributed to the article and approved the submitted version.

Funding

This work was funded by National Science Centre in Poland, grant Sonata Bis 2015/18/E/NZ3/00501. LO was supported by Sonata Bis grant 2019/34/E/NZ3/00014 from the National Science Centre, Poland.

Acknowledgments

We thank Marta Minkiewicz for skillful assistance in cell culture. We also thank Dr. Ellen M. Haugsten from the Institute for Cancer Research (Oslo University Hospital) for providing us U2OSR1-K514R cell line.

Conflict of interest

The authors declare that the research was conducted in the absence of any commercial or financial relationships that could be construed as a potential conflict of interest.

Publisher's note

Supplementary material

The Supplementary Material for this article can be found online at: https://www.frontiersin.org/articles/10.3389/fonc.2022.1011762/full#supplementary-material

References

1. Vasan N, Baselga J, Hyman DM. A view on drug resistance in cancer. *Nature* (2019) 575:299–309. doi: 10.1038/s41586-019-1730-1

2. Guo F, Zhang H, Jia Z, Cui M, Tian J. Chemoresistance and targeting of growth factors/cytokines signalling pathways: towards the development of effective therapeutic strategy for endometrial cancer. *Am J Cancer Res* (2018) 8:1317–31.

3. Jordan MA, Wilson L. Microtubules as a target for anticancer drugs. *Nat Rev Cancer* (2004) 4:253–65. doi: 10.1038/nrc1317

4. Housman G, Byler S, Heerboth S, Lapinska K, Longacre M, Snyder N, et al. Drug resistance in cancer: An overview. *Cancers (Basel)* (2014) 6:1769–92. doi: 10.3390/cancers6031769

5. Pan S-T, Li Z-L, He Z-X, Qiu J-X, Zhou S-F. Molecular mechanisms for tumour resistance to chemotherapy. *Clin Exp Pharmacol Physiol* (2016) 43:723–37. doi: 10.1111/1440-1681.12581

6. Dai Z, Huang Y, Sadee W. Growth factor signaling and resistance to cancer chemotherapy. *Curr Top Med Chem* (2004) 4:1345–54. doi: 10.2174/1568026043387746

7. Turner N, Grose R. Fibroblast growth factor signalling: From development to cancer. *Nat Rev Cancer* (2010) 10:116–29. doi: 10.1038/nrc2780

8. Ornitz DM, Itoh N. New developments in the biology of fibroblast growth factors. *WIREs Mech Dis* (2022). doi: 10.1002/wsbm.1549

9. Haugsten EM, Wiedlocha A, Olsnes S, Wesche J. Roles of fibroblast growth factor receptors in carcinogenesis. *Mol Cancer Res* (2010) 8:1439–52. doi: 10.1158/1541-7786.MCR-10-0168

10. Szymczyk J, Sluzalska KD, Materla I, Opalinski L, Otlewski J, Zakrzewska M. FGF/FGFR-dependent molecular mechanisms underlying anti-cancer drug resistance. *Cancers (Basel)* (2021) 13:5796. doi: 10.3390/cancers13225796

11. Song S, Guillaume Wientjes M, Gan Y, Au JLS. Fibroblast growth factors: An epigenetic mechanism of broad spectrum resistance to anticancer drugs. *Proc Natl Acad Sci U.S.A.* (2000) 97:8658–63. doi: 10.1073/pnas.140210697

12. Gan Y, Wientjes MG, Au JLS. Expression of basic fibroblast growth factor correlates with resistance to paclitaxel in human patient tumors. *Pharm Res* (2006) 23:1324–31. doi: 10.1007/s11095-006-0136-6

13. Kong S, Cao Y, Li X, Li Z, Xin Y, Meng Y. MiR-3116 sensitizes glioma cells to temozolomide by targeting FGFR1 and regulating the FGFR1/PI3K/AKT pathway. *J Cell Mol Med* (2020) 24:4677–86. doi: 10.1111/jcmm.15133

14. Zakrzewska M, Krowarsch D, Wiedlocha A, Otlewski J. Design of fully active FGF-1 variants with increased stability. *Protein Eng Des Sel* (2004) 17:603–11. doi: 10.1093/protein/gzh076

15. Krzyscik MA, Zakrzewska M, Sørensen V, Sokolowska-Wedzina A, Lobocki M, Swiderska KW, et al. Cytotoxic conjugates of fibroblast growth factor 2 (FGF2) with monomethyl auristatin e for effective killing of cells expressing FGF receptors. *ACS Omega* (2017) 2:3792–805. doi: 10.1021/acsomega.7b00116

16. Poźniak M, Porębska N, Krzyścik MA, Sokołowska-Wędzina A, Jastrzębski K, Sochacka M, et al. The cytotoxic conjugate of highly internalizing tetravalent antibody for targeting FGFR1-overproducing cancer cells. *Mol Med* (2021) 27:46. doi: 10.1186/s10020-021-00306-2

17. Weiss J, Sos ML, Seidel D, Peifer M, Zander T, Heuckmann JM, et al. Frequent and focal FGFR1 amplification associates with therapeutically tractable FGFR1 dependency in squamous cell lung cancer. *Sci Transl Med* (2010) 2:62ra93–3. doi: 10.1126/scitranslmed.3001451

18. Elakad O, Häupl B, Labitzky V, Yao S, Küffer S, von Hammerstein-Equord A, et al. Activation of CD44/PAK1/AKT signaling promotes resistance to FGFR1 inhibition in squamous-cell lung cancer. *NPJ Precis Oncol* (2022) 6:52. doi: 10.1038/s41698-022-00296-2

19. Lee S, Rauch J, Kolch W. Targeting MAPK signaling in cancer: Mechanisms of drug resistance and sensitivity. *Int J Mol Sci* (2020) 21:1–29. doi: 10.3390/ijms21031102

20. Brognard J, Clark AS, Ni Y, Dennis PA. Akt/pbotein kinace b is constitutively active in non-small cell lung cancer cells and promotes cellular survival and resistance to chemotherapy and radiation. *Cancer Res* (2001) 61:3986–97.

21. Clark AS, West K, Streicher S, Dennis PA. Constitutive and inducible akt activity promotes resistance to chemotherapy, trastuzumab, or tamoxifen in breast cancer cells. *Mol Cancer Ther* (2002) 1:707–17. doi: 10.1158/1535-7163.MCT-07-0434

22. Collins D, Bossenmaier B, Kollmorgen G, Niederfellner G. Acquired resistance to antibody-drug conjugates. *Cancers (Basel)* (2019) 11:394. doi: 10.3390/cancers11030394

23. Groenendijk FH, Bernards R. Drug resistance to targeted therapies: Déjà vu all over again. *Mol Oncol* (2014) 8:1067–83. doi: 10.1016/j.molonc.2014.05.004

24. Barreca M, Stathis A, Barraja P, Bertoni F. An overview on anti-tubulin agents for the treatment of lymphoma patients. *Pharmacol Ther* (2020) 211:107552. doi: 10.1016/j.pharmthera.2020.107552

25. Robey RW, Pluchino KM, Hall MD, Fojo AT, Bates SE, Gottesman MM. Revisiting the role of ABC transporters in multidrug-resistant cancer. *Nat Rev Cancer* (2018) 18:452–64. doi: 10.1038/s41568-018-0005-8

26. Hari M, Loganzo F, Annable T, Tan X, Musto S, Morilla DB, et al. Paclitaxel-resistant cells have a mutation in the paclitaxel-binding region of β-tubulin (Asp26Glu) and less stable microtubules. *Mol Cancer Ther* (2006) 5:270–8. doi: 10.1158/1535-7163.MCT-05-0190

27. Kavallaris M. Microtubules and resistance to tubulin-binding agents. *Nat Rev Cancer* (2010) 10:194–204. doi: 10.1038/nrc2803

28. Dorman SN, Baranova K, Knoll JHM, Urquhart BL, Mariani G, Carcangiu ML, et al. Genomic signatures for paclitaxel and gemcitabine resistance in breast cancer derived by machine learning. *Mol Oncol* (2016) 10:85–100. doi: 10.1016/j.molonc.2015.07.006

29. Karajannis MA, Vincent L, DiRenzo R, Shmelkov SV, Zhang F, Feldman EJ, et al. Activation of FGFR1β signaling pathway promotes survival, migration and resistance to chemotherapy in acute myeloid leukemia cells. *Leukemia* (2006) 20:979–86. doi: 10.1038/sj.leu.2404203

30. Byron SA, Loch DC, Pollock PM. Fibroblast growth factor receptor inhibition synergizes with paclitaxel and doxorubicin in endometrial cancer cells. *Int J Gynecol Cancer* (2012) 22:1517–26. doi: 10.1097/IGC.0b013e31826f6806

31. Anreddy N, Patel A, Sodani K, Kathawala RJ, Chen EP, Wurpel JND, et al. PD173074, a selective FGFR inhibitor, reverses MRP7 (ABCC10)-mediated MDR. *Acta Pharm Sin B* (2014) 4:202–7. doi: 10.1016/j.apsb.2014.02.003

32. Cha HJ, Choi JH, Park IC, Kim CH, An SK, Kim TJ, et al. Selective FGFR inhibitor BGJ398 inhibits phosphorylation of AKT and STAT3 and induces cytotoxicity in sphere-cultured ovarian cancer cells. *Int J Oncol* (2017) 50:1279–88. doi: 10.3892/ijo.2017.3913

33. Patel A, Tiwari AK, Chufan EE, Sodani K, Anreddy N, Singh S, et al. PD173074, a selective FGFR inhibitor, reverses ABCB1-mediated drug resistance in cancer cells. *Cancer Chemother Pharmacol* (2013) 72:189–99. doi: 10.1007/s00280-013-2184-z

34. Loganzo F, Discafani CM, Annable T, Beyer C, Musto S, Hari M, et al. HTI-286, a synthetic analogue of the tripeptide hemiasterlin, is a potent antimicrotubule agent that circumvents p-glycoprotein-mediated resistance. *Vitro vivo Cancer Res* (2003) 63:1838–45.

35. Loganzo F, Hari M, Annable T, Tan X, Morilla DB, Musto S, et al. Cells resistant to HTI-286 do not overexpress p-glycoprotein but have reduced drug accumulation and a point mutation in α-tubulin. *Mol Cancer Ther* (2004) 3:1319–27. doi: 10.1158/1535-7163.1319.3.10

36. Andersen RJ. Sponging off nature for new drug leads. *Biochem Pharmacol* (2017) 139:3–14. doi: 10.1016/j.bcp.2017.04.012

37. Poruchynsky MS, Kim JH, Nogales E, Annable T, Loganzo F, Greenberger LM, et al. Tumor cells resistant to a microtubule-depolymerizing hemiasterlin analogue, HTI-286, have mutations in α- or β-tubulin and increased microtubule stability. *Biochemistry* (2004) 43:13944–54. doi: 10.1021/bi049300+

38. Kostas M, Lampart A, Bober J, Wiedlocha A, Tomala J, Krowarsch D, et al. Translocation of exogenous FGF1 and FGF2 protects the cell against apoptosis independently of receptor activation. *J Mol Biol* (2018) 430:4087–101. doi: 10.1016/j.jmb.2018.08.004

39. Manousakidi S, Guillaume A, Pirou C, Bouleau S, Mignotte B, Renaud F, et al. FGF1 induces resistance to chemotherapy in ovarian granulosa tumor cells through regulation of p53 mitochondrial localization. *Oncogenesis* (2018) 7:18. doi: 10.1038/s41389-018-0033-y

40. Rodriguez-Enfedaque A, Bouleau S, Laurent M, Courtois Y, Mignotte B, Vayssière JL, et al. FGF1 nuclear translocation is required for both its neurotrophic activity and its p53-dependent apoptosis protection. *Biochim Biophys Acta - Mol Cell Res* (2009) 1793:1719–27. doi: 10.1016/j.bbamcr.2009.09.010

41. McCubrey JA, Abrams SL, Fitzgerald TL, Cocco L, Martelli AM, Montalto G, et al. Roles of signaling pathways in drug resistance, cancer initiating cells and cancer progression and metastasis. *Adv Biol Regul* (2015) 57:75–101. doi: 10.1016/j.jbior.2014.09.016

42. Turner N, Pearson A, Sharpe R, Lambros M, Geyer F, Lopez-Garcia MA, et al. FGFR1 amplification drives endocrine therapy resistance and is a therapeutic target in breast cancer. *Cancer Res* (2010) 70:2085–94. doi: 10.1158/0008-5472.CAN-09-3746

43. Zhang D, Han LL, Du F, Liu XM, Li J, Wang HH, et al. FGFR1 induces acquired resistance against gefitinib by activating AKT/mTOR pathway in NSCLC. *Onco Targets Ther* (2019) 12:9809–16. doi: 10.2147/OTT.S220462

44. Shimizu T, Tolcher AW, Papadopoulos KP, Beeram M, Rasco DW, Smith LS, et al. The clinical effect of the dual-targeting strategy involving PI3K/AKT/mTOR and RAS/MEK/ERK pathways in patients with advanced cancer. *Clin Cancer Res* (2012) 18:2316–25. doi: 10.1158/1078-0432.CCR-11-2381

45. Shariati M, Meric-Bernstam F. Targeting AKT for cancer therapy. *Expert Opin Investig Drugs* (2019) 28:977–88. doi: 10.1080/13543784.2019.1676726

46. Sathe A, Chalaud G, Oppolzer I, Wong KY, von Busch M, Schmid SC, et al. Parallel PI3K, AKT and mTOR inhibition is required to control feedback loops that limit tumor therapy. *PloS One* (2018) 13:1–18. doi: 10.1371/journal.pone.0190854

47. Roskoski R. The ErbB/HER family of protein-tyrosine kinases and cancer. *Pharmacol Res* (2014) 79:34–74. doi: 10.1016/j.phrs.2013.11.002

48. Garcia R, Franklin RA, McCubrey JA. EGF induces cell motility and multi-drug resistance gene expression in breast cancer cells. *Cell Cycle* (2006) 5:2820–6. doi: 10.4161/cc.5.23.3535

frontiers | Frontiers in Oncology

TYPE Original Research
PUBLISHED 12 October 2022
DOI 10.3389/fonc.2022.965455

OPEN ACCESS

EDITED BY
Brian Gabrielli,
The University of Queensland,
Australia

REVIEWED BY
Fabio Luis Forti,
University of São Paulo, Italy, Brazil
Lara Abramowitz,
National Institute of Diabetes and Digestive and Kidney Diseases (NIH), United States
Yousef Nami,
Agricultural Biotechnology Research Institute of Iran, Iran
Fangfang Duan,
Shenzhen Campus of Sun Yat-sen University, China
Ming Yi,
Zhejiang University, China

*CORRESPONDENCE
Dimitrios A. Skoufias
dimitrios.skoufias@ibs.fr

SPECIALTY SECTION
This article was submitted to Pharmacology of Anti-Cancer Drugs, a section of the journal Frontiers in Oncology

RECEIVED 09 June 2022
ACCEPTED 28 September 2022
PUBLISHED 12 October 2022

CITATION
Indorato R-L, DeBonis S, Garcia-Saez I and Skoufias DA (2022) Drug resistance dependent on allostery: A P-loop rigor Eg5 mutant exhibits resistance to allosteric inhibition by STLC.
Front. Oncol. 12:965455.
doi: 10.3389/fonc.2022.965455

Drug resistance dependent on allostery: A P-loop rigor Eg5 mutant exhibits resistance to allosteric inhibition by STLC

Rose-Laure Indorato, Salvatore DeBonis, Isabel Garcia-Saez and Dimitrios A. Skoufias*

Université Grenoble Alpes, CNRS, CEA, Institut de Biologie Structurale (IBS), Grenoble, France

The mitotic kinesin Eg5 has emerged as a potential anti-mitotic target for the purposes of cancer chemotherapy. Whether clinical resistance to these inhibitors can arise is unclear. We exploited HCT116 cancer cell line to select resistant clones to S-trityl-L-cysteine (STLC), an extensively studied Eg5 loop-L5 binding inhibitor. The STLC resistant clones differed in their resistance to other loop-L5 binding inhibitors but remained sensitive to the ATP class of competitive Eg5 specific inhibitors. Eg5 is still necessary for bipolar spindle formation in the resistant clones since the cells were sensitive to RNAi mediated depletion of Eg5. One clone expressing Eg5(T107N), a dominant point mutation in the P-loop of the ATP binding domain of the motor, appeared to be not only resistant but also dependent on the presence of STLC. Eg5 (T107N) expression was associated also with resistance to the clinical relevant loop-L5 Eg5 inhibitors, Arry-520 and ispinesib. Ectopic expression of the Eg5 (T107N) mutant in the absence of STLC was associated with strong non-exchangeable binding to microtubules causing them to bundle. Biochemical assays showed that in contrast to the wild type Eg5-STLC complex, the ATP binding site of the Eg5(T107N) is accessible for nucleotide exchange only when the inhibitor is present. We predict that resistance can be overcome by inhibitors that bind to other than the Eg5 loop-L5 binding site having different chemical scaffolds, and that allostery-dependent resistance to Eg5 inhibitors may also occur in cells and may have positive implications in chemotherapy since once diagnosed may be beneficial following cessation of the chemotherapeutic regimen.

KEYWORDS

mitosis, Eg5, rigor mutant, drug resistance, allostery

Introduction

Even though cancer therapy has improved significantly over the last decades, it often ultimately fails due to the development of drug resistance. The phenotypic plasticity associated with the inherent genomic instability of cancer cells serves as the primary cause of intrinsic or acquired therapy resistance and therapy failure allowing tumor relapse (1). Therefore, the discovery of new drugs and new targets in the already targeted pathways are urgently needed. To this goal, the kinesin motor protein Eg5 has been actively pursued in the last three decades for the development of inhibitors of mitosis (2) as putative alternative to anti-mitotic cancer chemotherapy based on agents targeting microtubules (3).

Eg5 is a homotetrameric kinesin motor protein arranged in two antiparallel dimers able to crosslink and slide antiparallel spindle microtubules (4), an activity which is necessary for the separation of the duplicated centrosomes in early mitosis and the formation of a bipolar spindle (5). Inhibition of Eg5 activity (6) or absence of Eg5 motor following RNAi depletion in cells (7) leads to mitotic failure with a characteristic monopolar spindle phenotype due to the inability of cells to slide antiparallel microtubules nucleated by the two unseparated centrosomes (8), forcing a cell cycle arrest in mitosis due to the activation of the mitotic spindle assembly checkpoint (9). The faith of the arrested cells appears to be cell type dependent (10, 11), but one thing is for sure, when Eg5 activity is absent or inhibited cells stop dividing normally.

Most, of the Eg5 inhibitors that entered clinical trials are allosteric in their mode of action (2). They bind to the helix α2/loop L5, and helix α3 pocket (12), which is approximately 10 Å away from the ATP binding site. Structural studies revealed that binding of a number of ligands to this pocket induces a rearrangement of loop L5, which allosterically transmits conformational changes in the ATP binding pocket, trapping the motor domain in an ATP like conformation, with ADP bound to it (13–20). As a consequence of the inhibitor binding to the α2/loop L5, and helix α3 pocket, the motor domain exhibits a low nucleotide exchange, and it can not reinitiate a new chemomechanical step. As a result, the motor activity remains inhibited as long as the inhibitor remains bound to the motor.

In the past, multiple efforts have been pursued to understand how acquired drug resistant may arise by the use of Eg5 inhibitors in cancer cells. First, the knowledge of the ligand-Eg5 motor binding pocket and extensive mutagenesis analysis in the helix α2/loop L5/helix α3 allosteric binding site of Eg5 has shown that certain amino acid substitutions can confer resistance to a variety of loop L5 inhibitors, including monastrol, S-trityl-L-cysteine (STLC), ispinesib and others (21–25). The identified amino acid substitutions in the inhibitor-binding pocket (including D130A; D130V; D133A and L214A, among others), although they do not alter appreciably the binding of monastrol or STLC to the motor domain (22), they can overcome inhibition by blocking the allosteric communication network to the ATP binding site. Furthermore, clonal selection of cells in the presence of Eg5 inhibitors such as ispinesib (26, 27), a loop L5 binding inhibitor, and BRD9647 that binds to the α4 and α6 helices (28), resulted in selection of resistant cells that express Eg5 mutants having amino acid substitutions in their respective inhibitor binding pockets. For example, the mutation D130V which is in the helix α2/loop L5/helix α3 allosteric binding site is associated with ispinesib resistance and the mutation Y104C, located in a distinct Eg5 allosteric binding site between the α4 and α6 helices associated with BRD9647 resistance.

In addition, clonal selection of cells in the presence of Eg5 inhibitors revealed another mode of resistance that was attributed to the functional plasticity of microtubule based motors substituting for loss of Eg5 function. For example, dynein and KIF15 have been shown to substitute for the loss of Eg5 function in the presence of STLC (29, 30).

In this report we used HCT116 cancer cell line to select clones that are capable of proliferating in the presence of STLC, a loop-L5 binding inhibitor of Eg5 (31). The STLC resistant clones remained sensitive to the ATP class of competitive Eg5 specific inhibitors (32) and were differentially resistant to other loop L5 binding inhibitors depending on the chemical scaffold of each inhibitor. Certain clones were not only resistant but also dependent on the presence of STLC as well as to the clinically relevant inhibitors, Arry-520 (33) and ispinesib (34–37). Dependency to STLC was associated with the expression of Eg5(T107N) mutant which when expressed in cells in the absence of the inhibitor caused strong microtubule bundling, due to a non-exchangeable association of the motor with the microtubules. Most importantly, and in contrast to the low exchange of the hydrolyzed nucleotide observed in the wild type Eg5-STLC complex, the mutant in the presence of the inhibitor retained the ability to exchange the ADP by ATP *in vitro*. We predict that resistance by dependence to allostery to Eg5 inhibitors may also occur in cells. We discuss the data in terms of their possible clinical significance.

Material and methods

Resistant colony isolation and colony formation assays

HCT116 p53+/+ cells were obtained from Dr. Vogelstein (Johns Hopkins University, Baltimore, MD) and were grown in McCoy medium supplemented with 10% FBS (Hyclone) and 1% L-glutamine and streptomycine/penicilline. For the selection purposes cells were plated in 15 cm plate and exposed to 10 μM STLC and the STLC (Novabiochem, Merck KGaA) containing medium was changed twice per week for 4 weeks.

Following ring selection, positive clones were kept under continuous presence of STLC. Colony formation assays, flow cytometry and immunofluorescence, were performed essentially as described in (38). Dimethylenastron (EgIII), EgVI and GSK-1 (EgVII) were purchased from Santa Cruz Biotechnology Inc whereas K858, Arry-520 and ispinesib were purchased from TOCRIS Bioscience. Proliferation of HCT116 cells and cell from the selected clones was assessed using an MTT colorimetric assay (Cell Proliferation Kit I, Roche) according to the manufacture's instructions. Cells were seeded at a concentration of 15,000 cells per well in 100 µl culture medium containing each inhibitor at the indicated concentration into 96 wells microplates (Falcon ref. 353072). Plates were incubated at 37°C and 5% CO2 for 72h. Plates were allowed to stand overnight in the incubator before measuring the spectrophotometrical absorbance at 570 nm and at the reference wavelength of 690 nm in a ClarioStar plate reader. The values of A570 nm–A690 nm were normalized relative to that obtained with vehicle (0.2% DMSO). Assays in the presence of STLC were carried our in 6 replicates and the assays in the presence of rest of the inhibitors were carried out in quadruplicates; data were subjected to a null hypothesis by student's t-test to compare each clone to the wild type.

RNA interference

Endogenous KIF11 expression is silenced by transient transfection with two Eg5 siRNAs (Dharmacon) targeting two 3'UTR sequences NNUGAGCCUUGUGUAUAGAUU and NNUGAGCUUAACAUAGGUAAA. Transfections were carried out in 6 wells plates with 100 nM of siRNA mixed with Oligofectamine, according the manufacturer's instructions. Following transfections of the cells, the transfection medium was replaced by fresh medium and the resistant cells were allowed to grow for two days in the presence of STLC. Naive cells in the absence of STLC were used as a control. Control and resistant cells were fixed for indirect immunofluorescence. Monopolar vs bipolar spindles were counted as described before and an unpaired samples t-test was performed to compare each clone to the untreated wild type.

Immunofluorescence microscopy

24h after the transfection, the coverslips were washed with PBS 1X, and then fixed with a solution of 2% paraformaldehyde in PBS 1X and incubated for 20 min at 37°C. After three washing steps with PBS 1X, they were permeabilized for 3 min with 0.2% triton and then washed 3 times with PBS 1X. Coverslips were placed in a humid chamber, incubated with a solution of primary antibodies: mouse monoclonal anti-tubulin clone TUB2.1 (Sigma: T4026) diluted at 1/450, human autoantibody against centromeres HCT-0100 (*Immunovision*) diluted at 1/450, mouse monoclonal anti-myc antibody (Covance, Berkeley, CA), rabbit polyclonal anti-TPX2 (Bethyl Laboratories, Motgomery, TX) diluted at 1/200 in antibody buffer (PBS 1X, sodium azide 0,02%, Tween 0,05%, and 3% (w/v) BSA) for 1 hour at 37°C. The coverslips were then washed 3 times for 5 min by immersion in PBS 1X. Coverslips were then incubated for 30 min at 37°C in a solution containing the corresponding Alexa fluo-488 and -568 conjugated goat anti-mouse, goat anti-rabbit and goat anti-human secondary antibodies (Invitrogen), diluted 1/400 in antibody buffer. Coverslips after washing 3 times in PBS 1X for 5 min, they were deposited onto a 5 µL of VECTASHIELD mounting media deposited on slides and sealed with nail polish. VECTASHIELD was used to protect samples from photobleaching and contains DAPI, a fluorescent molecule to stain DNA.

The cells are observed using Olympus microscope (IX 80), with an objective 60X equipped with a high-sensitivity camera. Excitation and emission filter wheels and signal processing were controlled by the Volocity software.

Purification and amplification of RNA from the resistant cells

Total RNA was isolated by using Trizol (Invitrogen) and the Nucleospin Kit® RNA II (Macherey-Nagel) according to the manufacturer's protocol, and KIF11 cDNA from the different clones was amplified by using Superscript™ One-Step RT-PCR RT/Platinum® *Taq* (Invitrogen), using the following primers Eg5_372 forward 5'-GTGGTGAGATGCAGACCATTTA-3' and Eg5_1228 reverse 5'-GGTGTTCTTTCTACAAGGGCAG-3' and then sequenced. Site-directed mutagenesis was performed by the use of Phusion® High-Fidelity DNA Polymerase (New England Biolabs) with pcDNA Myc-Eg5 as template (Blangy et al) and the following primers: T107N forward 5'-CACTATCTTTGCGTATGGCCAAAATGGCACTGGAAA-3'; T107N reverse 5'-TTTCCAGTGCCATTTTGGCCATACGCA AAGATAGTG-3'. All resulting plasmids were sequence verified.

Construction of pGFP-C1-Eg5 WT and mutants

The resulting 3729 bp fragment, following EcoRI digestion of the RcCMV-Eg5 vector (generous gift of Anne Blangy, CRBM Montpellier France), was ligated to the EcoRI linearized pGFP-C1 vector. The correct orientation of the insert was verified by HindIII digestion and the presence of a 2800bp fragment, in the case of the correct orientation, as opposed to the 1000bp fragment in the opposite orientation. The selected plasmids were further verified for the correct orientation by sequencing. The pGFPC1-Eg5(WT) vector was used for *in vitro* mutagenesis

to introduce the related mutations using the primers used above. All resulting plasmids were sequence verified.

Fluorescence recovery after photobleaching

48h after transfection, cells grown on glass coverslips were inverted with the cell face down in 2-well Labtek chambers and the medium was changed with DMEM/F-12 supplemented with 10% fetal bovine. Cells were then imaged in the M4D Cellular Imaging platform of IBS with a spinning disk confocal microscope (Olympus and Andor) configurated with a Nipkow wheel (Yogokawa CSU-X1) and 6 solid-state lasers for confocal imaging in real time. FRAP was achieved through the use of the photoconversion/photoactivation module. Areas of 1.5 μm^2 area were bleached from at least six cells for each population were photobleached and analyzed and their fluorescence recovery was monitored and images were acquired with an EMCCD camera (Andor iXon ultra). Analysis of the intensity traces were carried out using the easyFRAP software (39) and corrected for photobleaching and normalized with pre-bleaching intensity.

Bacterial expression vectors

A STOP codon was introduced to the pET28-Eg5 using a forward 5'CCTGAAGTGAATCAGAAATGAACCAAAA AAGCTTTGATTAAGG-3' and a reverse 5'-CCTTAATCAAA GCTTTTTTGGTTCATTTCTGATTCACTTCAGG-3' primers. Following sequence verification, the NcoI-HindIII insert of the pET28 Eg5 $_{(1\text{-}368)}$ was ligated into the pETM11 NcoI-HindIII linearized vector. The pETM11 $Eg5_{(1\text{-}368)}$ was then *in vitro* mutagenized by PCR using Phusion DNA Polymerase using the same primers as above. All resulting plasmids were sequence verified.

Purification of pET11 Eg5 $_{(1\text{-}368)}$ WT and mutants of Eg5 motor domain

BL21(DE3) cells carrying the pETM11 Eg5 $_{(1\text{-}368)}$ WT and mutant Eg5 were induced for expression with IPTG (0.5mM) overnight at 18°C. Bacterial pellets were resuspended in cold Lysis Buffer (50mM Tris pH 6.8, 250mM KCl, 2mM $MgCl_2$, 20mM imidazole) supplemented with 1⁄2 tablet of a mixture of protein inhibitors (Complete EDTA-free, Roche Applied Science), 2.5mg of lysozyme and 100µM phenylmethylsulfonyl fluoride (PMSF). Cells were lysed by sonication with 10 cycles of 30s of pulse and 60s of turn off at 50% amplitude in ice. Lysates were incubated with 1mM of DNAse and 10mM of $MgCl_2$ during 30 min at 4°C to digest the DNA, centrifuged at 4°C for 30 min at 15000 rpm and the supernatants were collected and filtered (diameter of the filter = 0.2um) before being loaded onto a HisTrap HP 5mL column (GE Healthcare), equilibrated (using an AKTA design FPLC system) with buffer A (50mM Tris at pH 6.8, 250mM KCl, 20mM imidazole and 2mM $MgCl_2$). The column was washed with 20 column volumes with buffer A. Finally, a gradient elution was performed over ten column volumes of buffer B (50mM Tris pH 6.8, 250mM KCl, 500mM imidazole, 2mM $MgCl_2$) and 1.5mL fractions were collected. Based on the chromatogram fractions the interesting fractions were selected and run on 10% SDS-PAGE electrophoresis. Fractions containing the Eg5 motor domain were pooled together and then digested with 6-His-TEV protease, previously purified in the laboratory (1mg TEV/20 mg of substrate). Digestion was carried out for 1 hr at room temperature and then the protein solution was dialyzed overnight with 1L of Dialysis Buffer (50mM Pipes, pH7.3,50 mMNaCl), using a 10kDa MW cut-off dialysis membrane. TEV cleavage was confirmed by SDS-PAGE electrophoresis and the uncleaved motor as well as the His-TEV was removed by a second purification on HisTrap HP 5mL column. The cleaved motor was recovered from the HisTrap unbound fraction and was concentrated using spin concentrators (10kDa MW cut-off; Millipore). Protein samples were concentrated and frozen in small aliquots in liquid nitrogen and kept frozen at -80°C. Protein concentration was determined using the Bradford reagent at Abs_{595} using BSA as a protein standard.

Mant-ADP release assay par fluorescence

Bacterially expressed and then isolated motor domain of Eg5 (WT) and Eg5(T107N) (1.5µM final) were injected in the cell compartment of the fluorimeter Bio-Logic MOS 250 that contained Mant-ADP (10µM final) and FRET was detected by measuring fluorescence emission at 395nm after excitation at 285nm. STLC (25µM final) was injected into the cell and Mant-ADP was chased with excess ATP (1mM final). Alternatively, Eg5(WT) and Eg5(T107N) motor domains (1.9um final) were incubated with Mant-ADP (10µM final) and STLC (18µM final) in 10mM $MgCl_2$, 6% DMSO (control) and the loss of FRET following addition of excess ATP (1.2mM final) was measured in black 384-well plates (Greiner ref. 781076, Greiner Bio-One) on a Clariostar plate reader (BMG Labtech) using a 285nm filter excitation at 285nm filter and 395nm emission filter and a LP565 dichroic mirror.

Basal and microtubule stimulated ATPase assays

The enzymatic activity of kinesin Eg5 were carried out using the pyruvate kinase (PK)-lactate dehydrogenase (LDH) coupled

assay in buffer A25 (40, 41). Experiments were performed in ATPase buffer A25 (25mM ACES/KOH (pH 6.9), 2mM magnesium acetate, 2mM potassium EGTA (SIGMA) (pH 8), 0.1mM potassium EDTA (SIGMA) (pH 8) and 1mM β-Mercaptoethanol) supplemented with 2mM PEP (SIGMA), 0.25mM NADH (SIGMA), 17.4 g/mL LDH (SIGMA) and 34ug/mL PK (SIGMA). Motor, microtubules, and ATP concentrations used were optimized. Kinetics were monitored in a TECAN-SUNRISE photometer using a 96-well plate (Greiner) by measuring the loss of NADH at OD_{340}. K_{cat} rates were determined from the change in OD_{340} per second after steady state has been reached, typically after a few minutes. All experiments were performed in triplicate at room temperature. Data were analysed using GraphPad Prism 7.

Results

Isolation of STLC-resistant cell lines

To determine whether human cancer cells can develop resistance to Eg5 inhibitors, we treated HCT116 cells with a cytotoxic concentration of STLC, a selective Eg5 inhibitor (31). HCT116 cells offer the advantage since they are defective in their DNA mismatch repair pathway that are hypermutagenic (42) and they might contain larger numbers of variants for selection under the conditions of our selection. In addition, HCT116 cells have no detectable P-glycoprotein (43), reducing the possibility of resistance due to induction of drug pumps. When $\sim 5 \times 10^6$ cells were continuously exposed for 4 weeks at 10 μM STLC, colonies appeared from which following ring selection, we generated 5 cell lines, designated R1 through R5. Detection of spindle formation in the STLC-resistant clones by indirect immunofluorescence microscopy revealed that indeed the cells were capable of forming bipolar spindles in the continuous presence of the Eg5 inhibitor and cells in various mitotic phases, notably anaphases, were present (Figure 1A). Cells from the selected clones were then subjected in proliferation assays for 72h and the ratio of number of cells in the presence of STLC over the number of cells in the absence of the inhibitor was determined from each clone (Figure 1B). The calculated ratio from the unselected, naive wild-type HCT166 cells was as expected lower than one (0,38 ± 0,008) since cells stopped to proliferate due to a mitotic block imposed by the spindle assembly checkpoint. However, the ratios for the cells of clones R1 and R2 were significantly higher compared to the wild-type and were close to one- or very close to one-, indicating that the presence of the inhibitor did not interfere with cell proliferation. Interestingly, the ratios for the cells from clones R3, R4 and R5 were significantly higher than one, indicating that in the absence of the inhibitor the cells of each of the clones do not proliferate. The low proliferation of the cells from clones R3, R4 and R5 in the absence of STLC coincides with the inability of the cells to form bipolar spindles in the absence of the inhibitor (Figure 1A). The monopolar spindles in the cells of clones R3, R4 and R5 in culture media without STLC resemble the monopolar spindles of cells treated with Eg5 inhibitors. In accordance with the above observations, ~1000 starting cells from the five clones, readily formed colonies at 10uM STLC after 14 days, whereas the naive unselected cells were potently inhibited; cells from clones R3, R4 and R5, were also not capable of growing in the absence of STLC (Figure 1C).

Eg5 presence is required for bipolar spindle formation in the STLC resistant cells

We then asked the question whether or not the formation of bipolar spindles in the STLC-resistant cells was still dependent on the presence of Eg5. We therefore treated the resistant cells with siRNA targeting Eg5 expression. Phenotypic analysis, by monitoring spindle assembly in the siRNA treated cells in the continuous presence of the STLC, revealed that the cells depleted of Eg5 were not capable of forming bipolar spindles as in all clones more than 90% of the spindles were monopolar, as they were in the depleted naive and untreated cells (Figure 2). Therefore, the data suggested that in the STLC-resistant cells the presence of Eg5 is necessary for the formation of spindles even in the presence of the inhibitor.

Differential resistance to Eg5 inhibitors of STLC-resistant clones

Since STLC belongs to the loop L5 binding class of Eg5 inhibitors, we tested if the STLC-resistant cell lines are also resistant to other loop L5 inhibitors with different chemical scaffolds such as K858 (44) and dimethylenastron (DME) (45), and to non-loop L5 inhibitors (ATP competitive inhibitors) EgVI and GSK-1 (32). Cells from the unselected wild type and the five selected STLC HCT116 resistant clones were analyzed in the presence and in the absence of each of the inhibitor in proliferation assays (Figure 3A) and the phenotype of the treated cells were analyzed by immuno-fluorescense microscopy (Figure 3B; Figure S1A). Following 72h exposure of the cells in the presence of the different Eg5 inhibitors, cells from all resistant clones were capable of proliferating in the presence of STLC, K858 and DME in contrast to the control whereas all cells were sensitive to the ATP competitive Eg5 inhibitors EgVI and GSK1. Microscopic analysis of the spindle phenotype of the treated cells revealed that for clones R1 and R2 the majority of the spindles were bipolar whereas in cells of clones R3, R4, and R5 were monopolar in the presence of the K858 and DME (Figure 3B; Figure S1A). All cells, however, were sensitive to the Eg5 ATP competitive inhibitors EgVI and GSK-1

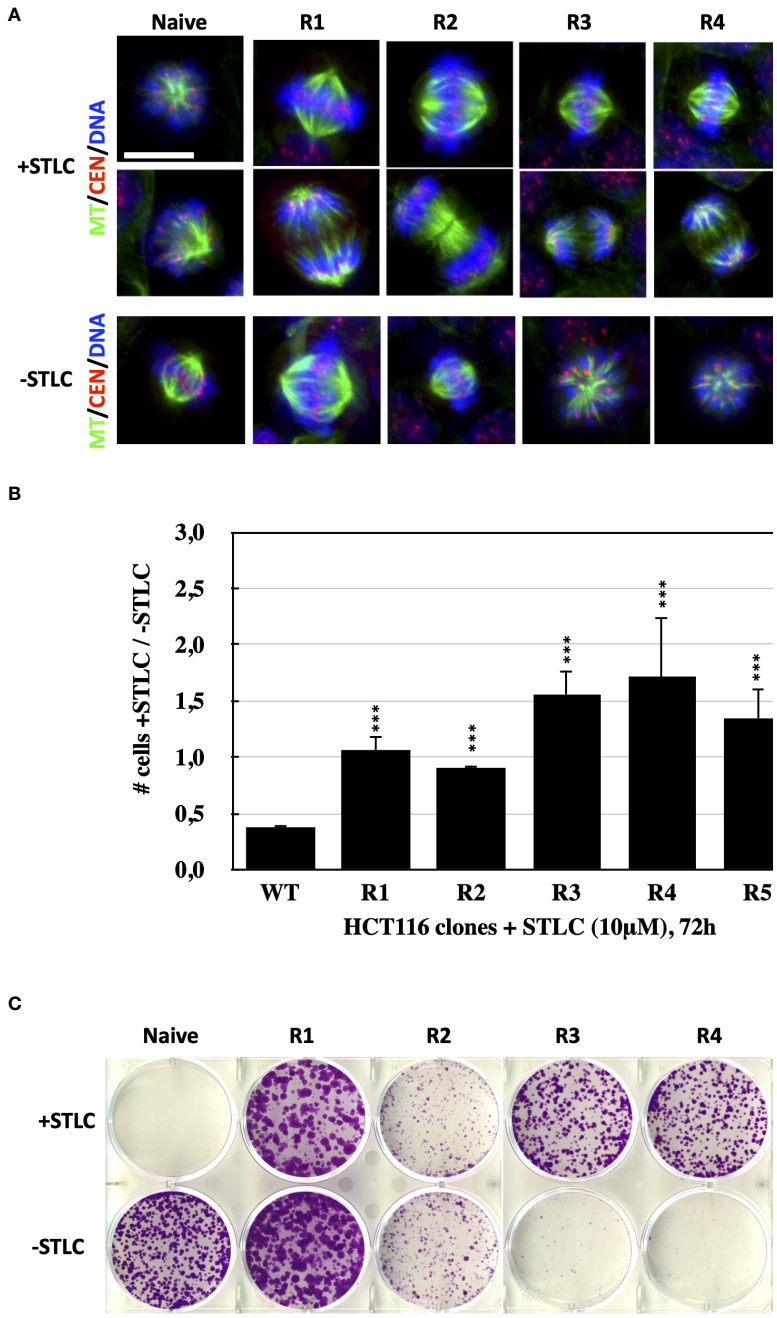

FIGURE 1
Bipolar spindle formation and proliferation of STLC-resistant cancer cells in the presence of STLC. **(A)** Immunofluorescence microscopy images of mitotic cells from naive and selected STLC resistant cells in the presence STLC 10 µM (upper two rows) and in the absence of STLC (lower row of images). Spindle microtubules were detected with an anti-tubulin antibody (green); centromeres with an auto-immune antibody (red) and chromatin with DAPI (blue). In contrast to the unselected naive cells, all resistant clones appeared to have normal bipolar spindles and were capable of proceeding to anaphase. STLC resistant clones R3, R4 and R5 in the absence of STLC had monopolar spindles. **(B)** Proliferations assays with the selected clones in the presence and in the absence of STLC. Ratio of the number of cells in the presence of STLC divided by the number of cells in the absence of inhibitor for unselected HCT116 cells and cells from the STLC resistant clones R1, R2, R3, R4 and R5, after 72h. Asterisks indicate significance values; *** $p < 0{,}0001$. **(C)** Crystal violet-stained colonies of parental HCT116 cells and drug-resistant lines (resistant clones R1, R2, R3, R4 and R5) after 14 days of exposure to STLC (upper panel) and following wash-out of the STLC (lower panel).

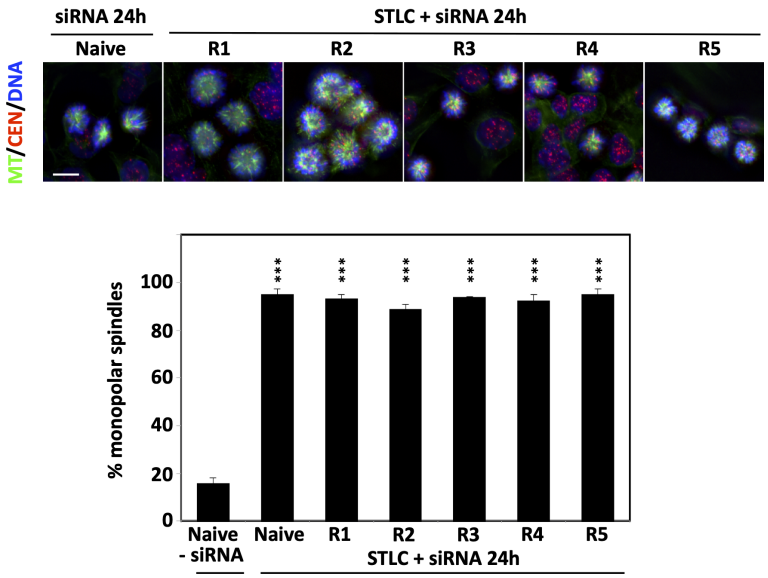

FIGURE 2
STLC resistant clones require the presence of Eg5 for growth in the presence of STLC. Immunofluorescence microscopy images of mitotic cells from unselected naive HCT116 cells and selected HCT116 STLC-resistant cells that were subjected to Eg5 siRNA mediated depletion of Eg5. Spindle microtubules were detected with an anti-tubulin antibody (green), centromeres with an auto-immune antibody (red) and chromatin with DAPI (blue). Scale bar in the images corresponds to 10 µm. The % of monopolar spindles following RNAi mediated Eg5 depletion in the presence of STLC was calculated for each the cell lines. Asterisks indicate significance values; *** p < 0,0001.

(Figures 3A, B). We have also assessed the ability of the resistant clones their ability to form cell colonies by carrying out long term colony formation assays in the presence of the inhibitors (Figure S1B). In accordance to the 72h proliferation assays and mitotic spindle formation capability of the resistant cells, 21 days exposure of cells in the different Eg5 inhibitors showed in contrast to the wild type cells, cells from clones R1 and R2 were capable of colony formation and cells from clones R3, R4 and R5 to a limited extend. However, all cells were not able to form colonies in the presence of the ATP competitive Eg5 inhibitors EgVI and GSK1. The results suggest that all STLC resistant clones are sensitive to ATP competitive inhibitors and there is a variable resistance to the other loop L5 binding inhibitors, such as K858 and DME.

Failure in mitosis in the absence of STLC in the STLC resistant and dependent cells

The cell cycle profile of the three cell clones that appeared to be STLC resistant and dependent were analyzed by flow cytometry and the ability of the cells to form bipolar spindles in a STLC concentration dependent manner. Cells from clones R3, R4, and R5 had a normal cell cycle profile in the presence of 10 µM STLC after 72h comparable to the naive untreated cells. However, in the absence of STLC as early as 24h after washing out the inhibitor, cells were enriched in G2/M (Figure 4A).

The enrichment of cells in G2/M in the R3, R4, R5 HCT116-clones in the absence of STLC was correlated with the presence of aberrant monopolar spindles (Figure 4B). There was an inverse correlation between the presence of bipolar spindles and decreasing concentrations of the inhibitor. In the absence and submicromolar concentrations of STLC the majority of the spindles were monopolar whereas at 5 and 10µM STLC more than 50% of the spindles were bipolar. The presence of bipolar spindles in the presence of the STLC offers an explanation why the cells continue to proliferate in the presence of the inhibitor and the lack of bipolar spindles in the absence of the inhibitor explain the dependency of the cells on the inhibitor.

Identification of Eg5 Mutations in the STLC resistant and dependent cells

We then asked whether the drug-resistance in drug-dependent cell lines might be due to mutations in Kif11, the gene coding for Eg5 motor protein. Sequencing Kif11 cDNAs from the drug-resistant clones revealed that all 3 STLC-dependent lines carried point mutations in Kif11, yielding 2 amino acid substitutions, namely cells in clone R4 expressed Eg5 (A103V) and clones R3 and R5 expressed Eg5(T107N) (Figure 4C). Therefore, we focused our attention to the Eg5 (T107N) STLC resistant and dependent cell line since the

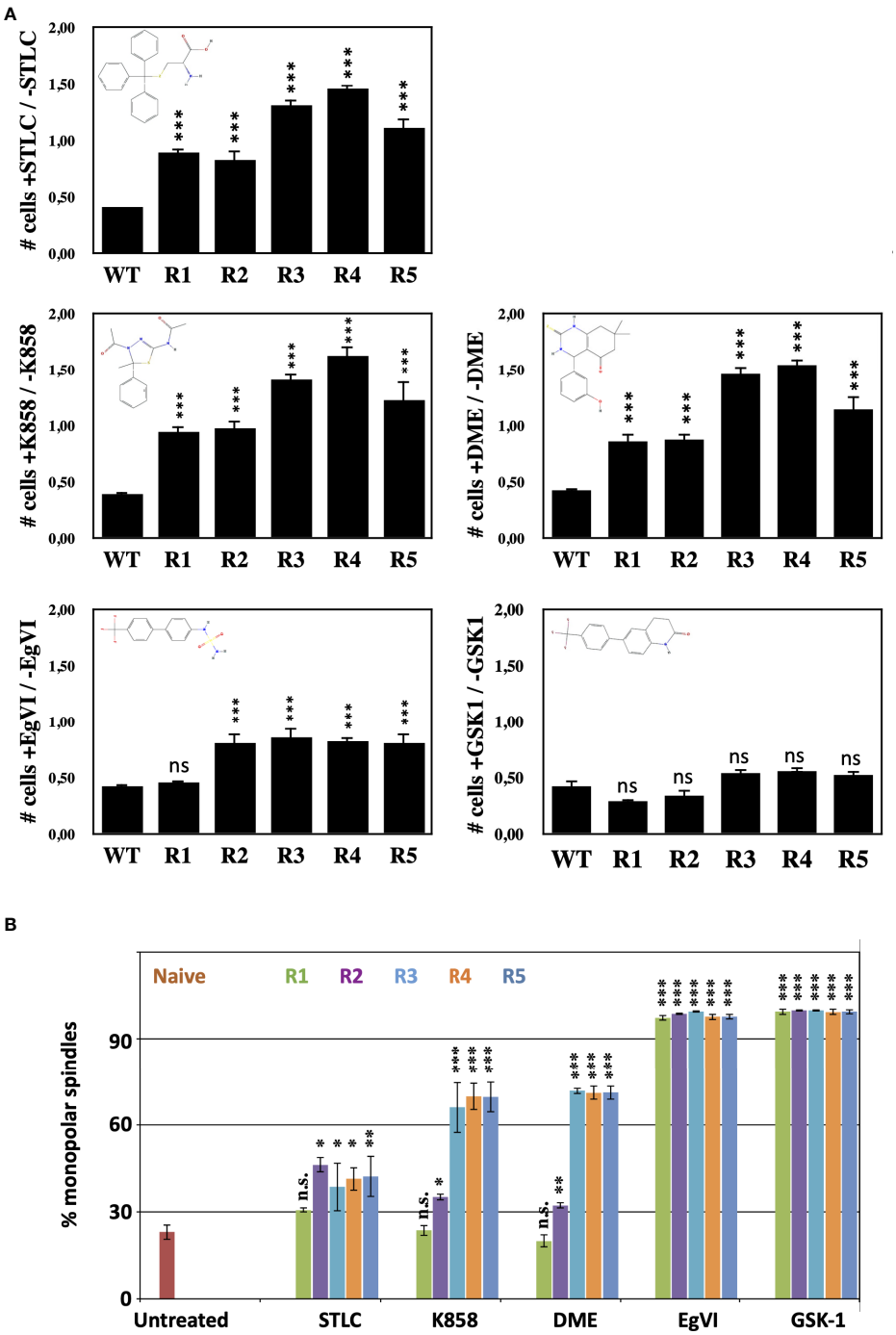

FIGURE 3
STLC resistant clones exhibit variable resitance to other Eg5 inhibitors **(A)** Proliferations assays with the selected clones in the presence and in the absence of STLC. Ratio of the number of cells in the presence of STLC (10μM) or K858 (7.5μM) or DME (5μM) or EgVI (5μM) or GSK-1 (0.5μM) divided by the number of cells in the absence of inhibitor for unselected HCT116 cells and cells from the STLC resistant clones R1, R2, R3, R4 and R5, after 72h. **(B)** The % of monopolar spindles in the presence of the different Eg5 inhibitors was calculated for each the cell lines from immunofluorescence microscopy images of mitotic cells (Supplementary Figure S1). Asterisks indicate significance values; ns – non-significant; * $p < 0,01$, ** $p < 0,001$, *** $p < 0,0001$.

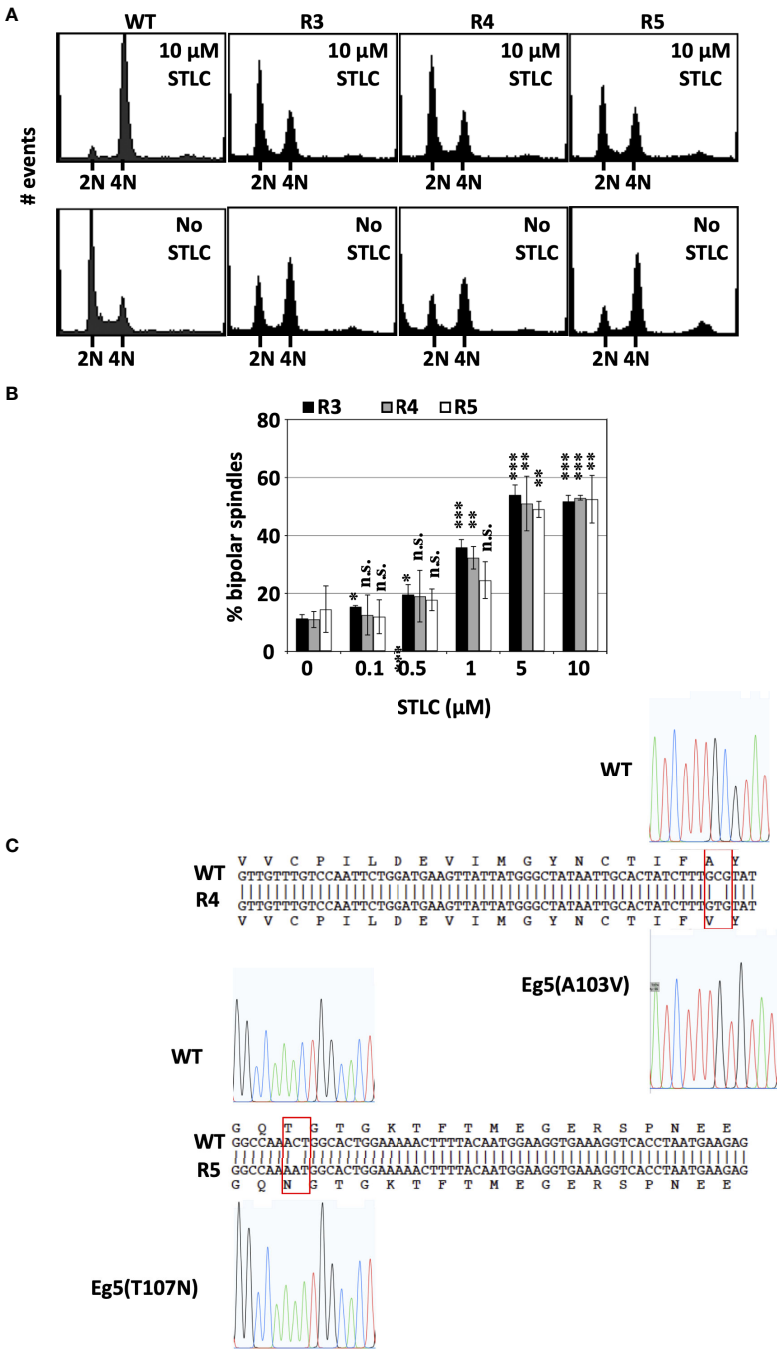

FIGURE 4
STLC resistance and dependence is linked to expression of mutant Eg5 **(A)** Cell-cycle profiles of unselected wild type HCT116 cells and STLC-resistant and -dependent clones, R3, R4 and R5 exposed to STLC (10 µM) (upper panels) and 24h following wash-out of STLC (lower panels). **(B)** The % of bipolar spindles in cell lines R3, R4 and R5 increase with increasing STLC concentration. Asterisks indicate significance values; ns – non-significant; * $p < 0,01$, **± $p < 0,001$, *** $p< 0,0001$. **(C)** DNA sequences of Eg5 (KIF11) cDNAs in WT and STLC-resistant and -dependent clones, R4 and R5 and the identified corresponding missense mutations. Clone R3 expressed the same T107N mutant Eg5 as the one identified in clone R5.

mutation A103V was identified independently in a previous study (46) and was not further pursued.

Resistance and dependence to clinical relevant Eg5 inhibitors

Due to the interesting STLC-resistance and at the same time STLC-dependent phenotype of the Eg5(T107N) expressing cells, we tested if they were also resistant and dependent to the clinical relevant Eg5 inhibitors, Arry-520 (47) and ispinesib (48), two inhibitors that entered clinical phase II clinical trials. The Eg5 (T107N) expressing cells of HCT116 clone R5 were able to proliferate (Figure 5A) and in long term colony formation assay to form colonies (Figure 5B) in contrast to the naive HCT116 cells that they were not able to neither proliferate nor form colonies in the presence of either Arry-520 or ispinesib. In agreement with the colony formation data, flow cytometric

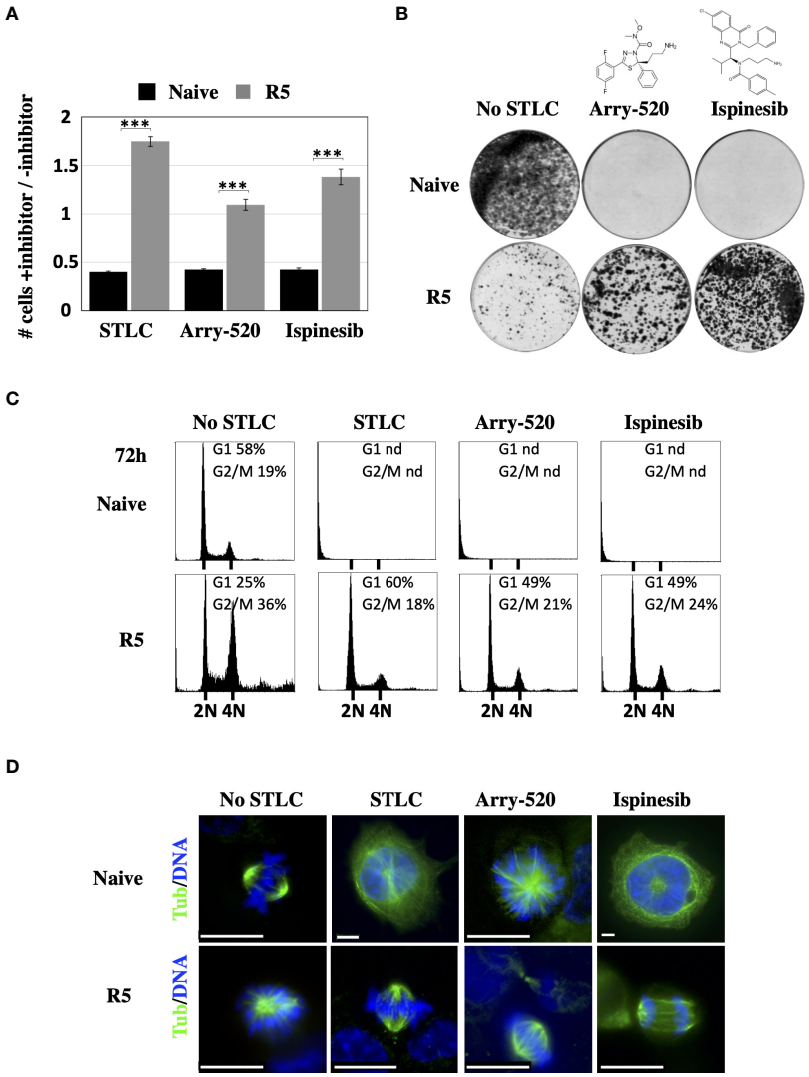

FIGURE 5
Response of the Eg5(T107) expressing cells to Arry-520 and ispinesib **(A)** Proliferation of STLC resistant and dependent cells in the presence and in the absence of STLC (10μM) or Arry-520 (10nM) or ispinesib (10nM). Ratio of the number of cells in the presence of STLC (10μM) or Arry-520 (10nM) or ispinesib (10nM) divided by the number of cells in the absence of the inhibitor for unselected HCT116 cells and cells from the STLC resistant clone R5, after 72h. Asterisks indicate significance values *** $p < 0,0001$;**(B)** Crystal violet-stained colonies of parental HCT116 cells and STLC-resistant and resistant clone R5 cells after 14 days exposed to either media or Eg5 inhibitors, Arry-520 (10nM) and ispinesib (10nM). **(C)** Cell-cycle progression of STLC-resistant and -dependent clone R5 exposed to STLC, Arry-520 and ispinesib for 72h. **(D)** Immunofluorescence microscopy images of mitotic cells from naive wild type (WT) and STLC -resistant and -dependent cell line clone R5, in the absence and in the presence of STLC, Arry-520 and ispinesib. Microtubules were detected with an anti-tubulin antibody (green) and chromatin with DAPI (blue). Scale bar in the images corresponds to 10 μm.

analysis of the treated cells after 72h showed normal cell cycle profiles in the presence of either Arry-520 or ispinesib as they did in the presence of STLC, whereas naive cells exposed to the either of the three inhibitors were absent since they could not proliferate (Figure 5C). Indirect immunofluorescence analysis of the treated cells also showed that the Eg5(T107N) expressing cells exhibited normal bipolar spindles and/or normal anaphase spindles in the presence of either of the three inhibitors whereas the naive cells after 72h were in either in interphase with an aberrant large nucleus, prominent centrosome, nucleated microtubules and/or monopolar spindles (Figure 5D).

Ectopic expression of Eg5(T107N) mutant restores bipolar spindle formation in the presence of STLC

To test whether the Eg5(T107N) mutant is sufficient to cause drug resistance, we ectopically expressed as Myc-tagged either the wild type Eg5(WT) or the mutant Eg5(T107N) in U2-OS cells (Figure 6A). The Myc-Eg5(WT) either in the absence or the presence of STLC appeared to be diffused in the cytoplasm and in mitotic cells there was some decoration of the spindle particularly in the spindle poles (Figure 6A upper panels). Strikingly, the Myc-tagged Eg5(T107N) in the absence of STLC appeared to exhibit a strong microtubule bundling activity in interphase cells; in mitotic cells there were also bundled microtubules and no bipolar spindles were present (Figure 6A; lower left panels). In marked contrast, in the STLC treated cells, expression of Myc-Eg5(T107N) in interphase showed no microtubule bundles and in mitotic cells the spindles were bipolar (Figure 6A; lower right panels). The obtained data offer an explanation why the cells in STLC dependent and resistant clone R5 are capable of proliferating in the presence of STLC and not in the absence of STLC.

Similar strong microtubule bundling after expression of Eg5 (T107N) has been previously reported in cells expressing two other Eg5 mutants, Eg5(G268V) (49) and Eg5(T112N) (50). The microtubule bundling activity of Eg5(G268V) was previously attributed to the fact that since the mutation is in the switch II ATP binding domain it drives the motor to be at its rigor state and therefore leading the four motor domains of the Eg5 tetramer to bind tightly to the microtubules in a non-exchangeable manner and forcing the microtubules to bundle. Since the Thr107 amino acid is located in the P-loop of the ATP binding site we tested if the mutant T107N, like the G268V, drives the motor to bind in a non-exchangeable manner to microtubules. First we constructed GFP-Eg5(WT) and GFP-Eg5 (T107N) mammalian expression vectors and determined if the GFP chimeras behave the same as the Myc-tagged Eg5. Similar to Myc-tagged constructs the GFP-Eg5(WT) was distributed in a diffuse manner in the cytoplasm of interphase cells and the GFP-Eg5(T107N) induce strong interphase bundles (Figure 6B).

Then, the dynamics of the microtubule binding properties of the GFP-Eg5(T107N) were compared with those of GFP-Eg5 (WT) by FRAP analysis in living U2-OS cells. In GFP-Eg5(WT) expressing cells, where the distribution of GFP-Eg5 appears as diffused in the cytoplasm similar to endogenous Eg5, following bleaching in the region of interest (ROI), the fluorescent signal gradually increased during the recovery phase (25s) because of the inflow of unbleached GFP-Eg5 into the bleached area (Figure 7A). In contrast to the WT, the GFP-Eg5(T107N) decorated strongly microtubule bundles in the cytoplasm of interphase cells (Figure 7A). The GFP-Eg5(T107N) exhibited almost no recovery (mobility fraction = 0,06) in the bleached ROI confirming the strong almost irreversible binding of the rigor mutant of Eg5 to microtubules at the time scale of the observation (Figures 7B, C). Therefore, the FRAP data suggest that the microtubule binding and bundling observed in GFP-Eg5 (T107N) expressing cells in the absence of the inhibitor is probably due to higher microtubule affinity properties of the mutant Eg5 compared to the control.

In vitro Activity of Eg5(T107N) mutant

Previous studies have suggested that Eg5 inhibitors can be divided into two classes, the loop-L5 type of inhibitors that actually promote weak binding of the motor to microtubules (15, 31, 51, 52), and the rigor-like inhibitors that are ATP competitive inhibitors and induce Eg5 strong microtubule-binding state (32, 53, 54). Furthermore, the loop L5 binding inhibitors are able to allosterically inhibit the exchange of the bound ADP with ATP and therefore the ATPase activity of the motor is inhibited and the motor cannot efficiently engage with the microtubules. The ternary Eg5-ADP-STLC complex might be able to bind MTs in a low-friction mode without productive ATP hydrolysis and coupled conformational changes. The mutant Eg5(T107N) behaves like a motor that is in rigor state and that in the presence of the STLC the motor is able to complete the chemomechanical step. In order to test the ability of the motor domain to bind and exchange the nucleotide in the ATP binding pocket in the absence and in the presence of STLC we determined the ability of the motor domain to bind a fluorescent analogue of ATP, Mant-ADP (55). Addition of the wild type motor domain in a Mant-ADP containing solution leads to an exchange of the motor bound ADP with Mant-ADP and with a resulting increase in fluorescence (excited at 285 nm) due to FRET from the tryptophan and tyrosine of Eg5 (Figure 8A, left panel). However, when the Eg5(T107N) motor domain was added to Mant-ADP there was no increase in FRET detected unless STLC was added (Figure 7A, right panel). Bound Mant-ATP could be then chased out by excess amount of ATP in both the wild type and the mutant. The data show that in the absence of microtubules the nucleotide pocket of Eg5(T107N) is in a state that cannot be accessed by a free nucleotide unless

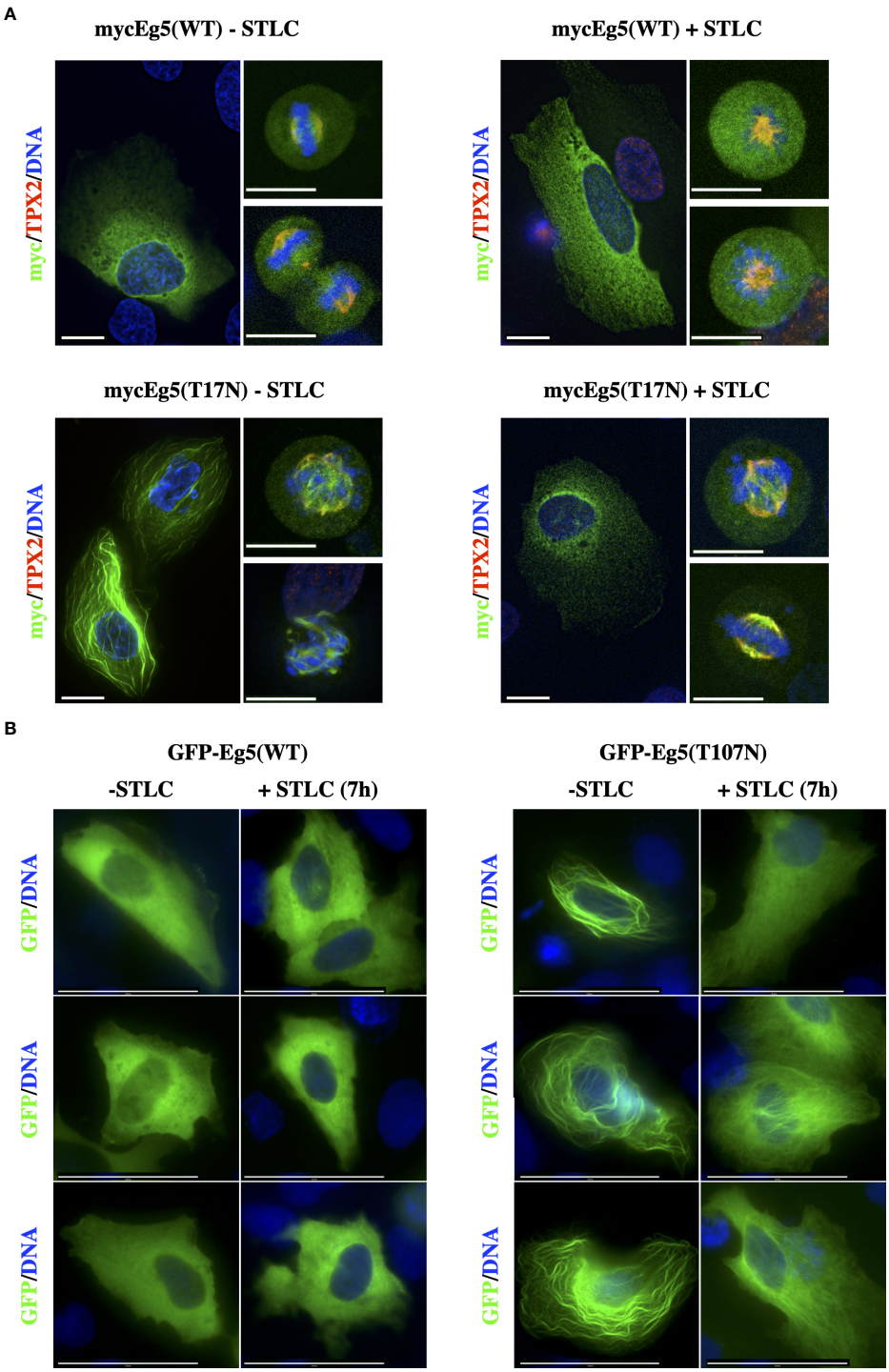

FIGURE 6
STLC resistant Eg5(T107N) variant binds and bundles microtubules in the absence of STLC. **(A)** Myc-tagged Eg5(WT) and -Eg5(T107N) were transfected for expression in U-2OS cells. Immunofluorescence microscopy images of cells untreated or in the presence of STLC (10μM) 24h post transfection fixed and stained; Eg5 was detected by an anti-myc (green) and mitotic spindle microtubules were detected by an anti-TPX2 (red) and chromatin by DAPI (blue). **(B)** GFP-tagged Eg5(WT) and -Eg5(T107N) were transfected for expression in U-2OS cells for 24h and fixed and stained for indirect immunofluorescence microscopy. Scale bar corresponds to 10 μm.

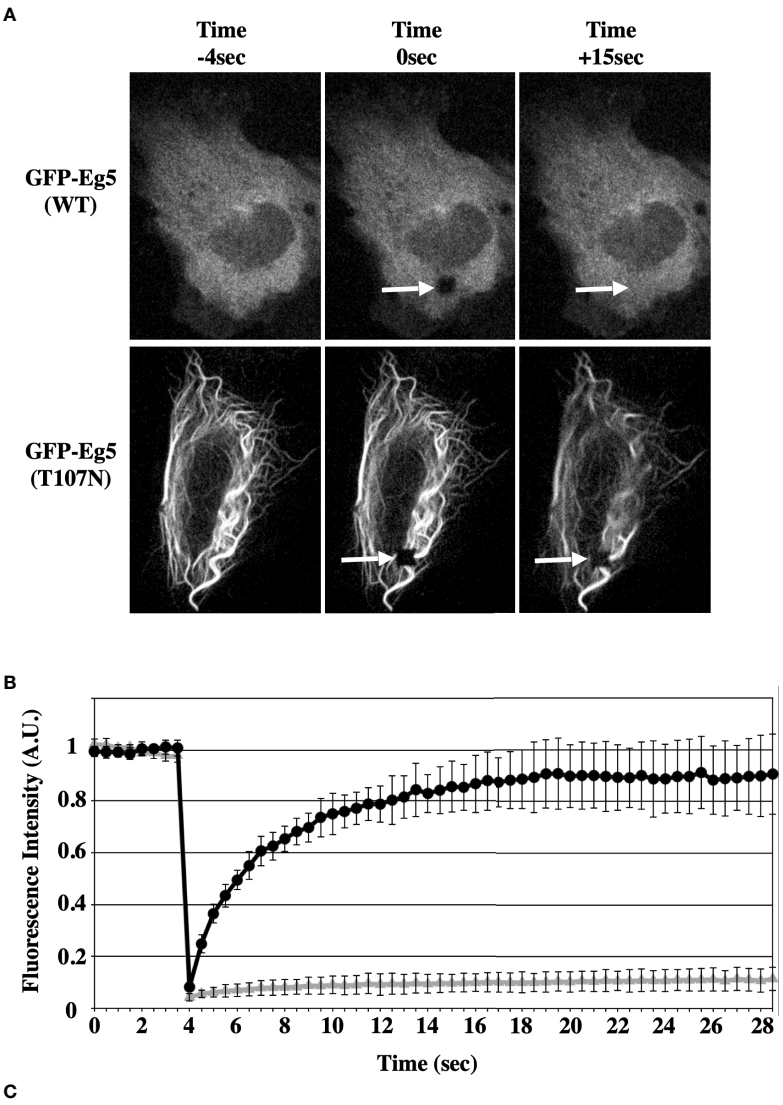

C

GFP-Eg5	$t_{1/2}$ (sec)	mob Fract	R square
WT	2,44	0,88	0,99
T107N	4,5	0,06	0,97

FIGURE 7
STLC resistant Eg5(T107N) variant binds microtubules in a non-reversible manner in the absence of STLC. **(A)** GFP-tagged Eg5(WT) and -Eg5 (T107N) were transfected for expression in U-2OS cells. Time lapse video microscopy images 48h following transfection before (-4 sec), immediately after FRAP (0 sec) and after FRAP (15 sec) are shown. Arrows indicate the site of the photobleaching. **(B)** Recovery of the fluorescence intensity after FRAP. **(C)** The measured mobile fraction and the half time represent the ability of GFP-Eg5 to actually replace the photobleached in cytoplasm of living cell during interphase.

there is some allosteric conformations that are transmitted to the nucleotide binding pocket following binding of STLC to the loop L5. Binding of the inhibitor opens the nucleotide binding pocket allowing the entry of the nucleotide.

We then asked if in the continuous presence of STLC bound to the motor domain the bound Mant-ADP can be chased out by cold ATP. As expected for the wild type, in the presence of STLC there was no nucleotide exchange whereas the Mant-ATP was

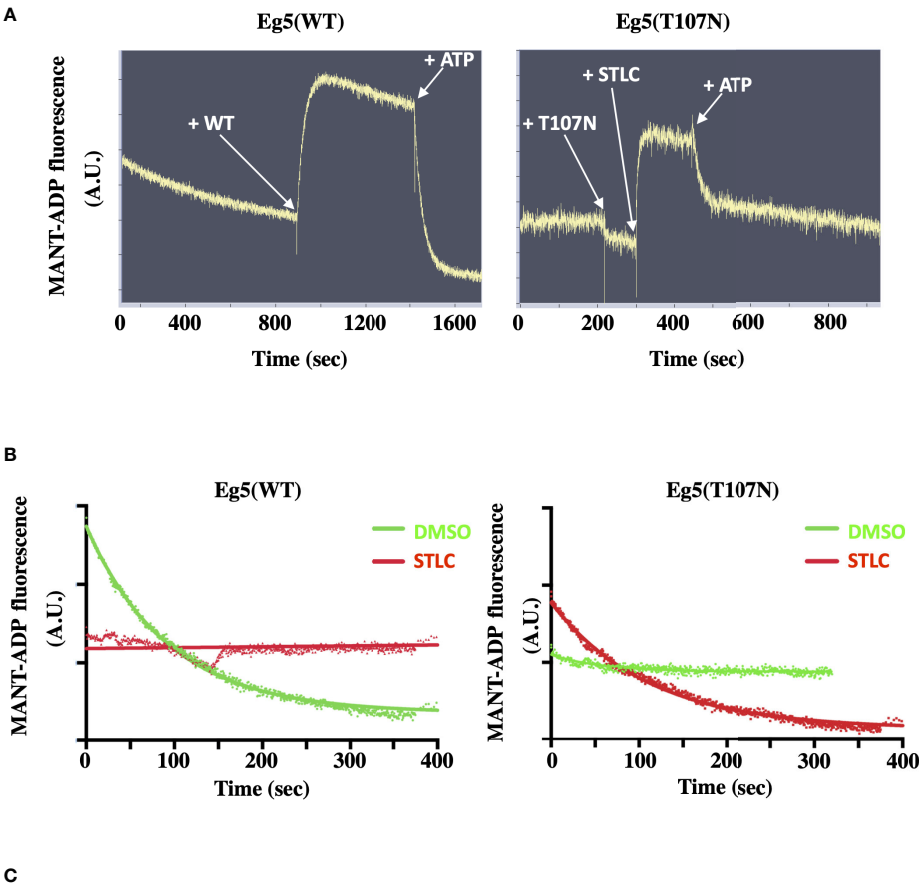

C

	Basal ATPase	MT stimulated ATPase	MT stimulated ATPase +STLC
	$K_{cat}(s^{-1})$	$K_{cat}(s^{-1})$	IC_{50} (μM)
Wild type	0,086 ± 0,0026	6,18±0,38	0,34
T107N	0,1355 ± 0,0045	1,48±0,07	0,9163

FIGURE 8
STLC dependent binding of ATP in the nucleotide pocket of Eg5(T107N) motor domain. **(A)** FRET of Mant-ADP is detected upon addition of the Eg5(WT) motor domain and is lost after been chased by the addition of cold ATP. In contrast, FRET of Mant-ADP is not detected upon addition of the Eg5(T107N) domain unless STLC is added. **(B)** Nucleotide exchange in the Eg5-STLC complex. Once STLC is bound to the Eg5(WT) pre-incubated with Mant-ADP the nucleotide is not exchangeable. Pre-incubation with DMSO allows the chase of Mant-ADP by ATP. In contrast, there is an exchange of the nucleotide in the Eg5(T107N)-STLC complex but not in the in the absence of STLC (DMSO control). **(C)** Kinetic parameters of the basal ATPAse activity of Eg5(WT) and Eg5(T107N) and the microtubule stimulated ATPase in the presence or the absence of STLC.

readily exchanged if the motor was pre-incubated with DMSO instead of STLC (Figure 8B left panel). However, in the case of the Eg5(T107N) motor domain pre-incubated with Mant-ADP in the presence or absence of STLC the Mant-ADP could be chased out by ATP only when STLC was present (Figure 8A right panel). The results suggest that in the Eg5(T107N), in contrast to the wild type-STLC complex, binding of STLC to loop-L5 permits the exchange of the bound ADP by ATP. Therefore, the next question we addressed was whether the mutant Eg5(T107N) can hydrolyze ATP in the presence of STLC.

The motor domain of the wild type Eg5, like all other kinesin motor proteins, is known to possess a basal ATPase activity (56) which is greatly stimulated in the presence of microtubules. We therefore measured the microtubule stimulated ATPase activity of wild type and that of Eg5(T107N) motor domains *in vitro 5* (Figures 2SA, B). The mutant displayed similar a k_{cat}value for basal ATPase activity (0,63fold increase) compared to the wild

type Eg5 (Figure 8C). Furthermore, there was only a 10.9x increase in k_{cat}value for the MT stimulated ATPase activity compared to the 71.8fold increase for the wild type. Although both wild type and mutant showed a dose response loss of activity in the presence of increasing concentrations of STLC, there was a 2,7fold increase in the IC_{50} for the mutant compared to the wild type (Figure 8C; Figures S2C, D). Therefore, the lower sensitivity (higher IC_{50}) of the mutant to STLC, coupled with the ability of the mutant to exchange the nucleotide only in the presence of the inhibitor in contrast to the wild type, offers a likely explanation why the mutant Eg5 motor is still active in cells in the presence of STLC.

Discussion

Eg5 is a valid target for the development of novel generation of specific anti-mitotic targets as cancer chemotherapeutic agents with less secondary effects compared to those linked to microtubule targeting agents (57). One hindering caveat of selective inhibitors to a given target is the emergence of subclones of tumour cells, preexisting or not, having mutations in the target, rendering the target resistant (58) (59). Previous data from our group and others have shown that indeed certain mutations in the helix α2/loop L5/helix α3 allosteric binding site of Eg5 can confer resistance to loop L5 inhibitors (26, 28, 38, 60).

In this report following the selection of HCT116 cells in the presence of the Eg5 inhibitor STLC, we have isolated five STLC resistant clones, arbitrarily named as R1, R2, R3, R4, and R5, that proliferate in the presence of the inhibitor at concentrations that block cellular growth due to an imposed mitotic block. Interestingly, three of the identified resistant clones were also STLC-dependent, the cells could not proliferate in the absence of STLC. The failure of cell proliferation of the STLC -resistant and -dependent cells was attributed to that the cells in the absence of STLC could not build bipolar spindles and therefore remained blocked in mitosis with the characteristic monopolar spindles, a phenotype widely observed when the Eg5 activity is missing either due to enzymatic inhibition or absence due to depletion by RNAi. Therefore, the STLC-resistance and dependency on Eg5 could most likely be attributed to the intrinsic properties of the Eg5 motor expressed in the cells.

Sequencing of the Eg5 cDNAs isolated from the three STLC-resistant and -dependent clones, raised in this report, identified two amino acid substitutions at positions, A103V and T107N that could be possible candidates for the observed resistance. The failure to detect Eg5 mutations in the two other clones may be related to the fact that the primers used for RT-PCR amplification covered only the part of the motor domain that included the helix α2/loop L5/helix α3 allosteric binding site of Eg5 open reading frame and not all the motor domain of Eg5. An additional contributing factor might be the functional plasticity of mitotic kinesins substituting for loss of Eg5 function (29, 30, 49).

In the absence of STLC, expression of the Eg5(T107N) mutant in cells led to strong microtubule cross linking in interphase and mitotic cells leading to mitotic failure. However, in the presence of STLC the mutant Eg5 had a diffused intracellular distribution resembling that of the wild type protein. FRAP assays in STLC devoid Eg5(T107N) expressing cells showed that the mutant protein is bound to microtubules in a non-exchangeable manner suggesting that the mutant motor is bound most likely in its rigor state. Since Eg5 is a tetramer, composed of two antiparallel dimers (4), the rigor state of the mutant would most definitely lead to a tight crosslinking of microtubules. Previous screening for resistance to STLC have led to the identification of Eg5(G268V) as being also responsible for the observed STLC resistance (49). The Eg5 residue G268 is located in the switch II nucleotide binding area and like the T107N mutant, the G268V traps the motor in a microtubule binding state leading to a strong microtubule crosslinking. Therefore, both mutants convert Eg5 from a motile force generator to a static microtubule crosslinker. Interestingly both resistant clones, G268V and T107N, appear to be dependent on the presence of the motor since the cells of both clones depleted of the Eg5 by siRNA do not proliferate. In the case of Eg5(G268V) expressing cells, acquired resistance was linked to the functional plasticity of mitotic kinesins, like KIF15, substituting for loss of Eg5 wild type function. KIF15 is a dimeric kinesin and through its two N-terminal motors and two C-terminal nonmotor MT-binding sites, is able to crosslink and slide MTs (61). In the G268V resistant clone, the mitotic kinesin KIF15, which is normally restricted to kinetochore-MTs because of its preferential binding to MT bundles, in the presence of Eg5 (G268V) induced crosslinking, changes its distribution and is enriched in the rest of spindle microtubules contributing to the formation of normal bipolar spindle (49). However, in the case of Eg5(T107N) expressing cells, microtubule crosslinking is present only in cells that are devoid of STLC. Therefore, the Eg5(T107N) acquired resistance appears not to be dependent on the plasticity of mitotic kinesins substituting for loss of Eg5 function. It appears to be due to intrinsic enzymatic properties of the mutant motor. Support for the need of Eg5 activity in the STLC-resistant and dependent cells is the fact that the resistant cells remain sensitive to Eg5 inhibition mediated by Eg5 inhibitors that are known to bind to a different binding site other than the helix α2/loop L5/helix α3 allosteric binding site and cause the inhibited motor domain to bind to microtubules.

The enzymatic data showed that the change of an invariant threonine (T) in the nucleotide-binding GQTGTGKT motif or P-loop of Eg5 by asparagine (N) is linked to cellular resistance to STLC, a loop L5 binding inhibitor. The presented nucleotide exchange data using Mant-ADP showed that nucleotide entry in the Eg5(T107N) is absolutely dependent on the binding of STLC

in the inhibitor binding site, α2/loop5/α3 allosteric pocket, which is approximately 10 Å away from the ATP-binding site. In Eg5, P-loop Thr107 is involved in the positioning of the γ-phosphoryl oxygen of ATP (62). Furthermore, according to the two-water mechanism of hydrolysis of ATP by Eg5 (62), during the chemomechanical step there is an opening of the nucleotide pocket allowing the release of P_i, which is coupled with the reorientation of the side chain of Thr107 allowing its binding to Glu270, as observed in the Eg5(WT)-ADP structure. The substitution of Thr107 with an amino acid with bulkier side chain, like Asn, may make the binding of the ATP less favorable and the reorientation of the P-loop impossible. However, the allosteric conformational changes imposed by the binding of STLC may open the nucleotide pocket and allow the entry of ATP leading to its hydrolysis and completing the necessary chemomechanical reaction leading to stepping of the motor.

It has been proposed that homotetrameric Eg5 crosslinks antiparallel MTs in spindles the same way as myosin crosslinks actin filaments in thick filaments (63). In both cases independent myosin or Eg5 motor heads can exert forces causing actin or microtubule filament sliding, respectively. In the presence of the Eg5(T107N), and in the absence of the inhibitor all the motor heads of the tetramer remain bound to the microtubules in a rigor state. The rigor state of the motor then is the cause of the observed strong microtubule bundling in the Eg5(T107N) expressing cells. In the presence of the inhibitor and because of the allosteric modifications transmitted into the nucleotide binding pocket of the motor domain, new ATP can enter in the nucleotide pocket releasing the motors from the microtubules, microtubules bundles are resolved and a new chemomechanical step of the four motor domains of the Eg5 tetramer can be initiated. However, how would Eg5(T107N) exert its motility functions in the presence of the inhibitor?. Firstly, because of the lower sensitivity of the mutant (2,7x higher IC_{50} for STLC compared to the wild type) even if only a few motor heads can complete ATP hydrolysis in the presence of STLC there will be enough to exert force-generating events necessary for directional microtubule sliding. Secondly, in addition to the ATP-consuming directional motion, Eg5 exhibits also a diffusive component not requiring ATP hydrolysis (64). This diffusional mode was also reported in the presence of Eg5 inhibitor monastrol (65), the prototype of the loop-L5 binding class of inhibitors (6) and it can also occur at physiological ionic strength (64). In the presence of the STLC that binds to the loop-L5 binding site as monastrol, following the exchange of the nucleotide in the Eg5(T107N) and the release from microtubules, the mutant motor can exhibit a diffusive mode of motility and in combination with its directional mode of motility, the tetrameric Eg5(T107N)-STLC complex will possess crosslinking and motile activity enough to contribute to the formation of a bipolar spindle. Therefore, the allosteric modifications that follow STLC binding are needed for the observed resistance to STLC in the Eg5(T107N) expressing cells.

The resistance dependent on the presence of the bound allosteric inhibitor reported here is an additional manifestation of resistance by allostery (66). Previous studies have shown that residue A133 is necessary for transmitting a perturbation pathway through the protein to the nucleotide-binding site when binding the inhibitor; when mutated to D133 the allosteric transmissions provoked by SB743921, another loop-L5 class of Eg5 binding inhibitors, are blocked conferring thus resistance. In the case of the Eg5(T107N) mutant, the perturbations that follow the binding of the inhibitor not only allow but they appear to be necessary for the exchange of the nucleotide in the ATP binding pocket, a step that is necessary for the completion of the ATP hydrolysis cycle and stepping of the motor (67).

It is interesting to also note that the STLC dependent cells remain sensitive to the class of inhibitors that are considered as ATP competitive and bind to a different site other than the STLC binding site. Furthermore, the resistance of the Eg5(T107N) cells appear not to be limited to STLC because the cells remain relatively insensitive to other loop L5 inhibitors that have entered clinical trails such as Arry-520 and ispinesib. However, the resistance and dependency it is not universal for all loop-L5 inhibitors since K858 and DME appear to inhibit growth in the STLC resistant and dependent cells. It is interesting to note that although DME has a different chemical scaffold compared to STLC or Arry-520 or ispinesib, K858 is a smaller, pre-optimised version of Arry-520 that lacks the key substituents necessary for potent inhibition. The results are consistent with our recent observation that subtle differences in ligand binding and flexibility in both compound and protein may alter allosteric transmission from the loop L5 site that do not necessarily result in reduced inhibitory activity in mutated Eg5 structures. Thus, it appears that resistance to Eg5 inhibition may be chemical scaffold dependent and suggest that a chemotherapeutic combination therapy employing different inhibitors targeting the same target may limit acquired resistance. More recently it was shown that cells expressing either Eg5(D130A) or Eg5 (L214A) are resistant to STLC and to Arry-520, a phase II clinical candidate. In contrast, the Eg5(L214A) expressing cells were sensitive to ispinesib an inhibitor that share the same binding site as STLC and Arry-520 (20). The data allow us to predict that resistance and dependence by allostery to Eg5 inhibitors may also occur in cells and once it is diagnosed it may be beneficial since cessation of the chemotherapeutic regimen may be beneficial to the patients because drug dependent tumor cells will cease to proliferate. The data also suggest that combining allosteric and orthosteric Eg5 inhibitors like the ATP competitive type of Eg5 inhibitors may be a good strategy to circumvent drug resistance.

The presented data bring attention to how different inhibitors to the same target could provoke different responses to treatment (due to their different biochemical structure) and mode of action, and how, in the case of Eg5 kinesin, a mutation

in the motor ATP binding site could possibly make the difference. Within the context of personalized and precision medicine, the data also point out the need of carefully considering that missense mutations in specific hotspots on the target may impair the function of some drugs but possibly not all of them. Therefore, our work highlights not only the importance of detecting mutations responsible for intrinsic resistance before even the beginning of the targeted therapy, but also the requirement to follow, through biopsy, the response to treatment in order to detect mutations that would confer an acquired resistance.

Data availability statement

The original contributions presented in the study are included in the article/Supplementary Materials. Further inquiries can be directed to the corresponding author.

Author contributions

R-LI carried out cell based assays and contributed in the construction and use of cDNAs. SD carried protein isolation and enzymatic characterization of the isolated motor proteins. IG-S contributed to the structural interpretation and analysis of the data. DS designed, supervised, and participated in the collection of the data, carried out microscopy and FRAP experiments and carried out analysis and interpretation of the entire presented data. All authors contributed to the article and approved the submitted version.

Funding

This work used the platforms of the Grenoble Instruct-ERIC Center (ISBG: UMS 3518 CNRS-CEA-UGA-EMBL) with support from FRISBI (ANR-10-INSB-05-02) and GRAL (ANR-10-LABX-49-01) within the Grenoble Partnership for Structural Biology (PSB). Part of this work was supported by La Ligue Contre Le Cancer Comité du Rhône.

Acknowledgments

This work used the platforms of the Grenoble Instruct-ERIC Center (ISBG: UMS 3518 CNRS-CEA-UGA-EMBL) with support from FRISBI (ANR-10-INSB-05-02) and GRAL (ANR-10-LABX-49-01) within the Grenoble Partnership for Structural Biology (PSB). We are indebted to Dr JP Kleman with his help on collecting the FRAP data. Part of this work was supported by La Ligue Contre Le Cancer Comité du Rhône (to DS).

Conflict of interest

The authors declare that the research was conducted in the absence of any commercial or financial relationships that could be construed as a potential conflict of interest.

Publisher's note

Supplementary material

The Supplementary Material for this article can be found online at: https://www.frontiersin.org/articles/10.3389/fonc.2022.965455/full#supplementary-material

SUPPLEMENTARY FIGURE 1
(A) Immunofluorescence microscopy images of mitotic cells from unselected naive HCT116 cells and selected HCT116 STLC-resistant cells that were exposed to Eg5 inhibitors, STLC (10μM) K858 (7.5μM), DME (5μM) EgVI (5μM) and GSK-1 (0.5μM) for 18h. Microtubules were detected with an anti-tubulin antibody (green) and chromatin with DAPI (blue). Scale bar in the images corresponds to 10 μm. **(B)** Crystal violet-stained colonies of parental HCT116 cells and STLC-resistant lines (resistant clones R1, R2, R3, R4 and R5) after 14 days exposed to either media or Eg5 inhibitors, STLC (10μM) K858 (7.5μM), DMEI (5μM) EgVI (5μM) and GSK-1 (0.5μM).

SUPPLEMENTARY FIGURE 2
(A) Basal ATPase activity of Eg5(WT) and Eg5(T107N) **(B)** Determination of the optimal microtubule concentration for screening the inhibition of the microtubule-stimulated Eg5 ATPase activity. **(C)** Inhibition of microtubule activated Eg5 ATPase activity of WT-Eg5 (red) and Eg5(T107N) motor domain by STLC.

References

1. Acar A, Nichol D, Fernandez-Mateos J, GD C, Barozzi I, SP H, et al. Exploiting evolutionary steering to induce collateral drug sensitivity in cancer. *Nat Commun* (2020) 11:1923. doi: 10.1038/s41467-020-15596-z

2. Garcia-Saez I, Skoufias DA. Eg5 targeting agents: From new anti-mitotic based inhibitor discovery to cancer therapy and resistance. *Biochem Pharmacol* (2021) 184:114364. doi: 10.1016/j.bcp.2020.114364

3. Dumontet C, Jordan MA. Microtubule-binding agents: a dynamic field of cancer therapeutics. *Nat Rev Drug Discovery* (2010) 9:790–803. doi: 10.1038/nrd3253

4. Scholey JE, Nithianantham S, Scholey JM, Al-Bassam J. Structural basis for the assembly of the mitotic motor kinesin-5 into bipolar tetramers. *Elife* (2014) 3: e02217. doi: 10.7554/eLife.02217

5. Mann BJ, Wadsworth P. Kinesin-5 regulation and function in mitosis. *Trends Cell Biol* (2019) 29:66–79. doi: 10.1016/j.tcb.2018.08.004

6. Kapoor TM, Mayer TU, Coughlin ML, Mitchison TJ. Probing spindle assembly mechanisms with monastrol, a small molecule inhibitor of the mitotic kinesin, Eg5. *J Cell Biol* (2000) 150:975–88. doi: 10.1083/jcb.150.5.975

7. Weil D, Garçon L, Harper M, Duménil D, Dautry F, Kress M. Targeting the kinesin Eg5 to monitor siRNA transfection in mammalian cells. *BioTechniques* (2002) 33:1244–8. doi: 10.2144/02336st01

8. Ferenz NP, Gable A, Wadsworth P. Mitotic functions of kinesin-5. *Semin Cell Dev Biol* (2010) 21:255–9. doi: 10.1016/j.semcdb.2010.01.019

9. Musacchio A. The molecular biology of spindle assembly checkpoint signaling dynamics. *Curr Biol* (2015) 25:R1002–1018. doi: 10.1016/j.cub.2015.08.051

10. Shi J, Orth JD, Mitchison T. Cell type variation in responses to antimitotic drugs that target microtubules and kinesin-5. *Cancer Res* (2008) 68:3269–76. doi: 10.1158/0008-5472.CAN-07-6699

11. Gascoigne KE, Taylor SS. Cancer cells display profound intra- and interline variation following prolonged exposure to antimitotic drugs. *Cancer Cell* (2008) 14:111–22. doi: 10.1016/j.ccr.2008.07.002

12. Yan Y, Sardana V, Xu B, Homnick C, Halczenko W, Buser CA, et al. Inhibition of a mitotic motor protein: where, how, and conformational consequences. *J Mol Biol* (2004) 335:547–54. doi: 10.1016/j.jmb.2003.10.074

13. Maliga Z, Xing J, Cheung H, Juszczak LJ, Friedman JM. Rosenfeld SS. a pathway of structural changes produced by monastrol binding to Eg5. *J Biol Chem* (2006) 281:7977–82. doi: 10.1074/jbc.M511955200

14. Garcia-Saez I, DeBonis S, Lopez R, Trucco F, Rousseau B, Thuéry P, et al. Structure of human Eg5 in complex with a new monastrol-based inhibitor bound in the r configuration. *J Biol Chem* (2007) 282:9740–7. doi: 10.1074/jbc.M608883200

15. Kaan HYK, Ulaganathan V, Hackney DD, Kozielski F. An allosteric transition trapped in an intermediate state of a new kinesin-inhibitor complex. *Biochem J* (2009) 425:55–60. doi: 10.1042/BJ20091207

16. Kaan HYK, Major J, Tkocz K, Kozielski F, Rosenfeld SS. "Snapshots" of ispinesib-induced conformational changes in the mitotic kinesin Eg5. *J Biol Chem* (2013) 288:18588–98. doi: 10.1074/jbc.M113.462648

17. Cox CD, Coleman PJ, Breslin MJ, Whitman DB, Garbaccio RM, Fraley ME, et al. Kinesin spindle protein (KSP) inhibitors. 9. discovery of (2S)-4-(2,5-difluorophenyl)-n-[(3R,4S)-3-fluoro-1-methylpiperidin-4-yl]-2-(hydroxymethyl)-N-methyl-2-phenyl-2,5-dihydro-1H-pyrrole-1-carboxamide (MK-0731) for the treatment of taxane-refractory cancer. *J Med Chem* (2008) 51:4239–52. doi: 10.1021/jm800386y

18. Talapatra SK, Schüttelkopf AW, Kozielski F. The structure of the ternary Eg5-ADP-ispinesib complex. *Acta Crystallogr D Biol Crystallogr* (2012) 68:1311–9. doi: 10.1107/S0907444912027965

19. Talapatra SK, Tham CL, Guglielmi P, Cirilli R, Chandrasekaran B, Karpoormath R, et al. Crystal structure of the Eg5 - K858 complex and implications for structure-based design of thiadiazole-containing inhibitors. *Eur J Med Chem* (2018) 156:641–51. doi: 10.1016/j.ejmech.2018.07.006

20. Indorato R-L, Talapatra SK, Lin F, Haider S, Mackay SP, Kozielski F, et al. Is the fate of clinical candidate arry-520 already sealed? predicting resistance in Eg5-inhibitor complexes. *Mol Cancer Ther* (2019) 18:2394–406. doi: 10.1158/1535-7163.MCT-19-0154

21. Maliga Z, Mitchison TJ. Small-molecule and mutational analysis of allosteric Eg5 inhibition by monastrol. *BMC Chem Biol* (2006) 6:2. doi: 10.1186/1472-6769-6-2

22. Brier S, Lemaire D, DeBonis S, Forest E, Kozielski F. Molecular dissection of the inhibitor binding pocket of mitotic kinesin Eg5 reveals mutants that confer resistance to antimitotic agents. *J Mol Biol* (2006) 360:360–76. doi: 10.1016/j.jmb.2006.04.062

23. Kim ED, Buckley R, Learman S, Richard J, Parke C, Worthylake DK, et al. Allosteric drug discrimination is coupled to mechanochemical changes in the kinesin-5 motor core. *J Biol Chem* (2010) 285:18650–61. doi: 10.1074/jbc.M109.092072

24. Sheth PR, Basso A, Duca JS, Lesburg CA, Ogas P, Gray K, et al. Thermodynamics of nucleotide and inhibitor binding to wild-type and ispinesib-resistant forms of human kinesin spindle protein. *Biochemistry* (2009) 48:11045–55. doi: 10.1021/bi900946r

25. Marshall CG, Torrent M, Williams O, Hamilton KA, Buser CA. Characterization of inhibitor binding to human kinesin spindle protein by site-directed mutagenesis. *Arch Biochem Biophys* (2009) 484:1–7. doi: 10.1016/j.abb.2009.01.015

26. Jackson JR, Auger KR, Gilmartin AG, Eng WK, Luo LS, Concha N, et al. A resistance mechanism for the KSP inhibitor ispinesib implicates point mutations in the compound binding sit. *Clin Cancer Res* (2005) 11(24):9150S–9151S.

27. Kasap C, Elemento O, Kapoor TM. DrugTargetSeqR: a genomics- and CRISPR-Cas9-based method to analyze drug targets. *Nat Chem Biol* (2014) 10:626–8. doi: 10.1038/nchembio.1551

28. Chattopadhyay S, Stewart AL, Mukherjee S, Huang C, Hartwell KA, Miller PG, et al. Niche-based screening in multiple myeloma identifies a kinesin-5 inhibitor with improved selectivity over hematopoietic progenitors. *Cell Rep* (2015) 10(5):755-70. doi: 10.1016/j.celrep.2015.01.017

29. Tanenbaum ME, Macůrek L, Galjart N, Medema RH. Dynein, Lis1 and CLIP-170 counteract Eg5-dependent centrosome separation during bipolar spindle assembly. *EMBO J* (2008) 27:3235–45. doi: 10.1038/emboj.2008.242

30. Tanenbaum ME, Macůrek L, Janssen A, Geers EF, Alvarez-Fernández M, Medema RH. Kif15 cooperates with eg5 to promote bipolar spindle assembly. *Curr Biol* (2009) 19:1703–11. doi: 10.1016/j.cub.2009.08.027

31. Skoufias DA, DeBonis S, Saoudi Y, Lebeau L, Crevel I, Cross R, et al. S-trityl-L-cysteine is a reversible, tight binding inhibitor of the human kinesin Eg5 that specifically blocks mitotic progression. *J Biol Chem* (2006) 281:17559–69. doi: 10.1074/jbc.M511735200

32. Luo L, Parrish CA, Nevins N, McNulty DE, Chaudhari AM, Carson JD, et al. ATP-competitive inhibitors of the mitotic kinesin KSP that function *via* an allosteric mechanism. *Nat Chem Biol* (2007) 3:722–6. doi: 10.1038/nchembio.2007.34

33. Algarín EM, Hernández-García S, Garayoa M, Ocio EM. Filanesib for the treatment of multiple myeloma. *Expert Opin Investig Drugs* (2020) 29:5–14. doi: 10.1080/13543784.2020.1703179

34. Beer TM, Goldman B, Synold TW, Ryan CW, Vasist LS, Van Veldhuizen PJ, et al. Southwest oncology group phase II study of ispinesib in androgen-independent prostate cancer previously treated with taxanes. *Clin Genitourin Cancer* (2008) 6:103–9. doi: 10.3816/CGC.2008.n.016

35. Knox JJ, Gill S, Synold TW, Biagi JJ, Major P, Feld R, et al. A phase II and pharmacokinetic study of SB-715992, in patients with metastatic hepatocellular carcinoma: a study of the national cancer institute of Canada clinical trials group (NCIC CTG IND.168). *Invest New Drugs* (2008) 26:265–72. doi: 10.1007/s10637-007-9103-2

36. Lee CW, Bélanger K, Rao SC, Petrella TM, Tozer RG, Wood L, et al. A phase II study of ispinesib (SB-715992) in patients with metastatic or recurrent malignant melanoma: a national cancer institute of Canada clinical trials group trial. *Invest New Drugs* (2008) 26:249–55. doi: 10.1007/s10637-007-9097-9

37. Tang PA, Siu LL, Chen EX, Hotte SJ, Chia S, Schwarz JK, et al. Phase II study of ispinesib in recurrent or metastatic squamous cell carcinoma of the head and neck. *Invest New Drugs* (2008) 26:257–64. doi: 10.1007/s10637-007-9098-8

38. Indorato R-L, DeBonis S, Kozielski F, Garcia-Saez I, Skoufias DA. STLC-resistant cell lines as tools to classify chemically divergent Eg5 targeting agents according to their mode of action and target specificity. *Biochem Pharmacol* (2013) 86:1441–51. doi: 10.1016/j.bcp.2013.09.003

39. Rapsomaniki MA, Kotsantis P, Symeonidou I-E, Giakoumakis N-N, Taraviras S, Lygerou Z. easyFRAP: an interactive, easy-to-use tool for qualitative and quantitative analysis of FRAP data. *Bioinformatics* (2012) 28:1800–1. doi: 10.1093/bioinformatics/bts241

40. Hackney DD, Jiang W. Assays for kinesin microtubule-stimulated ATPase activity. *Methods Mol Biol* (2001) 164:65–71.

41. DeBonis S, Skoufias DA, Lebeau L, Lopez R, Robin G, Margolis RL, et al. *In vitro* screening for inhibitors of the human mitotic kinesin Eg5 with antimitotic and antitumor activities. *Mol Cancer Ther* (2004) 3:1079–90.

42. Glaab WE, Tindall KR. Mutation rate at the hprt locus in human cancer cell lines with specific mismatch repair-gene defects. *Carcinogenesis* (1997) 18:1–8. doi: 10.1093/carcin/18.1.1

43. Teraishi F, Wu S, Zhang L, Guo W, Davis JJ, Dong F, et al. Identification of a novel synthetic thiazolidin compound capable of inducing c-jun NH2-terminal kinase–dependent apoptosis in human colon cancer cells. *Cancer Res* (2005) 65:6380–7. doi: 10.1158/0008-5472.CAN-05-0575

44. Nakai R, Iida S, Takahashi T, Tsujita T, Okamoto S, Takada C, et al. K858, a novel inhibitor of mitotic kinesin Eg5 and antitumor agent, induces cell death in cancer cells. *Cancer Res* (2009) 69:3901–9. doi: 10.1158/0008-5472.CAN-08-4373

45. Gartner M, Sunder-Plassmann N, Seiler J, Utz M, Vernos I, Surrey T, et al. Development and biological evaluation of potent and specific inhibitors of mitotic kinesin Eg5. *Chembiochem* (2005) 6:1173–7. doi: 10.1002/cbic.200500005

46. Wacker SA, Houghtaling BR, Elemento O, Kapoor TM. Using transcriptome sequencing to identify mechanisms of drug action and resistance. *Nat Chem Biol* (2012) 8:235–7. doi: 10.1038/nchembio.779

47. Woessner R, Tunquist B, Lemieux C, Chlipala E, Jackinsky S, Dewolf W, et al. ARRY-520, a novel KSP inhibitor with potent activity in hematological and taxane-resistant tumor models. *Anticancer Res* (2009) 29:4373–80.

48. Lad L, Luo L, Carson JD, Wood KW, Hartman JJ, Copeland RA, et al. Mechanism of inhibition of human KSP by ispinesib. *Biochemistry* (2008) 47:3576–85. doi: 10.1021/bi702061g

49. Sturgill EG, Norris SR, Guo Y, Ohi R. Kinesin-5 inhibitor resistance is driven by kinesin-12. *J Cell Biol* (2016) 213:213–27. doi: 10.1083/jcb.201507036

50. Blangy A, Chaussepied P, Nigg EA. Rigor-type mutation in the kinesin-related protein HsEg5 changes its subcellular localization and induces microtubule bundling. *Cell Motil Cytoskeleton* (1998) 40:174–82. doi: 10.1002/(SICI)1097-0169(1998)40

51. Crevel IM-TC, Alonso MC, Cross RA. Monastrol stabilises an attached low-friction mode of Eg5. *Curr Biol* (2004) 14:R411–412. doi: 10.1016/j.cub.2004.05.030

52. Larson AG, Naber N, Cooke R, Pate E, Rice SE. The conserved L5 loop establishes the pre-powerstroke conformation of the kinesin-5 motor, eg5. *Biophys J* (2010) 98:2619–27. doi: 10.1016/j.bpj.2010.03.014

53. Yokoyama H, Sawada J, Katoh S, Matsuno K, Ogo N, Ishikawa Y, et al. Structural basis of new allosteric inhibition in kinesin spindle protein Eg5. *ACS Chem Biol* (2015) 10:1128–36. doi: 10.1021/cb500939x

54. Chen G-Y, Kang YJ, Gayek AS, Youyen W, Tüzel E, Ohi R, et al. Eg5 inhibitors have contrasting effects on microtubule stability and metaphase spindle integrity. *ACS Chem Biol* (2017) 12:1038–46. doi: 10.1021/acschembio.6b01040

55. Hackney DD. Pathway of ADP-stimulated ADP release and dissociation of tethered kinesin from microtubules. *Implications extent processivity Biochem* (2002) 41:4437–46. doi: 10.1021/bi0159229

56. Cross RA. The kinetic mechanism of kinesin. *Trends Biochem Sci* (2004) 29:301–9. doi: 10.1016/j.tibs.2004.04.010

57. Good JAD, Skoufias DA, Kozielski F. Elucidating the functionality of kinesins: an overview of small molecule inhibitors. *Semin Cell Dev Biol* (2011) 22:935–45. doi: 10.1016/j.semcdb.2011.09.023

58. Rebucci M, Michiels C. Molecular aspects of cancer cell resistance to chemotherapy. *Biochem Pharmacol* (2013) 85:1219–26. doi: 10.1016/j.bcp.2013.02.017

59. McGranahan N, Swanton C. Biological and therapeutic impact of intratumor heterogeneity in cancer evolution. *Cancer Cell* (2015) 27:15–26. doi: 10.1016/j.ccell.2014.12.001

60. Tcherniuk S, van Lis R, Kozielski F, Skoufias DA. Mutations in the human kinesin Eg5 that confer resistance to monastrol and s-trityl-L-cysteine in tumor derived cell lines. *Biochem Pharmacol* (2010) 79:864–72. doi: 10.1016/j.bcp.2009.11.001

61. Sturgill EG, Das DK, Takizawa Y, Shin Y, Collier SE, Ohi MD, et al. Kinesin-12 Kif15 targets kinetochore fibers through an intrinsic two-step mechanism. *Curr Biol* (2014) 24:2307–13. doi: 10.1016/j.cub.2014.08.022

62. Parke CL, Wojcik EJ, Kim S, Worthylake DK. ATP hydrolysis in Eg5 kinesin involves a catalytic two-water mechanism. *J Biol Chem* (2010) 285:5859–67. doi: 10.1074/jbc.M109.071233

63. Kaseda K, Crevel I, Hirose K, Cross RA. Single-headed mode of kinesin-5. *EMBO Rep* (2008) 9:761–5. doi: 10.1038/embor.2008.96

64. Kapitein LC, Kwok BH, Weinger JS, Schmidt CF, Kapoor TM, Peterman EJG. Microtubule cross-linking triggers the directional motility of kinesin-5. *J Cell Biol* (2008) 182:421–8. doi: 10.1083/jcb.200801145

65. Kwok BH, Kapitein LC, Kim JH, Peterman EJG, Schmidt CF, Kapoor TM. Allosteric inhibition of kinesin-5 modulates its processive directional motility. *Nat Chem Biol* (2006) 2:480–5. doi: 10.1038/nchembio812

66. Viswanath ANI, Pae AN. Resistance by allostery: A novel perspective for Eg5-targeted drug design. *J Med Chem* (2013) 56:6314–6. doi: 10.1021/jm401071u

67. Talapatra SK, Anthony NG, Mackay SP, Kozielski F. Mitotic kinesin Eg5 overcomes inhibition to the phase I/II clinical candidate SB743921 by an allosteric resistance mechanism. *J Med Chem* (2013) 56:6317–29. doi: 10.1021/jm4006274

frontiers | Frontiers in Pharmacology

TYPE Original Research
PUBLISHED 17 October 2022
DOI 10.3389/fphar.2022.969611

OPEN ACCESS

EDITED BY
Christian Celia,
University of Studies G. d'Annunzio Chieti and Pescara, Italy

REVIEWED BY
Vrinda Gote,
Inventprise Inc., United States
Zhuo-Xun Wu,
St. John's University, United States

*CORRESPONDENCE
Weidong Chen,
wdchen@ahtcm.edu.cn
Fengling Wang,
syx050686wfl@163.com
Xiangyun Meng,
hfmxy70@163.com

†These authors have contributed equally to this work

SPECIALTY SECTION
This article was submitted to Pharmacology of Anti-Cancer Drugs, a section of the journal Frontiers in Pharmacology

RECEIVED 15 June 2022
ACCEPTED 27 September 2022
PUBLISHED 17 October 2022

CITATION
Ye X, Chen X, He R, Meng W, Chen W, Wang F and Meng X (2022), Enhanced anti-breast cancer efficacy of co-delivery liposomes of docetaxel and curcumin.
Front. Pharmacol. 13:969611.
doi: 10.3389/fphar.2022.969611

Enhanced anti-breast cancer efficacy of co-delivery liposomes of docetaxel and curcumin

Xi Ye[1,2,3†], Xin Chen[4†], Ruixi He[5,6], Wangyang Meng[7], Weidong Chen[6*], Fengling Wang[1,2,3*] and Xiangyun Meng[1,2,3*]

[1]Department of Pharmacy, The Second People's Hospital of Hefei, Hefei, China, [2]Hefei Hospital Affiliated to Anhui Medical University, Hefei, China, [3]Hefei Hospital Affiliated to Bengbu Medical College, Hefei, China, [4]Department of Pharmacy, Anhui Provincial Crops Hospital, Hefei, China, [5]Anhui University of Chinese Medicine, Hefei, China, [6]Institute of Drug Metabolism, School of Pharmaceutical Sciences, Anhui University of Chinese Medicine, Hefei, China, [7]Union Hospital, Tongji Medical College, Huazhong University of Science and Technology, Wuhan, China

The successful treatment of breast cancer is hampered by toxicity to normal cells, impaired drug accumulation at the tumor site, and multidrug resistance. We designed a novel multifunctional liposome, CUR-DTX-L, to co-deliver curcumin (CUR) and the chemotherapeutic drug docetaxel (DTX) for the treatment of breast cancer in order to address multidrug resistance (MDR) and the low efficacy of chemotherapy. The mean particle size, polydispersity index, zeta potential, and encapsulation efficiency of CUR-DTX-L were 208.53 ± 6.82 nm, 0.055 ± 0.001, −23.1 ± 2.1 mV, and 98.32 ± 2.37%, respectively. An *in vitro* release study and CCK-8 assays showed that CUR-DTX-L has better sustained release effects and antitumor efficacy than free drugs, the antitumor efficacy was verified by MCF-7 tumor-bearing mice, the CUR-DTX-L showed better antitumor efficacy than other groups, and the *in vivo* pharmacokinetic study indicated that the plasma concentration–time curve, mean residence time, and biological half-life time of CUR-DTX-L were significantly increased compared with free drugs, suggesting that it is a promising drug delivery system for the synergistic treatment of breast cancer.

KEYWORDS

co-delivery, curcumin, docetaxel, breast cancer, liposomes

1 Introduction

Cancer remains the second leading cause of death worldwide, with breast cancer being the most commonly diagnosed malignancy and the leading cause of cancer-related deaths in women worldwide, despite the fact that extensive research is being conducted worldwide to combat this dreadful and lethal disease (GBD 2017 Causes of Death Collaborators, 2018; Schmidt et al., 2017). In addition, the incidence of breast cancer, which affects one in eight women, is rising. Traditional breast cancer treatments include surgery, radiation, and chemotherapy, with chemotherapy being the most prevalent. Docetaxel (DTX), an artificial semi-synthetic yew chemical generated from the needles of European yew, is one of the first-line medications for breast cancer treatment that inhibits

the proliferation of cancer cells by interfering with their synthesis, migration, and division (Shi et al., 2015; Hua et al., 2017). However, the side effects caused by docetaxel have considerably overshadowed its clinical use. First, like most other classical chemotherapeutic drugs, DTX is distributed throughout the body in a non-specific manner, and second, due to the poor solubility of DTX in water, it can lead to adverse drug reactions (Persohn et al., 2005). In addition, multidrug resistance (MDR) has already been a major problem in clinical treatment that limits the efficacy of DTX; MDR can lead to rapid drug elimination and chemotherapy failure, and it may be associated with multiple mechanisms (Bukowski et al., 2020), among which drug efflux transporters are the main cause of MDR (Gote et al., 2021), which remove DTX from tumor cells and reduce the accumulation of drug-resistant cells. Therefore, in order to improve the antitumor efficacy and reduce side effects caused by the nonspecific delivery of DTX, it is imperative that the preparation and development of novel techniques be expedited (Kaushik et al., 2020).

In recent years, combination therapy of simultaneous administration of numerous medications has proven to be superior to the use of a single drug in clinical settings, thereby reducing the occurrence of MDR (Berríos-Caro et al., 2021). For instance, it is an effective strategy to alter the efficacy of anticancer agents by co-administration of reversal agents. Curcumin (CUR), a bioactive ingredient extracted from the rhizome of the herb turmeric, which has been recognized as a safe food additive by the FDA, is also being widely used in the prevention and treatment of a variety of cancers, including preclinical studies in breast cancer, colorectal cancer, stomach cancer, liver cancer, esophageal cancer, lung cancer, brain cancer, and leukemia (Chen et al., 2016; Hesari et al., 2019; Hong et al., 2019; Wong et al., 2019; Guo P. et al., 2020; Angeline et al., 2020; Schmidt et al., 2020). Furthermore, CUR is also well known to downregulate P-gp, MRP-1, and other components that contribute to MDR (Abouzeid et al., 2014). It has been demonstrated that the growth inhibitory and cell death-inducing effects of CUR and its analogs are not reduced by drug resistance in breast cancer MCF-7 cells (Labbozzetta et al., 2009). Growing interest has been focused on CUR-mediated combination of drug delivery systems. Studies have shown that the combination of CUR and chemotherapy drugs like paclitaxel and doxorubicin may improve treatment efficacy (Wang et al., 2019; Zhao et al., 2019). However, despite the promise of its pharmacological capabilities, the therapeutic application of CUR is now constrained by its insolubility in water and low bioavailability. If CUR is simply combined with other anti-cancer drugs to work directly on cancer cells, it will not achieve its full effect.

Nanoparticle drug delivery methods, such as liposomes, micelles, and nanoproducts, have gained increasing interest over the past decades due to their numerous advantages (Wang et al., 2011; Ran et al., 2014; Li et al., 2020). Among these, liposomes are considered to be a powerful drug delivery system due to their structural versatility, biocompatibility, biodegradability, non-toxicity, and non-immunogenicity (Mathiyazhakan et al., 2018). Liposomes are phospholipid vesicles formed by one or more concentric lipid bilayers surrounding discrete aqueous cavities. The liposome system has the unique ability to trap lipophilic and hydrophilic compounds, allowing a variety of drugs to be encapsulated by these vesicles (Sercombe et al., 2015). The process of medication release from liposomes is the disintegration of the phospholipid bilayer, and pharmaceuticals encapsulated in liposomes can be simultaneously released to exhibit their effectiveness (Yu et al., 2009).

In this report, we designed a CUR and DTX co-delivery strategy with liposomes as nanocarriers to synergistically induce apoptosis in human breast cancer. We formulated CUR-DTX-L by the ethanol injection method, which enabled the co-delivery of DTX and CUR in a single system. CUR-DTX-L was characterized in terms of particle size and zeta potential, and the *in vivo* pharmacokinetics of this liposome was investigated. Moreover, *in vitro* and *in vivo* pharmacodynamic studies of CUR-DTX-L were performed to evaluate its efficacy for antitumor activity in MCF-7 cells. This system is expected to achieve the stable and controlled release and active targeting of DTX and CUR to liposomes, improve synergistic anticancer effects, and reduce toxicity (Figure 1).

2 Materials and methods

2.1 Materials

Docetaxel (DTX), curcumin (CUR), and cholesterol (Chol) of analytical grade were acquired from Sinopharm Chemical Reagent Co., Ltd. (Shanghai, China). The supplier of egg phospholipid was A.V.T. (Shanghai) Pharmaceutical Co., Ltd. Merck was contacted to acquire methanol and acetonitrile of HPLC quality (Darmstadt, Germany). The remaining reagents were all of analytical grade.

2.2 Cells and animals

MCF-7 cells (Cell Bank of Shanghai Institute of Cell Biology, China) were cultured in DMEM supplemented with 10% (v/v) fetal bovine serum (FBS, Gibco), 4 ml glutamine, 4,500 mg/L glucose, 100 units/ml penicillin, and 100 units/ml streptomycin at 37°C in a humidified 5% CO_2 environment (Zhang et al., 2017).

Anhui Medical University's Experimental Animal Center supplied 220 ± 20 g of 5-week-old Sprague–Dawley (SD) rats and BALB/c nude female mice that were in good health (Hefei, China). All animals were housed in vented cages at a controlled

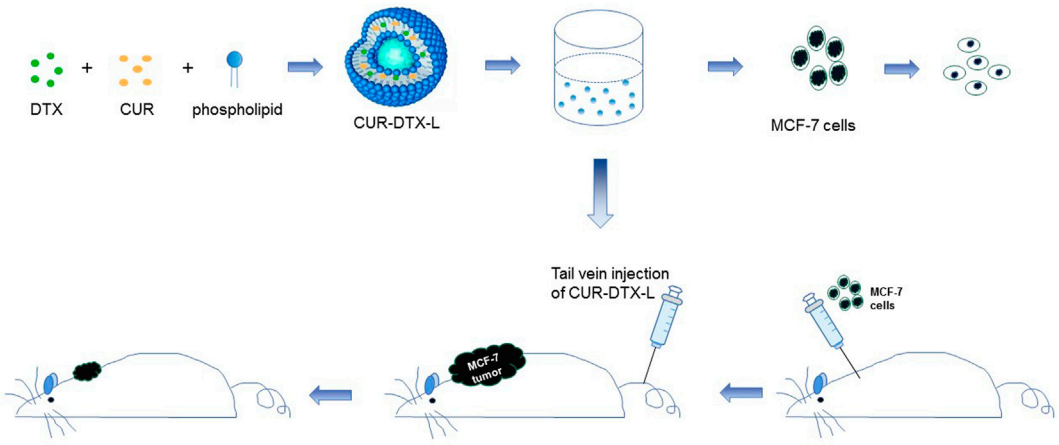

FIGURE 1
Schematic diagram of the assembly of CUR-DTX-L and its *in vitro* and *in vivo* efficacy tests. CUR-DTX-L was prepared by ethanol injection. The *in vitro* efficacy of CUR-DTX-L was investigated in the MCF-7 cell line, and its *in vivo* efficacy was investigated with an MCF-7 nude mouse model.

temperature of 24°C–26°C and relative humidity of 55%–65%, and they were permitted to consume regular feed and drink water *ad libitum* (Wu et al., 2016). All protocols involving experimental animals were performed in accordance with the guidelines evaluated and approved by the Institutional Animal Ethics Committee of Anhui Medical University (Hefei, China).

2.3 Preparation of liposomes

The CUR-DTX liposomes (CUR-DTX-L) were prepared by the ethanol injection method (Du and Deng, 2006; Vitor et al., 2017). Using single-factor experiments, the formulation process was optimized, and the optimization procedure is given as follows. Briefly, CUR (2 mg), DTX (4 mg), cholesterol (30 mg), and soybean phospholipid (120 mg) were dissolved in ethanol (3 ml) to generate the organic phase, and the mixed organic solution was deposited in a 55°C water bath. The solution was then rapidly injected into the agitated aqueous phase (20 ml of double-distilled water, 800 rpm). The aqueous phase was then agitated for 3 h at 55°C using an electric magnetic stirrer (DF-1 Electric Stirrer, JinTan, China) to produce a homogenous emulsion.

Single CUR-loaded liposomes (CUR-L) were prepared using the same procedure as CUR-DTX-L but without the addition of DTX to the organic phase. The amount of soybean phospholipid and cholesterol was changed to 130 mg and 20 mg, respectively.

Single DTX-loaded liposomes (DTX-L) were prepared using the same method as CUR-DTX-L but without the addition of CUR to the organic phase. The amount of soybean phospholipid and cholesterol was changed to 130 mg and 20 mg, respectively.

2.4 Encapsulation efficiency

The encapsulation efficiency (EE) was determined by measuring the unencapsulated drug concentration and total drug concentration by the high-performance liquid chromatography (HPLC) method (Wang et al., 2020). The unencapsulated DTX and CUR were separated from liposomes by size exclusion chromatography using a Sephadex G-50 column (1.5 cm × 20.0 cm) with distilled water as the eluent. Briefly, the isolated CUR-DTX-L, DTX-L, and CUR-L were dissolved in methanol and determined by HPLC. The EE% could be calculated as follows:

$$EE(\%) = WE/WT \times 100\%,$$

where WE refers to the weight of CUR/DTX encapsulated in liposomes and WT refers to the weight of the total CUR/DTX in the formulation.

2.5 Characterization of liposomes

Mean particle size, zeta potential, and polydispersity index (PDI) of the liposomes were measured by dynamic light scattering (DLS) using a Zetasizer Nano ZS90 Malvern particle size analyzer (Malvern, United Kingdom) after dilution with distilled water. The instrument was calibrated using standard latex liposomes. All particle size measurements were carried out after the liposomes were diluted 20-fold in distilled water. The zeta potential measurements of the prepared liposomes can be performed without dilution. The experimental data represented the mean of three distinct outcomes (Wu et al., 2020).

2.6 *In vitro* release of liposomes

In combination with the chemical properties of DTX and CUR, PBS (pH = 7.4) was selected as the release medium, and the solubility of DTX and CUR was enhanced by the addition of 0.5% Tween 80 to achieve the condition of tank leakage in order to observe the release characteristics of liposomes *in vitro*. In this experiment, samples containing 0.5 mg of drugs were placed in dialysis membrane bags (21 mm, MVCO 8000-14400 Da), tied, and submerged in a beaker containing 100 ml of the release medium at (37 ± 1)°C. Separate samples were taken at regular intervals, and an equal volume of the release medium was added to ensure sedimentation conditions. After passing the samples through a 0.22-μm filter membrane, the amount of DTX and CUR was determined using the HPLC technique (Ji et al., 2006).

2.7 Pharmacokinetic studies

In this investigation, male and female rats were randomly separated into six equal groups, and formulations were injected intravenously through the tail vein (n = 6 per group). Before administration, DTX-L, CUR-L, and CUR-DTX-L were freshly prepared. Each group was injected with free CUR, free DTX, free DTX-CUR, CUR-L, DTX-L, and CUR-DTX-L, and the CUR and DTX doses were 1.0 mg/kg and 2.0 mg/kg, respectively. Approximately, 0.3 ml of blood was taken in heparinized microcentrifuge tubes *via* the retro-orbital under isoflurane anesthesia immediately following a pre-determined post-injection time point (3, 10, 30, 60, 120, 240, 360, 480, 600, and 720 min). After the blood samples were centrifuged at 3,000 rpm for 10 min, plasma (150 L) was extracted and kept at −20°C until further HPLC analysis (Sun et al., 2018). The pharmacokinetic parameters of DTX and CUR were estimated using the software program DAS 2.0 (Shanghai Bojin Medical Technology Co., Ltd., Shanghai, China).

2.8 Cell viability assays

To examine cell viability, the Cell Counting Kit-8 (CCK-8) approach was chosen (Zhang et al., 2020). MCF-7 breast cancer cells were cultured at a density of 5,000 cells per well in 96-well plates and cultured at 37°C in a humidified room with 5% CO_2. After 24 h of culture, DTX-CUR-L, DTX-L, CUR-L, free DTX, and free CUR were applied to the adherent cells. Due to its limited water solubility, DMSO dissolves free DTX and CUR rapidly (final concentration of DMSO in medium ≤ 0.1%). The concentration gradients of DTX given to adherent cells were 25, 50, 75, 100, 120, 150, and 200 g/ml. The respective concentration gradients of CUR were 12.5, 25, 37.5, 50, 60, 75, and 100 g/ml. After 24 h of incubation at 37°C and 5% CO_2, the culture media were withdrawn from each well, and the cells were washed twice with PBS. Each well received 10 μl of CCK-8 solution (it should be noted not to develop air bubbles during the addition process), and the culture plate was incubated for an additional hour. At 490 nm, absorbance values were measured using an enzyme-linked immunosorbent assay reader (BioTek elx800 microplate reader, United States). Cell viability was calculated as the percentage of absorbance in the wells of treated cells relative to that of untreated cells. Assuming 100% survival of untreated cells, the percentage of viable cells can be calculated (Tian et al., 2018). In this study, all treatments were evaluated in triplicate, and the results are expressed as the mean standard deviation. The sample's half-maximal inhibitory concentration (IC_{50}) value was calculated.

2.9 *In vivo* antitumor study

2.9.1 Modeling and administration

MCF-7 cells were grown in DMEM media supplemented with 10% fetal bovine serum (FBS). When the cells reached the exponential growth phase, they are digested with 0.25% trypsin and spun at 1,200 rpm for 5 min. The serum from the cell precipitation was removed by rinsing it twice with PBS and resuspending the cells in PBS. Cells were counted under a microscope and diluted to 1×10^7 cells/ml. Afterward, 10^6 MCF-7 cells were implanted into the mammary fat pad close to the left axilla (Wang et al., 2015). After 10 days, the tumor-bearing mice were randomly divided into seven groups of three mice each: the saline group, CUR group, DTX group, CUR/DTX group, CUR-L group, DTX-L group, and CUR-DTX-L group. The groups received tail vein injections of corresponding medicines every third day four times, and the CUR and DTX doses were 0.1 mg/kg and 0.2 mg/kg, respectively. During therapy, each mouse was weighed, and the highest (D) and minimum 4) tumor diameters were measured with a caliper every other day. After the final injection, the mice were watched for a total of two treatment cycles. On day 14, all animals were sacrificed by cervical dislocation. Tumors and organs were removed, weighed, photographed, and then preserved in paraformaldehyde at 4% for subsequent studies.

2.9.2 The analysis of tumor growth inhibition and weight

Using a caliper, the maximum (D) and minimum (d) diameters of the tumors were determined. The volume (V) of the tumor was computed using the formula: V = Dd2/2 (Gao et al., 2013). The tumor growth inhibition curves for the different

groups are depicted using time as the horizontal axis and tumor volume as the vertical axis. Photographs of excised mouse tumors can directly indicate the efficacy of the drug. The weight of the tumor is a statistical measure of anticancer activity. Taking the tumor weight as the ordinate and the number of experimental groups as the abscissa, the differences in tumor weight between the groups were examined. According to the equation,

$$\text{Tumor inhibition rate (IRT\%)} = \frac{\left|(\text{W control} - \text{W experiment})\right|}{\text{W control}} \times 100\%.$$

the tumor inhibition rate of each prescription drug was calculated, and its antitumor efficacy was evaluated.

2.9.3 Histological examination and analysis

After washing the removed tumor with normal saline, it was fixed with 4% paraformaldehyde for more than 24 h, embedded in paraffin, stained with hematoxylin and eosin (H and E), and observed and examined at ×200 magnification using a microscope (He et al., 2010). The apoptosis of tumor cells was assessed by terminal deoxynucleotidyl transferase dUTP nick end labeling (TUNEL) stain labeling. The counterstain utilized was diaminobenzidine (DAB). In the TUNEL experiment, the apoptotic cell nuclei were stained brown. Tissue samples were routinely fixed with 4% paraformaldehyde, embedded in paraffin, stained with TUNEL, and sectioned (Nassir et al., 2019). Under a microscope, the sections were examined and photographed. The positive expression rates of apoptotic cells in the images of each group were compared.

2.10 Assessment of toxicity in MCF-7 tumor-bearing nude mice

Safety is mostly determined by observing the weight change of mice with tumors and the toxicity of drug-loaded micelles on the organs of mice by HE staining. The weight change curve is obtained by weighing and recording the weight of shaved mice every 2 days, and then, the time–weight curve is plotted. After removing the mouse's heart, liver, spleen, lung, and kidney, the removed organs were washed with normal saline, fixed with 4% paraformaldehyde, embedded in paraffin, stained with HE, and examined and studied at ×200 magnification using a microscope.

2.11 Statistical analysis

All data are provided as the mean ± SD. *T*-tests were used to compare two groups, while one-way analyses of variance (ANOVA) were utilized to compare multiple groups. *p*-values of 0.05 were statistically significant. Using SPSS 18.0 software, statistical analysis was performed.

TABLE 1 Characterization of different formulations (n = 3).

Parameter	Formulation		
	CUR-DTX-L	DTX-L	CUR-L
Size (nm)	208.53 ± 6.82	239.32 ± 4.95	212.95 ± 4.57
PDI	0.055 ± 0.001	0.134 ± 0.005	0.200 ± 0.012
Zeta potential (mV)	−23.1 ± 2.1	−20.5 ± 1.8	−19.4 ± 1.8
EE (%)	98.32 ± 2.37	95.63 ± 3.65	92.78 ± 3.07

3 Results

3.1 Characterization of liposomes

The properties of the drugs encapsulated in liposomes were analyzed. In this study, a nanoscale drug delivery system was used to encapsulate DTX and CUR, both of which are poorly water-soluble anticancer drugs (Frank et al., 2019). Drugs with strong lipid solubility and water solubility are typically loaded passively into liposomes. The injection method and thin-film ultrasonic dispersion method are the primary preparation methods. According to preliminary experiments, although the thin-film dispersion method could complete the preparation of liposomes in a short amount of time, the system was cloudy, the particle size distribution was uneven, the stability was poor, and the amount of residual organic solvents exceeded the standard. Injection-prepared liposomes with a high EE percentage, tiny particle size, uniform dispersion, and good stability met the parameters for liposome preparation. According to Table 1, the EE values of CUR-DTX-L, DTX-L, and CUR-L synthesized using this approach were 98.32 ± 2.37%, 95.63 ± 3.65%, and 92.78 ± 3.07%, respectively.

The mean particle size and PDI of liposomes have a substantial influence on the EE percentage, stability, half-life *in vivo*, and targeted selectivity. Consequently, determining the average particle size is crucial for assessing the quality of liposomes. PDI is an index for determining particle size distribution uniformity (Guo D. et al., 2020). The lower the PDI number, the more homogeneous the particle size distribution will be. The average particle size of DTX-CUR-L, DTX-L, and CUR-L, as shown in Table 1, is 208.53 ± 6.82 nm, 239.32 ± 4.95 nm, and 212.95 ± 4.57 nm, respectively. The combination of DTX-L and CUR-L did not significantly alter the dimensions of either material. Moreover, the formulations showed PDI values of approximately 0.055 ± 0.001, 0.134 ± 0.005, and 0.200 ± 0.012, indicating that the particle size distribution in these three formulations is narrow and the particle size is relatively uniform.

The zeta potential formed by the double electric layer on the liposome particle's surface is an additional essential component influencing its stability and action *in vivo*. It is generally believed

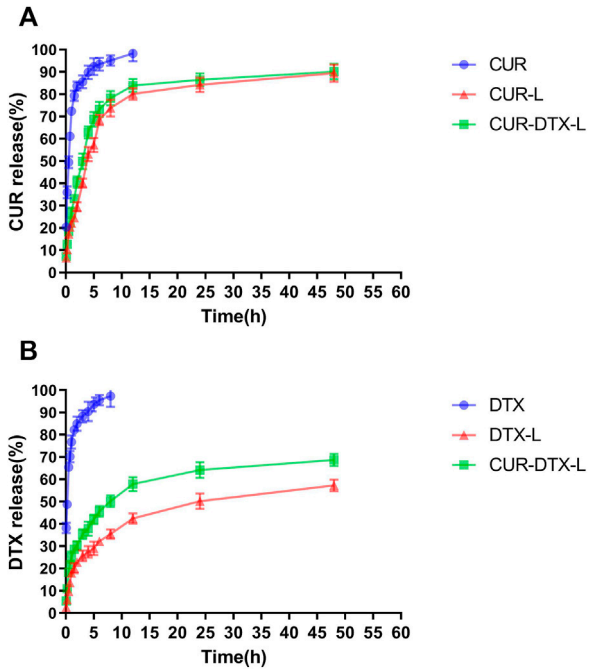

FIGURE 2
(A) Release profiles of DTX from DTX, DTX-L, and CUR-DTX-L in PBS (pH 7.4) at 37°C (n = 6). **(B)** Release profiles of CUR from CUR, CUR-L, and CUR-DTX-L in PBS (pH 7.4) at 37°C (n = 6).

that the bigger the absolute value of the zeta potential, the greater will be the electrostatic repulsion force between liposome particles, which can prevent the agglomeration and sedimentation of each particle in the dispersion system, and the physical stability is good (Alvebratt et al., 2020). Table 1 shows that all liposomes are negatively charged (−23.1 ± 2.1 mV for CUR-DTX-L, −20.5 ± 1.8 mV for DTX-L, and −19.4 ± 1.8 mV for CUR-L), indicating that the repulsive force prevents particles from aggregating, resulting in greater stability.

3.2 *In vitro* release kinetics

Due to the preliminary laboratory foundation, this experiment followed the preliminary experiment in the selection of a preparation method and the research of fundamental prescription, and on this basis, liposomes with a relatively high encapsulation rate and stability were obtained (Yu et al., 2017). The rate of drug release from the liposome is proportional to its permeability. *In vitro* release study circumstances can be utilized to imitate the physiological environment in the body, and the permeability and release rate of the medication can be initially understood, providing a firm foundation for future pharmacokinetics research. In PBS (pH = 7.4) without an additional surfactant, the solubility of DTX and CUR is exceedingly low, and it is challenging to achieve sink conditions. In this experiment, therefore, PBS containing 0.5% Tween 80 was selected as the release medium.

We studied the rate of DTX and CUR release from liposomes and free drug solutions for up to 48 h in order to determine the release profile of the formulations and free medication. Figure 2 shows that liposomes have a slow-release feature. The results revealed that, compared to the free DTX and CUR solution, liposome preparations can delay the release of DTX and CUR *in vitro* and retain higher concentrations for a longer period of time. As shown in Figure 2A, nearly 100% of the free DTX was measured within the first 24 h; however, only 59.27% DTX and 68.74% DTX were released from DTX-L and CUR-DTX-L, respectively. Figure 2B shows that almost all of the free CUR are measured within the first 12 h, whereas CUR in the formulation is not completely released until 48 h. Moreover, compared with the rapid release of the free drug group, *in vitro* release studies have shown that liposome formulations exhibit slow drug release characteristics without initial bursts, which may be due to the fact that affinity of the drug held by small fragments of the liposome membrane lipid properties, as well as drugs encapsulated in lipid membranes, is mainly released by dissolution and diffusion of the lipid bilayer (Cheng et al., 2019). In addition, the encapsulation of liposomes changed the *in vitro* release rate of DTX and CUR, suggesting the possibility of the sustained release of the preparation *in vivo*, and this sustained-release mode may be beneficial in that the drug is not released during normal vascular circulation, and most of the embedded drugs can be delivered directly to the tumor site.

TABLE 2 Pharmacokinetic parameters of CUR in formulations and free drugs (n = 6).

Parameter	Mean ± SD		
	CUR-DTX-L	CUR-L	Free CUR
T1/2 (min)	109.2 ± 19.7*	108.7 ± 22.5*	33.6 ± 3.3
Cmax (μg/ml)	8.1 ± 1.4*	8.0 ± 0.9*	7.2 ± 0.8
AUC(0-∞) (min·μg/mL)	901.2 ± 73.9*	834.6 ± 84.2*	287.2 ± 15.5
CL (ml/min/kg)	2.0 ± 0.3*	2.2 ± 0.3*	6.4 ± 0.3
MRT (min)	157.8 ± 32.9*	152.7 ± 26.8*	46.7 ± 3.3

*$p < 0.05$, compared with free CUR.

3.3 Pharmacokinetic studies

Pharmacokinetics is mainly a quantitative study of the process (absorption, distribution, metabolism, and excretion) of drugs in the body and uses mathematical principles and methods to elaborate the dynamic laws of drugs in the body (Cheng et al., 2019). In this work, rats were given intraperitoneal

TABLE 3 Pharmacokinetic parameters of DTX in formulations and free drugs (n = 6).

Parameter	Mean ± SD		
	CUR-DTX-L	DTX-L	Free DTX
$T_{1/2}$ (min)	214.8 ± 24*	188.1 ± 25.1*	106.6 ± 12.2
C_{max} (μg/ml)	22.1 ± 1.6*	21.4 ± 2.2*	19.8 ± 0.7
$AUC_{(0-\infty)}$ (min·μg/mL)	5050.9 ± 401*	4565.1 ± 335.1*	1750.7 ± 159.3
CL (ml/min/kg)	0.4 ± 0.0*	0.4 ± 0.0*	1.1 ± 0.1
MRT (min)	322.5 ± 17.0*	287.4 ± 19.5*	147.2 ± 5.0

*p < 0.05, compared with free DTX.

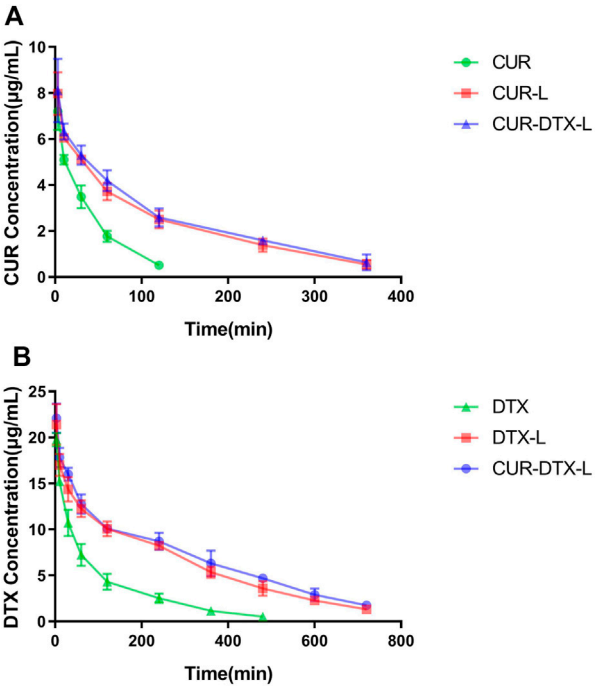

FIGURE 3
(A) Plasma concentrations vs. time curves of DTX in SD rats after intravenous injection of DTX, DTX-L, and CUR-DTX-L (n = 6). **(B)** Plasma concentrations vs. time curves of CUR in SD rats after intravenous injection of CUR, CUR-L, and CUR-DTX-L (n = 6).

dosages of 2.0 mg/kg (DTX) and 1.0 mg/kg (CUR). *In vivo* pharmacokinetic investigations were performed on CUR-L, DTX-L, and CUR-DTX-L, with free DTX and free CUR solutions serving as controls. The principal pharmacokinetic characteristics of the experiment are given in Tables 2, 3, and the plasma drug concentration–time curves are shown in Figure 3. As shown in Table 2, it can be clearly observed that compared to free DTX, the DTX-L and CUR-DTX-L formulations exhibit significantly higher $T_{1/2}$ (106.6 ± 12.2, 188.1 ± 25.1, and 214.8 ± 24 min, respectively), AUC (1750.7 ± 159.3, 4565.1 ± 335.1, and 5050.9 ± 401 min·μg/ml, respectively), and MRT (147.2 ± 5.0, 287.4 ± 19.5, and 322.5 ± 17.0 min, respectively), which indicated that the DTX-L and CUR-DTX-L formulations can significantly improve the relative bioavailability of DTX. Similar results were observed with CUR (Table 3), where the main pharmacokinetic parameters were significantly increased in formulation groups compared to free CUR. In addition, the pharmacokinetic characteristics and concentration–time curves of DTX and CUR indicate that CUR-DTX-L had superior pharmacokinetic performance in rats than DTX-L or CUR-L. This may be due to the interaction between CUR and DTX in rats, resulting in a delayed metabolism of both compounds *in vivo* (Rao et al., 2020). In addition, the longer circulation period of liposomes could limit the absorption of proteins and the uptake of RES, hence preventing the nanoparticles from being rapidly eliminated (Sun et al., 2017).

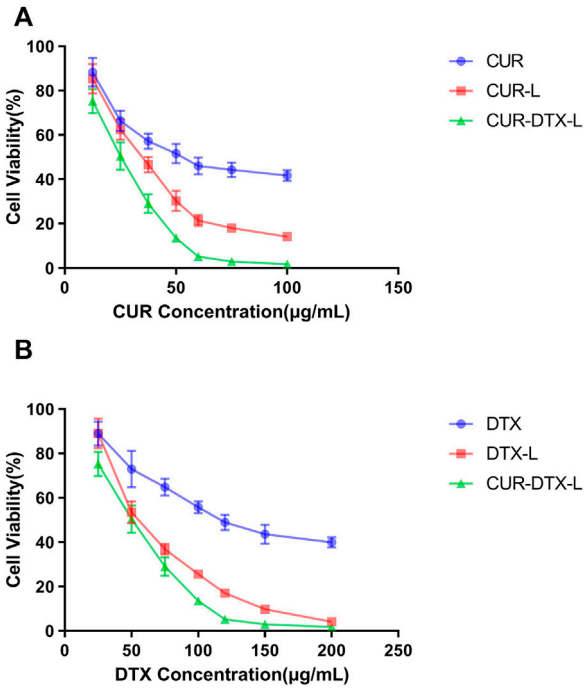

FIGURE 4
(A) MCF-7 cell viability vs. CUR concentration of CUR, CUR-L, and CUR-DTX-L (n = 3). **(B)** MCF-7 cell viability vs. DTX concentration of DTX, DTX-L, and CUR-DTX-L (n = 3).

3.4 *In vitro* cytotoxicity studies

CCK-8 assay was used to investigate the *in vitro* cytotoxicity of CUR-DTX-L, DTX-L, CUR-L, and free medicines on MCF-7

TABLE 4 IC_{50} values of formulations and free drugs in MCF-7 cells measured by the CCK-8 assay (n = 3).

IC_{50} (μg/ml)	Formulation				
	CUR-DTX-L	DTX-L	CUR-L	Free DTX	Free CUR
DTX	45.71 ± 3.15	57.81 ± 4.06	NA	125.03 ± 5.27	NA
CUR	22.86 ± 1.58	NA	36.24 ± 3.16	NA	53.26 ± 4.22

NA, not applicable.

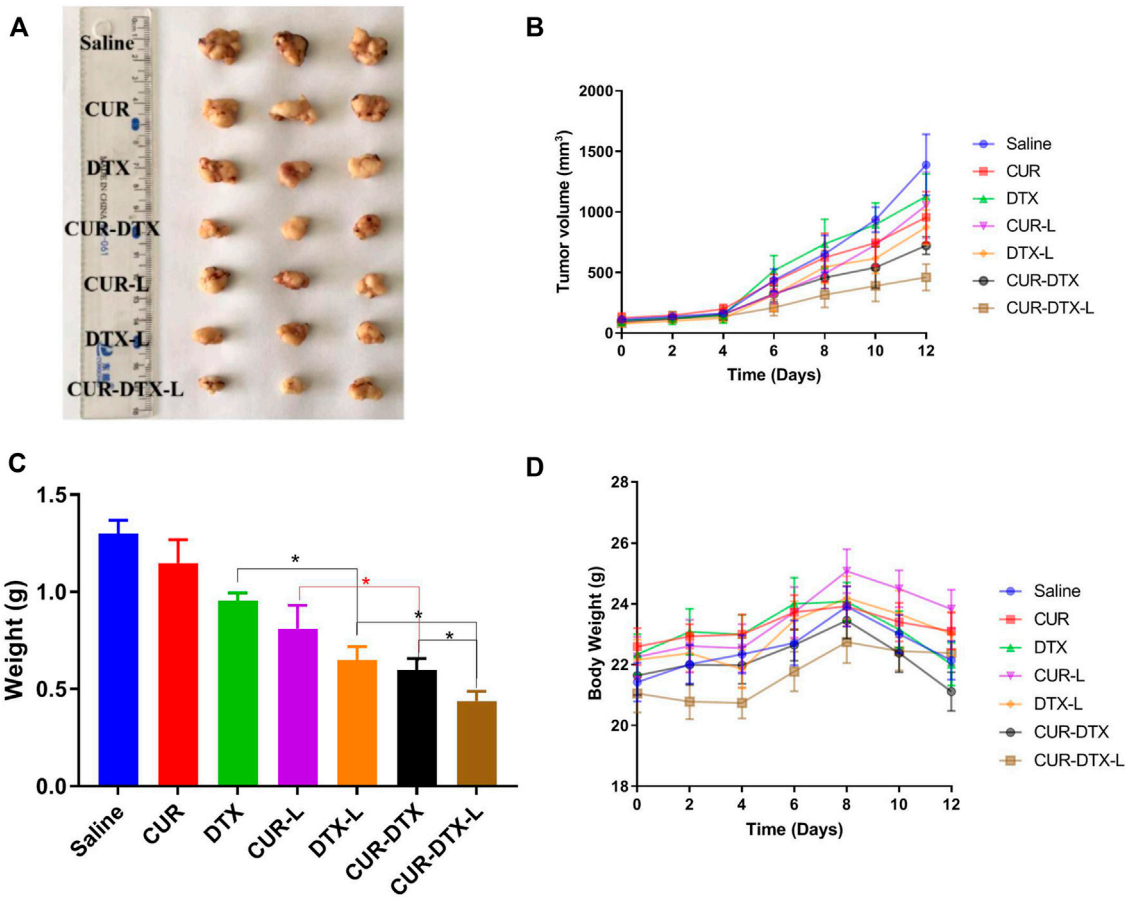

FIGURE 5
In vivo antitumor effect of tumor-bearing mice treated with saline, CUR, DTX, CUR-L, DTX-L, CUR-DTX, and CUR-DTX-L; *$p < 0.05$, **$p < 0.01$, and n = 3. **(A)** Tumor images of the different groups; **(B)** tumor volume curves; **(C)** weight of excised tumor tissues; **(D)** body weight changes of different groups during the whole therapy.

cells. Figure 4 shows the cell viability curves, from which it can be seen that free DTX and drug-loaded formulations inhibited cell proliferation dose-dependently in both cell types. In drug-loaded formulations, the vitality of MCF-7 cells was much lower than that of free DTX. After 24 h of incubation, seven distinct drug concentrations (DTX: 25, 50, 75, 100, 120, 150, and 200 g/ml; CUR: 12.5, 25, 37.5, 50, 60, 75, and 100 g/ml) exhibited significant differences in cell viability when compared to free drugs. In addition, the results demonstrated that CUR-DTX-L inhibited the proliferation of MCF-7 cells more effectively than DTX-L. The IC_{50} data (Table 4) demonstrated that CUR-DTX-L has the highest cytotoxicity compared to the other groups. On the

TABLE 5 Anti-tumor efficacy of tumor-bearing mice with saline, CUR, DTX, CUR-L, DTX-L, CUR-DTX, and CUR-DTX-L treatment (n = 3).

Group	Tumor weight (g)	Inhibition rate (%)
Saline	1.298 ± 0.07	—
CUR	1.148 ± 0.12	11.58
DTX	0.954 ± 0.04	26.50
CUR-L	0.811 ± 0.12	37.52
DTX-L	0.648 ± 0.02	50.80
CUR-DTX	0.597 ± 0.02	54.03
CUR-DTX-L	0.438 ± 0.14	66.23

one hand, liposomes can enhance the toxicity of medications, and on the other hand, CUR can reverse cell resistance and enhance the cytotoxicity of the treatment (Rejinold et al., 2018). Therefore, CUR-DTX-L may provide a novel insight into breast cancer treatment and palliation.

The IC_{50} values of various formulations are summarized in Table 4. It is obvious that CUR-DTX-L showed lower IC_{50} values (for DTX: 45.71 ± 3.15 μg/ml and for CUR: 22.86 ± 1.58 μg/ml) than DTX-L (57.81 ± 4.06 μg/ml), CUR-L (36.24 ± 3.16 μg/ml), and free drugs (for DTX: 125.03 ± 5.27 μg/ml and for CUR: 53.26 ± 4.22 μg/ml). These results indicate that CUR enhances DTX-mediated apoptosis in MCF-7 cells.

3.5 *In vivo* pharmacodynamic studies

3.5.1 Assessment of efficacy in MCF-7 tumor-bearing nude mice

The anticancer efficacy of CUR-DTX-L was investigated using MCF-7 tumor-bearing nude mice, which can simulate human breast cancer's proliferation and spread (Salem et al., 2020). As shown in Figure 5, the mean tumor volume in the saline-treated group increased more than 10-fold during the experiment. The results demonstrated that the tumor volume of mice treated with CUR was not significantly reduced compared to the saline group, whereas the tumor volume of mice treated with DTX was marginally reduced (Figures 5A,B). However, CUR-L, DTX-L, CUR-DTX, and CUR-DTX-L exhibit substantial antitumor actions and inhibit tumor growth significantly. Among them, the tumor volume and tumor weight of the CUR-DTX-L group were less than those treated with other medications (Figure 5C), and in Table 5, the IRT of the CUR-DTX-L group was the most significant at 66.23%, indicating that CUR-DTX-L inhibits tumor growth efficiently. Importantly, no substantial weight loss was detected in mice treated with CUR-DTX-L after the ninth day, in contrast to animals treated with other groups (Figure 5D), suggesting that CUR-DTX-L can mitigate the negative effects of CUR-L and DTX-L.

3.5.2 Histological examination and analysis

At the histology level, the anticancer effect of liposomes was studied using pathological sections. The top row in Figure 6 shows HE-stained tumor tissue from all seven groups. The treated group displayed a degree of necrosis. In the CUR-DTX-L group, tumor necrosis was the most severe. In contrast to the saline group, tumor necrosis was indicated by a lighter color in the other treatment groups. TUNEL staining revealed substantial differences as well. Rarely, tumors in the saline group exhibited immunoreactivity (brown). The single-drug-free group demonstrated incomplete positive spots (Shaik et al., 2004). Positive spots were observed in the CUR-DTX, CUR-L, and DTX-L groups. In contrast, the CUR-DTX-L group displayed several positive puncta in the form of dots. The cell death in tumor tissues can be efficiently reflected by TUNEL labeling. These results revealed that therapy with CUR-DTX-L could limit the growth of the tumor in a synergistic manner (Cai et al., 2021), which was consistent with the CCK-8 results.

3.6 Assessment of toxicity in nude mice

The safety test was evaluated by HE staining of vital organs including the heart, liver, spleen, lung, and kidney, as shown in Figure 7. After treatment, there were only a few inflammatory cells infiltrated in the pulmonary alveoli, and interstation in DTX groups was consistent with previously reported results (Abbasi et al., 2015), with even attenuation in the combination treatment group. In addition, regardless of the control group, monotherapy group, or combination therapy group, there were no notable pathological alterations in other organs. HE staining demonstrated that CUR-DTX-L caused the most damage to tumor tissue, and no damage to the heart, liver, spleen, lung, or kidney was observed. In addition, Figure 5D shows that after 9 days, nude mice in the CUR-DTX-L group did not experience any substantial weight loss, in stark contrast to the weight loss reported in the other treatment groups. Consequently, CUR-DTX-L not only significantly enhanced the antitumor effect but also reduced their exposure in non-targeted tissues, therefore diminishing the overall toxicity *in vivo*.

4 Discussion

The combination of chemotherapy has been broadly studied in recent years, and combination therapy shows great potential in enhancing the antitumor efficiency, especially in MDR (Assaraf et al., 2019; Xu et al., 2019). Furthermore, because chemotherapeutic drugs are usually non-specific small molecules that have poor pharmacokinetics, they are only distributed in a non-targeted manner throughout the body, resulting in their reduced effectiveness at the actual target site. Therefore, the development of a delivery system that modifies the

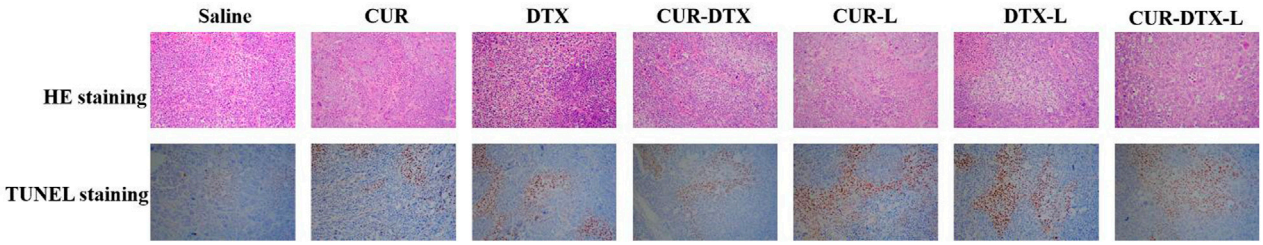

FIGURE 6
HE analysis and TUNEL immunohistochemical staining of tumor tissues (magnification ×200).

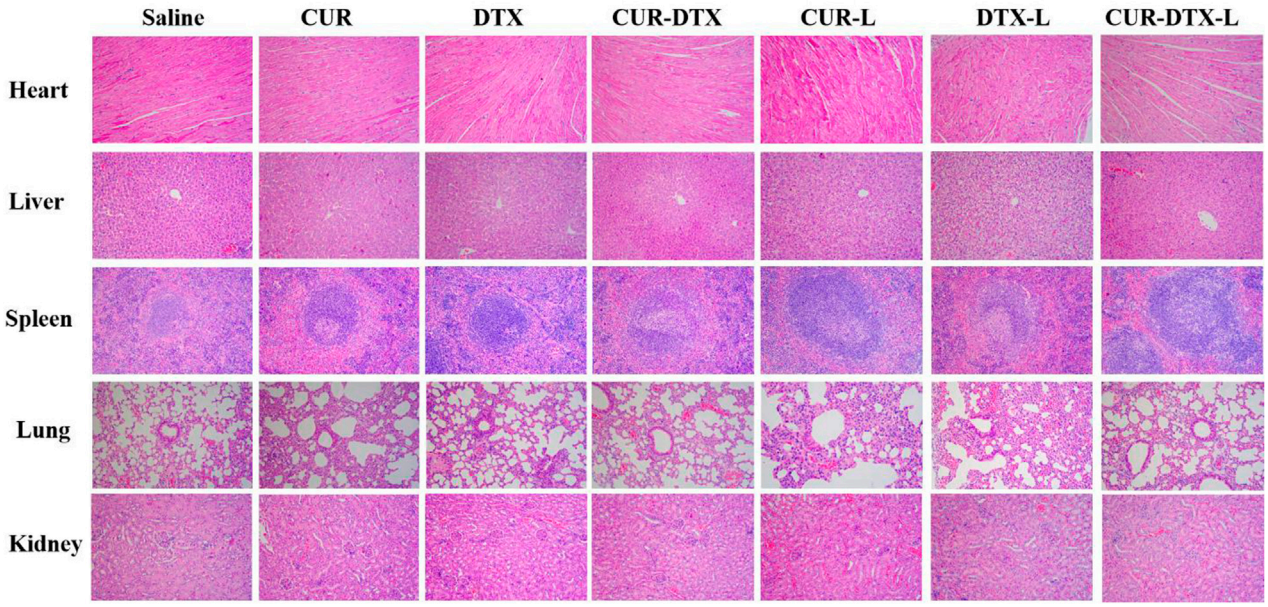

FIGURE 7
H and E staining images of the heart, liver, spleen, lung, liver, and kidney (magnification ×200).

in vivo distribution of chemotherapeutic drugs enhances their deposition at the tumor site and reduces their side effects, which is a requirement for cancer-specific therapy (Wang et al., 2019).

In this work, DTX and CUR were co-encapsulated and delivered by the liposomes for the treatment of breast cancer. The physicochemical properties showed that the liposomes have the ideal size and zeta potential, which provided the benign passive accumulation of liposomes in the tumor site. Furthermore, for an ideal drug delivery system, the speed of drug release is critical. Over 95% of DTX was released from the free DTX group in 10 h and about 60% of DTX was released from the DTX-L and DTX-CUR-L groups after using a dialysis system after 48 h; although DTX cannot be dissolved in the water, about 60% of DTX in the liposomes was released after 48 h, indicating that DTX could diffuse through the dialysis membrane. This may be due to the crystallization of free DTX as the phase separates inside the liposomes and leads to the sustained release, and this kind of release could reduce the damage of organs responsible for the drug and lessen side effects (Pawar et al., 2018). In addition, the pharmacokinetics assays demonstrated that free DTX was rapidly metabolized and cleared *in vivo*, and the liposomes provided a foundation for long-term therapy of breast cancer and retention of drugs. The pharmacokinetic parameters of $T_{1/2}$, AUC, and MRT also laid the groundwork for the accumulation and retention of drugs *in vivo* (He et al., 2019). These results are also consistent with those of other studies on DTX or co-delivery

systems (Bowerman et al., 2017; Wang et al., 2019), which indicated that liposomes attenuated the rapid phagocytosis of the bloodstream by macrophages and prolonged the retention time of DTX and CUR in the body circulation.

The results of the CCK-8 assay showed that the liposomes could achieve better inhibition of cell growth in MCF-7 cells *in vitro* than the two free drugs alone and the liposomes encapsulated with CUR and DTX. Moreover, in order to assess the efficacy of CUR-DTX-L *in vivo*, we investigated the efficacy of the liposomes in MCF-7 breast cancer model nude mice. As shown in Figures 4, 5, the combination of CUR and DTX resulted in stronger anticancer efficacy than the two drugs alone. The results of the synergistic study of CUR with DTX were similar to those of previous reports (Hu et al., 2020; Tanaudommongkon et al., 2020), which may be attributed to the reversal of the MDR effect of DTX by CUR. At the same time, co-delivery allows for a reduced number of carriers with synergistic effects and relatively easy preparation compared to the respective encapsulated CUR and DTX. The synergistic anti-tumor effect of CUR in combination with DTX has been documented through the reversal of MDR by CUR [(Hu et al., 2020), (Sahu et al., 2016)]. But further studies are still needed to confirm whether CUR in CUR-DTX-L exerts synergistic anti-tumor effects by reversing MDR and, if so, what the mechanism for reversing MDR is.

Any drug has a dual nature, being both beneficial and detrimental to the body. To investigate whether CUR-DTX-L has an effect on normal organs, the differences in body weight and HE staining between tissues were used to evaluate the side effect. The results showed that the mice treated with DTX-CUR-L had no significant pathological changes, indicating that DTX-CUR-L not only has better anti-tumor effects but also has lower side effects. These results could further confirm the reduced toxicity and enhanced efficiency effects of liposomes.

5 Conclusion

In this study, nanosized liposomes called CUR-DTX-L were created for the simultaneous administration of DTX and CUR to breast cancer. The preparation method is straightforward and reproducible. Systematically, the particle size, PDI, and EE were evaluated.

Then, we evaluated the *in vitro* and *in vivo* behaviors of CUR-DTX-L. DTX and CUR were able to sustain release from liposomes compared to free drugs, and *in vivo* investigations revealed that liposomes may lengthen the drug's retention period. The *in vivo* trial confirmed that the sustained release of medicine not only reduces side effects but also increases the drug's anticancer activity. CCK-8 experiments demonstrated that CUR-DTX-L was able to reverse MDR and improve DTX-induced cytotoxicity and apoptosis. In the mice of the MCF-7 tumor model, CUR-DTX-L generated much larger tumor volume reductions and less systemic toxicity than other groups. On the other hand, CUR could reverse the drug resistance of DTX, and the liposomes may enhance the therapeutic efficacy of combination medications. Therefore, we believe that CUR-DTX-L can be a potential treatment for breast cancer.

Data availability statement

The original contributions presented in the study are included in the article/Supplementary Materials; further inquiries can be directed to the corresponding authors.

Ethics statement

The animal study was reviewed and approved by the Institutional Animal Ethics Committee of Anhui Medical University.

Author contributions

Writing of the manuscript: XY, XC and RH; developing the idea for the manuscript and critically revising it: XY, XC, and WM; supervision: WC, FW and XM. All of the authors have read and approved the final version of the manuscript.

Funding

This research was supported by the National Natural Science Foundation of China (No. 82003849), the Science Foundation of Anhui Medical University (No. 2019xkj090), the Key Project of the Natural Science Foundation of Bengbu Medical College (No. BYKY2019298ZD), the Medical Science Research Foundation of the Beijing Medical Health Public Welfare Foundation (No. YWJKJJHKYJJ-B183063), the Research Project of Hefei Second People's Hospital (No. 2019-45-52), the Hefei Sixth-cycle Key Medical Specialty, and the Traditional Chinese Medicine Research Project of Hefei. The authors acknowledge the assistance of the students of the Pharmacokinetics Lab, Anhui University of Chinese Medicine, in conducting this study.

Conflict of interest

The authors declare that the research was conducted in the absence of any commercial or financial relationships that could be construed as a potential conflict of interest.

Publisher's note

References

Abbasi, A. Z., Prasad, P., Cai, P., He, C., Foltz, W. D., Amini, M. A., et al. (2015). Manganese oxide and docetaxel co-loaded fluorescent polymer nanoparticles for dual modal imaging and chemotherapy of breast cancer. *J. Control. Release* 209, 186–196. doi:10.1016/j.jconrel.2015.04.020

Abouzeid, A. H., Patel, N. R., and Torchilin, V. P. (2014). Polyethylene glycol-phosphatidylethanolamine (PEG-PE)/vitamin E micelles for co-delivery of paclitaxel and curcumin to overcome multi-drug resistance in ovarian cancer. *Int. J. Pharm.* 464 (1-2), 178–184. doi:10.1016/j.ijpharm.2014.01.009

Alvebratt, C., Dening, T. J., Åhlén, M., Cheung, O., Strømme, M., Gogoll, A., et al. (2020). *In vitro* performance and chemical stability of lipid-based formulations encapsulated in a mesoporous magnesium carbonate carrier. *Pharmaceutics* 12 (5), E426. doi:10.3390/pharmaceutics12050426

Angeline, N., Suhito, I. R., Kim, C. H., Hong, G. P., Park, C. G., Bhang, S. H., et al. (2020). A fibronectin-coated gold nanostructure composite for electrochemical detection of effects of curcumin-carrying nanoliposomes on human stomach cancer cells. *Analyst* 145 (2), 675–684. doi:10.1039/c9an01553a

Assaraf, Y. G., Brozovic, A., Gonçalves, A. C., Jurkovicova, D., Linē, A., Machuqueiro, M., et al. (2019). The multi-factorial nature of clinical multidrug resistance in cancer. *Drug resist. updat.* 46, 100645. doi:10.1016/j.drup.2019.100645

Berríos-Caro, E., Gifford, D. R., and Galla, T. (2021). Competition delays multi-drug resistance evolution during combination therapy. *J. Theor. Biol.* 509, 110524. doi:10.1016/j.jtbi.2020.110524

Bowerman, C. J., Byrne, J. D., Chu, K. S., Schorzman, A. N., Keeler, A. W., Sherwood, C. A., et al. (2017). Docetaxel-loaded PLGA nanoparticles improve efficacy in taxane-resistant triple-negative breast cancer. *Nano Lett.* 17 (1), 242–248. doi:10.1021/acs.nanolett.6b03971

Bukowski, K., Kciuk, M., and Kontek, R. (2020). Mechanisms of multidrug resistance in cancer chemotherapy. *Int. J. Mol. Sci.* 21 (9), E3233. doi:10.3390/ijms21093233

Cai, F. Y., Yao, X. M., Jing, M., Kong, L., Liu, J. J., Fu, M., et al. (2021). Enhanced antitumour efficacy of functionalized doxorubicin plus schisandrin B co-delivery liposomes via inhibiting epithelial-mesenchymal transition. *J. Liposome Res.* 31 (2), 113–129. doi:10.1080/08982104.2020.1745831

Chen, Y., Pan, L., Jiang, M., Li, D., and Jin, L. (2016). Nanostructured lipid carriers enhance the bioavailability and brain cancer inhibitory efficacy of curcumin both *in vitro* and *in vivo*. *Drug Deliv.* 23 (4), 1383–1392. doi:10.3109/10717544.2015.1049719

Cheng, C., Wu, Z., McClements, D. J., Zou, L., Peng, S., Zhou, W., et al. (2019). Improvement on stability, loading capacity and sustained release of rhamnolipids modified curcumin liposomes. *Colloids Surf. B Biointerfaces* 183, 110460. doi:10.1016/j.colsurfb.2019.110460

Du, S., and Deng, Y. (2006). Studies on the encapsulation of oxymatrine into liposomes by ethanol injection and pH gradient method. *Drug Dev. Ind. Pharm.* 32 (7), 791–797. doi:10.1080/03639040600760556

Frank, A. C., Ebersberger, S., Fink, A. F., Lampe, S., Weigert, A., Schmid, T., et al. (2019). Apoptotic tumor cell-derived microRNA-375 uses CD36 to alter the tumor-associated macrophage phenotype. *Nat. Commun.* 10 (1), 1135. doi:10.1038/s41467-019-08989-2

Gao, J. Q., Lv, Q., Li, L. M., Tang, X. J., Li, F. Z., Hu, Y. L., et al. (2013). Glioma targeting and blood-brain barrier penetration by dual-targeting doxorubincin liposomes. *Biomaterials* 34 (22), 5628–5639. doi:10.1016/j.biomaterials.2013.03.097

GBD 2017 Causes of Death Collaborators (2018). Global, regional, and national age-sex-specific mortality for 282 causes of death in 195 countries and territories, 1980-2017: A systematic analysis for the global burden of disease study 2017. *Lancet (London, Engl.* 392 (10159), 1736–1788. doi:10.1016/S0140-6736(18)32203-7

Gote, V., Nookala, A. R., Bolla, P. K., and Pal, D. (2021). Drug resistance in metastatic breast cancer: Tumor targeted nanomedicine to the rescue. *Int. J. Mol. Sci.* 22 (9), 4673. doi:10.3390/ijms22094673

Guo, D., Liu, J., Fan, Y., Cheng, J., Shi, Y., Zou, J., et al. (2020). Optimization, characterization and evaluation of liposomes from Malus hupehensis (Pamp.) Rehd. extracts. *J. Liposome Res.* 30 (4), 366–376. doi:10.1080/08982104.2019.1651334

Guo, P., Pi, C., Zhao, S., Fu, S., Yang, H., Zheng, X., et al. (2020). Oral co-delivery nanoemulsion of 5-fluorouracil and curcumin for synergistic effects against liver cancer. *Expert Opin. Drug Deliv.* 17 (10), 1473–1484. doi:10.1080/17425247.2020.1796629

He, H., Lu, Y., Qi, J., Zhu, Q., Chen, Z., and Wu, W. (2019). Adapting liposomes for oral drug delivery. *Acta Pharm. Sin. B* 9 (1), 36–48. doi:10.1016/j.apsb.2018.06.005

He, Z. Y., Zheng, X., Wu, X. H., Song, X. R., He, G., Wu, W. F., et al. (2010). Development of glycyrrhetinic acid-modified stealth cationic liposomes for gene delivery. *Int. J. Pharm.* 397 (1-2), 147–154. doi:10.1016/j.ijpharm.2010.06.029

Hesari, A., Azizian, M., Sheikhi, A., Nesaei, A., Sanaei, S., Mahinparvar, N., et al. (2019). Chemopreventive and therapeutic potential of curcumin in esophageal cancer: Current and future status. *Int. J. Cancer* 144 (6), 1215–1226. doi:10.1002/ijc.31947

Hong, Y., Che, S., Hui, B., Yang, Y., Wang, X., Zhang, X., et al. (2019). Lung cancer therapy using doxorubicin and curcumin combination: Targeted prodrug based, pH sensitive nanomedicine. *Biomed. Pharmacother. = Biomedecine Pharmacother.* 112, 108614. doi:10.1016/j.biopha.2019.108614

Hu, Y., Ran, M., Wang, B., Lin, Y., Cheng, Y., and Zheng, S. (2020). Co-delivery of docetaxel and curcumin via nanomicelles for enhancing anti-ovarian cancer treatment. *Int. J. Nanomedicine* 15, 9703–9715. doi:10.2147/IJN.S274083

Hua, H., Zhang, N., Liu, D., Song, L., Liu, T., Li, S., et al. (2017). Multifunctional gold nanorods and docetaxel-encapsulated liposomes for combined thermo- and chemotherapy. *Int. J. Nanomedicine* 12, 7869–7884. doi:10.2147/IJN.S143977

Ji, C., Na, W., Fei, X., Sheng-Jun, C., and Jia-Bi, Z. (2006). Characterization, lung targeting profile and therapeutic efficiency of dipyridamole liposomes. *J. Drug Target.* 14 (10), 717–724. doi:10.1080/10611860600916586

Kaushik, L., Srivastava, S., Panjeta, A., Chaudhari, D., Ghadi, R., Kuche, K., et al. (2020). Exploration of docetaxel palmitate and its solid lipid nanoparticles as a novel option for alleviating the rising concern of multi-drug resistance. *Int. J. Pharm.* 578, 119088. doi:10.1016/j.ijpharm.2020.119088

Labbozzetta, M., Notarbartolo, M., Poma, P., Maurici, A., Inguglia, L., Marchetti, P., et al. (2009). Curcumin as a possible lead compound against hormone-independent, multidrug-resistant breast cancer. *Ann. N. Y. Acad. Sci.* 1155, 278–283. doi:10.1111/j.1749-6632.2009.03699.x

Li, S., Shan, X., Wang, Y., Chen, Q., Sun, J., He, Z., et al. (2020). Dimeric prodrug-based nanomedicines for cancer therapy. *J. Control. Release* 326, 510–522. doi:10.1016/j.jconrel.2020.07.036

Mathiyazhakan, M., Wiraja, C., and Xu, C. (2018). A concise review of gold nanoparticles-based photo-responsive liposomes for controlled drug delivery. *Nanomicro. Lett.* 10 (1), 10. doi:10.1007/s40820-017-0166-0

Nassir, A. M., Ibrahim, I. A. A., Md, S., Waris, M., Ain, M. R., Ahmad, I., et al.Tanuja (2019). Surface functionalized folate targeted oleuropein nano-liposomes for prostate tumor targeting: Invitro and invivo activity. *Life Sci.* 220, 136–146. doi:10.1016/j.lfs.2019.01.053

Pawar, V. A., Manjappa, A. S., Murumkar, P. R., Gajaria, T. K., Devkar, R. V., Mishra, A. K., et al. (2018). Drug-fortified liposomes as carriers for sustained release of NSAIDs: The concept and its validation in the animal model for the treatment of arthritis. *Eur. J. Pharm. Sci.* 125, 11–22. doi:10.1016/j.ejps.2018.09.009

Persohn, E., Canta, A., Schoepfer, S., Traebert, M., Mueller, L., Gilardini, A., et al. (2005). Morphological and morphometric analysis of paclitaxel and docetaxel-induced peripheral neuropathy in rats. *Eur. J. Cancer* 41 (10), 1460–1466. doi:10.1016/j.ejca.2005.04.006

Ran, R., Liu, Y., Gao, H., Kuang, Q., Zhang, Q., Tang, J., et al. (2014). Enhanced gene delivery efficiency of cationic liposomes coated with PEGylated hyaluronic acid for anti P-glycoprotein siRNA: A potential candidate for overcoming multi-drug resistance. *Int. J. Pharm.* 477 (1-2), 590–600. doi:10.1016/j.ijpharm.2014.11.012

Rao, S. Q., Xu, G. W., Zeng, H. W., Zheng, X. F., Hu, Q., Wang, Q. Y., et al. (2020). Physicochemical and antibacterial properties of fabricated ovalbumin-carvacrol gel nanoparticles. *Food Funct.* 11 (6), 5133–5141. doi:10.1039/d0fo00755b

Rejinold, N. S., Yoo, J., Jon, S., and Kim, Y. C. (2018). Curcumin as a novel nanocarrier system for doxorubicin delivery to MDR cancer cells: *In vitro* and *in vivo* evaluation. *ACS Appl. Mat. Interfaces* 10 (34), 28458–28470. doi:10.1021/acsami.8b10426

Sahu, B. P., Hazarika, H., Bharadwaj, R., Loying, P., Baishya, R., Dash, S., et al. (2016). Curcumin-docetaxel co-loaded nanosuspension for enhanced anti-breast cancer activity. *Expert Opin. Drug Deliv.* 13 (8), 1065–1074. doi:10.1080/17425247.2016.1182486

Salem, A. R., Martínez Pulido, P., Sanchez, F., Sanchez, Y., Español, A. J., and Sales, M. E. (2020). Effect of low dose metronomic therapy on MCF-7 tumor cells growth and angiogenesis. Role of muscarinic acetylcholine receptors. *Int. Immunopharmacol.* 84, 106514. doi:10.1016/j.intimp.2020.106514

Schmidt, B., Ferreira, C., Alves Passos, C. L., Silva, J. L., and Fialho, E. (2020). Resveratrol, curcumin and piperine alter human glyoxalase 1 in MCF-7 breast cancer cells. *Int. J. Mol. Sci.* 21 (15), E5244. doi:10.3390/ijms21155244

Schmidt, T., van Mackelenbergh, M., Wesch, D., and Mundhenke, C. (2017). Physical activity influences the immune system of breast cancer patients. *J. Cancer Res. Ther.* 13 (3), 392–398. doi:10.4103/0973-1482.150356

Sercombe, L., Veerati, T., Moheimani, F., Wu, S. Y., Sood, A. K., and Hua, S. (2015). Advances and challenges of liposome assisted drug delivery. *Front. Pharmacol.* 6, 286. doi:10.3389/fphar.2015.00286

Shaik, M. S., Chatterjee, A., and Singh, M. (2004). Effects of monensin liposomes on the cytotoxicity, apoptosis and expression of multidrug resistance genes in doxorubicin-resistant human breast tumour (MCF-7/dox) cell-line. *J. Pharm. Pharmacol.* 56 (7), 899–907. doi:10.1211/0022357023772

Shi, C., Zhang, Z., Shi, J., Wang, F., and Luan, Y. (2015). Co-delivery of docetaxel and chloroquine via PEO-PPO-PCL/TPGS micelles for overcoming multidrug resistance. *Int. J. Pharm.* 495 (2), 932–939. doi:10.1016/j.ijpharm.2015.10.009

Sun, H., Cao, D., Wu, H., Liu, H., Ke, X., and Ci, T. (2018). Development of low molecular weight heparin based nanoparticles for metastatic breast cancer therapy. *Int. J. Biol. Macromol.* 112, 343–355. doi:10.1016/j.ijbiomac.2018.01.195

Sun, X., Yan, X., Jacobson, O., Sun, W., Wang, Z., Tong, X., et al. (2017). Improved tumor uptake by optimizing liposome based RES blockade strategy. *Theranostics* 7 (2), 319–328. doi:10.7150/thno.18078

Tanaudommongkon, I., Tanaudommongkon, A., Prathipati, P., Nguyen, J. T., Keller, E. T., and Dong, X. (2020). Curcumin nanoparticles and their cytotoxicity in docetaxel-resistant castration-resistant prostate cancer cells. *Biomedicines* 8 (8), E253. doi:10.3390/biomedicines8080253

Tian, M. P., Song, R. X., Wang, T., Sun, M. J., Liu, Y., and Chen, X. G. (2018). Inducing sustained release and improving oral bioavailability of curcumin via chitosan derivatives-coated liposomes. *Int. J. Biol. Macromol.* 120, 702–710. doi:10.1016/j.ijbiomac.2018.08.146

Vitor, M. T., Bergami-Santos, P. C., Zômpero, R. H. F., Cruz, K. S. P., Pinho, M. P., Barbuto, J. A. M., et al. (2017). Cationic liposomes produced via ethanol injection method for dendritic cell therapy. *J. Liposome Res.* 27 (4), 249–263. doi:10.1080/08982104.2016.1196702

Wang, C., Wang, X., Zhong, T., Zhao, Y., Zhang, W. Q., Ren, W., et al. (2015). The antitumor activity of tumor-homing peptide-modified thermosensitive liposomes containing doxorubicin on MCF-7/ADR: *In vitro* and *in vivo*. *Int. J. Nanomedicine* 10, 2229–2248. doi:10.2147/IJN.S79840

Wang, F., Zhang, D., Zhang, Q., Chen, Y., Zheng, D., Hao, L., et al. (2011). Synergistic effect of folate-mediated targeting and verapamil-mediated P-gp inhibition with paclitaxel -polymer micelles to overcome multi-drug resistance. *Biomaterials* 32 (35), 9444–9456. doi:10.1016/j.biomaterials.2011.08.041

Wang, Q. S., Gao, L. N., Zhu, X. N., Zhang, Y., Zhang, C. N., Xu, D., et al. (2019). Co-delivery of glycyrrhizin and doxorubicin by alginate nanogel particles attenuates the activation of macrophage and enhances the therapeutic efficacy for hepatocellular carcinoma. *Theranostics* 9 (21), 6239–6255. doi:10.7150/thno.35972

Wang, S., Liu, C., Wang, C., Ma, J., Xu, H., Guo, J., et al. (2020). Arsenic trioxide encapsulated liposomes prepared via copper acetate gradient loading method and its antitumor efficiency. *Asian J. Pharm. Sci.* 15 (3), 365–373. doi:10.1016/j.ajps.2018.12.002

Wong, K. E., Ngai, S. C., Chan, K. G., Lee, L. H., Goh, B. H., and Chuah, L. H. (2019). Curcumin nanoformulations for colorectal cancer: A review. *Front. Pharmacol.* 10, 152. doi:10.3389/fphar.2019.00152

Wu, H., Luo, Y., Xu, D., Ke, X., and Ci, T. (2020). Low molecular weight heparin modified bone targeting liposomes for orthotopic osteosarcoma and breast cancer bone metastatic tumors. *Int. J. Biol. Macromol.* 164, 2583–2597. doi:10.1016/j.ijbiomac.2020.08.068

Wu, H., Zhong, Q., Zhong, R., Huang, H., Xia, Z., Ke, Z., et al. (2016). Preparation and antitumor evaluation of self-assembling oleanolic acid-loaded Pluronic P105/d-α-tocopheryl polyethylene glycol succinate mixed micelles for non-small-cell lung cancer treatment. *Int. J. Nanomedicine* 11, 6337–6352. doi:10.2147/IJN.S119839

Xu, X. L., Kang, X. Q., Qi, J., Jin, F. Y., Liu, D., and Du, Y. Z. (2019). Novel antibacterial strategies for combating bacterial multidrug resistance. *Curr. Pharm. Des.* 25 (44), 4717–4724. doi:10.2174/1381612825666191022163237

Yu, B., Zhao, X., Lee, L. J., and Lee, R. J. (2009). Targeted delivery systems for oligonucleotide therapeutics. *AAPS J.* 11 (1), 195–203. doi:10.1208/s12248-009-9096-1

Yu, L., Liu, J., Xu, X., Zhang, L., Hu, R., Liu, J., et al. (2017). Ilmenite nanotubes for high stability and high rate sodium-ion battery anodes. *ACS Nano* 11 (5), 5120–5129. doi:10.1021/acsnano.7b02136

Zhang, W., Zheng, X., Meng, T., You, H., Dong, Y., Xing, J., et al. (2017). SET protein overexpression contributes to paclitaxel resistance in MCF-7/S cells through PI3K/Akt pathway. *J. Drug Target.* 25 (3), 255–263. doi:10.1080/1061186X.2016.1245307

Zhang, Y., He, W., Du, Y., Du, Y., Zhao, C., Zhang, Y., et al. (2020). Dimeric artesunate phospholipid-conjugated liposomes as promising anti-inflammatory therapy for rheumatoid arthritis. *Int. J. Pharm.* 579, 119178. doi:10.1016/j.ijpharm.2020.119178

Zhao, M. D., Li, J. Q., Chen, F. Y., Dong, W., Wen, L. J., Fei, W. D., et al. (2019). Co-delivery of curcumin and paclitaxel by "Core-Shell" targeting amphiphilic copolymer to reverse resistance in the treatment of ovarian cancer. *Int. J. Nanomedicine* 14, 9453–9467. doi:10.2147/IJN.S224579

Frontiers in Oncology

Advances knowledge of carcinogenesis and tumor progression for better treatment and management

The third most-cited oncology journal, which highlights research in carcinogenesis and tumor progression, bridging the gap between basic research and applications to imrpove diagnosis, therapeutics and management strategies.

Discover the latest Research Topics

See more →

Frontiers

Avenue du Tribunal-Fédéral 34
1005 Lausanne, Switzerland
frontiersin.org

Contact us

+41 (0)21 510 17 00
frontiersin.org/about/contact